

# **THE PATHOGENIC YERSINIAE – ADVANCES IN THE UNDERSTANDING OF PHYSIOLOGY AND VIRULENCE, VOLUME II**

EDITED BY: Matthew S. Francis and Victoria Auerbuch

PUBLISHED IN: Frontiers in Cellular and Infection Microbiology



# frontiers

## Frontiers Copyright Statement

© Copyright 2007-2019 Frontiers Media SA. All rights reserved.

All content included on this site, such as text, graphics, logos, button icons, images, video/audio clips, downloads, data compilations and software, is the property of or is licensed to Frontiers Media SA ("Frontiers") or its licensees and/or subcontractors. The copyright in the text of individual articles is the property of their respective authors, subject to a license granted to Frontiers.

The compilation of articles constituting this e-book, wherever published, as well as the compilation of all other content on this site, is the exclusive property of Frontiers. For the conditions for downloading and copying of e-books from Frontiers' website, please see the Terms for Website Use. If purchasing Frontiers e-books from other websites or sources, the conditions of the website concerned apply.

Images and graphics not forming part of user-contributed materials may not be downloaded or copied without permission.

Individual articles may be downloaded and reproduced in accordance with the principles of the CC-BY licence subject to any copyright or other notices. They may not be re-sold as an e-book.

As author or other contributor you grant a CC-BY licence to others to reproduce your articles, including any graphics and third-party materials supplied by you, in accordance with the Conditions for Website Use and subject to any copyright notices which you include in connection with your articles and materials.

All copyright, and all rights therein, are protected by national and international copyright laws.

The above represents a summary only. For the full conditions see the Conditions for Authors and the Conditions for Website Use.

ISSN 1664-8714

ISBN 978-2-88963-051-6

DOI 10.3389/978-2-88963-051-6

## About Frontiers

Frontiers is more than just an open-access publisher of scholarly articles: it is a pioneering approach to the world of academia, radically improving the way scholarly research is managed. The grand vision of Frontiers is a world where all people have an equal opportunity to seek, share and generate knowledge. Frontiers provides immediate and permanent online open access to all its publications, but this alone is not enough to realize our grand goals.

## Frontiers Journal Series

The Frontiers Journal Series is a multi-tier and interdisciplinary set of open-access, online journals, promising a paradigm shift from the current review, selection and dissemination processes in academic publishing. All Frontiers journals are driven by researchers for researchers; therefore, they constitute a service to the scholarly community. At the same time, the Frontiers Journal Series operates on a revolutionary invention, the tiered publishing system, initially addressing specific communities of scholars, and gradually climbing up to broader public understanding, thus serving the interests of the lay society, too.

## Dedication to Quality

Each Frontiers article is a landmark of the highest quality, thanks to genuinely collaborative interactions between authors and review editors, who include some of the world's best academicians. Research must be certified by peers before entering a stream of knowledge that may eventually reach the public - and shape society; therefore, Frontiers only applies the most rigorous and unbiased reviews.

Frontiers revolutionizes research publishing by freely delivering the most outstanding research, evaluated with no bias from both the academic and social point of view. By applying the most advanced information technologies, Frontiers is catapulting scholarly publishing into a new generation.

## What are Frontiers Research Topics?

Frontiers Research Topics are very popular trademarks of the Frontiers Journals Series: they are collections of at least ten articles, all centered on a particular subject. With their unique mix of varied contributions from Original Research to Review Articles, Frontiers Research Topics unify the most influential researchers, the latest key findings and historical advances in a hot research area! Find out more on how to host your own Frontiers Research Topic or contribute to one as an author by contacting the Frontiers Editorial Office: [researchtopics@frontiersin.org](mailto:researchtopics@frontiersin.org)



# THE PATHOGENIC YERSINIAE – ADVANCES IN THE UNDERSTANDING OF PHYSIOLOGY AND VIRULENCE, VOLUME II

Topic Editors:

**Matthew S. Francis**, Umeå University, Sweden

**Victoria Auerbuch**, University of California, Santa Cruz, United States



"Transmission electron microscopic observation of Yersinia flagella". Image: Ikenna Obi in collaboration with Umeå Core Facility for Electron Microscopy (Umeå University, Sweden).

Pathogenic Yersinia consist of the prominent human pathogens *Y. pestis*, *Y. enterocolitica*, and *Y. pseudotuberculosis*, the fish pathogen *Y. ruckeri*, as well as a number of insect pathogens. Facilitated by the ease of in vitro culturing, genetic tractability, and availability of relevant infection models, studies of pathogenic Yersinia have revealed a great deal about physiological processes at the molecular level that contribute to pathogen adaptation to the ever changing environments both inside and outside of the host. Comprehensive genome sequencing analyses has further benefitted understanding of this bacterial pathogen evolution. Critically, many of these detailed molecular studies also identified potential targets for the design and development of anti-bacterial therapeutic drugs that could help to fight the

ever-increasing problem of resistance to conventional antibiotics. New developments in several of these areas are highlighted in this edition of the Research Topic "The Pathogenic Yersiniae – Advances in the Understanding of Physiology and Virulence, Second Edition".

**Citation:** Francis, M. S., Auerbuch, V., eds. (2019). The Pathogenic Yersiniae – Advances in the Understanding of Physiology and Virulence, Volume II. Lausanne: Frontiers Media. doi: 10.3389/978-2-88963-051-6

# Table of Contents

## **06 Editorial: The Pathogenic *Yersiniae*—Advances in the Understanding of Physiology and Virulence, Second Edition**

Matthew S. Francis and Victoria Auerbuch

### **SECTION 1**

#### **PROTEIN SECRETION**

##### **11 Chromosomally-Encoded *Yersinia pestis* Type III Secretion Effector Proteins Promote Infection in Cells and in Mice**

Sara Schesser Bartra, Cherish Lorica, Lianfen Qian, Xin Gong, Wael Bahnan, Henry Barreras Jr., Rosmely Hernandez, Zhongwei Li, Gregory V. Plano and Kurt Schesser

##### **20 Heterologous Complementation Studies With the *YscX* and *YscY* Protein Families Reveals a Specificity for *Yersinia pseudotuberculosis* Type III Secretion**

Jyoti M. Gurung, Ayad A. A. Amer, Monika K. Francis, Tiago R. D. Costa, Shiyun Chen, Anton V. Zavialov and Matthew S. Francis

##### **36 Type VI Secretion Systems Present New Insights on Pathogenic *Yersinia***

Xiaobing Yang, Junfeng Pan, Yao Wang and Xihui Shen

### **SECTION 2**

#### **NICHE ADAPTATION**

##### **46 Changes in Transcriptome of *Yersinia pseudotuberculosis* IP32953 Grown at 3 and 28°C Detected by RNA Sequencing Shed Light on Cold Adaptation**

Jussa-Pekka Virtanen, Riikka Keto-Timonen, Kaisa Jaakkola, Noora Salin and Hannu Korkeala

##### **65 Prevalence of *Yersinia* Species in the Ileum of Crohn's Disease Patients and Controls**

Guillaume Le Baut, Claire O'Brien, Paul Pavli, Maryline Roy, Philippe Seksik, Xavier Tréton, Stéphane Nancey, Nicolas Barnich, Madeleine Bezault, Claire Auzolle, Dominique Cazals-Hatem, Jérôme Viala, Matthieu Allez, The REMIND GROUP, Jean-Pierre Hugot and Anne Dumay

### **SECTION 3**

#### **GENE EXPRESSION CONTROL**

##### **74 *OmpR*-Mediated Transcriptional Regulation and Function of Two Heme Receptor Proteins of *Yersinia enterocolitica* Bio-Serotype 2/O:9**

Karolina Jaworska, Marta Nieckarz, Marta Ludwiczak, Adrianna Raczowska and Katarzyna Brzostek

##### **93 *Yersinia pseudotuberculosis* *BarA-UvrY* Two-Component Regulatory System Represses Biofilms via *CsrB***

Jeffrey K. Schachterle, Ryan M. Stewart, M. Brett Schachterle, Joshua T. Calder, Huan Kang, John T. Prince and David L. Erickson



**104 *BfvR, an AraC-Family Regulator, Controls Biofilm Formation and pH6 Antigen Production in Opposite Ways in Yersinia pestis Biovar Microtus***

Haihong Fang, Lei Liu, Yiquan Zhang, Huiying Yang, Yanfeng Yan, Xiaojuan Ding, Yanping Han, Dongsheng Zhou and Ruifu Yang

**SECTION 4**

**MICROBIOLOGY AND PATHOGENESIS OF NON-MAMMALIAN YERSINIA INFECTIONS**

**115 *The Infection Process of Yersinia ruckeri: Reviewing the Pieces of the Jigsaw Puzzle***

José A. Guijarro, Ana I. García-Torrico, Desirée Cascales and Jessica Méndez

**125 *pYR4 From a Norwegian Isolate of Yersinia ruckeri is a Putative Virulence Plasmid Encoding Both a Type IV Pilus and a Type IV Secretion System***

Agnieszka Wrobel, Claudio Ottoni, Jack C. Leo and Dirk Linke

**139 *Insecticidal Toxicity of Yersinia frederiksenii Involves the Novel Enterotoxin YacT***

Katharina Springer, Philipp-Albert Sängler, Christian Moritz, Angela Felsl, Thomas Rattei and Thilo M. Fuchs

**SECTION 5**

**NEW FRONTIERS IN YERSINIA BIOLOGY RESEARCH**

**152 *An Experimental Pipeline for Initial Characterization of Bacterial Type III Secretion System Inhibitor Mode of Action Using Enteropathogenic Yersinia***

Jessica M. Morgan, Hanh N. Lam, Jocelyn Delgado, Justin Luu, Sina Mohammadi, Ralph R. Isberg, Helen Wang and Victoria Auerbuch

**169 *Discovering RNA-Based Regulatory Systems for Yersinia Virulence***

Vanessa Knittel, Ines Vollmer, Marcel Volk and Petra Dersch

**184 *All Yersinia are not Created Equal: Phenotypic Adaptation to Distinct Niches Within Mammalian Tissues***

Kimberly M. Davis



# Editorial: The Pathogenic *Yersiniae*—Advances in the Understanding of Physiology and Virulence, Second Edition

Matthew S. Francis<sup>1\*</sup> and Victoria Auerbuch<sup>2\*</sup>

<sup>1</sup> Department of Molecular Biology, Umeå Centre for Microbial Research, Umeå University, Umeå, Sweden, <sup>2</sup> Department of Microbiology and Environmental Toxicology, University of California, Santa Cruz, Santa Cruz, CA, United States

**Keywords:** phenotypic and niche adaptation, protein secretion, biofilm, small regulatory RNAs, two-component systems, virulence blockers, Crohn's disease, fish- and insect-pathogen

## Editorial on the Research Topic

### The Pathogenic *Yersiniae*—Advances in the Understanding of Physiology and Virulence, Second Edition

## OPEN ACCESS

### Edited and reviewed by:

John S. Gunn,  
The Research Institute at Nationwide  
Children's Hospital, United States

### \*Correspondence:

Matthew S. Francis  
matthew.francis@umu.se  
Victoria Auerbuch  
vastone@ucsc.edu

### Specialty section:

This article was submitted to  
Molecular Bacterial Pathogenesis,  
a section of the journal  
Frontiers in Cellular and Infection  
Microbiology

**Received:** 20 March 2019

**Accepted:** 03 April 2019

**Published:** 18 April 2019

### Citation:

Francis MS and Auerbuch V (2019)  
Editorial: The Pathogenic  
*Yersiniae*—Advances in the  
Understanding of Physiology and  
Virulence, Second Edition.  
Front. Cell. Infect. Microbiol. 9:119.  
doi: 10.3389/fcimb.2019.00119

Of the 18 known *Yersinia* species, *Y. pestis*, *Y. pseudotuberculosis*, and *Y. enterocolitica* are pathogenic to humans and animals and are widely characterized. The zoonotic obligate pathogen *Y. pestis* is the causal agent of plague, a systemic disease that is usually fatal if left untreated (Zietz and Dunkelberg, 2004; Zhou et al., 2006). Free-living *Y. enterocolitica* and *Y. pseudotuberculosis* are the agents of yersiniosis, a rarely systemic gastrointestinal disease (Galindo et al., 2011). The remaining species are mostly harmless to humans, although *Y. ruckeri* is an enteric fish pathogen affecting mainly salmonids, while a few others display toxicity toward insects (Sulakvelidze, 2000; Tobback et al., 2007; Fuchs et al., 2008; Chen et al., 2010). At the forefront of *Yersinia* research are studies of classical microbiology, pathogenesis, protein secretion, niche adaptation, and regulation of gene expression. In pursuit of these endeavors, new frontiers are being forged on waves of methodological and technological innovation. In this second edition of the special research topic on the pathogenic *Yersiniae* is a compilation of reviews and research articles that summarize current knowledge and future research directions in the *Yersinia* pathophysiology field.

## PROTEIN SECRETION

Type III secretion (T3S) is prominent protein delivery process in a large number of Gram-negative bacteria that confers to them an ability to interact in pathogenic or symbiotic relationships with either vertebrate or invertebrate hosts (Buttner, 2012; Deng et al., 2017). The Ysc-Yop T3S system (T3SS) is encoded on a virulence plasmid common to all human pathogenic *Yersinia* (Cornelis et al., 1998). This so-called “injectisome” has long been believed to provide a conduit through which a restricted set of just six or seven plasmid-encoded host-modulating Yop effectors are delivered from the bacterial cytoplasm into the eukaryotic cell cytosol (Pha and Navarro, 2016; Grabowski et al., 2017). Using a transposon site hybridization based genome wide screen, Schesser-Bartra et al. identified three chromosomally-encoded proteins that promote *Y. pestis* infection in cells and in mice. With features indicative of host-modulating Yop effectors, they identify the first non-plasmid

encoded secretion substrates of the Ysc-Yop T3SS. In another study that performed heterologous complementation analyses with the YscX and YscY protein families, Gurung et al. reveal that the YscX and YscY protein complex produced by *Y. pseudotuberculosis* is specifically critical for biogenesis and/or function of the Ysc-Yop T3SS. The authors go on to discuss what might be the molecular basis for this specificity.

While pathogenic potential of *Yersinia* for humans and animals is heavily correlated to the plasmid encoded Ysc-Yop T3SS, Yang et al. provide new insight into the four independent Type VI secretion system (T6SS) copies present in human pathogenic *Yersinia*. The impact of these multiple systems on *Yersinia* physiology and pathogenesis is likely to be very large given how T6SSs have capacity to deliver multiple effectors into either prokaryotic or eukaryotic cells, and are known to affect diverse biological processes such as virulence, anti-virulence, stress resistance and competition (Alteri and Mobley, 2016; Lien and Lai, 2017).

## NICHE ADAPTATION

Enteropathogenic *Yersinia* are foodborne pathogens. Therefore it comes as no surprise that they thrive at refrigeration temperatures (Brocklehurst and Lund, 1990; Goverde et al., 1994; Azizoglu and Kathariou, 2010; Keto-Timonen et al., 2018), and in this environment even remain primed for infection (Asadishad et al., 2013). To understand the molecular mechanisms by which psychotropic *Yersinia* thrive in cold environments may give rise to strategies by which growth can be restricted, and this would be a strategically important preventative measure for the food processing industry. To investigate the genome-wide cold adaptation behavior of *Y. pseudotuberculosis*, Virtanen et al. used RNA-Seq technology to identify genes that were significantly more expressed in a cell density specific manner at cold temperature. Among the many genes that were up-regulated were nutrient acquisition genes, cold shock protein genes, DEAD-box RNA helicase genes, genes handling compatible solutes, genes involved in transcription termination and translation initiation, and genes involved in cell wall modification. This suggests that *Y. pseudotuberculosis* establishes a core network of cold responsive proteins to drive ribosome biogenesis and function at low temperature.

It follows that psychotropic *Yersinia* are enriched in a variety of foods on a global scale (Hilbert et al., 2003; Ozdemir and Arslan, 2015; Le Guern et al., 2016). Moreover, changing food consumption practices and globalization of the international food trade have contributed to increased frequency of yersiniosis (Gupta et al., 2015). At the same time, orally ingested *Yersinia* have the potential to survive passage through the gastrointestinal tract. It has been postulated that surviving bacteria may contribute to the onset or persistence of gut inflammation (Hugot et al., 2003). Although experimental mouse models of Crohn's disease do not discount contributions made by infecting enteropathogenic *Yersinia* (Meinzer et al., 2008; Murthy et al., 2014; Fonseca et al., 2015; Han et al., 2017), support stemming from cohort studies of *Yersinia* infected clinical material is underwhelming (Kallinowski et al., 1998;

Lamps et al., 2003; Knosel et al., 2009; Chiodini et al., 2013; Leu et al., 2013). To further investigate this issue, Le Baut et al. analyzed the prevalence of *Yersinia* species in a total of 470 ileal samples taken from Crohn's disease patients and healthy controls. Significantly, *Yersinia* species were detected with equal frequency in both disease and healthy ileum tissue, suggesting that they are well adapted to this niche. Hence, there is now a need to characterize the effect of resident *Yersinia* on maturation and regulation of the mucosal immune response.

## GENE EXPRESSION CONTROL

Behind every successful niche adaptation is a complex regulatory circuitry that controls specific gene expression profiles. For example, the two-component or histidine-aspartate phosphorelay systems are vital for the monitoring of environmental and intracellular signals to produce changes in gene expression or behavioral responses (Stock et al., 2000; Laub and Goulian, 2007). In *Yersinia*, a large number of two-component systems are known (Marceau, 2005), with a few of them making recognized contributions to *Yersinia* survivability in the environment or in an infected host (Flamez et al., 2008; Reboul et al., 2014). A notable two component system is EnvZ/OmpR that enables many bacteria to alter gene expression in response to osmotic and acid stress (Walthers et al., 2005; Chakraborty and Kenney, 2018). The work of Jaworska et al. reports on OmpR-mediated control of iron acquisition via transcriptional repression of the HemR1 and HemR2 heme receptors. This regulatory circuit works in conjunction with the transcriptional repressor Fur to prevent over-accumulation of iron/heme by *Y. enterocolitica*.

Another two component system is BarA/UvrY. Responding to metabolic end products such as short chain fatty acids, BarA/UvrY signaling is the primary regulator of the widespread Csr global regulatory system, and in this way can profoundly influence multiple metabolic, behavioral and virulence traits in many bacteria (Vakulskas et al., 2015). In the report by Schachterle et al. BarA/UvrY signaling was found to repress the formation of *Y. pseudotuberculosis* biofilms through activation of the CsrB regulatory RNA. It is likely that this is pleiotropic repression affecting multiple elements of biofilm formation and maintenance by *Y. pseudotuberculosis*.

The primary requirement for mature biofilm formation by *Yersinia* is the production of an exopolysaccharide (EPS) that requires the *hmsHFRS* locus to coordinate its synthesis and transport (Bobrov et al., 2008). Moreover, c-di-GMP enhances EPS production, and the levels of this signaling molecule are tightly controlled by the opposing actions of two diguanylate cyclases (encoded by *hmsT* and *hmsD*) and a phosphodiesterase (*hmsP*) (Kirillina et al., 2004; Bobrov et al., 2011). The study of Fang et al. describes a novel AraC-like transcriptional activator termed BfvR that controls *Y. pestis* biofilm formation via stimulating transcription from the *hmsHFRS* and *hmsCDE* operons to elevate EPS and c-di-GMP production. This identifies BfvR as the first AraC family transcription regulator reported to control biofilm formation in *Yersinia*.



## MICROBIOLOGY AND PATHOGENESIS OF NON-MAMMALIAN *YERSINIA* INFECTIONS

Although not known to be harmful to humans, the enteric fish pathogen *Y. ruckeri* is still a pathogen of great interest as it has capacity to cause significant economic losses in the aquaculture industry (Tobback et al., 2007). This is reflected by a recent surge of reports that offer improved understanding of the biological processes contributing to *Y. ruckeri* infection and pathogenicity. The review by Guijarro et al. assimilates this new knowledge to provide up-to-date insight into the molecular mechanisms of the *Y. ruckeri* infection process. Complementing this review is a report by Wrobel et al. that analyzed the complete DNA sequence of the unique pYR4 plasmid from a highly virulent isolate of *Y. ruckeri*. This cryptic plasmid has potential to impact positively on *Y. ruckeri* virulence since it encodes for a type IV pilus and a type IV secretion system that are well established virulence associated factors in other bacteria (Craig et al., 2004; Giltner et al., 2012; Gonzalez-Rivera et al., 2016; Grohmann et al., 2018).

Moreover, there has been great interest in the function and taxonomical distribution of insecticidal genes among *Yersinia* spp., owing in part to their potential in contributing new knowledge to the ecology, evolution and pathogenicity of human pathogenic *Yersinia* (Pinheiro and Ellar, 2007; Fuchs et al., 2008, 2011; Hares et al., 2008; Spinner et al., 2012, 2013; Alenizi et al., 2016). Using *Y. frederiksenii* as a model system that displays toxicity toward insects, Springer et al. were able to demonstrate a distinct contribution of the novel heat-stable cytotoxic enterotoxin to oral and intrahemocoelic toxicity of infected insects. These findings led the authors to discuss how the ability to enter invertebrates may constitute a selective advantage to *Yersinia* isolates in environmental survival and evolution of virulence.

## NEW FRONTIERS IN *YERSINIA* BIOLOGY RESEARCH

Conventional antibiotics have saved the lives of many by decreasing the morbidity and mortality of bacterial infectious diseases. However, the global emergence of bacteria resistant to these antibiotics means that they no longer work effectively, and this presents a major healthcare issue that creates tremendous global social and economic suffering (Aminov, 2010). Consequently, alternative solutions to this healthcare crisis that are effective and reliable must be swiftly identified. In recent years, one such alternate approach has been to isolate anti-bacterials that function by targeting a virulence determinant (Clatworthy et al., 2007; Maura et al., 2016). Ideally, these so called “anti-infectives” or “virulence blockers” would be specific for pathogenic bacteria and have a bacteriostatic effect that would synergize with the immune system to clear the infection. A classic example of this endeavor is the identification of novel chemical inhibitors of the T3SS (Keyser et al., 2008; Duncan et al., 2012). Despite the success of identifying chemical inhibitors of the T3SS, none of these have yet reached the market. This issue is addressed in a

report by Morgan et al. which describes the development of an experimental pipeline that would help transition from high throughput screening to inhibitor validation and initial determination of their mode of action. In so doing, the authors consider important new possible modes of action for T3SS inhibitors.

Bacterial virulence regulation is exquisitely fine-tuned so that subsets of virulence factors are expressed only at times of need. Alterations in the local environment account for triggering changes in this virulence gene expression profile. Responses are rapid, and it is now clear that post-transcriptional regulatory effects, such as small non-coding RNAs contribute to the rapidity of this re-programming. Benefitting from progressive developments in genome-wide omics-based methods of exploration, several RNA-based regulatory systems have been discovered in pathogenic *Yersinia*. These discoveries have been reviewed by Knittel et al. in the context of *Yersinia* niche colonization, metabolic adaptation, acute and chronic infection, and evolution. By inference, at least some RNA-based regulatory systems could serve as a suitable target of anti-infective drug development.

The second edition of this research topic, provides many examples demonstrating the great capacity of *Yersinia* species to adapt and thrive in diverse environmental niches. This is reiterated by the timely review by Davis, which sheds light on the ability of *Yersinia* sub-populations to phenotypically diversify during an infection in order to balance the need to maintain bacterial growth while resisting attack from different cellular elements of an activated immune system. Underpinning this phenotypic diversification is the ability of subsets of bacteria to make temporal and spatial adjustments to their gene expression profiles in response to the microenvironment. Having the technology to detect gene expression profiles in distinct sub-populations of bacteria offers a unique opportunity to understand the yin and yang of interactions between individual bacteria and specific immune cell types. In turn, this may eventually enable the generation of more efficacious approaches to treat infections by having the option of tailoring novel antibacterials or their immunomodulatory counterparts that can favorably influence the outcome of this bacteria-immune cell interplay.

## AUTHOR CONTRIBUTIONS

MF developed the initial concept and outline. Both MF and VA contributed to the final version of the manuscript.

## FUNDING

MF received research funding from the Swedish Research Council (Vetenskapsrådet) under award numbers 2009-5628, 2014-2105 and 2018-02676, the Foundation for Medical Research at Umeå University and the Faculty of Science and Technology at Umeå University. VA received research funding from the National Institute of Allergy and Infectious Diseases of the National Institutes of Health under award numbers R01AI106930 and R01AI119082.

## REFERENCES

- Alenizi, D., Ringwood, T., Redhwan, A., Bouraha, B., Wren, B. W., Prentice, M., et al. (2016). All *Yersinia enterocolitica* are pathogenic: virulence of phylogroup 1 *Y. enterocolitica* in a *Galleria mellonella* infection model. *Microbiology* 162, 1379–1387. doi: 10.1099/mic.0.000311
- Alteri, C. J., and Mobley, H. L. (2016). The versatile type VI secretion system. *Microbiol. Spectr.* 4:VMBF-0026-2015. doi: 10.1128/microbiolspec.VMBF-0026-2015
- Aminov, R. I. (2010). A brief history of the antibiotic era: lessons learned and challenges for the future. *Front. Microbiol.* 1:134. doi: 10.3389/fmicb.2010.00134
- Asadishad, B., Ghoshal, S., and Tufenkji, N. (2013). Role of cold climate and freeze-thaw on the survival, transport, and virulence of *Yersinia enterocolitica*. *Environ. Sci. Technol.* 47, 14169–14177. doi: 10.1021/es403726u
- Azizoglu, R. O., and Kathariou, S. (2010). Impact of growth temperature and agar versus liquid media on freeze-thaw tolerance of *Yersinia enterocolitica*. *Foodborne Pathog. Dis.* 7, 1125–1128. doi: 10.1089/fpd.2009.0526
- Bobrov, A. G., Kirillina, O., Forman, S., Mack, D., and Perry, R. D. (2008). Insights into *Yersinia pestis* biofilm development: topology and co-interaction of Hms inner membrane proteins involved in exopolysaccharide production. *Environ. Microbiol.* 10, 1419–1432. doi: 10.1111/j.1462-2920.2007.01554.x
- Bobrov, A. G., Kirillina, O., Ryjenkov, D. A., Waters, C. M., Price, P. A., Fetherston, J. D., et al. (2011). Systematic analysis of cyclic di-GMP signalling enzymes and their role in biofilm formation and virulence in *Yersinia pestis*. *Mol. Microbiol.* 79, 533–551. doi: 10.1111/j.1365-2958.2010.07470.x
- Brocklehurst, T. F., and Lund, B. M. (1990). The influence of pH, temperature and organic acids on the initiation of growth of *Yersinia enterocolitica*. *J. Appl. Bacteriol.* 69, 390–397. doi: 10.1111/j.1365-2672.1990.tb01529.x
- Buttner, D. (2012). Protein export according to schedule: architecture, assembly, and regulation of type III secretion systems from plant- and animal-pathogenic bacteria. *Microbiol. Mol. Biol. Rev.* 76, 262–310. doi: 10.1128/MMBR.05017-11
- Chakraborty, S., and Kenney, L. J. (2018). A new role of OmpR in acid and osmotic stress in salmonella and *E. coli*. *Front. Microbiol.* 9:2656. doi: 10.3389/fmicb.2018.02656
- Chen, P. E., Cook, C., Stewart, A. C., Nagarajan, N., Sommer, D. D., Pop, M., et al. (2010). Genomic characterization of the *Yersinia* genus. *Genome Biol.* 11:R1. doi: 10.1186/gb-2010-11-1-r1
- Chiodini, R. J., Dowd, S. E., Davis, B., Galandiuk, S., Chamberlin, W. M., Kuenstner, J. T., et al. (2013). Crohn's disease may be differentiated into 2 distinct biotypes based on the detection of bacterial genomic sequences and virulence genes within submucosal tissues. *J. Clin. Gastroenterol.* 47, 612–620. doi: 10.1097/MCG.0b013e31827b4f94
- Clatworthy, A. E., Pierson, E., and Hung, D. T. (2007). Targeting virulence: a new paradigm for antimicrobial therapy. *Nat. Chem. Biol.* 3, 541–548. doi: 10.1038/nchembio.2007.24
- Cornelis, G. R., Boland, A., Boyd, A. P., Geuijen, C., Iriarte, M., Neyt, C., et al. (1998). The virulence plasmid of *Yersinia*, an antihost genome. *Microbiol. Mol. Biol. Rev.* 62, 1315–1352.
- Craig, L., Pique, M. E., and Tainer, J. A. (2004). Type IV pilus structure and bacterial pathogenicity. *Nat. Rev. Microbiol.* 2, 363–378. doi: 10.1038/nrmicro885
- Deng, W., Marshall, N. C., Rowland, J. L., McCoy, J. M., Worrall, L. J., Santos, A. S., et al. (2017). Assembly, structure, function and regulation of type III secretion systems. *Nat. Rev. Microbiol.* 15, 323–337. doi: 10.1038/nrmicro.2017.20
- Duncan, M. C., Linington, R. G., and Auerbuch, V. (2012). Chemical inhibitors of the type three secretion system: disarming bacterial pathogens. *Antimicrob. Agents Chemother.* 56, 5433–5441. doi: 10.1128/AAC.00975-12
- Flamez, C., Ricard, I., Arafah, S., Simonet, M., and Marceau, M. (2008). Phenotypic analysis of *Yersinia pseudotuberculosis* 32777 response regulator mutants: new insights into two-component system regulon plasticity in bacteria. *Int. J. Med. Microbiol.* 298, 193–207. doi: 10.1016/j.ijmm.2007.05.005
- Fonseca, D. M., Hand, T. W., Han, S. J., Gerner, M. Y., Glatman Zaretsky, A., Byrd, A. L., et al. (2015). Microbiota-dependent sequelae of acute infection compromise tissue-specific immunity. *Cell* 163, 354–366. doi: 10.1016/j.cell.2015.08.030
- Fuchs, T. M., Brandt, K., Starke, M., and Rattei, T. (2011). Shotgun sequencing of *Yersinia enterocolitica* strain W22703 (biotype 2, serotype O:9): genomic evidence for oscillation between invertebrates and mammals. *BMC Genomics* 12:168. doi: 10.1186/1471-2164-12-168
- Fuchs, T. M., Bresolin, G., Marcinowski, L., Schachtner, J., and Scherer, S. (2008). Insecticidal genes of *Yersinia* spp.: taxonomical distribution, contribution to toxicity towards *Manduca sexta* and *Galleria mellonella*, and evolution. *BMC Microbiol.* 8:214. doi: 10.1186/1471-2180-8-214
- Galindo, C. L., Rosenzweig, J. A., Kirtley, M. L., and Chopra, A. K. (2011). Pathogenesis of *Y. enterocolitica* and *Y. pseudotuberculosis* in Human Yersiniosis. *J. Pathog.* 2011:182051. doi: 10.4061/2011/182051
- Giltner, C. L., Nguyen, Y., and Burrows, L. L. (2012). Type IV pilin proteins: versatile molecular modules. *Microbiol. Mol. Biol. Rev.* 76, 740–772. doi: 10.1128/MMBR.00035-12
- Gonzalez-Rivera, C., Bhatti, M., and Christie, P. J. (2016). Mechanism and function of type IV secretion during infection of the human host. *Microbiol. Spectr.* 4:VMBF-0024-2015. doi: 10.1128/microbiolspec.VMBF-0024-2015
- Goverde, R. L., Kusters, J. G., and Huis in 't Veld, J. H. (1994). Growth rate and physiology of *Yersinia enterocolitica*; influence of temperature and presence of the virulence plasmid. *J. Appl. Bacteriol.* 77, 96–104. doi: 10.1111/j.1365-2672.1994.tb03050.x
- Grabowski, B., Schmidt, M. A., and Ruter, C. (2017). Immunomodulatory *Yersinia* outer proteins (Yops)-useful tools for bacteria and humans alike. *Virulence* 8, 1124–1147. doi: 10.1080/21505594.2017.1303588
- Grohmann, E., Christie, P. J., Waksman, G., and Backert, S. (2018). Type IV secretion in Gram-negative and Gram-positive bacteria. *Mol. Microbiol.* 107, 455–471. doi: 10.1111/mmi.13896
- Gupta, V., Gulati, P., Bhagat, N., Dhar, M. S., and Virdi, J. S. (2015). Detection of *Yersinia enterocolitica* in food: an overview. *Eur. J. Clin. Microbiol. Infect. Dis.* 34, 641–650. doi: 10.1007/s10096-014-2276-7
- Han, S. J., Glatman Zaretsky, A., Andrade-Oliveira, V., Collins, N., Dzutsev, A., Shaik, J., et al. (2017). White adipose tissue is a reservoir for memory T cells and promotes protective memory responses to infection. *Immunity* 47, 1154–1168. doi: 10.1016/j.immuni.2017.11.009
- Hares, M. C., Hinchliffe, S. J., Strong, P. C., Eleftherianos, I., Dowling, A. J., Ffrench-Constant, R. H., et al. (2008). The *Yersinia pseudotuberculosis* and *Yersinia pestis* toxin complex is active against cultured mammalian cells. *Microbiology* 154, 3503–3517. doi: 10.1099/mic.0.2008/018440-0
- Hilbert, F., Mayrhofer, S., and Smulders, F. J. (2003). Rapid urease screening of *Yersinia* on CIN agar plates. *Int. J. Food Microbiol.* 84, 111–115. doi: 10.1016/S0168-1605(02)00397-5
- Hugot, J. P., Alberti, C., Berrebi, D., Bingen, E., and Cezard, J. P. (2003). Crohn's disease: the cold chain hypothesis. *Lancet* 362, 2012–2015. doi: 10.1016/S0140-6736(03)15024-6
- Kallinowski, F., Wassmer, A., Hofmann, M. A., Harmsen, D., Heesemann, J., Karch, H., et al. (1998). Prevalence of enteropathogenic bacteria in surgically treated chronic inflammatory bowel disease. *Hepatogastroenterology* 45, 1552–1558.
- Keto-Timonen, R., Pontinen, A., Aalto-Araneda, M., and Korkeala, H. (2018). Growth of *Yersinia pseudotuberculosis* strains at different temperatures, pH values, and NaCl and ethanol concentrations. *J. Food Prot.* 81, 142–149. doi: 10.4315/0362-028X.JFP-17-223
- Keyser, P., Eloffsson, M., Rosell, S., and Wolf-Watz, H. (2008). Virulence blockers as alternatives to antibiotics: type III secretion inhibitors against Gram-negative bacteria. *J. Intern. Med.* 264, 17–29. doi: 10.1111/j.1365-2796.2008.01941.x
- Kirillina, O., Fetherston, J. D., Bobrov, A. G., Abney, J., and Perry, R. D. (2004). HmsP, a putative phosphodiesterase, and HmsT, a putative diguanylate cyclase, control Hms-dependent biofilm formation in *Yersinia pestis*. *Mol. Microbiol.* 54, 75–88. doi: 10.1111/j.1365-2958.2004.04253.x
- Knosel, T., Schewe, C., Petersen, N., Dietel, M., and Petersen, I. (2009). Prevalence of infectious pathogens in Crohn's disease. *Pathol. Res. Pract.* 205, 223–230. doi: 10.1016/j.prp.2008.04.018
- Lamps, L. W., Madhusudhan, K. T., Havens, J. M., Greenson, J. K., Bronner, M. P., Chiles, M. C., et al. (2003). Pathogenic *Yersinia* DNA is detected in bowel and mesenteric lymph nodes from patients with Crohn's disease. *Am. J. Surg. Pathol.* 27, 220–227. doi: 10.1097/0000478-200302000-00011
- Laub, M. T., and Goulian, M. (2007). Specificity in two-component signal transduction pathways. *Annu. Rev. Genet.* 41, 121–145. doi: 10.1146/annurev.genet.41.042007.170548

- Le Guern, A. S., Martin, L., Savin, C., and Carniel, E. (2016). Yersiniosis in France: overview and potential sources of infection. *Int. J. Infect. Dis.* 46, 1–7. doi: 10.1016/j.ijid.2016.03.008
- Leu, S. B., Shulman, S. C., Steelman, C. K., Lamps, L. W., Bulut, O. P., Abramowsky, C. R., et al. (2013). Pathogenic *Yersinia* DNA in intestinal specimens of pediatric patients with Crohn's disease. *Fetal Pediatr. Pathol.* 32, 367–370. doi: 10.3109/15513815.2013.768744
- Lien, Y. W., and Lai, E. M. (2017). Type VI secretion effectors: methodologies and biology. *Front. Cell. Infect. Microbiol.* 7:254. doi: 10.3389/fcimb.2017.00254
- Marceau, M. (2005). Transcriptional regulation in *Yersinia*: an update. *Curr. Issues Mol. Biol.* 7, 151–177. Available online at: <http://www.caister.com/cimb/v/v7/151.pdf>
- Maura, D., Ballok, A. E., and Rahme, L. G. (2016). Considerations and caveats in anti-virulence drug development. *Curr. Opin. Microbiol.* 33, 41–46. doi: 10.1016/j.mib.2016.06.001
- Meinzer, U., Esmiol-Welterlin, S., Barreau, F., Berrebi, D., Dussallant, M., Bonacorsi, S., et al. (2008). Nod2 mediates susceptibility to *Yersinia pseudotuberculosis* in mice. *PLoS ONE* 3:e2769. doi: 10.1371/journal.pone.0002769
- Murthy, A., Li, Y., Peng, I., Reichelt, M., Katakam, A. K., Noubade, R., et al. (2014). A Crohn's disease variant in Atg16l1 enhances its degradation by caspase 3. *Nature* 506, 456–462. doi: 10.1038/nature13044
- Ozdemir, F., and Arslan, S. (2015). Genotypic and phenotypic virulence characteristics and antimicrobial resistance of *Yersinia* spp. isolated from meat and milk products. *J. Food Sci.* 80, M1306–1313. doi: 10.1111/1750-3841.12911
- Pha, K., and Navarro, L. (2016). *Yersinia* type III effectors perturb host innate immune responses. *World J. Biol. Chem.* 7, 1–13. doi: 10.4331/wjbc.v7.i1.1
- Pinheiro, V. B., and Ellar, D. J. (2007). Expression and insecticidal activity of *Yersinia pseudotuberculosis* and *Photobacterium luminescens* toxin complex proteins. *Cell. Microbiol.* 9, 2372–2380. doi: 10.1111/j.1462-5822.2007.00966.x
- Reboul, A., Lemaitre, N., Titecat, M., Merchez, M., Deloison, G., Ricard, I., et al. (2014). *Yersinia pestis* requires the 2-component regulatory system OmpR-EnvZ to resist innate immunity during the early and late stages of plague. *J. Infect. Dis.* 210, 1367–1375. doi: 10.1093/infdis/jiu274
- Spinner, J. L., Carmody, A. B., Jarrett, C. O., and Hinnebusch, B. J. (2013). Role of *Yersinia pestis* toxin complex family proteins in resistance to phagocytosis by polymorphonuclear leukocytes. *Infect. Immun.* 81, 4041–4052. doi: 10.1128/IAI.00648-13
- Spinner, J. L., Jarrett, C. O., Larock, D. L., Miller, S. I., Collins, C. M., and Hinnebusch, B. J. (2012). *Yersinia pestis* insecticidal-like toxin complex (Tc) family proteins: characterization of expression, subcellular localization, and potential role in infection of the flea vector. *BMC Microbiol.* 12:296. doi: 10.1186/1471-2180-12-296
- Stock, A. M., Robinson, V. L., and Goudreau, P. N. (2000). Two-component signal transduction. *Annu. Rev. Biochem.* 69, 183–215. doi: 10.1146/annurev.biochem.69.1.183
- Sulakvelidze, A. (2000). *Yersinia* other than *Y. enterocolitica*, *Y. pseudotuberculosis*, and *Y. pestis*: the ignored species. *Microbes Infect.* 2, 497–513. doi: 10.1016/S1286-4579(00)00311-7
- Tobback, E., Decostere, A., Hermans, K., Haesebrouck, F., and Chiers, K. (2007). *Yersinia ruckeri* infections in salmonid fish. *J. Fish Dis.* 30, 257–268. doi: 10.1111/j.1365-2761.2007.00816.x
- Vakulskas, C. A., Potts, A. H., Babitzke, P., Ahmer, B. M., and Romeo, T. (2015). Regulation of bacterial virulence by Csr (Rsm) systems. *Microbiol. Mol. Biol. Rev.* 79, 193–224. doi: 10.1128/MMBR.00052-14
- Walthers, D., Go, A., and Kenney, L. J. (2005). “Regulation of porin gene expression by the two-component regulatory system EnvZ/OmpR,” in *Bacterial and Eukaryotic Porins: Structure, Function, Mechanism*, ed R. Benz (Weinheim: Wiley-VCH), 1–24.
- Zhou, D., Han, Y., and Yang, R. (2006). Molecular and physiological insights into plague transmission, virulence and etiology. *Microbes Infect.* 8, 273–284. doi: 10.1016/j.micinf.2005.06.006
- Zietz, B. P., and Dunkelberg, H. (2004). The history of the plague and the research on the causative agent *Yersinia pestis*. *Int. J. Hyg. Environ. Health* 207, 165–178. doi: 10.1078/1438-4639-00259

**Conflict of Interest Statement:** The authors declare that the research was conducted in the absence of any commercial or financial relationships that could be construed as a potential conflict of interest.

Copyright © 2019 Francis and Auerbuch. This is an open-access article distributed under the terms of the Creative Commons Attribution License (CC BY). The use, distribution or reproduction in other forums is permitted, provided the original author(s) and the copyright owner(s) are credited and that the original publication in this journal is cited, in accordance with accepted academic practice. No use, distribution or reproduction is permitted which does not comply with these terms.





# Chromosomally-Encoded *Yersinia pestis* Type III Secretion Effector Proteins Promote Infection in Cells and in Mice

Sara Schesser Bartra<sup>1</sup>, Cherish Lorica<sup>1,2</sup>, Lianfen Qian<sup>3</sup>, Xin Gong<sup>4</sup>, Wael Bahnan<sup>1</sup>, Henry Barreras Jr.<sup>1</sup>, Rosmely Hernandez<sup>1</sup>, Zhongwei Li<sup>4</sup>, Gregory V. Plano<sup>1</sup> and Kurt Schesser<sup>1\*</sup>

<sup>1</sup> Department of Microbiology and Immunology, University of Miami Miller School of Medicine, Miami, FL, United States, <sup>2</sup> Division of Pediatric Infectious Diseases, Department of Pediatrics, University of Miami Miller School of Medicine, Miami, FL, United States, <sup>3</sup> Department of Mathematics, Charles E. Schmidt College of Science, Florida Atlantic University, Boca Raton, FL, United States, <sup>4</sup> Department of Biomedical Science, Charles E. Schmidt College of Medicine, Florida Atlantic University, Boca Raton, FL, United States

## OPEN ACCESS

### Edited by:

Matthew S. Francis,  
Umeå University, Sweden

### Reviewed by:

Nikhil A. Thomas,  
Dalhousie University, Canada  
Andreas Diepold,  
Max-Planck-Institut für terrestrische  
Mikrobiologie, Germany  
Luís Jaime Mota,  
Universidade Nova de Lisboa,  
Portugal

### \*Correspondence:

Kurt Schesser  
kschesser@med.miami.edu

### Specialty section:

This article was submitted to  
Molecular Bacterial Pathogenesis,  
a section of the journal  
Frontiers in Cellular and Infection  
Microbiology

**Received:** 09 August 2018

**Accepted:** 22 January 2019

**Published:** 22 February 2019

### Citation:

Schesser Bartra S, Lorica C, Qian L,  
Gong X, Bahnan W, Barreras H Jr,  
Hernandez R, Li Z, Plano GV and  
Schesser K (2019)  
Chromosomally-Encoded *Yersinia*  
*pestis* Type III Secretion Effector  
Proteins Promote Infection in Cells  
and in Mice.  
Front. Cell. Infect. Microbiol. 9:23.  
doi: 10.3389/fcimb.2019.00023

*Yersinia pestis*, the causative agent of plague, possesses a number of virulence mechanisms that allows it to survive and proliferate during its interaction with the host. To discover additional infection-specific *Y. pestis* factors, a transposon site hybridization (TraSH)-based genome-wide screen was employed to identify genomic regions required for its survival during cellular infection. In addition to several well-characterized infection-specific genes, this screen identified three chromosomal genes (*y3397*, *y3399*, and *y3400*), located in an apparent operon, that promoted successful infection. Each of these genes is predicted to encode a leucine-rich repeat family protein with or without an associated ubiquitin E3 ligase domain. These genes were designated *Yersinia* leucine-rich repeat gene A (*ylrA*), B (*ylrB*), and C (*ylrC*). Engineered strains with deletions of *y3397* (*ylrC*), *y3399* (*ylrB*), or *y3400* (*ylrA*), exhibited infection defects both in cultured cells and in the mouse. C-terminal FLAG-tagged YlrA, YlrB, and YlrC were secreted by *Y. pestis* in the absence but not the presence of extracellular calcium and deletions of the DNA sequences encoding the predicted N-terminal type III secretion signals of YlrA, YlrB, and YlrC prevented their secretion, indicating that these proteins are substrates of the type III secretion system (T3SS). Further strengthening the connection with the T3SS, YlrB was readily translocated into HeLa cells and expression of the YlrA and YlrC proteins in yeast inhibited yeast growth, indicating that these proteins may function as anti-host T3S effector proteins.

**Keywords:** *Yersinia*, type III secretion, pathogenesis, leucine rich repeats, plague, mice

## INTRODUCTION

*Yersinia pestis*, the etiologic agent of plague, causes a variety of serious diseases in humans and animals. The clinical syndromes in humans include bubonic, pneumonic, and septicemic plague (Perry and Fetherston, 1997). Fleas transmit *Y. pestis* from infected domestic rats to humans causing bubonic plague. *Y. pestis* also can be transmitted via respiratory secretions following contact with

another infected human, leading to pneumonic plague. Currently, plague is still a public health threat in certain regions of Asia, Africa, North and South America (Centers for Disease Control Prevention., 2013). In recent years in the U.S., most cases of plague have occurred in children in whom diagnosis has been delayed. Among 183 U.S. pediatric cases from 1947 to 2001, 91% presented primarily as bubonic and one third of these cases developed secondary complications, such as sepsis, meningitis, and pneumonia. Children were more likely than adults to manifest with bubonic plague (91 vs. 79%), develop complications (32 vs. 27%), and to die (17 vs. 14%) (Dennis and Chow, 2004). Because plague is highly contagious, *Y. pestis* can be used in biological warfare and is considered a Category A agent of bioterrorism (Inglesby et al., 2000).

Among the virulence factors identified in *Y. pestis*, the plasmid pCD1 encoded type III secretion system (T3SS) is one of the best-studied. The T3SS is a complex protein machinery shared by numerous Gram-negative pathogens that injects effector proteins directly into the cytosol of an infected eukaryotic cell (Cornelis, 2002a). The translocation of effector proteins requires direct contact between the bacterium and the host cell. In *Y. pestis*, the T3S apparatus is called the Ysc injectosome and the effector proteins are termed Yops (Yersinia outer proteins). The Yops disrupt host signaling pathways that normally lead to bacterial phagocytosis and the production of pro-inflammatory cytokines (Cornelis and Van Gijsegem, 2000). To date, six Yop effectors have been identified—YopH, YopE, YopT, YpkA/YopO, YopP/YopJ, and YopM (Cornelis, 2002b). Following its identification as a virulence factor in the mouse model, YopM was initially described as an inhibitor of platelet aggregation (Leung and Straley, 1989). Later YopM was linked to a variety of activities associated with the host innate immune response including depletion of inflammatory monocytes and natural killer (NK) cells and induction of specific cytokines (Kerschen et al., 2004; Ye et al., 2009; McPhee et al., 2010). Once translocated into eukaryotic cells, YopM directly interacts with a number of host proteins including kinases and caspase-1 to inhibit signaling pathways and inflammasome activation (McDonald et al., 2003; Hentschke et al., 2010; LaRock and Cookson, 2012; Chung et al., 2014).

Structurally YopM is primarily composed of a number of leucine-rich repeats (LRR) (Evdokimov et al., 2001). Recently it has been shown that *Y. pestis*, as well as a number of other *Yersinia* species (but not *Y. enterocolitica*), possesses a chromosomal locus that potentially encodes three YopM-like proteins (Hu et al., 2016). Sequence analysis showed that the plasmid-encoded YopM was evolutionarily distinct from these three chromosomal-encoded YopM-like proteins and that two of these YopM-like proteins possessed E3 ligase domains in their C-terminal regions (Hu et al., 2016). Here we describe the independent identification and characterization of the genes encoding these three chromosomally-encoded YopM-like proteins in an unbiased screen for *Y. pestis* factors that promote its survival following its infection of macrophages.

## MATERIALS AND METHODS

### Bacterial Strains

The *Escherichia coli* DH5 $\alpha$  and *Y. pestis* strains were routinely grown in heart infusion broth (HIB) or on tryptone blood agar (TBA) base plates (Difco, Detroit, MI) at 27°C (*Y. pestis*) or 37°C (*E. coli*). Appropriate antibiotics were added to culture media when needed with ampicillin (50  $\mu$ g/ml), kanamycin (50  $\mu$ g/ml), chloramphenicol (20  $\mu$ g/ml), and streptomycin (50  $\mu$ g/ml). Non-polar deletion of *Y. pestis* KIM5 chromosomal DNA sequences *ylrC* (y3397; codons 29-515), *ylrB* (y3399; codons 29-261), and *ylrA* (y3400; codons 23-529) was accomplished using lambda Red recombination as described by Datsenko and Wanner (2000). PCR products used to construct the gene replacement were amplified using the template plasmid pKD4 (Km<sup>r</sup>). The resulting PCR products were gel purified, ethanol precipitated, and resuspended in 10  $\mu$ l of distilled water. *Y. pestis* KIM5 strain carrying plasmid pKD46, which encodes the Red recombinase, was induced with 0.2% L-arabinose for 2 h prior to harvest. Electrocompetent cells were electroporated with the purified PCR products. The transformations were plated onto TBA plates containing kanamycin (50  $\mu$ g/ml). Plasmid pCP20, which encodes the FLP recombinase, was electroporated into the Km<sup>r</sup> resistant strains to facilitate the removal of the FLP recognition target-flanked *kan* cassette and plasmid pKD46 simultaneously. Plasmid pCP20 was cured from the *Y. pestis* deletion strains by overnight growth at 39°C. Additionally, a deletion strain of the three gene sequences *ylrC*-codon 29 to *ylrA*-codon 529 was constructed using lambda Red-recombination as described above.

### Transposon Site Hybridization (TraSH)-Based Screening

A TraSH-based approach was used to map and quantify the relative abundance of the different transposon mutants in order to identify transposon mutant insertion sites that are underrepresented in the population of mutants exposed to RAW264.7 murine macrophage-like cells. The details of the mutagenesis, infection, and TraSH-screen and data analysis are described in Bartra et al. (2012).

### Infection Assays

Cell infection assays were performed essentially as described by Rosenzweig et al. (2005). RAW 264.7 murine macrophage-like cells and HeLa cells were cultured in Dubelcco's modified Eagle's medium (DMEM, Gibco) containing 10% heat-inactivated fetal bovine serum (Cellgro) at 37°C in the presence of 5% CO<sub>2</sub>. Cells were seeded in 24-well plates at densities of 2.5–4.0  $\times$  10<sup>5</sup> per well. Bacterial cell cultures were grown in tissue culture (TC) medium overnight at 27°C, diluted into fresh TC media and incubated with shaking at 27°C for 2 h and then shifted to 37°C for 1 h prior to being added to the cultured macrophages at a multiplicity of infection (MOI) of 30. After a 30 min attachment period, fresh DMEM medium was added to each well. At the 0 h and 8 h time points, the infected cells were lysed with 500  $\mu$ l of distilled H<sub>2</sub>O and a portion of which was plated on

TBA plates. Colony forming units (CFU) were counted after 2–3 days. For mouse infections, all procedures were in strict accordance with federal and state government guidelines for the Care and Use of Laboratory Animals of the National Institutes of Health and their use was approved for this entire study by the University of Miami institutional animal care and use committee (protocol number 15-081). Mice were infected intravenously with a total of 2000 CFU (1000 CFU each of the parental *Y. pestis* KIM5 and the isogenic  $\Delta yopB$  or  $\Delta ylrABC$  strains). Mice were humanely sacrificed at 48 h post infection, spleens were removed and homogenized in sterile water containing 0.05% triton X-100 by grinding through a fine wire mesh. The resulting homogenates were diluted and plated on media containing either chloramphenicol (CM) to select for the CM-resistant parental strain, as well as antibiotic-free media that allowed growth of both

the parental strain and the CM-sensitive mutant strains. Two to three days later colonies were enumerated and the competition index (CI) for the parental/  $\Delta yopB$  and parental/  $\Delta ylrABC$  co-infected animals was computed by dividing the CFU of the mutant by the CFU of the parental strain.

## Construction of YlrA, YlrB, and YlrC Expression Plasmids

DNA fragments used encoding YlrA, YlrB, and YlrC were PCR amplified from chromosomal DNA of *Y. pestis* KIM5. The resultant DNA fragments were digested with HindIII and BglII and inserted into HindIII- and BglII-digested pFLAG-CTC vector (Sigma-Aldrich). These vectors express full-length C-terminal FLAG-tagged YlrA-FLAG, YlrB-FLAG, and YlrC-FLAG. In addition, DNA sequences predicted to encode the

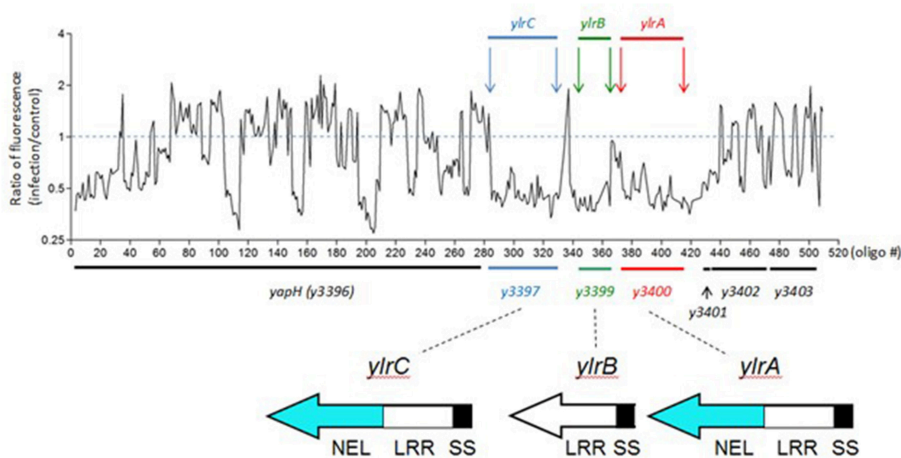


**FIGURE 1** | A TraSH screen indicates that the *ylrABC* locus promotes the survival of *Y. pestis* during infection. A pool of 90,000 unique *Y. pestis* transposon variants were used to infect cultured RAW 264.7 macrophages. Following infection bacterial DNA was isolated and the relative abundance of specific regions of the *Y. pestis* genome was determined. Shown in the abundance at the *ylr* locus indicating that *Y. pestis* variants possessing transposon insertion at this locus were under-represented at the termination of the infection period. Protein domains are labeled as Novel E3 Ubiquitin Ligase (NEL), Leucine-Rich Repeat (LRR), and T3SS Secretion and Translocation Signal (SS) domains.

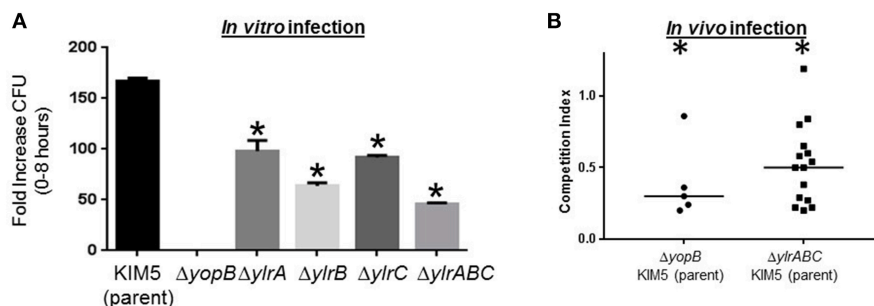


**FIGURE 2** | Infection defects of engineered *ylr* mutants. **(A)** Cultured RAW264.7 macrophages were infected with *Y. pestis* KIM5,  $\Delta yopB$ ,  $\Delta ylrA$ ,  $\Delta ylrB$ ,  $\Delta ylrC$ , or  $\Delta ylrABC$  strains at an MOI of 1. After a 30 min attachment period, unattached bacteria were removed and cell-associated bacteria (cfu) were determined by plating at the 0 and 8 h time points. Three independent wells per strain were analyzed and the average fold increase in cfu recovered for each strain over the 8 h infection period is shown (\* $P < 0.05$  by Student *t*-test of a single representative experiment performed multiple times). **(B)** Mice were infected intravenously with an equal mixture of wild-type *Y. pestis* KIM5 and either the  $\Delta yopB$  or  $\Delta ylrABC$  strains and 2 days later mice were humanely euthanized and the relative abundance of each strain in the spleen was determined. Each data point represents an individual mouse and the medium competition index is indicated. Statistically significant reductions in splenic colonization by the mutant strain is labeled by an asterisk ( $P < 0.05$  by Student *t*-test of multiple cohorts of mice in separate infections).



YlrA, YlrB, and YlrC N-terminal T3S signal (SS) (amino acid residues 2 to 10) were deleted from each expression vector using whole plasmid PCR (Imai et al., 1991), generating plasmids pYlrA-FLAG- $\Delta$ SS, pYlrB-FLAG- $\Delta$ SS, and pYlrC-FLAG- $\Delta$ SS. Oligonucleotide pairs used were YlrASS-F and YlrASS-R, YlrBSS-F and YlrBSS-R, and YlrCSS-F and YlrCSS-R. The resultant Ylr expression plasmids were transformed into *Y. pestis* KIM8 $\Delta$ 4 (Bartra et al., 2006).

## Construction of Vectors for $\beta$ -Lactamase Translocation Studies

Expression plasmids encoding full length YlrA, YlrB, and YlrC carrying a C-terminal  $\beta$ -lactamase gene were constructed by the PCR-ligation-PCR technique (Ali and Steinkasserer, 1995). Individual *Y. pestis* KIM genes and upstream sequences that include each gene's ribosomal binding site were amplified by PCR from vectors encoding full-length FLAG-YlrA, FLAG-YlrB, and FLAG-YlrC, respectively, using oligonucleotides primer pairs YlrA-KpnI-F and YlrA-FL-R, YlrB-KpnI-F and YlrB-FL-R, and YlrC-KpnI-F and YlrC-FL-R. The DNA fragments encoding the Bla gene were amplified from plasmid pBSKII- using primers Bla-25-F and Bla-STOP-HindIII-R. Obtained DNA fragments were gel purified, kinased and ligated. The reaction was used for a second PCR using primers YlrA-KpnI-F and Bla-STOP-HindIII-R, YlrB-KpnI-F and Bla-STOP-HindIII-R, and YlrC-KpnI-F and Bla-STOP-HindIII-R. The resulting DNA fragments were ethanol precipitated, digested with KpnI and HindIII, and inserted into KpnI and HindIII-digested pBad<sub>18</sub>-Cm<sup>r</sup>. The resultant plasmids were transformed into a *Y. pestis* strain lacking YopE, YopJ, YopM, YopT, YopH, and YpkA.

## Yeast Studies

DNA fragments encoding YlrA, YlrB and YlrC were amplified by PCR from pFLAG-YlrA, pFLAG-YlrB, and pFLAG-YlrC, respectively, using oligonucleotides primer pairs YlrA-XhoI and YlrA-BamHI, YlrB-XhoI and YlrB-BamHI, and YlrC-XhoI and YlrC-BamHI listed in Table 2. The resultant DNA fragments were digested with BamHI and XhoI and inserted into BamHI- and XhoI-digested pREP3X. The pREP-3X vector contains the inducible *nmt1* promoter (Maundrell, 1993) and the presence of thiamine (15  $\mu$ M) in the medium represses the promoter. If thiamine is not present in the media, the promoter becomes activated resulting in the transcription of the *ylr* gene cloned downstream. Plasmids generated were pREP-3X-YlrA, pREP-3X-YlrB, and pREP-3X-YlrC. In addition, site-specific mutation of three catalytic residues of the putative NEL domain of YlrA was done using the whole plasmid PCR method (Imai et al., 1991) generating plasmids pREP-3X-YlrA-C386S, pREP-3X-YlrA-R389A, and pREP-3X-YlrA-S449F. *Schizosaccharomyces pombe* h<sup>-</sup> ade6-704 leu1-32 ura4-D18 was grown in Pombe Glutamate medium (PMG) at 32°C. The plasmid vector pREP3x (*nmt13x* Thiamine repressible promoter) was used to express the Ylr genes in fission yeast. The plasmid vectors were transformed using the lithium acetate protocol (Morita and Takegawa, 2004). The yeast strains were grown in PMG supplemented with the appropriate amino acids as well as thiamine to maintain selection for 2 days in logarithmic growth to an optical density (OD)

of 0.1–0.4 at 595 nm. After growth, the cells were centrifuged at 4,000  $\times$  g, washed 3 times with distilled sterile water, and diluted for an overnight growth in media lacking thiamine. The following day, the OD of the cultures at 595 nm was measured and the cultures were diluted to an OD of 0.1. Three 10-fold serial dilutions of the cultures were made, and 5  $\mu$ L of each dilution was spotted onto an agar plate with and without thiamine and grown at 32°C for 3 days.

## Secretion Assay

For standard secretion assays, *Y. pestis* strains were grown in thoroughly modified Higuchi's (TMH) medium in the presence or absence of 2.5 mM CaCl<sub>2</sub> for 1 h at 27°C and then shifted to 37°C for the next 5 h as previously described (Jackson et al., 1998). FLAG-tagged Ylr proteins (pFLAG-CTC vector) were induced with 0.05 mM IPTG (isopropyl- $\beta$ -D-thiogalactopyranoside) at the temperature shift.

## SDS-PAGE and Immunoblotting

Cultures of bacteria were harvested by centrifugation at 14,000  $\times$  g for 10 min at room temperature. Pellets of whole-cell bacteria and trichloroacetic acid (TCA)-precipitated supernatant proteins were resuspended according to the harvest OD<sub>620</sub> and subjected to SDS-PAGE and immunoblotting as previously described (Jackson et al., 1998). LcrV was detected with rabbit polyclonal antisera (1:20,000) raised against the full-length LcrV proteins. FLAG-tagged proteins were detected with anti-FLAG M2 monoclonal antibody (Sigma-Aldrich) (1:1,000).

## $\beta$ -Lactamase Translocation Assay

HeLa cells were seeded to a six-well plate to achieve a 40–50% confluence 1 day prior to infection. *Y. pestis* strains were grown at 27°C for 2 h in HIB with antibiotics as appropriate and then shifted to 37°C for 1 h to induce expression of T3SS proteins. At temperature shift, 0.2% L-arabinose was added to the cultures. Bacteria were added at MOI = 50 to HeLa cells. The infected cells were incubated at 37°C with 5% CO<sub>2</sub>. Two negative controls (without *Y. pestis* cells and *Y. pestis*

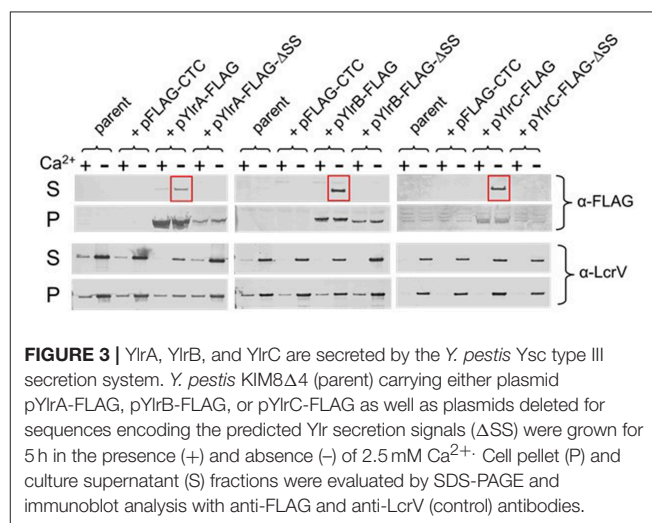


**FIGURE 3** | YlrA, YlrB, and YlrC are secreted by the *Y. pestis* Ysc type III secretion system. *Y. pestis* KIM8 $\Delta$ 4 (parent) carrying either plasmid pYlrA-FLAG, pYlrB-FLAG, or pYlrC-FLAG as well as plasmids deleted for sequences encoding the predicted Ylr secretion signals ( $\Delta$ SS) were grown for 5 h in the presence (+) and absence (–) of 2.5 mM Ca<sup>2+</sup>. Cell pellet (P) and culture supernatant (S) fractions were evaluated by SDS-PAGE and immunoblot analysis with anti-FLAG and anti-LcrV (control) antibodies.

with pBAD18-pYscF<sub>1</sub>-Bla) and a positive control were used to determine the background blue and green fluorescence. After infection for 3 h, the growth medium from the cells was removed and the cells were washed with 500  $\mu$ L of 1x of GIBCO Hank's Balanced Salt Solution (HBSS). 6X CCF-AM (Invitrogen) was added to each sample to obtain a final concentration of 1X per manufacturer's instructions. The plate was covered and incubated in room temperature for 1 h. Cells were then visualized by confocal-fluorescent microscopy (Leica TCS SP5 Inverted Confocal Microscope).

## RESULTS

### Pro-survival Activity of *Y. pestis* Leucine-Rich Proteins During Cellular Infection

Previously we described a transposon site hybridization (TraSH)-based screen to identify *Y. pestis* loci that are required during infection of cultured mouse macrophage-like RAW 264.7 cells (Bartra et al., 2012). From a pool of approximately 90,000 unique variants, 44 *Y. pestis* ORFs were identified that appeared to be required for pathogen survival during its interaction with the macrophage. A number of these ORFs (17) are encoded on the extrachromosomal plasmids pCD1 and pPCP1 and express components of the T3SS and Pla protease that both play critical roles in *Y. pestis* virulence (Viboud and Bliska, 2005). One such pCD1-encoded locus among this set of 17 identified ORFs, YopM, possesses Leucine-Rich Repeats (LRRs), and is associated

with a variety of infection phenotypes (see Introduction). Among the 27 chromosomally-encoded pro-survival ORFs, there were three, *y3397*, *y3399*, and *y3400*, that were previously predicted to possess LRRs (Hu et al., 2016) and here will be designated as *Yersinia* leucine-rich repeat A (*ylrA*), B (*ylrB*), and C (*ylrC*), respectively (Figure 1). In addition to LRR-encoding sequences, these three ORFs also possess predicted secretion signals (SS) for the T3SS at their N-termini and YlrA and YlrC are additionally predicted to encode novel ubiquitin E3 ligase (NEL) domains (Wang et al., 2013; Marchler-Bauer et al., 2017).

### Defective Infection Phenotypes of Engineered $\Delta$ ylr Strains

The aforementioned TraSH screen involves infecting macrophages with a mixture of *Y. pestis* variants followed by a quantification of under-represented genetic loci. To test whether the Ylr-encoding loci play a pro-survival function for *Y. pestis* during a single-strain infection, individual  $\Delta$ ylrA,  $\Delta$ ylrB, and  $\Delta$ ylrC mutant strains were constructed and tested in a colony-forming unit (CFU)-based infection assay. Similar to what has been shown previously, the fold-increases of the parental *Y. pestis* KIM5 strain and the T3SS mutant strain ( $\Delta$ yopB) during a 8 h infection, were 170 and 3, respectively (Figure 2A; Rosenzweig et al., 2005). The infectivity of the single gene deletion  $\Delta$ ylrA,  $\Delta$ ylrB, and  $\Delta$ ylrC mutant strains, as well as the triple gene deletion  $\Delta$ ylrABC mutant strain were intermediate between the parental and T3SS mutant strains (Figure 2A). This intermediate *in vitro* infection phenotype is similar to that observed in *Yersinia* mutants individually deleted

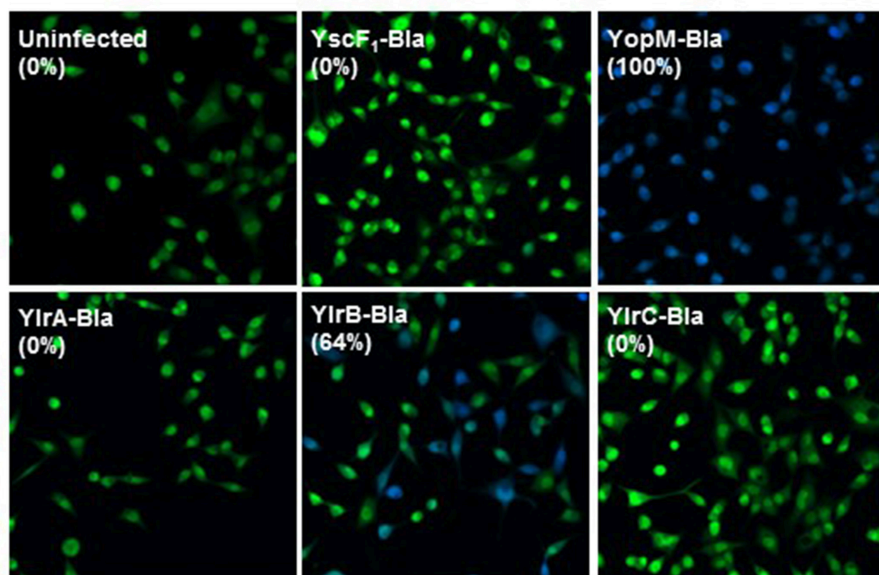


**FIGURE 4 |** YlrB is translocated into eukaryotic cells. HeLa cells were infected with Yp589 (*Y. pestis* strain with deletion of YopE, YopJ, YopM, SycT, and YpKA) carrying YscF<sub>1</sub>-Bla (possessing the *yscF* 5' UTR and the initiation codon), pMM85 YopM-Bla, YlrA-Bla, YlrB-Bla, or YlrC-Bla and were then incubated at 37°C for 3 h. CCF2-AM was added to HeLa cells and visualized by fluorescence microscopy. HeLa cells infected with the strain carrying the YlrB-Bla were positive for cytoplasmic  $\beta$ -lactamase activity (blue fluorescence), indicating that these cells had been injected with YlrB-Bla. Shown is a single representative experiment performed multiple times.

for the YopE and YopH T3SS effectors (Bartra et al., 2001). These data validated the findings of the TraSH screen indicating that the Ylr-encoding genes promote the survival of *Y. pestis* during their interaction with macrophages.

The *Y. pestis*  $\Delta ylrABC$  strain was tested in a mouse-based infection model to determine whether the Ylr-encoding loci promote the pathogen survival *in vivo*. A competition infection assay was used to compare the proliferation of the parental KIM5 strain to that of the mutant strain within individual mice. Accordingly, in the control experiment mice were infected with an equal mixture of the parental KIM5 and the isogenic T3SS mutant  $\Delta yopB$  strains and after 2 days the mice were humanely sacrificed and the presence of each strain in the spleen was determined by CFU assay. In contrast to the equal ratio of the parental and  $\Delta yopB$  stains in the “input” (i.e., the dosed inoculum), the parental strain was greatly over-represented in the “output” (i.e., the splenic homogenates derived from mice infected for 2 days) (Figure 2B). Mice similarly infected with an equal mixture of the parental KIM5 and the isogenic  $\Delta ylrABC$  strains also yielded a statistically significant over-representation of the parental strain following 2 days of infection (Figure 2B). There was no detectable differences in growth rates between the parental KIM5 and the isogenic  $\Delta ylrABC$  strains (Supplementary Figure 1). Collectively these data indicate that the *ylr* locus promotes *Y. pestis* infection both in cells and in mice.

### YlrA, YlrB, and YlrC Are Secreted by the *Y. pestis* Ysc Type III Secretion System

Sequence analysis of the *ylrA*, *ylrB*, and *ylrC* genes indicated that they each potentially encode at their amino-terminus a recognition sequence for the type III secretion system (T3SS)

(Hu et al., 2016). To determine if the YlrA, YlrB, and YlrC proteins are secreted by the T3SS, expression vectors containing full-length C-terminal FLAG-tagged proteins were constructed. In addition, DNA sequences predicted to encode YlrA, YlrB, and YlrC N-terminal T3SS signal residues 2 to 10 were deleted from each of the expression vectors. Generated plasmids were placed in *Y. pestis* KIM8 $\Delta$ 4, a strain containing a modified pCD1 virulence plasmid that contains all of the genes necessary to assemble a functional T3SS but lacks all other effector proteins (Bartra et al., 2006). The strains were tested for expression and secretion in the presence and absence of 2.5 mM of calcium and bacterial pellet and supernatant were analyzed. FLAG-tagged YlrA, YlrB, and YlrC were expressed in the presence and absence of calcium, but were secreted only in the absence of calcium (Figure 3; red boxes; and Data Sheet 1). There was no secretion of the YlrA, YlrB, and YlrC proteins when the putative T3SS signal of each protein was deleted. Finally, there was no secretion of YlrA-FLAG, YlrB-FLAG, or YlrC-FLAG detected by *Y. pestis* strain KIM8 (pCD1-) or *Y. pestis*  $\Delta yscF$ , both of which are unable to assemble a functional Ysc injectisome (Supplementary Figures 2–4). Together, these results demonstrate that YlrA, YlrB and YlrC are T3S substrates and that they are recognized and secreted by the *Y. pestis* T3SS.

### YlrB Is Translocated Into Mammalian Cells

A  $\beta$ -lactamase reporter system was used to determine whether Ylr proteins are translocated into cultured cells during infection (Marketon et al., 2005). Upon diffusion into cultured cells, CCF2-AM is cleaved into the membrane-impermeable CCF2 by endogenous cytoplasmic esterases, emitting a green fluorescence. When  $\beta$ -lactamase fusion proteins are injected into the cells, CCF2 can be cleaved further, changing the fluorescent emission to blue (Charpentier and Oswald, 2004). Cells that were either uninfected or infected with a *Y. pestis* strain expressing YscF1-Bla, which is expressed but not secreted by the T3SS, retained their initial green fluorescence (Figure 4). In striking contrast, essentially all CCF2-labeled cells infected with a *Y. pestis* strain expressing YopM-Bla, which, as discussed in the Introduction, is a plasmid-encoded virulence factor, fluoresce blue indicating that YopM-Bla is readily translocated into the infected cell cytosol. Cells infected with *Y. pestis* strains expressing either YlrA-Bla or YlrC-Bla retained their green fluorescence indicating that these proteins were not detectably translocated as assayed by this method despite being readily expressed as assayed by western blotting (Figure 4; Supplementary Figure 5). In contrast, blue fluorescing cells were readily detected following infection with a *Y. pestis* strain expressing YlrB-Bla. These show that the YlrB is translocated by *Y. pestis* during infection.

### Intracellular Activity of Ylr

Previous studies of the *Yersinia* Yop virulence factors have shown a robust correlation between their growth inhibition in yeast and their activity in mammalian cells (Lesser and Miller, 2001; Wiley et al., 2009). Yeast provide a relatively simple genetic model system for the study of the eukaryotic genes and is based on the premise that yeast share many molecular, genetic, and biochemical features with mammalian

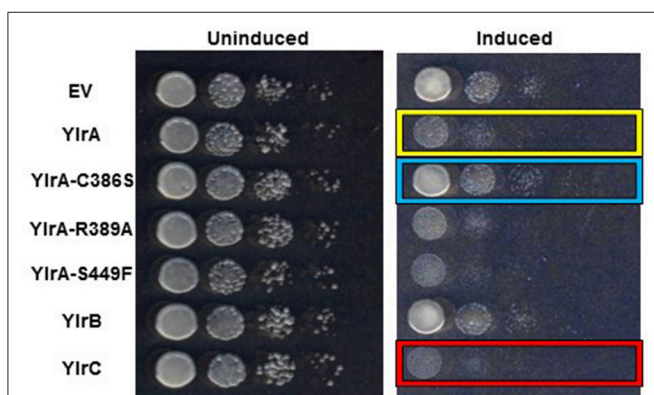


**FIGURE 5 |** YlrA and YlrC, but not YlrB, disrupt yeast growth. Yeast transformed with either an empty vector (EV) control plasmid or the indicated Ylr proteins under the control of an inducible promoter. Comparable growth was observed when strains were plated on non-inducing media (left panel). However, when strains were plated on inducing media (right panel), the YlrA- and YlrC-expressing strains (yellow and red boxes, respectively) displayed a growth defect compared to the EV and YlrB-expressing strains. Also, mutation of the putative catalytic cysteine residue of the NEL domain of YlrA reversed the disruptive effect of YlrA on yeast growth (blue box); whereas mutation of the other residues did not have any effect. Shown is the result of a single experiment performed three times with similar outcomes.



cells (Zhao and Lieberman, 1995). Accordingly, the fission yeast *Schizosaccharomyces pombe* was transformed with either an empty vector control plasmid or inducible expression plasmids encoding either YlrA, YlrB, or YlrC and plated either on media in which the Ylr proteins were not expressed (“uninduced”) or on media in which Ylr expression occurs (“induced”). All *S. pombe* transformant strains grew equally well on uninduced media (Figure 5). However, on induced media, there was a marked differences between the relatively rapid growth of the empty vector and YlrB transformants (rows 1 and 6) and that of the relatively poorer growth of the YlrA and YlrC transformants (rows 2 and 7). Previous work has shown that IpaH effectors and SspH2 have a conserved catalytic cysteine residue that is absolutely required for ubiquitin ligase activity (Rohde et al., 2007; Quezada et al., 2009). To determine if this residue and other conserved residues of the NEL domain of YlrA will affect its growth-inhibiting activity in yeast, these residues were substituted generating plasmids expressing YlrA-C386S, YlrA-R389A, and YlrA-S449F. There was a clear reduction in growth inhibition for the *S. pombe* strain expressing the YlrA-C386S variant compared to the strain expressing wild-type YlrA (Figure 5, rows 2 and 3). In contrast, there was no detectable loss of growth inhibitory activity in the *S. pombe* strains expressing either the YlrA-R389A or YlrA-S449F (rows 4 and 5). These data suggest that the ubiquitin ligase activity of YlrA is required for its growth inhibitory activity in eukaryotic cells.

## DISCUSSION

In this study, we demonstrate that the *Y. pestis* chromosomally-encoded proteins YlrA, YlrB, and YlrC are secreted and recognized by the T3SS and are required for the optimal survival of this pathogen both in the presence of cells as well as in mice. Although many chromosomally-encoded *Y. pestis* virulence factors have been described, to the best of our knowledge the Ylr are the first chromosomally-encoded virulence factors secreted by the pCD1-encoded T3SS.

YlrA, YlrB, and YlrC are leucine rich repeat proteins (LRR) with (YlrA and YlrC) or without (YlrB) an E3 ligase domain (NEL). The Ylr proteins belong to a diverse group of molecules distinguished by a consensus sequence consisting predominantly of leucines, hence the term leucine-rich repeat. Similar proteins are found in other Gram-negative bacteria that possess T3SSs, including *Yersinia* (YopM) (Kobe and Deisenhofer, 1994), *Shigella* (IpaH family proteins) (Ashida et al., 2007), *Salmonella* (SspH1, SspH2 and SlrP) (Miao et al., 1999; Tsolis et al., 1999; Bernal-Bayard et al., 2010) and other bacterial pathogens. In addition to possessing detectable membrane-penetrating activity, LRR domains offer adaptable structural frameworks that mediate protein-protein interactions, coupling enzymatic domains to substrate-binding domains, function to determine substrate specificity, and to suppress the enzymatic activity of the NEL domain prior to substrate binding (Kobe and Kajava, 2001; Quezada et al., 2009; Rüter et al., 2010). The NEL domains function as ubiquitin E3 ligases which mimic the activities of host E3 ubiquitin ligases and ubiquitinate specific target proteins

(Rohde et al., 2007; Quezada et al., 2009). YlrA and YlrC contain an N-terminal LRR domain and a predicted C-terminal novel E3 ligase domain (NEL) (Hu et al., 2016). E3 ligase activity has been demonstrated for the *Shigella* effectors IpaH4.5 and IpaH9.8 and *Salmonella* effectors SspH1, SspH2, and SlrP (Rohde et al., 2007; Singer et al., 2008; Zhu et al., 2008; Bernal-Bayard and Ramos-Morales, 2009; Quezada et al., 2009). Bacterial E3 ubiquitin ligases transported into host cells mimic the activities of host E3 ubiquitin ligases and ubiquitinate specific target proteins. For example, IpaH 4.5 appears to dampen the innate immune system of human cells by inhibiting nuclear factor KB (NF-KB) signaling in response to an intracellular infection with *Shigella* (Ashida et al., 2010). The *Salmonella* virulence effector SlrP targets the mammalian thioredoxin-1 (Trx) leading to ubiquitination of Trx and causes a decrease in its redox activity (Bernal-Bayard and Ramos-Morales, 2009).

We have demonstrated that YlrB is translocated into the eukaryotic cell, whereas there was no evidence of translocation of the YlrA and YlrC using a  $\beta$ -lactamase reporter system. These results are difficult to interpret. Both full-length YlrA and YlrC are expressed and secreted, albeit at lower levels than YlrB (see Figure 3 and Supplementary Figure 5); therefore we expect them to be translocated as well. In addition, the fact that they contain an E3 ligase domain suggests that these proteins work inside the eukaryotic cell. Lack of detectable translocation in our experiments could be due to the large size of the proteins (~600 amino acids). Further experiments are needed using smaller-sized constructs expressing the translocation domains of both proteins. The most compelling data we present that YlrA and YlrC actually function within eukaryotic cells is the fact that they both disrupt the growth of the fission yeast *S. pombe*. Furthermore, to test if the conserved catalytic cysteine residue in YlrA is important to the activity of the protein, it was replaced with a serine residue. This resulted to the loss of the growth-inhibiting activity of YlrA. We speculate that the deleterious effect of YlrA and YlrC is due to the activity of their NEL domain. In a study using a yeast model, Rohde et al. (2007) have shown that *S. flexneri* IpaH9.8 inhibit yeast pheromone response signaling by ubiquitination and by promoting proteasome-dependent destruction of the mitogen-activated protein kinase kinase (MAPKK) Ste7. It was also demonstrated in the same study that the cysteine residue conserved in the NEL domain of all IpaH family members is required for the IpaH9.8 activities in yeast. The *Salmonella* effector SspH2 also has a conserved cysteine residue (Quezada et al., 2009). This catalytic cysteine residue and all other NEL active site residues are absolutely conserved between YlrA, YlrC and SspH2. We conclude that both YlrA and YlrC are strong candidates to join the list of bacterial virulence proteins that target the mammalian ubiquitination system.

To date, little is known about the leucine-rich repeat proteins in *Yersinia* with the exception of YopM. Miao et al. (1999) described three leucine-rich repeat open reading frames (ORFs) in *Y. pestis* that share significant homology with SspH2. These ORFs seem to be *ylrA*, *ylrB* and *ylrC*, since the ORFs were described to be present in an operon-like structure in the chromosome. Later, Evdokimov et al. (2001) described that these



three ORFs share similar structure with *Salmonella* effectors SlrP, SspH1, SspH2; *Shigella* effector IpaH; and *Yersinia* effector YopM. Chou et al. (2012) PCR amplified *Y. pestis* y3400 (*ylrA*), expressed and purified the previously uncharacterized protein in *E. coli* and demonstrated that the purified protein possessed constitutive, not autoinhibited, ubiquitin E3 ligase activity. Finally, Soundararajan et al. (2011) were the first to identify and analyze the structure-function relation of a protein which appears to be the protein product of y3397 (YlrC) (McPhee and Bliska, 2011). More systematic studies are needed to characterize the expression, secretion, translocation, molecular functions and host target of these novel effector proteins. Research on these *ylr* gene products will lead to a better understanding of *Y. pestis* pathogenesis and possibly to the identification of the proteins as novel vaccine candidates or potential targets for therapeutics.

In conclusion, the *ylrA*, *ylrB*, and *ylrC* gene products represent the first chromosome-encoded T3S effector proteins of *Y. pestis* and are required for the optimal survival of this pathogen in the presence of macrophages. The gene products share significant similarity with T3S effector proteins from other

bacterial pathogens and hence they are strong candidates to join the list of bacterial virulence proteins.

## AUTHOR CONTRIBUTIONS

SS, CL, XG, WB, ZL, GP, and KS planned and performed the majority of the experiments. HB and RH provided technical assistance. LQ analyzed the results of the TraSH screen. SS, CL, and KS wrote the manuscript.

## FUNDING

This study was funded in part by NIH AI119450 (GP/KS) and U.S. Army Research, Development and Engineering Command (RDECOM), Contract W911SR-07-C-0084 (ZL).

## SUPPLEMENTARY MATERIAL

The Supplementary Material for this article can be found online at: <https://www.frontiersin.org/articles/10.3389/fcimb.2019.00023/full#supplementary-material>

## REFERENCES

- Ali, S. A., and Steinkasserer, A. (1995). PCR-ligation-PCR mutagenesis: a protocol for creating gene fusions and mutations. *BioTechniques* 18, 746–750.
- Ashida, H., Kim, M., Schmidt-Supprian, M., Ma, A., Ogawa, M., and Sasakawa, C. (2010). A bacterial E3 ubiquitin ligase IpaH9.8 targets NEMO/IKK $\gamma$  to dampen the host NF- $\kappa$ B-mediated inflammatory response. *Nat. Cell Biol.* 12, 66–73. doi: 10.1038/ncb2006
- Ashida, H., Toyotome, T., Nagai, T., and Sasakawa, C. (2007). *Shigella* chromosomal IpaH proteins are secreted via the type III secretion system and act as effectors. *Mol. Microbiol.* 63, 680–693. doi: 10.1111/j.1365-2958.2006.05547.x
- Bartra, S., Cherepanov, P., Forsberg, A., and Schesser, K. (2001). The *Yersinia* YopE and YopH type III effector proteins enhance bacterial proliferation following contact with eukaryotic cells. *BMC Microbiol.* 1:22. doi: 10.1186/1471-2180-1-22
- Bartra, S. S., Gong, X., Loric, C. D., Jain, C., Nair, M. K., Schifferli, D., et al. (2012). The outer membrane protein A (OmpA) of *Yersinia pestis* promotes intracellular survival and virulence in mice. *Microb. Pathog.* 52, 41–46. doi: 10.1016/j.micpath.2011.09.009
- Bartra, S. S., Jackson, M. W., Ross, J. A., and Plano, G. V. (2006). Calcium-regulated type III secretion of yop proteins by an *Escherichia coli* hha mutant carrying a *Yersinia pestis* pCD1 virulence plasmid. *Infect. Immun.* 74, 1381–1386. doi: 10.1128/IAI.74.2.1381-1386.2006
- Bernal-Bayard, J., Cardenal-Munoz, E., and Ramos-Morales, F. (2010). The *Salmonella* type III secretion effector, *Salmonella* leucine-rich repeat protein (SlrP), targets the human chaperone ERdj3. *J. Biol. Chem.* 285, 16360–16368. doi: 10.1074/jbc.M110.100669
- Bernal-Bayard, J., and Ramos-Morales, F. (2009). *Salmonella* type III secretion effector SlrP is an E3 ubiquitin ligase for mammalian thioredoxin. *J. Biol. Chem.* 284, 27587–27595. doi: 10.1074/jbc.M109.010363
- Centers for Disease Control and Prevention. (2013). *Plague: Map and Statistics*. Available online at: <http://www.cdc.gov/plague/maps/index.html>
- Charpentier, X., and Oswald, E. (2004). Identification of the secretion and translocation domain of the enteropathogenic and enterohemorrhagic *Escherichia coli* effector cif, using TEM-1 beta-lactamase as a new fluorescence-based reporter. *J. Bacteriol.* 186, 5486–5495. doi: 10.1128/JB.186.16.5486-5495.2004
- Chou, Y. C., Keszei, A. F., Rohde, J. R., Tyers, M., and Sicheri, F. (2012). Conserved structural mechanisms for autoinhibition in IpaH ubiquitin ligases. *J. Biol. Chem.* 287, 268–275. doi: 10.1074/jbc.M111.316265
- Chung, L. K., Philip, N. H., Schmidt, V. A., Koller, A., Strowig, T., Flavell, R. A., et al. (2014). IQGAP1 is important for activation of caspase-1 in macrophages and is targeted by *Yersinia pestis* type III effector YopM. *MBio* 5:e01402-14. doi: 10.1128/mBio.01402-14
- Cornelis, G. R. (2002a). The *Yersinia* ysc-yop ‘type III’ weaponry. *Nat. Rev. Mol. Cell Biol.* 3, 742–752. doi: 10.1038/nrm932
- Cornelis, G. R. (2002b). *Yersinia* type III secretion: send in the effectors. *J. Cell Biol.* 158, 401–408. doi: 10.1083/jcb.200205077
- Cornelis, G. R., and Van Gijsegem, F. (2000). Assembly and function of type III secretory systems. *Annu. Rev. Microbiol.* 54, 735–774. doi: 10.1146/annurev.micro.54.1.735
- Datsenko, K. A., and Wanner, B. L. (2000). One-step inactivation of chromosomal genes in *Escherichia coli* K-12 using PCR products. *Proc. Natl. Acad. Sci. U S A.* 97, 6640–6645. doi: 10.1073/pnas.120163297
- Dennis, D. T., and Chow, C. C. (2004). Plague. *Pediatr. Infect. Dis. J.* 23, 69–71. doi: 10.1097/01.inf.0000106918.18570.dd
- Evdokimov, A. G., Anderson, D. E., Routzahn, K. M., and Waugh, D. S. (2001). Unusual molecular architecture of the *Yersinia pestis* cytotoxin YopM: a leucine-rich repeat protein with the shortest repeating unit. *J. Mol. Biol.* 312, 807–821. doi: 10.1006/jmbi.2001.4973
- Hentschke, M., Berneking, L., Belmar Campos, C., Buck, F., Ruckdeschel, K., and Aepfelbacher, M. (2010). *Yersinia* virulence factor YopM induces sustained RSK activation by interfering with dephosphorylation. *PLoS ONE* 5:e13165. doi: 10.1371/journal.pone.0013165
- Hu, Y., Huang, H., Hui, X., Cheng, X., White, A. P., Zhao, Z., et al. (2016). Distribution and evolution of *Yersinia* leucine-rich repeat proteins. *Infect Immun.* 84, 2243–2254. doi: 10.1128/IAI.00324-16
- Imai, Y., Matsushima, Y., Sugimura, T., and Terada, M. (1991). A simple and rapid method for generating a deletion by PCR. *Nucleic Acids Res.* 19:2785. doi: 10.1093/nar/19.10.2785
- Inglesby, T. V., Dennis, D. T., Henderson, D. A., Bartlett, J. G., Ascher, M. S., Eitzen, E., et al. (2000). Plague as a biological weapon: medical and public health management. Working group on civilian biodefense. *JAMA* 283, 2281–2290. doi: 10.1001/jama.283.17.2281
- Jackson, M. W., Day, J. B., and Plano, G. V. (1998). YscB of *Yersinia pestis* functions as a specific chaperone for YopN. *J. Bacteriol.* 180, 4912–4921.

- Kerschen, E. J., Cohen, D. A., Kaplan, A. M., and Straley, S. C. (2004). The plague virulence protein YopM targets the innate immune response by causing a global depletion of NK cells. *Infect. Immun.* 72, 4589–4602. doi: 10.1128/IAI.72.8.4589-4602.2004
- Kobe, B., and Deisenhofer, J. (1994). The leucine-rich repeat: a versatile binding motif. *Trends Biochem. Sci.* 19, 415–421. doi: 10.1016/0968-0004(94)90090-6
- Kobe, B., and Kajava, A. V. (2001). The leucine-rich repeat as a protein recognition motif. *Curr. Opin. Struct. Biol.* 11, 725–732. doi: 10.1016/S0959-440X(01)00266-4
- LaRock, C. N., and Cookson, B. T. (2012). The *Yersinia* virulence effector YopM binds caspase-1 to arrest inflammasome assembly and processing. *Cell Host Microbe* 12, 799–805. doi: 10.1016/j.chom.2012.10.020
- Lesser, C. F., and Miller, S. I. (2001). Expression of microbial virulence proteins in *Saccharomyces cerevisiae* models mammalian infection. *EMBO J.* 20, 1840–1849. doi: 10.1093/emboj/20.8.1840
- Leung, K. Y., and Straley, S. C. (1989). The yopM gene of *Yersinia pestis* encodes a released protein having homology with the human platelet surface protein GPIb alpha. *J. Bacteriol.* 171, 4623–4632. doi: 10.1128/jb.171.9.4623-4632.1989
- Marchler-Bauer, A., Bo, Y., Han, L., He, J., Lanczycki, C. J., Lu, S., et al. (2017). CDD/SPARCLE: functional classification of proteins via subfamily domain architectures. *Nucleic Acids Res.* 45, D200–D203. doi: 10.1093/nar/gkw1129
- Marketon, M. M., DePaolo, R. W., DeBord, K. L., Jabri, B., and Schneewind, O. (2005). Plague bacteria target immune cells during infection. *Science* 309, 1739–1741. doi: 10.1126/science.1114580
- Maundrell, K. (1993). Thiamine-repressible expression vectors pREP and pRIP for fission yeast. *Gene* 123, 127–130. doi: 10.1016/0378-1119(93)90551-D
- McDonald, C., Vacratsis, P. O., Bliska, J. B., and Dixon, J. E. (2003). The yersinia virulence factor YopM forms a novel protein complex with two cellular kinases. *J. Biol. Chem.* 278, 18514–18523. doi: 10.1074/jbc.M301226200
- McPhee, J. B., and Bliska, J. B. (2011). Letter to the editor and response. *Innate Immun.* 17, 558–559. doi: 10.1177/1753425911426251
- McPhee, J. B., Mena, P., and Bliska, J. B. (2010). Delineation of regions of the *Yersinia* YopM protein required for interaction with the RSK1 and PRK2 host kinases and their requirement for interleukin-10 production and virulence. *Infect. Immun.* 78, 3529–3539. doi: 10.1128/IAI.00269-10
- Miao, E. A., Scherer, C. A., Tsolis, R. M., Kingsley, R. A., Adams, L. G., Bäuml, A. J., et al. (1999). *Salmonella typhimurium* leucine-rich repeat proteins are targeted to the SPI1 and SPI2 type III secretion systems. *Mol. Microbiol.* 34, 850–864. doi: 10.1046/j.1365-2958.1999.01651.x
- Morita, T., and Takegawa, K. (2004). A simple and efficient procedure for transformation of *Schizosaccharomyces pombe*. *Yeast* 21, 613–617. doi: 10.1002/yea.1104
- Perry, R. D., and Fetherston, J. D. (1997). *Yersinia pestis*—etiologic agent of plague. *Clin. Microbiol. Rev.* 10, 35–66. doi: 10.1128/CMR.10.1.35
- Quezada, C. M., Hicks, S. W., Galan, J. E., and Stebbins, C. E. (2009). A family of *salmonella* virulence factors functions as a distinct class of autoregulated E3 ubiquitin ligases. *Proc. Natl. Acad. Sci. USA.* 106, 4864–4869. doi: 10.1073/pnas.0811058106
- Rohde, J. R., Breitkreutz, A., Chenal, A., Sansonetti, P. J., and Parsot, C. (2007). Type III secretion effectors of the IpaH family are E3 ubiquitin ligases. *Cell Host Microbe* 1, 77–83. doi: 10.1016/j.chom.2007.02.002
- Rosenzweig, J. A., Weltman, G., Plano, G. V., and Schesser, K. (2005). Modulation of yersinia type three secretion system by the S1 domain of polynucleotide phosphorylase. *J. Biol. Chem.* 280, 156–163. doi: 10.1074/jbc.M405662200
- Rüter, C., Buss, C., Scharnert, J., Heussipp, G., and Schmidt, M. A. (2010). A newly identified bacterial cell-penetrating peptide that reduces the transcription of pro-inflammatory cytokines. *J. Cell. Sci.* 123(Pt 13):2190–2198. doi: 10.1242/jcs.063016
- Singer, A. U., Rohde, J. R., Lam, R., Skarina, T., Kagan, O., Dileo, R., et al. (2008). Structure of the shigella T3SS effector IpaH defines a new class of E3 ubiquitin ligases. *Nat. Struct. Mol. Biol.* 15, 1293–1301. doi: 10.1038/nsmb.1511
- Soundararajan, V., Patel, N., Subramanian, V., Sasisekharan, V., and Sasisekharan, R. (2011). The many faces of the YopM effector from plague causative bacterium *Yersinia pestis* and its implications for host immune modulation. *Innate Immun.* 17, 548–557. doi: 10.1177/1753425910377099
- Tsolis, R. M., Townsend, S. M., Miao, E. A., Miller, S. I., Ficht, T. A., Adams, L. G., et al. (1999). Identification of a putative *Salmonella enterica* serotype typhimurium host range factor with homology to IpaH and YopM by signature-tagged mutagenesis. *Infect. Immun.* 67, 6385–6393.
- Viboud, G. I., and Bliska, J. B. (2005). *Yersinia* outer proteins: role in modulation of host cell signaling responses and pathogenesis. *Annu. Rev. Microbiol.* 59, 69–89. doi: 10.1146/annurev.micro.59.030804.121320
- Wang, Y., Sun, M., Bao, H., Zhang, Q., and Guo, D. (2013). Effective identification of bacterial type III secretion signals using joint element features. *PLoS ONE* 8:e59754 doi: 10.1371/journal.pone.0059754
- Wiley, D. J., Shrestha, N., Yang, J., Atis, N., Dayton, K., and Schesser K. (2009). The activities of the *Yersinia* protein kinase A (YpkA) and outer protein J (YopJ) virulence factors converge on an eIF2α kinase. *J. Biol. Chem.* 284, 24744–24753. doi: 10.1074/jbc.M109.010140
- Ye, Z., Kerschen, E. J., Cohen, D. A., Kaplan, A. M., van Rooijen, N., and Straley, S. C. (2009). Gr1+ cells control growth of YopM-negative *Yersinia pestis* during systemic plague. *Infect. Immun.* 77, 3791–3806. doi: 10.1128/IAI.00284-09
- Zhao, Y., and Lieberman, H. B. (1995). *Schizosaccharomyces pombe*: a model for molecular studies of eukaryotic genes. *DNA Cell Biol.* 14, 359–371. doi: 10.1089/dna.1995.14.359
- Zhu, Y., Li, H., Hu, L., Wang, J., Zhou, Y., Pang, Z., et al. (2008). Structure of a shigella effector reveals a new class of ubiquitin ligases. *Nat. Struct. Mol. Biol.* 15, 1302–1308. doi: 10.1038/nsmb.1517

**Conflict of Interest Statement:** The authors declare that the research was conducted in the absence of any commercial or financial relationships that could be construed as a potential conflict of interest.

Copyright © 2019 Schesser Bartra, Lorica, Qian, Gong, Bahnan, Barreras, Hernandez, Li, Plano and Schesser. This is an open-access article distributed under the terms of the Creative Commons Attribution License (CC BY). The use, distribution or reproduction in other forums is permitted, provided the original author(s) and the copyright owner(s) are credited and that the original publication in this journal is cited, in accordance with accepted academic practice. No use, distribution or reproduction is permitted which does not comply with these terms.



# Heterologous Complementation Studies With the YscX and YscY Protein Families Reveals a Specificity for *Yersinia pseudotuberculosis* Type III Secretion

Jyoti M. Gurung<sup>1,2</sup>, Ayad A. A. Amer<sup>1,2</sup>, Monika K. Francis<sup>1,2</sup>, Tiago R. D. Costa<sup>1,2†</sup>, Shiyun Chen<sup>3</sup>, Anton V. Zavialov<sup>4</sup> and Matthew S. Francis<sup>1,2\*</sup>

## OPEN ACCESS

### Edited by:

Sophie Bleves,  
Aix-Marseille Université, France

### Reviewed by:

Luís Jaime Mota,  
Faculdade de Ciências e Tecnologia  
da Universidade Nova de Lisboa,  
Portugal  
Eric Faudry,  
CEA Grenoble, France

### \*Correspondence:

Matthew S. Francis  
matthew.franis@umu.se

### † Present Address:

Tiago R. D. Costa,  
MRC Centre for Molecular  
Bacteriology and Infection,  
Department of Life Sciences, Imperial  
College London, London,  
United Kingdom

**Received:** 16 December 2017

**Accepted:** 28 February 2018

**Published:** 16 March 2018

### Citation:

Gurung JM, Amer AAA, Francis MK, Costa TRD, Chen S, Zavialov AV and Francis MS (2018) Heterologous Complementation Studies With the YscX and YscY Protein Families Reveals a Specificity for *Yersinia pseudotuberculosis* Type III Secretion. *Front. Cell. Infect. Microbiol.* 8:80. doi: 10.3389/fcimb.2018.00080

<sup>1</sup> Department of Molecular Biology, Umeå University, Umeå, Sweden, <sup>2</sup> Umeå Centre for Microbial Research, Umeå University, Umeå, Sweden, <sup>3</sup> Key Laboratory of Special Pathogens and Biosafety, Wuhan Institute of Virology, Chinese Academy of Sciences Wuhan, Wuhan, China, <sup>4</sup> Department of Chemistry, University of Turku, Turku, Finland

Type III secretion systems harbored by several Gram-negative bacteria are often used to deliver host-modulating effectors into infected eukaryotic cells. About 20 core proteins are needed for assembly of a secretion apparatus. Several of these proteins are genetically and functionally conserved in type III secretion systems of bacteria associated with invertebrate or vertebrate hosts. In the Ysc family of type III secretion systems are two poorly characterized protein families, the YscX family and the YscY family. In the plasmid-encoded Ysc-Yop type III secretion system of human pathogenic *Yersinia* species, YscX is a secreted substrate while YscY is its non-secreted cognate chaperone. Critically, neither an yscX nor yscY null mutant of *Yersinia* is capable of type III secretion. In this study, we show that the genetic equivalents of these proteins produced as components of other type III secretion systems of *Pseudomonas aeruginosa* (PscX and PscY), *Aeromonas* species (AscX and AscY), *Vibrio* species (VscX and VscY), and *Photobacterium luminescens* (SctX and SctY) all possess an ability to interact with its native cognate partner and also establish cross-reciprocal binding to non-cognate partners as judged by a yeast two-hybrid assay. Moreover, a yeast three-hybrid assay also revealed that these heterodimeric complexes could maintain an interaction with YscV family members, a core membrane component of all type III secretion systems. Despite maintaining these molecular interactions, only expression of the native yscX in the near full-length yscX deletion and native yscY in the near full-length yscY deletion were able to complement for their general substrate secretion defects. Hence, YscX and YscY must have co-evolved to confer an important function specifically critical for *Yersinia* type III secretion.

**Keywords:** T3S chaperone, secretion hierarchy, substrate sorting, LcrH/SycD, YscV, protein-protein interaction

## INTRODUCTION

Type III secretion (T3S) is an effective means for many different Gram-negative bacteria to deliver proteins into diverse eukaryotic cell types. This is a common virulence mechanism of many harmful pathogens (Buttner, 2012; Portaliou et al., 2016), but is also useful for bacteria relying on a symbiotic lifestyle or for survival in the environment (Pallen et al., 2005), and for the biosynthesis of the flagella apparatus (Erhardt et al., 2010). Upon artificial induction, a T3S system (T3SS) can also secrete substrates into laboratory culture media and this requires a complex of ~20 proteins that all together span both bacterial membranes (inner and outer), the peptidoglycan layer and which also protrudes out from the surface. This apparatus has been purified from a few different bacteria, taking on the appearance of a syringe equipped with needle (often termed the “needle complex”) (Kubori et al., 1998; Blocker et al., 1999, 2001; Kimbrough and Miller, 2000; Tamano et al., 2000, 2002; Sekiya et al., 2001; Sukhan et al., 2001; Journet et al., 2003; Marlovits et al., 2004; Mueller et al., 2005). Generally, protein cargo is thought to be secreted through the needle complex (Radics et al., 2014), and these can be divided into three categories—“early” substrates that make up the outer needle, “middle” substrates comprising the pore-forming translocon proteins and “late” host-modulating effector proteins that with assistance from the translocon are targeted to the eukaryotic cell interior (Osborne and Coombes, 2011; Buttner, 2012; Dewoody et al., 2013).

About 10 proteins exist in the needle complex that are common to all known non-flagella and flagella T3SSs (Francis et al., 2004; Buttner, 2012; Portaliou et al., 2016). Moreover, thorough analysis of sequence similarities can classify all T3SSs into evolutionary distinct nodes (Troisfontaines and Cornelis, 2005; Abby and Rocha, 2012). Among the non-flagella T3SSs, a major node is the *inv/spa* system encoded by the *Salmonella* pathogenicity island 1 (SPI-1) of *Salmonella enterica* and including systems from *Shigella* sp. (*mxil/spa*), *Escherichia coli* (*evilepa*) and *Burkholderia* sp. (*inv/spa*). Another major node is characterized by the *ysc* system, encoded on a common virulence plasmid of human pathogenic *Yersinia* sp., and includes systems found in *Pseudomonas aeruginosa* (*psc*), selected *Aeromonas* sp. (*asc*), *Photobacterium luminescens* (*lsc/sct*) and certain *Vibrio* sp. (*vsc*). Unique to this node are a number of genetically distinct T3SS components not represented in other nodes. Two examples of this are the components YscX and YscY.

The functional role of YscX and YscY in T3S remains enigmatic. In *Yersinia*, a mutant lacking either *yscX* or *yscY* allele poorly synthesizes Yop substrates and their secretion is abolished (Iriarte and Cornelis, 1999; Day and Plano, 2000; Bröms et al., 2005). Moreover, YscX is a T3SS substrate that prior to secretion is stabilized in the cytoplasm by the YscY chaperone (Iriarte and Cornelis, 1999; Day and Plano, 2000). Interestingly, an *in silico* analysis revealed that YscY possesses three tandem tetratricopeptide repeats (Pallen et al., 2003) that are important for function of the translocator class of T3S chaperones (Bröms et al., 2006; Edqvist et al., 2006; Buttner et al., 2008; Lunelli et al., 2009; Job et al., 2010; Singh et al., 2013; Kim et al., 2014). These studies taken together indicate that YscX could be a

structural component of the needle complex, while YscY would be necessary to stabilize pre-made pools of YscX and to ensure correct temporal YscX secretion. However, a recent study could find no support for YscX association with the needle, but rather together with YscY was found associated with YscV (alternatively known as LcrD), a core structural inner membrane component of all T3SSs (Diepold et al., 2012).

In a study of *P. aeruginosa* T3S, it was reported that the YscY homolog, Pcr4 (from here on termed PscY for consistency), is actually the secreted component, and not the YscX homolog, Pcr3 (here on termed PscX) (Yang et al., 2007). Despite this anomaly, the YscX/PscX and YscY/PscY components otherwise appear to serve somewhat analogous functions in their respective T3SSs (Bröms et al., 2005; Yang et al., 2007). Moreover, expression of *yscX* and *yscY* in the corresponding *P. aeruginosa* mutants can efficiently restore T3S (Bröms et al., 2005). Yet specific differences must exist since neither *pscX* nor *pscY* alone, or even when expressed in combination, could complement the T3S defects observed in *Yersinia* mutants lacking the corresponding alleles (Bröms et al., 2005). A known difference is the YscY interaction with the LcrH chaperone (also known as SycD) that has an undisclosed role in T3SS regulation in *Yersinia* (Francis et al., 2001; Bröms et al., 2005); the equivalent interaction between PscY and the PcrH chaperone in *P. aeruginosa* has not been detected (Bröms et al., 2003; Bröms et al., 2005). Moreover, it is not yet known whether PscX and PscY complex with PscV (the YscV homolog) as do the three equivalent *Yersinia* components (Diepold et al., 2012).

Hence, in this study we further investigated the notion that an YscX-YscY complex has evolved molecular attributes unique to T3SS function in *Yersinia*. We analyzed T3S from *Yersinia* *yscX* or *yscY* mutants ectopically expressing *in trans* homologous alleles from *Aeromonas salmonicida* and *A. hydrophila* (termed *ascX<sub>As</sub>/ascX<sub>Ah</sub>* and *ascY<sub>As</sub>/ascY<sub>Ah</sub>*), *P. luminescens* (termed *sctX* or *sctY*), *V. harveyi* and *V. parahaemolyticus* (termed *vscX<sub>Vh</sub>/vscX<sub>Vp</sub>* and *vscY<sub>Vh</sub>/vscY<sub>Vp</sub>*) or *P. aeruginosa* (PscX and PscY). No combination resulted in restoration of T3S, despite confirmation of reciprocal interactions giving rise to the equivalent of YscX-YscY bipartite and YscX-YscY-YscV tripartite complexes. This suggested that the YscX-YscY complex serves an exclusive T3SS function in *Yersinia*.

## MATERIALS AND METHODS

### Strains, Plasmids, and Growth Conditions

Bacterial strains and plasmids used in this study are listed in Table S1. Bacteria were routinely cultivated in Lysogeny broth (LB) (Bertani, 2004) or LB agar at either 26°C (*Yersinia pseudotuberculosis*) or 37°C (*E. coli*) with aeration. When required, the antibiotics carbenicillin (Cb), kanamycin (Km) and gentamicin (Gm) were added to laboratory culture media at the final concentrations of 100 µg per ml, 50 µg per ml and 20 µg per ml, respectively. Analysis of T3SS by *Y. pseudotuberculosis* occurred at 37°C in Brain Heart Infusion (BHI) broth. Media containing Ca<sup>2+</sup> ions was the non-inducing condition (BHI supplemented with 2.5 mM CaCl<sub>2</sub>), while media devoid of Ca<sup>2+</sup> ions was the inducing



condition (BHI supplemented with 20 mM MgCl<sub>2</sub> and 5 mM Ethylene glycol-bis-( $\beta$ -aminoethyl ether)-N,N,N',N'-tetraacetic acid). To stimulate promoter activity from the expression vectors pMMB67EHgm and/or pMMB208, isopropyl  $\beta$ -D-1-thiogalactopyranoside (IPTG) at a final concentration of 0.4 mM was added.

The *Saccharomyces cerevisiae* reporter strain AH109 or Y190 was maintained by growth at 30°C in YEP broth [2% (w/v) peptone, 1% (w/v) yeast extract, 2% (v/v) glucose] or agar [YEP broth with 2% (w/v) agar]. pGBKT7 derived plasmids were sustained in yeast by growth on SD synthetic minimal medium (0.67% (w/v) Yeast nitrogen base without amino acids, 300  $\mu$ gml<sup>-1</sup> L-isoleucine, 1.5 mgml<sup>-1</sup> L-valine, 200  $\mu$ gml<sup>-1</sup> L-adenine hemisulphate salt, 200  $\mu$ gml<sup>-1</sup> L-arginine HCl, 200  $\mu$ gml<sup>-1</sup> L-histidine HCl monohydrate, 1 mgml<sup>-1</sup> L-leucine, 300  $\mu$ gml<sup>-1</sup> L-lysine HCl, 200  $\mu$ gml<sup>-1</sup> L-methionine, 500  $\mu$ gml<sup>-1</sup> L-phenylalanine, 2 mgml<sup>-1</sup> L-threonine) while pBridge derived plasmids were grown on the same media minus methionine. Yeast containing pGADT7 derivatives were cultured on similar SD media with the exception that leucine was replaced with 200  $\mu$ gml<sup>-1</sup> L-tryptophan.

## PCR Amplification and Sequence Analysis

Amplified DNA fragments were obtained by PCR using the appropriate oligonucleotide combinations listed as online Supplementary Information (Table S2). These were synthesized by either DNA Technology A/S (Aarhus, Denmark), TAG Copenhagen A/S (Copenhagen, Denmark) or Sigma-Aldrich Sweden AB (Stockholm, Sweden). Amplified fragments were confirmed to be mutation free by first cloning into pCR<sup>®</sup>4-TOPO TA (Invitrogen AB, Stockholm, Sweden) or pTZ57R using the InsTAclone PCR cloning kit (Thermo Fisher Scientific, Gothenburg, Sweden) and then via commercial sequencing (Eurofins MWG Operon, Ebersberg, Germany or GATC Biotech AB, Solna, Sweden).

## Phylogenetic Analysis of YscX and YscY Protein Families

Protein sequences corresponding to YscX and YscY protein family were mined from National Center for Biotechnology Information (<https://www.ncbi.nlm.nih.gov/sites/entrez>) and phylogenetic trees obtained by the Neighbor-Joining method using MEGA6 (Molecular Evolutionary Genetics Analysis) (Tamura et al., 2013). Briefly, proteins were aligned by ClustalW using default settings and the unaligned regions and gaps were trimmed. The significance of the phylogenetic grouping was assessed using confidence level for 1,000 replicates. The trees were rooted with genetically related *Bordetella pertussis* 1475 YscX-like or YscY-like protein as the respective out-groups.

## Generation of Bacterial Protein Expression Constructs

Constructs containing the *yscX* and *yscY* alleles from *Y. pseudotuberculosis* and *pscX* and *pscY* alleles from *P. aeruginosa* have been described previously (Bröms et al., 2005). *ascX* and *ascY* were amplified from both *A. salmonicida* subsp. *salmonicida* JF2267 (a gift from Joachim Frey, Universität Bern,

Switzerland) and *A. hydrophila* AH-3 (Juan Tomás, Universidad de Barcelona, Spain). *yscX* and *yscY* were amplified from both *Vibrio harveyi* BB120 (Debra Milton, Umeå University, Sweden) and *V. parahaemolyticus* RIMD2210633 (Tetsuya Iida, Osaka University, Japan). Finally, *sctX* and *sctY* were amplified from *P. luminescens* TT01 (Rif<sup>R</sup>) (David Clarke, University of Bath, United Kingdom). For the complementation assay in *Y. pseudotuberculosis*, with one exception all alleles were cloned individually or together as a dual expression construct into *EcoRI*-*BamHI* digested pMMB67EHgm. (The *yscY* allele from *V. harveyi* was digested by *BamHI*-*PstI*.) To examine stable protein expression in *Y. pseudotuberculosis*, with two exceptions all PCR amplified alleles with a 5-prime FLAG<sup>TM</sup> epitope were cloned individually into *BamHI*-*EcoRI* digested pMMB208. (The *yscY* allele from *Y. pseudotuberculosis* and the *yscY* allele from *V. harveyi* was digested by *PstI*-*BamHI*.) The same approach was utilized to generate expression constructs of codon-optimized gene variants.

## Construction of Yeast Plasmids

To investigate reciprocal binding between the products of *yscY*, *yscX* and related alleles, a series of constructs were generated in the yeast two-hybrid vectors pGBKT7 and pGADT7 (Clontech Laboratories, Palo Alto, CA). Constructs expressing the *yscY* and *pscY* alleles fused to the GAL4 DNA binding domain in pGBKT7 are already described (Francis et al., 2001; Bröms et al., 2005). PCR amplified *ascY*, *yscY*, and *sctY* alleles were fused to the GAL4 DNA binding domain by cloning into *EcoRI*-*BamHI* digested pGBKT7. Plasmids expressing the *yscX* and *pscX* alleles fused to the GAL4 activation domain in pGADT7 are already established (Bröms et al., 2005). PCR amplified *ascX*, *yscX*, and *sctX* alleles were fused to the GAL4 activation domain by cloning into *EcoRI*-*BamHI* digested pGADT7.

Reciprocal interaction between YscX, YscY, YscV, and related family members were assessed with a yeast three hybrid approach by utilizing a three hybrid GAL4 DNA binding domain pBridge vector (Clontech Laboratories, Palo Alto, CA) and Gal4 activation domain pGADT7 vector. Constructs expressing *yscY* and related alleles were expressed as Gal4 DNA binding fusion protein by introducing into *EcoRI*-*PstI* digested pBridge downstream of *ADHI* promoter. Additionally, the coding sequences of *yscX* and related alleles were cloned into *NotI*-*BglII* sites of pBridge downstream of *MET25* promoter to finally yield pBridge-*yscY*-*yscX* and its variants. Likewise, *yscV* and related members were expressed as GAL4 activation fusion protein from pGADT7. While PCR-amplified *yscV*, *ascV* and *sctV* alleles were cloned into *EcoRI*-*XhoI* sites, PCR-amplified *pscV* and *yscV* were inserted into *NdeI*-*BamHI* sites of pGADT7.

## Yeast Transformation and the n-Hybrid Assays

For yeast two-hybrid assay, transformation of the *S. cerevisiae* reporter strain AH109 was performed as described earlier (Francis et al., 2000; Bröms et al., 2005; Amer et al., 2016). Protein interactions from multiple independent transformations were determined by measuring the activation of the *ADE2* reporter gene activation and the *HIS3* reporter gene during growth on



tryptophan and leucine minus SD synthetic minimal medium also lacking either adenine or histidine, respectively. The latter also required the addition of 4 mM 3-aminotriazole in the growth media to overcome any risk of false positives (James et al., 1996). Analysis of protein stability in yeast was performed as previously described (Francis et al., 2000).

The yeast three-hybrid assay was performed in *S. cerevisiae* reporter strain Y190 as described previously (Carlo et al., 2007; Glass et al., 2015). Briefly, yeast were co-transformed with pBridge and pGADT7-based vectors and a master plate established by initial growth at 30°C on SD synthetic minimal medium lacking leucine, tryptophan and methionine. The extent of protein interactions were then measured via the activation of the *HIS3* reporter gene upon growth on the above mentioned medium also lacking histidine, but supplemented with 40 mM 3-aminotriazole (3-AT) to neutralize the inherent leakiness of the reporter. Equal amount of colony from each of the transformants were resuspended in water and subjected to 5-fold serial dilutions. An aliquot of each serial dilution was then transferred onto two sets of plates: (1) master plate (SD -Leu, -Trp, -Met) and (2) selective plate (SD -Leu, -Trp, -Met, -His + 40 mM 3-AT). The growth of yeast on the selective plate indicated a positive interaction. As a control, 1 mM methionine was used for near complete repression of *MET25* repressible promoter (Her et al., 2003).

## Analysis of Gene Transcription by Qualitative RT-PCR

Total RNA was isolated from T3SS-induced *Yersinia* cultures as previously described (Carlsson et al., 2007a,b). Briefly, overnight cultures of *Yersinia* grown in a secretion permissive condition (BHI minus  $\text{Ca}^{2+}$ ) were diluted into 5 ml fresh media to an optical density (OD) at 600 nm of 0.1. After incubating at 26°C for 30 min, cultures were shifted to 37°C and grown for approximately 90 min to an OD at 600 nm of 0.4 to 0.8. RNA was immediately stabilized by mixing two volumes of RNA protect bacterial reagent (QIAGEN GmbH, Hilden, Germany) with one volume of the bacterial culture. Total RNA was isolated using the NucleoSpin RNA II method (Macherey Nagel, Düren, Germany) that included an on-column DNase treatment. For reverse transcription, 0.2 µg of total RNA was used to generate cDNA by RevertAid H Minus Reverse Transcriptase (RT) system (Thermo Scientific, Vilnius, Lithuania). RNA samples that were not treated with RT were used as negative controls to confirm the absence of contaminating DNA. PCR to confirm the presence of specific transcript was performed using gene-specific primers as listed in Table S2 and the cDNA generated above as template (Carlsson et al., 2007a,b).

Qualitative RT-PCR to determine the stability of mRNA transcript was performed as described elsewhere (Okan et al., 2006; Jeters et al., 2009; Chen and Anderson, 2011) with some modifications. Briefly, *Yersinia* cultures were grown in BHI media lacking  $\text{Ca}^{2+}$  at 37°C to an OD at 600 nm of 0.4 to 0.8. At time point zero, one volume of bacterial culture was removed and rifampicin to a final concentration of 100 µg/ml was added to the bacterial culture to inhibit *de novo* RNA synthesis. Thereafter,

one volume of bacterial cultures was taken at 5, 10, and 20 min time points. RNA was always stabilized by the addition of two volumes of RNA protect bacterial reagent (QIAGEN GmbH, Hilden, Germany). Isolation of total RNA, synthesis of cDNA and qualitative presence of transcript by PCR was performed as described above.

## Synthesis and Secretion of Type III-Secreted Substrates

Induction of type III substrate synthesis and secretion from *Y. pseudotuberculosis* was performed as previously described (Francis et al., 2000, 2001). All protein samples were normalized to the amount of bacterial cells at an optical density of 600 nm. Protein associated with whole bacteria was assessed by sampling from pelleted bacterial cultures. Total fraction contained proteins associated within intact bacteria and secreted to the culture medium. Sampling of the cell-free supernatant assessed the secreted protein levels. All protein fractions were separated by SDS-PAGE and subjected to immunoblotting. Detection of *Yersinia* substrates used rabbit polyclonal antisera raised against secreted YopE, YopD, and YopB (AgriSera AB, Vännäs, Sweden).

## Quantification of Protein Production in *Y. pseudotuberculosis*

Relative protein levels were quantified from protein bands on scanned western blot X-ray films using the gel analysis tool in ImageJ (Schneider et al., 2012). In every case, the lane profile plot area of each protein band of interest was normalized to the corresponding protein band appearing in the same lane in the loading control blot.

## RESULTS

### Amino Acid Identity Among the YscX and YscY Protein Families

*In silico* analysis has identified up to 9 core structural components in all T3SSs (Francis et al., 2004). Additional common components restricted to genetically related T3SS sub-families can also be found. A genetically related T3SS exists in the notable human and animal pathogens *Y. pestis*, *Yersinia enterocolitica*, *Y. pseudotuberculosis*, and *P. aeruginosa*, the marine pathogens *Aeromonas hydrophila*, *A. salmonicida*, *V. harveyi*, and *V. parahaemolyticus*, and the insect pathogen *P. luminescens*. Components common only to these systems include the YscX and YscY protein families. To ascertain genetic relatedness between representatives of the YscX and YscY protein families, amino acid sequences were retrieved from the sequenced genomes at <http://www.ncbi.nlm.nih.gov/sites/entrez> of the above mentioned bacteria and then aligned with ClustalW (<http://www.ebi.ac.uk/Tools/clustalw/index.html>). The evolutionary pattern was then examined by generating a phylogenetic tree rooted against the genetically related YscX-like and/or YscY-like protein from *B. pertussis* I475 by using the neighbor-joining method (Tamura et al., 2013; Bhattacharyya et al., 2017).

Based on amino acid sequence, the percent amino acid identity to YscX (122 aa) ranged from 54.1% over a 122 residue overlap (*A. salmonicida*) to 36.5% across a 126 residue overlap (*V. parahaemolyticus*) (Figure 1A). Apart from the near complete identity of YscX among the three *Yersinia* species, most relatedness occurred between the AscX proteins produced by the two *Aeromonas* species (~97% identical) and the VscX proteins produced by the two *Vibrio* species (~75%) (Figure 1A). Consistent with this, a phylogenetic tree analysis revealed that they each formed a separate clade distinct from other homologs (Figure 1C).

Similarly, amino acid sequence identity to YscY (114 aa) from *Yersinia* ranged between 52.6% (*A. hydrophila*) over a 116 residue overlap down to 32.5% (*V. harveyi*) over a 114 residue overlap (Figure 1B). Apart from the YscY proteins, the AscY proteins displayed most similarity to each other (~91% identical), followed by the VscY proteins (~68%), consistent with them forming separate phylogenetic clades (Figure 1D). In addition, the *P. luminescens* proteins SctX and SctY were most similar to the AscX and AscY counterparts from *Aeromonas* species (~63 and ~61%, respectively) (Figures 1A,B) and they all grouped close together on the phylogenetic tree (Figures 1C,D). Finally, among the three human pathogenic *Yersinia* species, YscY amino acid sequence was identical, whereas in YscX the amino acid glutamine at position 29 in both *Y. pseudotuberculosis* and *Y. pestis* existed as an aspartate residue in *Y. enterocolitica* (Figure S1). This subtle sequence divergence of YscX from *Y. enterocolitica* is reflected in the phylogenetic tree (Figure 1C).

In summary, this analysis reveals that YscX and YscY generally share most genetic relatedness with equivalent proteins from the two *Aeromonas* sp. Moreover, the YscX and YscY homologs that have diverged the most stem from the two *Vibrio* sp. This is in concordance with the phylogeny of non-flagella-T3SS of other core Ysc structural components (Troisfontaines and Cornelis, 2005; Romano et al., 2016).

## Reciprocal Chaperone-Substrate Interactions

A cornerstone of YscX and YscY function appears to be their ability to interact with each other (Day and Plano, 2000; Bröms et al., 2005), and this seems true also of PscX and PscY function in *P. aeruginosa* T3S (Bröms et al., 2005; Yang et al., 2007). The yeast two-hybrid system has proven to be a reliable tool to demonstrate reciprocal interactions of YscX/PscX with YscY/PscY (Francis et al., 2001; Bröms et al., 2005). Thus, we utilized this approach to examine the interaction reciprocity between the representative YscX and YscY family members detailed in Figure 1. The PCR amplified *yscX*-related alleles were all separately cloned into the pGADT7 vector to establish fusions to the C-terminus of the GAL4 activation domain (AD). Additionally, the PCR amplified *yscY*-related alleles were all individually cloned into the pGBKT7 vector to establish fusions to the C-terminus of the GAL4 DNA binding domain (BD). The various pair-wise combinations of vectors expressing a AD and BD fusion were established in *S. cerevisiae* AH109 containing an *ADE2* and *HIS3* reporter gene. Interactions between YscX-like and YscY-like proteins were determined by the ability of transformed yeast to grow on either minimal media lacking histidine (but

supplemented with 3-aminotriazole at a final concentration of 4 mM) or adenine. Interaction specificity was confirmed by the failure of a particular strain to grow on this same media after being cured of either the AD or BD expressing plasmid (data not shown). Reciprocal chaperone (YscY-like)-substrate (YscX-like) interactions could be observed for every possible combination (Figure 2, Figure S2). However, YscY-like variants derived from *Y. pseudotuberculosis*, *P. aeruginosa*, *Aeromonas* species, and *P. luminescens* all interacted better with YscX-like proteins also derived from these same bacteria. In contrast, these proteins consistently displayed weaker interactions with their more distantly related counterparts originating from *Vibrio* species (Figure 2, Figure S2). Importantly however, this was not a reflection of reduced protein expression, since cognate proteins derived from *V. harveyi* and *V. parahaemolyticus* demonstrated strong reciprocal binding with each other (Figure 2, Figure S2). Hence, reciprocal interactions between YscY- and YscX-like proteins are all generated in a yeast two-hybrid system. Conservation of these interactions is suggestive of a common functional requirement in T3S.

## Reciprocal Ternary Interactions Between YscX, YscY and the Inner Membrane Component YscV Indicate Formation of a Conserved Substrate Secretion Sorting Complex

Together YscX and YscY co-interact with YscV, a highly conserved T3SS component that makes up part of the inner membrane export apparatus (Diepold et al., 2012). This YscX-YscY-YscV tripartite complex helps to facilitate the temporal export of early T3S substrates (Diepold et al., 2012). We utilized the yeast three hybrid approach to verify that YscX and YscY together form a ternary complex with YscV (Figure 3). Y190 yeast competent cells were co-transformed with pBridge vector carrying PADH1-BD-YscY/pMET25-YscX and pGADT7 carrying PADH1-AD-YscV. Transformed yeast cells were grown on SD minimal medium lacking histidine (but supplemented with 40 mM 3-aminotriazole) either in the absence or presence of methionine as a means to control output from the leaky MET25 promoter (Carlo et al., 2007). Expression of *yscX* under the control of MET25 promoter can be repressed in the presence of 1 mM methionine and activated in methionine-free media. Based on the extent of yeast growth in the absence of methionine, we could verify the formation of a YscY-YscX-YscV complex (Figure 3, panel 7). Importantly, the interaction was comparatively diminished upon growing yeast transformants on media containing 1 mM methionine. As expected, YscX did not bind to YscV in the absence of YscY (unpublished data), nor did YscY bind to YscV in the absence of YscX (Figure 3, panel 5). Moreover, transformation of empty vectors, YscV or YscX-YscY alone did not permit auto-activation of *HIS3* reporter gene. These data demonstrated the suitability of the yeast three hybrid system for detecting the YscY-YscX-YscV interaction. Hence, we then tested if YscY-like, YscX-like, and YscV-like proteins from *P. aeruginosa*, *A. hydrophila*, *V. parahaemolyticus*, and *P. luminescens* have evolved to maintain the tripartite interaction with their specific counterparts. A significant amount

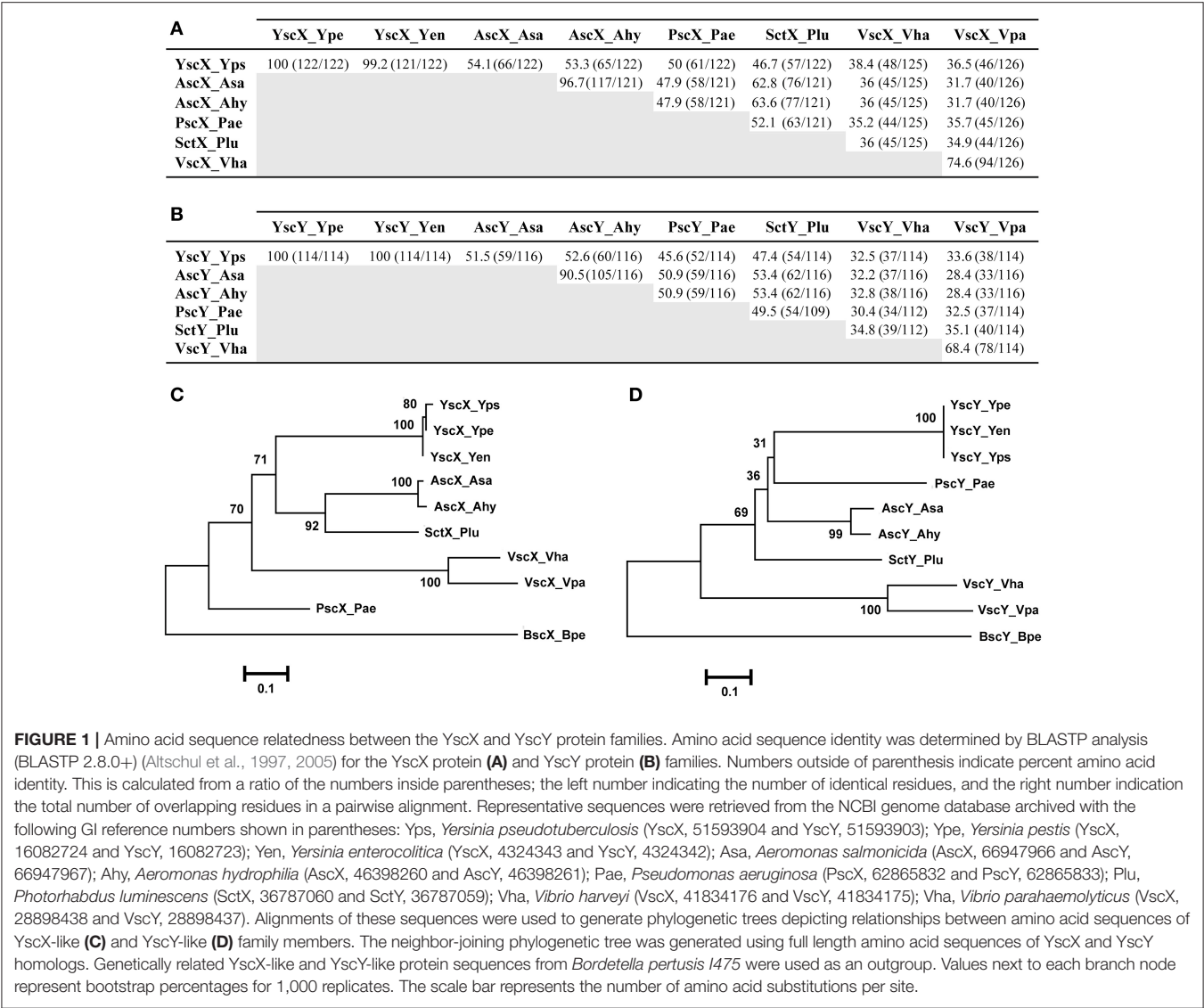


**FIGURE 1 |** Amino acid sequence relatedness between the YscX and YscY protein families. Amino acid sequence identity was determined by BLASTP analysis (BLASTP 2.8.0+) (Altschul et al., 1997, 2005) for the YscX protein (A) and YscY protein (B) families. Numbers outside of parenthesis indicate percent amino acid identity. This is calculated from a ratio of the numbers inside parentheses; the left number indicating the number of identical residues, and the right number indicating the total number of overlapping residues in a pairwise alignment. Representative sequences were retrieved from the NCBI genome database archived with the following GI reference numbers shown in parentheses: Yps, *Yersinia pseudotuberculosis* (YscX, 51593904 and YscY, 51593903); Ype, *Yersinia pestis* (YscX, 16082724 and YscY, 16082723); Yen, *Yersinia enterocolitica* (YscX, 4324343 and YscY, 4324342); Asa, *Aeromonas salmonicida* (AscX, 66947966 and AscY, 66947967); Ahy, *Aeromonas hydrophila* (AscX, 46398260 and AscY, 46398261); Pae, *Pseudomonas aeruginosa* (PscX, 62865832 and PscY, 62865833); Plu, *Photobacterium luminescens* (SctX, 36787060 and SctY, 36787059); Vha, *Vibrio harveyi* (VscX, 41834176 and VscY, 41834175); Vpa, *Vibrio parahaemolyticus* (VscX, 28898438 and VscY, 28898437). Alignments of these sequences were used to generate phylogenetic trees depicting relationships between amino acid sequences of YscX-like (C) and YscY-like (D) family members. The neighbor-joining phylogenetic tree was generated using full length amino acid sequences of YscX and YscY homologs. Genetically related YscX-like and YscY-like protein sequences from *Bordetella pertussis* I475 were used as an outgroup. Values next to each branch node represent bootstrap percentages for 1,000 replicates. The scale bar represents the number of amino acid substitutions per site.

of interaction between the cognate partners was evident in all YscY, YscX, YscV homologs tested (Figure 3, panel 16–19). Given the ability of YscY, YscX, and YscV homologs to maintain tripartite interactions, we then tested the possibility of reciprocal interactions involving the different combinations of family members. A reciprocal interaction between the members of ternary complex was observed in all combinations (Figure 3, panel 8–15). Thus, conservation of this interaction suggests that YscY-like, YscX-like, and YscV-like proteins have coevolved to perform a common T3S function, which is to facilitate the temporal export of early T3S substrates (Diepold et al., 2012).

**Production of YscX and YscY Is a Strict Requirement for T3SS Assembly and Function in *Y. pseudotuberculosis***

Next we asked whether members of the YscX and YscY protein families could restore T3S function to a respective  $\Delta yscX$  or

$\Delta yscY$  null mutant of *Y. pseudotuberculosis*. To achieve this, the various PCR-amplified *yscX*- and *yscY*-like alleles were cloned either separately or together under the control of an IPTG inducible promoter in the expression vector pMMB67EHgm and then conjugated into the appropriate *Y. pseudotuberculosis* background. Following standardization against bacterial cell number, the level of T3S substrates associated with the total bacteria (a mixture of proteins contained within intact bacteria and secreted to the culture supernatant) and secreted free into the culture media was examined from bacteria grown in both T3S restrictive (BHI plus  $Ca^{2+}$ ) and permissive (BHI minus  $Ca^{2+}$ ) conditions. Expectantly, YscX when expressed in a  $\Delta yscX$  null mutant (Figure 4A) and YscY when expressed in a  $\Delta yscY$  null mutant (Figure 4B) restored functional T3S in *Y. pseudotuberculosis*. Moreover, YscX derived from *Y. enterocolitica* could readily complement the T3S defect in the  $\Delta yscX$  null mutant (data not shown). Furthermore, dual expression of both YscX and YscY together in a  $\Delta yscX$ , *yscY*

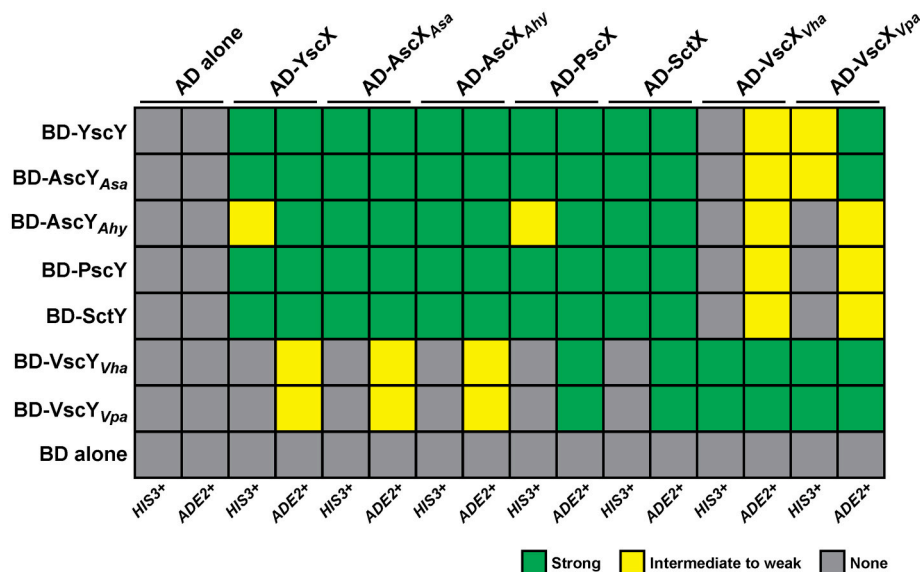


**FIGURE 2 |** Summary of the reciprocal binding between members of the YscX and YscY protein families. Protein–protein interactions were determined using the yeast two-hybrid assay. YscX family members were fused to the GAL4 activation domain (in pGADT7), whereas YscY family members were fused to the GAL4 DNA binding domain (in pGBKT7). Pairwise transformations were performed in *S. cerevisiae* AH109 (Clontech Laboratories) that contained the *HIS3* and *ADE2* reporter genes. Strength of interactions were determined by the extent of growth on minimal medium devoid of histidine or adenine and recorded after day 4. Green shade indicates robust yeast growth (strong binary interaction), yellow shade reflects modest growth (moderate interaction) and gray shade specifies no growth (no interaction). Due to an intrinsic leakiness with the *HIS3* reporter, 4 mM 3-aminotriazole was added to histidine dropout media to suppress false positives (James et al., 1996).

double mutant also restored functional T3S (Figure 5). On the other hand, no expressed YscX-like or YscY-like protein could restore functional T3S to a  $\Delta yscX$  null mutant (Figure 4A) or to a  $\Delta yscY$  null mutant (Figure 4B), respectively. Additionally, co-expression of the cognate substrate-chaperone pair did not help to restore T3S to a  $\Delta yscX$ ,  $yscY$  double mutant (Figure 5). These data are consistent with an earlier study which concluded that PscX and PscY from *P. aeruginosa* could not complement the Yop synthesis and secretion defect apparent in a *Y. pseudotuberculosis* mutant lacking the *yscX* and *yscY* alleles respectively (Bröms et al., 2005). Taken all together, these data suggest that YscX–YscY interplay has functional consequences unique to T3S by *Yersinia*.

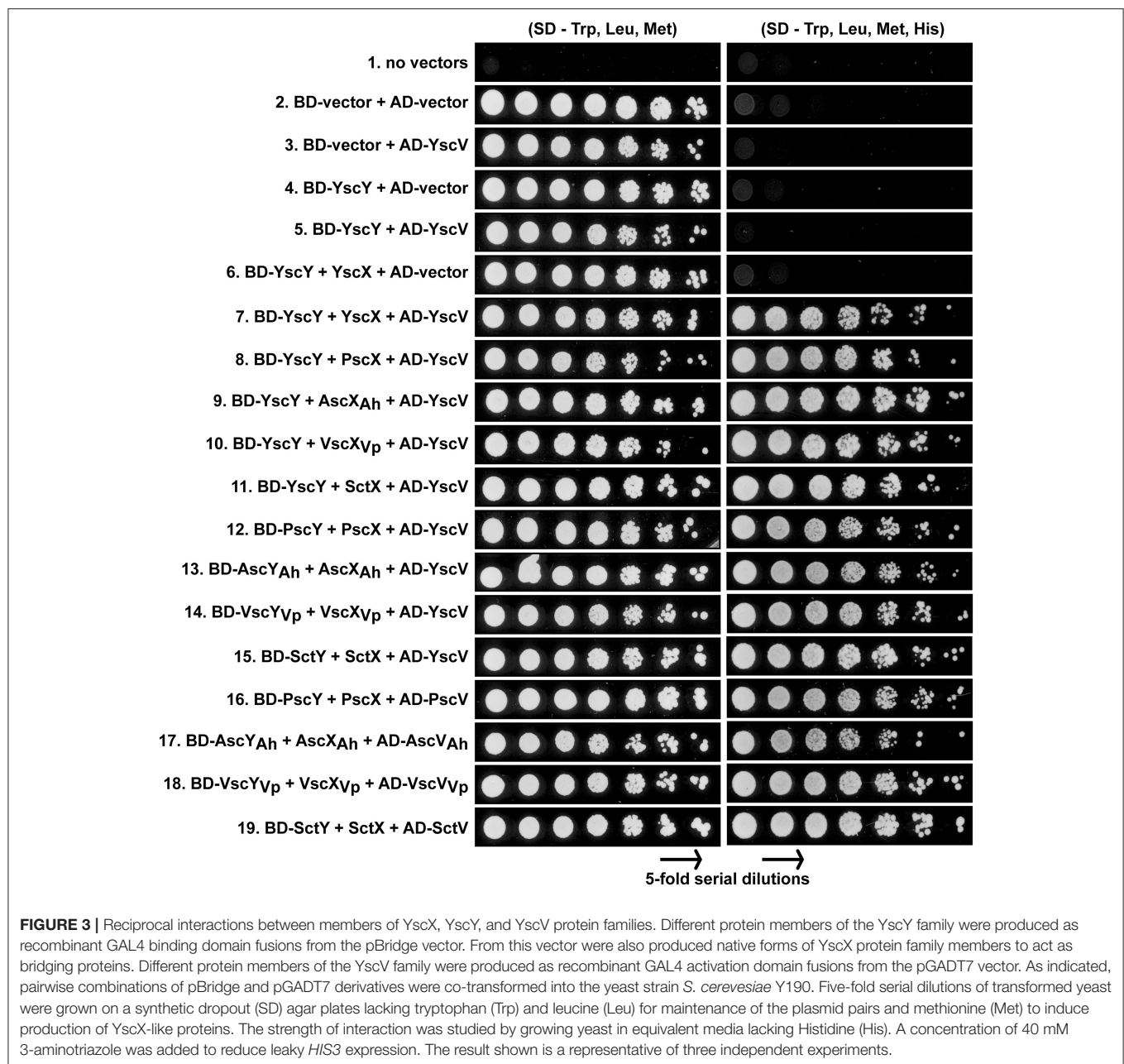
### Codon Optimization Fails to Improve the Complementation Efficiency of Non-endogenous *yscX*- and *yscY*-Like Alleles

Complementation may have failed because the non-cognate alleles were not sufficiently expressed. Due to the absence of available antibodies, production of YscX-like and YscY-like proteins in *Y. pseudotuberculosis* was assessed by appending an N-terminal FLAG<sup>TM</sup> epitope, followed by immunoblotting using an anti-FLAG<sup>TM</sup> monoclonal antibody. Accumulated levels of recombinant PscX, VscX<sub>Vp</sub>, SctX and to a much lesser extent VscX<sub>Vh</sub> could be detected (Figure S3A). Additionally, accumulated levels of recombinant PscY, VscX<sub>Vh</sub>, VscX<sub>Vp</sub>, and to a lesser extent SctY could be detected (Figure S3B). However, accumulated levels of all four recombinant Asc proteins were

undetectable under these assay conditions (Figure S3). A number of reasons could contribute to the wide disparity in heterologous protein production in *Yersinia*, although it can often be attributed to species-specific GC content and species-specific codon usage (Gustafsson et al., 2004; Yu et al., 2015; Zhou et al., 2016). Indeed, the percent GC content of the individual genomes targeted here do vary considerably—*Y. pseudotuberculosis* (47.6% GC content), *Aeromonas* sp. (61.6%), *P. aeruginosa* (66.6%), *Vibrio* sp. (45.4%), and *P. luminescens* (42.8%) (<http://archaea.ucsc.edu/>) (Schneider et al., 2006; Chan et al., 2012), and this variance can be assumed to tailor the codon usage within each individual allele that may be incompatible with optimal translation in *Y. pseudotuberculosis* (Gustafsson et al., 2004; Yu et al., 2015; Zhou et al., 2016).

Interestingly, an analysis of codon usage scores in the *yscX* and *yscY*-like gene families based on the codon adaption index (CAI) revealed the presence of codon usage biases of different genes (Figure S4). Hence, we synthesized commercially a series of synthetic alleles that were optimized for production in *Y. pseudotuberculosis* by actively considering (i) codon usage bias, (ii) GC content, and (iii) mRNA secondary structure. In all cases the decoded amino acid sequence remained identical to that encoded by the native gene sequences. In the optimized synthetic genes, the number of unfavorable codons was reduced by upgrading the CAI value to ~0.9 and by adjusting the GC content more closely resembling that of *Yersinia* (Figures S4, S5). Predicted mRNA secondary structure was not affected by optimization (data not shown). To assess protein production, we cloned both native and synthetically optimized gene sequences as N-terminal FLAG<sup>TM</sup>-tagged variants into pMMB208 vector





under the control of an IPTG-inducible promoter. Following introduction into *Y. pseudotuberculosis* and subsequent growth in BHI minus  $\text{Ca}^{2+}$ , bacterial pellets standardized against bacterial cell number were examined for accumulation of FLAG<sup>TM</sup>-tagged protein. Except for the SctX and VscY<sub>Vh</sub> variants, codon optimization led to improved production of all the YscX-like and YscY-like variants with accumulated levels ranging between 1.3- and 7.0-fold more abundant than their native (non-optimized) counterparts (Figure S6). Interestingly, despite the successful efforts to codon optimize, accumulated levels of some recombinant proteins such as those originally derived from *Aeromonas* sp. still failed to reach a level close to that achieved for the native *Yersinia* proteins (Figure 6).

Significantly, this low level protein production was not due to an inferior transcriptional output because accumulated mRNA levels transcribed from all *yscX*-like (Figure S7A) and *yscY*-like (Figure S7B) genes was similar, which is consistent with transcription being driven by an identical promoter and transcriptional start site architecture in every case. Furthermore, the stability of accumulated *ascX* mRNA transcripts (Figure S7C) and *ascY* mRNA transcripts (Figure S7D) was equivalent to *yscX* and *yscY* mRNA transcripts. Thus, additional hitherto unknown regulatory elements must be limiting AscX and AscY production in *Y. pseudotuberculosis*.

Nevertheless, given that in most cases elevated production arose from codon optimization, we assessed if these codon



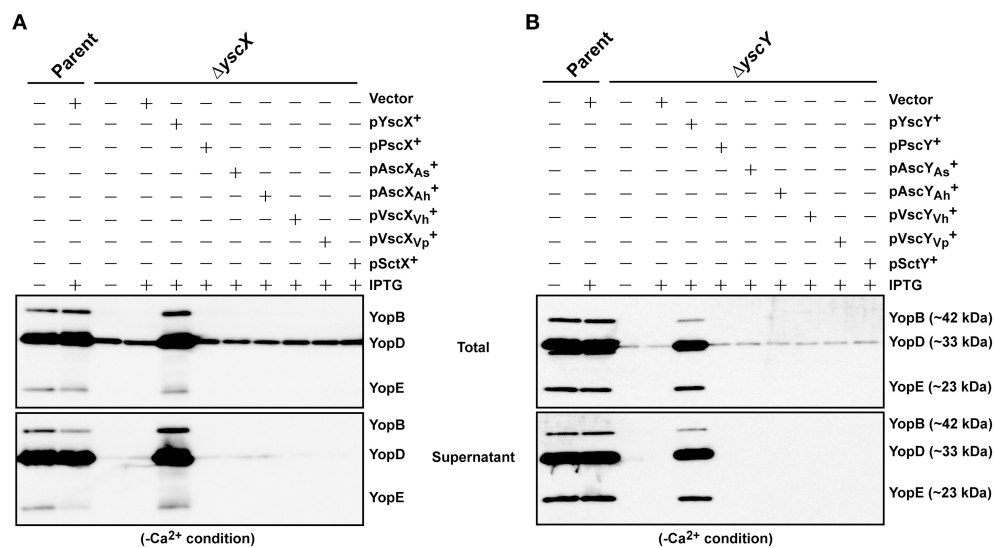


**FIGURE 4 |** Assessing complementation of YscX and/or YscY function in *Yersinia* type III secretion. Bacteria were grown in BHI medium under secretion-permissive conditions (absence of Ca<sup>2+</sup>). Proteins contained within intact bacteria and secreted to the culture medium (Total) or secreted free to the extracellular medium (Supernatant) were fractionated on a 12% SDS-PAGE and analyzed by immunoblotting using polyclonal rabbit anti-YopB, anti-YopD and anti-YopE antiserum. IPTG was added to a final concentration of 0.4 mM where indicated. **(A)** Parent *Y. pseudotuberculosis* and  $\Delta yscX$  complemented with pMMB67EHgm or pMMB67EHgm-encoded YscX family members. Strains: Parent (YP111/p1B102); Complemented YP111/p1B102, pMMB67EHgm (Vector);  $\Delta yscX$  (YP111/p1B880); complemented YP111/p1B880, pMMB67EHgm (Vector); complemented YP111/p1B880, pJEB291 (YscX<sup>+</sup>); complemented YP111/p1B880, pJEB295 (PscX<sup>+</sup>); complemented YP111/p1B880, pMF720 (AscX<sub>As</sub><sup>+</sup>); complemented YP111/p1B880, pMF722 (AscX<sub>Ah</sub><sup>+</sup>); complemented YP111/p1B880, pMF724 (VscX<sub>Vh</sub><sup>+</sup>); complemented YP111/p1B880, pMF725 (VscX<sub>Vp</sub><sup>+</sup>); complemented YP111/p1B880, pMF727 (SctX<sup>+</sup>). **(B)** Parent *Y. pseudotuberculosis* and  $\Delta yscY$  complemented with pMMB67EHgm or pMMB67EHgm-encoded YscY family members. Strains: Parent (YP111/p1B102);  $\Delta yscY$  (YP111/p1B890); complemented YP111/p1B890, pMMB67EHgm (Vector); complemented YP111/p1B890, pJEB292 (YscY<sup>+</sup>); complemented YP111/p1B890, pJEB296 (PscY<sup>+</sup>); complemented YP111/p1B890, pMF721 (AscY<sub>As</sub><sup>+</sup>); complemented YP111/p1B890, pMF723 (AscY<sub>Ah</sub><sup>+</sup>); complemented YP111/p1B890, pMF796 (VscY<sub>Vh</sub><sup>+</sup>); complemented YP111/p1B890, pMF726 (VscY<sub>Vp</sub><sup>+</sup>); complemented YP111/p1B890, pMF728 (SctY<sup>+</sup>). Molecular mass values shown in parentheses were deduced from primary amino acid sequences.

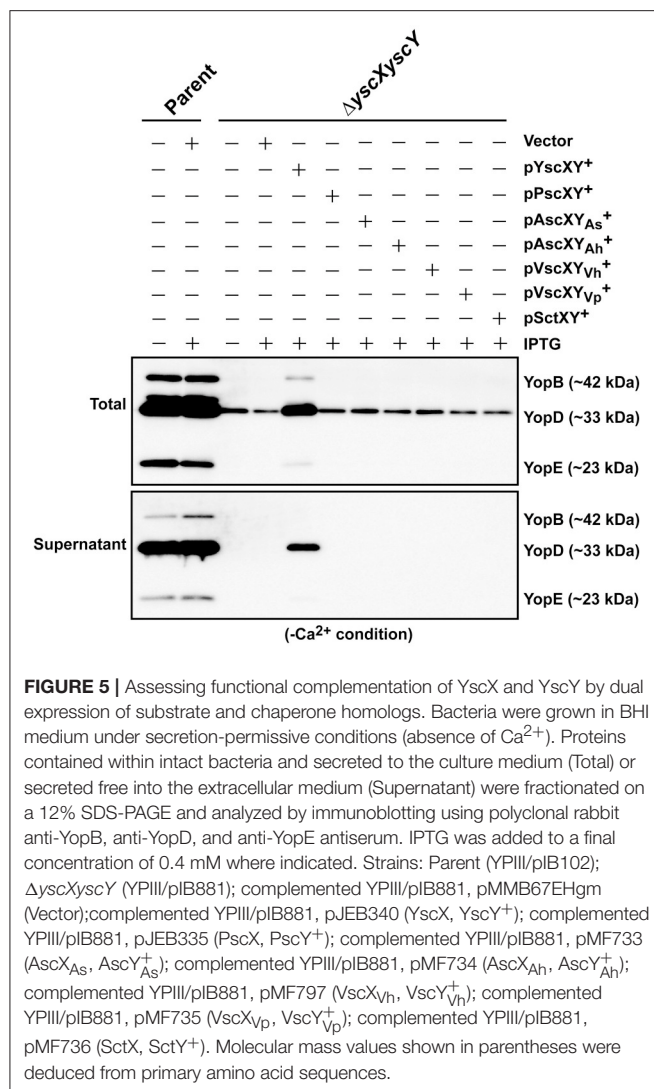
optimized YscX-like and YscY-like protein variants could restore T3S to the  $\Delta yscX$  null mutant and  $\Delta yscY$  null-mutant, respectively. The optimized *yscX*-like and *yscY*-like genes were cloned individually into pMMB67EHgm and Yops production associated with total bacterial culture and Yops secretion associated with bacterial supernatants were monitored in secretion permissive growth conditions. Once again however, Yops production and secretion could be restored only when the  $\Delta yscX$  null mutant was complemented with native YscX protein (**Figure 6A**) and  $\Delta yscY$  null mutant with native YscY protein (**Figure 6B**).

To be sure that all other codon-optimized homologs were sufficiently produced to permit complementation, we compared these levels to the minimal amount of YscX and YscY sufficient to restore T3S to the  $\Delta yscX$  and  $\Delta yscY$  null mutants respectively. Critically, an undetectable amount of native YscX and YscY ectopically produced during growth in the presence of 0.02 mM of IPTG was already sufficient to restore high capacity T3S to the  $\Delta yscX$  null mutant (**Figure 6C**) and  $\Delta yscY$  null mutant (**Figure 6D**), respectively. These levels were quite noticeably much less than accumulated amounts detected for all of the non-complementing YscX-like (**Figure 6E**) and YscY-like (**Figure 6F**) variants when bacteria were grown in the presence of 0.4 mM IPTG. From this data we infer that insufficient expression of non-native YscX- and YscY-like

family members cannot explain their inability to function in *Y. pseudotuberculosis*.

## Codon Optimized Alleles Do Not Suppress a Functional *Yersinia* T3SS

Despite the YscX- and YscY-like homologs being unable to substitute for the respective loss of *yscX* or *yscY* in *Y. pseudotuberculosis*, we still wondered if they possess any activity at all when expressed in *Y. pseudotuberculosis*. To assess this, we examined for the ability of produced homologs to exert a dominant negative effect on *Yersinia* T3SS. All of the codon-optimized homologs of YscX and YscY under control of the IPTG inducible promoter of pMMB67EHgm were introduced in parental *Y. pseudotuberculosis* harboring an intact and fully functional T3SS. Firstly, we examined the protein expression profile of YscX and YscY family members in parental *Yersinia* background and found them to be comparable to what we had previously observed in the knockout strain backgrounds (data not shown). We then assessed the impact of this production on T3SS function as measured by Yops production and secretion. Significantly, neither the production of codon-optimized YscX-like (**Figure 7A**) nor YscY-like (**Figure 7B**) homologs interfered with T3SS activity by parental bacteria. The complete absence of any dominant negative effect implies that none of the YscX-like or YscY-like proteins are recognized by the *Yersinia* T3SS,



which underscores that these proteins are truly non-functional in *Yersinia* bacteria. Taken altogether, our data indicates that an undisclosed feature(s) inherent in the native YscX and YscY products is necessary for proper T3S function in *Yersinia*, and one or more of these features cannot be substituted for by a genetically related gene from another bacterial source.

## DISCUSSION

On the basis that a number of core T3SS basal body components associated with bacterial inner and outer membranes are highly conserved, these have been the focus of studies to establish at least eight phylogenetically distinct T3SS sub-families among sequenced bacteria (Troisfontaines and Cornelis, 2005; Abby and Rocha, 2012). In addition, there exist critical components that are present only in a restricted T3SS sub-family. For example, the poorly studied proteins YscX and YscY exist only in the Ysc T3SS sub-family, and the prototype of this family is the

plasmid encoded Ysc-Yop system of human pathogenic species of *Yersinia*. In this study, we have reported on the evolutionary conservation among the YscX and YscY protein families. We also explored their function in two ways. The first approach examined the binary interactions between all YscX-like and YscY-like family members, and the ability of this YscX-YscY complex to interact with the core basal body component YscV. The second approach examined the ability of all YscX-like and YscY-like family members to complement a type III secretion defect in *Y. pseudotuberculosis* brought about by a deletion of *yscX* and/or *yscY*. Our focus was on six different homologs sourced from *P. aeruginosa*, *A. hydrophila*, *A. salmonicida*, *V. harveyi*, *V. parahaemolyticus* and *P. luminescens*. Despite showing robust and interchangeable binary YscX-YscY interactions and ternary YscX-YscY-YscV interactions, none of the homologs could restore T3S to *Y. pseudotuberculosis* lacking functional YscX and/or YscY. Thus, it seems that this YscX-YscY-YscV system is functionally conserved in Ysc-like T3SSs, but that each set exhibits functional specificity to assemble their own apparatus, and this could include recognition of their own set of substrates.

Events allowing YscX to form stable complexes with the known cognate chaperone YscY, and for the YscX-YscY complex to interact with the core T3SS structural component YscV, are considered to constitute integral elements of T3SS assembly and function (Day and Plano, 2000; Diepold et al., 2012). Our n-hybrid analyses suggests that these interactions are a key attribute of all YscX-like, YscY-like and YscV-like homologs, serving an important T3SS assembly function that is evolutionarily conserved. In fact, the need to form a bipartite and a tripartite interaction is most likely an ancient role of these protein families, and maybe the reason why YscX and YscY could functionally substitute for the absence of PscX and PscY in mutants of *P. aeruginosa* (Bröms et al., 2005). However, merely having the ability to establish these known reciprocal interactions was clearly not enough to permit any of the homologs to mediate functional exchange in *Y. pseudotuberculosis*. Indeed this suggests that both YscX and YscY possess other molecular targets that are arguably unique to Ysc-Yop T3SS function. An approach to identify these putative targets within soluble bacterial lysate or solubilized bacterial membrane fractions would be to combine pull down technology using the Flag-YscX or Flag-YscY as a bait with mass spectroscopy detection. We can only assume that this need for additional molecular interactions arose as a consequence of *Yersinia* evolving the ability to thrive in a particular ecological niche. This notion is consistent with previous findings that correlate a diversification of bacterial T3SSs with known bacterial-host interactions (Abby and Rocha, 2012).

Sequence alignments revealed several obvious regions of uniqueness within the YscX and YscY amino acid sequence, respectively. At first glance, these are too numerous to perform targeted mutagenesis to screen for loss-of-function in the *Yersinia* proteins or gain-of-function in the heterologous proteins. Hence, we are now attempting to first map potentially critical functional domains unique to YscX and YscY, prior to embarking on a site-directed mutagenesis strategy. A series of chimeric alleles between *yscX* and *yscX*-like homologs as well as

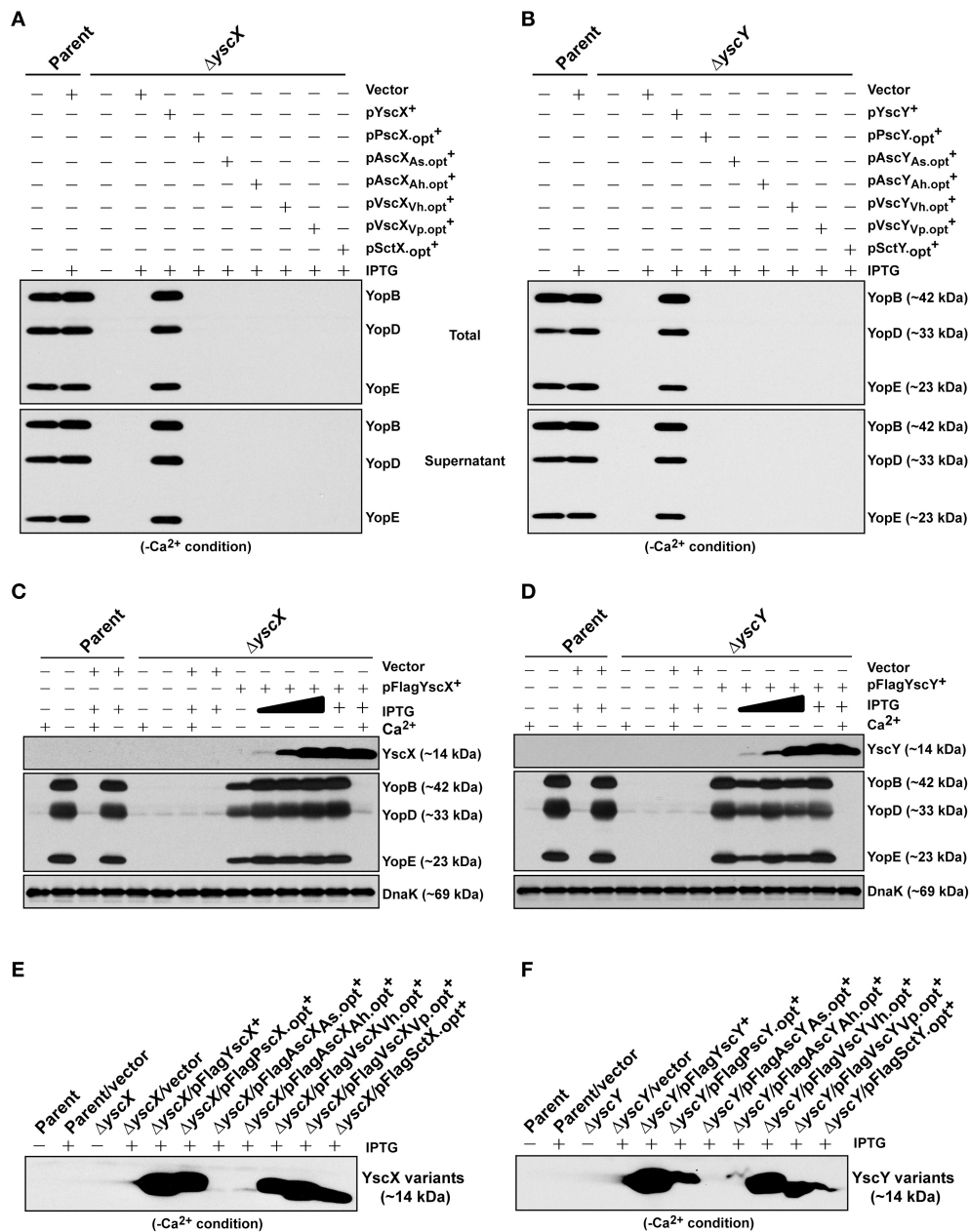


**FIGURE 6 |** Assessing functional complementation by codon-optimized *yscX*- and *yscY*-like alleles. Synthesized Yop's associated with total fractions (proteins contained within intact bacteria and secreted to the culture medium) or with supernatant (secreted free to the extracellular medium) were analyzed in  $\Delta yscX$  null-mutant complemented with YscX and codon-optimized YscX-like protein family members (**A**) or in  $\Delta yscY$  null-mutant complemented with YscY and codon-optimized YscY-like protein family (**B**). Polyclonal anti-YopB, anti-YopD and anti-YopE were used for detection of Yops. The “+” symbol indicates the addition of IPTG to a final concentration of 0.4 mM. Proteins associated with bacterial pellet from *Y. pseudotuberculosis* cultures harboring either pFLAG-YscX (**C**) or pFLAG-YscY (**D**) grown in secretion-permissive condition (absence of Ca<sup>2+</sup>) and supplemented with increasing concentration of IPTG were analyzed by Western immunoblot using anti-FLAG<sup>TM</sup>, anti-YopB, anti-YopD, anti-YopE, and anti-DnaK. The “-” symbol indicates absence of a particular component, while the “+” symbol indicates the presence of a particular component. In the case of IPTG, the “+” symbol indicates a final concentration of 0.4 mM IPTG was added, while the filled in graduation symbol reflects an incremental increase of IPTG according to the following final concentrations of 0.01, 0.02, and 0.1 mM. Steady state accumulation in the bacterial pellet of YscX protein family (**E**) and YscY protein family (**F**) produced from codon-optimized alleles following growth of *Y. pseudotuberculosis* in secretion-permissive conditions (absence of Ca<sup>2+</sup>). Protein was fractionated by SDS-PAGE and detected by immunoblot using monoclonal anti-FLAG<sup>TM</sup> antiserum. The “-” symbol indicates bacterial growth in the absence of IPTG, while “+” symbol indicates a final concentration of 0.4 mM was added. Strains: Parent (YPIII/pIB102); Complemented YPIII/pIB102, pMMB208 (Vector);  $\Delta yscX$  (YPIII/pIB880); complemented YPIII/pIB880, pMMB208 (Vector); complemented YPIII/pIB880, pJMG242 (FLAG<sup>TM</sup>-YscX<sup>+</sup>); complemented YPIII/pIB880, pJMG261 (FLAG<sup>TM</sup>-PscX<sub>opt</sub><sup>+</sup>); complemented YPIII/pIB880, pJMG262 (FLAG<sup>TM</sup>-AscX<sub>As, opt</sub><sup>+</sup>); complemented YPIII/pIB880, pJMG263 (FLAG<sup>TM</sup>-AscX<sub>Ah, opt</sub><sup>+</sup>); complemented YPIII/pIB880, pJMG264 (FLAG<sup>TM</sup>-VscX<sub>Vh, opt</sub><sup>+</sup>); complemented YPIII/pIB880, pJMG265 (FLAG<sup>TM</sup>-VscX<sub>Vp, opt</sub><sup>+</sup>); complemented YPIII/pIB880, pJMG266 (FLAG<sup>TM</sup>-SctX<sub>opt</sub><sup>+</sup>).

(Continued)





YscY (Francis et al., 2001; Bröms et al., 2005). Thus, LcrH-YscY complex formation is likely to feed into the post-transcriptionally active complex of YopD, LcrH, and *yop* mRNA with the sole purpose to further fine-tune temporal and spatial control of substrate secretion. It is not anticipated to assist in assembly of a secretion-competent apparatus *per se*. On this basis, we do not believe that the specificity of LcrH-YscY interaction in *Yersinia* is the reason why heterologous protein expression cannot support T3S. Hence, we will continue to pursue evidence for a unique non-reciprocal interaction involving YscX and YscY that is essential for the physical assembly of the Ysc-Yop T3SS, rather than one involved in substrate secretion control.

Through sequence alignments we did observe that only native YscX contained two cysteine residues in codon positions that were absolutely conserved. At this stage we do not know if these cysteine residues are reduced or participate in inter- or intra-disulfide bond formation. If they do participate in disulfide bond formation, this would be a unique feature of native YscX, and gives a reason as to why heterologous YscX-like proteins that lack these two conserved cysteines are not functional in *Yersinia*. It is well-established that disulfide bonds are an important structural element of the secretome of bacterial pathogens (De Geyter et al., 2016; Bocian-Ostrzycka et al., 2017). This is true also for human pathogenic *Yersinia* sp., where a role for thiol bonding is reported for the Ysc-Yop T3SS, the Caf1 chaperone-usher system, and the invasin autotransporter (Leong et al., 1993; Zav'yalov et al., 1997; Jackson and Plano, 1999; Mitchell et al., 2017). Thus, a logical next step is to use site-directed mutagenesis to investigate possible inter- or intra-disulfide bond formation in YscX.

Following completion of the needle assembly in *Y. enterocolitica*, YscX secretion into the extracellular milieu occurs (Diepold et al., 2012). However, the purpose of YscX secretion is enigmatic. Our ongoing studies have so far revealed that secretion of YscX is absolutely required for a functional T3SS in *Y. pseudotuberculosis* (unpublished data). One reason for YscX secretion might be to free up a complex of YscY-YscV to recognize and secrete other later subsets of T3S substrates, namely the translocators that are necessary to trigger the next stage of injectisome assembly and the host-modulating effectors that are injected into eukaryotic cells (Dewoody et al., 2013). In parallel, secreted YscX might comprise a minor component of the external needle, although experimental evidence to support this is completely lacking. Alternatively, secreted YscX may comprise a structural component within the needle assembly platform, such as via a cooperation with the YscI inner rod. Hence, to understand the role of YscX secretion in T3SS function is important. This pursuit is made all the more intriguing on the basis that PscY is the secreted component of the T3SS of *P. aeruginosa*, not PscX as one may have expected (Yang et al., 2007).

Given that all indicators point to the fact that YscX secretion is essential for T3SS function in *Yersinia*, it follows that a functional requirement for complementation of the  $\Delta yscX$  deletion mutant would likely be secretion of the corresponding YscX-like homologs. Taking account of the already stated PscY secretion exception (Yang et al., 2007), we are aware of only one other YscX-like homolog that has been proven experimentally to be a

T3SS substrate—the AscX substrate of *A. salmonicida* (Vanden Bergh et al., 2013). We attempted to examine secretion of all YscX-like proteins by parental *Y. pseudotuberculosis* containing a fully functional Ysc-Yop T3SS. However, this was complicated by the need to produce all YscX-like variants as a FLAG<sup>TM</sup> fusion to facilitate their immune-detection, for this tag may impact on fusion protein secretion efficiency. Indeed, the amount of FLAG<sup>TM</sup>-YscX secreted was only a fraction of the amount that was produced (data not shown). Furthermore, we could not corroborate the findings of Vanden Bergh et al. (2013), for the yields of AscX were routinely too low to assess its secretion. Consistent with this, most other FLAG<sup>TM</sup>-tagged variants were not even detected in the secretion fraction, including PscX that is not a T3S substrate (Yang et al., 2007) (data not shown). The exception to this was the observation that FLAG<sup>TM</sup>-YscX<sub>Vp</sub> and FLAG<sup>TM</sup>-SctX were active substrates of a fully intact Ysc-T3SS of *Y. pseudotuberculosis* (data not shown). Hence, at present we cannot establish a clear correlation between lack of secretion and lack of functional complementation.

One final observation of interest stemming from this study concerned the poor production of the two AscX proteins and the two AscY proteins in the *Y. pseudotuberculosis* background. This occurred despite (1) YscX and AscX as well as YscY and AscY sharing a sequence identity above the 50 percentile, (2) an abundance of comparatively stable mRNA being initiated from an identical promoter used to support the expression of all other genes studied in this report, and (3) the use of synthetic genes that had been codon optimized to maximize efficient translation in *Y. pseudotuberculosis*. Hence, some hitherto unknown phenomenon is responsible for the lack of heterologous production of these proteins in *Yersinia*. A straightforward reason for this is that they are normally stabilized by species-specific protein-protein interactions. The YscY chaperone is thought to function as an YscX stabilizer (Iriarte and Cornelis, 1999; Day and Plano, 2000). Indeed, this motivated the dual expression complementation experiment performed in this study. However, co-expression of AscX with cognate AscY did not increase the production of either protein. A conclusion from this work is that AscY alone is probably insufficient for AscX stabilization, meaning that the complex of AscX-AscY requires stabilizing influence from additional protein-protein interactions not supported by expression in a heterologous host like *Yersinia*. Another reason for poor AscX and AscY yield could also be that some aspect of mRNA sequence and/or structure defined by the *ascX* and *ascY* open reading frames influences that rate of their translation in *Yersinia*. As a means to pin-point the reason for low yield, we are currently analyzing allelic chimeras between *ascX* and *yscX* as well as *ascY* and *yscY*. This approach has the possibility to locate the genetic regions in AscX and AscY that are either (1) the interface for species-specific protein-protein interactions that are necessary for protein stability, or (2) the site of novel posttranscriptional control mechanisms that have potential to influence the spatial and temporal control of T3SS.

In summary, on the basis of complementation assays measuring the capacity for *in vitro* synthesis and secretion of Yops, it appears that the function of native YscX and

YscY is evolutionary optimized to contribute unique and essential information for the physical assembly of the Ysc-Yop T3SS by pathogenic *Yersinia* sp. Thus, the challenge that lies ahead is to define the function of both YscX and YscY, and to decipher whether this function requires the recruitment of additional molecular components. In contrast, from this work we now know that the established bipartite YscX-YscY interaction and the tripartite YscX-YscY-YscV interaction is not a unique feature restricted only to native components of *Yersinia*. Rather, these interactions are preserved among all heterologous YscX-like and YscY-like family members, and this probably reflects an ancient and evolutionarily conserved universal function of these proteins.

## AUTHOR CONTRIBUTIONS

JG, AA, MKF, TC, and MSF conceived and planned the experiments. SC and MSF contributed essential materials. JG, AA, MKF, and TC carried out the experiments and contributed to sample preparation. JG, AA, MKF, TC, SC, AZ, and MSF contributed to the interpretation of the results. JG and MSF took the lead in writing the manuscript. All authors provided critical feedback and helped shape the research, analysis, and manuscript.

## REFERENCES

- Abby, S. S., and Rocha, E. P. (2012). The non-flagellar type III secretion system evolved from the bacterial flagellum and diversified into host-cell adapted systems. *PLoS Genet.* 8:e1002983. doi: 10.1371/journal.pgen.1002983
- Altschul, S. F., Madden, T. L., Schaffer, A. A., Zhang, J., Zhang, Z., Miller, W., et al. (1997). Gapped BLAST and PSI-BLAST: a new generation of protein database search programs. *Nucleic Acids Res.* 25, 3389–3402. doi: 10.1093/nar/25.17.3389
- Altschul, S. F., Wootton, J. C., Gertz, E. M., Agarwala, R., Morgulis, A., Schaffer, A. A., et al. (2005). Protein database searches using compositionally adjusted substitution matrices. *FEBS J.* 272, 5101–5109. doi: 10.1111/j.1742-4658.2005.04945.x
- Amer, A. A., Gurung, J. M., Costa, T. R., Ruuth, K., Zavialov, A. V., Forsberg, A., et al. (2016). YopN and TyeA hydrophobic contacts required for regulating Ysc-Yop Type III secretion activity by *Yersinia pseudotuberculosis*. *Front. Cell. Infect. Microbiol.* 6:66. doi: 10.3389/fcimb.2016.00066
- Anderson, D. M., Ramamurthi, K. S., Tam, C., and Schneewind, O. (2002). YopD and LcrH regulate expression of *Yersinia enterocolitica* YopQ by a posttranscriptional mechanism and bind to yopQ RNA. *J. Bacteriol.* 184, 1287–1295. doi: 10.1128/JB.184.5.1287-1295.2002
- Bertani, G. (2004). Lysogeny at mid-twentieth century: P1, P2, and other experimental systems. *J. Bacteriol.* 186, 595–600. doi: 10.1128/JB.186.3.595-600.2004
- Bhattacharyya, C., Bakshi, U., Mallick, I., Mukherji, S., Bera, B., and Ghosh, A. (2017). Genome-guided insights into the plant growth promotion capabilities of the physiologically versatile *Bacillus aryabhata* strain AB211. *Front. Microbiol.* 8:411. doi: 10.3389/fmicb.2017.00411
- Blocker, A., Gounon, P., Larquet, E., Niebuhr, K., Cabiaux, V., Parsot, C., et al. (1999). The tripartite type III secretion of *Shigella flexneri* inserts IpaB and IpaC into host membranes. *J. Cell Biol.* 147, 683–693. doi: 10.1083/jcb.147.3.683
- Blocker, A., Jouihri, N., Larquet, E., Gounon, P., Ebel, F., Parsot, C., et al. (2001). Structure and composition of the *Shigella flexneri* “needle complex”, a part of its type III secretion. *Mol. Microbiol.* 39, 652–663. doi: 10.1046/j.1365-2958.2001.02200.x

## FUNDING

This work has been supported by grants from the Swedish Research Council (2009-5628 and 2014-2105), the Foundation for Medical Research at Umeå University and the Faculty of Science and Technology at Umeå University.

## ACKNOWLEDGMENTS

This work was performed within the framework of the Umeå Centre for Microbial Research at Umeå University. We appreciate the contributions made by undergraduate students of the Umeå University Life science and Biomedicine programs. Andreas Diepold is acknowledged for valuable discussion surrounding YscX and YscY function. We express gratitude to Hans Wolf-Watz for antibodies to YopE, YopD, and YopB. We are also grateful to Joachim Frey, Juan Tomás, Debra Milton, Tetsuya Iida, and David Clarke for the gift of strains and/or chromosomal DNA.

## SUPPLEMENTARY MATERIAL

The Supplementary Material for this article can be found online at: <https://www.frontiersin.org/articles/10.3389/fcimb.2018.00080/full#supplementary-material>

- Bocian-Ostrzycka, K. M., Grzeszczuk, M. J., Banas, A. M., and Jagusztyn-Krynicka, E. K. (2017). Bacterial thiol oxidoreductases - from basic research to new antibacterial strategies. *Appl. Microbiol. Biotechnol.* 101, 3977–3989. doi: 10.1007/s00253-017-8291-8
- Bröms, J. E., Edqvist, P. J., Carlsson, K. E., Forsberg, Å., and Francis, M. S. (2005). Mapping of a YscY binding domain within the LcrH chaperone that is required for regulation of *Yersinia* type III secretion. *J. Bacteriol.* 187, 7738–7752. doi: 10.1128/JB.187.22.7738-7752.2005
- Bröms, J. E., Edqvist, P. J., Forsberg, Å., and Francis, M. S. (2006). Tetratricopeptide repeats are essential for PcrH chaperone function in *Pseudomonas aeruginosa* type III secretion. *FEMS Microbiol. Lett.* 256, 57–66. doi: 10.1111/j.1574-6968.2005.00099.x
- Broms, J. E., Forslund, A. L., Forsberg, A., and Francis, M. S. (2003). PcrH of *Pseudomonas aeruginosa* is essential for secretion and assembly of the type III translocon. *J. Infect. Dis.* 188, 1909–1921. doi: 10.1086/379898
- Buttner, C. R., Sorg, I., Cornelis, G. R., Heinz, D. W., and Niemann, H. H. (2008). Structure of the *Yersinia enterocolitica* type III secretion translocator chaperone SycD. *J. Mol. Biol.* 375, 997–1012. doi: 10.1016/j.jmb.2007.11.009
- Buttner, D. (2012). Protein export according to schedule: architecture, assembly, and regulation of type III secretion systems from plant- and animal-pathogenic bacteria. *Microbiol. Mol. Biol. Rev.* 76, 262–310. doi: 10.1128/MMBR.05017-11
- Carlo, J. M., Osman, A., Niles, E. G., Wu, W., Fantappie, M. R., Oliveira, F. M., et al. (2007). Identification and characterization of an R-Smad ortholog (SmSmaD1B) from *Schistosoma mansoni*. *FEBS J.* 274, 4075–4093. doi: 10.1111/j.1742-4658.2007.05930.x
- Carlsson, K. E., Liu, J., Edqvist, P. J., and Francis, M. S. (2007a). Extracytoplasmic-stress-responsive pathways modulate type III secretion in *Yersinia pseudotuberculosis*. *Infect. Immun.* 75, 3913–3924. doi: 10.1128/IAI.01346-06
- Carlsson, K. E., Liu, J., Edqvist, P. J., and Francis, M. S. (2007b). Influence of the Cpx extracytoplasmic-stress-responsive pathway on *Yersinia* sp.-eukaryotic cell contact. *Infect. Immun.* 75, 4386–4399. doi: 10.1128/IAI.01450-06

- Chan, P. P., Holmes, A. D., Smith, A. M., Tran, D., and Lowe, T. M. (2012). The UCSC archaeal genome browser: 2012 update. *Nucleic Acids Res.* 40, D646–D652. doi: 10.1093/nar/gkr990
- Chen, Y., and Anderson, D. M. (2011). Expression hierarchy in the *Yersinia* type III secretion system established through YopD recognition of RNA. *Mol. Microbiol.* 80, 966–980. doi: 10.1111/j.1365-2958.2011.07623.x
- Day, J. B., and Plano, G. V. (2000). The *Yersinia pestis* YscY protein directly binds YscX, a secreted component of the type III secretion machinery. *J. Bacteriol.* 182, 1834–1843. doi: 10.1128/JB.182.7.1834-1843.2000
- De Geyter, J., Tsigotaki, A., Orfanoudaki, G., Zorzini, V., Economou, A., and Karamanou, S. (2016). Protein folding in the cell envelope of *Escherichia coli*. *Nat. Microbiol.* 1, 16107. doi: 10.1038/nmicrobiol.2016.107
- Dewoody, R. S., Merritt, P. M., and Marketon, M. M. (2013). Regulation of the *Yersinia* type III secretion system: traffic control. *Front. Cell. Infect. Microbiol.* 3:4. doi: 10.3389/fcimb.2013.00004
- Diepold, A., Wiesand, U., Amstutz, M., and Cornelis, G. R. (2012). Assembly of the *Yersinia* injectisome: the missing pieces. *Mol. Microbiol.* 85, 878–892. doi: 10.1111/j.1365-2958.2012.08146.x
- Edqvist, P. J., Bröms, J. E., Betts, H. J., Forsberg, Å., Pallen, M. J., and Francis, M. S. (2006). Tetratricopeptide repeats in the type-III-secretion chaperone, LcrH: their role in substrate binding and secretion. *Mol. Microbiol.* 59, 31–44. doi: 10.1111/j.1365-2958.2005.04923.x
- Erhardt, M., Namba, K., and Hughes, K. T. (2010). Bacterial nanomachines: the flagellum and type III injectisome. *Cold Spring Harb. Perspect. Biol.* 2:a000299. doi: 10.1101/cshperspect.a000299
- Francis, M. S., Aili, M., Wiklund, M. L., and Wolf-Watz, H. (2000). A study of the YopD-LcrH interaction from *Yersinia pseudotuberculosis* reveals a role for hydrophobic residues within the amphipathic domain of YopD. *Mol. Microbiol.* 38, 85–102. doi: 10.1046/j.1365-2958.2000.02112.x
- Francis, M. S., Lloyd, S. A., and Wolf-Watz, H. (2001). The type III secretion chaperone LcrH co-operates with YopD to establish a negative, regulatory loop for control of Yop synthesis in *Yersinia pseudotuberculosis*. *Mol. Microbiol.* 42, 1075–1093. doi: 10.1046/j.1365-2958.2001.02702.x
- Francis, M. S., Schesser, K., Forsberg, Å., and Wolf-Watz, H. (2004). “Type III secretion systems in animal- and plant-interacting bacteria,” in *Cellular Microbiology, 2nd Edn.*, eds P. Cossart, P. Boquet, S. Normark, and R. Rappuoli (Washington, DC: American Society for Microbiology Press), 361–392.
- Glass, F., Hartel, B., Zehrmann, A., Verbitskiy, D., and Takenaka, M. (2015). MEF13 requires MORF3 and MORF8 for RNA editing at eight targets in mitochondrial mRNAs in *Arabidopsis thaliana*. *Mol. Plant* 8, 1466–1477. doi: 10.1016/j.molp.2015.05.008
- Gustafsson, C., Govindarajan, S., and Minshull, J. (2004). Codon bias and heterologous protein expression. *Trends Biotechnol.* 22, 346–353. doi: 10.1016/j.tibtech.2004.04.006
- Her, C., Wu, X., Griswold, M. D., and Zhou, F. (2003). Human MutS homologue MSH4 physically interacts with von Hippel-Lindau tumor suppressor-binding protein 1. *Cancer Res.* 63, 865–872. Available online at: <http://cancerres.aacrjournals.org/content/63/4/865>
- Iriarte, M., and Cornelis, G. R. (1999). Identification of SycN, YscX, and YscY, three new elements of the *Yersinia* yop virulon. *J. Bacteriol.* 181, 675–680.
- Jackson, M. W., and Plano, G. V. (1999). DsbA is required for stable expression of outer membrane protein YscC and for efficient Yop secretion in *Yersinia pestis*. *J. Bacteriol.* 181, 5126–5130.
- James, P., Halladay, J., and Craig, E. A. (1996). Genomic libraries and a host strain designed for highly efficient two-hybrid selection in yeast. *Genetics* 144, 1425–1436.
- Jeters, R. T., Wang, G. R., Moon, K., Shoemaker, N. B., and Salyers, A. A. (2009). Tetracycline-associated transcriptional regulation of transfer genes of the *Bacteroides* conjugative transposon CTnDOT. *J. Bacteriol.* 191, 6374–6382. doi: 10.1128/JB.00739-09
- Job, V., Mattei, P. J., Lemaire, D., Attree, I., and Dessen, A. (2010). Structural basis of chaperone recognition of type III secretion system minor translocator proteins. *J. Biol. Chem.* 285, 23224–23232. doi: 10.1074/jbc.M110.111278
- Journet, L., Agrain, C., Broz, P., and Cornelis, G. R. (2003). The needle length of bacterial injectisomes is determined by a molecular ruler. *Science* 302, 1757–1760. doi: 10.1126/science.1091422
- Kim, J. S., Kim, B. H., Jang, J. I., Eom, J. S., Kim, H. G., Bang, I. S., et al. (2014). Functional insight from the tetratricopeptide repeat-like motifs of the type III secretion chaperone SicA in *Salmonella enterica* serovar Typhimurium. *FEMS Microbiol. Lett.* 350, 146–153. doi: 10.1111/1574-6968.12315
- Kimbrough, T. G., and Miller, S. I. (2000). Contribution of *Salmonella typhimurium* type III secretion components to needle complex formation. *Proc. Natl. Acad. Sci. U.S.A.* 97, 11008–11013. doi: 10.1073/pnas.200209497
- Kopaskie, K. S., Ligtenberg, K. G., and Schneewind, O. (2013). Translational regulation of *Yersinia enterocolitica* mRNA encoding a type III secretion substrate. *J. Biol. Chem.* 288, 35478–35488. doi: 10.1074/jbc.M113.504811
- Kubori, T., Matsushima, Y., Nakamura, D., Uralil, J., Lara-Tejero, M., Sukhan, A., et al. (1998). Supramolecular structure of the *Salmonella typhimurium* type III protein secretion system. *Science* 280, 602–605. doi: 10.1126/science.280.5363.602
- Leong, J. M., Morrissey, P. E., and Isberg, R. R. (1993). A 76-amino acid disulfide loop in the *Yersinia pseudotuberculosis* invasins protein is required for integrin receptor recognition. *J. Biol. Chem.* 268, 20524–20532.
- Lunelli, M., Lokareddy, R. K., Zychlinsky, A., and Kolbe, M. (2009). IpaB-IpgC interaction defines binding motif for type III secretion translocator. *Proc. Natl. Acad. Sci. U.S.A.* 106, 9661–9666. doi: 10.1073/pnas.0812900106
- Marlovits, T. C., Kubori, T., Sukhan, A., Thomas, D. R., Galan, J. E., and Unger, V. M. (2004). Structural insights into the assembly of the type III secretion needle complex. *Science* 306, 1040–1042. doi: 10.1126/science.1102610
- Mitchell, A., Tam, C., Elli, D., Charlton, T., Osei-Owusu, P., Fazlollahi, F., et al. (2017). Glutathionylation of *Yersinia pestis* LcrV and its effects on plague pathogenesis. *MBio* 8:e00646-17. doi: 10.1128/mBio.00646-17
- Mueller, C. A., Broz, P., Muller, S. A., Ringler, P., Erne-Brand, F., Sorg, I., et al. (2005). The V-antigen of *Yersinia* forms a distinct structure at the tip of injectisome needles. *Science* 310, 674–676. doi: 10.1126/science.1118476
- Okan, N. A., Bliska, J. B., and Karzai, A. W. (2006). A Role for the SmpB-SsrA system in *Yersinia pseudotuberculosis* pathogenesis. *PLoS Pathog.* 2:e6. doi: 10.1371/journal.ppat.0020006
- Osborne, S. E., and Coombes, B. K. (2011). Expression and secretion hierarchy in the nonflagellar type III secretion system. *Future Microbiol.* 6, 193–202. doi: 10.2217/fmb.10.172
- Pallen, M. J., Beatson, S. A., and Bailey, C. M. (2005). Bioinformatics, genomics and evolution of non-flagellar type-III secretion systems: a Darwinian perspective. *FEMS Microbiol. Rev.* 29, 201–229. doi: 10.1016/j.femsre.2005.01.001
- Pallen, M. J., Francis, M. S., and Futterer, K. (2003). Tetratricopeptide-like repeats in type-III-secretion chaperones and regulators. *FEMS Microbiol. Lett.* 223, 53–60. doi: 10.1016/S0378-1097(03)00344-6
- Portaliou, A. G., Tsois, K. C., Loos, M. S., Zorzini, V., and Economou, A. (2016). Type III secretion: building and operating a remarkable nanomachine. *Trends Biochem. Sci.* 41, 175–189. doi: 10.1016/j.tibs.2015.09.005
- Radics, J., Konigsmair, L., and Marlovits, T. C. (2014). Structure of a pathogenic type 3 secretion system in action. *Nat. Struct. Mol. Biol.* 21, 82–87. doi: 10.1038/nsmb.2722
- Romano, S., Fernandez-Guerra, A., Reen, F. J., Glockner, F. O., Crowley, S. P., O'sullivan, O., et al. (2016). Comparative genomic analysis reveals a diverse repertoire of genes involved in prokaryote-eukaryote interactions within the *Pseudovibrio* genus. *Front. Microbiol.* 7:387. doi: 10.3389/fmicb.2016.00387
- Schneider, C. A., Rasband, W. S., and Eliceiri, K. W. (2012). NIH Image to ImageJ: 25 years of image analysis. *Nat. Methods* 9, 671–675. doi: 10.1038/nmeth.2089
- Schneider, K. L., Pollard, K. S., Baertsch, R., Pohl, A., and Lowe, T. M. (2006). The UCSC archaeal genome browser. *Nucleic Acids Res.* 34, D407–410. doi: 10.1093/nar/gkj134
- Sekiya, K., Ohishi, M., Ogino, T., Tamano, K., Sasakawa, C., and Abe, A. (2001). Supermolecular structure of the enteropathogenic *Escherichia coli* type III secretion system and its direct interaction with the EspA-sheath-like structure. *Proc. Natl. Acad. Sci. U.S.A.* 98, 11638–11643. doi: 10.1073/pnas.191378598
- Singh, S. K., Boyle, A. L., and Main, E. R. (2013). LcrH, a class II chaperone from the type three secretion system, has a highly flexible native structure. *J. Biol. Chem.* 288, 4048–4055. doi: 10.1074/jbc.M112.395889
- Sukhan, A., Kubori, T., Wilson, J., and Galán, J. E. (2001). Genetic analysis of assembly of the *Salmonella enterica* serovar Typhimurium type III secretion-associated needle complex. *J. Bacteriol.* 183, 1159–1167. doi: 10.1128/JB.183.4.1159-1167.2001
- Tamano, K., Aizawa, S., Katayama, E., Nonaka, T., Imajoh-Ohmi, S., Kuwae, A., et al. (2000). Supramolecular structure of the *Shigella* type III secretion

- machinery: the needle part is changeable in length and essential for delivery of effectors. *EMBO J.* 19, 3876–3887. doi: 10.1093/emboj/19.15.3876
- Tamano, K., Aizawa, S., and Sasakawa, C. (2002). Purification and detection of Shigella type III secretion needle complex. *Methods Enzymol.* 358, 385–392. doi: 10.1016/S0076-6879(02)58104-0
- Tamura, K., Stecher, G., Peterson, D., Filipski, A., and Kumar, S. (2013). MEGA6: Molecular Evolutionary Genetics Analysis version 6.0. *Mol. Biol. Evol.* 30, 2725–2729. doi: 10.1093/molbev/mst197
- Troisfontaines, P., and Cornelis, G. R. (2005). Type III secretion: more systems than you think. *Physiology* 20, 326–339. doi: 10.1152/physiol.00011.2005
- Vanden Bergh, P., Heller, M., Braga-Lagache, S., and Frey, J. (2013). The *Aeromonas salmonicida* subsp. *salmonicida* exoproteome: determination of the complete repertoire of Type-Three Secretion System effectors and identification of other virulence factors. *Proteome Sci.* 11, 42. doi: 10.1186/1477-5956-11-42
- Wattiau, P., Bernier, B., Deslee, P., Michiels, T., and Cornelis, G. R. (1994). Individual chaperones required for Yop secretion by *Yersinia*. *Proc. Natl. Acad. Sci. U.S.A.* 91, 10493–10497. doi: 10.1073/pnas.91.22.10493
- Yang, H., Shan, Z., Kim, J., Wu, W., Lian, W., Zeng, L., et al. (2007). Regulatory role of PopN and its interacting partners in type III secretion of *Pseudomonas aeruginosa*. *J. Bacteriol.* 189, 2599–2609. doi: 10.1128/JB.01680-06
- Yu, C. H., Dang, Y., Zhou, Z., Wu, C., Zhao, F., Sachs, M. S., et al. (2015). Codon usage influences the local rate of translation elongation to regulate co-translational protein folding. *Mol. Cell* 59, 744–754. doi: 10.1016/j.molcel.2015.07.018
- Zav'yalov, V. P., Chernovskaya, T. V., Chapman, D. A., Karlyshev, A. V., MacIntyre, S., Zavialov, A. V., et al. (1997). Influence of the conserved disulphide bond, exposed to the putative binding pocket, on the structure and function of the immunoglobulin-like molecular chaperone Caf1M of *Yersinia pestis*. *Biochem J.* 324 (Pt 2), 571–578. doi: 10.1042/bj3240571
- Zhou, Z., Dang, Y., Zhou, M., Li, L., Yu, C. H., Fu, J., et al. (2016). Codon usage is an important determinant of gene expression levels largely through its effects on transcription. *Proc. Natl. Acad. Sci. U.S.A.* 113, E6117–E6125. doi: 10.1073/pnas.1606724113

**Conflict of Interest Statement:** The authors declare that the research was conducted in the absence of any commercial or financial relationships that could be construed as a potential conflict of interest.

Copyright © 2018 Gurung, Amer, Francis, Costa, Chen, Zavialov and Francis. This is an open-access article distributed under the terms of the Creative Commons Attribution License (CC BY). The use, distribution or reproduction in other forums is permitted, provided the original author(s) and the copyright owner are credited and that the original publication in this journal is cited, in accordance with accepted academic practice. No use, distribution or reproduction is permitted which does not comply with these terms.





# Type VI Secretion Systems Present New Insights on Pathogenic *Yersinia*

Xiaobing Yang<sup>1,2†</sup>, Junfeng Pan<sup>2†</sup>, Yao Wang<sup>2</sup> and Xihui Shen<sup>1,2\*</sup>

<sup>1</sup> State Key Laboratory of Crop Stress Biology for Arid Areas, College of Life Sciences, Northwest A&F University, Yangling, China, <sup>2</sup> Shaanxi Key Laboratory of Agricultural and Environmental Microbiology, College of Life Sciences, Northwest A&F University, Yangling, China

The type VI secretion system (T6SS) is a versatile secretion system widely distributed in Gram-negative bacteria that delivers multiple effector proteins into either prokaryotic or eukaryotic cells, or into the extracellular milieu. T6SS participates in various physiological processes including bacterial competition, host infection, and stress response. Three pathogenic *Yersinia* species, namely *Yersinia pestis*, *Yersinia pseudotuberculosis*, and *Yersinia enterocolitica*, possess different copies of T6SSs with distinct biological functions. This review summarizes the pathogenic, antibacterial, and stress-resistant roles of T6SS in *Yersinia* and the ion-transporting ability in *Y. pseudotuberculosis*. In addition, the T6SS-related effectors and regulators identified in *Yersinia* are discussed.

**Keywords:** pathogenic *Yersinia*, type VI secretion system (T6SS), function, effectors, regulation

## OPEN ACCESS

### Edited by:

Matthew S. Francis,  
Umeå University, Sweden

### Reviewed by:

Cristina Elisa Alvarez-Martinez,  
Universidade Estadual de Campinas,  
Brazil  
Erwan Gueguen,  
Université de Lyon, France  
Christopher Alteri,  
University of Michigan, United States

### \*Correspondence:

Xihui Shen  
xihuishen@nwsuaf.edu.cn

<sup>†</sup> These authors have contributed  
equally to this work.

**Received:** 02 May 2018

**Accepted:** 13 July 2018

**Published:** 31 July 2018

### Citation:

Yang X, Pan J, Wang Y and Shen X  
(2018) Type VI Secretion Systems  
Present New Insights on Pathogenic  
*Yersinia*.  
*Front. Cell. Infect. Microbiol.* 8:260.  
doi: 10.3389/fcimb.2018.00260

## INTRODUCTION

The genus *Yersinia* comprises three species of bacterial pathogens, namely *Y. pestis*, *Y. enterocolitica*, and *Y. pseudotuberculosis*, that are causative agents of human diseases. *Y. pestis* is the etiological agent of plague, often transmitted by flea bites or aerosols. It infects regional lymph nodes or lungs and causes the highly lethal disease in humans. *Y. pseudotuberculosis* and *Y. enterocolitica* are enteric pathogens, which usually grow in the environment and can be transmitted to mammalian hosts through ingestion of contaminated food or water. They typically cause a broad range of gastrointestinal diseases, from enteritis to mesenteric lymphadenitis (Bibikova, 1977; Brubaker, 1991; Bottone, 1997; Putzker et al., 2001; Pujol and Bliska, 2005). These three bacterial species have been used in experimental models of infection to study their pathogenicity for the mammalian host.

Despite differences in pathogenesis, these virulent *Yersinia* species have several common virulence factors, including the 70-kb virulence plasmid (pCD1 in *Y. pestis* and pYV in enteropathogenic *Yersinia*) and the yersiniabactin (Ybt) system (Brubaker, 1991; Heesemann et al., 1993; Cornelis et al., 1998). The 70-kb plasmid contains dozens of genes encoding structural components of a type III secretion system (T3SS), and also encodes several T3SS effector proteins called *Yersinia* outer proteins (Yops) and their dedicated chaperones to subvert the innate immune system of the hosts (Bliska et al., 2013; Schwiesow et al., 2015). Since enzymes/toxins/ effectors delivered by secretion systems play a crucial role in the interaction between pathogens and their hosts or competitors, the various types of secretion systems attract interest in the research on pathogenic bacteria.

Several virulence associated secretion (*vas*) genes in T6SS gene clusters were identified in bacterial pathogens before, but till the year of 2006 the Type VI secretion system was proposed and defined as a contact-dependent secretion mechanism (Mougous et al., 2006; Pukatzki et al., 2006). T6SS was found distributed in about 25% of all sequenced Gram-negative bacteria with high

conservation (Boyer et al., 2009; Salomon and Orth, 2015). The T6SS is a proteinaceous machinery that directly injects effector proteins into target cells in a one-step process with a bacteriophage-like cell-puncturing device (Zoued et al., 2014), although the membrane puncturing process has not been directly observed to date. The versatile T6SS weapons allow bacteria to compete with other bacteria or attack simple or higher eukaryotes. The main function of T6SS was implicated in virulence, commensalism or symbiosis, and interbacterial competition (Jani and Cotter, 2010). Apart from the conserved components and similar structures, various functions of T6SSs have been exploited in the past decade, and the newly discovered effectors and their dedicated chaperones secreted by T6SS are also being updated. In the three pathogenic *Yersinia* species, different series of T6SS seem to possess different functions. This review focuses on the detailed description of T6SSs function in *Yersinia*.

## COMPARISON OF T6SS GENE CLUSTERS IN *YERSINIA* SPECIES

### Component, Structure, and Energetics of T6SSs

The core components of T6SS contain 13 subunits, which comprise the typical T6SS structure similar to the T4 bacteriophage, with tail, spike, sheath, hub or baseplate proteins (Boyer et al., 2009; Cascales and Cambillau, 2012). The typical T6SS structure is composed of three subunits: the membrane complex, the baseplate complex, and the injection apparatus. The membrane complex is composed of proteins TssJLM, which anchor the baseplate complex (TssAEFGK) to the membrane and provide structural support. The injection apparatus contains needle sheath (TssBC), tail tube (TssD/Hcp) and spike complex (TssI/VgrG and PAAR motifs) (Silverman et al., 2012; Brunet et al., 2015; Cianfanelli et al., 2016). Generally, various effectors and chaperones could bind to this injection apparatus when they were needed to be secreted out through the T6SS apparatus, and the secretion of Hcp or VgrG is often regarded as the hallmark of a functional T6SS in many bacterial species (Mougous et al., 2006; Pukatzki et al., 2006; Wang et al., 2011). The PAAR (Proline-Alanine-Alanine-aRginine) repeat containing proteins were regarded as an additional component of the T6SS machinery. PAAR-repeat could form a sharp conical extension on the tip of the VgrG spike, which is further involved in the effector recruitment and attaching effector domains to the spike (Shneider et al., 2013; Bondage et al., 2016). The 13 core components of typical T6SS are listed in **Table 1**.

The secretion of T6SS is a dynamic cycle of assembly/extension, contraction/puncture, and disassembly of the sheath, accompanying the energy supply and effector transportation (Basler et al., 2012). The initial stage of the T6SS assembly is to form the membrane complex, followed by the recruitment of baseplate proteins for anchor and extension of the outer sheath and the inner tube (Brunet et al., 2015). This indicated that the T6SS shares a common

assembly pathway of tail tubes with bacteriophage (Brunet et al., 2014). During the attack process, the sheath-like structure propels an inner tube through contraction, and the membrane-puncturing spike is pierced into the target cells. Then effectors and chaperones are delivered into target cells with this expelled structure in a one-step manner (Cianfanelli et al., 2016).

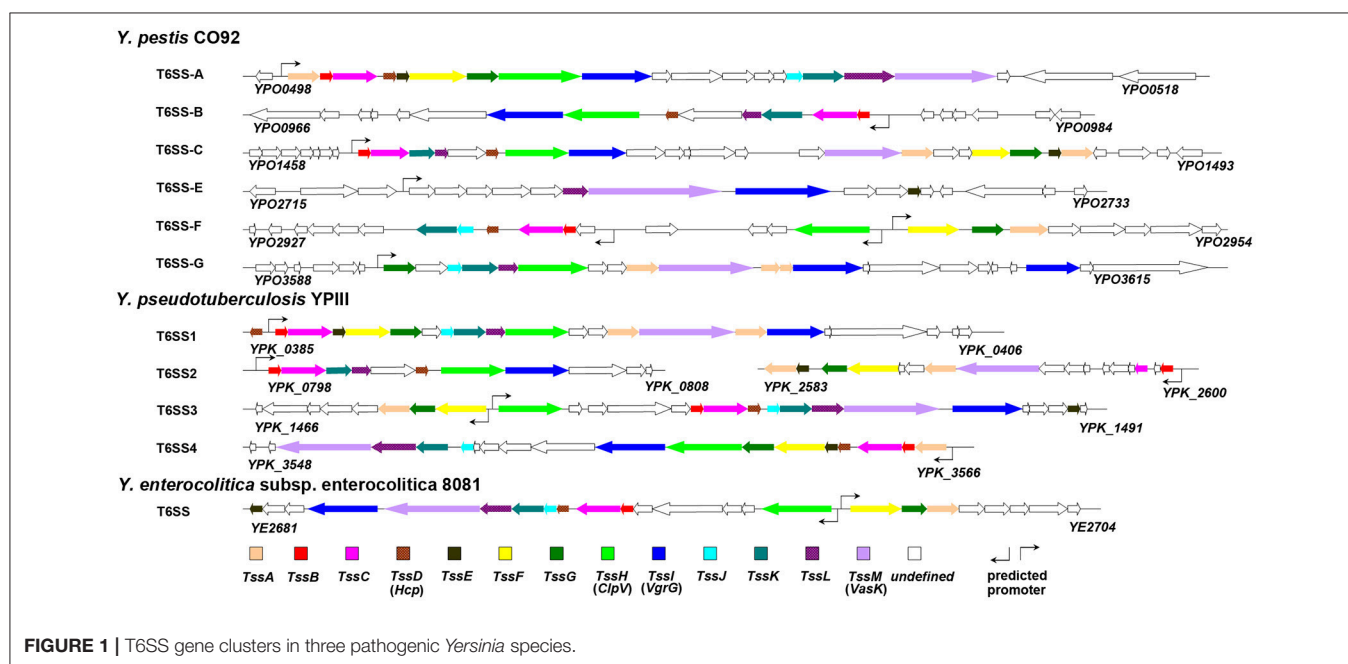
### Different Series of T6SS in Three *Yersinia* Species

T6SS displays a single copy in majority of the bacterial species, yet multiple distinct copies are found in several bacterial species (Boyer et al., 2009). In the *Yersinia* species, six and four T6SS clusters were identified in *Y. pestis* (Andersson et al., 2017) and *Y. pseudotuberculosis* (Zhang et al., 2011b), respectively, while only one copy was found in *Y. enterocolitica* (Jaakkola et al., 2015). The T6SS gene clusters in *Yersinia* are shown in **Figure 1**.

It is noteworthy that the multiple distinct T6SS copies are not functionally redundant; for example, T6SS-1 and T6SS-5 in *B. thailandensis* mediate the bacterial antagonism and macrophage infection, respectively (Schwarz et al., 2010). In *Y. pestis*, the T6SS region YPO0498-YPO0516 (the T6SS Cluster A in **Figure 1**) is preferentially expressed at 26 vs. 37°C (Cathelyn et al., 2006; Robinson et al., 2009), which suggests this gene cluster may function in natural conditions rather than in its mammalian host. Deletion of the T6SS Cluster A locus reduced the uptake by J774.1 murine macrophages (Robinson et al., 2009). However, it had no effect on virulence in bubonic or pneumonic murine plague models compared to the parental *Y. pestis* CO92 strain (Robinson et al., 2009; Andersson et al., 2017). An Hcp-like protein encoded by *ypo0502* was found to play important roles in autoagglutination (AA), indicating that the T6SS Cluster A is involved in intraspecies interaction of bacteria (Podladchikova et al., 2011). A similar thermoregulated gene cluster in *Y. pseudotuberculosis* was identified as T6SS4 (*ypk\_3548-ypk\_3566*), which is precisely regulated by temperature, growth phase, and AHL-dependent quorum sensing systems, and plays a crucial role in resistance to environmental stresses (Zhang et al., 2011b). The T6SS Cluster A in *Y. pestis* and T6SS4 in *Y. pseudotuberculosis* could both be induced by room temperature conditions (about 25°C). The phylogenetic analysis based on TssL of *Yersinia* T6SSs showed a close genetic distance between T6SS Cluster A in *Y. pestis* and T6SS4 in *Y. pseudotuberculosis* (**Figure 2**). Furthermore, the two T6SS clusters have similar genomic organization, suggesting they may both play crucial roles in environment adaptability. From **Figure 1** it showed the T6SS-E and F clusters in *Y. pestis* only contain 4 and 9 T6SS genes, respectively. Considering these components seemed complementary, and the two T6SS clusters locate in vicinity to each other, it speculated they may represent an integral set of T6SS. It is worth noting that *Y. pestis* has 6 clusters but only one with a complete set of T6SS genes, while *Y. pseudotuberculosis* has 4 clusters with full set of genes. Note that some clusters encode an incomplete set of T6SS genes and could be non-functional. The function of these incomplete T6SSs should be experimental verified in the future.

**TABLE 1** | The 13 conserved components of typical T6SS.

COG No.	Protein name	Alternative names	Location/activity	Homologous proteins
COG3515	TssA	BimE	Baseplate	
COG3516	TssB	VipA/iglA	Contractile sheath	phage T4 gp18
COG3517	TssC	VipB/iglB	Contractile sheath	phage T4 gp18
COG3157	TssD	Hcp	Form the secreted hexameric tube	phage T4 gp19
COG3518	TssE	HsiF	Baseplate	phage T4 gp25
COG3519	TssF	VasA	Baseplate	
COG3520	TssG		Baseplate	
COG0542	TssH	ClpV	Sheath recycling AAA+ ATPase	
COG3501	TssI	VgrG	Tail spike	phage T4 gp27/5
COG3521	TssJ	Lip, SciN	Membrane anchoring complex	
COG3522	TssK		Baseplate	
COG3455	TssL	IcmH/DotU, VasF	Membrane anchoring complex	T4bSS IcmH
COG3523	TssM	IcmF, VasK	Membrane anchoring complex	T4bSS IcmF

**FIGURE 1** | T6SS gene clusters in three pathogenic *Yersinia* species.

## THE FUNCTIONS OF T6SS IN *YERSINIA*

### Virulence

At the beginning, genes of T6SS cluster in *Vibrio cholerae* and *Pseudomonas aeruginosa* were identified as *vas* (virulence-associated secretion) genes for their roles in pathogenesis (Mougous et al., 2006; Pukatzki et al., 2006). Afterwards, the virulence-related functions of T6SS in the host were verified in several organisms including *Edwardsiella tarda* (Zheng and Leung, 2007), *Aeromonas hydrophila* (Suarez et al., 2008), *Salmonella enterica* (Blondel et al., 2010), *Campylobacter jejuni* (Lertpiriyapong et al., 2012), and *Burkholderia pseudomallei* (Schwarz et al., 2014).

In 2008, five T6SS gene clusters in *Y. pestis* KIM were identified through a phylogenetic analysis (Bingle et al., 2008),

while six T6SS clusters in *Y. pestis* CO92 were predicted based on *in silico* analysis (Boyer et al., 2009). Actually, six T6SS clusters are distributed in genome of *Y. pestis* KIM and CO92 according to the SecReT6 database, which is a web-based resource for type VI secretion systems found in bacteria (Li et al., 2015). However, the virulence of T6SS in *Y. pestis* to hosts was confirmed through laboratory experiments till 2015. Using an *in vivo* signature-tagged mutagenesis (STM) screening approach, Ponnusamy et al. identified three T6SS genes with virulence potential in *Y. pestis* CO92. In-frame deletion of *vasK* (YPO3603, a component of the T6SS cluster G) in *Y. pestis* CO92 resulted in significant attenuation of the bacterium in murine models of infection, and this attenuation could be fully complemented (Ponnusamy et al., 2015). In addition, the five deletion mutants of T6SS clusters (B, C, E-G) showed varying levels of attenuation when evaluated in

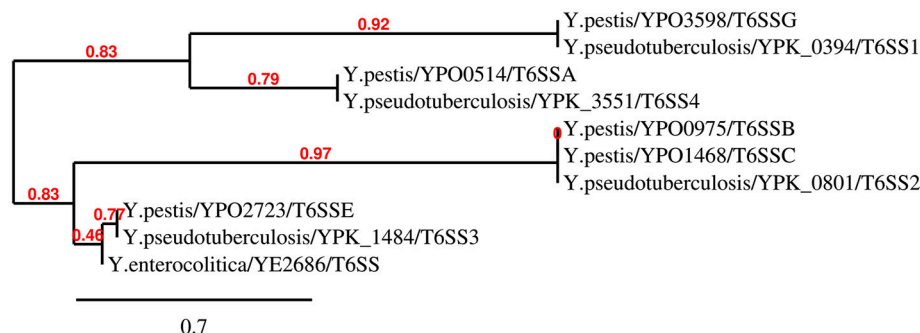


**FIGURE 2 |** Neighbour-Joining tree of TssL proteins of *Yersinia* T6SSs. The phylogenetic tree was generated using BioNJ with 100 bootstrap replicates based on the alignment of TssL sequences (Gascuel, 1997). As the TssL is missed in T6SS gene cluster F in *Y. pestis*, the T6SS gene cluster F was not present in this N-J dendrogram.

a mouse model of pneumonic plague, but not all T6SS clusters of *Y. pestis* are equally functional. Deletion mutants for Cluster C and Cluster F exhibited limited, 14%, or no attenuation, respectively, while deletion mutants for Cluster B, Cluster E, and Cluster G, exhibited significant levels of attenuation in infection of a bubonic plague model. A further augmented attenuation was detected in mutants lacking multiple T6SSs. The  $\Delta ypo2720-2733\Delta hcp3$  (Cluster E and *hcp* homolog 3) double deletion mutant showed 60% of attenuation in comparison to WT CO92. This result further supports the involvement of T6SSs in *Y. pestis* virulence (Andersson et al., 2017). Moreover, most of the attenuated T6SS deletion mutant strains showed decreased host cell cytotoxicity and intracellular survival in comparison to WT CO92 (Andersson et al., 2017).

*Y. pseudotuberculosis* YPIII mutants lacking T6SS-4 or *yezP* (*ypk\_3549*, an effector gene in T6SS-4 cluster) are defective in virulence in mice (Wang et al., 2015). The enteropathogenic *Y. enterocolitica* causes infections similar to *Y. pseudotuberculosis*, but has several different characteristics related to epidemiology and ecology, and only one type of T6SS was found in the *Y. enterocolitica* genome. It is speculated that the lack of multiple T6SS might be beneficial for escaping the host immune system, because a T6SS with toxic effectors might encumber the invasion and survival of *Y. enterocolitica* cells in mammalian hosts (Jaakkola et al., 2015). This function can be regarded as anti-virulence, which has been discussed previously (Jani and Cotter, 2010).

## Bacteria-Bacteria Interaction

Bacteria have evolved various mechanisms to kill bacterial competitors and defense against predators in their environment. The T6SS has membrane-penetrating tails similar to bacteriophages, suggesting that T6SS may be involved in cell-cell interactions of bacteria (Pell et al., 2009). Bacteria could utilize T6SS to intimately interface with other bacteria, efficiently killing or inhibiting competitors with T6SS toxins and protecting itself with immune proteins, which has been reported in *P. aeruginosa* (HSI-1) (Hood et al., 2010), *B. thailandensis* (T6SS-1) (Schwarz et al., 2010), *V. cholerae* (MacIntyre et al., 2010; Ishikawa et al.,

2012), and *Serratia marcescens* (Murdoch et al., 2011). Different from the traditional offensive and defensive model of T6SS mediated bacterial competition (Russell et al., 2012; Lien and Lai, 2017; Yang et al., 2018), swarming *Proteus mirabilis* discriminate non-identical population via T6SS-dependent delivery of toxic effectors, thus forming a visible demarcation line (Dienes line) between different *Proteus* isolates (Alteri et al., 2013). Although this phenomenon of self-recognition during swarming in *P. mirabilis* has been known for decades it was only ascribed to the T6SS recently.

Through DNA microarrays analysis of *Y. pestis* CO92, an IAHP (IcmF-Associated Homologous Protein) locus (*YPO0498-0516*) was found regulated by RovA, which was specifically required for bubonic plague (Cathelyn et al., 2006). However, another study indicated that mutation in this locus had no effect in laboratory models of infected oriental rat flea *X. cheopis*, or in virulence using bubonic or pneumonic murine plague models (Robinson et al., 2009). Similarly, in-frame deletion of *YPO0498* did not affect virulence *in vivo* (Ponnusamy et al., 2015). Recently, this locus was classified as T6SS cluster A in *Y. pestis* CO92, and was confirmed not required for pathogenesis (Andersson et al., 2017). Nevertheless, deletion of the T6SS Cluster A locus resulted in increased uptake and intracellular growth of *Y. pestis* in the macrophage-like J774.A1 cells, indicating a role of T6SS in interaction with host cells (Robinson et al., 2009). Among this T6SS cluster, YPO0502, identified as a Hcp-like protein that forms pilus-like structure, determines *Y. pestis* autoagglutination (AA). This suggests that at least one (T6SS Cluster A) of the 6 T6SS clusters in *Y. pestis* is involved in bacterial interaction (Podladchikova et al., 2011). However, whether *Yersinia* T6SSs are involved in bacterial competition and Dienes line formation needs to be verified in the future.

## Stress Response

Many of the earliest studies on T6SS focused on their roles in virulence and the interactions between pathogens and hosts. In 2009, it was reported that a T6SS in *Vibrio anguillarum* acts as a sensor for an unknown extracytoplasmic signal that modulates RpoS (Weber et al., 2009). RpoS is the main regulator of gene



expression during stationary phase and stress conditions, and it positively regulates VanT linking quorum sensing (QS) to stress response and general physiology of *V. anguillarum* (Weber et al., 2008). Therefore, this study suggested a new function for T6SS in the ecology of bacteria, that T6SS played a crucial role in bacterial stress response and cell survival after exposure to various environmental challenges (Weber et al., 2009).

In *Y. pseudotuberculosis*, RpoS was found to be important in resistance to multiple stressors including oxidative stress, acid stress, osmotic stress, and 42°C heat shock, and was also crucial for motility, biofilm formation, and T6SS expression. The electrophoretic mobility shift assay (EMSA) showed that RpoS regulates T6SS4 expression by directly binding to the T6SS4 promoter (Guan et al., 2015). However, compared with the two reported YpsRI QS system (Atkinson et al., 2008) and the OmpR regulator (Zhang et al., 2013), RpoS plays a less crucial role in T6SS4 activation. T6SS4 is only partly responsible for the stress-resistance activity of RpoS, consistent with the relatively weak role of RpoS in activating T6SS4 expression in *Y. pseudotuberculosis* (Guan et al., 2015). Similarly, the PppA-PpkA pair of H1-T6SS in *P. aeruginosa* plays roles in bacterial resistance to oxidative and osmotic stress, and *pppA-ppkA* deletion affects the expression of the RpoS and QS regulons (Goldova et al., 2011).

In 2013, an OmpR-T6SS4 regulation pathway for stress resistance in *Y. pseudotuberculosis* was characterized in two studies, both of which confirmed the direct binding of OmpR on the T6SS-4 promoter region *in vitro* (Gueguen et al., 2013; Zhang et al., 2013). In an earlier study, OmpR was found to be essential for low pH adaptation by positively regulating the expression of urease in *Y. pseudotuberculosis* (Hu et al., 2009). Here, it was indicated that T6SS4 contributed to acid survival by maintaining a steady-state intracellular pH in *Y. pseudotuberculosis*. The acid resistance ability is dependent upon the ATPase activity of ClpV4 that participates in H<sup>+</sup> extrusion, and this process is positively regulated by the global regulator OmpR (Zhang et al., 2013).

In addition, the T6SS-4 expression mediated by OmpR is also induced in high osmolarity conditions or in the presence of sodium deoxycholate. Besides T6SS4 gene cluster, OmpR activates additional genes involved in tolerance to high osmolarity, because the *ompR* transposon mutant cells were more severely affected than the *tssF4* cells (Gueguen et al., 2013). Similarly, an earlier study showed that deletion of T6SS increased the susceptibility of *C. jejuni* to a bile salt, deoxycholic acid (DCA), and the reason for which was attributed to an increase in the intracellular influx of DCA mediated by T6SS (Lertpiriyapong et al., 2012).

## Ion Transport

Recently, T6SS4 in *Y. pseudotuberculosis* was found to have a notable function of transporting zinc ions (Zn<sup>2+</sup>) from the environment into bacterial cells to mitigate the detrimental hydroxyl radicals induced by multiple stressors (Wang et al., 2015). Generally, bacteria utilize the classical ZnuABC transport system to acquire Zn<sup>2+</sup> to maintain zinc balance. In *Y. pseudotuberculosis*, the ZnuABC transporter contributes to reduce the intracellular ROS levels and thus prevents

oxidative damage to cells (Wang et al., 2016). While in *Y. pestis*, the yersiniabactin (Ybt, a zincophore for Zn<sup>2+</sup> acquisition) synthetase HMWP2, together with ZnuABC, are critical for lethal infections in a mouse model of septicemic plague (Bobrov et al., 2014). Interestingly, in *Y. pseudotuberculosis* a T6SS4-mediated substrate YezP (YPK\_3549), a novel Zn<sup>2+</sup>-binding protein, has the capacity to rescue the sensitivity to oxidative stress exhibited by T6SS4 mutants when added to extracellular milieu. Zn<sup>2+</sup> acquisition achieved by YezP is co-regulated with T6SS4 by OxyR, which is a global oxidative stress regulator that senses diverse environmental cues (Wang et al., 2015).

Similar capability of ion transport by T6SS was found in *B. thailandensis* and *P. aeruginosa*. In *B. thailandensis*, a proteinaceous zincophore (TseZ) secreted through T6SS4 interacts with the outer membrane heme transporter HmuR to acquire zinc under oxidative stress (Si et al., 2017a). In addition, the T6SS4 in *B. thailandensis* facilitated the uptake of Mn<sup>2+</sup> by secreting a Mn<sup>2+</sup>-binding effector TseM during oxidative stress. The Mn<sup>2+</sup> load on TseM could be delivered to MnoT, a Mn<sup>2+</sup>-specific TonB-dependent outer membrane transporter, and then transported into cells to fulfill the increased cellular demand for Mn<sup>2+</sup> under oxidative stress (Si et al., 2017b). While in *P. aeruginosa*, a H3-T6SS secreted effector TseF (PA2374) is involved in iron uptake by interacting with outer membrane vesicles (OMVs) and the Pseudomonas Quinolone Signal (PQS) system (Lin et al., 2017). These studies highlight the newly characterized function of ion transport through T6SSs. Whether and how *Yersinia* T6SSs transport other metal ions besides Zn<sup>2+</sup> needs to be investigated in the future.

## Other Potential Functions

More functions were identified in other bacterial species in addition to *Yersinia*. T6SS is also implicated in biofilm formation in several bacterial pathogens. For example, Hcp participates in biofilm formation in *P. aeruginosa* PAO1 (Southey-Pillig et al., 2005), and H1-T6SS is associated with biofilm-specific antibiotic resistance in *P. aeruginosa* PA14 (Zhang et al., 2011a). In *Acidovorax citrulli*, four mutants of T6SS components were reduced in biofilm formation (Tian et al., 2015). Recently, T6SS was shown to be associated with cell autophagy. VgrG2, a translocon of T6SS2 in *Vibrio parahaemolyticus*, induces autophagy in macrophages (Yu et al., 2015). A Type VI secretion PGAP1-like effector TplE, belonging to Tle4 phospholipase family in *P. aeruginosa* (Russell et al., 2013), induced autophagy through disruption of endoplasmic reticulum (ER) homeostasis (Jiang et al., 2016). In addition, the T6SS in *P. mirabilis* plays a role in self-recognition during swarming via delivery of toxic effectors (Alteri et al., 2013). Further research and analysis need to be performed to verify these potential T6SS functions in *Yersinia* species.

## EFFECTORS SECRETED BY T6SS IN *YERSINIA*

With a bacteriophage tail-like structure, T6SS apparatus can deliver various effectors into bacterial competitors for

**TABLE 2 |** Putative PAAR motif-containing effectors in *Yersinia* T6SS clusters.

	T6SS Cluster	Predicted effectors with PAAR motif	Other Pfam	Function	HHpred
<i>Y. pestis</i>	T6SS-A	YPO0511a	DUF4150, ScdA_N	Against oxidative/nitrosative stress	Tail-associated lysozyme
	T6SS-B	YPO0866	Pyocin_S	Bacterial membrane proteins	Tail-associated lysozyme
		YPO0873		Bacteriocin	S-type Pyocin family protein endonuclease activity
	T6SS-C	YPO1484	Ntox44	RNase toxin	Tail-associated lysozyme
	T6SS-G	YPO3615	RHS_repeat, RHS DUF4595	Bacterial membrane proteins	Tail-associated lysozyme
<i>Y. pseudotuberculosis</i>	T6SS1	YPK_0403	RHS_repeat, RHS DUF4595, Ntox47	ABC toxin complex	TccC3
	T6SS2	YPK_2589	Ntox44	RNase toxin	Tail-associated lysozyme PMID: 22731697
					Tail-associated lysozyme, S-type pyocin
	T6SS3	YPK_0952	Pyocin_S	Bacteriocin	Endonuclease activity PMID: 12409205
		YPK_0959		Bacterial membrane proteins	Tail-associated lysozym
	T6SS4	YPK_1487	DUF4150, ScdA_N	Bacterial membrane proteins	Tail-associated lysozyme
		YPK_3554		Against oxidative/nitrosative stress	Tail-associated lysozyme
	<i>Y. enterocolitica</i>	T6SS	YE2683a		Bacterial membrane proteins

interbacterial competition (Cianfanelli et al., 2016), into eukaryotic hosts for pathogenesis (Durand et al., 2014) or into extracellular milieu for nutritional demands (Wang et al., 2015; Lin et al., 2017; Si et al., 2017a). The antibacterial T6SS effector usually has a chaperone immunity protein that provides protection to the organism itself. These effectors could be divided into three categories as targeting the membrane, cell wall, or nucleic acid (Russell et al., 2014). The eukaryotic host-targeted T6SS effectors are diverse in biological and biochemical functions. For example, VgrG-1 in *V. cholerae* can cause actin crosslinking for intestinal inflammation (Ma and Mekalanos, 2010), VgrG2b in *P. aeruginosa* interacts with microtubules for successful invasion of epithelial cells (Sana et al., 2015), and VgrG-5 in *B. thailandensis* could induce the host cell membrane fusions by interacting directly with a neighboring host cell receptor or by engaging in homotypic interactions within or between cells (Schwarz et al., 2014). A recent publication summarizes the T6SS effectors identified in recent years (Lien and Lai, 2017).

Many T6SS secretion effectors have been identified in bacterial organisms. However, apart from the hallmark of T6SS effectors Hcp or VgrG, only two effectors were functionally characterized in *Yersinia* species according to published papers. They are YezP (YPK\_3549) in *Y. pseudotuberculosis*, which is a novel Zn<sup>2+</sup>-binding protein substrate (Wang et al., 2015), and YPO0502 in *Y. pestis* CO92, which is a low-molecular-weight component with siderophore activity and regarded as the autoagglutination factor (Podladchikova et al., 2011). In addition, three T6SS associated proteins, y3673/Hcp, y3674 and

y3675, were detected in the outer-membrane proteome in *Y. pestis* KIM6+ using 2DGE gel electrophoresis (Pieper et al., 2009). However, the y3674/y3675 genes possess VipB/VipA motif according to the KEGG database, which suggests these two proteins may comprise the contractile sheath of T6SS. With high-throughput signature-tagged mutagenesis (STM) approach, three T6SS components or effector-encoding genes (*vasK/ypo3603*, *ypo0498*, and *ypo1484*) were identified in *Y. pestis* CO92 (Ponnusamy et al., 2015). VasK was confirmed to be important during *Y. pestis* infection in mouse models of plague (Andersson et al., 2017). With a conserved “MxiM” motif, YPO0498 may be a lipoprotein, while YPO1484 is likely to be an RNase toxin with a sharp conical extension complex of “PAAR” (Proline-Alanine-Alanine-arginine) (Shneider et al., 2013). However, more experiments need to be performed to explain the connection between these proteins and T6SS apparatus. Recently, Andersson et al generated three PAAR motif repeat-containing T6SS effector encoding gene deletion mutants ( $\Delta ypo0873$ ,  $\Delta ypo1484$ , and  $\Delta ypo3615$ ). Only  $\Delta ypo1484$  exhibited a limited level of attenuation, 20% survivability, in comparison to WT CO92 in a mouse model of pneumonic plague. This attenuation was similar to the level of attenuation, 14%, reported in the T6SS Cluster C (*ypo1458-1484*) deletion mutant, which contains the *ypo1484* gene (Andersson et al., 2017). As multiple copies of T6SS have been confirmed in *Yersinia* species, it seems that more potential undiscovered effectors remain to be identified. Here, we presented the hypothetical effectors with “PAAR” motif in *Yersinia* T6SS clusters (as shown in **Table 2**).

**TABLE 3** | The identified transcriptional regulators for T6SSs in *Yersinia*.

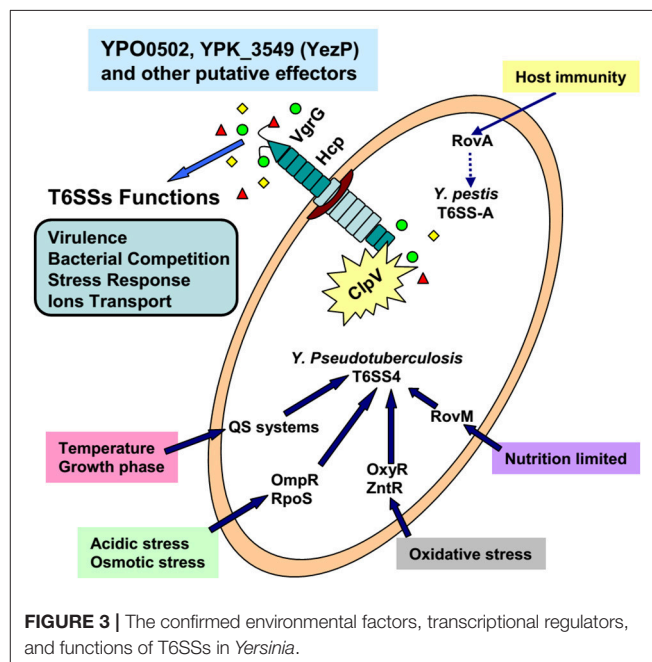
Regulator	Mode	Environment cues	T6SS copies of Organisms	References
RovA	Positively/Indirectly	Host immunity	<i>Y. pestis</i> T6SS cluster A	Cathelyn et al., 2006
YpsI/Ytl (QS)	Positively/not sure	Growth phase	<i>Y. pseudotuberculosis</i> T6SS4	Zhang et al., 2011b
OmpR	Positively/directly	Acidic or osmotic stresses	<i>Y. pseudotuberculosis</i> T6SS4	Gueguen et al., 2013; Zhang et al., 2013
OxyR	Positively/directly	Oxidative stress	<i>Y. pseudotuberculosis</i> T6SS4	Wang et al., 2015
ZntR	Positively/directly	Oxidative stress	<i>Y. pseudotuberculosis</i> T6SS4	Wang et al., 2017
RpoS	Positively/directly	Osmotic, acid stresses	<i>Y. pseudotuberculosis</i> T6SS4	Guan et al., 2015
RovM	Positively/directly	Nutrition limited	<i>Y. pseudotuberculosis</i> T6SS4	Song et al., 2015

## T6SS REGULATION IN *YERSINIA*

T6SS gene clusters are found both in pathogenic and non-pathogenic bacteria, which are distributed in various environments including marine, soil, rhizosphere, higher plants and mammalian hosts, implying their diverse functions (Boyer et al., 2009). As the assembly, contraction, and disassembly cycle of the T6SS is likely to be energetically costly to the bacterial cell, the T6SS organelle is tightly regulated when organisms alternate in various environmental conditions (Silverman et al., 2012). It has been reported that T6SS in bacterial species responds to various environmental factors including salinity (Salomon et al., 2013), iron-concentration (Chakraborty et al., 2011), temperature (Pieper et al., 2009), QS-dependent cell density (Zheng et al., 2010; Kitaoka et al., 2011), host immune system, and other stressors (Brooks et al., 2013).

Temperature is a common environmental factor for most pathogens, and changes widely when organisms alternate in various environmental conditions. The expression of T6SS cluster A (YPO0498-YPO0516 in *Y. pestis* CO92 or y3658-y3677 in *Y. pestis* KIM) is induced by lowering the temperature from 37 to 26°C (Pieper et al., 2009; Robinson et al., 2009). In *Y. pseudotuberculosis*, all the four T6SS clusters are differentially thermoregulated. In addition to the induction of T6SS4 at 26°C, the T6SS1 expression is obviously induced at 37°C, while T6SS2, T6SS3, and T6SS4 was completely repressed at 37°C, which suggested that the T6SS1 played a more important role in bacterial virulence during mammalian host infection than other 3 T6SS loci. In addition, T6SS is precisely regulated by growth phase and acylated homoserine lactones (AHLs) dependent quorum sensing (QS) systems (Zhang et al., 2011b). Furthermore, T6SS4 in *Y. pseudotuberculosis* has been shown to respond to oxidative stress (Wang et al., 2015).

T6SS could be activated by different transcriptional regulators to combat multiple stresses and host immunity, and several transcriptional regulators have been identified in *Yersinia* species. In *Y. pseudotuberculosis*, the OmpR-regulated T6SS4 plays important roles under acidic and osmotic stress conditions (Gueguen et al., 2013; Zhang et al., 2013). It was proposed that T6SS4 was activated by RpoS and partly mediated the roles of RpoS in osmotic and acid resistance (Guan et al., 2015). Furthermore, T6SS4 could be regulated by OxyR or ZntR to cope with oxidative stress by removing ROS produced by host immunity or harmful environments (Wang et al., 2015,

**FIGURE 3** | The confirmed environmental factors, transcriptional regulators, and functions of T6SSs in *Yersinia*.

2017). We have summarized the identified regulators of T6SS in *Yersinia* in Table 3.

In addition to the research on *Yersinia*, other transcriptional regulators of T6SSs have been identified in more bacterial species. In *P. aeruginosa*, a T6SS is controlled by the global virulence regulator proteins RetS and LadS (Mougous et al., 2006). In *Salmonella enterica*, T6SS genes were controlled by the SsrA/SsrB two-component regulatory system (Parsons and Heffron, 2005). Furthermore, T6SS is regulated by AggR in enteroaggregative *Escherichia coli* (Dudley et al., 2006), by VirA/G in *Burkholderia mallei* (Schell et al., 2007), and similarly by quorum sensing mechanism in the plant pathogen *Pectobacterium atrosepticum* (Liu et al., 2008). By contrast, few post-transcriptional regulators have been identified so far. Lon, a posttranslational regulator, is known to affect a variety of physiological traits in many bacteria. It suggested that T6SS was regulated by LonA in *V. cholerae*, as well as biofilm formation, swimming motility, intracellular levels of cyclic diguanylate (Rogers et al., 2016). In *P. aeruginosa*, a screen to identify T6SS regulatory elements found that the posttranscriptional regulator RsmA imposes a

concerted repression on all three T6SS clusters. RsmA and a transcriptional regulator AmrZ orchestrate the assembly of all three T6SSs in *P. aeruginosa* (Allsopp et al., 2017).

## CONCLUSIONS

Over the past decade, pathogenic bacteria *P. aeruginosa* and *V. cholerae* have been widely used to study T6SS, and significant advancements have been made on the understanding of their structure, activation signals, and regulatory pathways (Chen et al., 2015; Joshi et al., 2017). As important pathogenic bacteria, three *Yersinia* species also attracted increasing attention because of their multiple T6SS copies. As a summary, we drew a schematic diagram based on the current achievement of research on T6SSs in *Yersinia* (Figure 3). However, many questions need to be addressed. We believe that the future work in *Yersinia* T6SS research will involve at least six points: 1, The T6SS activation conditions; 2, The T6SS regulators and the regulation network; 3, Identification of T6SS secreted effectors and their new functions; 4, Based on the knowledge of T6SS attack and protection ability,

the ways to prevent the T6SS<sup>+</sup> pathogens; 5, The different functions and connection of different T6SS clusters; 6, The exploitation of new methods or techniques for further T6SS studies. The progress of *Yersinia* T6SS research will provide new knowledge and challenges, as well as further our understanding of the T6SS complexities in other important human pathogens. This research will also influence clinical medicine, microbial community ecology, and physiology.

## AUTHOR CONTRIBUTIONS

XY, JP, and YW collected and assessed the references; YW and XS contributed in the proposal and guideline of the review; XY, JP, and XS wrote the paper.

## FUNDING

The authors thank the National Natural Science Foundation of China (Nos. 31725003, 31670053, and 31370150) for the financial support.

## REFERENCES

- Allsopp, L. P., Wood, T. E., Howard, S. A., Maggiorini, F., Nolan, L. M., Wettstadt, S., et al. (2017). RsmA and AmrZ orchestrate the assembly of all three type VI secretion systems in *Pseudomonas aeruginosa*. *Proc. Natl. Acad. Sci. U.S.A.* 114, 7707–7712. doi: 10.1073/pnas.1700286114
- Alteri, C. J., Himpfl, S. D., Pickens, S. R., Lindner, J. R., Zora, J. S., Miller, J. E., et al. (2013). Multicellular bacteria deploy the type VI secretion system to preemptively strike neighboring cells. *PLoS Pathog.* 9:e1003608. doi: 10.1371/journal.ppat.1003608
- Andersson, J. A., Sha, J., Erova, T. E., Fitts, E. C., Ponnusamy, D., Kozlova, E. V., et al. (2017). Identification of new virulence factors and vaccine candidates for *Yersinia pestis*. *Front. Cell. Infect. Microbiol.* 7:448. doi: 10.3389/fcimb.2017.00448
- Atkinson, S., Chang, C. Y., Patrick, H. L., Buckley, C. M., Wang, Y., Sockett, R. E., et al. (2008). Functional interplay between the *Yersinia pseudotuberculosis* YpsRI and YtbRI quorum sensing systems modulates swimming motility by controlling expression of flhDC and fliA. *Mol. Microbiol.* 69, 137–151. doi: 10.1111/j.1365-2958.2008.06268.x
- Basler, M., Pilhofer, M., Henderson, G. P., Jensen, G. J., and Mekalanos, J. J. (2012). Type VI secretion requires a dynamic contractile phage tail-like structure. *Nature* 483, 182–186. doi: 10.1038/nature10846
- Bibikova, V. A. (1977). Contemporary views on the interrelationships between fleas and the pathogens of human and animal diseases. *Ann. Rev. Entomol.* 22, 23–32. doi: 10.1146/annurev.en.22.010177.000323
- Bingle, L. E., Bailey, C. M., and Pallen, M. J. (2008). Type VI secretion: a beginner's guide. *Curr. Opin. Microbiol.* 11, 3–8. doi: 10.1016/j.mib.2008.01.006
- Bliska, J. B., Wang, X., Viboud, G. I., and Brodsky, I. E. (2013). Modulation of innate immune 387 responses by *Yersinia* type III secretion system translocators and effectors. *Cell. Microbiol.* 15, 1622–1631. doi: 10.1111/cmi.12164
- Blondel, C. J., Yang, H. J., Castro, B., Chiang, S., Toro, C. S., Zaldivar, M., et al. (2010). Contribution of the type VI secretion system encoded in SPI-19 to chicken colonization by *Salmonella enterica* serotypes Gallinarum and Enteritidis. *PLoS ONE* 5:e11724. doi: 10.1371/journal.pone.0011724
- Bobrov, A. G., Kirillina, O., Fetherston, J. D., Miller, M. C., Burlison, J. A., and Perry, R. D. (2014). The *Yersinia pestis* siderophore, yersiniabactin, and the ZnuABC system both contribute to zinc acquisition and the development of lethal septicemic plague in mice. *Mol. Microbiol.* 93, 759–775. doi: 10.1111/mmi.12693
- Bondage, D. D., Lin, J. S., Ma, L. S., Kuo, C. H., and Lai, E. M. (2016). VgrG C terminus confers the type VI effector transport specificity and is required for binding with PAAR and adaptor-effector complex. *Proc. Natl. Acad. Sci. U.S.A.* 113, E3931–E3940. doi: 10.1073/pnas.1600428113
- Bottone, E. J. (1997). *Yersinia enterocolitica*: the charisma continues. *Clin. Microbiol. Rev.* 10, 257–276.
- Boyer, F., Fichant, G., Berthod, J., Vandenbrouck, Y., and Attree, I. (2009). Dissecting the bacterial type VI secretion system by a genome wide *in silico* analysis: what can be learned from available microbial genomic resources? *BMC Genomics* 10:104. doi: 10.1186/1471-2164-10-104
- Brooks, T. M., Unterwiesing, D., Bachmann, V., Kostiuik, B., and Pukatzki, S. (2013). Lytic activity of the *Vibrio cholerae* type VI secretion toxin VgrG-3 is inhibited by the antitoxin TsaB. *J. Biol. Chem.* 288, 7618–7625. doi: 10.1074/jbc.M112.436725
- Brubaker, R. R. (1991). Factors promoting acute and chronic diseases caused by *Yersinia*. *Clin. Microbiol. Rev.* 4, 309–324. doi: 10.1128/CMR.4.3.309
- Brunet, Y. R., Henin, J., Celia, H., and Cascales, E. (2014). Type VI secretion and bacteriophage tail tubes share a common assembly pathway. *EMBO Rep.* 15, 315–321. doi: 10.1002/embr.201337936
- Brunet, Y. R., Zoued, A., Boyer, F., Douzi, B., and Cascales, E. (2015). The type VI secretion TssEFGK-VgrG phage-like baseplate is recruited to the TssJLM membrane complex via multiple contacts and serves as assembly platform for tail tube/sheath polymerization. *PLoS Genet.* 11:e1005545. doi: 10.1371/journal.pgen.1005545
- Cascales, E., and Cambillau, C. (2012). Structural biology of type VI secretion systems. *Philos. Trans. R. Soc. Lond. B Biol. Sci.* 367, 1102–1111. doi: 10.1098/rstb.2011.0209
- Cathelyn, J. S., Crosby, S. D., Lathem, W. W., Goldman, W. E., and Miller, V. L. (2006). RovA, a global regulator of *Yersinia pestis*, specifically required for bubonic plague. *Proc. Natl. Acad. Sci. U.S.A.* 103, 13514–13519. doi: 10.1073/pnas.0603456103
- Chakraborty, S., Sivaraman, J., Leung, K. Y., and Mok, Y. K. (2011). Two-component PhoB-PhoR regulatory system and ferric uptake regulator sense phosphate and iron to control virulence genes in type III and VI secretion systems of *Edwardsiella tarda*. *J. Biol. Chem.* 286, 39417–39430. doi: 10.1074/jbc.M111.295188
- Chen, L., Zou, Y., She, P., and Wu, Y. (2015). Composition, function, and regulation of T6SS in *Pseudomonas aeruginosa*. *Microbiol. Res.* 172, 19–25. doi: 10.1016/j.micres.2015.01.004



- Cianfanelli, F. R., Monlezun, L., and Coulthurst, S. J. (2016). Aim, load, fire: the type VI Secretion System, a bacterial nanoweapon. *Trends Microbiol.* 24, 51–62. doi: 10.1016/j.tim.2015.10.005
- Cornelis, G. R., Boland, A., Boyd, A. P., Geuijen, C., Iriarte, M., Neyt, C., et al. (1998). The virulence plasmid of *Yersinia*, an antihost genome. *Microbiol. Mol. Biol. Rev.* 62, 1315–1352.
- Dudley, E. G., Thomson, N. R., Parkhill, J., Morin, N. P., and Nataro, J. P. (2006). Proteomic and microarray characterization of the AggR regulon identifies a pheU pathogenicity island in enteroaggregative *Escherichia coli*. *Mol. Microbiol.* 61, 1267–1282. doi: 10.1111/j.1365-2958.2006.05281.x
- Durand, E., Cambillau, C., Cascales, E., and Journet, L. (2014). VgrG, Tae, Tle, and beyond: the versatile arsenal of type VI secretion effectors. *Trends Microbiol.* 22, 498–507. doi: 10.1016/j.tim.2014.06.004
- Gascuel, O. (1997). BIONJ: an improved version of the NJ algorithm based on a simple model of sequence data. *Mol. Biol. Evol.* 14, 685–695. doi: 10.1093/oxfordjournals.molbev.a025808
- Goldova, J., Ulrych, A., Hercik, K., and Branny, P. (2011). A eukaryotic-type signalling system of *Pseudomonas aeruginosa* contributes to oxidative stress resistance, intracellular survival and virulence. *BMC Genomics* 12:437. doi: 10.1186/1471-2164-12-437
- Guan, J., Xiao, X., Xu, S., Gao, F., Wang, J., Wang, T., et al. (2015). Roles of RpoS in *Yersinia pseudotuberculosis* stress survival, motility, biofilm formation and type VI secretion system expression. *J. Microbiol.* 53, 633–642. doi: 10.1007/s12275-015-0099-6
- Gueguen, E., Durand, E., Zhang, X. Y., d'Amalric, Q., Journet, L., and Cascales, E. (2013). Expression of a *Yersinia pseudotuberculosis* type VI secretion system is responsive to envelope stresses through the ompR transcriptional activator. *PLoS ONE* 8:e66615. doi: 10.1371/journal.pone.0066615
- Heesemann, J., Hantke, K., Vocke, T., Saken, E., Rakin, A., Stojiljkovic, I., et al. (1993). Virulence of *Yersinia-Enterocolitica* is closely associated with siderophore production, expression of an iron-repressible outer-membrane polypeptide of 65000 Da and pesticin sensitivity. *Mol. Microbiol.* 8, 397–408. doi: 10.1111/j.1365-2958.1993.tb01583.x
- Hood, R. D., Singh, P., Hsu, F., Guvener, T., Carl, M. A., Trinidad, R. R., et al. (2010). A type VI secretion system of *Pseudomonas aeruginosa* targets a toxin to bacteria. *Cell Host Microbe* 7, 25–37. doi: 10.1016/j.chom.2009.12.007
- Hu, Y., Lu, P., Wang, Y., Ding, L., Atkinson, S., and Chen, S. (2009). OmpR positively regulates urease expression to enhance acid survival of *Yersinia pseudotuberculosis*. *Microbiology* 155, 2522–2531. doi: 10.1099/mic.0.028381-0
- Ishikawa, T., Sabharwal, D., Broms, J., Milton, D. L., Sjostedt, A., Uhlin, B. E., et al. (2012). Pathoadaptive conditional regulation of the type VI secretion system in *Vibrio cholerae* O1 strains. *Infect. Immun.* 80, 575–584. doi: 10.1128/IAI.05510-11
- Jaakkola, K., Somervuo, P., and Korkeala, H. (2015). Comparative genomic hybridization analysis of *Yersinia enterocolitica* and *Yersinia pseudotuberculosis* identifies genetic traits to elucidate their different ecologies. *Biomed. Res. Int.* 2015:760494. doi: 10.1155/2015/760494
- Jani, A. J., and Cotter, P. A. (2010). Type VI secretion: not just for pathogenesis anymore. *Cell Host Microbe* 8, 2–6. doi: 10.1016/j.chom.2010.06.012
- Jiang, F., Wang, X., Wang, B., Chen, L., Zhao, Z., Waterfield, N. R., et al. (2016). The *Pseudomonas aeruginosa* type VI secretion PGAP1-like effector induces host autophagy by activating endoplasmic reticulum stress. *Cell Rep.* 16, 1502–1509. doi: 10.1016/j.celrep.2016.07.012
- Joshi, A., Kostiuik, B., Rogers, A., Teschler, J., Pukatzki, S., and Yildiz, F. H. (2017). Rules of engagement: the type VI secretion system in *Vibrio cholerae*. *Trends Microbiol.* 25, 267–279. doi: 10.1016/j.tim.2016.12.003
- Kitaoka, M., Miyata, S. T., Brooks, T. M., Unterwiesing, D., and Pukatzki, S. (2011). VasH is a transcriptional regulator of the type VI secretion system functional in endemic and pandemic *Vibrio cholerae*. *J. Bacteriol.* 193, 6471–6482. doi: 10.1128/JB.05414-11
- Lertpiriyapong, K., Gamazon, E. R., Feng, Y., Park, D. S., Pang, J., Botka, G., et al. (2012). *Campylobacter jejuni* type VI secretion system: roles in adaptation to deoxycholic acid, host cell adherence, invasion, and *in vivo* colonization. *PLoS ONE* 7:e42842. doi: 10.1371/journal.pone.0042842
- Li, J., Yao, Y., Xu, H. H., Hao, L., Deng, Z., Rajakumar, K., et al. (2015). SecReT6: a web-based resource for type VI secretion systems found in bacteria. *Environ. Microbiol.* 17, 2196–2202. doi: 10.1111/1462-2920.12794
- Lien, Y. W., and Lai, E. M. (2017). Type VI secretion effectors: methodologies and biology. *Front. Cell. Infect. Microbiol.* 7:254. doi: 10.3389/fcimb.2017.00254
- Lin, J., Zhang, W., Cheng, J., Yang, X., Zhu, K., Wang, Y., et al. (2017). A *Pseudomonas* T6SS effector recruits PQS-containing outer membrane vesicles for iron acquisition. *Nat. Commun.* 8:14888. doi: 10.1038/ncomms14888
- Liu, H., Coulthurst, S. J., Pritchard, L., Hedley, P. E., Ravensdale, M., Humphris, S., et al. (2008). Quorum sensing coordinates brute force and stealth modes of infection in the plant pathogen *Pectobacterium atrosepticum*. *PLoS Pathog.* 4:e1000093. doi: 10.1371/journal.ppat.1000093
- Ma, A. T., and Mekalanos, J. J. (2010). *In vivo* actin cross-linking induced by *Vibrio cholerae* type VI secretion system is associated with intestinal inflammation. *Proc. Natl. Acad. Sci. U.S.A.* 107, 4365–4370. doi: 10.1073/pnas.0915156107
- MacIntyre, D. L., Miyata, S. T., Kitaoka, M., and Pukatzki, S. (2010). The *Vibrio cholerae* type VI secretion system displays antimicrobial properties. *Proc. Natl. Acad. Sci. U.S.A.* 107, 19520–19524. doi: 10.1073/pnas.1012931107
- Mougous, J. D., Cuff, M. E., Raunser, S., Shen, A., Zhou, M., Gifford, C. A., et al. (2006). A virulence locus of *Pseudomonas aeruginosa* encodes a protein secretion apparatus. *Science* 312, 1526–1530. doi: 10.1126/science.1128393
- Murdoch, S. L., Trunk, K., English, G., Fritsch, M. J., Pourkarimi, E., and Coulthurst, S. J. (2011). The opportunistic pathogen *Serratia marcescens* utilizes type VI secretion to target bacterial competitors. *J. Bacteriol.* 193, 6057–6069. doi: 10.1128/JB.05671-11
- Parsons, D. A., and Heffron, F. (2005). *sciS*, an *icmF* homolog in *Salmonella enterica* serovar Typhimurium, limits intracellular replication and decreases virulence. *Infect. Immun.* 73, 4338–4345. doi: 10.1128/IAI.73.4.4338-4345.2005
- Pell, L. G., Kanelis, V., Donaldson, L. W., Howell, P. L., and Davidson, A. R. (2009). The phage lambda major tail protein structure reveals a common evolution for long-tailed phages and the type VI bacterial secretion system. *Proc. Natl. Acad. Sci. U.S.A.* 106, 4160–4165. doi: 10.1073/pnas.0900044106
- Pieper, R., Huang, S. T., Robinson, J. M., Clark, D. J., Alami, H., Parmar, P. P., et al. (2009). Temperature and growth phase influence the outer-membrane proteome and the expression of a type VI secretion system in *Yersinia pestis*. *Microbiology* 155, 498–512. doi: 10.1099/mic.0.022160-0
- Podladchikova, O., Antonenka, U., Heesemann, J., and Rakin, A. (2011). *Yersinia pestis* autoagglutination factor is a component of the type six secretion system. *Int. J. Med. Microbiol.* 301, 562–569. doi: 10.1016/j.ijmm.2011.03.004
- Ponnusamy, D., Fitts, E. C., Sha, J., Erova, T. E., Kozlova, E. V., Kirtley, M. L., et al. (2015). High-throughput, signature-tagged mutagenic approach to identify novel virulence factors of *Yersinia pestis* CO92 in a mouse model of infection. *Infect. Immun.* 83, 2065–2081. doi: 10.1128/IAI.02913-14
- Pujol, C., and Bliska, J. B. (2005). Turning *Yersinia* pathogenesis outside in: subversion of macrophage function by intracellular yersiniae. *Clin. Immunol.* 114, 216–226. doi: 10.1016/j.clim.2004.07.013
- Pukatzki, S., Ma, A. T., Sturtevant, D., Krastins, B., Sarracino, D., Nelson, W. C., et al. (2006). Identification of a conserved bacterial protein secretion system in *Vibrio cholerae* using the Dictyostelium host model system. *Proc. Natl. Acad. Sci. U.S.A.* 103, 1528–1533. doi: 10.1073/pnas.0510322103
- Putzker, M., Sauer, H., and Sobbe, D. (2001). Plague and other human infections caused by *Yersinia* species. *Clin. Lab.* 47, 453–466.
- Robinson, J. B., Telepnev, M. V., Zudina, I. V., Bouyer, D., Monteneri, J. A., Bearden, S. W., et al. (2009). Evaluation of a *Yersinia pestis* mutant impaired in a thermoregulated type VI-like secretion system in flea, macrophage and murine models. *Microb. Pathog.* 47, 243–251. doi: 10.1016/j.micpath.2009.08.005
- Rogers, A., Townsley, L., Gallego-Hernandez, A. L., Beyhan, S., Kwuan, L., and Yildiz, F. H. (2016). The LonA protease regulates biofilm formation, motility, virulence, and the type VI secretion system in *Vibrio cholerae*. *J. Bacteriol.* 198, 973–985. doi: 10.1128/JB.00741-15
- Russell, A. B., LeRoux, M., Hathazi, K., Agnello, D. M., Ishikawa, T., Wiggins, P. A., et al. (2013). Diverse type VI secretion phospholipases are functionally plastic antibacterial effectors. *Nature* 496, 508–512. doi: 10.1038/nature12074
- Russell, A. B., Peterson, S. B., and Mougous, J. D. (2014). Type VI secretion system effectors: poisons with a purpose. *Nat. Rev. Microbiol.* 12, 137–148. doi: 10.1038/nrmicro3185
- Russell, A. B., Singh, P., Brittnacher, M., Bui, N. K., Hood, R. D., Carl, M. A., et al. (2012). A widespread bacterial type VI secretion effector superfamily identified using a heuristic approach. *Cell Host Microbe* 11, 538–549. doi: 10.1016/j.chom.2012.04.007

- Salomon, D., Gonzalez, H., Updegraff, B. L., and Orth, K. (2013). *Vibrio parahaemolyticus* type VI secretion system 1 is activated in marine conditions to target bacteria, and is differentially regulated from system 2. *PLoS ONE* 8:e61086. doi: 10.1371/journal.pone.0061086
- Salomon, D., and Orth, K. (2015). Type VI secretion system. *Curr. Biol.* 25, R265–R266. doi: 10.1016/j.cub.2015.02.031
- Sana, T. G., Baumann, C., Merdes, A., Soscia, C., Rattei, T., Hachani, A., et al. (2015). Internalization of *Pseudomonas aeruginosa* strain PAO1 into epithelial cells is promoted by interaction of a T6SS effector with the microtubule network. *MBio* 6:e00712. doi: 10.1128/mBio.00712-15
- Schell, M. A., Ulrich, R. L., Ribot, W. J., Brueggemann, E. E., Hines, H. B., Chen, D., et al. (2007). Type VI secretion is a major virulence determinant in *Burkholderia mallei*. *Mol. Microbiol.* 64, 1466–1485. doi: 10.1111/j.1365-2958.2007.05734.x
- Schwarz, S., Singh, P., Robertson, J. D., LeRoux, M., Skerrett, S. J., Goodlett, D. R., et al. (2014). VgrG-5 is a *Burkholderia* type VI secretion system-exported protein required for multinucleated giant cell formation and virulence. *Infect. Immun.* 82, 1445–1452. doi: 10.1128/IAI.01368-13
- Schwarz, S., West, T. E., Boyer, F., Chiang, W. C., Carl, M. A., Hood, R. D., et al. (2010). *Burkholderia* type VI secretion systems have distinct roles in eukaryotic and bacterial cell interactions. *PLoS Pathog.* 6:e1001068. doi: 10.1371/journal.ppat.1001068
- Schwiesow, L., Lam, H., Dersch, P., and Auerbuch, V. (2015). *Yersinia* type III secretion system master regulator LcrF. *J. Bacteriol.* 198, 604–614. doi: 10.1128/JB.00686-15
- Shneider, M. M., Buth, S. A., Ho, B. T., Basler, M., Mekalanos, J. J., and Leiman, P. G. (2013). PAAR-repeat proteins sharpen and diversify the type VI secretion system spike. *Nature* 500, 350–353. doi: 10.1038/nature12453
- Si, M., Wang, Y., Zhang, B., Zhao, C., Kang, Y., Bai, H., et al. (2017a). The type VI secretion system engages a redox-regulated dual-functional heme transporter for zinc acquisition. *Cell Rep.* 20, 949–959. doi: 10.1016/j.celrep.2017.06.081
- Si, M., Zhao, C., Burkinshaw, B., Zhang, B., Wei, D., Wang, Y., et al. (2017b). Manganese scavenging and oxidative stress response mediated by type VI secretion system in *Burkholderia thailandensis*. *Proc. Natl. Acad. Sci. U.S.A.* 114, E2233–E2242. doi: 10.1073/pnas.1614902114
- Silverman, J. M., Brunet, Y. R., Cascales, E., and Mougous, J. D. (2012). Structure and regulation of the type VI secretion system. *Ann. Rev. Microbiol.* 66, 453–472. doi: 10.1146/annurev-micro-121809-151619
- Song, Y., Xiao, X., Li, C., Wang, T., Zhao, R., Zhang, W., et al. (2015). The dual transcriptional regulator RovM regulates the expression of AR3- and T6SS4-dependent acid survival systems in response to nutritional status in *Yersinia pseudotuberculosis*. *Environ. Microbiol.* 17, 4631–4645. doi: 10.1111/1462-2920.12996
- Southey-Pillig, C. J., Davies, D. G., and Sauer, K. (2005). Characterization of temporal protein production in *Pseudomonas aeruginosa* biofilms. *J. Bacteriol.* 187, 8114–8126. doi: 10.1128/JB.187.23.8114-8126.2005
- Suarez, G., Sierra, J. C., Sha, J., Wang, S., Erova, T. E., Fadl, A. A., et al. (2008). Molecular characterization of a functional type VI secretion system from a clinical isolate of *Aeromonas hydrophila*. *Microb. Pathog.* 44, 344–361. doi: 10.1016/j.micpath.2007.10.005
- Tian, Y., Zhao, Y., Wu, X., Liu, F., Hu, B., and Walcott, R. R. (2015). The type VI protein secretion system contributes to biofilm formation and seed-to-seedling transmission of *Acidovorax citrulli* on melon. *Mol. Plant Pathol.* 16, 38–47. doi: 10.1111/mpp.12159
- Wang, M., Luo, Z., Du, H., Xu, S., Ni, B., Zhang, H., et al. (2011). Molecular characterization of a functional type VI secretion system in *Salmonella enterica* serovar Typhi. *Curr. Microbiol.* 63, 22–31. doi: 10.1007/s00284-011-9935-z
- Wang, T., Chen, K., Gao, F., Kang, Y., Chaudhry, M. T., Wang, Z., et al. (2017). ZntR positively regulates T6SS4 expression in *Yersinia pseudotuberculosis*. *J. Microbiol.* 55, 448–456. doi: 10.1007/s12275-017-6540-2
- Wang, T., Si, M., Song, Y., Zhu, W., Gao, F., Wang, Y., et al. (2015). Type VI secretion system transports  $Zn^{2+}$  to combat multiple stresses and host immunity. *PLoS Pathog.* 11:e1005020. doi: 10.1371/journal.ppat.1005020
- Wang, T. T., Yang, X. B., Gao, F., Zhao, C., Kang, Y. W., Wang, Y., et al. (2016). Zinc acquisition via ZnuABC in *Yersinia pseudotuberculosis* facilitates resistance to oxidative stress. *Ann. Microbiol.* 66, 1189–1197. doi: 10.1007/s13213-016-1205-7
- Weber, B., Croxatto, A., Chen, C., and Milton, D. L. (2008). RpoS induces expression of the *Vibrio anguillarum* quorum-sensing regulator VanT. *Microbiology* 154, 767–780. doi: 10.1099/mic.0.2007/014167-0
- Weber, B., Hasic, M., Chen, C., Wai, S. N., and Milton, D. L. (2009). Type VI secretion modulates quorum sensing and stress response in *Vibrio anguillarum*. *Environ. Microbiol.* 11, 3018–3028. doi: 10.1111/j.1462-2920.2009.02005.x
- Yang, X., Long, M., and Shen, X. (2018). Effector(-)immunity pairs provide the T6SS nanomachine its offensive and defensive capabilities. *Molecules* 23:E1009. doi: 10.3390/molecules23051009
- Yu, Y., Fang, L., Zhang, Y., Sheng, H., and Fang, W. (2015). VgrG2 of type VI secretion system 2 of *Vibrio parahaemolyticus* induces autophagy in macrophages. *Front. Microbiol.* 6:168. doi: 10.3389/fmicb.2015.00168
- Zhang, L., Hinz, A. J., Nadeau, J. P., and Mah, T. F. (2011a). *Pseudomonas aeruginosa* tssC1 links type VI secretion and biofilm-specific antibiotic resistance. *J. Bacteriol.* 193, 5510–5513. doi: 10.1128/JB.00268-11
- Zhang, W., Wang, Y., Song, Y., Wang, T., Xu, S., Peng, Z., et al. (2013). A type VI secretion system regulated by OmpR in *Yersinia pseudotuberculosis* functions to maintain intracellular pH homeostasis. *Environ. Microbiol.* 15, 557–569. doi: 10.1111/1462-2920.12005
- Zhang, W., Xu, S., Li, J., Shen, X., Wang, Y., and Yuan, Z. (2011b). Modulation of a thermoregulated type VI secretion system by AHL-dependent quorum sensing in *Yersinia pseudotuberculosis*. *Arch. Microbiol.* 193, 351–363. doi: 10.1007/s00203-011-0680-2
- Zheng, J., and Leung, K. Y. (2007). Dissection of a type VI secretion system in *Edwardsiella tarda*. *Mol. Microbiol.* 66, 1192–1206. doi: 10.1111/j.1365-2958.2007.05993.x
- Zheng, J., Shin, O. S., Cameron, D. E., and Mekalanos, J. J. (2010). Quorum sensing and a global regulator TsrA control expression of type VI secretion and virulence in *Vibrio cholerae*. *Proc. Natl. Acad. Sci. U.S.A.* 107, 21128–21133. doi: 10.1073/pnas.1014998107
- Zoued, A., Brunet, Y. R., Durand, E., Aschtgen, M. S., Logger, L., Douzi, B., et al. (2014). Architecture and assembly of the type VI secretion system. *Biochim. Biophys. Acta* 1843, 1664–1673. doi: 10.1016/j.bbamcr.2014.03.018

**Conflict of Interest Statement:** The authors declare that the research was conducted in the absence of any commercial or financial relationships that could be construed as a potential conflict of interest.

Copyright © 2018 Yang, Pan, Wang and Shen. This is an open-access article distributed under the terms of the Creative Commons Attribution License (CC BY). The use, distribution or reproduction in other forums is permitted, provided the original author(s) and the copyright owner(s) are credited and that the original publication in this journal is cited, in accordance with accepted academic practice. No use, distribution or reproduction is permitted which does not comply with these terms.



# Changes in Transcriptome of *Yersinia pseudotuberculosis* IP32953 Grown at 3 and 28°C Detected by RNA Sequencing Shed Light on Cold Adaptation

Jussa-Pekka Virtanen, Riikka Keto-Timonen\*, Kaisa Jaakkola, Noora Salin and Hannu Korkeala

Department of Food Hygiene and Environmental Health, Faculty of Veterinary Medicine, University of Helsinki, Helsinki, Finland

## OPEN ACCESS

### Edited by:

Victoria Auerbuch,  
University of California, Santa Cruz,  
United States

### Reviewed by:

Karl M. Thompson,  
Howard University, United States  
Michael Marceau,  
Université Lille Nord de France, France

### \*Correspondence:

Riikka Keto-Timonen  
riikka.keto-timonen@helsinki.fi

### Specialty section:

This article was submitted to  
Molecular Bacterial Pathogenesis,  
a section of the journal  
Frontiers in Cellular and Infection  
Microbiology

**Received:** 07 May 2018

**Accepted:** 09 November 2018

**Published:** 27 November 2018

### Citation:

Virtanen J-P, Keto-Timonen R,  
Jaakkola K, Salin N and Korkeala H  
(2018) Changes in Transcriptome of  
*Yersinia pseudotuberculosis* IP32953  
Grown at 3 and 28°C Detected by  
RNA Sequencing Shed Light on Cold  
Adaptation.  
Front. Cell. Infect. Microbiol. 8:416.  
doi: 10.3389/fcimb.2018.00416

*Yersinia pseudotuberculosis* is a bacterium that not only survives, but also thrives, proliferates, and remains infective at cold-storage temperatures, making it an adept foodborne pathogen. We analyzed the differences in gene expression between *Y. pseudotuberculosis* IP32953 grown at 3 and 28°C to investigate which genes were significantly more expressed at low temperature at different phases of growth. We isolated and sequenced the RNA from six distinct corresponding growth points at both temperatures to also outline the expression patterns of the differentially expressed genes. Genes involved in motility, chemotaxis, phosphotransferase systems (PTS), and ATP-binding cassette (ABC) transporters of different nutrients such as fructose and mannose showed higher levels of transcripts at 3°C. At the beginning of growth, especially genes involved in securing nutrients, glycolysis, transcription, and translation were upregulated at 3°C. To thrive as well as it does at low temperature, *Y. pseudotuberculosis* seems to require certain cold shock proteins, especially those encoded by *yptb3585*, *yptb3586*, *yptb2414*, *yptb2950*, and *yptb1423*, and transcription factors, like Rho, IF-1, and RbfA, to maintain its protein synthesis. We also found that genes encoding RNA-helicases CsdA (*yptb0468*), RhlE (*yptb1214*), and DbpA (*yptb1652*), which unwind frozen secondary structures of nucleic acids with cold shock proteins, were significantly more expressed at 3°C, indicating that these RNA-helicases are important or even necessary during cold. Genes involved in excreting poisonous spermidine and acquiring compatible solute glycine betaine, by either uptake or biosynthesis, showed higher levels of transcripts at low temperatures. This is the first finding of a strong connection between the aforementioned genes and the cold adaptation of *Y. pseudotuberculosis*. Understanding the mechanisms behind the cold adaptation of *Y. pseudotuberculosis* is crucial for controlling its growth during cold storage of food, and will also shed light on microbial cold adaptation in general.

**Keywords:** cold stress, stress tolerance, compatible solute, RNA helicase, cold shock protein, transcription factor

## INTRODUCTION

*Yersinia pseudotuberculosis* is an enteropathogenic bacterium that causes the foodborne infection yersiniosis. Although it has an optimum growth temperature of around 28°C, *Y. pseudotuberculosis* can grow and multiply at cold-storage temperatures, even as low as 0°C (Keto-Timonen et al., 2018). Long storage at low temperature favors the growth of psychrotrophs like *Y. pseudotuberculosis*, as they can proliferate without much competition. Outbreaks of *Y. pseudotuberculosis* have been associated with vegetables, raw milk, and drinking untreated water (Sato and Komazawa, 1991; Nuorti et al., 2004; Rimhanen-Finne et al., 2009; Pärn et al., 2015). In order to survive the various ecological niches through which it could enter the food chain, *Y. pseudotuberculosis* carries many tools in its genome, such as operons for the transport of substrates more abundant in plants and soil than animal tissue, as well as type VI secretion systems (Jaakkola et al., 2015). The bacterium has been found in the intestines of many animals like domestic pigs, goats, sheep, wild lagomorphs, birds, rodents, and shrews (Niskanen et al., 2003; Laukkanen et al., 2008; Giannitti et al., 2014; Le Guern et al., 2016; Joutsen et al., 2017). It can also thrive in soil as well as in certain protozoans and nematodes (Buzoleva and Somov, 2003; Gengler et al., 2015; Santos-Montañez et al., 2015).

Adaptation to cold and long-term growth at low temperatures poses many challenges to bacteria. Low temperature decreases the fluidity of cell membranes, thereby interfering with normal membrane protein function. It also slows down protein folding, ribosomes, and translation as well as excessively stabilizes nucleic acid structures (Palonen et al., 2010). Cold also induces radical oxygen species production by both slowing metabolism and increasing oxygen solubility (Chattopadhyay et al., 2011). Psychrotrophic bacteria have many methods to deal with these problems. For example, bacteria can increase membrane fluidity by introducing unsaturated lipids that no longer fit as snugly together (Suutari and Laakso, 1994). Unsaturated fatty acids dominate the fatty acid composition of *Y. pseudotuberculosis* at low temperatures (Bakholdina et al., 2004).

Cold shock proteins (Csp) are small proteins whose mRNA carries a cold shock domain that enables its translation at low temperatures. Csps, along with helicases and translation factors exhibiting similar stabilizing secondary structures, unwind mRNA and support the translational apparatus at low temperatures. *Y. pseudotuberculosis* has nine *csp* genes, homologous to those of *Escherichia coli*, five of which are induced at low temperature in *E. coli* (Keto-Timonen et al., 2016). The bacterium also has five helicases with a conserved DEAD-box motif: CsdA (*yptb0486*), RhlE (*yptb1214*), RhlB (*yptb0165*), DbpA (*yptb1652*), and SrmA (*yptb2900*).

The main goal of this study was to determine how *Y. pseudotuberculosis* manages to thrive at refrigerator temperature. We identified which genes showed significantly more transcripts at 3°C when compared to 28°C, at each growth phase, mainly focusing on the beginning of growth and logarithmic phase. Of all cold shock proteins, those encoded by *yptb1423*, *yptb3585*, *yptb3586*, and especially *yptb2414* and *yptb2950*, showed significantly more transcripts at low temperature,

seemingly forming the backbone of cold acclimation of *Y. pseudotuberculosis*. Furthermore, we found that, in addition to CsdA, helicases RhlE, and DbpA were significantly upregulated at low temperature, which speaks to their importance in surviving low temperatures. The bacterium also seems to accumulate glycine betaine by uptake and biosynthesis, as the corresponding genes were upregulated at low temperature. Transcription termination factor Rho, along with IF-1 and RbfA, both acting on ribosomes, were also upregulated, which would seem to suggest that they play an important role. None of these genes and proteins have, to our knowledge, been linked to cold acclimation of *Y. pseudotuberculosis* before.

## MATERIALS AND METHODS

### Bacterial Strain and Growth Conditions

Single *Y. pseudotuberculosis* IP32953 colonies grown on blood agar plates at 28°C were inoculated and grown separately in LB broth (Luria-Bertani; Sigma-Aldrich, St. Louis, MO, USA) at 28°C with shaking overnight. Overnight broths were diluted (1:100) in LB broth and divided into two groups so that four cultures (biological replicates) were grown with shaking both at 3°C and at 28°C. Biological replicates were used to better model true biological variability and improve the accuracy of statistical methods. Samples for total RNA extraction were collected at six corresponding points at different phases of growth across both temperatures (Figure 1). For total RNA extraction 1.25 ml of bacterial culture was mixed with 250 µl cold phenol-ethanol mixture (1:10) and kept on ice for 30 min. After incubation, samples were centrifuged at 4°C at 13,200 rpm for 2 min and the resulting cell pellets were stored at −70°C until RNA isolation.

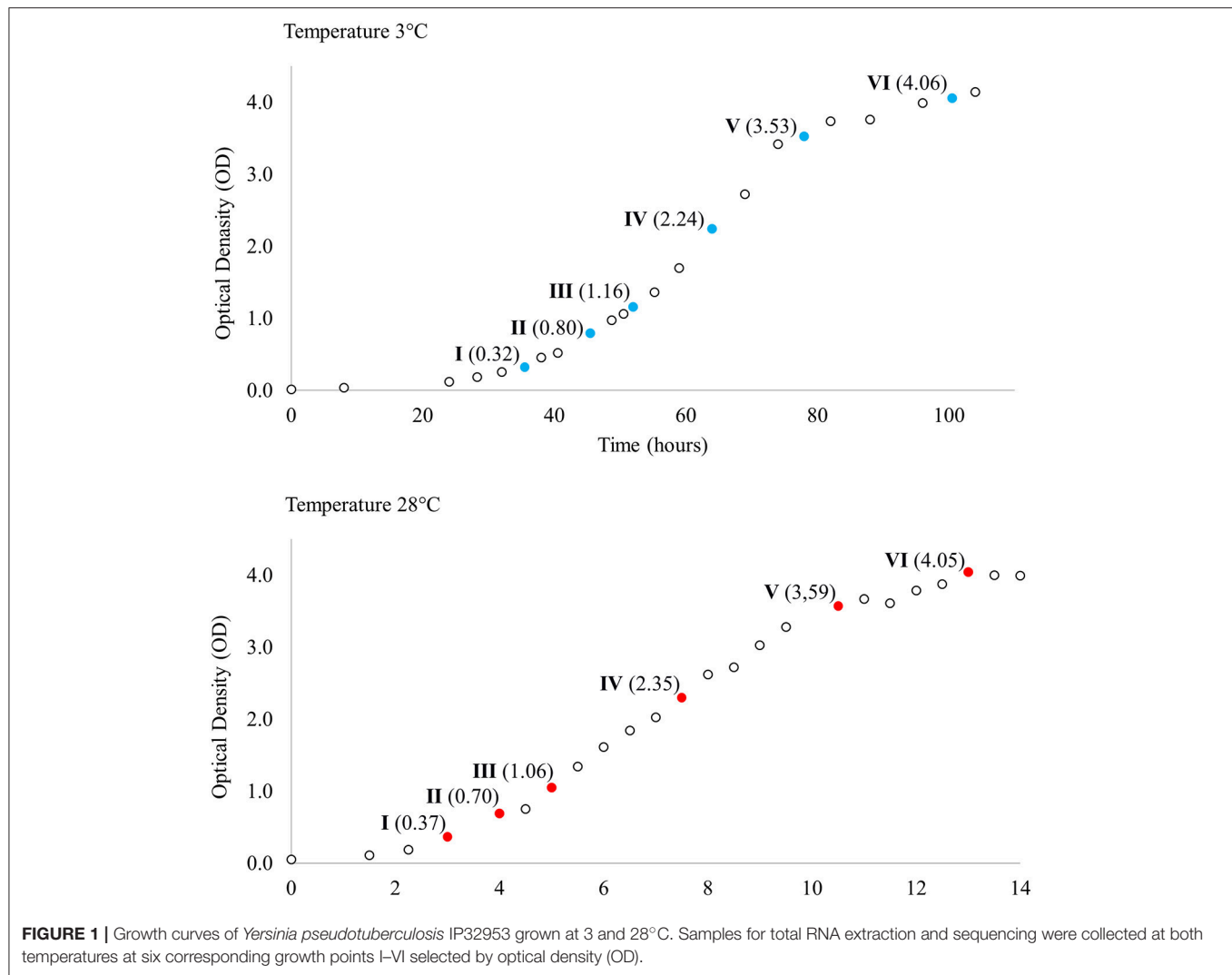
### RNA Isolation

Total RNA was isolated using GeneJET RNA Purification Kit (Thermo Fisher Scientific, Waltham, MA, USA) and treated with DNA-Free DNA Removal Kit (Ambion, Life Technologies, Carlsbad, CA, USA) according to manufacturers' instructions. The quantity and quality of RNA was examined with a Nanodrop ND-1000 Spectrophotometer (Thermo Fisher Scientific) and Agilent 2100 Bioanalyzer (Agilent Technologies, Santa Clara, CA, USA). RNA was stored at −70°C until RNA-seq library preparation.

### Library Preparation and Sequencing

Ribosomal RNA was depleted from total RNA using Ribo-Zero rRNA Removal Kit for Bacteria (Epicenter, Madison, WI, USA) following the manufacturer's protocol. cDNA libraries were prepared using Script-Seq v2 RNA-Seq Library Preparation Kit (Epicenter) following the manufacturer's instructions. The libraries were amplified twice by PCR and barcoded. PCR was performed using Phusion High-Fidelity DNA Polymerase Kit (Thermo Fisher Scientific). The libraries were purified using AMPure XP System (Beckman Coulter, Brea CA, USA) after both PCR procedures. The libraries were sequenced (75 bp single read) using the Illumina NextSeq500 platform at the Institute of Biotechnology, University of Helsinki, yielding four sets of sequence reads (biological replicates) per growth point at both





3 and 28°C. Raw sequences were deposited in the Sequence Read Archive (<http://www.ncbi.nlm.nih.gov/sra>) under accession number SRP144570.

### cDNA Synthesis and RT-qPCR

To confirm the differences of transcript levels identified in the RNA-sequence expression analysis, RT-qPCR validation was performed for selected genes (*betB*, *csdA*, *fabF*, *infA*, *mdtI*, *proX*, *rhIE*, and *rho*) at growth points I and III at both temperatures (3 and 28°C). These genes or operons they represent are discussed in detail in this paper. A total of 500 ng of each RNA sample from three biological replicates per growth point was reverse-transcribed into cDNA in duplicate by using Maxima cDNA Synthesis Kit (Thermo Fisher Scientific) according to manufacturer's instructions. Primers for RT-qPCR were designed using Primer-BLAST software ((Ye et al., 2012); **Table 1**). Two replicate qPCR reactions for each cDNA sample were performed using the Dynamo Flash SYBR Green qPCR Kit (Thermo Scientific). Each reaction consisted of 1x Master Mix, 0.5 μM of forward and reverse primer and 4 μl of 1:20 (gene of interest)

or 1:100,000 (16S *rrn*) diluted cDNA in a total volume of 20 μl. Rotor-Gene Q thermal cycler (Qiagen GmbH, Hilden Germany) was used in PCR runs with the cycling protocol consisting of initial heating step at 95°C for 7 min, followed by 40 cycles of denaturation at 95°C for 10 s, annealing at 60°C for 15 s, extension at 72°C for 20 s, and a final extension at 60°C for 1 min. After each run a melt curve analysis was done to confirm specificity. Amplification reaction efficiencies for each primer pair were obtained from RT-qPCR standard curves prepared from serial dilutions of pooled cDNA samples. The duplicate  $C_q$  values for PCR replicates were averaged. The relative quantification of gene of interest transcript levels at 3°C, normalized to reference gene (16S *rrn*) transcript levels and calibrated to the samples taken at the same growth point at 28°C, were calculated using the Pfaffl method (Pfaffl, 2001). Given near equal primer efficiencies, the logFC values of Pfaffl gene expression ratios between 3 and 28°C should be proportional to the logFC values acquired by RNA-Seq. A linear regression analysis was performed on corresponding logFC values of RNA-Seq and RT-qPCR.

**TABLE 1** | Primers used in quantitative real-time reverse transcription-PCR.

Gene	Forward primer (5' → 3')	Reverse primer (5' → 3')
16S rRNA gene	GCTCGTGTGTGAATGTTGG	TATGTGGTCCGCTGGCTCT
<i>betB</i>	AGGATTTGAACCGTGCCCAT	GCTGATACCGTTTTACGGC
<i>csdA</i>	GTGATGTTGGCGAGATGGAG	ATCGTTGAGTGGGAAGCAAA
<i>fabF</i>	ATGCTGATGTCATGGTGGCT	TGCTGCTTGTGGTTATCGT
<i>infA</i>	TCTTGATACGCTGCCGAACA	TGACTTTGTACCCGTCAGG
<i>mdtI</i>	CCCGCCAGCAGTAAGATCAA	ATGTGGGGCGGTTTTGGTAT
<i>proX</i>	GATAACCTGTGCCAAGCCT	GATGCAACCTATCTGGCGGT
<i>rhlE</i>	ATAGCGGCAAGGTGAAACCA	ATCCTGCGTGCTGTTGAAGA
<i>rho</i>	CGTTAGTTTTCGCAGTCGCC	CCGCTCTGGTACCCGTAAG

## Alignment and Annotation of RNA-Seq Data

We aligned, annotated, and analyzed the sequence reads with Bioconductor (Huber et al., 2015). The complete reference genome sequence and genomic features of *Y. pseudotuberculosis* IP32953 (Johnson et al., 2015) were acquired from the Pathosystems Resource Integration Center, PATRIC (Wattam et al., 2014). The sequence reads were both aligned to the reference genome, allowing a maximum of 10 hits, and annotated with Bioconductor package QuasR (Gaidatzis et al., 2015).

## Differential Gene Expression Analysis

One of the replicates of growth point IV at 28°C was discarded for its low alignment quality. The remaining annotated transcript counts were analyzed using Bioconductor package baySeq (Hardcastle and Kelly, 2010). Low count reads were filtered out. The replicate counts for each growth point at 3°C were compared to the counts of the respective growth point at 28°C. The prior distributions were acquired using a negative binomial distribution whose parameters were estimated by quasi-maximum-likelihood methods with a sample size of 10,000. The posterior likelihoods were established using 10 iterations to re-estimate the priors. Results were normalized by library size and results with FDR > 0.05 were discarded. Log<sub>2</sub> fold changes (logFC) across the two temperatures were calculated using transcript count averages of replicates, and genes with logFC ≥ 2 were considered significantly expressed at 3°C. For ease of viewing, genes were further grouped into operons retrieved from ProOpDB (Taboada et al., 2012). Amino acid sequence similarities were derived from multiple sequence alignment by Clustal Omega (Sievers et al., 2011). Upregulated genes sharing similar functions were classified into functional units (modules), acquired from the KEGG database (Kanehisa and Goto, 2000), using Bioconductor package clusterProfiler (Yu et al., 2012). *P*-values were adjusted for multiple comparisons by controlling the false discovery rate, using the Benjamini & Hochberg method implemented in clusterProfiler (Benjamini and Hochberg, 1995).

## Clustering

Expression profiles of genes that were significantly more expressed at low temperature, at least at one growth point, were

clustered using Pearson correlation distance. Count data was normalized for visualization by using median ratio normalization implemented in Bioconductor package DESeq2 (Love et al., 2014). Averages of replicate counts were used instead of individual counts. Normalized data for each gene (rows) across all growth points (columns) was then plotted in a heatmap (Figure 2).

## RESULTS

Expression profiles of *Y. pseudotuberculosis* IP32953 grown at 3 and 28°C were compared at corresponding phases of the growth based on growth curves determined by the optical density. We found 570 genes in total that showed significantly more transcripts at 3°C than 28°C at least at one of the growth points I–VI (Table 2). Motility and chemotaxis genes were at the top throughout growth since *Y. pseudotuberculosis* is non-motile at 28°C. The total number of upregulated genes was 482 when motility, chemotaxis, and tRNA genes were filtered out. Growth point VI held the fewest significantly expressed genes (*N* = 125) whereas growth points II and IV held the most (*N* = 162; Table 2). The difference in expression was largest for genes involved in motility, with a maximum logFC of 7.42.

A gene that was expressed both differentially and in great numbers at 3°C probably plays an important role in cold growth. We clustered expression profiles of genes that at least once during growth showed more transcripts at 3°C than at 28°C. Five subclusters (A–E) could be identified in the expression profile heatmap (Figure 2). The genes of most interest in the context of cold growth express highly at the beginning and logarithmic phases of growth, clustered into subclusters B–E (see details in Supplementary Material). Subcluster A mostly held genes that were expressed highly at the stationary phase.

## Validation of RNA Sequencing Results With RT-qPCR

The expression profiles of eight differentially expressed genes at two different growth points were evaluated by RT-qPCR and compared with the RNA-seq analysis results. In linear regression analysis between the RNA-seq and RT-qPCR logFC values (Figure 3), a 0.93 Pearson correlation coefficient value (*R*<sup>2</sup> = 0.85) was observed, which confirmed the reproducibility and reliability of the RNA-seq method (Figure 3).

## Differentially Expressed Genes by Growth Point

At growth point I, genes involved in acquiring compatible solutes and various nutrients showed significantly more transcripts at 3°C, and this pattern continued until stationary phase (Figure 4). For example, a significant increase in transcripts at 3°C was displayed in the following genes: genes encoding a glycine betaine transporter (*yptb2959–61*); phosphotransferase systems (PTS) to import fructose (*yptb1329–31*; Figure 5), N-acetylglucosamine (*yptb1120*, *yptb3075–82*), and L-ascorbate (*yptb2600–2*; Figure 5); and ATP-binding cassette (ABC) transporters of maltose (*yptb2521*, *yptb3095–102*) and

### Expression profiles of differentially expressed genes at 3°C

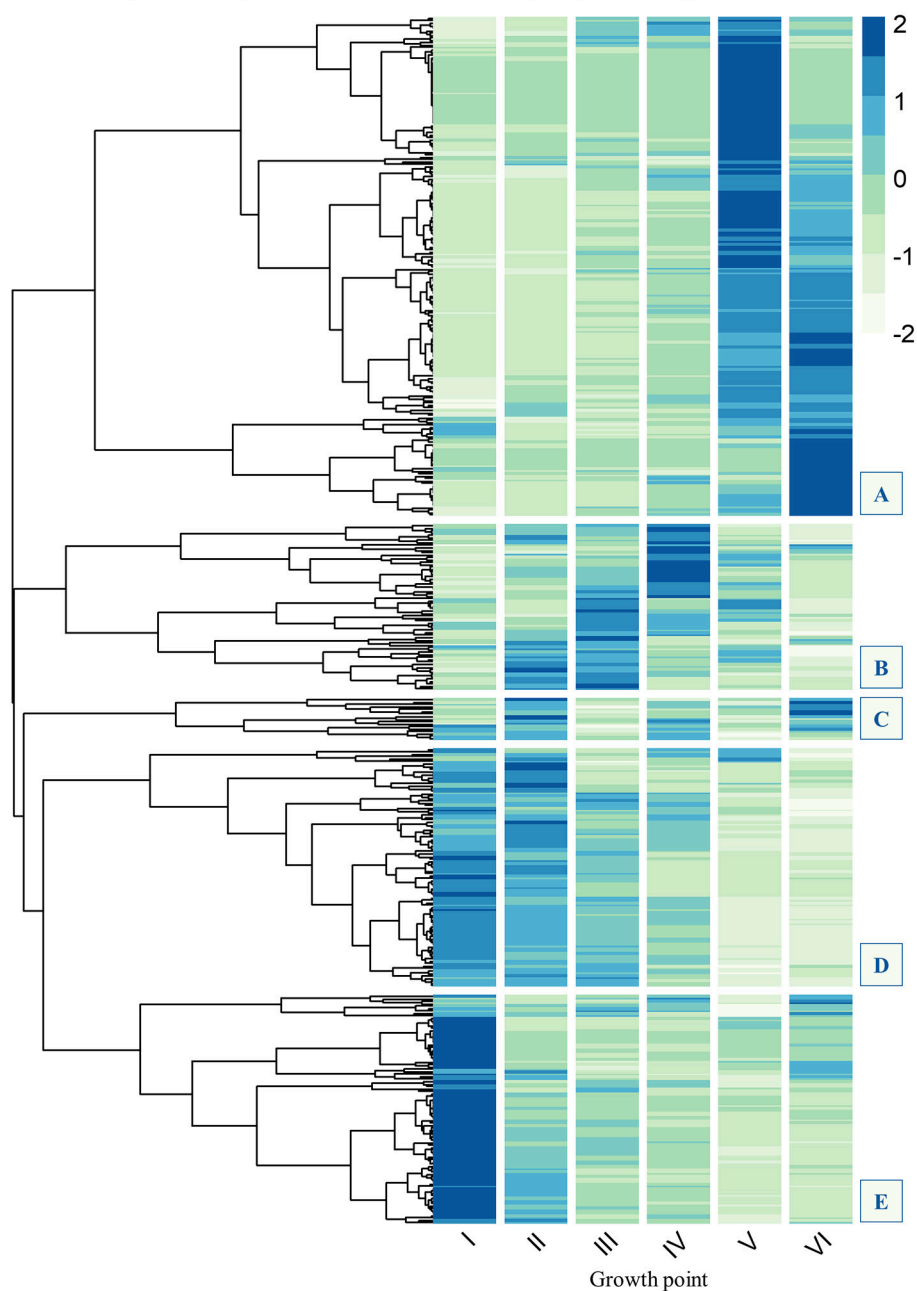


**FIGURE 2 |** Gene expression profile clustering of *Yersinia pseudotuberculosis* strain IP32953 genes that showed significantly more transcripts ( $\log_{2}FC \geq 2$ ,  $FDR \leq 0.05$ ) at 3°C than 28°C at least once during growth. The tree has been cut to five subclusters (A–E). Subclusters (B–E) are of most interest because they comprise genes that express highly at the beginning and logarithmic phase of growth. Subcluster A consists of genes whose expression mainly peaks at stationary phase. Flagellar assembly (Figure S1) and chemotaxis genes (Figure S2) have been left out as *Y. pseudotuberculosis* is not motile at 28°C. In addition, tRNA-genes (Figure S3) have been filtered out, so that the final  $N = 482$ . The darker the color in the heatmap, the more transcripts the gene showed at that growth point.

aldopentoses (*yptb3591–6*). A significant portion of upregulated genes at this growth point were associated with different PTSs and glycine betaine transport (Figure 4). As expected, genes encoding chaperone molecules such as helicase RhIE (*yptb1214*) and Csp's (*yptb2950*, *yptb2414*, *yptb3585*, and *yptb3586*), which

destabilize nucleic acid secondary structures, showed more transcripts at 3°C.

At growth point II, genes involved in further processing of compatible solutes, spermidine efflux, synthesizing desaturated membrane lipids, biosynthesis of ribosomes, securing translation

**TABLE 2** | The number of *Yersinia pseudotuberculosis* strain IP32953 genes expressed significantly more at 3°C than at 28°C by growth point.

Growth point (OD)	logFC	
	≥2	≥4
I (0.32–0.37)	134	27
II (0.69–0.80)	162	13
III (1.05–1.17)	139	9
IV (2.24–2.30)	162	9
V (3.53–3.57)	129	7
VI (4.05–4.06)	125	8

Flagellar assembly and chemotaxis genes have been disregarded as *Y. pseudotuberculosis* is not motile at 28°C; and tRNA-genes have also been filtered out.

under cold stress, and posttranscriptional modification of RNA molecules showed significantly more transcripts at 3°C. Modules of different amino acid transporters and betaine synthesis were overexpressed (**Figure 4**). Genes encoding translation factors IF-1 (*yptb1395*) and Rho factor (*yptb0167*) peaked at this growth point. New additions to differentially expressed chaperone genes were helicase gene *dbpA* (*yptb1652*) and a new Csp gene (*yptb1423*).

At growth point III, a urease operon (*yptb2938–44*) and PTSs to import fructose (**Figure 5**), N-acetylglucosamine, and mannose showed significantly more transcripts at 3°C than 28°C. The gene encoding superoxide dismutase (*yptb3925*) also showed more transcripts at 3°C at this growth point. At growth point IV, it seems the nutrient strategy shifted as an operon involved in sulfur metabolism (*yptb2309–14*) was expressed more at 3°C than 28°C. In addition to genes encoding IF-1 and Rho factor, a new translation factor gene *rbfA* (*yptb0481*) showed more transcripts at 3°C at this point of growth.

At growth points V and VI, the nutrient strategy continued shifting as operons involved in the metabolism of histidine (*yptb1965–9*, *yptb3851–2*; **Figure 5**), cystine (*yptb1717–20*; **Figure 5**), methionine (*yptb2973–5*; **Figure 5**), and nitrogen compounds (*yptb0022–3*) showed more transcripts at 3°C. At the same time, Csp gene expression levels and differences tapered off. The gene encoding helicase CsdA (*yptb0486*) was significantly more expressed at 3°C at growth point III, but at 28°C at growth points V and VI. An operon encoding a system that utilizes autoinducer AI-2 showed significantly more transcripts at growth point V.

## Expression of Cold Shock Protein Genes

Of all the Csp genes, *yptb2414* showed most transcripts at 3°C from the beginning of growth throughout the logarithmic growth phase (**Figure 6**). Its difference in expression between 3 and 28°C was significant at all growth points and the largest of all Csp genes. Gene *yptb1624* was expressed significantly more at 28°C (**Figure 6**). Gene *yptb2950* showed many more transcripts at 3°C at growth points I–IV, with a peak logFC of over 7 (**Figure 6**). Its transcription counts dipped after growth point I and decreased toward stationary phase. Gene *yptb1423* was expressed at lower levels, but showed significantly more transcripts at 3°C throughout growth points II–IV (**Figure 6**).

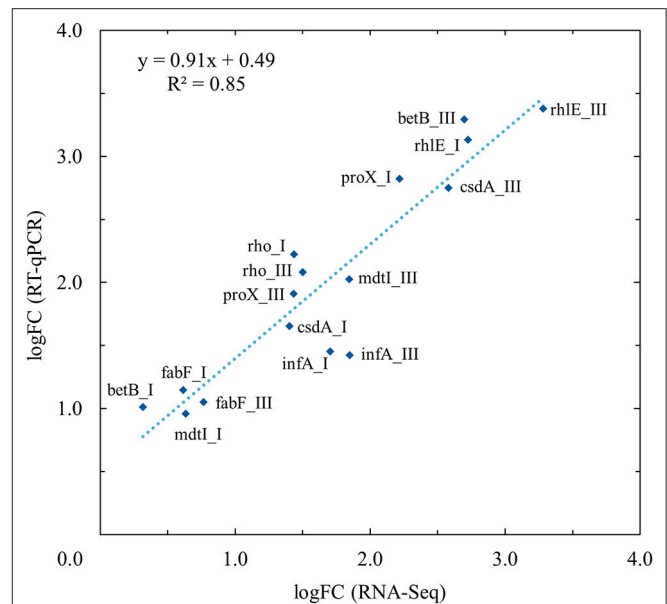


**FIGURE 3** | Validation of RNA-Seq results with quantitative real-time reverse-transcription PCR (RT-qPCR) using linear regression analysis. RT-qPCR validation was performed for selected genes (*betB*, *csdA*, *fabF*, *infA*, *mdtI*, *proX*, *rhIE*, and *rho*) at growth points I and III at both temperatures (3 and 28°C). Linear regression analysis showed an  $R^2$  coefficient of determination value of 0.85 between the RNA-Seq and RT-qPCR  $\log_2$  fold changes (logFC).

Nearly identical genes, *yptb3585* and *yptb3586*, were expressed highly at growth point I, but their expression levels dipped right after (**Figure 7**). However, the differences in their expression between 3 and 28°C consistently favored cold at significant levels. Expression levels of *yptb3587* and *yptb1088* rose toward the stationary phase at 3°C, but the difference between 3 and 28°C was not significant. After starting growth, *yptb3587* appeared slightly downregulated (**Figure 7**). Gene *yptb1392* was expressed much in the same way, but showed significantly more transcripts at 28°C at the stationary phase of growth (**Figure 7**).

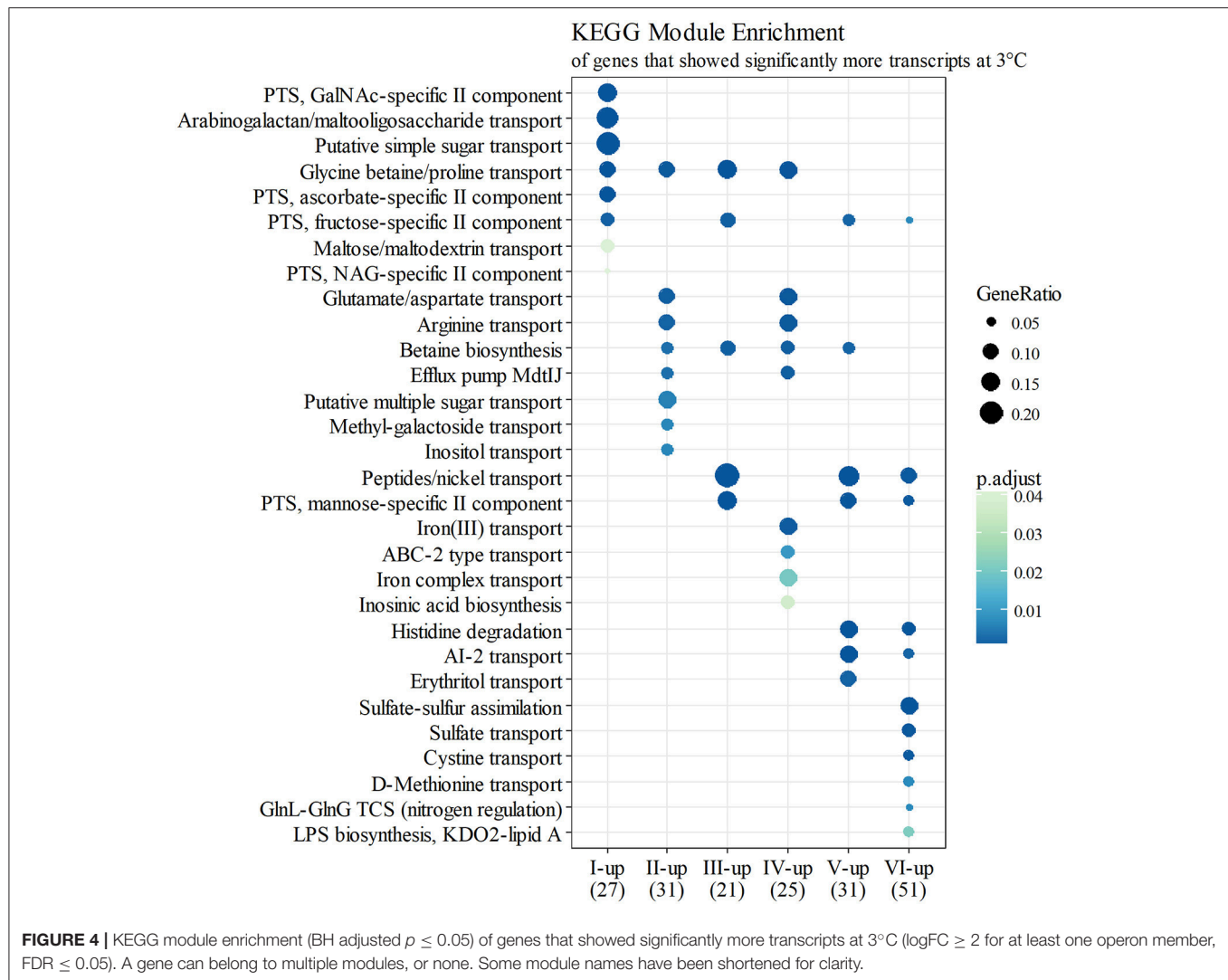
## Expression of DEAD-Box RNA Helicase Genes

*Y. pseudotuberculosis* has five helicases with a conserved DEAD-box motif: CsdA (*yptb0486*), RhlE (*yptb1214*), RhlB (*yptb0165*), DbpA (*yptb1652*), and SrmA (*yptb2900*). All the helicase genes were expressed more at 3°C throughout growth (**Figure 8**), but the difference was significant for *csdA* (*yptb0486*) at growth point III, *rhIE* (*yptb1214*) at growth points I–IV, and *dbpA* (*yptb1652*) at growth points II and IV.

## Expression of Genes Handling Compatible Solutes

Genes *yptb2959–61* form the *proU* operon that encodes a transport system for glycine betaine and proline; genes *yptb1195–98* form the *betIBA–betT* divergent operon that is involved in glycine betaine biosynthesis; and genes *yptb2052* and *yptb2051* form the *mdtII* operon that encodes a spermidine efflux





pump. Operon *proU* showed significantly more transcripts at 3°C at growth points I–IV (Figure 9), operon *betIBA-betT* at growth points II–IV (Figure 10), and operon *mdtIJ* at II and IV (Figure 11). Corresponding functional modules were also overexpressed at growth points I–IV for operon *proU*, points II–V for operon *betIBA-betT*, and points II and IV for operon *mdtIJ* (Figure 4). Another glycine betaine and L-proline transporter encoding gene *proP* (*yptb0608*) showed more transcripts at 3°C throughout the growth, but not quite at significant levels (Figure 9).

### Expression of Genes Encoding Rho Factor, IF-1, and RbfA

Genes *rho* (*yptb0167*), *infA* (*yptb1395*), and *rbfA* (*yptb0481*) encode the homologs of Rho factor, the translation initiation factor IF-1, and ribosome binding factor RbfA, respectively. The three factor genes were expressed highly from the beginning of growth to the end of the logarithmic phase (Figure 12). Their difference in expression between 3 and 28°C was significant at

growth points II and IV, over 16-fold at the largest for *yptb1395*, but the three genes showed more transcripts at 3°C consistently throughout the growth.

### Expression of Genes Involved in Modifying Membrane Lipid Composition

Genes *yptb1450* and *yptb2469*, encoding FabA and FabF, were expressed highly at the beginning of growth whereas gene *yptb2426* encoding FabB at stationary phase (Figure 13). Gene *yptb2469* showed significantly more transcripts at 3°C at growth point II, although the difference favored cold during most of the growth.

## DISCUSSION

We identified several upregulated genes that may be important to cold adaptation of *Y. pseudotuberculosis*. We also analyzed gene expression profiles to better understand what happens at different phases of growth in cold. To tackle problems

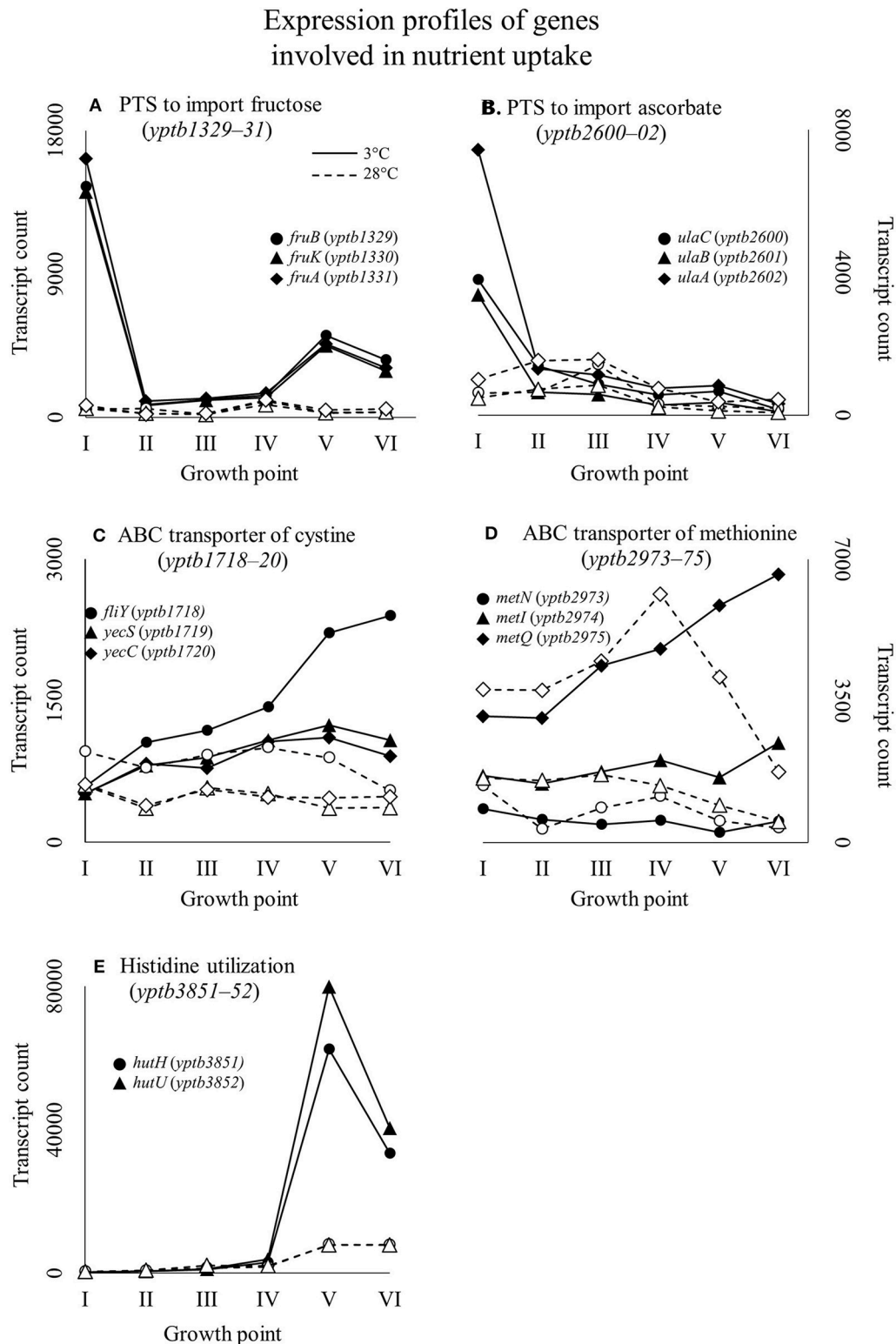
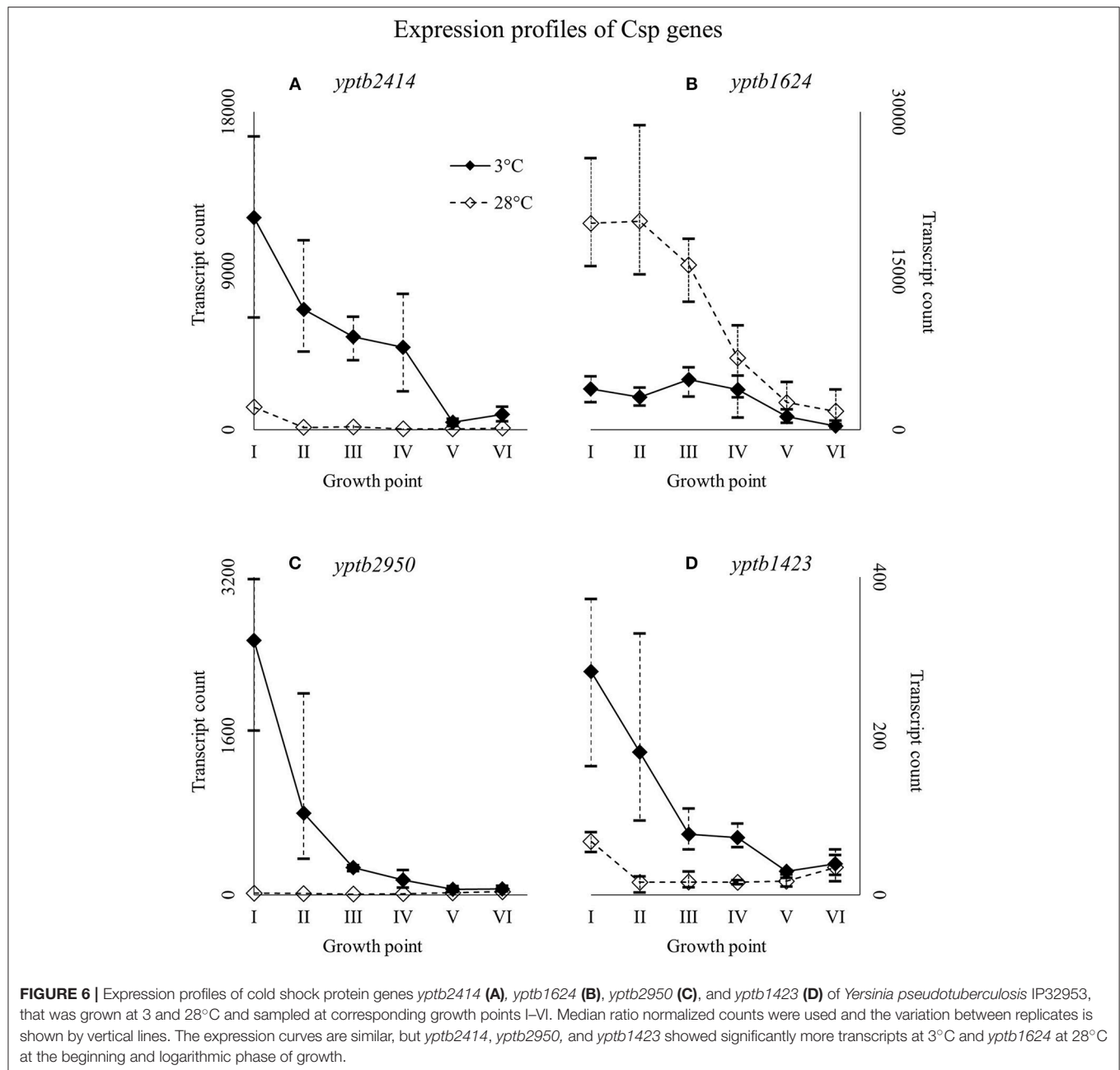


**FIGURE 5 |** Expression profiles of example genes involved in nutrient uptake: *fru*-operon encoding a phosphotransferase system (PTS) to import fructose (**A**); *ula*-operon encoding a PTS to import ascorbate (**B**); ATP binding cassette (ABC) transporter of cystine, dimer form of cysteine (**C**); ABC transporter of methionine (**D**); and part of the histidine utilization system (**E**) of *Yersinia pseudotuberculosis* IP32953, that was grown at 3 and 28°C and sampled at corresponding growth points I–VI. Median ratio normalized counts were used. A large significant difference in expression of sugar importers between 3 and 28°C can be observed at the beginning of growth. Toward the end of growth at 3°C, amino acid utilization takes precedence when sugar importer expression tapers off.



posed by refrigerator temperatures, *Y. pseudotuberculosis* has an extensive toolbox that includes Csps, DEAD-box RNA-helicases, compatible solutes, transcription factors, and fatty acid saturases.

## Nutrient Acquisition

*Y. pseudotuberculosis* expresses many genes involved in securing nutrients significantly more at 3°C compared to 28°C (Figures 4,5), as successful growth in low temperatures requires more energy. In our results, a shift in nutrient utilization over time is observed. At the beginning of growth, transporters of fructose, ascorbate, maltooligosaccharides,

and maltose were upregulated at 3°C. At the beginning of logarithmic phase, transporters of glutamate, aspartate, and arginine were upregulated. Toward the stationary phase, in addition to an operon turning histidine to glutamate, transporters of cystine, methionine, and sulfates were upregulated.

PTSs allow quick acquisition of carbohydrates from the environment (Postma et al., 1993). PTSs have also been linked to regulatory functions during cold stress (Wouters et al., 2000; Monedero et al., 2007). *Y. pseudotuberculosis* expresses several PTSs especially at the beginning of growth significantly more at 3°C than 28°C, as it is in dire need of carbon to sustain

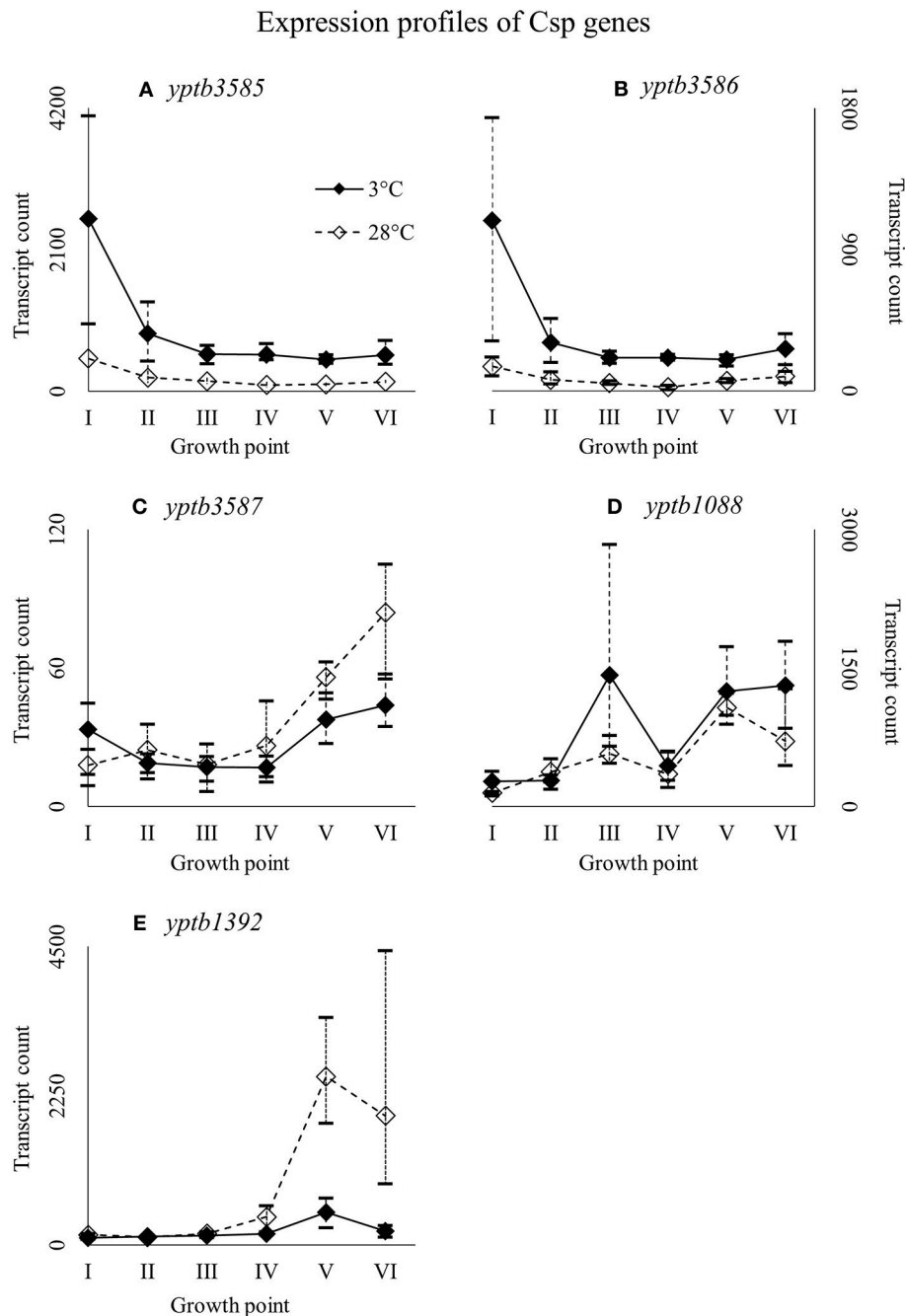


**FIGURE 7 |** Expression profiles of cold shock protein genes *yptb3585* (A), *yptb3586* (B), *yptb3587* (C), *yptb1088* (D), and *yptb1392* (E) of *Yersinia pseudotuberculosis* IP32953, that was grown at 3 and 28°C and sampled at corresponding growth points I–VI. Median ratio normalized counts were used and the variation between replicates is shown by vertical lines. Expression of *yptb3585–86* decreased toward stationary phase whereas that of *yptb3687*, *yptb1088*, and *yptb1392* increased.

its laborious growth. Another large peak in expression of a fructose PTS can be observed at growth point V at 3°C, whereas the peak is located at growth point IV at 28°C. However, this is probably due to slower regulatory processes at 3°C. In *Y. pestis*, the *malMBKEFG*-operon, which is involved in maltose intake, was highly upregulated after cold shock (Han et al., 2005).

Maltose can act as a cryoprotectant in addition to being a carbon source (Jain and Roy, 2009). In our results, parts of the *mal*-operon were upregulated especially at the beginning of growth.

*E. coli* has been shown to accumulate certain amino acids, including aspartic acid, glutamic acid, and methionine,



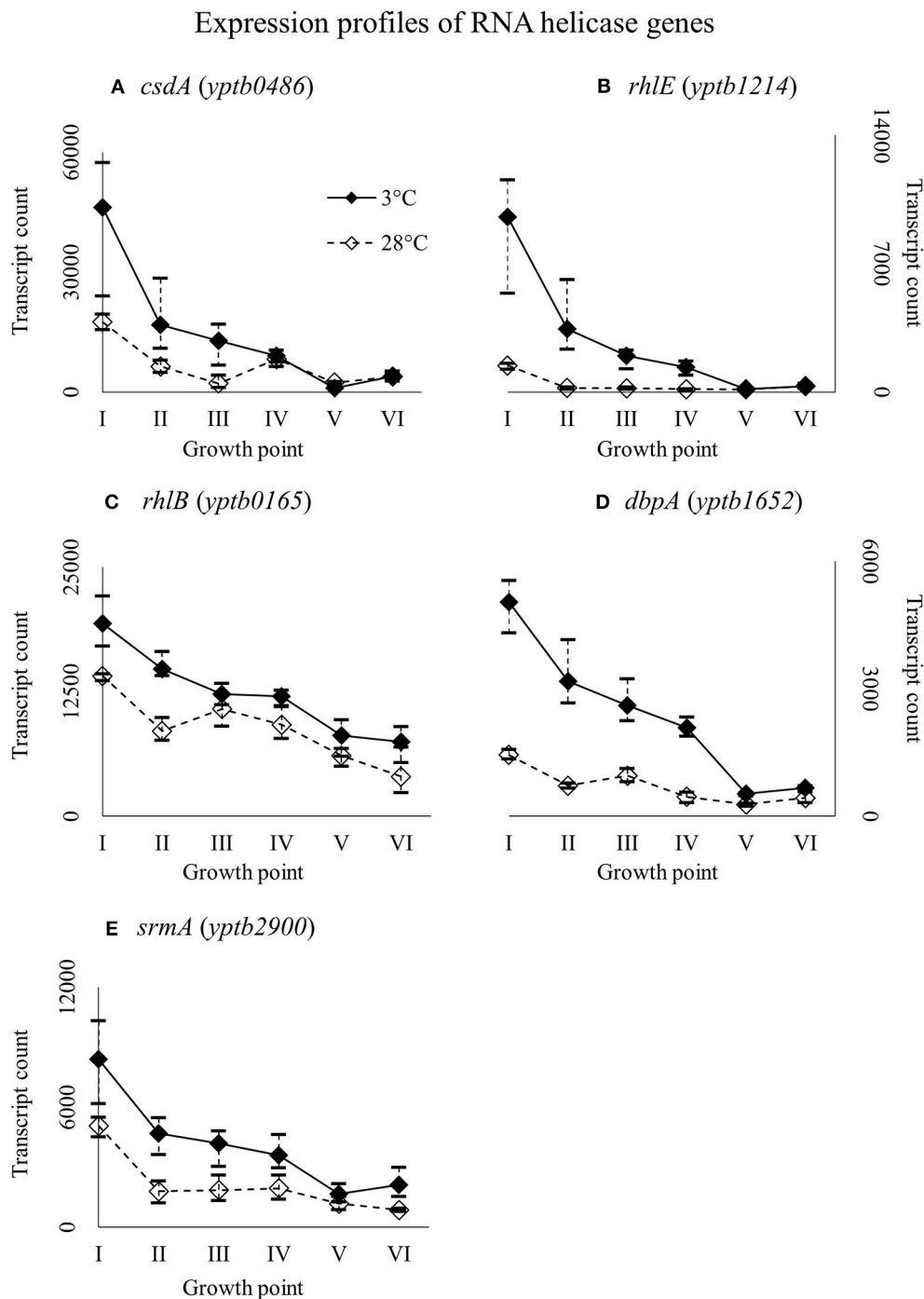


**FIGURE 8 |** Expression profiles of DEAD-box RNA helicase genes *csdA* (A), *rhIE* (B), *rhIB* (C), *dbpA* (D), and *srmA* (E) of *Yersinia pseudotuberculosis* IP32953, that was grown at 3 and 28°C and sampled at corresponding growth points I–VI. Median ratio normalized counts were used and the variation between replicates is shown by vertical lines. Gene *csdA* showed significantly more transcripts at growth point III, *rhIE* at growth points I–IV, and *dbpA* at growth points II and IV, although all the genes expressed more at 3°C at least from the beginning through logarithmic phase.

when subjected to suboptimal temperatures (Jozefczuk et al., 2010). Accumulation has been theorized to result from protein degradation. In our results, ABC transporters for cystine and methionine were upregulated in cold at the stationary phase.

## Cold Shock Proteins

*Y. pseudotuberculosis* seems to express Csp's encoded by *yptb2414* and *yptb2950* almost exclusively at low temperature, i.e., with the highest significant difference of all Csp's, and at high

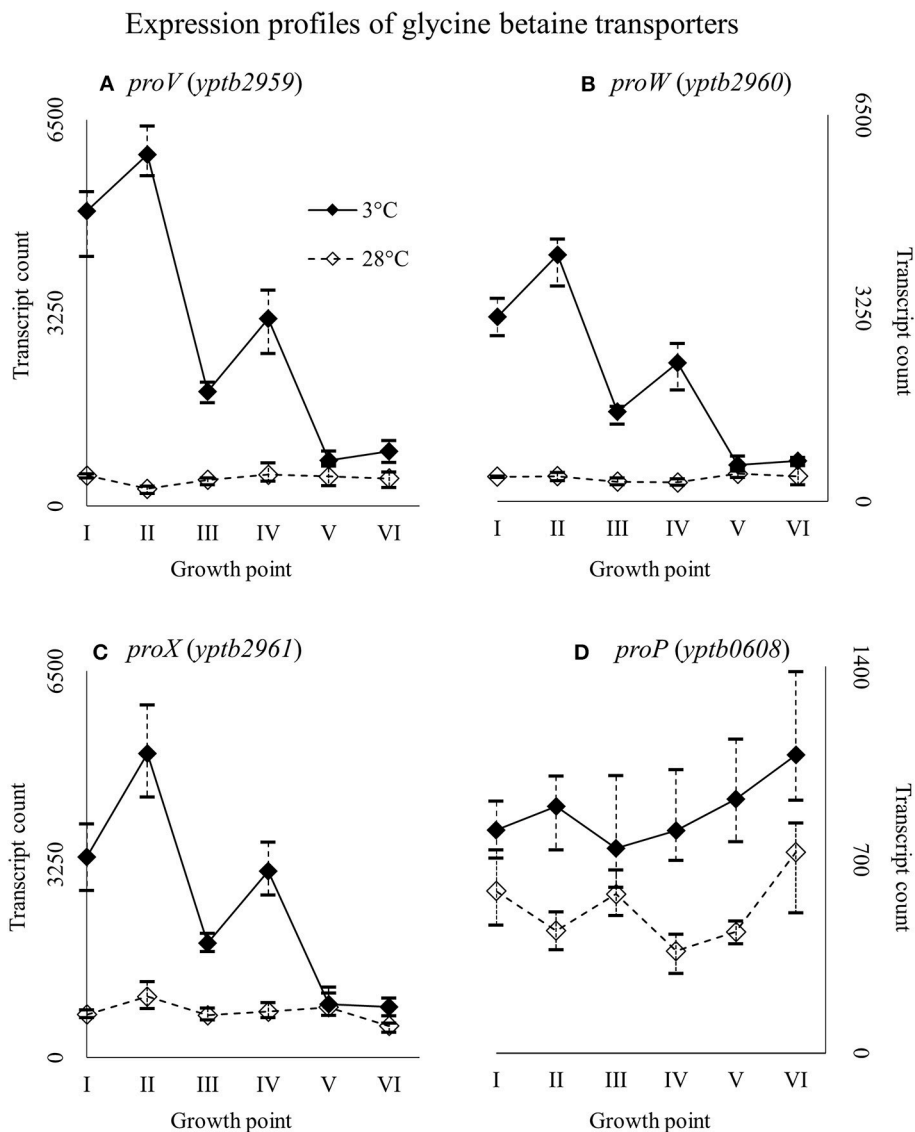


**FIGURE 9 |** Expression profiles of genes encoding glycine betaine transporters, the *proU* operon (*proVWX*, **A–C**), and *proP* (**D**) of *Yersinia pseudotuberculosis* IP32953, that was grown at 3 and 28°C and sampled at corresponding growth points I–VI. Median ratio normalized counts were used and the variation between replicates is shown by vertical lines. The *proU* operon is hardly expressed at all at 28°C and *proP* also showed more transcripts at 3°C.

levels. Additionally, *yptb3585*, *yptb3586*, and *yptb1423* were upregulated throughout the growth. Csps encoded by *yptb2950* and *yptb3585/6* are comparable to CspG and CspB of *E. coli*, respectively (Keto-Timonen et al., 2016). Csp encoded by *yptb2414* is 80% similar to CspC and CspE of *E. coli* K-12 W3110.

Csp encoded by *yptb1088*, which is almost identical to CspE of *E. coli* (Keto-Timonen et al., 2016), showed more transcripts at 3°C, but not at significant levels. However, its transcript count rose toward stationary phase like has been shown to happen in *E. coli* (Czapski and Trun, 2014). In *E. coli*, CspE was also the most abundant of all *csps* after cold shock and present in the bacterium at all times. The expression of *yptb1392*,

similar to CspD of *E. coli*, ramped up at stationary phase in 28°C and a similar but less dramatic bump can be seen in expression profile in 3°C. In *E. coli*, CspD is not cold-induced and is expressed mainly at stationary phase (Yamanaka et al., 2001). It is involved in persister cell and biofilm formation (Kim and Wood, 2010).

In *E. coli*, the genes *cspA*, *cspB*, *cspE*, and *cspG* all must be deleted to achieve a cold-sensitive phenotype, and the deletion of only one or two genes leads to overexpression of the rest (Xia et al., 2001). In addition, CspC and CspE seem to double as regulatory elements in stress responses (Phadtare and Inouye, 2001; Phadtare et al., 2006). The two proteins have been shown to be required for expression of fructose

## Expression profiles of genes involved in glycine betaine biosynthesis

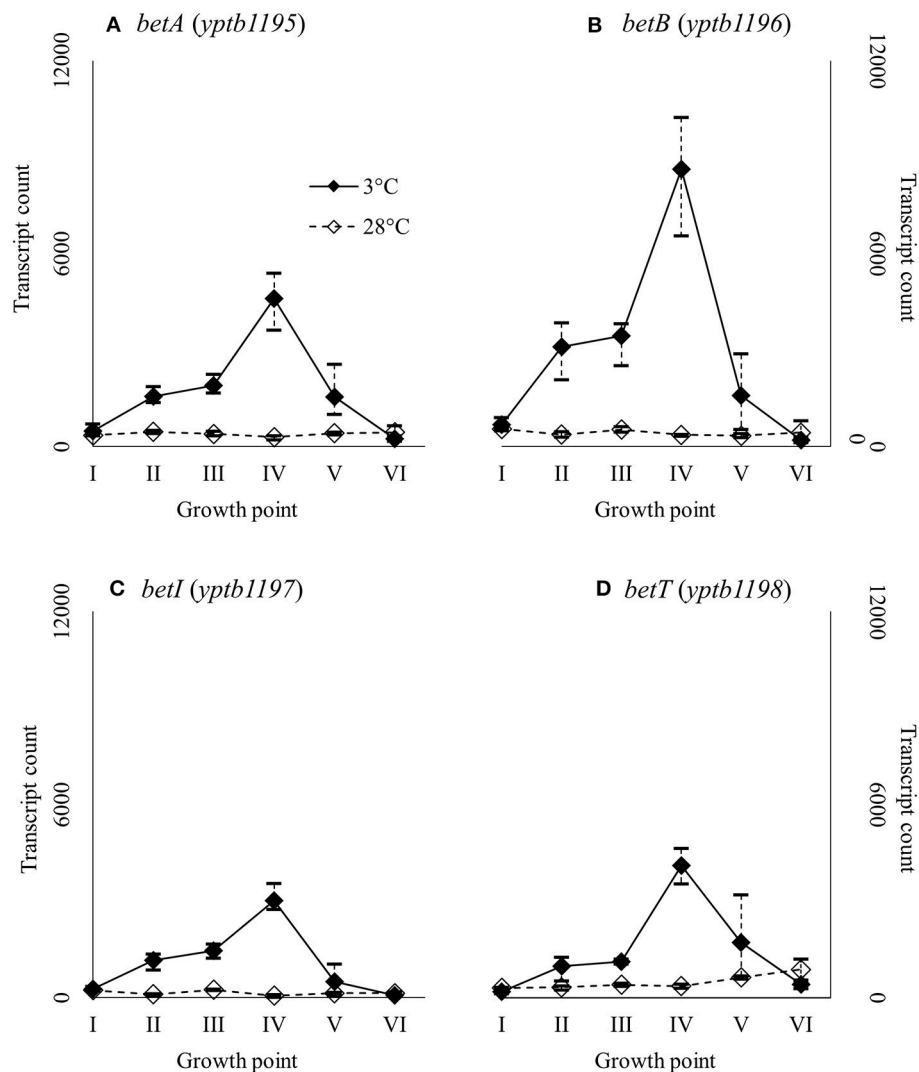
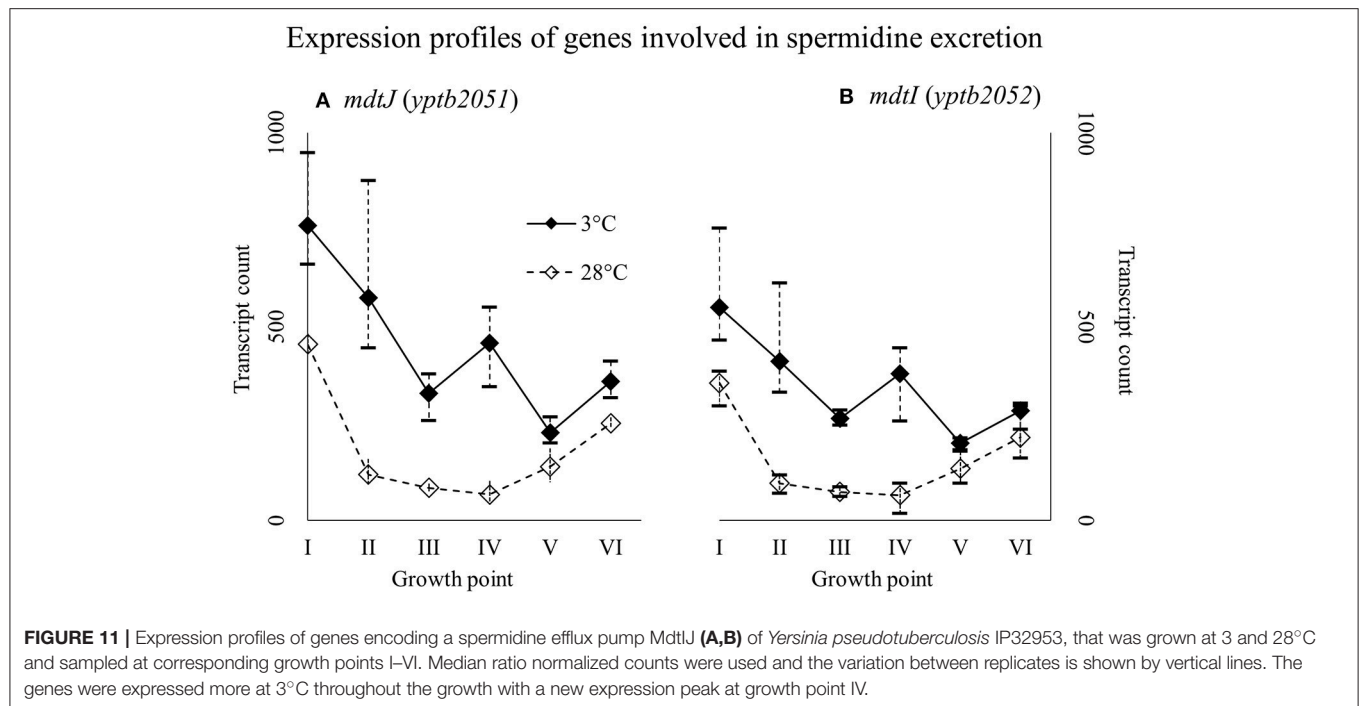


**FIGURE 10 |** Expression profiles of genes involved in glycine betaine biosynthesis, the *betI*BA-*betT* divergent operon (A–D), of *Yersinia pseudotuberculosis* IP32953, that was grown at 3 and 28°C and sampled at corresponding growth points I–VI. Median ratio normalized counts were used and the variation between replicates is shown by vertical lines. The expression of the operon is all but diminished at 28°C.

PTS at suboptimal temperatures (Phadtare et al., 2006). *E. coli* expresses *cspA*, *cspB*, and *cspG* even when its protein synthesis is inhibited by antimicrobials (Etchegaray and Inouye, 1999). In *Clostridium botulinum*, deletion of *cspB*, or *cspC* leads to a cold-sensitive phenotype, and *cspC* deletion even hinders growth at 37°C (Söderholm et al., 2011). Genes *cspB* and *cspC* also provide the bacterium resistance to NaCl, pH, and ethanol stress (Derman et al., 2015). In *Staphylococcus aureus*, *cspB* mutation renders the bacterium susceptible to cold and various antimicrobials (Duval et al., 2010). By contrast, CspC has been shown to induce more strongly in response to antimicrobials, hydrogen peroxide, and arsenate than cold (Chanda et al., 2009).

In our experiment, the expression of the genes *yptb3585–86*, comparable to *cspB* of *E. coli* (Keto-Timonen et al., 2016), dipped after the beginning of growth at 3°C but showed more transcripts at 3°C throughout the growth. Pathogenic *Yersinia* have been shown to hold a tandem gene duplication *cspA1/A2* (Neuhaus et al., 1999), which is very nearly identical to genes *yptb3585–87* and needs to be downregulated after the initial cold shock for growth to continue (Neuhaus et al., 2000). In *Yersinia enterocolitica*, *cspA* and *cspB* were the very first genes expressed after cold-shock with their transcript levels decreasing after the beginning (Bresolin et al., 2006). Similarly, *cspA* and *cspB* expression fluctuated accordingly with temperature cycling in *E. coli* (Ivancic et al., 2013). In light of our



results, *yptb3585–86* might play an important role in the initial regulation of cold-inducible genes also in *Y. pseudotuberculosis*. Genes *yptb2414* and *yptb2950* seem to be important at low temperature growth considering their differential expression and transcript levels. It is also probable that most Csp of *Y. pseudotuberculosis* are interchangeable. Csp encoded by *yptb1423* is an odd one out, with a similarity of 54% at best to other Csp of *Y. pseudotuberculosis* (Keto-Timonen et al., 2016), with a peak similarity of 50% to the Csp of *E. coli* K-12 W3110.

## DEAD-Box RNA Helicases

*Y. pseudotuberculosis* is unable to grow at 3°C without a functional RNA helicase gene *csdA* (*yptb0486*) (Palonen et al., 2012). Of other foodborne pathogens, *Listeria monocytogenes* and *C. botulinum* have been shown to require RNA-helicases, including a CsdA homolog, to grow at suboptimal temperatures (Markkula et al., 2012; Söderholm et al., 2015). In fact, CsdA was the most abundant protein extracted from the microbial mats of Lake Joyce in Antarctica (Koo et al., 2016). CsdA and SrmB of *E. coli* are directly involved in the biogenesis of large ribosomal subunits, presumably at subsequent steps with some functional overlap, and deletion of either gene stunts growth at low temperatures (Charollais et al., 2003, 2004). The deletion of *dbpA* in *E. coli* did not lead to similar accumulation of ribosome precursors and stunted growth at either 25 or 37°C (Peil et al., 2008).

Our results suggest that DbpA (encoded by *yptb1652*) may indeed be important at low temperatures, at least in *Y. pseudotuberculosis*. DbpA is missing completely from *Pasteurellales*, an order of symbionts and parasites growing at unchanging, high-temperature, nutrient-rich niches, which

suggests that DbpA, like other DEAD-box helicases, has become specialized to operate in adverse growth conditions (Iost and Dreyfus, 2006). Amino acid similarities between corresponding helicases of *Y. pseudotuberculosis* IP32953 and *E. coli* K-12 W3110 range from 69 to 90%.

Gene *yptb1214* coding RhlE had the largest and most consistent significant difference in expression in favor of 3°C. It has been suggested by Jain (2008) that RhlE may modulate the function of CsdA and SrmB in priming immature ribosomal RNA. This would also help explain the gene's prominence at low temperature in our results at the beginning and during logarithmic phase when ribosomal activity is at its highest. In *E. coli*, RhlE has been shown to complement the function of both CsdA and RhlB (Khemici et al., 2004; Awano et al., 2007), but deletion of *rhlE* did not affect growth at 37°C in *E. coli* (Phadtare, 2011).

## Compatible Solutes

Our results show that *Y. pseudotuberculosis* expresses genes involved in glycine betaine intake and biosynthesis significantly more at 3°C during critical points of growth, i.e., the beginning and logarithmic phase. It has been shown that *Y. enterocolitica*, with almost identical *proU* and *proP* operons, accumulates glycine betaine at low temperature, but glycine betaine only protects it against osmotic stress (Park et al., 1995; Annamalai and Venkitanarayanan, 2009). However, glycine betaine has been shown to also grant cold protection to gram-positive *L. monocytogenes*, *B. subtilis*, and gram-negative *Vibrio anguillarum* (Ko et al., 1994; Hoffmann and Bremer, 2011; Ma et al., 2017). Furthermore, choline/carnitine/betaine transporter gene of *C. botulinum* was upregulated in cold shock (Dahlsten et al., 2014). The precise



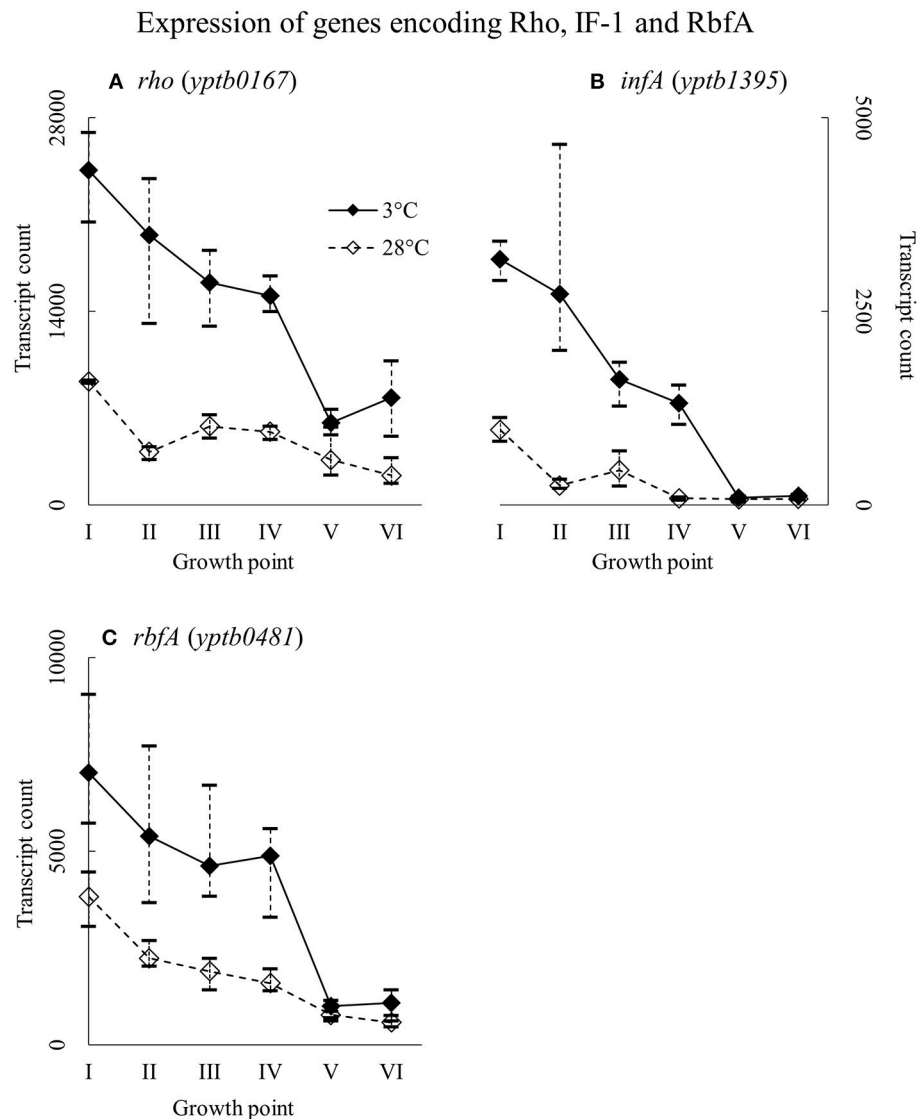


**FIGURE 12 |** Expression profiles of genes encoding transcription termination factor Rho (A), translation initiation factor IF-1 (B), and ribosome binding factor RbfA (C) of *Yersinia pseudotuberculosis* IP32953, that was grown at 3 and 28°C and sampled at corresponding growth points I–VI. Median ratio normalized counts were used and the variation between replicates is shown by vertical lines. All three factors showed more transcripts at 3°C at least to the end of logarithmic phase.

mechanism behind glycine betaine mediated cold protection is unclear, but the molecule has been suggested to hinder ice crystal formation and displace water around macromolecules, reducing aggregation and denaturation (Hoffmann and Bremer, 2011).

In our results, an operon encoding spermidine efflux pump MdtI was expressed significantly more at 3°C. Bacteria need spermidine for various purposes, but at low temperatures excess spermidine is detrimental (Higashi et al., 2008). Spermidine displaces magnesium-ions from ribosomes, thus deactivating them, but it also prolongs synthesis of Csp's after cold shock (Limsuwun and Jones, 2000). It has been shown that prolonged synthesis of Csp's after cold shock occupies all available ribosomes effectively stopping growth in *Y. enterocolitica* (Neuhaus et al.,

2000). Our results suggest that also *Y. pseudotuberculosis* ejects excess spermidine to avoid these problems.

### Rho Factor, IF-1, and RbfA

Translation factors like IF-1 and RbfA act directly on ribosomes, securing protein synthesis. Initiation factor IF-1 separates the overly stabilized large and small subunits of ribosomes so that they can fuse and begin translating again elsewhere (Giangrossi et al., 2007), while RbfA primes 16S rRNA for new small subunits (Xia et al., 2003). Both IF-1 and RbfA have been shown to be significantly more expressed during cold shock in *E. coli* (Xia et al., 2003; Giangrossi et al., 2007). *E. coli* IF-1 resembles the CspA homologs (Phadtare et al., 2007), whereas in *Y.*

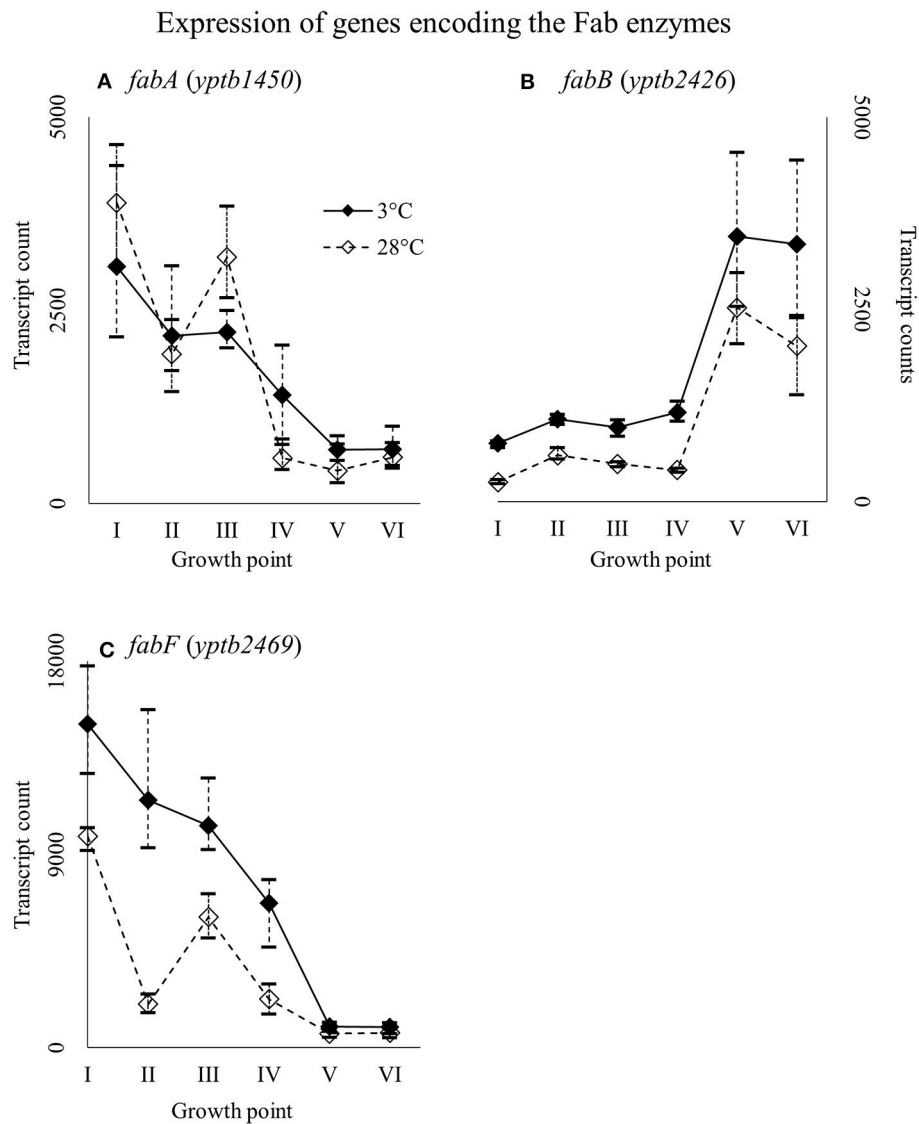


**FIGURE 13 |** Expression profiles of genes encoding the Fab enzymes *fabA* (A), *fabB* (B), and *fabF* (C) of *Yersinia pseudotuberculosis* IP32953, that was grown at 3 and 28°C and sampled at corresponding growth points I–VI. Median ratio normalized counts were used and the variation between replicates is shown by vertical lines. Gene *fabB* and *fabF* showed more transcripts at 3°C during most of the growth.

*pseudotuberculosis* they are only 42–50% similar in nucleic acid and 14–21% in amino acid sequence.

The *rho* gene is associated with bacteria that are subjected to various stresses in their environment (D'hegère et al., 2013). Rho factor is needed at low temperature to clear the bacterial DNA of frozen ribosomes and polymerases (D'hegère et al., 2013), and the structure of its RNA-binding subunit is similar to that of a cold shock domain (Briercheck et al., 1996). Rho factor also coordinates homeostasis of magnesium ions, which are needed by ribosomes, by controlling transporter genes (Kriner and Groisman, 2015). The Rho factor has been shown to be upregulated at low temperature in at least *Acidithiobacillus ferrooxidans* (Mykytczuk et al., 2011), *Pseudomonas haloplanktis* strain TAC125 (Piette et al., 2010), and *Bacillus subtilis* (Quirk

et al., 1993). To our knowledge, none of these factors have been linked to cold growth in *Yersinia* genus before.

*Y. pseudotuberculosis* expressed the genes encoding IF-1, RbfA, and Rho all through the critical phases of growth at high levels but also significantly more at 3°C. Massive difference of IF-1 (*yptb1395*) expression in favor of cold during logarithmic phase suggests that the initiation factor is important for continued growth at low temperature. It is probable that IF-1 and RbfA of *Y. pseudotuberculosis* provide the bacterium with working ribosomes at low temperature. *Y. pseudotuberculosis* might need Rho factor not only to terminate inefficient transcription but also to provide ribosomes with much needed magnesium ions. The upregulation of *mgt* transporter genes at 3°C throughout the growth supports this theory.

## Cell Membranes

Lipid synthesis and cell growth cease in cyanobacteria until an adequate membrane lipid composition has been achieved (Sinetova and Los, 2016). However, gram-negative cyanobacteria and gram-positive *Bacillus subtilis* possess a two-component system, DesK-DesR, that senses increasing membrane rigidity at low temperatures (Beranová et al., 2010; Sinetova and Los, 2016). Although a corresponding two-component system has not been identified in *Y. pseudotuberculosis* (Palonen et al., 2011), the ratio of unsaturated to saturated fatty acids in its membranes rises at low temperature (Bakholdina et al., 2004). In another gram-negative bacterium, *E. coli*, temperature drop directly affects activity of the FabF enzyme in its cytosol and this enzyme is involved in unsaturated lipid synthesis with FabA and FabB (Mansilla et al., 2004). Cold stress has also been shown to induce the transcription of *fabF* in *Y. pestis* (Han et al., 2005).

It is also possible that the csp encoded by *yptb2414*, a homolog of *E. coli* CspC and CspE, is involved in cold adaptation of membranes in *Y. pseudotuberculosis*. CspC and CspE bind specific uracil-rich segments of mRNA, and these segments often encode hydrophobic structures of membrane proteins (Benhalevy et al., 2015). It has been suggested that bacteria use these segments as addresses for directing membrane protein mRNA to where they are needed in the cell (Benhalevy et al., 2015).

## CONCLUSIONS

*Y. pseudotuberculosis* has extensive tools to keep its protein synthesis running at low temperature. It is probable, that the functions of its Csps, RNA helicases and factors acting on ribosomes overlap greatly and thus form a robust network to protect nucleic acids from cold damage. Csps encoded by *yptb1423*, *yptb2414*, *yptb2950*, *yptb3585–86*, and RNA helicases CsdA, RhlE, and DbpA, seem to form the backbone of cold survival of *Y. pseudotuberculosis* with their regulatory and nucleic acid unwinding functions. IF-1, RbfA, and by extension, Rho, keep the ribosomes of *Y. pseudotuberculosis* running even at suboptimal temperatures. Rho factor also terminates frozen ribosomes and RNA polymerases, freeing scant resources under cold stress.

## REFERENCES

- Annamalai, T., and Venkitanarayanan, K. (2009). Role of *proP* and *proU* in betaine uptake by *Yersinia enterocolitica* under cold and osmotic stress conditions. *Appl. Environ. Microbiol.* 75, 1471–1477. doi: 10.1128/AEM.01644-08
- Awano, N., Xu, C., Ke, H., Inoue, K., Inouye, M., and Phadtare, S. (2007). Complementation analysis of the cold-sensitive phenotype of the *Escherichia coli* *csdA* deletion strain. *J. Bacteriol.* 189, 5808–5815. doi: 10.1128/JB.00655-07
- Bakholdina, S. I., Sanina, N. M., Krasikova, I. N., Popova, O. B., and Solov'eva, T. F. (2004). The impact of abiotic factors (temperature and glucose) on physicochemical properties of lipids from *Yersinia pseudotuberculosis*. *Biochimie* 86, 875–881. doi: 10.1016/j.biochi.2004.10.011
- Benhalevy, D., Bochkareva, E. S., Biran, I., and Bibi, E. (2015). Model uracil-rich RNAs and membrane protein mRNAs interact specifically

Increased expression of motility, chemotaxis, and nutrient uptake genes at low temperature suggests that *Y. pseudotuberculosis* actively tries to find and secure sufficient resources to grow in refrigerator temperatures. The nutrients acquired are diverse and the nutrient profile seems to shift as growth progresses. The bacterium also possibly changes its membrane lipid composition with Fab enzymes, much like *E. coli*, to battle increasing membrane rigidity.

The exact role of glycine betaine in cold resistance is uncertain, but *Y. pseudotuberculosis* seems to accumulate it during cold growth like many other bacteria. Genes involved in defense against foreign DNA as well as oxidative stress were upregulated at 3°C, which would seem to suggest that stress responses are linked in some way.

## AUTHOR CONTRIBUTIONS

RK-T and HK designed the study. NS and RK-T performed the experiments. J-PV and KJ performed the transcriptome analysis. J-PV, KJ, RK-T, and HK contributed to the data analysis and interpretation. J-PV drafted the manuscript. RK-T, NS, and HK contributed to manuscript revision. All authors have read and approved the final manuscript.

## FUNDING

This work was funded by the Finnish Veterinary Foundation and the Walter Ehrström Foundation.

## ACKNOWLEDGMENTS

We gratefully acknowledge Dr. Elisabeth Carniel, Institut Pasteur, Paris, France for providing the *Y. pseudotuberculosis* IP32953 strain. We thank Henna Niinivirta, Erika Pitkänen, and Kirsi Ristkari for technical assistance.

## SUPPLEMENTARY MATERIAL

The Supplementary Material for this article can be found online at: <https://www.frontiersin.org/articles/10.3389/fcimb.2018.00416/full#supplementary-material>

with cold shock proteins in *Escherichia coli*. *PLoS ONE* 10:e0134413. doi: 10.1371/journal.pone.0134413

- Benjamini, Y., and Hochberg, Y. (1995). Controlling the false discovery rate: a practical and powerful approach to multiple testing. *J. R. Stat. Soc. Ser. B Methodol.* 57, 289–300.
- Beranová, J., Mansilla, M. C., De Mendoza, D., Elhottová, D., and Konopásek, I. (2010). Differences in cold adaptation of *Bacillus subtilis* under anaerobic and aerobic conditions. *J. Bacteriol.* 192, 4164–4171. doi: 10.1128/JB.00384-10
- Bresolin, G., Neuhaus, K., Scherer, S., and Fuchs, T. M. (2006). Transcriptional analysis of long-term adaptation of *Yersinia enterocolitica* to low-temperature growth. *J. Bacteriol.* 188, 2945–2958. doi: 10.1128/JB.188.8.2945-2958.2006
- Briercheck, D. M., Allison, T. J., Richardson, J. P., Ellena, J. F., Wood, T. C., and Rule, G. S. (1996). <sup>1</sup>H, <sup>15</sup>N and <sup>13</sup>C resonance assignments and secondary structure determination of the RNA-binding domain of *E. coli* Rho protein. *J. Biomol. NMR* 8, 429–444. doi: 10.1007/BF00228145

- Buzoleva, L. S., and Somov, G. P. (2003). Adaptation variability of *Yersinia pseudotuberculosis* during long-term persistence in soil. *Bull. Exp. Biol. Med.* 135, 456–459. doi: 10.1023/A:1024915409187
- Chanda, P. K., Mondal, R., Sau, K., and Sau, S. (2009). Antibiotics, arsenate and H<sub>2</sub>O<sub>2</sub> induce the promoter of *Staphylococcus aureus* cspC gene more strongly than cold. *J. Basic Microbiol.* 49, 205–211. doi: 10.1002/jobm.200800065
- Charollais, J., Dreyfus, M., and Iost, I. (2004). CsdA, a cold-shock RNA helicase from *Escherichia coli*, is involved in the biogenesis of 50S ribosomal subunit. *Nucleic Acids Res.* 32, 2751–2759. doi: 10.1093/nar/gkh603
- Charollais, J., Pflieger, D., Vinh, J., Dreyfus, M., and Iost, I. (2003). The DEAD-box RNA helicase SrmB is involved in the assembly of 50S ribosomal subunits in *Escherichia coli*. *Mol. Microbiol.* 48, 1253–1265. doi: 10.1046/j.1365-2958.2003.03513.x
- Chattopadhyay, M. K., Raghu, G., Sharma, Y. V. R. K., Biju, A. R., Rajasekharan, M. V., and Shivaji, S. (2011). Increase in oxidative stress at low temperature in an antarctic bacterium. *Curr. Microbiol.* 62, 544–546. doi: 10.1007/s00284-010-9742-y
- Czapski, T. R., and Trun, N. (2014). Expression of csp genes in *E. coli* K-12 in defined rich and defined minimal media during normal growth, and after cold-shock. *Gene* 547, 91–97. doi: 10.1016/j.gene.2014.06.033
- Dahlsten, E., Isokallio, M., Somervuo, P., Lindström, M., and Korkeala, H. (2014). Transcriptomic analysis of (Group I) *Clostridium botulinum* ATCC 3502 cold shock response. *PLoS ONE* 9:e89958. doi: 10.1371/journal.pone.0089958
- Derman, Y., Söderholm, H., Lindström, M., and Korkeala, H. (2015). Role of csp genes in NaCl, pH, and ethanol stress response and motility in *Clostridium botulinum* ATCC 3502. *Food Microbiol.* 46, 463–470. doi: 10.1016/j.fm.2014.09.004
- D'heygère, F., Rabhi, M., and Boudvillain, M. (2013). Phyletic distribution and conservation of the bacterial transcription termination factor Rho. *Microbiology* 159, 1423–1436.
- Duval, B. D., Mathew, A., Satola, S. W., and Shafer, W. M. (2010). Altered growth, pigmentation, and antimicrobial susceptibility properties of *Staphylococcus aureus* due to loss of the major cold shock gene cspB. *Antimicrob. Agents Chemother.* 54, 2283–2290. doi: 10.1128/AAC.01786-09
- Etchegaray, J. P., and Inouye, M. (1999). CspA, CspB, and CspG, major cold shock proteins of *Escherichia coli*, are induced at low temperature under conditions that completely block protein synthesis. *J. Bacteriol.* 181, 1827–1830.
- Gaidatzis, D., Lerch, A., Hahne, F., and Stadler, M. B. (2015). QuasR: quantification and annotation of short reads in R. *Bioinformatics* 31, 1130–1132. doi: 10.1093/bioinformatics/btu781
- Gengler, S., Laudisoit, A., Batoko, H., and Wattiau, P. (2015). Long-Term Persistence of *Yersinia pseudotuberculosis* in entomopathogenic nematodes. *PLoS ONE* 10:e0116818. doi: 10.1371/journal.pone.0116818
- Giangrossi, M., Brandi, A., Giuliadori, A. M., Gualerzi, C. O., and Pon, C. L. (2007). Cold-shock-induced *de novo* transcription and translation of *infA* and role of IF1 during cold adaptation. *Mol. Microbiol.* 64, 807–821. doi: 10.1111/j.1365-2958.2007.05699.x
- Giannitti, F., Barr, B. C., Brito, B. P., Uzal, F. A., Villanueva, M., and Anderson, M. (2014). *Yersinia pseudotuberculosis* infections in goats and other animals diagnosed at the California animal health and food safety laboratory system: 1990–2012. *J. Vet. Diagn. Invest.* 26, 88–95. doi: 10.1177/1040638713516624
- Han, Y., Zhou, D., Pang, X., Zhang, L., Song, Y., Tong, Z., et al. (2005). DNA microarray analysis of the heat- and cold-shock stimulons in *Yersinia pestis*. *Microbes Infect.* 7, 335–348. doi: 10.1016/j.micinf.2004.11.005
- Hardcastle, T. J., and Kelly, K. A. (2010). baySeq: Empirical Bayesian methods for identifying differential expression in sequence count data. *BMC Bioinformatics* 11:422. doi: 10.1186/1471-2105-11-422
- Higashi, K., Ishiguro, H., Demizu, R., Uemura, T., Nishino, K., Yamaguchi, A., et al. (2008). Identification of a spermidine excretion protein complex (MdtJI) in *Escherichia coli*. *J. Bacteriol.* 190, 872–878. doi: 10.1128/JB.01505-07
- Hoffmann, T., and Bremer, E. (2011). Protection of *Bacillus subtilis* against cold stress via compatible-solute acquisition. *J. Bacteriol.* 193, 1552–1562. doi: 10.1128/JB.01319-10
- Huber, W., Carey, V. J., Gentleman, R., Anders, S., Carlson, M., Carvalho, B. S., et al. (2015). Orchestrating high-throughput genomic analysis with Bioconductor. *Nat. Methods* 12:115. doi: 10.1038/nmeth.3252
- Iost, I., and Dreyfus, M. (2006). DEAD-box RNA helicases in *Escherichia coli*. *Nucl. Acids Res.* 34, 4189–4197. doi: 10.1093/nar/gkl500
- Ivancic, T., Jamnik, P., and Stopar, D. (2013). Cold shock CspA and CspB protein production during periodic temperature cycling in *Escherichia coli*. *BMC Res. Notes* 6:248. doi: 10.1186/1756-0500-6-248
- Jaakkola, K., Somervuo, P., and Korkeala, H. (2015). Comparative genomic hybridization analysis of *Yersinia enterocolitica* and *Yersinia pseudotuberculosis* identifies genetic traits to elucidate their different ecologies. *BioMed. Res. Int.* 2015:760494. doi: 10.1155/2015/760494
- Jain, C. (2008). The *E. coli* RhlE RNA helicase regulates the function of related RNA helicases during ribosome assembly. *RNA* 14, 381–389. doi: 10.1261/rna.800308
- Jain, N. K., and Roy, I. (2009). Effect of trehalose on protein structure. *Protein Sci.* 18, 24–36. doi: 10.1002/pro.3
- Johnson, S. L., Daligault, H. E., Davenport, K. W., Jaisle, J., Frey, K. G., Ladner, J. T., et al. (2015). Thirty-two complete genome assemblies of nine *Yersinia* species, including *Y. pestis*, *Y. pseudotuberculosis*, and *Y. enterocolitica*. *Genome Announc.* 3:e00148–15. doi: 10.1128/genomeA.00148-15
- Joutsen, S., Laukkanen-Niinios, R., Henttonen, H., Niemimaa, J., Voutilainen, L., Kallio, E. R., et al. (2017). *Yersinia* spp. in Wild Rodents and Shrews in Finland. *Vector-Borne Zoonotic Dis.* 17, 303–311. doi: 10.1089/vbz.2016.2025
- Jozefczuk, S., Klie, S., Catchpole, G., Szymanski, J., Cuadros-Inostroza, A., Steinhauser, D., et al. (2010). Metabolomic and transcriptomic stress response of *Escherichia coli*. *Mol. Syst. Biol.* 6:364. doi: 10.1038/msb.2010.18
- Kanehisa, M., and Goto, S. (2000). KEGG: kyoto encyclopedia of genes and genomes. *Nucleic Acids Res.* 28, 27–30. doi: 10.1093/nar/28.1.27
- Keto-Timonen, R., Hietala, N., Palonen, E., Hakakorpi, A., Lindström, M., and Korkeala, H. (2016). Cold shock proteins: a minireview with special emphasis on csp-family of enteropathogenic *Yersinia*. *Front. Microbiol.* 7:1151. doi: 10.3389/fmicb.2016.01151
- Keto-Timonen, R., Pontinen, A., Aalto-Araneda, M., and Korkeala, H. (2018). Growth of *Yersinia pseudotuberculosis* strains at different temperatures, pH values, and NaCl and ethanol concentrations. *J. Food Prot.* 81, 142–149. doi: 10.4315/0362-028X.JFP-17-223
- Khemici, V., Toesca, I., Poljak, L., Vanzo, N. F., and Carpousis, A. J. (2004). The RNase E of *Escherichia coli* has at least two binding sites for DEAD-box RNA helicases: functional replacement of RhlB by RhlE. *Mol. Microbiol.* 54, 1422–1430. doi: 10.1111/j.1365-2958.2004.04361.x
- Kim, Y., and Wood, T. K. (2010). Toxins Hha and CspD and small RNA regulator Hfq are involved in persister cell formation through MqsR in *Escherichia coli*. *Biochem. Biophys. Res. Commun.* 391, 209–213. doi: 10.1016/j.bbrc.2009.11.033
- Ko, R., Smith, L. T., and Smith, G. M. (1994). Glycine betaine confers enhanced osmotolerance and cryotolerance on *Listeria monocytogenes*. *J. Bacteriol.* 176, 426–431. doi: 10.1128/jb.176.2.426-431.1994
- Koo, H., Hakim, J. A., Fisher, P. R. E., Grueneberg, A., Andersen, D. T., and Bej, A. K. (2016). Distribution of cold adaptation proteins in microbial mats in Lake Joyce, Antarctica: analysis of metagenomic data by using two bioinformatics tools. *J. Microbiol. Methods* 120, 23–28. doi: 10.1016/j.mimet.2015.11.008
- Kriner, M. A., and Groisman, E. A. (2015). The bacterial transcription termination factor Rho coordinates Mg<sup>2+</sup> homeostasis with translational signals. *J. Mol. Biol.* 427, 3834–3849. doi: 10.1016/j.jmb.2015.10.020
- Laukkanen, R., Martínez, P. O., Siekkinen, K.-M., Ranta, J., Majjala, R., and Korkeala, H. (2008). Transmission of *Yersinia pseudotuberculosis* in the Pork Production Chain from Farm to Slaughterhouse. *Appl. Environ. Microbiol.* 74, 5444–5450. doi: 10.1128/AEM.02664-07
- Le Guern, A.-S., Martin, L., Savin, C., and Carniel, E. (2016). Yersiniosis in France: overview and potential sources of infection. *Int. J. Infect. Dis.* 46, 1–7. doi: 10.1016/j.ijid.2016.03.008
- Limsuwun, K., and Jones, P. G. (2000). Spermidine acetyltransferase is required to prevent spermidine toxicity at low temperatures in *Escherichia coli*. *J. Bacteriol.* 182, 5373–5380. doi: 10.1128/JB.182.19.5373-5380.2000
- Love, M. I., Huber, W., and Anders, S. (2014). Moderated estimation of fold change and dispersion for RNA-seq data with DESeq2. *Genome Biol.* 15:550. doi: 10.1186/s13059-014-0550-8
- Ma, Y., Wang, Q., Gao, X., and Zhang, Y. (2017). Biosynthesis and uptake of glycine betaine as cold-stress response to low temperature in fish pathogen *Vibrio anguillarum*. *J. Microbiol.* 55, 44–55. doi: 10.1007/s12275-017-6370-2
- Mansilla, M. C., Cybulski, L. E., Albanesi, D., and De Mendoza, J. (2004). Control of membrane lipid fluidity by molecular thermosensors. *J. Bacteriol.* 186, 6681–6688. doi: 10.1128/JB.186.20.6681-6688.2004



- Markkula, A., Mattila, M., Lindström, M., and Korkeala, H. (2012). Genes encoding putative DEAD-box RNA helicases in *Listeria monocytogenes* EGD-e are needed for growth and motility at 3°C. *Environ. Microbiol.* 14, 2223–2232. doi: 10.1111/j.1462-2920.2012.02761.x
- Monedero, V., Maze, A., Boel, G., Zuniga, M., Beaufils, S., Hartke, A., et al. (2007). The phosphotransferase system of *Lactobacillus casei*: regulation of carbon metabolism and connection to cold shock response. *J. Mol. Microbiol. Biotechnol.* 12, 20–32. doi: 10.1159/000096456
- Myktyczuk, N. C. S., Trevors, J. T., Foote, S. J., Leduc, L. G., Ferroni, G. D., and Twine, S. M. (2011). Proteomic insights into cold adaptation of psychrotrophic and mesophilic *Acidithiobacillus ferrooxidans* strains. *Antonie van Leeuwenhoek* 100, 259–277. doi: 10.1007/s10482-011-9584-z
- Neuhaus, K., Francis, K. P., Rapposch, S., Görg, A., and Scherer, S. (1999). Pathogenic *Yersinia* species carry a novel, cold-inducible major cold shock protein tandem gene duplication producing both bicistronic and monocistronic mRNA. *J. Bacteriol.* 181, 6449–6455.
- Neuhaus, K., Rapposch, S., Francis, K. P., and Scherer, S. (2000). Restart of exponential growth of cold-shocked *Yersinia enterocolitica* occurs after down-regulation of *cspA1/A2* mRNA. *J. Bacteriol.* 182, 3285–3288. doi: 10.1128/JB.182.11.3285-3288.2000
- Niskanen, T., Waldenström, J., Fredriksson-Ahomaa, M., Olsen, B., and Korkeala, H. (2003). *virF*-Positive *Yersinia pseudotuberculosis* and *Yersinia enterocolitica* found in migratory birds in Sweden. *Appl. Environ. Microbiol.* 69, 4670–4675. doi: 10.1128/AEM.69.8.4670-4675.2003
- Nuorti, J. P., Niskanen, T., Hallanvuo, S., Mikkola, J., Kela, E., Hatakka, M., et al. (2004). A widespread outbreak of *Yersinia pseudotuberculosis* O:3 infection from iceberg lettuce. *J. Infect. Dis.* 189, 766–774. doi: 10.1086/381766
- Palonen, E., Lindström, M., Karttunen, R., Somervuo, P., and Korkeala, H. (2011). Expression of signal transduction system encoding genes of *Yersinia pseudotuberculosis* IP32953 at 28°C and 3°C. *PLoS ONE* 6:e25063. doi: 10.1371/journal.pone.0025063
- Palonen, E., Lindström, M., and Korkeala, H. (2010). Adaptation of enteropathogenic *Yersinia* to low growth temperature. *Crit. Rev. Microbiol.* 36, 54–67. doi: 10.3109/10408410903382581
- Palonen, E., Lindström, M., Somervuo, P., Johansson, P., Björkroth, J., and Korkeala, H. (2012). Requirement for RNA Helicase CsdA for Growth of *Yersinia pseudotuberculosis* IP32953 at low temperatures. *Appl. Environ. Microbiol.* 78, 1298–1301. doi: 10.1128/AEM.07278-11
- Park, S., Smith, L. T., and Smith, G. M. (1995). Role of glycine betaine and related osmolytes in osmotic stress adaptation in *Yersinia enterocolitica* ATCC 9610. *Appl. Environ. Microbiol.* 61, 4378–4381.
- Pärn, T., Hallanvuo, S., Salmenlinna, S., Pihlajasaari, A., Heikkinen, S., Telkki-Nykänen, H., et al. (2015). Outbreak of *Yersinia pseudotuberculosis* O:1 infection associated with raw milk consumption, Finland, spring 2014. *Eurosurveillance* 20:30033. doi: 10.2807/1560-7917.ES.2015.20.40.30033
- Peil, L., Virumäe, K., and Remme, J. (2008). Ribosome assembly in *Escherichia coli* strains lacking the RNA helicase Dcd/CsdA or DbpA. *FEBS J.* 275, 3772–3782. doi: 10.1111/j.1742-4658.2008.06523.x
- Pfaffl, M. W. (2001). A new mathematical model for relative quantification in real-time RT-PCR. *Nucleic Acids Res.* 29:e45. doi: 10.1093/nar/29.9.e45
- Phadtare, S. (2011). Unwinding activity of cold shock proteins and RNA metabolism. *RNA Biol.* 8, 394–397. doi: 10.4161/rna.8.3.14823
- Phadtare, S., and Inouye, M. (2001). Role of CspC and CspE in regulation of expression of RpoS and UspA, the stress response proteins in *Escherichia coli*. *J. Bacteriol.* 183, 1205–1214. doi: 10.1128/JB.183.4.1205-1214.2001
- Phadtare, S., Kazakov, T., Bubunenkov, M., Court, D. L., Pestova, T., and Severinov, K. (2007). Transcription antitermination by translation initiation factor IF1. *J. Bacteriol.* 189, 4087–4093. doi: 10.1128/JB.00188-07
- Phadtare, S., Tadigotla, V., Shin, W.-H., Sengupta, A., and Severinov, K. (2006). Analysis of *Escherichia coli* global gene expression profiles in response to overexpression and deletion of CspC and CspE. *J. Bacteriol.* 188, 2521–2527. doi: 10.1128/JB.188.7.2521-2527.2006
- Piette, F., D'amico, S., Struvay, C., Mazzucchelli, G., Renaut, J., Tutino, M. L., et al. (2010). Proteomics of life at low temperatures: trigger factor is the primary chaperone in the Antarctic bacterium *Pseudoalteromonas haloplanktis* TAC125. *Mol. Microbiol.* 76, 120–132. doi: 10.1111/j.1365-2958.2010.07084.x
- Postma, P. W., Lengeler, J. W., and Jacobson, G. R. (1993). Phosphoenolpyruvate: carbohydrate phosphotransferase systems of bacteria. *Microbiol. Rev.* 57, 543–594.
- Quirk, P. G., Dunkley, E. A., Lee, P., and Krulwich, T. A. (1993). Identification of a putative *Bacillus subtilis* rho gene. *J. Bacteriol.* 175, 647–654. doi: 10.1128/jb.175.3.647-654.1993
- Rimhanen-Finne, R., Niskanen, T., Hallanvuo, S., Makary, P., Haukka, K., Pajunen, S., et al. (2009). *Yersinia pseudotuberculosis* causing a large outbreak associated with carrots in Finland, 2006. *Epidemiol. Infect.* 137, 342–347. doi: 10.1017/S0950268807000155
- Santos-Montañez, J., Benavides-Montano, J. A., Hinz, A. K., and Vadyvaloo, V. (2015). *Yersinia pseudotuberculosis* IP32953 survives and replicates in trophozoites and persists in cysts of *Acanthamoeba castellanii*. *FEMS Microbiol. Lett.* 362:fnv091. doi: 10.1093/femsle/fnv091
- Sato, K., and Komazawa, M. (1991). *Yersinia pseudotuberculosis* infection in children due to untreated drinking water. *Contrib. Microbiol. Immunol.* 12, 5–10.
- Sievers, F., Wilm, A., Dineen, D., Gibson, T. J., Karplus, K., Li, W., et al. (2011). Fast, scalable generation of high-quality protein multiple sequence alignments using Clustal Omega. *Mol. Syst. Biol.* 7:539. doi: 10.1038/msb.2011.75
- Sinetova, M. A., and Los, D. A. (2016). New insights in cyanobacterial cold stress responses: Genes, sensors, and molecular triggers. *Biochim. Biophys. Acta* 1860, 2391–2403. doi: 10.1016/j.bbagen.2016.07.006
- Söderholm, H., Derman, Y., Lindström, M., and Korkeala, H. (2015). Functional *csdA* is needed for effective adaptation and initiation of growth of *Clostridium botulinum* ATCC 3502 at suboptimal temperature. *Int. J. Food Microbiol.* 208, 51–57. doi: 10.1016/j.jfoodmicro.2015.05.013
- Söderholm, H., Lindström, M., Somervuo, P., Heap, J., Minton, N., Lindén, J., et al. (2011). *cspB* encodes a major cold shock protein in *Clostridium botulinum* ATCC 3502. *Int. J. Food Microbiol.* 146, 23–30. doi: 10.1016/j.jfoodmicro.2011.01.033
- Suutari, M., and Laakso, S. (1994). Microbial Fatty Acids and Thermal Adaptation. *Crit. Rev. Microbiol.* 20, 285–328. doi: 10.3109/10408419409113560
- Taboada, B., Ciria, R., Martinez-Guerrero, C. E., and Merino, E. (2012). ProOpDB: prokaryotic operon database. *Nucleic Acids Res.* 40, D627–D631. doi: 10.1093/nar/gkr1020
- Wattam, A. R., Abraham, D., Dalay, O., Disz, T. L., Driscoll, T., Gabbard, J. L., et al. (2014). PATRIC, the bacterial bioinformatics database and analysis resource. *Nucleic Acids Res.* 42, D581–D591. doi: 10.1093/nar/gkt1099
- Wouters, J. A., Kamphuis, H. H., Hugenholtz, J., Kuipers, O. P., De Vos, W. M., and Abee, T. (2000). Changes in glycolytic activity of *Lactococcus lactis* induced by low temperature. *Appl. Environ. Microbiol.* 66, 3686–3691. doi: 10.1128/AEM.66.9.3686-3691.2000
- Xia, B., Ke, H., and Inouye, M. (2001). Acquisition of cold sensitivity by quadruple deletion of the *cspA* family and its suppression by PNPase S1 domain in *Escherichia coli*. *Mol. Microbiol.* 40, 179–188. doi: 10.1046/j.1365-2958.2001.02372.x
- Xia, B., Ke, H., Shinde, U., and Inouye, M. (2003). The role of RbfA in 16S rRNA processing and cell growth at low temperature in *Escherichia coli*. *J. Mol. Biol.* 332, 575–584. doi: 10.1016/S0022-2836(03)00953-7
- Yamanaka, K., Zheng, W., Crooke, E., Wang, Y.-H., and Inouye, M. (2001). CspD, a novel DNA replication inhibitor induced during the stationary phase in *Escherichia coli*. *Mol. Microbiol.* 39, 1572–1584. doi: 10.1046/j.1365-2958.2001.02345.x
- Ye, J., Coulouris, G., Zaretskaya, I., Cutcutache, I., Rozen, S., and Madden, T. L. (2012). Primer-BLAST: a tool to design target-specific primers for polymerase chain reaction. *BMC Bioinform.* 13:134. doi: 10.1186/1471-2105-13-134
- Yu, G., Wang, L.-G., Han, Y., and He, Q.-Y. (2012). ClusterProfiler: an R package for comparing biological themes among gene clusters. *J. Integr. Biol.* 16, 284–287. doi: 10.1089/omi.2011.0118

**Conflict of Interest Statement:** The authors declare that the research was conducted in the absence of any commercial or financial relationships that could be construed as a potential conflict of interest.

Copyright © 2018 Virtanen, Keto-Timonen, Jaakkola, Salin and Korkeala. This is an open-access article distributed under the terms of the Creative Commons Attribution License (CC BY). The use, distribution or reproduction in other forums is permitted, provided the original author(s) and the copyright owner(s) are credited and that the original publication in this journal is cited, in accordance with accepted academic practice. No use, distribution or reproduction is permitted which does not comply with these terms.



# Prevalence of *Yersinia* Species in the Ileum of Crohn's Disease Patients and Controls

Guillaume Le Baut<sup>1,2</sup>, Claire O'Brien<sup>3,4</sup>, Paul Pavli<sup>3,4</sup>, Maryline Roy<sup>1</sup>, Philippe Seksik<sup>5</sup>, Xavier Tréton<sup>1,6</sup>, Stéphane Nancey<sup>7,8</sup>, Nicolas Barnich<sup>9</sup>, Madeleine Bezault<sup>10</sup>, Claire Auzolle<sup>10</sup>, Dominique Cazals-Hatem<sup>1,6</sup>, Jérôme Viala<sup>1,11</sup>, Matthieu Allez<sup>10</sup>, The REMIND GROUP, Jean-Pierre Hugot<sup>1,11\*†</sup> and Anne Dumay<sup>1†</sup>

## OPEN ACCESS

### Edited by:

Matthew S. Francis,  
Umeå University, Sweden

### Reviewed by:

Maristela Gomes De Almeida,  
Hospital Edmundo Vasconcelos, Brazil  
Wojciech Marlicz,  
Pomeranian Medical University,  
Poland

### \*Correspondence:

Jean-Pierre Hugot  
jp.hugot@orange.fr

†These authors have contributed  
equally to this work

### Specialty section:

This article was submitted to  
Molecular Bacterial Pathogenesis,  
a section of the journal  
Frontiers in Cellular and Infection  
Microbiology

Received: 13 July 2018

Accepted: 30 August 2018

Published: 21 September 2018

### Citation:

Le Baut G, O'Brien C, Pavli P, Roy M, Seksik P, Tréton X, Nancey S, Barnich N, Bezault M, Auzolle C, Cazals-Hatem D, Viala J, Allez M, The REMIND GROUP, Hugot J-P and Dumay A (2018) Prevalence of *Yersinia* Species in the Ileum of Crohn's Disease Patients and Controls. *Front. Cell. Infect. Microbiol.* 8:336. doi: 10.3389/fcimb.2018.00336

<sup>1</sup> UMR1149 INSERM, Research Centre on Inflammation, Université Paris Diderot-Sorbonne Paris-Cité, Paris, France, <sup>2</sup> Department of Gastroenterology and Nutrition, Centre Hospitalier Universitaire de Caen, Caen, France, <sup>3</sup> IBD Research Group, Canberra Hospital, Canberra, ACT, Australia, <sup>4</sup> Australian National University Medical School, Canberra, ACT, Australia, <sup>5</sup> Gastroenterology Unit, CNRS, INSERM, ERL 1157, LBM, APHP, Saint Antoine Hospital, Sorbonne Universités, UPMC Univ Paris 06, Ecole Normale Supérieure, Paris, France, <sup>6</sup> Departments of Gastroenterology and Pathology, Hôpital Beaujon, Assistance Publique Hôpitaux de Paris, Paris, France, <sup>7</sup> Department of Gastroenterology, Hospices Civils de Lyon, Lyon-Sud Hospital, Pierre-Bénite, France, <sup>8</sup> INSERM U1111, International Center for Research in Infectiology, Lyon, France, <sup>9</sup> UMR 1071 Inserm/Université d'Auvergne, USC-INRA 2018, Microbes, Intestin, Inflammation et Susceptibilité de l'Hôte (M2ISH), CRNH Auvergne, Clermont-Ferrand, France, <sup>10</sup> Department of Gastroenterology, Saint-Louis Hospital, APHP, INSERM U1160, University Denis Diderot, Paris, France, <sup>11</sup> Department of Pediatric Gastroenterology, Hôpital Robert Debré, Assistance-Publique Hôpitaux de Paris, Paris, France

*Yersinia* are common contaminants of food products, but their prevalence in the human gut is poorly documented. *Yersinia* have been implicated in Crohn's Disease (CD, an inflammatory bowel disease) however their role in CD is controversial. We performed highly sensitive PCR assays of specific sequences for the *gyrB* gene of *Y. aldovae*, *Y. bercovieri*, *Y. enterocolitica*, *Y. intermedia*, *Y. mollaretii* and the *inv* gene of *Y. pseudotuberculosis*. We analyzed a total of 470 ileal samples taken from 338 participants (262 CD patients and 76 controls) belonging to three independent cohorts. All patients and controls were phenotyped and genotyped for the main CD susceptibility variants: *NOD2*, *ATG16L1*, and *IRGM*. *Yersinia* were found in 7.7% of ileal samples (respectively 7.9 and 7.6% in controls and CD patients) corresponding to 10% of participants (respectively 11.8 and 9.5% in controls and CD patients). *Y. enterocolitica*, *Y. pseudotuberculosis* and *Y. intermedia* were the most frequently identified species. The bacteria were more frequent in resected specimens, lymph nodes and Peyer's patches. *Yersinia* were no more likely to be detected in CD tissues than tissues from inflammatory and non-inflammatory controls. CD patients treated with immunosuppressants were less likely to be *Yersinia* carriers. In conclusion, this work shows that *Yersinia* species are frequently found at low levels in the human ileum in health and disease. The role of *Yersinia* species in this ecosystem should now be explored.

**Keywords:** *yersinia*, Crohn's disease, gut microbiota, ileal mucosa, innate immunity, mucosal immune system, molecular test

## INTRODUCTION

The genus *Yersinia* comprises 18 species, 3 of which are well-recognized human pathogens: *Y. pestis*, the causative agent of plague, and the two enteropathogenic species *Y. pseudotuberculosis* and *Y. enterocolitica*. The 15 other species are *Y. aldovae*, *Y. aleksiciae*, *Y. bercovieri*, *Y. entomophaga*, *Y. frederiksenii*, *Y. intermedia*, *Y. kristensenii*, *Y. massiliensis*, *Y. mollaretii*, *Y. nurmii*, *Y. pekkanenii*, *Y. rohdei*, *Y. ruckeri*, *Y. similis*, and *Y. wautersii*.

Various culture-dependent, immunological, and molecular techniques are currently available for the detection of pathogenic *Yersinia* (Gupta et al., 2015). The presence of *Y. enterocolitica* and *Y. pseudotuberculosis* can be determined quantitatively by direct culture on selective agar plates but confirmatory tests require a combination of cold enrichment and subcultures. Culture-independent methods have been developed to detect pathogenic *Y. enterocolitica* and *Y. pseudotuberculosis*. These PCR assays usually target the *yadA* or *virF* gene located on the pYV plasmid, and thus only detect virulent strains. Consequently, little is known about the presence of non-pathogenic *Yersinia* species in most of studied samples. *Yersinia* prevalence in food products, especially for low virulence species is thus undoubtedly underestimated, especially considering that *Yersinia* surveillance is not systematic in industrial processes.

Despite these limitations, *Yersinia* (mainly *enterocolitica*) have been associated with a variety of foods, including milk and milk products, raw meat (beef, pork, chicken, and lamb), poultry, eggs, vegetables, bean sprouts, tofu, seafood, and others. *Yersinia* species are able to propagate in vacuum-packed foods and at refrigeration temperature. Refrigeration of contaminated foods at manufacturing and consumer sites may provide *Yersinia* species an opportunity to survive and thrive in food. A recent shift toward the increased consumption of processed foods wherein contamination can occur after pasteurization has also potentiated the risk of outbreaks. Expansion in international food trade and changes in livestock farming and food industry have also led to the emergence of yersiniosis globally (Gupta et al., 2015).

As an example, a recent study performed in Turkey found 84 (28%) out of 300 food samples were contaminated by *Yersinia* species (Özdemir and Arslan, 2015). Of the food samples analyzed, 41% of 120 meat products and 19% of 180 milk products contained *Yersinia* species. *Y. enterocolitica* was the most frequently detected species ( $N = 18$ ), followed by *Y. rohdei* ( $N = 15$ ), *Y. intermedia* ( $N = 14$ ), *Y. pseudotuberculosis* ( $N = 12$ ), *Y. ruckeri* ( $N = 12$ ), *Y. mollaretii* ( $N = 5$ ), and *Y. bercovieri* ( $N = 4$ ). In another study from Austria, 90/120 (75%) of meat or fish samples contained *Yersinia* (Hilbert et al., 2003). In France, *Yersinia* was detected in eggs, vegetables, pastries, and others (Le Guern et al., 2016). Exposure to *Yersinia* in our food products appears to be common across continents.

Following food ingestion, about 10% of bacteria survive the acidic gastric environment. If they do survive, they may translocate the gut barrier via the follicle-associated epithelium, which comprises Peyer's patches in the small bowel, and isolated lymphoid follicles in the large bowel. Following translocation,

*Yersinia* may be phagocytosed by macrophages and drain to neighboring lymph nodes via lymphatic vessels, and less often to the portal blood stream.

It has been proposed that *Yersinia* species may contribute to the occurrence or persistence of gut inflammation in Crohn's Disease (CD) patients (Hugot et al., 2003), which is a chronic relapsing inflammatory condition of the digestive tract. CD can occur anywhere along the gastrointestinal tract, but most commonly affects the terminal ileum. Like yersiniosis, CD inflammation is initially focused around the follicle-associated epithelium (Fujimura et al., 1996; Krauss et al., 2012) and may progress into deeper, more diffuse ulcerations. Lymphatic vessels have been shown to play a key role in the dissemination in both yersiniosis (Von Der Weid and Rainey, 2010) and CD (Randolph et al., 2016). CD is characterized by an increased and persistent reactivity against the gut microbiota and similar observations have been made in mice infected with *Yersinia* (Fonseca et al., 2015). Several *NOD2* gene variants and a variant on the *ATG16L1* gene are strongly associated with CD. In mice, *Nod2* mutations homologous to the human CD-associated mutations favor the survival of animals orally infected with *Y. pseudotuberculosis* (Meinzer et al., 2012). Similarly, the CD-associated *Atg16l1* mutation has been associated with decreased clearance of *Y. enterocolitica* and a concurrent increase in inflammatory cytokine production (Murthy et al., 2014).

*Yersinia* infection in CD patients has been explored using conventional methods. Sera from CD patients were found to be reactive to enteropathogenic *Yersinia* more often than control sera (Saebo et al., 2005). Five studies used *Yersinia*-specific sequence primers to detect *Yersinia* species in CD tissues (Kallinowski et al., 1998; Lamps et al., 2003; Knösel et al., 2009; Chiodini et al., 2013; Leu et al., 2013). Overall 0–63% of CD samples were positive compared to 0–31% of inflammatory or non-inflammatory controls. In all studies, *Yersinia* were found in CD and/or controls suggesting that *Yersinia* is a common inhabitant of the human gastrointestinal tract. Differences in patient and control cohorts, tissues analyzed, and PCR methods may explain the large variations reported. Of note, Knösel et al. found more *Yersinia* species in control than CD archived tissues. In their study, PCR signals were weak suggesting that a non-specific sequence may have been amplified or alternatively that contaminations may have occurred. In none of the above studies, except for Chiodini's work, were the PCR products sequenced in order to confirm their specificity.

To further document the presence of *Yersinia* in intestinal tissues of CD patients and controls, we analyzed samples from three cohorts, representing a total 470 samples from 338 participants. All patients and controls were phenotyped and genotyped for the most strongly associated CD susceptibility gene variants. All samples were analyzed under the same conditions, using a validated sensitive PCR method capable of detecting six *Yersinia* species. PCR products were systematically sequenced to confirm the presence of *Yersinia*. Correlations between *Yersinia* positivity and clinical or genetic parameters were assessed.



**TABLE 1** | Characteristics of patients included in the three cohorts.

		Cohort 1, (O'Brien et al., 2014)	Cohort 2, (unpublished)	Cohort 3, (Fumery et al., 2017)
All participants		n = 65	n = 62	n = 211
Disease status	CD	52%	27%	100%
	UC	12%	24%	0%
	No-IBD controls	35%	48%	0%
Gender	Males	60%	53%	45%
Age (year)	Median (interquartile range)	45.1 (23–95) <sup>a</sup>	23.6 (9.5–62) <sup>b</sup>	33.8 (25–70) <sup>b</sup>
Smoking habits	Never smokers	NA	58%	38%
	Past smokers		21%	28%
	Active smokers		21%	34%
Genotyping	<i>NOD2</i> wt	68%	89%	56%
	<i>NOD2</i> mutated*	32%	11%	44%
	<i>ATG16L1</i> (AA)	18%	29%	21%
	<i>ATG16L1</i> (AG + GG)	82%	70%	79%
	<i>IRGM</i> (CC)	85%	74%	62%
	<i>IRGM</i> (CT + TT)	15%	26%	38%
CD patients only		n = 34	n = 17	n = 211
Age at diagnosis	A1 (<17 years)	16%	55%	10%
	A2 (17–40 years)	59%	45%	80%
	A3 (>40 years)	25%	0%	10%
Disease Location	L1 (ileum)	59%	20%	60%
	L2 (colon)	13%	50%	1%
	L3 (ileocolon)	25%	30%	38%
	L4 (upper gastrointestinal)	3%	0%	2%
Disease Behavior	B1 (inflammatory)	6%	80%	16%
	B2 (stricturing)	72%	0%	48%
	B3 (penetrating)	22%	20%	36%

CD, Crohn's Disease; UC, Ulcerative Colitis; IBD, Inflammatory Bowel Disease; <sup>a</sup>at diagnosis; <sup>b</sup>at enrolment; \*one or more of the R702W, G908R, or L1007fs-insC mutations. Cohort 1 and 3: post-surgical resected tissues, cohort 2: endoscopic mucosal biopsies. Montreal Classification is reported for CD patients (Satsangi et al., 2006).

## MATERIALS AND METHODS

### Patients

Three cohorts were used in this study. Cohort 1 is an Australian cohort of 65 patients [34 CD, 7 Ulcerative Colitis (UC), 24 others] previously published by O'Brien et al. (2014). Samples were taken from involved ( $n = 59$ ) and uninvolved ( $n = 53$ ) areas on ileal resected specimens and mesenteric lymph nodes ( $n = 53$ ). Cohort 2 is a French cohort of 62 patients (17 CD, 14 UC and 31 non-inflammatory controls). Mucosal biopsies were collected at diagnosis, and represent 45 Peyer's patches and 51 non-inflammatory ileal mucosa. Cohort 3 consisted of 211 CD resected bowel specimens from the REMIND study (Fumery et al., 2017), representing 211 inflamed ileal samples. The main characteristics of the three cohorts are summarized in **Table 1**.

All participants provided a written informed consent and the study was approved by the relevant ethic committees in France and Australia [Australian National University Human Ethics Committee approval (ref 2012/596), ACT Health Human

Research Ethics Committee approval (ref ETH.5.07.464), AFFSAPS approval (ref IDRCB: 2009-A00205-52) and French ethic committee Hôpital Saint Louis (ref 2009/17)].

### DNA Extraction and Amplification

For cohort 1, DNA was extracted using DNeasy Blood and Tissue kit (Qiagen) as previously described (O'Brien et al., 2014). For cohort 2, DNAs were extracted using QIAamp DNA mini kit (QIAGEN) according to standard protocols. For the third cohort, DNA extraction was performed from specimens preserved in RNAlater, using Trizol reagent (Invitrogen life technologie) with NucleoSpin Tissue (Macherey-Nagel).

DNA quantity and quality were checked for all samples using a Nanodrop ND-1000 spectrophotometer (NanoDrop Technologies, USA). Of the total of 509 DNA samples, 39 with DNA concentrations less than 20 ng/μl were removed. DNA samples were pre-amplified using the GenomiPhi V2 DNA Amplification kit (GE Healthcare) according to the manufacturer's instructions. Briefly, 25 ng of each DNA sample was heat-denatured at 95°C. After addition of the enzyme solution, the sample was incubated at 30°C for 90 min. DNA polymerases were then heat-inactivated at 65°C for 10 min and samples were stored at −20°C until use.

### Yersinia Identification

Unlike of previous studies, we wanted to identify several *Yersinia* species frequently encountered in contaminated food. We focused on *Yersinia*-specific sequences present in the genome regardless their pathogenicity and ability to differentiate *Yersinia* species. *In silico* analyses directed us to focus on *gyrB*, a gene coding for a subunit of DNA gyrase. Proteins encoded by *gyrB* exhibit considerable variation between species (Mun Huang, 1996). Their substitution rates have been estimated to be 4-fold higher than RNA 16S and *gyrB* has therefore been used to differentiate species and genera phylogenetically. **Figure 1A** shows the main differences between DNA sequences of different species of *Yersinia* and *E. coli*. In addition to *gyrB*, we determined the presence of *inv*, a virulence gene present in 100% of *Y. pseudotuberculosis* strains (Thoerner et al., 2003), and *ail*, a gene which is a marker of pathogenicity of *Y. enterocolitica*.

PCR assays were performed with 1.2 μl of pre-amplified DNA in a 20 μl volume containing Platinum blue reagent (Invitrogen life technologie) together with reverse and forward primers (0.2 μM of each). Our PCR assays were specific for the following six species: *Y. aldovae*, *Y. bercovieri*, *Y. enterocolitica*, *Y. intermedia*, *Y. mollaretii*, and *Y. pseudotuberculosis*. The primer sequences are provided in **Table 2**. PCR reactions were carried out using an Eppendorf Mastercycler (Eppendorf, Germany). An initial denaturation was performed at 95°C for 10 min, followed by 35 cycles of 95°C for 30 s, annealing temperature for 30 s and 72°C for 30 s. A second PCR reaction of 35 cycles was performed using 1.2 μl of the first-round PCR products, using the same conditions described above. All PCR reactions included negative controls.

PCR products were then analyzed on 1.5% agarose gels and stained with SYBR-safe (Invitrogen). Sequencing was



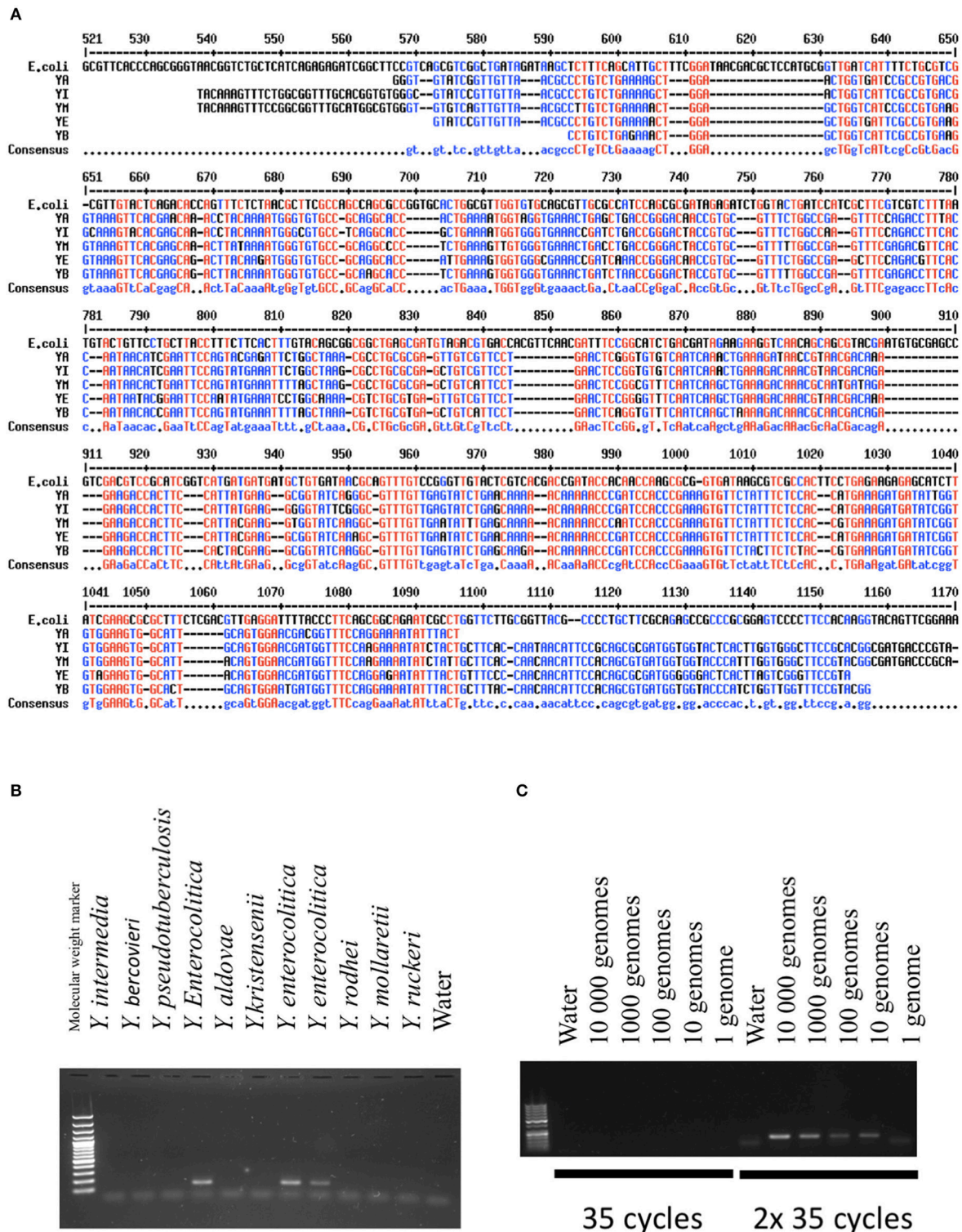


**FIGURE 1 |** Validation of the PCR methods. **(A)** Comparison of GyrB sequences between different *Yersinia* species and *E. coli*. In red are indicated the nucleic acids present in all species. In blue is indicated the consensus sequence (Corpet, 1998). YA, *Yersinia aldovae*; YB, *Yersinia bercovieri*; YE, *Yersinia enterocolitica*; YI, *Yersinia intermedia*; YM, *Yersinia Mollaretii*. **(B)** Specificity of the PCR methods developed for *Y. frederiksenii* (GyrB). DNAs from several species of *Yersinia* were amplified with the PCR technique and loaded on an agarose gel. A band indicates the presence of the specific PCR product specific to *Y. frederiksenii*. **(C)** Sensitivity of the PCR method developed for *Y. enterocolitica* (GyrB). The quantity of amplified DNA is expressed as genome equivalents. The method was highly sensitive when two cycles of 35 amplifications were performed.

**TABLE 2 |** Primers used for *Yersinia* species identification.

<i>Yersinia</i> species	Gene name	Forward and reverse primers sequences (5'-3')	Size of PCR product (bp)	Annealing temp (°C)
<i>Y. enterocolitica</i>	<i>ail</i>	ACTCGATGATACTGGGGAG CCCCCAGTAATCCATAAAGG	170	56
<i>Y. enterocolitica</i>	<i>gyrB</i>	AACCGATCAAACCGGGACAA AGCTTGATTGAAACCCCGGA	138	60
<i>Y. pseudotuberculosis</i>	<i>inv</i>	CGGTACGGCTCAAGTTAATCTG CCGTTCTCCAATGTACGTATCC	183	60
<i>Y. bercovieri</i>	<i>gyrB</i>	CGCAAGCACCTCTGAAAGTG CCGTACGGAAACCAACCAGA	414	60
<i>Y. mollaretii</i>	<i>gyrB</i>	AACTGACCTGACCGGGACTA GGAAGCCACCAAATGGGTA	380	60
<i>Y. intermedia</i>	<i>gyrB</i>	AAGTTTCTGGCGGTTTGAC CAGATCGGTTTCACCCACCA	138	60
<i>Y. aldovae</i>	<i>gyrB</i>	GATCCGCGGTGACGGTAAAG GCCCTGATACCGCCTTCATA for nested-PCR: CGCAGGCACCACTGAAAATG TGACACACCCGAGTTCAGGA	158	60

subsequently performed on all gel-purified PCR products (QIAquick extraction kit, Qiagen). Bi-allelic direct DNA sequencing was applied using BigDye Terminator v1.1 reagent (Applied Biosystems, USA), on an ABI 3730 automated genetic analyzer and analyzed using the 4peaks software. Sequences were then compared with those present in the NCBI public databases using BLAST. The presence of *Yersinia* was assumed if BLAST returned a homology score with *Yersinia* of at least 95%.

### NOD2, ATG16L1 and IRGM Genotyping

Allelic discrimination assays were used to genotype patients and controls for five susceptibility variants: *NOD2* SNPs rs2066844 (assay ID: C\_11717468\_20), rs2066845 (assay ID: C\_11717466\_20), and rs2066847 (custom assay); *ATG16L1* SNP rs2241880 (assay ID: C\_9095577\_20); and *IRGM* SNP rs10065172 (assay ID: C\_30593568\_10). These SNPs were analyzed using real-time PCR as recommended by the manufacturer (Applied Biosystems, USA). Reactions were carried out using a LightCycler 480 Systems (Roche). An initial denaturation step was performed at 95°C for 10 min, followed by 40 cycles of 92°C for 15 s and 1 min at 60°C.

### Statistics

Comparisons between groups were done using Fisher exact test for quantitative data, combined with a student *T*-test for qualitative data. Tests were performed using Xlstat V1.2. A *P*-value <0.05 was retained as significant.

## RESULTS

### Validation of the PCR Methods

Validation of the PCR techniques was based on the analysis of DNA from 10 *Yersinia* species (*Y. intermedia*, *Y. bercovieri*, *Y. pseudotuberculosis*, *Y. entomophaga*, *Y. aldovae*, *Y. frederiksenii*, *Y. mollaretii*, *Y. kristensenii*, *Y. ruckeri*, and *Y. rohdei*) kindly provided by Elisabeth Carniel from the

international reference center of *Yersinia*, Institut Pasteur, Paris, France. PCRs were performed using 5 ng of DNA (corresponding to  $\sim 10^6$  genomes). All species except *Y. rohdei* were detected by the selected primers. **Figure 1B** shows the results obtained with *gyrB* specific primers for *Y. enterocolitica*.

To evaluate the sensitivity of the PCR methods, we serially diluted the DNA samples between 1 to 10,000 genomes based on an estimated genome weight of  $\sim 4.7 \times 10^{-6}$  ng. The serial DNA dilutions underwent 35 PCR cycles, but no PCR products were observed in the majority of cases (**Figure 1C**). We thus performed a second round of 35 cycles, which allowed us to detect the bacteria. In these conditions, the thresholds were estimated between 1 and 100 equivalent genomes.

We also determined if the PCR techniques were efficient in detecting *Yersinia* in a DNA sample containing human genomic DNA. The presence of eukaryotic DNA did not alter the sensitivity of the methods (data not shown). We also confirmed that genomic pre-amplification did not significantly change the capacity of the PCR to detect *Yersinia* DNA (data not shown). Of note, when performed on human samples, the specificities of the PCR methods were lower than previously described with purified *Yersinia* DNA only. Indeed, several non-specific PCR products were evident for ileal samples, indicating that sequencing was always necessary to validate the presence of *Yersinia*-specific sequences in tissues.

Ultimately, we retained the PCR assays for *Y. aldovae*, *Y. bercovieri*, *Y. enterocolitica*, *Y. intermedia*, *Y. mollaretii*, and *Y. pseudotuberculosis*. For the other species, the sensitivity and/or specificity of the techniques were deemed to be insufficient.

### Yersinia in CD and Controls

We analyzed a total of 140 samples from 76 controls (ischemic colitis, intestinal obstructions, diverticular diseases and others) (**Table 3**). Seventy nine samples were from cohort 1 and consisted of mucosal tissues and lymph nodes. We found 6/54 specimens and 3/25 lymph nodes positive for *Yersinia* corresponding to a

**TABLE 3 |** Detection of *Yersinia* species in samples from the three cohorts.

Disease status	Cohort 1 (O'Brien et al., 2014)						Cohort 2 (unpublished)				Cohort 3 (Fumery et al., 2017)	
	CD (n = 34)			controls (n = 31)			CD (n = 17)		controls (n = 45)		CD (n = 211)	
	NIA (28)	IA (30)	LN (28)	NIA (25)	IA (29)	LN (25)	PP (17)	IM (16)	PP (26)	IM (35)	IA (211)	
<i>gyrB</i> for YE	0	3	1	3	2	2	0	0	2	0	9	
<i>ail</i> for YE	0	1	0	0	0	0	0	0	0	0	2	
<i>inv</i> for YP	1	0	0	0	0	1	1	0	0	0	2	
<i>gyrB</i> for YB	0	0	0	0	0	0	0	0	0	0	0	
<i>gyrB</i> for YM	0	0	0	1	0	0	0	0	0	0	1	
<i>gyrB</i> for YA	0	0	0	0	0	0	0	0	0	0	1	
<i>gyrB</i> for YI	1	0	0	2	0	0	0	0	0	0	2	
Positive samples	2 (7%)	4 (13%)	1 (4%)	4* (16%)	2 (7%)	3 (12%)	1 (6%)	0 (0%)	2 (7%)	0 (0%)	17 (8%)	

CD, Crohn's Disease; NIA, Non-inflammatory area; IA, inflammatory area; LN, lymph node; PP, Peyer's patch; IM, ileal mucosa; YE, *Y. enterocolitica*; YP, *Y. pseudotuberculosis*; YB, *Y. bercovieri*; YM, *Y. molarctii*; YA, *Y. aldovae*; YI, *Y. intermedia*. \*one patient was positive for 3 *Yersinia* species.

total of 11%. When several samples were available for the same individual, some were found positive, while others were not. This result indicated that the status of a given individual was highly dependent on the number of samples studied but also on the number of PCR reactions conducted on the same DNA sample (data not shown). In cohort 2, we found *Yersinia* DNA in 2/26 Peyer's patches (8%) and 0/35 mucosal biopsies, corresponding to a total of 3%. Thus a total of 8% of positive samples were found in the combined cohorts.

In cohorts 1 and 2, *Yersinia* species identified in controls were *Y. enterocolitica* ( $n = 9$ ), *Y. intermedia* ( $n = 2$ ), *Y. pseudotuberculosis* ( $n = 1$ ), and *Y. molarctii* ( $n = 1$ ). No differences were found between inflammatory and non-inflammatory controls.

In CD patients (all cohorts), as for the control group, biopsies were less often positive (1/33, 3%) than resected specimens or lymph nodes (24/297, 8%). On average, no clear difference was observed between CD cases and inflammatory or non-inflammatory controls. The *Yersinia* species encountered in CD patients were *Y. enterocolitica* ( $n = 13$ ), *Y. intermedia* ( $n = 3$ ), *Y. pseudotuberculosis* ( $n = 4$ ), *Y. molarctii* ( $n = 1$ ), and *Y. aldovae* ( $n = 1$ ) (Table 3). These results are similar to those of the control groups. Of note, only 3/13 *Y. enterocolitica* contained the *ail* gene suggesting that most of the strains present in the mucosa were not fully virulent (Sihvonen et al., 2011).

## Impact of Genetic and Clinical Parameters on the Presence of *Yersinia* Species

To look for an association between clinical, genetic or therapeutic parameters and the presence of *Yersinia* in CD patients we analyzed the data from cohorts 1 and 3 which were fully phenotyped and genotyped (Table 4). Positivity rates were roughly identical when gender, Montreal classification [age at diagnosis, behavior, and location] (Satsangi et al., 2006)] and genotypes were included in the analysis. Most of the therapeutic regimens also did not affect the frequency of detection, however

a borderline association between the use of immunosuppressants and the absence of *Yersinia* was found in cohorts 1 ( $P = 0.08$ ) and 3 ( $P = 0.08$ ). This association reached significance when pooling the two cohorts ( $P = 0.035$ ).

Most patients from cohort 3 were followed prospectively for at least 6 months after surgery. It was thus possible to evaluate the prognostic value of the presence of *Yersinia* at surgery on disease recurrence risk. The Rutgeerts endoscopic severity index, based on the presence of small bowel ulcerations, is widely used to monitor the presence of post-operative recurrence ( $i > 1$ ) or not ( $i < 2$ ). The Rutgeerts index calculated at least 6 months after surgery was not associated with the presence of *Yersinia* at surgery, suggesting that a sample positive for *Yersinia* is not predictive of an early recurrence.

## DISCUSSION

This study is the largest report of the presence of *Yersinia* in the human ileum. It is based on a total of 470 samples, taken from controls (140 samples) and CD patients (330 samples). The samples consisted of non-inflammatory ileal mucosa, Peyer's patches, resected bowel specimens, and lymph nodes. We looked for six different species of *Yersinia* with a highly sensitive PCR method, and sequenced all of the PCR products to confirm the presence of *Yersinia*-specific DNA.

This study proposes a new set of PCR tests based on the amplification of *gyrB* sequences, capable of identifying *Y. aldovae*, *Y. bercovieri*, *Y. enterocolitica*, *Y. intermedia*, and *Y. molarctii*. Despite a very high specificity of the tests *in vitro*, PCR products must always be sequenced to confirm the presence of *Yersinia* in tissues, because non-specific sequences are frequently encountered *in vivo*. These tests are highly sensitive, with detection thresholds between 1 and 100 bacteria per sample.

Given the low thresholds of bacterial detection, sampling plays an important role in the assay's results: increasing the number

**TABLE 4 |** Presence of *Yersinia* in ileal samples according to clinical and genetic classification of CD patients.

		Cohort 1			Cohort 3		
		Total	<i>Yersinia</i> +n (%)	P-value	Total	<i>Yersinia</i> +n (%)	P-value
Gender	Female	13	3 (23)	1	109	10 (9)	0.80
	Male	20	4 (20)		90	7 (8)	
Age at diagnosis	A1 (<17 years)	5	2 (40)	0.60	20	1 (5)	0.63
	A2 (17–40 years)	19	4 (21)		159	13 (8)	
	A3 (>40 years)	8	1 (12)		20	3 (15)	
Disease behavior	B1 (inflammatory)	2	0 (0)	1	32	4 (13)	0.23
	B2 (stricturing)	23	5 (22)		96	5 (5)	
	B3 (penetrating)	7	2 (29)		71	8 (11)	
Disease location	L1 (ileum)	19	4 (21)	1	120	8 (7)	0.45
	L2 (colon)	4	1 (25)		1	0 (0)	
	L3 (ileocolon)	8	2 (25)		75	9 (12)	
	L4 (upper gastrointestinal)	1	0 (0)		3	0 (0)	
Genotype	<i>NOD2</i> wt	20	4 (20)	0.92	118	11 (9)	0.61
	<i>NOD2</i> mutated*	14	3 (21)		93	6 (6)	
	<i>ATG16L1</i> (AA)	6	1 (17)	1	45	6 (13)	0.21
	<i>ATG16L1</i> (AG + GG)	28	6 (21)		165	11 (7)	
	<i>IRGM</i> (CC)	28	6 (21)	1	130	10 (8)	0.80
	<i>IRGM</i> (CT + TT)	6	1 (17)		80	7 (9)	
Medications at surgery	Antibiotics	9	1 (11)	0.64	65	7 (11)	0.43
	No antibiotics	22	5 (22)		134	10 (7)	
	Anti-TNF	8	2 (25)	0.64	99	6 (6)	0.31
	No anti-TNF	22	4 (18)		99	11 (11)	
	Immunosuppressants	15	1 (7)	0.08	60	2 (3)	0.08
	No immunosuppressants	14	5 (36)		138	15 (11)	
	Corticosteroids	17	1 (6)	0.06	67	9 (13)	0.10
	No corticosteroids	13	5 (38)		131	8 (6)	
	5-ASA	7	2 (29)	0.61	16	2 (12)	0.63
	No 5-ASA	22	4 (18)		183	15 (8)	
Rutgeerts score	i0 + i1	NA			87	10 (11)	0.26
	i2 + i3 + i4				70	4 (6)	

\*one or more of the R702W, G908R or L1007fs-insC mutations; 5-ASA, 5 aminosalicylates.

of samples tested increases the number of positive results on a per patient basis. This point is well illustrated by cohort 1 where three samples were tested for most patients with a positivity of 21% at the patient level but only 10% at the sample level. As a consequence, it is possible that *Yersinia* species could be found in the ileum of many people (may be all) if one performs enough tests. As a whole, the percentage and significance of negative results in patients remains to be evaluated. The concordance between this new test and other methods like serological tests or immunohistochemistry methods also needs to be explored.

If our work suggests that *Yersinia* carriage is common, it also indicates that there are generally low numbers in the ileum. This result is consistent with the fact that *Yersinia* are rarely found in stool and mucosal samples from either CD patients or controls in gut microbiota analyses (Sihvonen et al., 2011). These are designed to explore the dominant species, and are not appropriate for detecting low abundance of *Yersinia* species.

Low bacterial loads are also in line with a common exposure to the few bacteria assumed to be present in contaminated food. The main bacteria encountered in the ileum are *Y. enterocolitica* which represent about 2/3 of the identified bacteria. *Y. pseudotuberculosis* and *Y. intermedia* are the second most commonly found here. Even if we did not test all the panel of *Yersinia* species, these relative frequencies seem to reflect the relative frequencies of *Yersinia* species in food products (Özdemir and Arslan, 2015). Among *Y. enterocolitica*, most of the strains did not carry the *ail* gene indicating that they are not fully virulent. In other words, bacteria appear to be mainly non-virulent, or transient (allochthonous), and their retrieval from the gut may simply be a marker of food contamination. Additional works looking at a relationship between food habits and the presence of *Yersinia* in the gut would help to resolve this question.

On the other hand, looking at *Yersinia* species as inoffensive bystanders passively transported by the luminal flow can be



questioned. *Yersinia* species are able to survive in the ileum due to their facultative anaerobic properties and tolerance to the bile acids (Bottone, 1997). They are able to interact with the gut associated lymphoid tissue and we confirm here the tropism of *Yersinia* for M-cells, the bacteria being mainly found in superficial biopsies centered on Peyer's patches. However, superficial biopsies tended to be positive less often than resected bowel specimens ( $P = 0.058$ ). This may be related to technical differences in sample collection and storage. But it may also indicate that the bacteria are more commonly detectable within the inner intestinal layers. This point is in accordance with a previous study showing the presence of *Yersinia* in the submucosal layer of the intestine (Chiodini et al., 2013). The relatively high frequency of bacteria in mesenteric lymph nodes also supports this idea. If true, this finding indicates that *Yersinia*, even low virulence strains, are able to translocate through the gut epithelial barrier and putatively the gut-vascular barrier (Spadoni et al., 2015).

It is important to note that bacteria were equally frequent in non-inflammatory, and inflammatory controls and CD patients, and that *Yersinia* could be found in inflammatory and non-inflammatory parts of the ileum in CD patients. Thus, CD cannot be seen as an infection by *Yersinia* species: the disease is not defined by its presence in the intestinal tissues. However, it cannot be dismantled that CD patients have an abnormal response toward *Yersinia*. Indeed, *Yersinia* have been associated with long-term sequelae after acute infection in mice, including destruction of the lymphatic network and loss of antigen tolerance, similar to CD (Fonseca et al., 2015). Furthermore, CD is characterized by increased adipose tissue around the lesions (fat wrapping). White adipose tissue has been recently shown to play a key role in the long-term memory of infection by *Yersinia* (Han et al., 2017). Thus CD could be characterized by an excessive response toward *Yersinia*. The abnormal inflammatory response to *Yersinia* in mice carrying either *Nod2* or *Atg16l1* CD-associated mutations (Meinzer et al., 2008; Murthy et al., 2014) further supports this idea.

This work failed to detect an association between phenotypic or genotypic subgroups of patients. Mutations in *NOD2* (a gene involved in the innate immunity and bacterial sensing) or *ATG16L1* and *IRGM*, (two genes involved in autophagy and xenophagy) are not associated with *Yersinia* positivity despite their roles in the host response to the bacteria. The age at onset is also not associated with the presence of *Yersinia*. It is more difficult to demonstrate an association between disease location and behavior (L and B values of the Montreal classification). Indeed, fistulizing, and penetrating ileal diseases are over-represented in surgical patients, which represented the largest contingent of the studied cohorts.

Common medications used to treat CD patients, including antibiotics, are not associated with the presence of *Yersinia*. This finding is not surprising if we consider that they are often administered prior to surgery. As a result, bacteria, including dead cells, remain detectable by PCR. Steroids, immunosuppressants or anti-TNF antibodies could be expected to decrease bacterial clearance and promote *Yersinia* detection. However, the presence of bacteria at very low rates in the mucosa must be distinguished from an invasive infection and the impact of immunosuppressive agents is likely to be different in these two situations. At the opposite, immunosuppressants tended to be associated with a lower rate of positive samples in two cohorts. An hypothesis to explain this finding is that azathioprine (which is the most commonly used immunosuppressant in CD), modulates intracellular GTP levels and thus interferes with the function of Rac1, a Rho GTPase (Tiede et al., 2003). Rho GTPase activities are important for bacterial internalization by host cells and subsequent dissemination and survival of bacteria (Schweer et al., 2013). A defect of bacterial internalization could be disadvantageous for bacterial survival and azathioprine could thus have a beneficial role in CD, not only via its immunosuppressive properties, but also via the reduction of *Yersinia* burden in the gut mucosa.

In summary, this work provides for the first time the demonstration that *Yersinia* species are common in human ileum. The presence of different species seems to be proportional to assumed rates of exposure in contaminated foods. *Yersinia* are found in the same proportions in controls and CD patients, whatever their clinical presentation. It is important now to characterize the mucosal immune response toward *Yersinia* species in CD patients.

## AUTHOR CONTRIBUTIONS

GL, AD, and J-PH were involved in study design, data acquisition, analyses and writing. CO, PP were involved in study design, data acquisition, and analyses for cohort 1. JV, J-PH, DC-H, and MA were involved in data acquisition for cohort 2. PS, XT, SN, MB, CA, and The REMIND Group were involved in study design, data acquisition and analyses for cohort 3. NB, MR, and AD were involved in participants genotyping PCR analyses.

## ACKNOWLEDGMENTS

This work has been supported by Investissements d'Avenir programme ANR-11-IDEX-0005-02, Sorbonne Paris Cite, Laboratoire d'excellence INFLAMEX. We thank all investigators (researchers, clinicians and surgeons) of the REMIND group who collected the ileal samples. We thank Rida Zouak for technical assistance and Elisabeth Carniel who gave us the reference *Yersinia* strains.

## REFERENCES

- Bottone, E. J. (1997). *Yersinia enterocolitica*: the charisma continues. *Clin. Microbiol. Rev.* 10, 257–276.
- Chiodini, R. J., Dowd, S. E., Davis, B., Galandiuk, S., Chamberlin, W. M., Kuenstner, J. T., et al. (2013). Crohn's disease may be differentiated into 2 distinct biotypes based on the detection of bacterial genomic sequences and virulence genes within submucosal tissues. *J. Clin. Gastroenterol.* 47, 612–620. doi: 10.1097/MCG.0b013e31827b4f94
- Corpet, F. (1998). Multiple sequence alignment with hierarchical clustering. *Nucleic Acids Res.* 16, 10881–10890.
- Fonseca, D. M., Hand, T. W., Han, S.-J., Gerner, M. Y., Zaretsky, A. G., Byrd, A. L., et al. (2015). Microbiota-dependent sequelae of acute infection compromise tissue-specific immunity. *Cell* 163, 354–366. doi: 10.1016/j.cell.2015.08.030
- Fujimura, Y., Kamoi, R., and Iida, M. (1996). Pathogenesis of aphthoid ulcers in Crohn's disease: correlative findings by magnifying colonoscopy, electron microscopy, and immunohistochemistry. *Gut* 38, 724–732. doi: 10.1136/gut.38.5.724
- Fumery, M., Seksik, P., Auzolle, C., Munoz-Bongrand, N., Gornet, J.-M., Boschetti, G., et al. (2017). Postoperative complications after ileocecal resection in Crohn's Disease: a prospective study from the REMIND Group. *Am. J. Gastroenterol.* 112, 337–345. doi: 10.1038/ajg.2016.541
- Gupta, V., Gulati, P., Bhagat, N., Dhar, M. S., and Virdi, J. S. (2015). Detection of *Yersinia enterocolitica* in food: an overview. *Eur. J. Clin. Microbiol. Infect. Dis.* 34, 641–650. doi: 10.1007/s10096-014-2276-7
- Han, S.-J., Glatman Zaretsky, A., Andrade-Oliveira, V., Collins, N., Dzutsev, A., Shaik, J., et al. (2017). White adipose tissue is a reservoir for memory T cells and promotes protective memory responses to infection. *Immunity* 47, 1154–1168.e6. doi: 10.1016/j.immuni.2017.11.009
- Hilbert, F., Mayrhofer, S., and Smulders, F. J. (2003). Rapid urease screening of yersinia on CIN agar plates. *Int. J. Food Microbiol.* 84, 111–115. doi: 10.1016/S0168-1605(02)00397-5
- Hugot, J.-P., Alberti, C., Berrebi, D., Bingen, E., and Cézard, J.-P. (2003). Crohn's disease: the cold chain hypothesis. *Lancet* 362, 2012–2015. doi: 10.1016/S0140-6736(03)15024-6
- Kallinowski, F., Wassmer, A., Hofmann, M. A., Harmsen, D., Heesemann, J., Karch, H., et al. (1998). Prevalence of enteropathogenic bacteria in surgically treated chronic inflammatory bowel disease. *Hepatogastroenterology* 45, 1552–1558.
- Knösel, T., Schewe, C., Petersen, N., Dietel, M., and Petersen, I. (2009). Prevalence of infectious pathogens in Crohn's disease. *Pathol. Res. Pract.* 205, 223–230. doi: 10.1016/j.prp.2008.04.018
- Krauss, E., Agaimy, A., Neumann, H., Schulz, U., Kessler, H., Hartmann, A., et al. (2012). Characterization of lymphoid follicles with red ring signs as first manifestation of early Crohn's disease by conventional histopathology and confocal laser endomicroscopy. *Int. J. Clin. Exp. Pathol.* 5, 411–421.
- Lamps, L. W., Madhusudan, K. T., Havens, J. M., Greenson, J. K., Bronner, M. P., Chiles, M. C., et al. (2003). Pathogenic *Yersinia* DNA is detected in bowel and mesenteric lymph nodes from patients with Crohn's disease. *Am. J. Surg. Pathol.* 27, 220–227. doi: 10.1097/00000478-200302000-00011
- Le Guern, A.-S., Martin, L., Savin, C., and Carniel, E. (2016). Yersiniosis in France: overview and potential sources of infection. *Int. J. Infect. Dis.* 46, 1–7. doi: 10.1016/j.ijid.2016.03.008
- Leu, S. B., Shulman, S. C., Steelman, C. K., Lamps, L. W., Bulut, O. P., Abramowsky, C. R., et al. (2013). Pathogenic yersinia DNA in intestinal specimens of pediatric patients with crohn's disease. *Fetal Pediatr. Pathol.* 32, 367–370. doi: 10.3109/15513815.2013.768744
- Meinzer, U., Barreau, F., Esmiol-Welterlin, S., Jung, C., Villard, C., Léger, T., et al. (2012). *Yersinia pseudotuberculosis* effector YopJ subverts the Nod2/RICK/TAK1 pathway and activates caspase-1 to induce intestinal barrier dysfunction. *Cell Host Microbe* 11, 337–351. doi: 10.1016/j.chom.2012.02.009
- Meinzer, U., Esmiol-Welterlin, S., Barreau, F., Berrebi, D., Dussaillant, M., Bonacorsi, S., et al. (2008). Nod2 mediates susceptibility to *Yersinia pseudotuberculosis* in mice. *PLoS ONE* 3:e2769. doi: 10.1371/journal.pone.0002769
- Mun Huang, W. (1996). Bacterial diversity based on type II DNA topoisomerase genes. *Annu. Rev. Genet.* 30, 79–107. doi: 10.1146/annurev.genet.30.1.79
- Murthy, A., Li, Y., Peng, L., Reichelt, M., Katakam, A. K., Noubade, R., et al. (2014). A Crohn's disease variant in Atg16l1 enhances its degradation by caspase 3. *Nature* 506, 456–462. doi: 10.1038/nature13044
- O'Brien, C. L., Pavli, P., Gordon, D. M., and Allison, G. E. (2014). Detection of bacterial DNA in lymph nodes of Crohn's disease patients using high throughput sequencing. *Gut* 63, 1596–1606. doi: 10.1136/gutjnl-2013-305320
- Özdemir, F., and Arslan, S. (2015). Genotypic and phenotypic virulence characteristics and antimicrobial resistance of *Yersinia* spp. isolated from meat and milk products: virulence factors of *Yersinia* spp. *J. Food Sci.* 80, M1306–M1313. doi: 10.1111/1750-3841.12911
- Randolph, G. J., Bala, S., Rahier, J.-F., Johnson, M. W., Wang, P. L., Nalbantoglu, I., et al. (2016). Lymphoid aggregates remodel lymphatic collecting vessels that serve mesenteric lymph nodes in crohn disease. *Am. J. Pathol.* 186, 3066–3073. doi: 10.1016/j.ajpath.2016.07.026
- Saebo, A., Vik, E., Lange, O. J., and Matuszkiewicz, L. (2005). Inflammatory bowel disease associated with *Yersinia enterocolitica* O:3 infection. *Eur. J. Intern. Med.* 16, 176–182. doi: 10.1016/j.ejim.2004.11.008
- Satsangi, J., Silverberg, M. S., Vermeire, S., and Colombel, J. F. (2006). The Montreal classification of inflammatory bowel disease: controversies, consensus, and implications. *Gut* 55, 749–753. doi: 10.1136/gut.2005.082909
- Schweer, J., Kulkarni, D., Kochut, A., Pezoldt, J., Pisano, F., Pils, M. C., et al. (2013). The cytotoxic necrotizing factor of *Yersinia pseudotuberculosis* (CNFY) enhances inflammation and yop delivery during infection by activation of rho GTPases. *PLoS Pathog.* 9:e1003746. doi: 10.1371/journal.ppat.1003746
- Sihvonen, L. M., Hallanvuori, S., Haukka, K., Skurnik, M., and Siitonen, A. (2011). The ail gene is present in some yersinia enterocolitica biotype 1A strains. *Foodborne Pathog. Dis.* 8, 455–457. doi: 10.1089/fpd.2010.0747
- Spadoni, I., Zagato, E., Bertocchi, A., Paolinelli, R., Hot, E., Di Sabatino, A., et al. (2015). A gut-vascular barrier controls the systemic dissemination of bacteria. *Science* 350, 830–834. doi: 10.1126/science.1250135
- Thoerner, P., Bin Kingombe, C. I., Bogli-Stubler, K., Bissig-Choisat, B., Wassenaar, T. M., Frey, J., et al. (2003). PCR detection of virulence genes in *Yersinia enterocolitica* and *Yersinia pseudotuberculosis* and investigation of virulence gene distribution. *Appl. Environ. Microbiol.* 69, 1810–1816. doi: 10.1128/AEM.69.3.1810-1816.2003
- Tiede, I., Fritz, G., Strand, S., Poppe, D., Dvorsky, R., Strand, D., et al. (2003). CD28-dependent Rac1 activation is the molecular target of azathioprine in primary human CD4+ T lymphocytes. *J. Clin. Invest.* 111, 1133–1145. doi: 10.1172/JCI16432
- Von Der Weid, P.-Y., and Rainey, K. J. (2010). Review article: lymphatic system and associated adipose tissue in the development of inflammatory bowel disease: review: lymphatics, fat and IBD. *Aliment. Pharmacol. Ther.* 32, 697–711. doi: 10.1111/j.1365-2036.2010.04407.x

**Conflict of Interest Statement:** The authors declare that the research was conducted in the absence of any commercial or financial relationships that could be construed as a potential conflict of interest.

Copyright © 2018 Le Baut, O'Brien, Pavli, Roy, Seksik, Tréton, Nancey, Barnich, Bezault, Auzolle, Cazals-Hatem, Viala, Allez, The REMIND GROUP, Hugot and Dumay. This is an open-access article distributed under the terms of the Creative Commons Attribution License (CC BY). The use, distribution or reproduction in other forums is permitted, provided the original author(s) and the copyright owner(s) are credited and that the original publication in this journal is cited, in accordance with accepted academic practice. No use, distribution or reproduction is permitted which does not comply with these terms.



# OmpR-Mediated Transcriptional Regulation and Function of Two Heme Receptor Proteins of *Yersinia enterocolitica* Bio-Serotype 2/O:9

Karolina Jaworska, Marta Nieckarz, Marta Ludwiczak, Adrianna Raczowska\* and Katarzyna Brzostek

Department of Applied Microbiology, Institute of Microbiology, Faculty of Biology, University of Warsaw, Warsaw, Poland

## OPEN ACCESS

### Edited by:

Victoria Auerbuch,  
University of California, Santa Cruz,  
United States

### Reviewed by:

Michael Marceau,  
Université Lille Nord de France, France  
Xihui Shen,  
Northwest A&F University, China

### \*Correspondence:

Adrianna Raczowska  
araczko@biol.uw.edu.pl

### Specialty section:

This article was submitted to  
Molecular Bacterial Pathogenesis,  
a section of the journal  
Frontiers in Cellular and Infection  
Microbiology

**Received:** 10 July 2018

**Accepted:** 29 August 2018

**Published:** 20 September 2018

### Citation:

Jaworska K, Nieckarz M,  
Ludwiczak M, Raczowska A and  
Brzostek K (2018) OmpR-Mediated  
Transcriptional Regulation and  
Function of Two Heme Receptor  
Proteins of *Yersinia enterocolitica*  
Bio-Serotype 2/O:9.  
Front. Cell. Infect. Microbiol. 8:333.  
doi: 10.3389/fcimb.2018.00333

We show that *Yersinia enterocolitica* strain Ye9 (bio-serotype 2/O:9) utilizes heme-containing molecules as an iron source. The Ye9 genome contains two multigenic clusters, *hemPRSTUV-1* and *hemPRST-2*, encoding putative heme receptors HemR1 and HemR2, that share 62% amino acid identity. Expression of these proteins in an *Escherichia coli* mutant defective in heme biosynthesis allowed this strain to use hemin and hemoglobin as a source of porphyrin. The *hemPRSTUV-1* and *hemPRST-2* clusters are organized as operons, expressed from the  $p_{\text{hem-1}}$  and weaker  $p_{\text{hem-2}}$  promoters, respectively. Expression of both operons is negatively regulated by iron and the iron-responsive transcriptional repressor Fur. In addition, OmpR, the response regulator of two component system (TCSs) EnvZ/OmpR, represses transcription of both operons through interaction with binding sequences overlapping the  $-35$  region of their promoters. Western blot analysis of the level of HemR1 in *ompR*, *fur*, and *ompRfur* mutants, showed an additive effect of these mutations, indicating that OmpR may regulate HemR expression independently of Fur. However, the effect of OmpR on the activity of the  $p_{\text{hem-1}}$  promoter and on HemR1 production was observed in both iron-depleted and iron-replete conditions, i.e., when Fur represses the iron-regulated promoter. In addition, a hairpin RNA thermometer, composed of four uracil residues (FourU) that pair with the ribosome-binding site in the 5'-untranslated region (5'-UTR) of *hemR1* was predicted by *in silico* analysis. However, thermoregulated expression of HemR1 could not be demonstrated. Taken together, these data suggest that Fur and OmpR control iron/heme acquisition via a complex mechanism based on negative regulation of *hemR1* and *hemR2* at the transcriptional level. This interplay could fine-tune the level of heme receptor proteins to allow *Y. enterocolitica* to fulfill its iron/heme requirements without over-accumulation, which might be important for pathogenic growth within human hosts.

**Keywords:** OmpR, Fur, *Yersinia enterocolitica*, HemR1, HemR2

## INTRODUCTION

*Yersinia enterocolitica*, a member of the genus *Yersinia* in the family *Enterobacteriaceae* is a human enteropathogen which causes yersiniosis, i.e., gut-associated diseases such as enteritis, diarrhea, and mesenterial lymphadenitis (Bottone, 1997). Multiple virulence factors encoded by chromosomal and plasmid pYV-located genes are involved in *Y. enterocolitica* virulence (Cornelis, 2002). In addition, iron-acquisition systems are considered important pathogenicity determinants. The concentration of iron in the environment is critical for the control of bacterial metabolism. Iron limitation in the host can abolish bacterial growth, whereas a high intracellular iron concentration may damage bacterial cells due to the formation of harmful reactive oxygen species (ROS). Thus, the transport, storage, and metabolism of iron have to be tightly controlled to maintain iron homeostasis (Hantke, 2001).

A variety of mechanisms are employed by *Y. enterocolitica* to take up iron from the host body, including siderophore-mediated uptake and systems for acquiring iron from abundant heme or hemoproteins (Caza and Kronstad, 2013). Pathogenic strains can be divided into two groups: those producing the siderophore yersiniabactin (biotype 1B) and those unable to produce this siderophore but able to use ectogenic siderophores released by other bacteria, such as ferrioxamin B and E or ferrichrome (biotypes 2–5) (Heesemann, 1987; Bäumlér et al., 1993). About 70% of the iron in the human host is present within heme and/or hemoproteins (hemoglobin, myoglobin, cytochromes). A heme uptake system was identified previously in *Y. enterocolitica* bio-serotype 1B/O:8 strain WA-C (Stojiljkovic and Hantke, 1992, 1994). This system, involved in the acquisition and transport of the entire heme moiety into the cytoplasm, consists of the receptor HemR, an ATP-binding cassette (ABC) transporter HemTUV, and a putative heme-degrading protein HemS. The energy for heme uptake is transferred from the inner to the outer membrane via the TonB/ExbB/ExbD system (Krewulak and Vogel, 2011). The protein TonB spans the periplasm and can physically interact with a highly conserved region of the receptor HemR called the TonB box. A conformational change in the heme receptor caused by this interaction permits the transport of the ligand across the OM into the periplasm (Nau and Konisky, 1989; Braun et al., 1991). Gene clusters responsible for the uptake and transport of heme have been identified in several bacterial species, including *Yersinia pestis* (*hmuRSTUV*) (Thompson et al., 1999), *Yersinia pseudotuberculosis* (*hmuRSTUV*) (Schwiesow et al., 2018), *Shigella dysenteriae* (*shu* genes) (Wyckoff et al., 1998), and *Vibrio cholerae* (*hut* genes) (Occhino et al., 1998), although their organization varies. The heme gene cluster of *Y. enterocolitica* bio-serotype 1B/O:8 strain WA-C contains six open reading frames (ORFs) *hemPRSTUV*, organized in an operon whose expression is enhanced by iron deprivation (Stojiljkovic and Hantke, 1992, 1994). To avoid high concentrations of free intracellular iron, the ferric uptake regulator (Fur) with Fe<sup>2+</sup> cofactor efficiently represses the transcription of appropriate genes. Fur is a global transcriptional regulator that tightly controls the transport, storage, and metabolism of iron in many Gram-negative bacteria (Hantke, 2001). In addition, Fur

represses the expression of genes involved in the regulation of multiple cellular functions such as the oxidative stress response, energy metabolism, acid tolerance, and virulence (Hassett et al., 1996; Ochsner and Vasil, 1996; Bijlsma et al., 2002; van Vliet et al., 2003).

Bacterial cells are constantly challenged by various environmental stresses in their natural habitats. *Y. enterocolitica* faces several different challenges during infection and colonization of the human body. Efficient adaptation to changing environmental conditions is possible due to the activity of sensory regulators such as TCSs, e.g., the EnvZ/OmpR signaling pathway. This prototype TCS, first identified and characterized in non-pathogenic *Escherichia coli* K-12, consists of the transmembrane histidine kinase EnvZ and the response regulator OmpR. EnvZ senses changes in the environment, undergoes autophosphorylation and then a phosphate group is transferred to OmpR. Conformational changes in the phosphorylated OmpR allow it to bind to DNA as a dimer and modulate gene expression (Kenney, 2002). EnvZ/OmpR is involved in the transcriptional regulation, in a positive or negative manner, of several genes/operons of *E. coli* in response to changes in osmolarity, pH, temperature, and the concentration of nutrients in the environment (Slauch and Silhavy, 1989; Higashitani et al., 1993; Shin and Park, 1995; Vidal et al., 1998; Yamamoto et al., 2000; Jubelin et al., 2005). OmpR was recognized as a pleiotropic regulator that controls the expression of genes involved in many different cellular processes such as chemotaxis, motility, drug sensitivity, or acid resistance, and virulence of pathogenic bacteria (Bernardini et al., 1990; Chatfield et al., 1991; Shin and Park, 1995; Bang et al., 2002; Feng et al., 2003; Stincone et al., 2011).

The relationship between virulence and the activity of the OmpR protein has also been described for *Y. enterocolitica* O:8 (Dorman et al., 1989) and *Y. enterocolitica* 2/O:9 (our studies). We have shown that OmpR is involved in the control of various cellular processes and functions in *Y. enterocolitica*, including adhesion, invasion, motility, Yop production, biofilm formation, and multidrug and serum resistance (Brzostek et al., 2003, 2007, 2012; Raczowska et al., 2010, 2011a,b, 2015; Brzóstkowska et al., 2012; Skorek et al., 2013). Taken together, these findings have revealed the important role of OmpR in remodeling the cell surface and in the adaptation of *Y. enterocolitica* to different environmental niches, including the host body.

Comparative proteomic LC-MS/MS analysis of outer membranes prepared from *Y. enterocolitica* bio-serotype 2/O:9 strain Ye9 and its isogenic *ompR* deletion mutant AR4 identified HemR, an ortholog of enterobacterial heme receptor proteins, including HemR of *Y. enterocolitica* strain 8081 of bio-serotype 1B/O:8 (99% amino acid identity), as subject to negative regulation by OmpR. Moreover, preliminary data suggested an indirect role for OmpR in regulating *hemR* expression (Nieckarz et al., 2016).

Here, we demonstrate that the *Y. enterocolitica* Ye9 genome contains two multigene clusters, *hemPRSTUV*-1 and *hemPRST*-2, encoding homologous heme receptor proteins HemR1 and HemR2. Furthermore, we show that both clusters are organized as operons that are negatively regulated by Fur. More



importantly, OmpR directly represses the expression of *hemR1* and *hemR2* through interaction with binding sequences located in the promoter regions of their respective operons. In addition, a zipper-like RNA structure closely resembling a FourU RNA thermosensor was recognized within the *hemR1* 5'-untranslated region (5'-UTR), but *hemR1* expression was not subject to thermoregulation at the post-transcriptional level. Our results suggest that OmpR controls HemR1 expression in both the absence and presence of the Fur repressor. Finally, we evaluated the importance of both heme receptor proteins in iron/heme acquisition by *Y. enterocolitica* and *E. coli* cells.

## MATERIALS AND METHODS

### Bacterial Strains and Growth Conditions

The bacterial strains used in this study are described in Table S1. *E. coli* strains for plasmid manipulation and propagation were grown at 37°C in LB medium (10 g/l tryptone, 5 g/l yeast extract, 5 g/l NaCl). *E. coli* strain SASX77 ( $\Delta$ *hemA* mutant), was grown in the presence of 50 mM aminolevulinic acid (ALA; Sigma-Aldrich) unless otherwise indicated. *Y. enterocolitica* strains were cultured at 26 or 37°C in LB medium. To achieve iron-depleted conditions, cultures were grown in LBD medium, i.e., LB supplemented with an inhibitory concentration of 150  $\mu$ M 2,2'-dipyridyl (DPD; Sigma-Aldrich). Antibiotics were used at the following concentrations: nalidixic acid (Nal), 30  $\mu$ g/ml; chloramphenicol (Cm), 25  $\mu$ g/ml; kanamycin (Km), 50  $\mu$ g/ml; gentamicin (Gm), 40  $\mu$ g/ml; tetracycline (Tet), 12.5  $\mu$ g/ml; spectinomycin (Sp), 100  $\mu$ g/ml.

### Assay for Utilization of Heme-Containing Compounds as an Iron Source

*Y. enterocolitica* strain Ye9 grown under iron-depleted conditions was tested for the ability to obtain iron from heme-containing compounds. Initially, the growth yield (OD<sub>600</sub>) of this strain in LB supplemented with the iron chelator (DPD) to final concentrations of 0, 100, 150, 200, and 300  $\mu$ M, was assessed. Cultures were incubated at 26 or 37°C for 28 h. Subsequently, heme and hemoglobin at final concentrations of 10 and 2.5  $\mu$ M, respectively, were added to LBD (150  $\mu$ M DPD) and the growth yield determined as above.

### Growth of *E. coli* Strain SASX77 ( $\Delta$ *hemA* Mutant) Carrying Plasmids Expressing *Y. enterocolitica* HemR1 or HemR2 Proteins

The *E. coli*  $\Delta$ *hemA* strain SASX77, which is defective in ALA synthetase, was transformed with the plasmid pACYC184 or its derivatives pHEM1 and pHEM2, and maintained on LB agar supplemented with 50  $\mu$ M ALA and Tet. Overnight cultures of these strains were adjusted to an OD<sub>600</sub> of 0.1 and 1 ml was harvested by centrifugation (2,400  $\times$  g, 2 min, RT). The pelleted cells were resuspended in 100  $\mu$ l of 0.9% (w/v) NaCl, then mixed with 3 mL of 0.75% (w/v) agarose, and spread on LB agar plates. After solidification of the agarose, 5-mm diameter circles of Whatman filter paper (thickness 0.88 mm) were placed on the

plates and these were wetted with 10  $\mu$ l of different test solutions: 10 mM hemin, 0.1 mM hemoglobin, 0.9% (w/v) NaCl, or 50 mM ALA. The plates were photographed after incubation at 37°C for 48 h.

### CAS Assay

Chrome azurol S (CAS) agar plates, prepared as described previously (Schwyn and Neilands, 1987; Neilands, 1994), were used to monitor siderophore production. CAS is an iron-dye complex that changes color from blue to orange when iron (Fe<sup>3+</sup>) is removed by the action of siderophores. Strains were grown overnight in LBD medium at 26°C and 10  $\mu$ l aliquots were spotted onto the plates. The plates were photographed after incubation at 26°C for 48 h.

### Molecular Biology Techniques

All DNA manipulations, polymerase chain reactions (PCRs), restriction digests, ligations, and DNA electrophoresis, were performed as previously described (Sambrook and Russell, 2001). Plasmid and genomic DNA were isolated using a Plasmid Miniprep DNA purification Kit and Bacteria & Yeast Genomic DNA Purification Kit (EurX), respectively. When the amplified fragments were used for cloning, PCR was performed using DreamTaq DNA polymerase or Phusion High-Fidelity DNA polymerase (Thermo Scientific). Oligonucleotide primers for PCR and sequencing were purchased from Sigma Aldrich and are listed in Table S2. DNA fragments amplified by PCR were purified using a PCR/DNA Clean Up kit (EurX). The plasmids used in this study are described in Table S1. DNA sequencing was performed by Genomed S.A. (Warsaw, Poland).

### Semi-quantitative Reverse Transcription (RT)-PCR Gene Expression Analysis

Cultures of *Y. enterocolitica* Ye9 were grown until OD<sub>600</sub> ~1 in LBD medium at 37°C and then total RNA was isolated from 10<sup>9</sup> cells using a High Pure RNA Isolation Kit (Roche). Following treatment with RNase-free DNase I (TURBO DNA-free™ Kit, Invitrogen), the RNA was reverse-transcribed using Maxima H Minus reverse transcriptase (Thermo Scientific) primed with random hexamers. The cDNA was used as the template in PCRs (RNA as a negative control) with primer pairs RThPR1F/RThPR1R, RThRS1F/RThRS1R, and RThPR1F/RThPV1R (Table S2), specific for *hemPR-1*, *hemRS-1*, and *hemPRSTUV-1*, respectively, or RThPR2F/RThPR2R, RThRS2F/RThRS2R, RThRS2F/RThPV2R, and RThPR2F/RThPV2R specific for the *hemPR-2*, *hemRS-2*, *hemRST-2*, and *hemPRST-2* mRNAs, respectively. The amplified fragments were mixed with RunSAFE stain (Cleaver Scientific), resolved by electrophoresis on 2% (w/v) agarose gels and visualized with a GE Healthcare AI600 Imager.

### Construction of Transcriptional Fusion Plasmids *p<sub>hem-1</sub>::lacZ* and *p<sub>hem-2</sub>::lacZ*

To obtain transcriptional fusions of the *P<sub>hem-1</sub>* and *P<sub>hem-2</sub>* promoters with the *lacZ* gene, fragments of the *hemPRSTUV-1* and *hemPRST-2* operons containing the predicted promoters

were first amplified from *Y. enterocolitica* Ye9 genomic DNA by PCR using the primer pairs hemP1F/hemP1R and hemP2F/hemP2R, respectively (Table S2). The obtained amplicons were digested with the restriction endonucleases EcoRI/KpnI and cloned into the corresponding sites of reporter vector pCM132Gm [derivative of plasmid pCM132 (Marx and Lidstrom, 2001) containing a Gm resistance cassette] upstream of a promoterless *lacZ* gene. The resulting constructs were verified by PCR using the primer pair pCM132GmSpr1/pCM132Spr2 (flanking the EcoRI and KpnI sites) followed by sequencing of the amplicons. The two constructs, named pCM1 ( $p_{\text{hem-1}}::lacZ$ ) and pCM2 ( $p_{\text{hem-2}}::lacZ$ ), were introduced into *E. coli* BW25113. These constructs were also introduced into *E. coli* S17-1  $\lambda$ pir and transferred by conjugation into *Y. enterocolitica* Ye9N and the *ompR* mutant AR4. Selection of transconjugants was carried out on LB plates containing Gm and Nal (Ye9N) or Gm and Km (AR4). The presence of the plasmids in the *Y. enterocolitica* strains was confirmed by plasmid isolation and PCR with the primer pair pCM132GmSpr1/pCM132Spr2.

## Construction of a HemR1'-GFP Translational Fusion

To measure post-transcriptional regulation of *hemR1* expression, a translational fusion with GFP was constructed in plasmid pFX-P (Schmidtke et al., 2013) using the Golden Gate technique (Engler et al., 2008). A DNA fragment carrying the 5'-UTR of *hemR1* plus the first 16 codons of the gene was amplified by PCR using the primer pair hemR-fw/hemR-rev and Ye9 genomic DNA as the template. In a separate PCR a fragment containing the *lacZ* promoter was amplified using primer pair OR181-plac-fw/OR182-plac-rv and plasmid pFX-P as template. The PCR primers contained BsaI sites and additional sequences designed to generate ends compatible with BsaI-cleaved vector pFX-P (Table S2). In a 20  $\mu$ l Golden Gate cloning reaction, 40 fmol of vector were mixed with 40 fmol of each PCR product, 5 units of Eco31I (BsaI isoschizomer, Thermo Scientific), and 4.5 units of T4 DNA ligase (Thermo Scientific) in ligase buffer. The reaction was incubated at 37°C for 1 h, 5 min at 50°C, followed by 5 min at 80°C, and then it was used to transform *E. coli* BW25113. Clones were selected on LB agar supplemented with Sp and their identity confirmed by PCR and plasmid DNA sequencing.

## Construction of *fur* Deletion Mutants

The  $\Delta fur::Gm$  deletion mutants of *Y. enterocolitica* Ye9N and the *ompR* mutant AR4 were obtained by homologous recombination using suicide vector pDS132 (Philippe et al., 2004). A *fur* gene mutated by the insertion of a Gm<sup>R</sup> cassette was constructed by overlap extension PCR using primers listed in Table S2. As the first step, three DNA fragments were PCR-amplified using *Y. enterocolitica* genomic DNA (for flanking regions) or plasmid pBBR1MCS-5 Gm<sup>R</sup> (for the Gm<sup>R</sup> cassette) as the templates. Fragment A, extending from 403 bp upstream of *fur* to 6 bp within the ORF was amplified using primer pair Fur1/Fur2; fragment B, an 803-bp Gm<sup>R</sup> cassette was amplified using primer pair Fur2/Fur3; fragment C, comprising the last 20 bp of the *fur* ORF plus 557 bp downstream of this ORF was amplified using primer pair Fur5/Fur6. A mixture of these three

amplicons was then used as the template with flanking primers (Fur1/Fur6) in a PCR to generate the mutagenic fragment (1,860 bp). This was purified, digested with XbaI, and then cloned into the corresponding site of suicide vector pDS132. The resulting plasmid pDSfur was propagated in *E. coli* S17-1  $\lambda$ pir, with selection on Cm and Gm, and then sequenced to confirm the absence of errors. This plasmid was introduced into two *Y. enterocolitica* strains, Ye9N and AR4, by biparental mating. Transconjugants created by single crossovers to integrate the allelic exchange plasmid into the Ye9N or AR4 genomes were selected in LB supplemented with Cm, Gm plus Nal (Ye9N), or Km (for AR4). Plasmid integration after a single crossover was verified by PCR. To force the second recombination, the transconjugant strains were plated on LB agar containing Gm and 10% (w/v) sucrose, and incubated at room temperature for 48 h. Sucrose-resistant colonies were screened for the loss of Cm resistance (encoded by the vector). The correct allelic exchange was verified for these *fur* mutants by PCR using the primer pair Fur0/Fur7 (Table S2) and by sequencing.

## Gel Electrophoresis, Preparation of Cell Extracts, and Western Blotting

For immunological detection of the HemR1 and HemR1'-GFP proteins, *Y. enterocolitica* strains were grown under the desired conditions and extracts prepared from equal numbers of cells. The protein concentrations in the extracts were determined using the RC-DC protein assay (Bio-Rad) and if necessary they were diluted in Laemmli buffer to achieve equal loading (Sambrook and Russell, 2001). Samples were separated by electrophoresis on 12% TGX Stain-Free FastCast Acrylamide gels. Each gel was then Stain-Free activated by a 5 min exposure to UV and imaged using a GE Healthcare AI600 Imager. In some experiments, the loading of equivalent amounts of protein was controlled by Coomassie blue staining of an identical gel run in parallel. Next, the proteins were transferred to nitrocellulose membrane (Amersham Protran Western blotting membrane, nitrocellulose, pore size 0.2  $\mu$ m; GE Healthcare) using a wet electroblotting system (Bio-Rad). The blots were probed with polyclonal rabbit antibodies against HemR1 (1:10,000, generous gift of Jürgen Heesemann) or GFP (Sigma Aldrich, 1:10,000). Sheep anti-rabbit IgG, conjugated to horseradish peroxidase (HRP, Promega) was used as the secondary antibody (1:15,000). Positive immunoreaction was visualized using Clarity ECL Blotting Substrate (Bio-Rad) for HRP-based chemiluminescent detection (GE Healthcare AI600 Imager).

## $\beta$ -Galactosidase Assays

$\beta$ -Galactosidase assays were performed essentially as described by Thibodeau et al. (2004), using 96-well microtiter plates (Nest Sc. Biotech.) and a Sunrise plate reader (Tecan). Briefly, cultures grown to stationary phase were diluted to an OD<sub>600</sub> of 0.3–0.5 and 80  $\mu$ l of each cell suspension were then mixed with 20  $\mu$ l of POPCulture Reagent (EMD Millipore Corp) and incubated for 15 min to cause cell lysis. In the wells of a microtiter plate, 20  $\mu$ l of each cell lysate were mixed with 130  $\mu$ l of Z-Buffer and 30  $\mu$ l of ONPG (4 mg/ml), as described by Miller (1992). For kinetic assays, the absorbance at 415 nm (relative

to a blank) was measured at time intervals of 10 s, with 2 s of shaking before each reading. The assays were performed at 26°C and monitored for up to 20 min. The  $\beta$ -galactosidase activity was expressed in Miller units calculated as described previously (Thibodeau et al., 2004). Each assay was performed at least in triplicate.

## Electrophoretic Mobility Shift Assays (EMSAs)

For *in vitro* DNA-binding studies, recombinant OmpR-His<sub>6</sub> was expressed and purified as described previously (Nieckarz et al., 2016). Briefly, the N-terminal His-tagged OmpR protein (OmpR-His<sub>6</sub>, 29.78 kDa) was expressed from plasmid pETOmpR in *E. coli* BL21(DE3) and purified using Ni-NTA resin (Qiagen). The concentration of the purified OmpR protein was determined using the RC DC protein assay (Bio-Rad). DNA fragments comprising the regulatory regions upstream *hem-1* and *hem-2* clusters of the *Y. enterocolitica* Ye9 were amplified by PCR using primers listed in Table S2 with Ye9 genomic DNA as the template. The amplicons were purified using a Gene Matrix PCR/DNA Clean-Up kit (EurX) and the concentration of DNA was determined with a NanoDrop 2000. EMSA reactions (10  $\mu$ l), contained 0.05 pmol of each DNA fragment, OmpR binding buffer (50 mM Tris-HCl pH 8.0, 100 mM KCl, 1 mM EDTA, 1 mM DTT, 20 mM MgCl<sub>2</sub>, 12% glycerol, 100  $\mu$ g/ml BSA, 0.1% Triton X-100), and increasing amounts of OmpR-His<sub>6</sub>. After incubation at room temperature for 15 min, 2  $\mu$ l of 30% (v/v) glycerol were added and the reactions were loaded onto a 4.2% native polyacrylamide gel (19:1 acrylamide/bisacrylamide, 0.2X TBE, 2% glycerol) that had been pre-run in 0.2X TBE running buffer for 40 min at 80 V. After loading, the electrophoresis was continued for 3 h at 110 V. The gels were then soaked in SYBRgreen 1X solution (Invitrogen) and visualized using a GE Healthcare AI600 imager.

## Sequence Alignments and *in silico* Modeling

Bioinformatic analyses examined the complete genome sequences of *Y. enterocolitica* subsp. *paleartica* Y11 and *Y. enterocolitica* subsp. *enterocolitica* 8081 (GenBank; <http://www.ncbi.nlm.nih.gov/genbank/>). Homology searches were performed with BLAST software (<https://blast.ncbi.nlm.nih.gov/Blast.cgi>). Promoter prediction was conducted using the web-based software BPROM in the Softberry package (<http://linux1.softberry.com/berry.phtml?topic=bprom&group=programs&subgroup=gfindb>; Solovyev and Salamov, 2011). Predicted secondary structures of the partial and complete *hemR1* 5'-UTR were obtained using Mfold software (<http://mfold.rna.albany.edu>; Zuker, 2003). Western blot images were analyzed with Amersham Imager 600 Analysis Software V1.0.0 (GE Healthcare).

## Statistical Analyses

Statistical analyses were performed using Prism 7 software (v. 7.02, GraphPad). One-way ANOVA was used to determine statistically significant differences.

## RESULTS

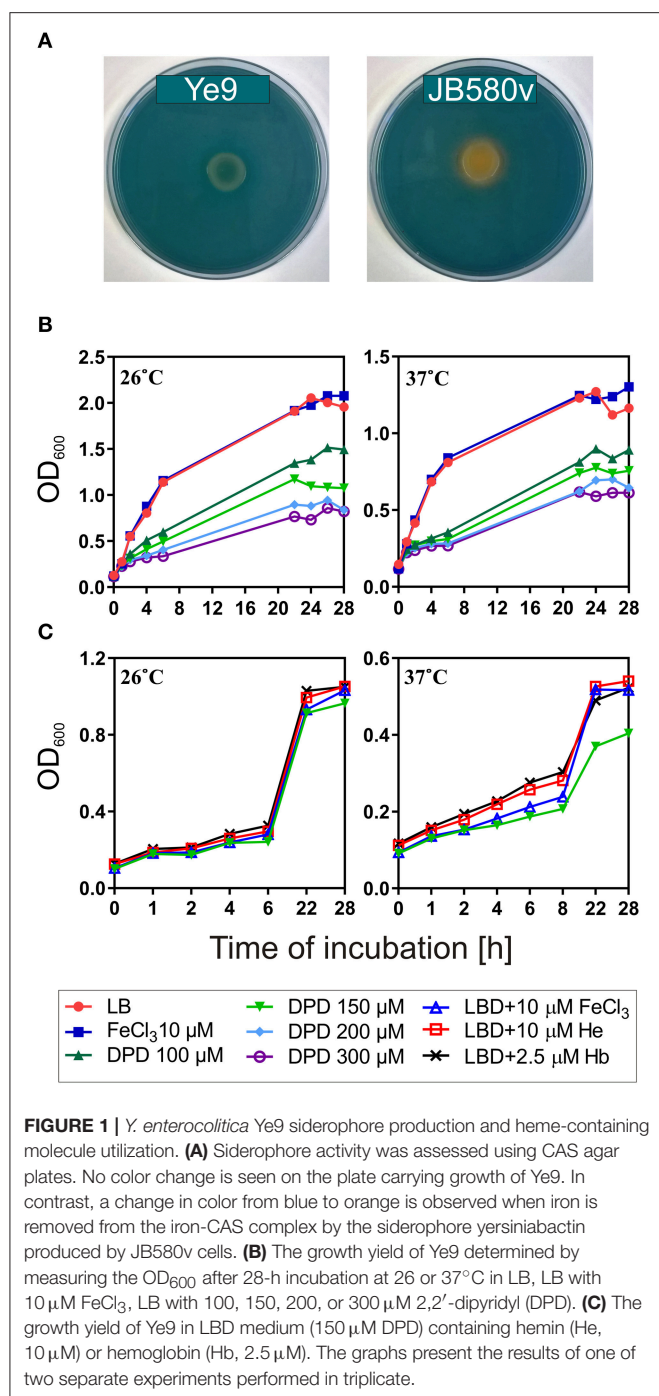
### *Y. enterocolitica* Ye9 Utilizes Heme-Containing Molecules as an Iron Source

The wild-type strain Ye9 is a low-level pathogenic strain belonging to *Y. enterocolitica* bio-serotype 2/O:9. In contrast to more highly pathogenic *Y. enterocolitica* strains from bio-serotype 1B/O:8, it lacks the high-pathogenicity island (HPI), a chromosomal cluster of iron-regulated genes involved in the biosynthesis of siderophore yersiniabactin (Ybt) and the uptake of Fe-Ybt into cells (Pelludat et al., 1998; Carniel, 2001). To study the ability of *Y. enterocolitica* strains to produce siderophores, the strains Ye9 and JB580v (bio-serotype 1B/O:8) were spotted onto agar containing CAS and incubated at 26°C for 48 h (Figure 1A). As anticipated, an orange halo was observed around the colonies of JB580v, demonstrating its ability to synthesize yersiniabactin (Figure 1A), while Ye9 growth failed to produce any color change on the CAS plates, suggesting that it does not produce siderophores. Strain Ye9 was further characterized for its ability to utilize heme-containing molecules as an iron source. The growth yield of Ye9 incubated at 26 or 37°C in LB medium supplemented with 100–300  $\mu$ M of the iron chelator 2,2'-dipyridyl (LBD) was significantly lower than in LB medium or LB with 10  $\mu$ M FeCl<sub>3</sub>, and varied according to the chelator concentration (Figure 1B). However, the addition of hemin (He, 10  $\mu$ M) or hemoglobin (Hb, 2.5  $\mu$ M) caused moderate stimulation of the growth of Ye9 in LBD (150  $\mu$ M 2,2'-dipyridyl) at 37°C, demonstrating that this strain can utilize heme-bound iron from hemin or hemoglobin (Figure 1C).

### Identification of Two Multigenic Clusters Encoding Putative Outer Membrane Heme Receptor Proteins HemR1 and HemR2 in the Genome of *Y. enterocolitica* Ye9

The *hemR* gene was previously recognized within the multigenic *hemPRSTUV* cluster responsible for the uptake and transport of hemin in highly pathogenic *Y. enterocolitica* (1B/O:8) strain WA-C (Stojiljkovic and Hantke, 1992). We established the presence of the *hemPRSTUV* cluster of *Y. enterocolitica* Ye9 (2/O:9) by PCR amplifications using primers designed from the Y11 (4/O:3) genome sequence (GenBank Acc. No. FR729477). Sequencing of these amplicons confirmed the presence of six ORFs *hemPRSTUV-1* (*hem-1* locus) (Figure S1). The sequence of this gene cluster was identical to that found in the Y11 (4/O:3) genome and it shared 99% sequence identity with *hemPRSTUV* of strain 8081 of bio-serotype 1B/O:8 (data not shown). The *Y. enterocolitica* *hemR1* gene encoding the outer membrane heme receptor protein HemR1 (687 amino acids) is situated downstream of the *hemP1* ORF encoding a small protein HemP1 (64 amino acids) of uncharacterized function (Figure 2A). The amino acid sequences of the HemR1 protein of *Y. enterocolitica* (2/O:9) strain Ye9 and *Y. enterocolitica* (1B/O:8) strain 8081 share 99% identity (data not shown). The deduced amino acid sequences of the proteins encoded by *hemSTUV-1* in Ye9 are similar to the equivalent sequences of proteins of the 8081 strain.





HemS1 is possibly involved in the release of iron from heme, and HemTUV-1 comprise subunits of a periplasmic/inner membrane ABC heme permease (Stojiljkovic and Perkins-Balding, 2002).

Bioinformatic analysis using BLAST software revealed the presence of a second multigenic cluster *hemPRST-2* (*hem-2* locus), encoding putative hemin transporter protein HemR2, in the genomes of *Y. enterocolitica* strains of low (2/O:9) and high pathogenicity (8081 strain, 1B/O:8) (Figure 2A). As for *hem-1*, we determined the sequence of the *hem-2* locus in *Y.*

*enterocolitica* strain Ye9 (Figure S1). Analysis of the structure of this novel heme transport locus revealed four intact ORF *hemPRST-2* organized in an order similar to the hemin transport cluster *hem-1*. The predicted translation products of the *hem-2* locus genes exhibit a high degree of amino acid sequence similarity to those encoded by the corresponding ORFs of *hem-1* (HemP 52%, HemR 62%, HemS 53%, HemT 60% identity, respectively) (Figure S2, Figure 2B). The nomenclature for the *hem-2* genes at locus 2 follows that of the highly homologous *hem* genes at locus 1, and the putative proteins encoded are named HemP2, HemR2, HemS2, and HemT2, respectively. Interestingly, the lack of *hemUV2* genes in this cluster suggests that the putative *hem-2* heme permease is non-functional. This does not exclude the possibility that HemR2 might function as a receptor protein involved in heme uptake by utilizing components of the ABC transport system encoded by the *hem-1* locus.

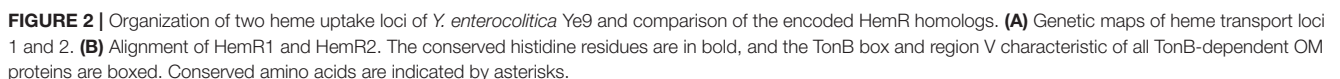
Alignment of HemR2 with the well-characterized HemR1 showed high amino acid sequence identity. These homologous proteins have typical TonB boxes at their amino-termini, conserved histidine residues, plus region V, which is characteristic of TonB-dependent proteins. These conserved motifs and residues were shown to be essential for heme transport through the receptor channel (Thompson et al., 1999) (Figure 2B).

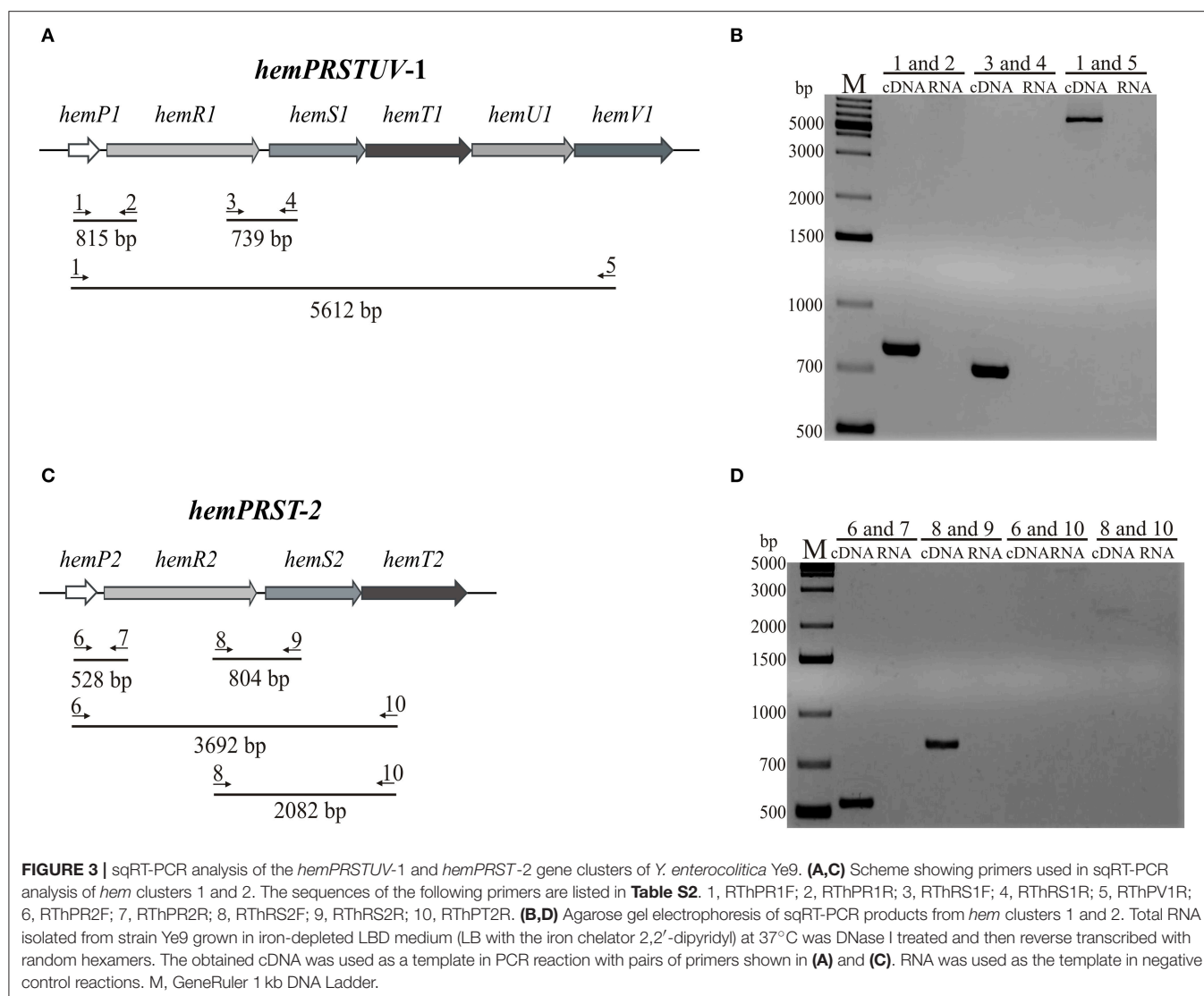
### Genes Within the *hemPRSTUV-1* and the *hemPRST-2* Clusters Are Organized as Operons

There are six and four genes within the *hemPRSTUV-1* (*hem-1*) and the *hemPRST-2* (*hem-2*) clusters of *Y. enterocolitica* Ye9, respectively (Figure 2A). To determine whether the genes within these two loci might be transcribed as one transcriptional unit, sqRT-PCR analysis was performed on total RNA isolated from *Y. enterocolitica* Ye9 grown in iron-depleted medium (LBD). The locations of the primers used in this analysis are shown in Figures 3A,C and their sequences are given in Table S1. For the *hemPRSTUV-1* cluster, the obtained RT-PCR products (815 and 739 bp) confirmed co-transcription of the *hemPR-1* and *hemRS-1* genes, respectively. The operon organization of *hemPRSTUV-1* was conclusively demonstrated by the amplification of a 5,612-bp RT-PCR product (Figure 3B).

The operon organization of the *hemPRST-2* cluster was also examined by sqRT-PCR analysis using the primers (Table S1) shown in Figure 3C. RT-PCR products of the expected sizes (528 and 804 bp) confirmed the co-transcription of the *hemPR-2* and *hemRS-2* genes, respectively. However, a 3,692-bp RT-PCR product spanning the entire *hemPRST-2* operon could not be obtained, despite repeated attempts. Therefore, co-transcription of the *hemRST-2* genes was tested. The presence of a faint RT-PCR product of the expected size (2,082 bp) confirmed the operon organization of the *hemPRST-2* cluster (Figure 3D). Based on these data, it seems that the *hemPRST-2* transcript might be particularly unstable or expressed at low levels at 37°C. Control PCRs with the tested primers and Ye9 genomic DNA as template gave positive results in all cases (data not shown).







## Role of HemR1 And HemR2 Proteins in Heme and Hemoprotein Utilization by *E. coli* $\Delta$ *hema* Strain SASX77

Previous studies have shown that a plasmid containing *hemPR*, part of the heme operon of *Y. enterocolitica* WA-C O:8, permits an *E. coli* strain lacking a functional *hema* gene to use heme as a porphyrin source (Stojiljkovic and Hantke, 1992, 1994). To examine the importance of the two *Y. enterocolitica* Ye9 HemR proteins in the utilization of heme and hemoglobin as sources of porphyrin, they were introduced into the *E. coli*  $\Delta$ *hema* strain SASX77, which is defective in ALA synthetase (auxotrophic for ALA, the heme biosynthetic precursor). The *hemPR* genes of the *hem-1* and *hem-2* operons with their native promoters were cloned into vector pACYC184 to obtain plasmids pHEM1 and pHEM2, respectively. These plasmids and the parent vector were introduced into *E. coli* SASX77. All transformant strains grew well in the presence of ALA, but no growth was observed on LB agar lacking this precursor.

To examine the effect of heme or hemoglobin on the growth of strain SASX77 harboring plasmids containing *hemPR1* or *hemPR2*, a plate assay was used to detect utilization of these porphyrin sources in iron-replete (LB) and iron-deficient conditions (LBD). The strains expressing the receptors HemR1 or HemR2 were able to utilize exogenously supplied heme and hemoglobin as porphyrin sources (**Table 1**, **Figure 4**). However, growth of the SASX77/pHEM1 (HemR1<sup>+</sup>) strain around the heme and hemoglobin discs was significantly stronger than that of strain SASX77/pHEM2 (HemR2<sup>+</sup>). Moreover, the HemR2-expressing bacteria grew only as single colonies. Control strain SASX77/pACYC184 was unable to use either heme or hemoglobin (**Figure 4A**). In iron-depleted conditions, the zone of growth stimulation was broad (up to 30 mm in diameter), but the colonies were very small and needed more time to develop (up to a week, in contrast to 1–2 days for the strains growing on LB) (data not shown). These results strongly suggest that both HemRs participate in the acquisition of heme and hemoproteins

in *Y. enterocolitica* Ye9, and that HemR1 is significantly more efficient than HemR2.

Next, the level of HemR1 receptor protein in the *E. coli* strain carrying pHEM1 was determined by Western blot analysis with anti-HemR1 polyclonal antibody (**Figure 4B**). Cells of *Y. enterocolitica* Ye9 and of the *E. coli* strain carrying pACYC184 were used as a positive and negative control, respectively. All strains were grown in both iron-replete (LB+FeCl<sub>3</sub>) and iron-deficient (LBD) conditions. Extracts of cells grown to stationary phase at 37°C were immunoblotted and a strong HemR1 signal was produced by the samples from the Ye9 strain and *E.*

*coli* DH5α/pHEM1 grown in LBD medium. As expected, no immunoreactive band was observed in the case of *E. coli*/pHEM2. This result indicated the absence of cross-reactivity between anti-HemR1 antibodies and the protein HemR2. Since no HemR2 antibody was available it was not possible to confirm expression of this protein in the *E. coli* strain carrying plasmid pHEM2. This experiment also demonstrated the induction of HemR1 protein in *Y. enterocolitica* grown under iron starvation conditions, confirmed that this gene can be expressed in a heterologous system from a recombinant plasmid, and showed that this expression is repressed by iron.

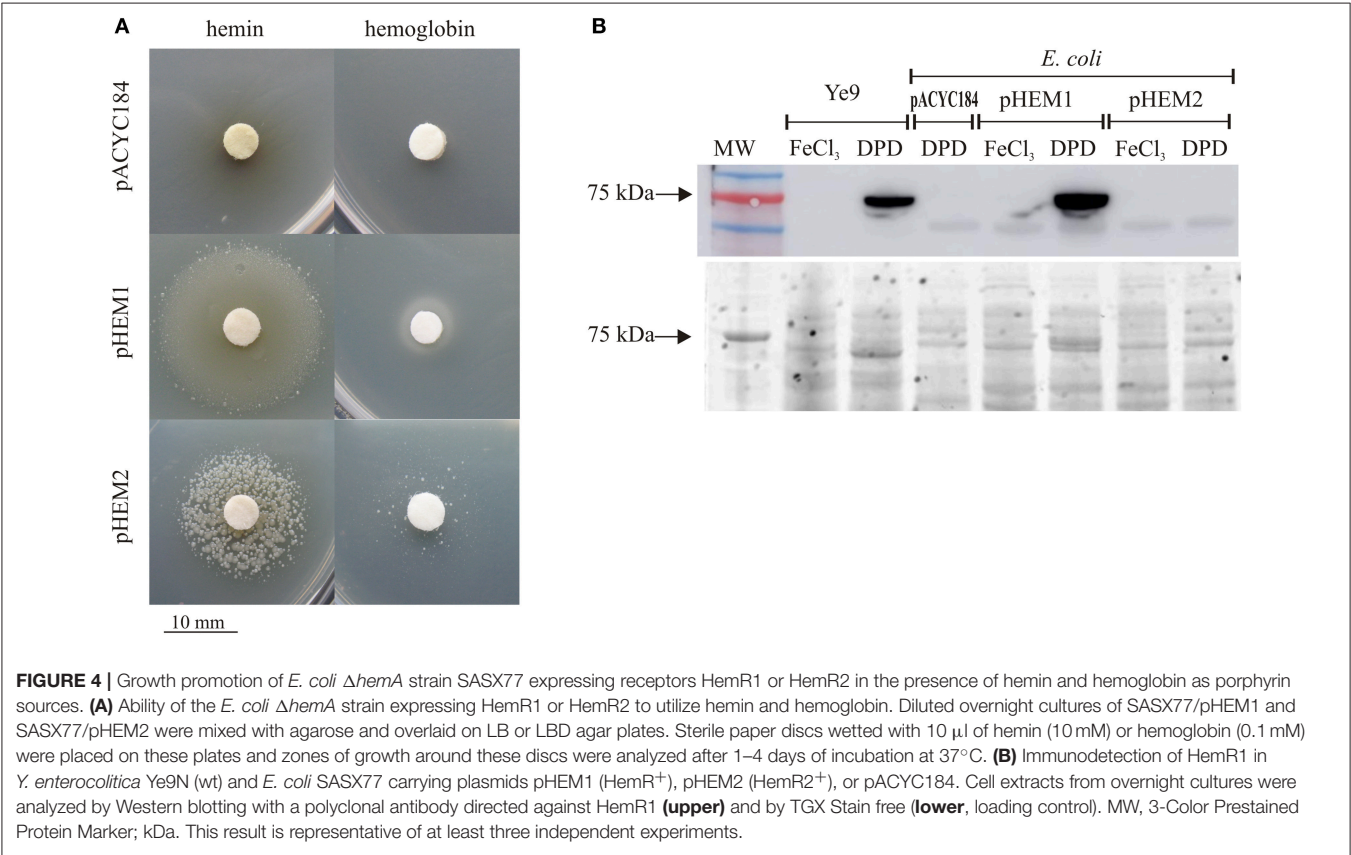
**TABLE 1 |** Assessment of HemR1 and HemR2 activity in hemin and hemoglobin transport in *E. coli* Δ*hemA* strain SASX77.

Strain	Growth on		
	LB/Hemin	LB/Hemoglobin	LB/ALA
SASX77/pACYC184	–	–	+++
SASX77/pHEM1	++	+	+++
SASX77/pHEM2	++ <sup>a</sup>	++ <sup>a</sup>	+++

– No growth.  
+ ~10 mm diameter growth zone around the discs.  
++ 20–25 mm diameter growth zone around the discs.  
+++ >30 mm diameter growth zone around the discs.  
<sup>a</sup>Growth as single colonies.

**OmpR Inhibits the Activity of the *hemPRSTUV-1* and *hemPRST-2* Promoters**

The putative promoters *p*<sub>hem-1</sub> and *p*<sub>hem-2</sub>, located 42 and 43 bp upstream of the *hemP* gene in the *hemPRSTUV-1* and *hemPRST-2* operons, respectively, of *Y. enterocolitica* Ye9, were identified using the program BPROM (Solovyev and Salamov, 2011). Sequence analysis of the *hemPRSTUV-1* and *hemPRST-2* regions also led to the identification of an internal, putative promoter in the intergenic region between *hemR* and *hemS*. These findings corroborate the previously described locations of *hemPRSTUV* operon promoters in *Y. enterocolitica* WA-C (Stojiljkovic and Hantke, 1992), *Y. pestis* (*hmu* locus, Thompson et al., 1999), and *Y. pseudotuberculosis* (*hmu* locus, Schwiesow et al., 2018). *In silico* analysis revealed the presence of potential



OmpR binding sites within the  $p_{hem-1}$  and  $p_{hem-2}$  promoters (see below), but not within the putative internal promoters, so their activity was not investigated further.

To examine the activity of the  $p_{hem-1}$  and  $p_{hem-2}$  promoters and the influence of iron and the regulator OmpR, we generated transcriptional fusions of the putative promoter sequences with the *lacZ* gene in vector pCM132Gm. The resulting plasmids pCM1 ( $p_{hem-1}::lacZ$ ) and pCM2 ( $p_{hem-2}::lacZ$ ) were introduced into *E. coli* BW25113 and two strains of *Y. enterocolitica*: the wild-type strain Ye9N (both fusions) and the isogenic *ompR* mutant AR4 (only fusion  $p_{hem-1}::lacZ$ ). The transformed strains were grown to stationary phase in LB or LBD and  $\beta$ -galactosidase activity was measured (Figure 5).

In the *E. coli* strains grown at 37°C in both iron-replete or iron-depleted conditions the expression of the  $p_{hem-1}::lacZ$  transcriptional fusion (pCM1) was significantly higher than that of  $p_{hem-2}::lacZ$  (pCM2), indicating that  $p_{hem-2}$  is a weaker promoter. In addition, the expression of both  $p_{hem-1}::lacZ$  and  $p_{hem-2}::lacZ$  was upregulated in the presence of the iron chelator (~3-fold and ~2.5-fold, respectively), demonstrating inhibition by inorganic iron (Figure 5A).

To investigate whether the *hem-1* and *hem-2* operons are subject to OmpR-dependent regulation,  $p_{hem-1}::lacZ$  and  $p_{hem-2}::lacZ$  activity was measured in the *Y. enterocolitica* strains differing in the amount of OmpR grown at 26 or 37°C in iron-replete or iron-depleted conditions. With the  $p_{hem-1}::lacZ$  fusion, a ~2-fold (26°C) and ~1.5-fold (37°C) up-regulation was observed under conditions of iron deficiency, confirming iron-dependent regulation of  $p_{hem-1}$ . Moreover,  $\beta$ -galactosidase activity was increased in the absence of OmpR at both studied temperatures in iron-replete or iron-depleted conditions (Figure 5B). The effect of complementation of the *ompR* mutation in strain AR4 or overexpression of OmpR in the wild-type strain were studied by introducing plasmid pBOmpR carrying the wild-type copy of *ompR*. An increase in the level of OmpR caused a clear reduction in the expression of  $p_{hem-1}::lacZ$  in cells grown in LB with FeCl<sub>3</sub> or LBD, showing that OmpR negatively regulates expression of this fusion. These results indicated that *hem-1* expression is controlled by an iron- and OmpR-dependent promoter located upstream of this operon. Both iron and OmpR participate in the negative regulation of *hem-1*.

To test the role of iron and OmpR in the regulation of  $p_{hem-2}::lacZ$ , the wild-type strain Ye9N transformed with plasmid pCM2 was grown at 26 or 37°C in iron-replete or iron-depleted conditions. A ~1.5-fold increase in  $\beta$ -galactosidase activity was detected in wild-type cells grown at 26°C under iron-deficiency (Figure 5C). However, the inhibitory effect of iron on  $p_{hem-2}::lacZ$  expression was not observed at 37°C, suggesting a more complex regulatory mechanism compared to the *hem-1* promoter. Attempts to study the activity of the  $p_{hem-2}::lacZ$  reporter fusion in the *ompR* mutant background were thwarted by the inability to transform strain AR4 with plasmid pCM2. Therefore, the wild-type *ompR* allele was introduced *in trans* (pBOmpR) into the Ye9N cells to monitor the effect of overexpression. The observed decrease in  $p_{hem-2}$  activity in the presence of *ompR* in multicopy in the wild-type strain grown

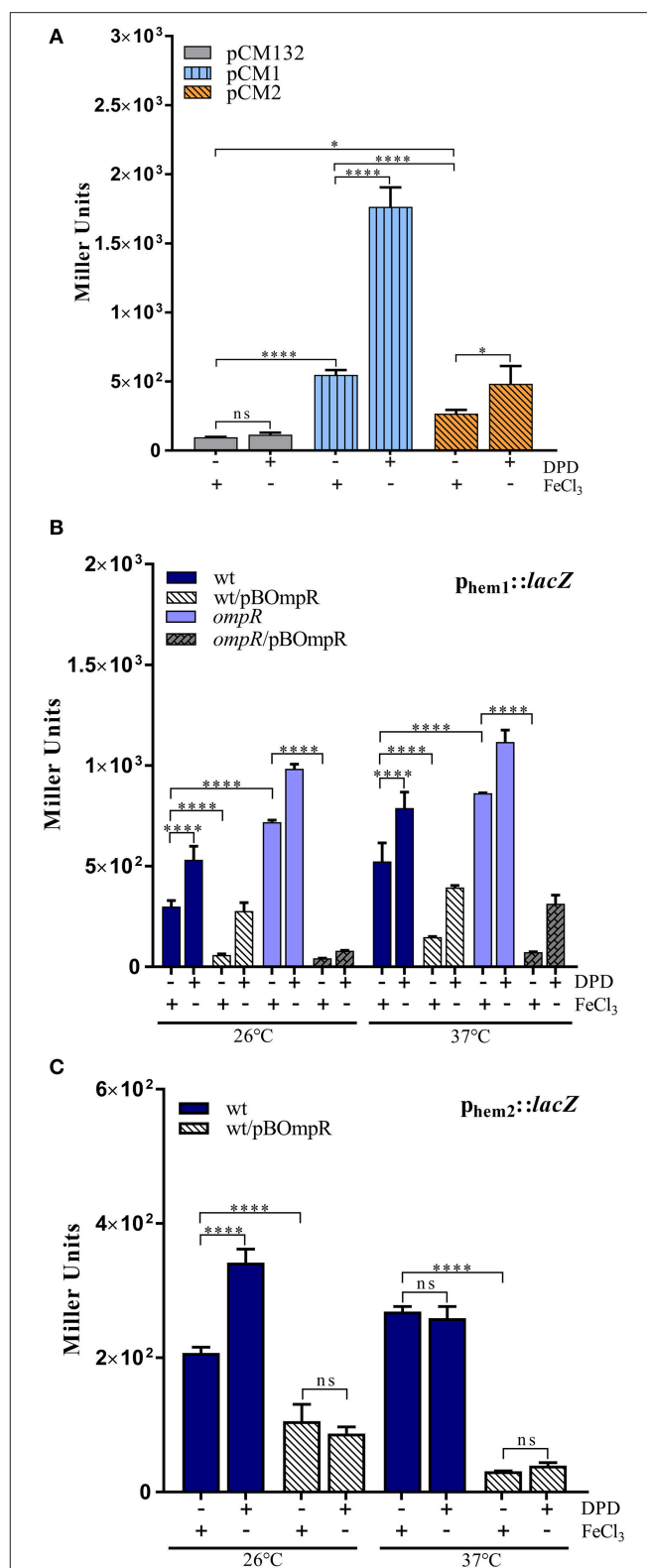


**FIGURE 5** | OmpR-dependent regulation of *hem-1* and *hem-2* operon expression. (A) Activity of the  $p_{hem-1}$  and  $p_{hem-2}$  promoters in *E. coli* BW25113 harboring the  $p_{hem-1}::lacZ$  (pCM1) or  $p_{hem-2}::lacZ$  (pCM2) fusion (Continued)



**FIGURE 5 |** plasmids, compared with the same strain carrying parent vector pCM132. Strains were grown overnight in LB+FeCl<sub>3</sub> or LBD medium at 37°C. **(B,C)** OmpR-dependent regulation of *hem-1* and *hem-2* expression in *Y. enterocolitica* strains grown to stationary phase in LB+FeCl<sub>3</sub> or LBD medium at 26 or 37°C. **(B)** The wild-type Ye9N (wt), wt/pBOmpR, AR4 (*ompR*), and *ompR*/pBOmpR, harboring fusion *p<sub>hem-1</sub>::lacZ* (pCM1). **(C)** The wild-type Ye9N (wt) and wt/pBOmpR harboring fusion *p<sub>hem-2</sub>::lacZ* (pCM2). Plasmid pBOmpR carries the wild-type *ompR* allele.  $\beta$ -galactosidase activity was determined for each culture and expressed in Miller units. The data represent mean activity values with standard deviation from two independent experiments, each performed using at least triplicate cultures of each strain. Significance was calculated using one-way ANOVA [ns (non-significant)  $P > 0.05$ , \* $P < 0.05$ , \*\*\*\* $P < 0.00001$ ].

at 26 or 37°C, suggested a negative role for OmpR in *hem-2* expression. Interestingly, the inhibitory effect of iron was absent in the wild-type strain containing plasmid pBOmpR grown at 26°C (Figure 5C).

### Impact of Fur and OmpR on HemR1 Receptor Production

The analysis of strains carrying the *p<sub>hem-1</sub>::lacZ* reporter fusion construct suggested that iron and OmpR negatively influence the expression of the *hem-1* operon at the transcriptional level. We next examined whether this regulatory effect was observable at the protein level. Western blot analysis with a polyclonal anti-HemR1 antibody was used to detect the HemR1 protein in cell extracts prepared from the following *Y. enterocolitica* strains: wild-type Ye9N, *ompR* mutant AR4, Ye9N/pBOmpR, AR4/pBOmpR, and strains with empty vector pBBR1. All strains were grown to stationary phase at 37°C in LB supplemented with FeCl<sub>3</sub> (iron-replete) or LBD (iron-depleted). As shown in Figures 6A,B, HemR1 protein production was significantly influenced by iron content, because HemR1 was undetectable in strain Ye9N grown under iron-replete conditions, and highly abundant in iron-depleted conditions. Moreover, HemR1 production was notably increased in the *ompR* mutant compared to the wild-type strain in both media. Plasmid pBOmpR carrying the wild-type *ompR* allele, used to complement the *ompR* mutation in strain AR4, caused a clear reduction in the level of HemR1, confirming that OmpR negatively regulates its expression. In addition, the strain Ye9N/pBOmpR, which overexpresses OmpR, produced less HemR1 than strain Ye9N in LBD medium (Figure 6B). The presence of the empty vector pBBR1 in the wild-type strain and the *ompR* mutant, grown in LBD medium (Figure 6B) did not have any impact on the level of HemR1. However, for some unknown reason, a difference in the abundance of HemR1 was observed in the *ompR* mutant vs. the *ompR* strain carrying the empty vector pBBR1, when grown in iron-replete conditions (Figure 6A).

These data corroborated the results of the transcriptional fusion analysis and suggested that the Fur may be involved in iron-dependent inhibition of *hem-1* operon expression, and thus HemR1 production.

In order to determine whether OmpR controls the level of HemR1 expression independently of the Fur repressor,

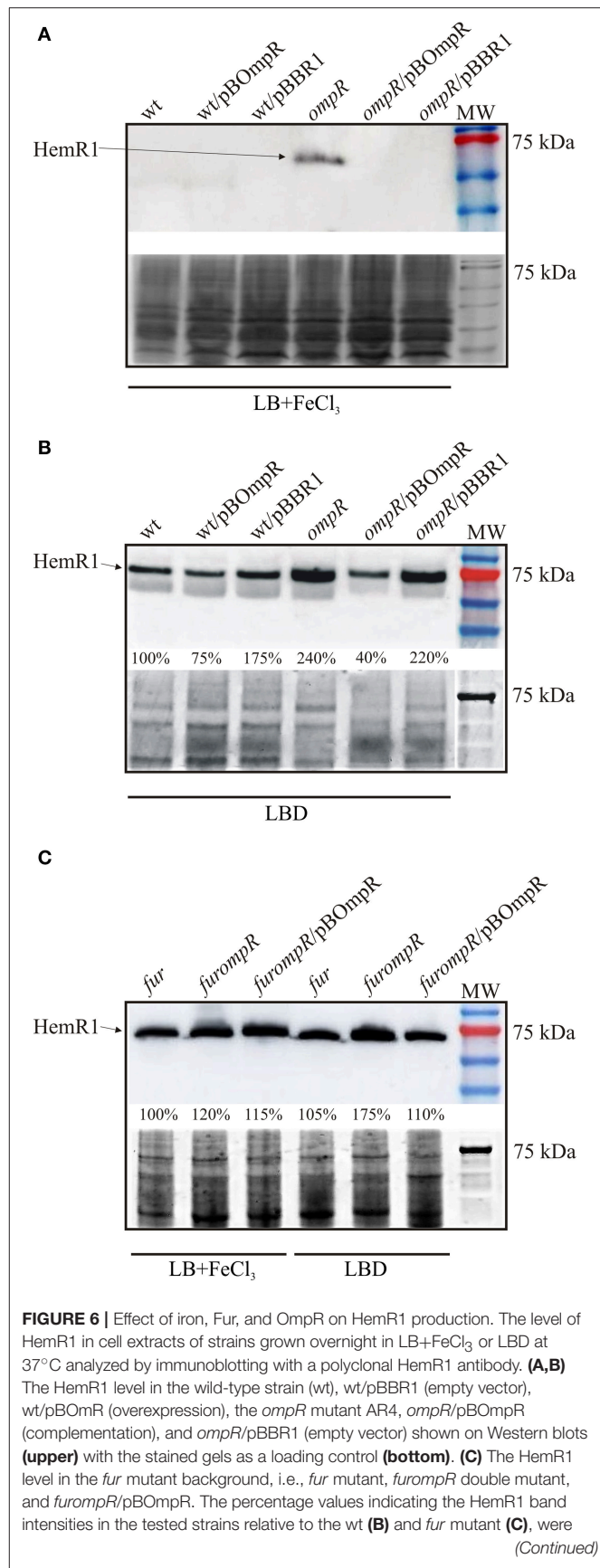


**FIGURE 6 |** Effect of iron, Fur, and OmpR on HemR1 production. The level of HemR1 in cell extracts of strains grown overnight in LB+FeCl<sub>3</sub> or LBD at 37°C analyzed by immunoblotting with a polyclonal HemR1 antibody. **(A,B)** The HemR1 level in the wild-type strain (wt), wt/pBBR1 (empty vector), wt/pBOmpR (overexpression), the *ompR* mutant AR4, *ompR*/pBOmpR (complementation), and *ompR*/pBBR1 (empty vector) shown on Western blots (upper) with the stained gels as a loading control (bottom). **(C)** The HemR1 level in the *fur* mutant background, i.e., *fur* mutant, *fuompR* double mutant, and *fuompR*/pBOmpR. The percentage values indicating the HemR1 band intensities in the tested strains relative to the wt **(B)** and *fur* mutant **(C)**, were (Continued)

**FIGURE 6 |** determined using Amersham Imager 600 Analysis Software V1.0.0 (GE Healthcare). Stained gels shown as a loading control: **(A,C)** TGX Stain-Free gels (BioRad), **(B)** Coomassie blue stained gel. MW, 3-Color Prestained Protein Marker, kDa. The size of the HemR1 band is approximately 75 kDa on the Western blots. This result is representative of at least three independent experiments.

the *fur* gene was deleted in both the wild-type strain Ye9N (Ye9*fur*) and the *ompR* mutant (AR4*fur*). HemR1 levels were then examined by immunoblotting of cell extracts prepared from the *fur*, *fuompR* and *fuompR*/pBOmpR strains grown to stationary phase in LB supplemented with FeCl<sub>3</sub> or LBD at 37°C (**Figure 6C**). The Western blot data showed a high level of HemR1 production in the *fur* mutant background (independently of iron concentration), confirming that the Fur represses the biosynthesis of HemR1 in *Y. enterocolitica*. Interestingly, the strain also lacking OmpR (*fuompR* mutant), grown in LBD medium, displayed a further increase in HemR1 protein abundance (ca. 70%), which suggested that OmpR inhibits the production of HemR1 independently of Fur. This effect was restored by complementation with plasmid pBOmpR carrying the wild-type *ompR* allele. Under iron-replete conditions the difference in HemR1 level between the *fur* and *fuompR* mutants was less evident. These data suggested that iron may influence OmpR-dependent HemR1 synthesis irrespective of Fur.

## Interactions of OmpR With Putative OmpR-Binding Sequences in the Promoter Regions of *hem-1* and *hem-2*

We next tested whether OmpR influences *hem-1* and *hem-2* operon expression directly or if other regulatory factors are involved. *In silico* analysis of the *Y. enterocolitica* Ye9 *hem-1* promoter region  $P_{hem-1}$ , conducted using the consensus Fur binding site sequence of *E. coli* [FBS, 5'-GATAATGAT(A/T)ATCATTATC-3'] (Stojiljkovic et al., 1994; Escolar et al., 1999), led to the identification of the element FBS-1, with 74% homology to the *E. coli* FBS, that overlaps the -10 element of  $P_{hem-1}$  (**Figure 7A**). In addition, a putative OmpR binding site OBS-1, overlapping the -35 element of  $P_{hem-1}$  was identified by comparison with the consensus OmpR-binding sequence of *E. coli* (OBS, 5'-TTTACTTTTGTG(A/T)AACATAT-3', Maeda et al., 1991). OBS-1 exhibits 60% identity to the *E. coli* OBS (**Figure 7A**).

*In silico* analysis of the *hem-2* promoter region  $P_{hem-2}$  revealed a putative Fur binding site (FBS-2), as well as a potential OmpR binding site (OBS-2) in similar locations to FBS-1 and OBS-1. FBS-2 and OBS-2 are 74 and 45% identical to the *E. coli* consensus sequences, respectively (**Figure 7B**).

The ability of OmpR to directly interact with the predicted OBS elements was tested in electrophoretic mobility shift assays (EMSAs) using DNA fragments with or without the putative OmpR-binding sites (**Figures 7C–E**). Three  $P_{hem-1}$  fragments were PCR-amplified with the pairs of primers listed in **Table S2**. Fragment F1 (415 bp) represented a sequence upstream of OBS-1, F2 (326 bp) carried OBS-1, while F3 (107 bp) was a

sequence downstream of OBS-1. When purified recombinant OmpR was mixed with equimolar amounts of these three  $P_{hem-1}$  fragments, shifted OmpR/DNA complexes started to appear at an OmpR concentration of 0.65  $\mu$ M, and their amount increased as the concentration of the protein was raised (**Figure 7D**). The formation of these complexes was related to the disappearance of fragment F2, so were attributed to specific binding to OBS-1.

The interaction of OmpR with the putative OBS-2 within the promoter region of *hem-2* was examined by incubating increasing amounts of recombinant OmpR with fragment F4 (303 bp), the region of  $P_{hem-2}$  containing OBS-2, or  $P_{hem-1}$  fragment F2 (326 bp), carrying OmpR binding site OBS-1. Specific OmpR/F4 complexes were observed at an OmpR concentration of 1.31  $\mu$ M, with the simultaneous disappearance of fragment F4. In comparison, the appearance of OmpR/F2 complexes occurred at the lower OmpR concentration of 0.65  $\mu$ M (**Figure 7E**). A 16S rDNA fragment (amplified with primer pair 16SF/16SR, **Table S2**), to which OmpR is unable to bind, was used as a negative control in both experiments. These results suggested that transcription of the *hem-1* and *hem-2* gene clusters is directly regulated by OmpR, and this regulation requires OmpR binding to specific sites in their promoter regions.

## The Impact of Temperature on Post-transcriptional HemR1 Expression

*Y. enterocolitica* HemR1 is a homolog (69% amino acid identity) of the *S. dysenteriae* ShuA receptor required for the utilization of heme as a source of iron (data not shown). Recently, thermoregulation of ShuA protein expression under iron-limited conditions was demonstrated, with low ShuA abundance at 25°C increased to high levels at 37°C (Kouse et al., 2013). Within the *shuA* 5'-UTR a regulatory element was recognized that closely resembles a FourU RNA thermometer: a zipper-like RNA structure that occludes the Shine-Dalgarno sequence at low temperatures, thus blocking translation of the *shuA* transcript.

Both HemR1 and ShuA are encoded within hemin transport loci, but the organization of these multigenic clusters differs considerably (Wyckoff et al., 1998). The *hemR1* gene of *Y. enterocolitica* is located 172 bp downstream of *hemP1*, the first gene of the *hemPRSTUV-1* operon. There is no *hemP1* homolog in the hemin transport locus in *S. dysenteriae*. Moreover, the intergenic non-translated *hemP1-hemR1* region (172 nt) is present in polycistronic mRNA of *hem-1*. In comparison, the predicted promoter of *shuA* is located 328 bp upstream of the translation start site in a monocistronic transcript.

To investigate the possible thermoregulation of *hemR1* expression we analyzed an extended 5'-UTR of *Y. enterocolitica* *hemR1* for the presence of secondary structures using Mfold software (Zuker, 2003). This analysis identified a hairpin sequestering the *hemR1* ribosomal binding site, containing four consecutive uracil residues characteristic of a FourU RNA thermometer (Waldminghaus et al., 2007; Böhme et al., 2012). However, compared to the FourU base-pair region in the 5'-UTR of *shuA* there was moderate sequence variation in the

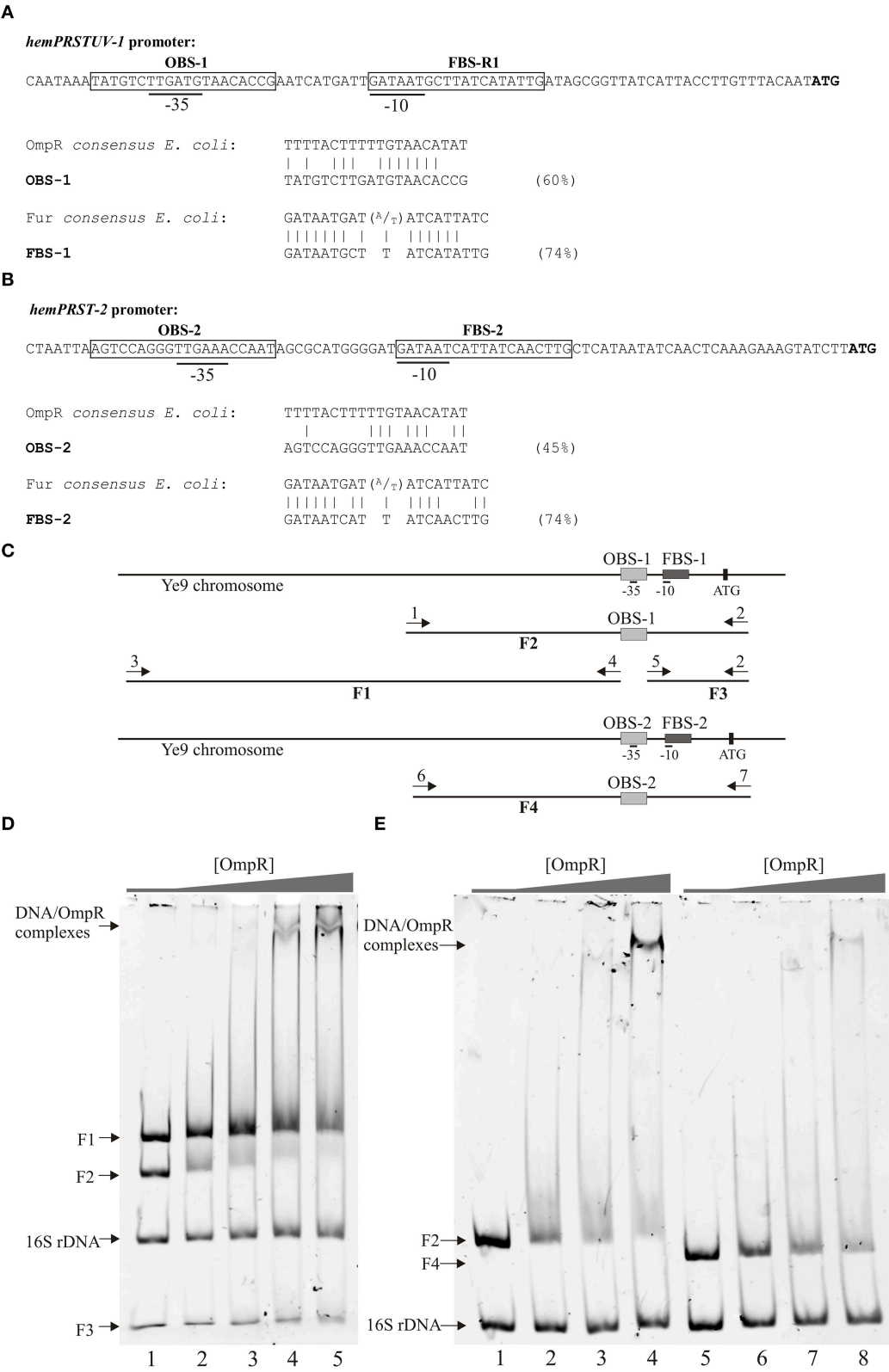


**FIGURE 7 |** OmpR binding to fragments of the *hem-1* and *hem-2* promoter regions. **(A,B)** OmpR- and Fur-binding sites identified in promoter regions of the two heme uptake loci. The −35 and −10 promoter elements are underlined and putative regulator-binding sites are boxed. The ATG start codon of the *first* ORF of each operon is shown in bold. FBS, Fur-binding site; OBS, OmpR-binding site. **(C)** Schematic representation of fragments used in EMSA experiments presented in **(D)** and **(E)**. The *(Continued)*

**FIGURE 7** | numbered arrows represent the primers used to amplify the DNA fragments used in EMSAs: 1, hem1F; 2, hem1R; 3, hem1-aF; 4, hem1-aR; 5, hem1-bF; 6, hem2F; 7, hem2R. **(D)** EMSA with fragment F2 (326 bp) containing OBS-1 and neighboring fragments F1 (415 bp, upstream) and F3 (107 bp, downstream). A 16S rDNA fragment (211 bp) was used as a negative control. The reaction mixtures contained 0.05 pmol of each fragment and increasing amounts of purified OmpR-His<sub>6</sub> were added: lane 1, no protein; lanes 2–5, 0.65, 1.31, 2.61, and 3.92  $\mu$ M of OmpR-His<sub>6</sub>, respectively. **(E)** Binding of purified OmpR-His<sub>6</sub> to fragments containing OBS-1 (F2, lanes 1–4) and OBS-2 (F4, lanes 5–8). The 16S rDNA fragment was used as a negative control. The reaction mixtures contained 0.05 pmol of each fragment and increasing amounts of purified OmpR-His<sub>6</sub> were added: lanes 1 and 5, no protein; lanes 2 and 6, 0.65  $\mu$ M; lanes 3 and 7, 1.31  $\mu$ M; lanes 4 and 8, 3.92  $\mu$ M.

surrounding regions (**Figure 8A**). No similar secondary structure was detected in the 5'-UTR of *hemR2* (data not shown).

The impact of temperature on HemR1 expression was assessed by immunoblotting of cell extracts prepared from the *fur* mutant following growth in LB medium to stationary phase at 26 or 37°C (**Figure 8B**). Identical levels of HemR1 were detected in the tested strain, irrespective of the growth temperature, which indicated that HemR1 production is not thermoregulated in *Y. enterocolitica* Ye9.

To further examine the potential thermoregulation of HemR1 expression at the post-transcriptional level, a plasmid pFX-P<sub>lac</sub>-hemR1, which carries the p<sub>lac</sub> promoter linked to the 5'-UTR and first 16 codons of *hemR1* fused in frame with *gfp*, was constructed. Plasmid pFX-P<sub>lac</sub>-hemR1 and control plasmids pFX-0, containing promoterless *gfp*, and pFX-1, carrying *gfp* fused to the p<sub>lac</sub> promoter (Schmidtke et al., 2013), were introduced into *E. coli* BW25113. Cultures of these strains were grown to stationary phase in LB medium at 26 or 37°C and green fluorescence intensity was measured (**Figure 8C**). Analysis of the strain carrying the *hemR1*'-'*gfp* fusion revealed a decrease in *hemR1* expression at 26°C relative to 37°C, however a slight reduction in fluorescence at this lower temperature was also observed for the control strain carrying pFX-1. In parallel, the impact of growth temperature on the GFP level was assessed by immunoblotting with an anti-GFP antibody (**Figure 8D**). The Western blot data corresponded well with the results of the fluorescence assay. A higher level of HemR1'-GFP fusion protein was produced at 37°C compared to 26°C, which may indicate that temperature-dependent post-transcriptional regulation of *hem-1* occur in *E. coli*. However, we could not exclude that observed effect may be explain also by the increased metabolic activity at the higher temperature.

## DISCUSSION

The acquisition of iron/heme is necessary for pathogenic bacteria to grow within the host and to survive during the progression of an infection (Mietzner and Morse, 1994; Lee, 1995; Braun et al., 1998). On the other hand, both iron and heme are toxic at high concentrations (Anzaldi and Skaar, 2010). Thus, tight regulation of iron/heme acquisition is essential to fulfill the iron requirements of a pathogen while preventing harmful over-accumulation.

Studies on the role of OmpR in pathogenic *Yersinia* strains have provided evidence that this response regulator might be involved in the adaptation of yersiniae to diverse environmental conditions, which allows the bacteria to grow in distinct niches within and outside the host body (Brzostek et al., 2003, 2007;

Raczkowska et al., 2011a,b, 2015; Brzostkowska et al., 2012; Skorek et al., 2013). In a recent shotgun proteomic study we revealed that the regulator OmpR affects, both positively and negatively, the production of over 100 membrane proteins in *Y. enterocolitica* strain Ye9 of bio-serotype 2/O:9, a low pathogenicity strain that is not lethal for mice at low doses (Nieckarz et al., 2016). The loss of OmpR positively affected the production of heme receptor HemR1 in *Y. enterocolitica* cells grown in LB medium at 37°C and preliminary data suggested indirect repression of *hemR1* by OmpR.

In this study, we investigated the molecular mechanisms underlying OmpR-dependent production of two potential heme receptor proteins encoded within *hemPRSTUV-1* (*hem-1* locus) and *hemPRST-2* (*hem-2* locus) gene clusters identified in *Y. enterocolitica* strain Ye9. Firstly, we demonstrated that strain Ye9 utilizes heme-containing molecules as an iron source. The *Y. enterocolitica* hemin uptake system involved in transporting the entire heme moiety into the cytoplasm was described previously in strain WA-C, a mouse-virulent strain of bio-serotype 1B/O:8 (Stojiljkovic and Hantke, 1992, 1994). In contrast to strain Ye9, this strain is able to produce and utilize the siderophore yersiniabactin (Ybt), encoded on a chromosomal HPI (36 kb) (Heesemann et al., 1993; Rakin et al., 1994, 2012; Pelludat et al., 1998).

Heme uptake systems have been identified in several pathogenic bacteria, including *Y. pestis* (Thompson et al., 1999), *Y. pseudotuberculosis* (Schwiesow et al., 2018), *S. dysenteriae* (Mills and Payne, 1995, 1997; Wyckoff et al., 1998), and *V. cholerae* (Henderson and Payne, 1994; Occhino et al., 1998). Partial redundancy of heme-acquisition systems is often observed in Gram-negative bacteria due to the presence of uptake systems with a specific outer membrane receptor for heme and heme-proteins and/or the production of secreted hemophores (Ochsner et al., 2000; Runyen-Janecky, 2013).

In this study, two multigenic clusters, *hemPRSTUV-1* and *hemPRST-2* were identified in the genome of Ye9. The genetic organization of these clusters is identical except that the *hem-2* locus lacks two ORFs, *hemU2* and *hemV2*, encoding potential components of the heme transport system. Evidence from sqRT-PCR analysis revealed that both the *hem-1* and *hem-2* clusters are organized as operons, and expressed from the promoters P<sub>hem-1</sub> and P<sub>hem-2</sub> located upstream of the respective *hemP* genes. Experiments with a *Y. enterocolitica* strain carrying a plasmid-located p<sub>hem-1</sub>::*lacZ* reporter fusion showed that P<sub>hem-1</sub> promoter activity is inhibited by iron, which suggested the involvement of Fe<sup>2+</sup>-Fur in this repression. It has been previously demonstrated in diverse microorganisms that Fur, activated upon binding ferrous iron, binds to specific genes to inhibit



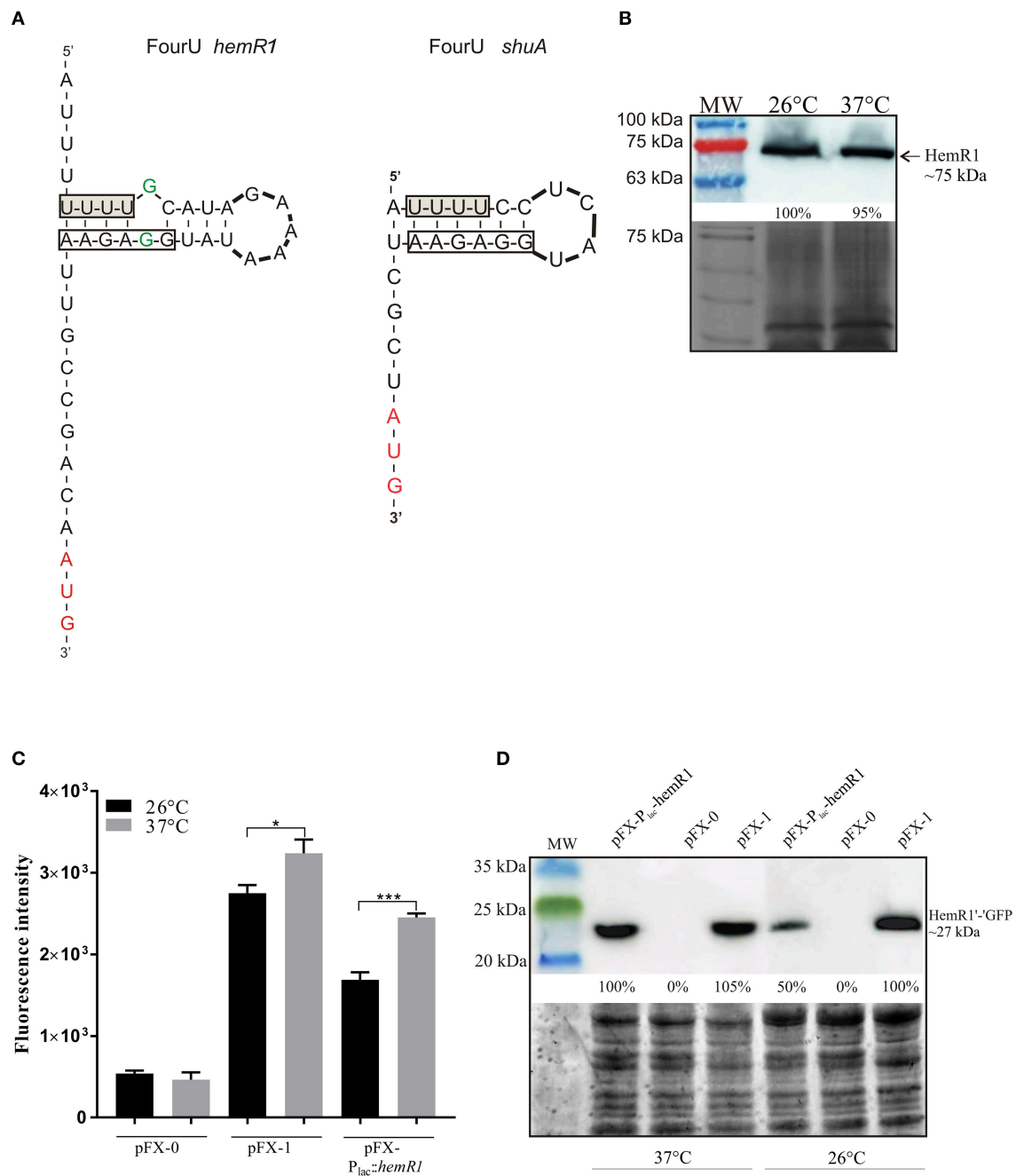


**FIGURE 8 |** Influence of temperature on *hemR1* expression. **(A)** Potential FourU thermometer RNA secondary structures in the 5'-UTRs of *Y. enterocolitica* Ye9 *hemR1* and *S. dysenteriae* *shuA*, composed of a stretch of FourU and the ribosomal binding site (RBS), revealed by Mfold analysis (<http://mfold.rna.albany.edu>). Boxes indicate the location of the FourU motif (shaded) and putative RBS, the translation start codon is marked red, and unpaired nucleotides within the predicted secondary structure are in green. **(B)** Temperature-dependent HemR1 expression in *Y. enterocolitica* examined by immunoblotting. The analyzed samples were cell lysates of the *fur* mutant grown at 26 or 37°C in LB medium. The top panel shows the Western blot probed with a polyclonal antibody against HemR1, the bottom panel shows the Coomassie blue-stained gel as a loading control. The percentage values on the blot, indicating the HemR1 band intensities relative to that of cells grown at 26°C, were determined using Amersham Imager 600 Analysis Software V1.0.0 (GE Healthcare). **(C)** Expression of a *hemR1'*-*gfp* translational fusion at different temperatures, monitored by fluorescence intensity. *E. coli* BW25113 harboring the reporter plasmid pFX-P<sub>lac</sub>-*hemR1* or control plasmids pFX-0 and pFX-1 were grown in LB medium at 26 or 37°C. The GFP fluorescence intensity (RFU) of overnight cultures was determined. The data represent the averages  $\pm$  SD from at least three experiments with duplicate cultures. Significance was calculated using one-way ANOVA [ $P > 0.05$ ,  $^*P < 0.05$ ,  $^{***}P < 0.001$ ]. **(D)** GFP abundance examined by immunoblotting. The analyzed samples were cell lysates of *E. coli* BW25113 harboring the plasmids pFX-0, pFX-1 or pFX-P<sub>lac</sub>-*hemR1*. The top panel shows the immunoblot probed with antibody against GFP, the bottom panel shows the TGX Stain-Free gel as a loading control. MW, 3-Color Prestained Protein Marker; kDa. These results are representative of at least three independent experiments.

their transcription (Bagg and Neilands, 1987; de Lorenzo et al., 1987; Andrews et al., 2003). Based on experimental and/or bioinformatic analyses, almost all iron-acquisition systems of pathogenic yersiniae, i.e., *Y. pestis*, have been shown to be Fur-controlled (Gao et al., 2008). More importantly, the results we obtained using transcriptional fusions with the *lacZ* gene and by Western blot analysis demonstrated that OmpR negatively regulates  $p_{\text{hem-1}}$  activity and thus HemR1 protein expression under conditions of iron starvation. The precise role of OmpR in the repression of HemR1 expression was revealed in a *fur* mutant background. While the *ompR* and *fur* mutations alone led to an increase in HemR1 synthesis, the combination of the two produced an additive effect. These data showed that OmpR inhibits HemR1 production in the absence of Fur. However, the OmpR-dependent regulation of HemR1 expression seems to be much more complex, since the effect of OmpR was also observed at the transcriptional and HemR1 protein level in iron-replete conditions, when the Fur repressor is active.

EMSA analysis revealed that OmpR acts directly at the  $p_{\text{hem-1}}$  promoter. We observed that OmpR specifically recognizes and binds a  $p_{\text{hem-1}}$  promoter fragment containing the *in silico*-predicted OmpR-binding sequence. This result confirmed a direct role for OmpR in mediating *hemR1* repression. In the *hem-1* promoter, the predicted 19-bp Fur box (FSB-1) overlaps the  $-10$  promoter motif, and is only 10 bp downstream of the 20-bp putative OmpR-binding site (OBS-1) at the  $-35$  motif. Based on the location of these binding sites, we propose the following model for Fur- and OmpR-dependent repression of *hem-1*. Consistent with the notion that under iron-starved conditions Fur-dependent repression is abolished, OmpR may interact with OBS-1 and prevent the polymerase binding to the promoter, leading to inhibition of *hem-1* expression. In iron-replete medium, there are a number of possible ways in which OmpR could regulate *hem-1* expression. It is likely that binding of OmpR to the  $p_{\text{hem-1}}$  promoter leads to a DNA structure that is favorable for the function of  $\text{Fe}^{2+}$ -Fur. Recent reports have suggested that the OmpR of *Salmonella enterica* may influence DNA topology to control target promoter activity (Cameron and Dorman, 2012; Quinn et al., 2014). We do not rule out the possibility that OmpR-Fur protein interactions could stimulate the binding of Fur to the *hem-1* promoter, which would lead to inhibition of transcription initiation. Further research is required to characterize the molecular mechanisms modulating the activity of Fur at the *hem-1* promoter in the presence of OmpR.

Similarly to the *hem-1* locus, the *hem-2* gene cluster *hemPRST-2* is organized as an operon. However,  $p_{\text{hem-2}}$  promoter activity was much lower than  $p_{\text{hem-1}}$  and iron repression was detected only at  $26^{\circ}\text{C}$ . Although a sequence displaying 74% identity to the Fur box consensus was recognized in  $p_{\text{hem-2}}$  (at the  $-10$  motif), the potential regulatory role of  $\text{Fe}^{2+}$ -Fur might be dependent on other thermoregulated factors. The role of OmpR in the activity of  $p_{\text{hem-2}}$  was studied by analyzing the expression of a  $p_{\text{hem-2}}::\text{lacZ}$  fusion in the wild-type strain with a normal or raised OmpR content. This experiment revealed that OmpR negatively regulates *hem-2* expression. Interestingly, in the presence of an increased

level of OmpR, iron regulation was abolished. Moreover, in EMSAs, we were able to detect the specific interaction of OmpR with the putative OmpR binding site in  $p_{\text{hem-2}}$ , but with lower affinity than with OBS-1 in the *hem-1* promoter. The higher binding sequence degeneracy in  $p_{\text{hem-2}}$  (45% identity to the consensus sequence for OBS-2 vs. 60% identity for OBS-1) might explain the weaker interaction of OmpR with this promoter.

Taken together, these results demonstrated the importance of the OmpR regulator in *hem-1* and *hem-2* expression, and hence the production of the HemR1 and HemR2 heme receptors in *Y. enterocolitica*. Our findings suggest that the effects of OmpR on *hem-1* and *hem-2* transcription are likely to be direct, i.e., produced by binding to specific DNA sequence elements in the promoter regions. The negative effect of OmpR on *hem-1* transcription occurs in both the absence and presence of the Fur repressor. The role of OmpR in regulating *hem-2* expression is difficult to assess and needs further study.

Thermo-induced structural changes in mRNA play a fundamental role in temperature sensing in bacteria and influence virulence gene expression in many pathogens, including those of the genus *Yersinia* (Narberhaus et al., 2006; Narberhaus, 2010; Böhme et al., 2012). Analysis of the intergenic region of the *hemP1-hemR1* transcript in locus *hem-1*, but not in locus *hem-2*, in *Y. enterocolitica* Ye9, suggested the formation of a secondary structure in the *hemR1* 5'-UTR with a FourU element that may sequester the ribosome binding site. Such an RNA structure was previously shown to be sufficiently stable at moderate temperatures ( $25^{\circ}\text{C}$ ) to inhibit expression of the ShuA receptor in *S. dysenteriae*. Melting of the FourU motif at  $37^{\circ}\text{C}$  permits access of ribosomes and initiates *shuA* translation (Kouse et al., 2013). However, Western blot analysis revealed that HemR1 of *Y. enterocolitica* is not subject to thermoregulation. Despite the presence of a FourU sequence in the 5'-UTR of *hemR1*, the unpaired G-G sequence within the hairpin may destabilize this secondary structure. In *S. dysenteriae*, only a single nucleotide replacement within the *shuA* hairpin led to destabilization of this inhibitory structure and resulted in increased expression of this gene at the non-permissive temperature of  $25^{\circ}\text{C}$  (Kouse et al., 2013). A stretch of four uracils located within an intergenic region of the *yscW-lcrF* transcript in a pathogenic *Yersinia* has been linked with the thermally regulated expression of the transcript encoding LcrF, the transcriptional activator of *yop* and *ysc* genes of the type III secretion system (Böhme et al., 2012). It is notable that analyses of the expression of a *hemR1'-gfp* translational fusion and the level of a HemR1'-GFP fusion protein in *E. coli* showed a degree of temperature dependence, suggesting that a mechanism of thermoregulation, unconnected with the presence of a FourU RNA thermometer, is active in this heterologous genetic background.

HemR1 and the newly identified HemR2 protein exhibit a high degree of amino acid sequence similarity (62% identity), including the presence of signature motifs like the TonB box, the conserved V region associated with all TonB-dependent OM proteins, and histidine residues required for heme transport via the receptor channel (Kadner, 1990; Bracken et al., 1999).

Significant similarities between HemR1/HemR2 and hemin-binding proteins suggest that these two *Y. enterocolitica* proteins are involved in the binding and utilization of hemin and heme-proteins. The expression of the HemR1 or HemR2 protein from their native promoters in *E. coli* SASX77, a  $\Delta$ hemA mutant defective in the biosynthesis of a heme precursor and naturally lacking a heme binding protein in the outer membrane (Stojiljkovic and Hantke, 1994; Mills and Payne, 1995), permitted hemin and hemoglobin utilization. The strain expressing HemR2 was less efficient in utilizing hemin or hemoglobin, which might reflect lower activity of the  $p_{\text{hem-2}}$  promoter. It is also possible that structural or functional differences in these OM receptors may influence the transport of the heme moiety.

Taken together the findings of this study indicate that *Y. enterocolitica* HemR1 and HemR2 are outer membrane-receptors that play an important role in hemin and hemoglobin utilization. We hypothesize that HemR1 and HemR2 together with HemTUV-1, a periplasmic/inner membrane ABC heme transporter also encoded by the *hem-1* locus, may constitute a system involved in the acquisition of the heme moiety from host hemoproteins under the varied conditions encountered by *Y. enterocolitica* during an infection. It is also possible that HemR2 together with an as yet unidentified cytoplasmic transporter constitute an alternative system for the utilization of heme and host hemoproteins. Such a system might be able to counteract the loss/inactivation of the *Y. enterocolitica* heme uptake system based on the HemR receptor. Pathogenic bacteria frequently possess more than one transport system for iron or heme/hemoprotein uptake (Braun et al., 1998), so additional

systems besides those involving the TonB-dependent HemR1 and HemR2 receptors may help perform this vital function in *Y. enterocolitica*.

In conclusion, this study has demonstrated that the regulators Fur and OmpR participate in a complex mechanism governing the negative regulation of *Y. enterocolitica* *hemR1* and *hemR2*. This interplay might be responsible for fine-tuning the expression of HemR receptor proteins mediating iron/heme acquisition during infection, to permit rapid growth while avoiding toxicity.

## AUTHOR CONTRIBUTIONS

KJ, AR, and KB designed the study. KJ, MN, and ML performed the experiments. KB, AR, KJ, and ML analyzed the data. AR, KB, and KJ wrote the manuscript. KJ and MN designed and prepared the figures. KB provided financial support.

## FUNDING

This work was supported by a grant from the National Science Center, Poland (OPUS grant UMO-2016/21/B/N26/011009). Publication co-financed by the University of Warsaw.

## SUPPLEMENTARY MATERIAL

The Supplementary Material for this article can be found online at: <https://www.frontiersin.org/articles/10.3389/fcimb.2018.00333/full#supplementary-material>

## REFERENCES

- Andrews, S. C., Robinson, A. K., and Rodriguez-Quinones, F. (2003). Bacterial iron homeostasis. *FEMS Microbiol. Rev.* 27, 215–237. doi: 10.1016/S0168-6445(03)00055-X
- Anzaldi, L. L., and Skaar, E. P. (2010). Overcoming the heme paradox: heme toxicity and tolerance in bacterial pathogens. *Infect. Immun.* 78, 4977–4989. doi: 10.1128/IAI.00613-10
- Bagg, A., and Neilands, J. B. (1987). Ferric uptake regulation protein acts as a repressor, employing iron (II) as a cofactor to bind the operator of an iron transport operon in *Escherichia coli*. *Biochemistry* 26, 5471–5477. doi: 10.1021/bi00391a039
- Bang, I. S., Audia, J. P., Part, Y. K., and Foster, J. W. (2002). Autoinduction of the *ompR* response regulator by acid shock and control of the *Salmonella enterica* acid tolerance response. *Mol. Microbiol.* 44, 1235–1250. doi: 10.1046/j.1365-2958.2002.02937.x
- Bäumler, A., Koebnik, R., Stojiljkovic, I., Heesemann, J., Braun, V., and Hantke, K. (1993). Survey on newly characterized iron uptake systems of *Yersinia enterocolitica*. *Z. Bakteriologie* 278, 416–424. doi: 10.1016/S0934-8840(11)80858-3
- Bernardini, M. L., Fontaine, A., and Sansonetti, P. J. (1990). The two-component regulatory system *ompR-envZ* controls the virulence of *Shigella flexneri*. *J. Bacteriol.* 172, 6274–6281. doi: 10.1128/jb.172.11.6274-6281.1990
- Bijlsma, J. J., Waidner, B., Vliet, A. H., Hughes, N. J., Hag, S., Bereswill, S., et al. (2002). The *Helicobacter pylori* homologue of the ferric uptake regulator is involved in acid resistance. *Infect. Immun.* 70, 606–611. doi: 10.1128/IAI.70.2.606-611.2002
- Böhme, K., Steinmann, R., Kortmann, J., Seekircher, S., Heroven, A. K., Berger, E., et al. (2012). Concerted actions of a thermo-labile regulator and a unique intergenic RNA thermosensor control *Yersinia* virulence. *PLoS Pathog.* 8:e1002518. doi: 10.1371/journal.ppat.1002518
- Bottone, E. J. (1997). *Yersinia enterocolitica*: the charisma continues. *Clin. Microbiol. Rev.* 10, 257–276.
- Bracken, C. S., Baer, M. T., Abdur-Rashid, A., Helms, W., and Stojiljkovic, I. (1999). Use of heme-protein complexes by the *Yersinia enterocolitica* HemR receptor: histidine residues are essential for receptor function. *J. Bacteriol.* 181, 6063–6072.
- Braun, V., Günter, K., and Hantke, K. (1991). Transport of iron across the outer membrane. *Biol. Met.* 4, 14–22. doi: 10.1007/BF01135552
- Braun, V., Hantke, K., and Köster, W. (1998). Bacterial iron transport: mechanisms, genetics, and regulation. *Met. Ions Biol. Syst.* 35, 67–145.
- Brzostek, K., Brzostkowska, M., Bukowska, I., Karwicka, E., and Raczkowska, A. (2007). OmpR negatively regulates expression of invasin in *Yersinia enterocolitica*. *Microbiology* 153, 2416–2425. doi: 10.1099/mic.0.2006/003202-0
- Brzostek, K., Raczkowska, A., and Zasada, A. (2003). The osmotic regulator OmpR is involved in the response of *Yersinia enterocolitica* O:9 to environmental stresses and survival within macrophages. *FEMS Microbiol. Lett.* 228, 265–271. doi: 10.1016/S0378-1097(03)00779-1
- Brzostek, K., Skorek, K., and Raczkowska, A. (2012). OmpR, a central integrator of several cellular responses in *Yersinia enterocolitica*. *Adv. Exp. Med. Biol.* 954, 325–334. doi: 10.1007/978-1-4614-3561-7-40
- Brzostkowska, M., Raczkowska, A., and Brzostek, K. (2012). OmpR, a response regulator of the two-component signal transduction pathway, influences *inv* gene expression in *Yersinia enterocolitica* O9. *Front. Cell. Inf. Microbiol.* 2:153. doi: 10.3389/fcimb.2012.00153
- Cameron, A. D., and Dorman, C. J. (2012). A fundamental regulatory mechanism operating through OmpR and DNA topology controls expression of *Salmonella* pathogenicity islands SPI-1 and SPI-2. *PLoS Genet.* 8:e1002615. doi: 10.1371/journal.pgen.1002615
- Carniel, E. (2001). The *Yersinia* high-pathogenicity island: an iron-uptake island. *Microbes Infect.* 3, 561–569. doi: 10.1016/S1286-4579(01)01412-5

- Caza, M., and Kronstad, J. W. (2013). Shared and distinct mechanisms of iron acquisition by bacterial and fungal pathogens of humans. *Front. Cell. Infect. Microbiol.* 3:80. doi: 10.3389/fcimb.2013.00080
- Chatfield, S. N., Dorman, C. J., Hayward, C., and Dougan, G. (1991). Role of *ompR*-dependent genes in *Salmonella typhimurium* virulence: mutants deficient in both OmpC and OmpF are attenuated *in vivo*. *Infect. Immun.* 59, 449–452.
- Cornelis, G. R. (2002). *Yersinia* type III secretion: send in the effectors. *Cell Biol.* 158, 401–408. doi: 10.1083/jcb.200205077
- de Lorenzo, V., Wee, S., Herrero, M., and Neilands, J. B. (1987). Operator sequences of the aerobactin operon of plasmid ColV-K30 binding the ferric uptake regulation (*fur*) repressor. *J. Bacteriol.* 169, 2624–2630. doi: 10.1128/jb.169.6.2624-2630.1987
- Dorman, C. J., Chatfield, S., Higgins, C. F., Hayward, C., and Dougan, G. (1989). Characterization of porin and *ompR* mutants of a virulent strain of *Salmonella typhimurium*: *ompR* mutants are attenuated *in vivo*. *Infect. Immun.* 57, 2136–2140.
- Engler, C., Kandzia, R., and Marillonnet, S. (2008). A one pot, one step, precision cloning method with high throughput capability. *PLoS ONE* 3:e3647. doi: 10.1371/journal.pone.0003647
- Escobar, L., Pérez-Martín, J., and de Lorenzo, V. (1999). Opening the iron box: transcriptional metalloregulation by the Fur protein. *J. Bacteriol.* 181, 6223–6229.
- Feng, X., Oropeza, R., and Kenney, L. J. (2003). Dual regulation by phospho-OmpR of *ssrA/B* gene expression in *Salmonella* pathogenicity island 2. *Mol. Microbiol.* 48, 1131–1143. doi: 10.1046/j.1365-2958.2003.03502.x
- Gao, H., Zhou, D., Li, Y., Guo, Z., Han, Y., Song, Y., et al. (2008). The iron-responsive Fur regulon in *Yersinia pestis*. *J. Bacteriol.* 190, 3063–3075. doi: 10.1128/JB.01910-07
- Hantke, K. (2001). Iron and metal regulation in bacteria. *Curr. Opin. Microbiol.* 4, 172–177. doi: 10.1016/S1369-5274(00)00184-3
- Hassett, D. J., Sokol, P. A., Howell, M. L., Ma, J. F., Schweizer, H. T., Ochsner, U., et al. (1996). Ferric uptake regulator (Fur) mutants of *Pseudomonas aeruginosa* demonstrate defective siderophore-mediated iron uptake, altered aerobic growth, and decreased superoxide dismutase and catalase activities. *J. Bacteriol.* 178, 3996–4003. doi: 10.1128/jb.178.14.3996-4003.1996
- Heesemann, J. (1987). Chromosomal-encoded siderophores are required for mouse virulence of enteropathogenic *Yersinia* species. *FEMS Microbiol. Lett.* 48, 229–233. doi: 10.1111/j.1574-6968.1987.tb02547.x
- Heesemann, J., Hantke, K., Vocke, T., Saken, E., Rakin, A., Stojiljkovic, I., et al. (1993). Virulence of *Yersinia enterocolitica* is closely associated with siderophore production, expression of an iron-repressible outer membrane polypeptide of 65,000 Da and pesticin sensitivity. *Mol. Microbiol.* 8, 397–408. doi: 10.1111/j.1365-2958.1993.tb01583.x
- Henderson, D. P., and Payne, S. M. (1994). Characterization of the *Vibrio cholerae* outer membrane heme transport protein HutA: sequence of the gene, regulation of expression, and homology to the family of TonB-dependent proteins. *J. Bacteriol.* 176, 3269–3277. doi: 10.1128/jb.176.11.3269-3277.1994
- Higashitani, A., Nishimura, Y., Hara, H., Aiba, H., Mizuno, T., and Horiuchi, K. (1993). Osmoregulation of the fatty acid receptor gene *fadL* in *Escherichia coli*. *Mol. Gen. Genet.* 240, 339–347.
- Jubelin, G., Vianney, A., Beloin, C., Ghigo, J. M., Lazzaroni, J. C., Lejeune, P., et al. (2005). CpxR/OmpR interplay regulates curli gene expression in response to osmolarity in *Escherichia coli*. *J. Bacteriol.* 187, 2038–2049. doi: 10.1128/JB.187.6.2038-2049.2005
- Kadner, R. J. (1990). Vitamin B<sub>12</sub> transport in *Escherichia coli*: energy coupling between membranes. *Mol. Microbiol.* 4, 2027–2033. doi: 10.1111/j.1365-2958.1990.tb00562.x
- Kenney, L. J. (2002). Structure/function relationships in OmpR and other winged-helix transcription factors. *Curr. Opin. Microbiol.* 5, 135–141. doi: 10.1016/S1369-5274(02)00310-7
- Kouse, A. B., Righetti, F., Kortmann, J., Narberhaus, F., and Murphy, E. R. (2013). RNA-mediated thermoregulation of iron-acquisition genes in *Shigella dysenteriae* and pathogenic *Escherichia coli*. *PLoS ONE* 8:e63781. doi: 10.1371/journal.pone.0063781
- Krewulak, K. D., and Vogel, H. J. (2011). TonB or not TonB: is that the question? *Biochem. Cell. Biol.* 89, 87–97. doi: 10.1139/o10-141
- Lee, B. C. (1995). Quelling the red menace: haem capture by bacteria. *Mol. Microbiol.* 18, 383–390. doi: 10.1111/j.1365-2958.1995.mmi\_18030383.x
- Maeda, S., Takayanagi, K., Nishimura, Y., Maruyama, T., Sato, K., and Mizuno, T. (1991). Activation of the osmoregulated *ompC* gene by the OmpR protein in *Escherichia coli*: a study involving synthetic OmpR-binding sequences. *J. Biochem.* 110, 324–327.
- Marx, C. J., and Lidstrom, M. E. (2001). Development of improved versatile broad-host-range vectors for use in methylotrophs and other Gram-negative bacteria. *Microbiology* 147, 2065–2075. doi: 10.1099/00221287-147-8-2065
- Mietzner, T. A., and Morse, S. A. (1994). The role of iron-binding proteins in the survival of pathogenic bacteria. *Annu. Rev. Nutr.* 14, 471–493. doi: 10.1146/annurev.nu.14.070194.002351
- Miller, J. H. (1992). *Experiments in Molecular Genetics*. Cold Spring Harbor, NY: Cold Spring Harbor Laboratory.
- Mills, M., and Payne, S. M. (1995). Genetics and regulation of heme iron transport in *Shigella dysenteriae* and detection of an analogous system in *Escherichia coli* O157:H7. *J. Bacteriol.* 177, 3004–3009.
- Mills, M., and Payne, S. M. (1997). Identification of *shuA*, the gene encoding the heme receptor of *Shigella dysenteriae*, and analysis of invasion and intracellular multiplication of a *shuA* mutant. *Infect. Immun.* 65, 5358–5363.
- Narberhaus, F. (2010). Translational control of bacterial heat shock and virulence genes by temperature-sensing mRNAs. *RNA Biol.* 7, 84–89. doi: 10.4161/rna.7.1.10501
- Narberhaus, F., Waldmingham, T., and Chowdhury, S. (2006). RNA thermometers. *FEMS Microbiol. Rev.* 30, 3–16. doi: 10.1111/j.1574-6976.2005.004.x
- Nau, C. D., and Konisky, J. (1989). Evolutionary relationship between the TonB-dependent outer membrane transport proteins: nucleotide and amino acid sequences of the *Escherichia coli* colicin I receptor gene. *J. Bacteriol.* 171, 1041–1047.
- Neilands, J. B. (1994). Identification and isolation of mutants defective in iron acquisition. *Methods Enzymol.* 235, 352–356. doi: 10.1016/0076-6879(94)35153-8
- Nieckarz, M., Raczkowska, A., Debski, J., Kistowski, M., Dadlez, M., Heesemann, J., et al. (2016). Impact of OmpR on the membrane proteome of *Yersinia enterocolitica* in different environments: repression of major adhesin YadA and heme receptor HemR. *Env. Microbiol.* 18, 997–1021. doi: 10.1111/1462-2920.13165
- Occhino, D. A., Wyckoff, E. E., Henderson, D. P., Wrona, T. J., and Payne, S. M. (1998). *Vibrio cholerae* iron transport: haem transport genes are linked to one of two sets of *tonB*, *exbB*, *exbD* genes. *Mol. Microbiol.* 29, 1493–1507.
- Ochsner, U. A., Johnson, Z., and Vasil, M. L. (2000). Genetics and regulation of two distinct haem-uptake systems, *phu* and *has*, in *Pseudomonas aeruginosa*. *Microbiology* 146, 185–198. doi: 10.1099/00221287-146-1-185
- Ochsner, U. A., and Vasil, M. L. (1996). Gene repression by the ferric uptake regulator in *Pseudomonas aeruginosa*: cycle selection of iron-regulated genes. *Proc. Natl. Acad. Sci. USA* 93, 4409–4414.
- Pelludat, C., Rakin, A., Jacobi, C. A., Schubert, S., and Heesemann, J. (1998). The yersiniabactin biosynthetic gene cluster of *Yersinia enterocolitica*: organization and siderophore-dependent regulation. *J. Bacteriol.* 180, 538–546.
- Philippe, N., Alcaraz, J. P., Coursange, E., Geiselman, J., and Schneider, D. (2004). Improvement of pCVD442, a suicide plasmid for gene allele exchange in bacteria. *Plasmid* 51, 246–255. doi: 10.1016/j.plasmid.2004.02.003
- Quinn, H. J., Cameron, A. D., and Dorman, C. J. (2014). Bacterial regulon evolution: distinct responses and roles for the identical OmpR proteins of *Salmonella Typhimurium* and *Escherichia coli* in the acid stress response. *PLoS Genet.* 10:e1004215. doi: 10.1371/journal.pgen.1004215
- Raczkowska, A., Brzostkowska, M., Kwiatek, A., Bielecki, J., and Brzostek, K. (2011a). Modulation of *inv* gene expression by the OmpR two-component response regulator protein of *Yersinia enterocolitica*. *Folia Microbiol. (Praha)* 56, 313–319. doi: 10.1007/s12223-011-0054-9
- Raczkowska, A., Skorek, K., Bielecki, J., and Brzostek, K. (2010). OmpR controls *Yersinia enterocolitica* motility by positive regulation of *flhDC* expression. *Antonie Van Leeuwenhoek* 99, 381–394. doi: 10.1007/s10482-010-9503-8
- Raczkowska, A., Skorek, K., Brzostkowska, M., Łasinska, A., and Brzostek, K. (2011b). Pleiotropic effects of a *Yersinia enterocolitica ompR* mutation on adherent-invasive abilities and biofilm formation. *FEMS Microbiol. Lett.* 321, 43–49. doi: 10.1111/j.1574-6968.2011.02308.x



- Raczowska, A., Trzós, J., Lewandowska, O., Nieckarz, M., and Brzostek, K. (2015). Expression of the AcrAB components of the AcrAB-TolC multidrug efflux pump of *Yersinia enterocolitica* is subject to dual regulation by OmpR. *PLoS ONE* 10:e0124248. doi: 10.1371/journal.pone.0124248
- Rakin, A., Saken, E., Harmsen, D., and Heesemann, J. (1994). The pesticin receptor of *Yersinia enterocolitica*: a novel virulence factor with dual function. *Mol. Microbiol.* 13, 253–263. doi: 10.1111/j.1365-2958.1994.tb00420.x
- Rakin, A., Schneider, L., and Podladchikova, O. (2012). Hunger for iron: the alternative siderophore iron scavenging systems in highly virulent *Yersinia*. *Front. Cell. Infect. Microbiol.* 2:151. doi: 10.3389/fcimb.2012.00151
- Runyen-Janecky, L. J. (2013). Role and regulation of heme iron acquisition in gram-negative pathogens. *Front. Cell. Infect. Microbiol.* 3:55. doi: 10.3389/fcimb.2013.00055
- Sambrook, J., and Russell, D. W. (2001). *Molecular Cloning: A Laboratory Manual, 3rd Edn.* Cold Spring Harbor, NY: Cold Spring Harbor Laboratory Press.
- Schmidtke, C., Abendroth, U., Brock, J., Serrania, J., Becker, A., and Bonas, U. (2013). Small RNA sX13: a multifaceted regulator of virulence in the plant pathogen *Xanthomonas*. *PLoS Pathog.* 9:e1003626. doi: 10.1371/journal.ppat.1003626
- Schwiesow, L., Mettert, E., Wei, Y., Miller, H. K., Herrera, N. G., Balderas, D., et al. (2018). Control of *hmu* heme uptake genes in *Yersinia pseudotuberculosis* in response to iron sources. *Front. Cell. Infect. Microbiol.* 8:47. doi: 10.3389/fcimb.2018.00047
- Schwyn, B., and Neilands, J. B. (1987). Universal chemical assay for the detection and determination of siderophores. *Anal. Biochem.* 160, 47–56. doi: 10.1016/0003-2697(87)90612-9
- Shin, S., and Park, C. (1995). Modulation of flagellar expression in *Escherichia coli* by acetyl phosphate and the osmoregulator OmpR. *J. Bacteriol.* 177, 4696–4702.
- Skorek, K., Raczowska, A., Dudek, B., Mietka, K., Guz-Regner, K., Pawlak, A., et al. (2013). Regulatory protein OmpR influences the serum resistance of *Yersinia enterocolitica* O:9 by modifying the structure of the outer membrane. *PLoS ONE* 8:e79525. doi: 10.1371/journal.pone.0079525
- Slauch, J. M., and Silhavy, T. J. (1989). Genetic analysis of the switch that controls porin gene expression in *Escherichia coli* K-12. *J. Mol. Biol.* 210, 281–292.
- Solov'yev, V., and Salamov, A. (2011). "Automatic annotation of microbial genomes and metagenomic sequences," In *Metagenomics and Its Applications in Agriculture, Biomedicine and Environmental Studies*, ed R. W. Li (Hauppauge, NY: Nova Science Publishers), 61–78.
- Stincone, A., Daudi, N., Rahman, A. S., Antczak, P., Henderson, I., Cole, J., et al. (2011). A systems biology approach sheds new light on *Escherichia coli* acid resistance. *Nucleic Acids Res.* 39, 7512–7528. doi: 10.1093/nar/gkr338
- Stojiljkovic, I., Bäuml, A. J., and Hantke, K. (1994). Fur regulon in Gram-negative bacteria: identification and characterization of new iron-regulated *Escherichia coli* genes by a Fur titration assay. *J. Mol. Biol.* 236, 531–545. doi: 10.1006/jmbi.1994.1163
- Stojiljkovic, I., and Hantke, K. (1992). Hemin uptake system of *Yersinia enterocolitica*: similarities with other TonB-dependent systems in Gram-negative bacteria. *EMBO J.* 11, 4359–4367.
- Stojiljkovic, I., and Hantke, K. (1994). Transport of haemin across the cytoplasmic membrane through a haemin-specific periplasmic binding-protein-dependent transport system in *Yersinia enterocolitica*. *Mol. Microbiol.* 13, 719–732.
- Stojiljkovic, I., and Perkins-Balding, D. (2002). Processing of heme and heme-containing proteins by bacteria. *DNA Cell Biol.* 21, 281–295. doi: 10.1089/104454902753759708
- Thibodeau, S. A., Fang, R., and Joung, J. K. (2004). High-throughput beta-galactosidase assay for bacterial cell-based reporter systems. *Biotechniques* 36, 410–415. doi: 10.2144/04363BM07
- Thompson, J. M., Jones, H. A., and Perry, R. D. (1999). Molecular characterization of the hemin uptake locus (*hmu*) from *Yersinia pestis* and analysis of *hmu* mutants for hemin and hemoprotein utilization. *Infect. Immun.* 67, 3879–3892.
- van Vliet, A. H., Stoof, J., Poppelaars, S. W., Bereswill, S., Homuth, G., Kist, M., et al. (2003). Differential regulation of amidase- and formamidase mediated ammonia production by the *Helicobacter pylori* fur repressor. *J. Biol. Chem.* 278, 9052–9057. doi: 10.1074/jbc.M207542200
- Vidal, O., Longin, R., Prigent-Combaret, C., Dorel, C., Hooreman, M., and Lejeune, P. (1998). Isolation of an *Escherichia coli* K-12 mutant strain able to form biofilms on inert surfaces: involvement of a new *ompR* allele that increases curli expression. *J. Bacteriol.* 180, 2442–2449.
- Waldminghaus, T., Heidrich, N., Brantl, S., and Narberhaus, F. (2007). FourU: a novel type of RNA thermometer in *Salmonella*. *Mol. Microbiol.* 65, 413–424. doi: 10.1111/j.1365-2958.2007.05794.x
- Wyckoff, E. E., Duncan, D., Torres, A. G., Mills, M., Maase, K., and Payne, S. M. (1998). Structure of the *Shigella dysenteriae* haem transport locus and its phylogenetic distribution in enteric bacteria. *Mol. Microbiol.* 28, 1139–1152.
- Yamamoto, K., Nagura, R., Tanabe, H., Fujita, N., Ishihama, A., and Utsumi, R. (2000). Negative regulation of the *bolA1p* of *Escherichia coli* K-12 by the transcription factor OmpR for osmolarity response genes. *FEMS Microbiol. Lett.* 186, 257–262. doi: 10.1111/j.1574-6968.2000.tb09114.x
- Zuker, M. (2003). Mfold web server for nucleic acid folding and hybridization prediction. *Nucleic Acids Res.* 31, 3406–3415. doi: 10.1093/nar/gkg595

**Conflict of Interest Statement:** The authors declare that the research was conducted in the absence of any commercial or financial relationships that could be construed as a potential conflict of interest.

Copyright © 2018 Jaworska, Nieckarz, Ludwiczak, Raczowska and Brzostek. This is an open-access article distributed under the terms of the Creative Commons Attribution License (CC BY). The use, distribution or reproduction in other forums is permitted, provided the original author(s) and the copyright owner(s) are credited and that the original publication in this journal is cited, in accordance with accepted academic practice. No use, distribution or reproduction is permitted which does not comply with these terms.



# ***Yersinia pseudotuberculosis* BarA-UvrY Two-Component Regulatory System Represses Biofilms via CsrB**

Jeffrey K. Schachterle<sup>1</sup>, Ryan M. Stewart<sup>1</sup>, M. Brett Schachterle<sup>1</sup>, Joshua T. Calder<sup>1</sup>, Huan Kang<sup>2</sup>, John T. Prince<sup>2</sup> and David L. Erickson<sup>1\*</sup>

## OPEN ACCESS

### Edited by:

Matthew S. Francis,  
Umeå University, Sweden

### Reviewed by:

Yi-Cheng Sun,  
Institute of Pathogen Biology (CAMS),  
China

Gregory Anderson,  
Indiana University, Purdue University  
Indianapolis, United States

Nadim Majdalani,  
National Institutes of Health (NIH),  
United States

### \*Correspondence:

David L. Erickson  
david\_erickson@byu.edu

### Specialty section:

This article was submitted to  
Molecular Bacterial Pathogenesis,  
a section of the journal  
Frontiers in Cellular and Infection  
Microbiology

**Received:** 14 June 2018

**Accepted:** 24 August 2018

**Published:** 18 September 2018

### Citation:

Schachterle JK, Stewart RM,  
Schachterle MB, Calder JT, Kang H,  
Prince JT and Erickson DL (2018)  
*Yersinia pseudotuberculosis*  
BarA-UvrY Two-Component  
Regulatory System Represses  
Biofilms via CsrB.  
Front. Cell. Infect. Microbiol. 8:323.  
doi: 10.3389/fcimb.2018.00323

<sup>1</sup> Department of Microbiology and Molecular Biology, Brigham Young University, Provo, UT, United States, <sup>2</sup> Department of Chemistry and Biochemistry, Brigham Young University, Provo, UT, United States

The formation of biofilms by *Yersinia pseudotuberculosis* (*Yptb*) and *Y. pestis* requires the *hmsHFRS* genes, which direct production of a polysaccharide extracellular matrix (Hms-ECM). Despite possessing identical *hmsHFRS* sequences, *Yptb* produces much less Hms-ECM than *Y. pestis*. The regulatory influences that control *Yptb* Hms-ECM production and biofilm formation are not fully understood. In this study, negative regulators of biofilm production in *Yptb* were identified. Inactivation of the BarA/UvrY two-component system or the CsrB regulatory RNA increased binding of Congo Red dye, which correlates with extracellular polysaccharide production. These mutants also produced biofilms that were substantially more cohesive than the wild type strain. Disruption of *uvrY* was not sufficient for *Yptb* to cause proventricular blockage during infection of *Xenopsylla cheopis* fleas. However, this strain was less acutely toxic toward fleas than wild type *Yptb*. Flow cytometry measurements of lectin binding indicated that *Yptb* BarA/UvrY/CsrB mutants may produce higher levels of other carbohydrates in addition to poly-GlcNAc Hms-ECM. In an effort to characterize the relevant downstream targets of the BarA/UvrY system, we conducted a proteomic analysis to identify proteins with lower abundance in the *csrB::Tn5* mutant strain. Urease subunit proteins were less abundant and urease enzymatic activity was lower, which likely reduced toxicity toward fleas. Loss of CsrB impacted expression of several potential regulatory proteins that may influence biofilms, including the RcsB regulator. Overexpression of CsrB did not alter the Congo-red binding phenotype of an *rscB::Tn5* mutant, suggesting that the effect of CsrB on biofilms may require RcsB. These results underscore the regulatory and compositional differences between *Yptb* and *Y. pestis* biofilms. By activating CsrB expression, the *Yptb* BarA/UvrY two-component system has pleiotropic effects that impact biofilm production and stability.

**Keywords:** *Yersinia pseudotuberculosis*, biofilm, carbon storage regulator system A (CsrA), two-component regulation, fleas

## INTRODUCTION

Like many bacteria, *Yersinia pseudotuberculosis* (*Yptb*) in varied environments such as soil and water face temperature extremes, desiccation, nutrient deprivation, or nematode predation, and their survival is enhanced by efficient biofilm production. Transmission of *Yersinia pestis* by fleas is also significantly influenced by biofilm production. One transmission mechanism exhibited by some fleas requires *Y. pestis* to form biofilm on the spines that line the interior surface of the flea's proventriculus (Hinnebusch et al., 1996; Jarrett et al., 2004). Biofilm formation in both *Yptb* and *Y. pestis* is aided by the *hmsHFRS* gene products, which together direct the synthesis of an extracellular matrix (ECM) containing poly- $\beta$ -1,6 linked *N*-acetyl-D-glucosamine ( $\beta$ -1,6-GlcNAc) (Bobrov et al., 2008; Erickson et al., 2008; Hinnebusch and Erickson, 2008). HmsR and HmsS are inner-membrane proteins that may assemble polymers from UDP-*N*-acetylglucosamine in the cytoplasm. The polymer is likely deacetylated by HmsF prior to export and transport through the outer membrane porin HmsH. Hms-ECM production by *Yptb* and *Y. pestis* can be visualized as Congo red binding (pigmentation) on agar plates. All four of the *hmsHFRS* gene products are required for pigmentation and biofilm, and inactivation of the periplasmic, deacetylase, and glycosyl transferase domains of HmsH, F, and R, respectively, reduces Congo red binding and *in vitro* biofilm formation (Forman et al., 2006).

Recent efforts have focused on understanding how biofilm production in *Y. pestis* is regulated. Multiple regulatory influences of the Hms-ECM in *Y. pestis* have been identified including temperature (Perry et al., 2004), polyamines (Wortham et al., 2010), and the second messenger cyclic-diguanylate (c-di-GMP) (Kirillina et al., 2004; Bobrov et al., 2011). Hms-ECM is produced at growth temperatures  $\leq 26^\circ\text{C}$  (Perry et al., 1990; Hinnebusch et al., 1996; Darby et al., 2002; Jarrett et al., 2004). Temperature regulation is achieved in part by the reduced translation or stability of HmsH, HmsR and the diguanylate cyclase HmsT (Perry et al., 2004) at temperatures above  $28^\circ\text{C}$ . High levels of cyclic diguanylate in the cell may increase the glycosyl transferase activity of HmsR (Bobrov et al., 2008). *Y. pestis* contains an additional diguanylate cyclase (HmsD) that enhances biofilm formation in the flea digestive tract (Bobrov et al., 2011; Sun et al., 2011).

Less is known about the regulation of biofilm in *Yptb*. Although *Yptb*, like *Y. pestis*, forms Hms-dependent biofilms *in vitro* and on the outer mouthparts of *Caenorhabditis elegans* nematodes (Darby et al., 2002; Joshua et al., 2003), the majority of *Yptb* strains do not form pigmented colonies on Congo-red agar. Additionally, *Yptb* never forms biofilm on the flea proventriculus to cause blockage of the digestive tract, even though it can colonize the flea midgut (Erickson et al., 2006). Compositional changes in the ECM of *Y. pestis* and *Yptb* may contribute to this difference but it is now clear that during the evolution of *Y. pestis*, mutations in genes that affect the regulation of Hms protein synthesis or production and stability of the ECM have been selected. Functional regulatory mechanisms that repress Hms-dependent ECM production in *Yptb* such as the RcsA

transcriptional regulator (Sun et al., 2008; Guo et al., 2015), the NghA glycosyl hydrolase (Erickson et al., 2008), and additional enzymes that produce or degrade cyclic diguanylate (Bobrov et al., 2011) have been lost or altered during the emergence of *Y. pestis*, which have enhanced its biofilm production within fleas.

In this study we sought to identify additional regulatory mechanisms that repress production of extracellular polysaccharides in *Yptb*. A screen for mutants with enhanced Congo Red pigmentation phenotypes suggested a role for the BarA/UvrY two-component regulatory system. We tested the effect of *barA*, *uvrY* and *csrB* mutation in Congo Red binding and biofilm stability. We sought to correlate the changes we observed in biofilm stability and Congo-red binding with production of specific carbohydrates using fluorescently-labeled lectins and flow cytometry. Finally, we employed a proteomic approach to identify multiple downstream targets of the CsrB regulatory RNA that could influence biofilm formation.

## MATERIALS AND METHODS

### Bacterial Strains and Growth Conditions

*Y. pseudotuberculosis* strain IP32953 and *Y. pestis* KIM6+ were routinely grown at  $28^\circ\text{C}$  in Terrific broth (TB) or at  $21^\circ\text{C}$  in 1% heart infusion broth supplemented with 0.2% galactose (HIG). The transposon mutants in strain IP32953 were generated using the pRL27 Tn5 donor plasmid as described previously (Erickson et al., 2016). The mutants were plated onto HIG agar containing 0.01% Congo-Red dye. After growth on Congo-red agar plates for 48 h, mutants with increased pigmentation were selected and the location of their transposon insertions determined using arbitrary PCR and sequencing as previously described (Erickson et al., 2016).

To complement the transposon insertion mutants, copies of *barA*, *uvrY*, *rcaA*, and *rcaB* were amplified by PCR from IP32953 genomic DNA (all primers are listed in **Supplementary Table 1**) and inserted into pJET1.2. The CsrB expression plasmid contains the *csrB* sequence in plasmid pACYC184 and was generously supplied by Petra Dersch. The *csrA* gene was also overexpressed by cloning into pJET1.2. Plasmids were created in *E. coli* strain DH5 $\alpha$  and transferred to *Yptb* by electroporation.

### Biofilm Tests

Liquid biofilms were grown in 24-well plates in 1 ml of HIG broth. The plates were incubated at  $21^\circ\text{C}$  for 48 h with shaking at 100 rpm. The unattached cells were removed and the wells were gently washed with 1 ml water, and then the plates were dried for 30 min at  $80^\circ\text{C}$ . The attached cells were stained for 20 min with 0.1% crystal violet and rinsed 3 times with water. The bound dye was solubilized by adding 1 ml DMSO and then the absorbance was measured at 590 nm.

To measure biofilm stability, biofilms were grown on  $0.2\text{ }\mu\text{m}$  polycarbonate filters (25 mm) placed on HIG agar plates. After growth in liquid media overnight, 5  $\mu\text{l}$  of saturated culture was added to the filters and incubated for 72 h. The filters containing the biofilms were transferred to 50 ml conical tubes containing 40 ml of phosphate-buffered saline (PBS). The tubes were placed

horizontally and shaken at 100 rpm for 1 h. The density of the cells that were dislodged during this time was measured by spectrophotometry at 600 nm. The tubes were then vortexed vigorously for 5 min to suspend all of the bacteria that were present on the filters, and the density of the total population was measured. The absorbance of the biofilm cells that were initially dislodged was divided by the absorbance after vortexing to calculate the percent disruption after 1 h.

## Lectin Binding Flow Cytometry

Bacteria were grown on HIG agar plates for 24 h. Single colonies were washed and resuspended in 300  $\mu$ l of 20 mM HEPES buffer containing 0.1 mM each of  $MgCl_2$ ,  $CaCl_2$ ,  $MnCl_2$ . Washed bacteria were diluted 1:10 into HEPES buffer containing 0.2 mg/ml FITC-labeled lectin (Wheat germ agglutinin or *Ulex europaeus* agglutinin, Sigma). Samples were incubated on ice in the dark for 30 min and then washed twice in HEPES buffer and finally resuspended in HEPES containing 1% formaldehyde. The fluorescence of individual bacterial cells was measured using a BD FACSCanto II flow cytometer. Negative control samples contained bacteria with no lectin added. The specificity of the lectin binding was assessed by adding 10 mM N,N'-Diacetylchitobiose or L-(-)-Fucose (Sigma) to the WGA or UEA reactions, respectively.

## Flea Infections

*X. cheopis* were orally infected with *Yptb* through shaved mouse skins using a membrane feeder apparatus and monitored for survival and proventricular blockage as previously described (Erickson et al., 2006, 2007; Zhou et al., 2012). For each experiment, ~200 fleas were allowed to feed on 5 ml of heparinized human blood containing  $5-8 \times 10^8$  colony-forming units (CFU) *Yptb* wild type IP32953 or *uvrY::Tn5* per ml. Feedings lasted 1 h, and the blood was kept at 37°C during the feeding. Control fleas were fed under the same conditions, on the same blood source but without bacteria. All of the female fleas that ingested blood meals were separated and monitored for 24 h to determine acute toxicity. All of the male fleas were visually inspected for development of proventricular blockage characterized by appearance of fresh blood in the esophagus but not the midgut during twice-weekly feedings for 4 weeks. After 28 days, 20 fleas from each group were homogenized and plated on TB agar containing 1  $\mu$ g/ml irgasan, 0.5  $\mu$ g/ml crystal violet, and 1 mg/ml bile salts to determine the proportion of fleas that remained infected throughout the experiment.

## Proteome Samples

Samples for label-free proteomic analysis of wild-type and *csrB::Tn5* mutant were prepared using a filter aided sample preparation (FASP) protocol as described previously (Wiśniewski et al., 2009). Bacteria were grown for 24 h at 21°C on solid HIG media and then washed and frozen. Frozen cell pellets were dropped into 95°C SDT lysis buffer (4% sodium dodecyl sulfate, 100 mM Tris-HCl, 0.1M dithiothreitol) and incubated at 95°C for 10 min. Cell suspensions were sonicated for 30 s (3 Watts of power) and incubated for an additional 10 min at 95°C. Cell extracts were clarified, and clarified lysate was mixed with

UA (8 M urea, 100 mM Tris-HCl pH 8.5) in a ratio of 1:5 and applied to Vivacon-500 30,000 MWCO filters (Sartorius, Göttingen, Germany). The filters were washed twice with 100  $\mu$ L buffer UA. Filters were then incubated 20 min in the dark with 100  $\mu$ L buffer UA amended with 50 mM iodoacetamide and washed twice with UA and twice with 100  $\mu$ L 50 mM ammonium bicarbonate. Samples were then digested with trypsin (1  $\mu$ g proteomic grade trypsin added to 40  $\mu$ g of total protein in 50 mM ammonium bicarbonate). The filters were incubated at 37°C for 16 h. Peptides were eluted with 50 mM ammonium bicarbonate and acidified to 1% formic acid.

## Ultra-Performance Liquid Chromatography Coupled With Mass Spectrometry (UPLC-MS/MS) and Data Analysis

Tryptic peptides from the wild-type and the mutant *csrB::Tn5* were analyzed with reversed phase chromatography (RPC) on an Ultra Performance Liquid Chromatography (UPLC) Eksigent NanoLC system coupled with an LTQ Orbitrap XL mass spectrometer (Thermo Scientific) equipped with an electrospray ionization source (ESI). Specifically, 4  $\mu$ L of digested proteins were loaded on to a C18-trap column (Waters Corporation), and were desalted with 97% mobile phase A (0.1% formic acid in  $H_2O$ , Optima) and 3% of mobile phase B (0.1% formic acid in  $CH_3CN$ , Optima) at a flow rate of 4  $\mu$ L/min for 10 min. A linear gradient at a flow rate of 325 nL/min changing from 3 to 35% of mobile phase B was then applied to load the peptides onto an online Waters Peptide Separation Technology C18 column in 90 min, and further sprayed into LTQ Orbitrap XL MS. The mass spectrometer was operated in the positive ion mode, and MS1 was analyzed at a resolution of 60,000 at m/z 400. MS/MS fragmentation analysis was performed on the top 10 most abundant MS1 precursor ions with collision-induced dissociation at a collision energy of 35 V. The online XCalibur software (Thermo Fisher Scientific) was used for data collection. MaxQuant software (Max Plank Institute of Biochemistry) was utilized for MS-based proteomics data analysis, e.g., protein identification and quantification. A *Yptb* IP32953 FASTA file downloaded from Uniprot (The UniProt, 2017) was applied for protein identification with 1% false discovery rate (FDR). A label free quantification (LFQ) approach was utilized for screening differently expressed proteins, with LFQ min. ratio count set as 2.

## Urease Assay

Urease activity was quantified as previously described (Onal Okyay and Frigi Rodrigues, 2013) with modifications. Bacteria grown in HIG were pelleted, washed, and resuspended in PBS to an absorbance (600 nm) of 1.0. Stuart's broth (20 g/L urea, 0.1 g/L yeast extract, 0.095 g/L disodium phosphate, 0.091 g/L monopotassium phosphate, 0.01 g/L phenol red) was used as the assay medium. Bacterial suspensions (20  $\mu$ l) were added to 1 ml Stuart's broth and incubated at 21°C. Every 20 min for 4 h, the absorbance at 560 nm was measured, which corresponds to an increase in pH due to the hydrolysis of urea detected by the color change from yellow to pink of the phenol red indicator.



## RESULTS

### *Yptb* Mutants That Form Pigmented Colonies on Congo-Red Agar

To identify genes that repress the formation of the Hms-dependent ECM, we used random Tn5 mutagenesis of *Yptb* strain IP32953, which normally forms white or very light-pink colonies on Congo-red agar. From a screen of ~15,000 colonies from four different mutagenesis experiments, we isolated 35 mutants that consistently produced colonies that were noticeably darker than the wild-type when grown at 21°C on Congo-red agar. We identified the transposon insertion sites by sequencing arbitrary PCR products and comparing these sequences to the *Yptb* IP32953 genome. The locations of the insertions are listed in **Table 1**. As expected, we obtained insertion mutants in several known negative regulators of Hms expression, including the *rcsA* and *rcsB* transcriptional regulators of the Rcs phosphorelay system and the phosphodiesterase *hmsP*. Insertions were also found in or near genes not previously reported to affect Hms function, including transcriptional regulator *nhaR*, the chaperone *djlA*, and the DNA-binding protein *dps*. *NhaR* is a transcriptional activator of the *E. coli* *pgaABCD* genes, which are orthologs of the *hmsHFRS* operon (Goller et al., 2006; Cerca and Jefferson, 2008). *DjlA* is a member of the DnaJ family of inner membrane co-chaperone proteins, whose overexpression leads to increased production of *E. coli* colanic acid capsule via activation of the Rcs phosphorelay system (Clarke et al., 1997; Chen et al., 2001; Shiba et al., 2006).

We obtained several independent insertions in the genes encoding the BarA sensor kinase, the UvrY response regulator, and the CsrB small RNA that resulted in increased pigmentation on Congo-red plates. The CsrA regulatory protein is an RNA-binding protein that primarily represses translation of target mRNA molecules by binding at sites containing A/UCANGGANGU/A motifs, often at or near the Shine-Dalgarno sequence (Timmermans and Van Melder, 2010). The *pgaABCD* transcript in *E. coli* contains three CsrA-binding sites in its 5' untranslated region (Wang et al., 2005), and mutants that lack CsrA produce higher than normal levels of  $\beta$ -1,6-GlcNAc polysaccharide. CsrB and CsrC are small RNAs with high affinity for CsrA that when expressed can relieve CsrA-mediated inhibition of translation. In response to accumulation of by-products of glycolysis such as acetate and formate (Chavez et al., 2010), BarA phosphorylates UvrY, which then activates transcription of genes including the CsrB regulatory RNA (Suzuki et al., 2002). Thus, mutations in *barA*, *uvrY*, or *csrB* decrease  $\beta$ -1,6-GlcNAc production in *E. coli*. Our transposon mutagenesis results suggested that the opposite is true in *Yptb*, which led us to focus our investigation on this regulatory system.

### The Role of BarA/UvrY/CsrB on Biofilm Stability and Extracellular Polysaccharide Production

In order to verify that the transposon insertions did not affect expression of other genes, we complemented *uvrY::Tn5* and *barA::Tn5* strains with plasmids containing functional *barA*

**TABLE 1** | *Yptb* strain IP32953 Tn5 insertion mutants with increased Congo-red binding.

Tn5 insertion location	YPTB ORF	Name/function
66366	YPTB0055	hldD ADP-L-glycero-D-manno-heptose-6-epimerase
67035	YPTB0055	hldD ADP-L-glycero-D-manno-heptose-6-epimerase
233986	YPTB0194	uvrD helicase
420511	YPTB0355	Putative phage inhibition, colistin resistance protein
683674	YPTB0580	Putative Na <sup>+</sup> dependent nucleoside transporter-family protein
702455	YPTB0594	Putative Ca <sup>++</sup> transporting P-type ATPase
729594	YPTB0614	nhaR transcriptional activator protein
757451		intergenic, adjacent to <i>djlA</i> colanic acid regulator
903733	YPTB0750	barA sensor kinase
1211890	YPTB1009	gmd; GDP-mannose dehydratase
1212962	YPTB1010	fcl; GDP-fucose synthetase
1213231	YPTB1010	fcl; GDP-fucose synthetase
1504191	YPTB1258	rcsB; regulator of colanic acid
2093492	YPTB1735	uvrY response regulator
2093513	YPTB1735	uvrY response regulator
2093729	YPTB1735	uvrY response regulator
2093834	YPTB1735	uvrY response regulator
2093927	YPTB1735	uvrY response regulator
2757792	YPTB2335	ihf; integration host factor alpha subunit
2797859	YPTB2373	Putative fimbrial chaperone protein
2803602	YPTB2377	Putative solute/DNA competence effector
2931611	YPTB2486	rcsA; regulator of colanic acid
2931807	YPTB2486	rcsA; regulator of colanic acid
2931914	YPTB2486	rcsA; regulator of colanic acid
3012673	YPTB2546	dps; DNA binding during starvation
3013236	YPTB2546	dps; DNA binding during starvation
3458503	YPTB2924	seqA; negative regulator of cell division
3467542	YPTB2935	Putative periplasmic transport protein
3550221		csrB regulatory RNA
3550315		csrB regulatory RNA
3550460		csrB regulatory RNA
3819095	YPTB3244	Hypothetical protein
3819394	YPTB3244	Hypothetical protein
4450576	YPTB3750	Shikimate kinase I
4581248	YPTB3836	hmsP phosphodiesterase

or *uvrY* genes. Overexpression of *barA* restored the wild-type phenotype (non-pigmented colonies) in the *barA::Tn5* background. However, overexpression of *uvrY* in this strain resulted in an intermediate pigmentation phenotype, suggesting that phosphorylation of UvrY by BarA is required for UvrY to fully activate the relevant downstream targets. Overexpression of CsrB in both the *barA::Tn5* and *uvrY::Tn5* strains restored the non-pigmented phenotype, suggesting that the regulatory effect of BarA/UvrY occurs largely through CsrB and its regulation

of CsrA. When we overexpressed the CsrA regulatory protein in wild type *Yptb* the cells were highly pigmented, but they grew more slowly and many non-pigmented colonies appeared in the population (data not shown) suggesting a toxic effect. Thus, the effect of the BarA/UvrY/CsrB system most likely affects pigmentation by regulating CsrA activity.

To define the role of this system in biofilm production, we first tested the ability of *Yptb* mutants lacking BarA or UvrY to form biofilms in 24-well polystyrene plates (**Figure 1**). The *uvrY::Tn5* and *csrB::Tn5* strains formed slightly thicker biofilms than the wild type, whereas the *barA* mutant strain was not significantly different from wild type in this assay. Similar to the Congo-red binding, overexpression of CsrB was sufficient to reduce biofilm production in the *barA::Tn5* and *uvrY::Tn5* mutants.

We used an additional assay specifically to investigate the cohesiveness of the biofilms formed by these strains. We allowed biofilms to form on polycarbonate filters and then measured the tendency of the biofilm to become dislodged and cells to become suspended in solution. The biofilms were placed in tubes with saline and agitated. The proportion of the biofilm that was dislodged and suspended in the solution was measured after a 1-h period (**Figure 2**). This assay showed that the wild type biofilms were easily disrupted, whereas the *csrB::Tn5* and *uvrY::Tn5* biofilms strongly adhered together. The *barA::Tn5* biofilms were less cohesive than the *uvrY::Tn5* or *csrB::Tn5* biofilms but more than the wild type, similar to the Congo-red binding results.

Since the *uvrY::Tn5* mutant produces strongly cohesive biofilms *in vitro*, we considered whether this strain could form

biofilms in fleas and cause proventricular blockage similar to *Y. pestis*, or to *Yptb* mutants that lack *rcsA*, *hmsT* and *hmsD* (Sun et al., 2014). We infected *Xenopsylla cheopis* fleas with wild type *Yptb* or the *uvrY::Tn5* mutant, and monitored the fleas for 28 days for signs of proventricular blockage. Although both strains were able to colonize and maintain stable infections, none of the fleas were observed to develop blockage over this period. However, more fleas infected with the mutant strain survived the first 24 h after infection than with the wild type strain (**Figure 3**), suggesting that UvrY may regulate acute toxicity of *Yptb* within the flea digestive tract.

Pigmentation of *Yersinia* colonies on Congo-red agar is correlated with Hms-ECM production, but additional proteins and carbohydrates are also able to bind the dye. To more specifically assess the surface carbohydrate differences in these strains, we employed fluorescently-labeled lectins with affinity to specific sugars. Flow cytometry was used to measure the fluorescence of individual bacteria after labeling with wheat-germ agglutinin (WGA, **Figures 4A,B**), which binds to dimers or trimers of *N*-acetylglucosamine, or to *Ulex europaeus* agglutinin (UEA-1, **Figures 4C,D**), which binds to  $\alpha$ -linked fucose residues. We measured the percentage of bacteria within each sample with detectable lectin binding (% positive, **Figures 4A,C**) as well as the mean fluorescence of the entire population (**Figures 4B,D**). We found that the binding of WGA to *Y. pestis* KIM6+ was very high, and this binding was strongly inhibited by addition of competing

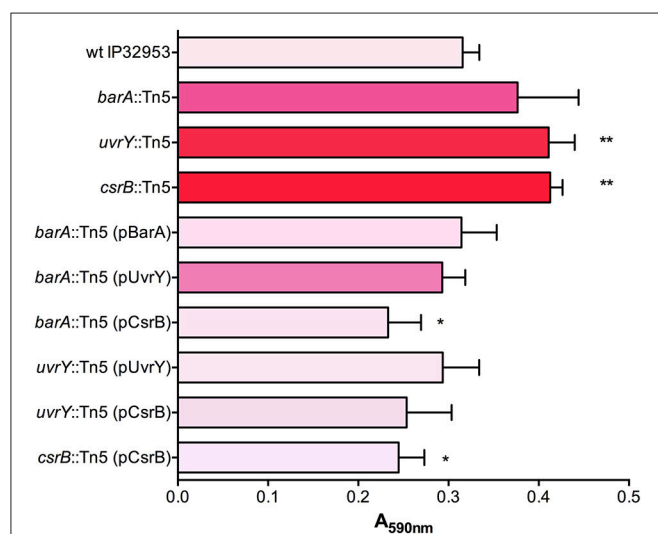


**FIGURE 1** | BarA, UvrY, and CsrB negatively regulate biofilm production in *Yptb* IP32953. Congo-red binding phenotypes were qualitatively assessed and categorized (light pink indicates little to no binding and red indicates strongly pigmented colonies). Biofilm attachment after 48 h to polystyrene plates was quantified by crystal violet staining ( $A_{590nm}$ ). Results are means and standard deviations for a representative experiment ( $n = 3$ ) that was performed three times. One-way ANOVA analysis was performed with Tukey's correction for multiple comparisons and strains significantly different from the wild type strain are indicated (\*adjusted  $P$ -value  $< 0.05$ , \*\*  $< 0.01$ ).

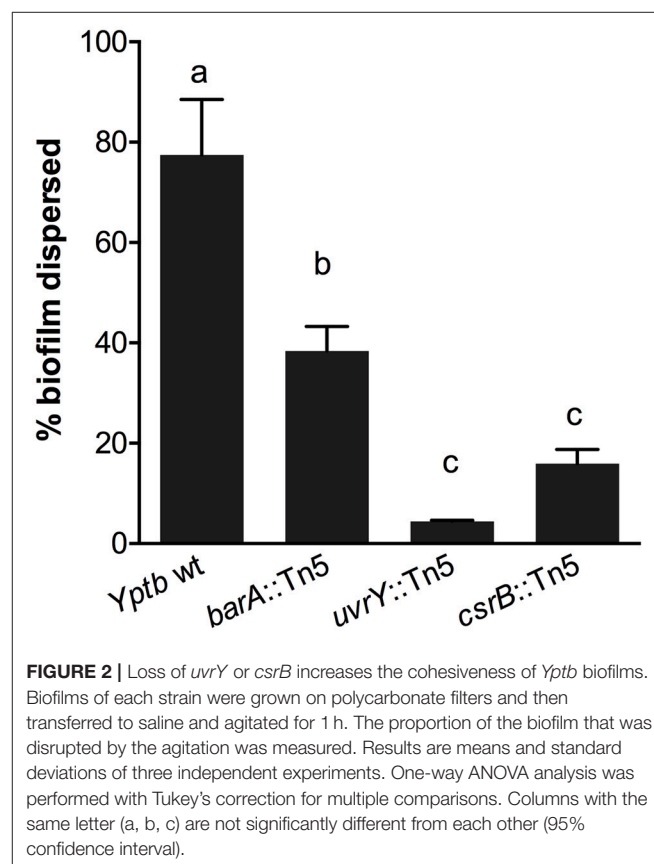


**FIGURE 2** | Loss of *uvrY* or *csrB* increases the cohesiveness of *Yptb* biofilms. Biofilms of each strain were grown on polycarbonate filters and then transferred to saline and agitated for 1 h. The proportion of the biofilm that was disrupted by the agitation was measured. Results are means and standard deviations of three independent experiments. One-way ANOVA analysis was performed with Tukey's correction for multiple comparisons. Columns with the same letter (a, b, c) are not significantly different from each other (95% confidence interval).

N-acetyl-chitobiose. UEA-1 bound only modestly to *Y. pestis*, consistent with the majority of the extracellular carbohydrate consisting of Hms-ECM. Surprisingly, the wild type *Yptb* strain did not bind detectably to WGA and only moderately to UEA-1.

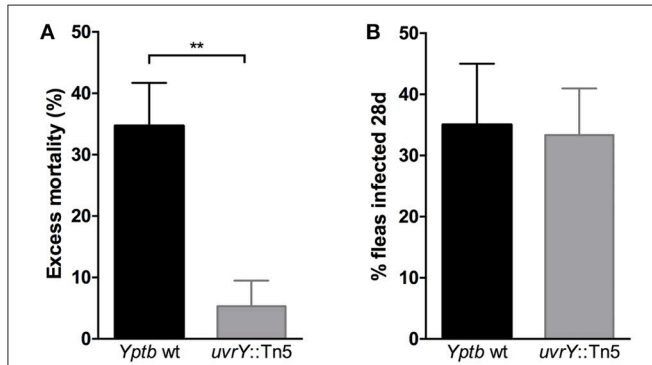


**FIGURE 3 |** Loss of *uvrY* does not affect *Yptb* colonization or blockage due to biofilm but does reduce acute oral toxicity toward *X. cheopis* fleas. Fleas were fed blood meals containing  $10^8$  CFU/ml wild type or *uvrY::Tn5* mutant strain. **(A)** The proportion of fed fleas that died within 24 h of infection was significantly less for the *uvrY::Tn5* mutant compared to the wild type strain (\*\* $p < 0.01$  by unpaired *T*-test) in three independent feeding experiments. **(B)** Proportions of fleas that remained infected with the *uvrY::Tn5* mutant or wild type strain after 28 days. No signs of proventricular blockage were observed in any *Yptb*-infected fleas (wild type or mutant) during twice-weekly feedings.

This binding was not inhibited by the addition of competing chitobiose (for WGA) or fucose (for UEA-1), suggesting the possibility of secondary or tertiary sugar preferences for lectin binding to these bacteria. The *csrB::Tn5* mutant strain bound more WGA lectin than the wild type strain, which is consistent with greater Hms-ECM production, but again the addition of competing chitobiose did not reduce lectin binding. Surprisingly, the *rcsB::Tn5* mutant strain, which is known to express high levels of cyclic diguanylate and Hms-ECM, bound more strongly to UEA-1 than to WGA. These results suggest differences in the extracellular matrix between *Y. pestis* and *Yptb*.

## Proteomic Investigation of BarA/UvrY Regulation Through CsrB

Phosphorylated UvrY upregulates CsrB expression in *E. coli* and *Yersinia*. Multiple copies of CsrA protein are bound by CsrB RNA, thus preventing it from binding its target mRNAs. In *E. coli*, CsrA binds to *pgaABCD* transcripts to repress their translation. CsrA is most often a translational repressor, but enhances translation of some target mRNAs (Potts et al., 2017). Unlike the *pgaABCD* upstream region, no obvious CsrA binding sites were identified within the coding sequences or in the 500 bp region immediately upstream of the *hmsH* start codon. We therefore considered whether the CsrA protein of *Yptb* could instead repress other negative regulators of Hms activity. We applied a proteomic approach on whole cell lysates prepared from wild type *Yptb* strain and the *csrB::Tn5* mutant using LC-MS/MS

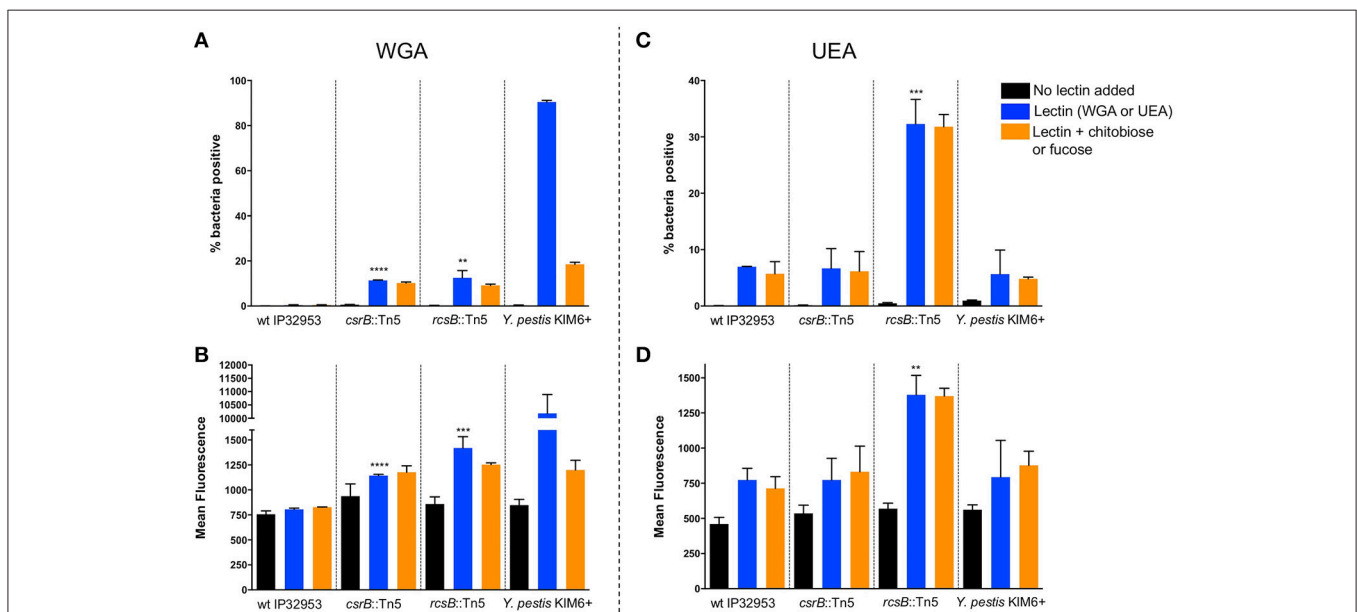


**FIGURE 4 |** Loss of *rcsB* and *csrB* alters lectin binding to bacterial surfaces. Bacteria were incubated with FITC-labeled WGA **(A,B)** or UEA **(C,D)** lectins. Flow cytometry was used to measure the proportion of bacteria with any detectable binding **(A,C)** or the mean fluorescence of the population **(B,D)**. For each strain that was tested, a control with no lectin was included to establish baseline fluorescence, as well as samples with competing sugars (chitobiose or fucose). Results are means and standard deviations for a representative experiment that was performed four times. To see if the *csrB::Tn5* or *rcsB::Tn5* mutants bound lectin differently than the wild type strain, one-way ANOVA analysis was performed with Tukey's correction for multiple comparisons using the lectin-treated samples (blue bars). The *csrB::Tn5* and *rcsB::Tn5* mutants bound significantly more WGA than the wild type strain, but only the *rcsB::Tn5* mutant bound more UEA than wild type. *Y. pestis* binding was tested as a control, and it bound to WGA far more efficiently than *Yptb* (\*\* $p < 0.01$ , \*\*\* $p < 0.001$ , \*\*\*\* $p < 0.0001$ ).

analysis and mapping the peptide fragments to the *Yptb* IP32953 database. We selected proteins that were at least 1.5-fold changed in abundance between the two strains (**Supplementary Table 2**). As expected, the vast majority of the differentially expressed proteins were less abundant in the *csrB* mutant, consistent with the role of CsrA protein as mainly a repressor of translation.

The global changes in transcript abundance in a *Yptb* strain YPIII *csrA* mutant were recently reported by Bückner et al. (2014). Many of the genes that are upregulated in their study showed lower protein levels in this analysis of strain IP32953 *csrB::Tn5* mutant. The RovA (SlyA) protein is known to be repressed by CsrA (Heroven et al., 2008), and our data indicated a 28-fold decrease in RovA abundance. RovA is controlled by CsrA through the RovM protein, which is activated by CsrA (Heroven et al., 2008). RovM peptides were not detected among the wild type samples, but were in the *csrB::Tn5* mutant (**Supplementary Table 2**). Several additional regulatory proteins that could regulate biofilm production were repressed in the *csrB::Tn5* mutant strain. Nucleoid-associated proteins, including Integration Host Factor alpha (IHf $\alpha$ , 11.8-fold reduction) and histone-like nucleoid structuring protein (H-NS, 24-fold reduction) function to silence and activate gene expression on a global scale (Dillon and Dorman, 2010). IHf $\alpha$  was also identified in our initial transposon screen for mutants that exhibit enhanced Congo-red binding (**Table 1**). H-NS represses expression of horizontally acquired genes (Lucchini et al., 2006), and the *hmsHFRS* operon is contained within the mobile *Yersinia* high-pathogenicity island (Lillard et al., 1997). H-NS also represses expression of *pgaABCD* and biofilm production in *Actinobacillus pleuropneumoniae* (Bossé et al., 2010). H-NS is believed to be essential for *Yersinia* survival (Ellison and Miller, 2006), so we were unlikely to identify it in our transposon screen.

We identified transposon insertions in both *rcaA* and *rcaB* in our screen for Congo-red binding mutants (**Table 1**). The *Yptb* RcsB transcriptional regulatory protein, together with RcsA, represses transcription of the diguanylate cyclases *hmsT* and *hmsD*, thereby reducing biofilm production. *Y. pestis* *rcaA* has a frameshift mutation, thus eliminating this repression and enhancing biofilms (Sun et al., 2008, 2014; Sun Y. C. et al., 2012; Guo et al., 2015). To ensure that the transposon insertions in *rcaA* and *rcaB* were not affecting other genes, we complemented both mutants via plasmids containing functional copies of these genes. The *rcaB::Tn5* mutant was complemented with a plasmid containing *rcaB*. The *rcaA::Tn5* mutant was able to be complemented via *rcaA* from *Yptb* but not from *Y. pestis*, consistent with the frameshift mutation in *Y. pestis* *rcaA*. Our proteomic data revealed that *csrB::Tn5* produced 8-fold less RcsB protein than the wild type strain (**Supplementary Table 2**). CsrA has not been previously shown to repress expression of RcsB directly or indirectly. To test the relationship between *rcaB* and CsrB further, we overexpressed CsrB in the *Yptb* *rcaA::Tn5* or *rcaB::Tn5* mutant strains (**Figure 5**). Unlike in the *uvrY::Tn5* or *barA::Tn5* mutants, CsrB expression did not reduce Congo-red binding in the *rcaA* or *rcaB* mutants. This suggests the possibility that CsrB competes with *rcaB* transcripts for CsrA binding. The predicted secondary structure of the *rcaB* transcript

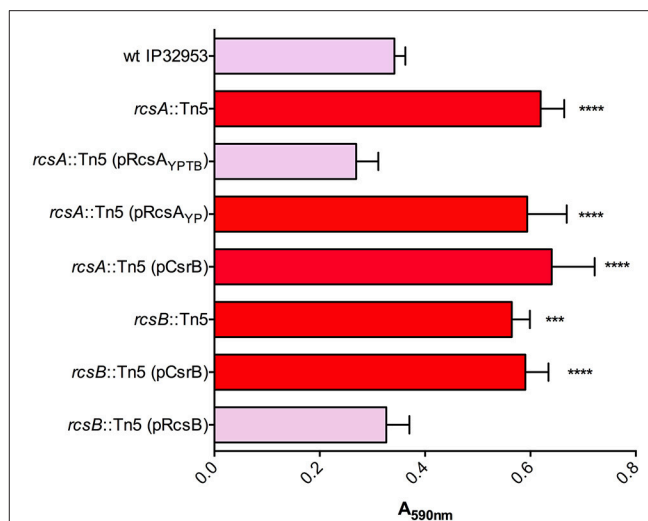


**FIGURE 5** | Biofilm and Congo-red binding by *rcaA* and *rcaB* mutants is not affected by overexpression of CsrB. Congo-red binding phenotypes and biofilm attachment in polystyrene plates after 48 h were measured in wild type *Yptb* and in *rcaA::Tn5* or *rcaB::Tn5* mutants. The effects of plasmids containing *rcaA* from *Yptb* (pRcsA<sub>YPTB</sub>) or *Y. pestis* (pRcsA<sub>YP</sub>) were determined in the *rcaA::Tn5* mutant strain. The *rcaB::Tn5* mutant was complemented with a plasmid containing *rcaB* from *Yptb*. Overexpression of CsrB (pCsrB), which reduced Congo-red binding and biofilm production in *barA::Tn5* and *uvrY::Tn5* mutants (**Figure 1**), was also tested in the *rcaA* and *rcaB* mutants. Results are means and standard deviations for a representative experiment ( $n = 3$ ) that was performed four times. One-way ANOVA analysis was performed with Tukey's correction for multiple comparisons. Values that were significantly different from the wild type are indicated (\*\*\*adjusted  $P$ -value < 0.001, \*\*\*\* adjusted  $P$ -value < 0.0001).

contains a stem-loop with an exposed GGA motif overlapping the Shine-Delgarno sequence (**Supplementary Figure 1**), which is characteristic of CsrA targets (Romeo and Babitzke, 2018). Alternatively, the absence of a functional Rcs phosphorelay could overpower the negative regulatory effects of CsrB.

Urease subunit proteins were also substantially reduced in the *csrB::Tn5* mutant (**Supplementary Table 2**). The urease structural proteins (UreA 59-fold, UreB 21-fold, UreC 21-fold), and the accessory proteins (UreE 1423-fold, UreF undetected, UreG 45-fold, UreD 71-fold), make up the multimeric urease enzyme. *Y. pestis* lacks a functional UreD subunit, which is sufficient to eliminate urease activity (Sebbane et al., 2001). Unlike *Y. pestis*, *Yptb* strains are acutely toxic to *X. cheopis* fleas (Erickson et al., 2007), and restoration of urease also restores toxicity to *Y. pestis* (Chouikha and Hinnebusch, 2014). Since the *uvrY::Tn5* mutant was also less toxic to fleas, we tested whether this strain produces less urease enzyme. The wild type strain produced much more urease than the *uvrY::Tn5* mutant (**Figure 6**). The *csrB::Tn5* mutant also produced much less urease, and no urease activity was detected using *Y. pestis* KIM6+. During the preparation of this manuscript, it was also reported by Dai et al. that CsrA represses urease production in *Yptb* strain YPIII, which is consistent with our results (Dai et al., 2018).



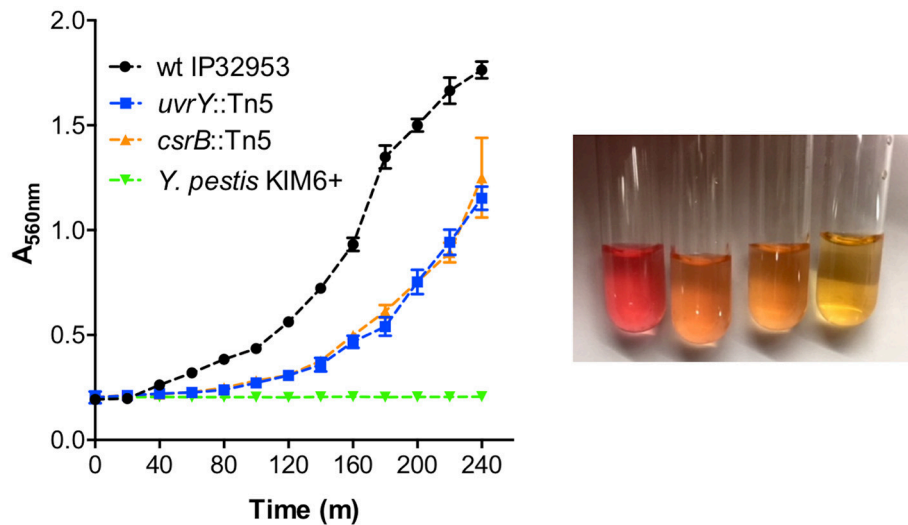


**FIGURE 6 |** UvrY and CsrB positively regulate urease. Equal numbers of bacteria were suspended in Stuart's broth and pH change due to hydrolysis of urea was detected by color change from yellow to pink (picture from left to right: wild type *Yptb*, *uvrY*::Tn5, *csrB*::Tn5, and *Y. pestis* after 4 h). Urease was quantified by measuring the absorbance at 560 nm (left panel) every 20 min. Results are means and standard deviations of three independent experiments. Multiple *t*-tests of the data were performed with a false-discovery rate (Q) value set to 1.000%, without assuming a consistent SD. The *uvrY*::Tn5 and *csrB*::Tn5 mutant strains were significantly different ( $p < 0.05$ ) from the wild type strain at every time point after 60 min.

## DISCUSSION

Switching between planktonic and sessile modes of growth is a tightly controlled process involving multiple levels of transcriptional and post-transcriptional regulation. Successful navigation of this transition is critically important to the success of pathogenic yersiniae (Chen et al., 2016). In this study we demonstrated that the BarA/UvrY two component system as well as the small RNA CsrB repress biofilm production in *Yptb*. Disruption of CsrB increased biofilm production while at the same time reducing urease-mediated toxicity toward fleas. Many bacterial pathogens, including *Yersinia* (Bobrov et al., 2011; Zhao et al., 2013; Redelman et al., 2014), exhibit an inverse relationship between biofilm production and acute virulence. The regulatory networks that govern transition between highly toxic phenotypes and the biofilm mode of growth are of interest as possible therapeutic targets. CsrB is known to exert its effects by occupying CsrA proteins, thereby altering expression of CsrA-controlled regulatory proteins and cell-envelope structures that have pleiotropic effects.

Previous work has shown that in *Yptb* strain YPIII, UvrY (and CsrB) expression is normally repressed by the cyclic AMP-Crp complex except during times of nutrient deprivation (Heroven et al., 2012). Starvation conditions would therefore be predicted to promote motility and reduce biofilm formation by reducing the concentration of free CsrA proteins. The downstream targets of CsrA that mediate the biofilm-specific effects are not completely known and may be different between individual strains of *Yptb* or in *Y. pestis*. In *Yptb* strain YPIII, CsrA indirectly activates expression of the RovM transcriptional regulatory protein (Heroven et al., 2008). RovM binds the promoter regions of the *flhDC* flagellar regulatory genes, the

*hmsHFRS* operon, and the *rovA* virulence regulator (Heroven et al., 2008; Zhao et al., 2017). Binding of RovM represses *flhDC* and enhances *hmsHFRS* and *rovA* transcription. Others have also shown that CsrA enhances biofilms in *Y. pestis* (Willias et al., 2015). However, loss of CsrA did not change *Y. pestis* *hmsHFRS*, *hmsT*, or *hmsP* transcription as occurs in *Yptb*. It will be interesting to determine if RovM activates *hmsHFRS* in *Y. pestis*, or whether RovM is controlled by CsrA in the same fashion as in *Yptb*. We did not identify any transposon insertions in the *rovM* gene (YPTB2588) in our screen for Congo-red binding mutants. This could be because the expression of *rovM* is very low in nutrient-rich conditions such as were used in our study (Heroven and Dersch, 2006). Indeed, RovM protein levels in the wild type strain were below the limit of detection in our proteomic analysis. However, RovM peptides were detected in the *csrB* mutant samples, consistent with CsrA being an activator of RovM expression in *Yptb* strain IP32953. We also did not obtain any transposon insertion mutants in the CsrC regulatory RNA gene in our screen. In contrast to *E. coli*, expression of CsrC is not activated by UvrY in *Yptb* strain YPIII (Heroven et al., 2008). Rather, when CsrB expression is triggered by UvrY, CsrC is repressed by a mechanism that is yet to be determined.

In addition to RovM, our results suggest that other regulatory proteins that control biofilm attachment and stability are under the influence of CsrA. These include the RcsA and RcsB transcriptional regulatory proteins. The Rcs phosphorelay system contains a sensor kinase RcsC that autophosphorylates upon detection of signals that include cellular stress. The phosphate is then transferred through RcsD to RcsB, which then dimerizes and binds to specific promoter sequences. RcsB may also form heterodimers with RcsA, and RcsAB binding represses

transcription of diguanylate cyclases *hmsD* and *hmsT*, as well as the *hmsHFRS* operon (Sun Y. C. et al., 2012; Fang et al., 2015). The *rcaA* gene has been disrupted in *Y. pestis*, which was a key event in the evolution of *Y. pestis* transmission by fleas because it greatly enhanced cyclic di-GMP and biofilm production (Sun et al., 2008, 2014). We found that when *rcaA* or *rcaB* were non-functional, overexpression of CsrB did not reduce Congo-red pigmentation or prevent biofilm formation. In our analysis of the *csrB::Tn5* mutant proteins, RcsA and RcsB proteins were both decreased compared to the wild type strain. These results are suggestive of a possible direct interaction between CsrA and *rcaA* or *rcaB* transcripts, particularly in the case of *rcaB*.

Disruption of *uvrY* or *csrB* had a very strong effect on the cohesiveness of *Yptb* biofilms. We considered that the most likely explanation for this would be increased abundance of extracellular polysaccharide contained in the biofilm matrix, specifically the Hms-ECM in these mutants. *Yersinia* biofilms are often described as bacteria encased in a homopolymer of N-acetyl-D-glucosamine (Hms-ECM) (Zhou and Yang, 2011; Sun F. et al., 2012). Hms-ECM is almost certainly present in *Y. pestis* and *Yptb* biofilms, based on antigenic cross-reactivity of *Y. pestis* biofilms with antibodies directed against purified poly-N-acetylglucosamine (Erickson et al., 2006) and from the extensive genetic data showing the impact of *hmsHFRS* on biofilms in both species. However, our results also suggest that loss of CsrB could control biofilm production by affecting expression of other cell surface molecules. The binding of WGA lectin to *Yptb* mutants that were strongly pigmented on Congo-red agar was far less than what we observed for *Y. pestis*, and binding was barely detectable for the wild type IP32953 strain. Binding of UEA-1 lectin, which is specific for fucose, was increased in the *rcaB* mutant to a greater degree than WGA lectin, which is specific for N-acetylglucosamine. However, these results are complicated by the fact that addition of competing sugars did not reduce lectin binding, except for WGA and *Y. pestis*. The possibility of other proteins, carbohydrates, or nucleic acids within *Yersinia* biofilms deserves further investigation, particularly in *Yptb*. It is likely that Hms-ECM is increased on the surface of *uvrY*, *csrB* and *rcaB*

*Yptb* mutants, but other macromolecules within the biofilm matrix may interfere with efficient WGA lectin binding. The presence of additional carbohydrates within *Yersinia* biofilms is suggested by previous lectin binding experiments in other *Yptb* strains (Tan and Darby, 2004) as well as genetic studies showing that lipopolysaccharide genes are required for efficient biofilm production in *Y. pestis* (Liu et al., 2016). *Yptb* biofilm extracellular matrix also contains extracellular DNA (Atkinson et al., 2011). The protein component of *Yersinia* biofilms has not been well-studied, but even when lacking the Hms polysaccharide, *Y. pestis* can form biofilm-like aggregates that resist killing by neutrophils (Jarrett et al., 2004). The biochemical nature of the components within these aggregates is unknown, but may suggest that specific *Yersinia* proteins that perform stabilizing and attachment (Fong and Yildiz, 2015) or immune evasion functions within the ECM await discovery.

## AUTHOR CONTRIBUTIONS

JS, JB, and DE conceived and designed the experimental procedures, JS, RS, MS, JC, HK, and DE performed the experiments and carried out data analysis, JS and DE wrote the manuscript.

## FUNDING

This work was funded by a Mentoring Environment Grant from Brigham Young University.

## ACKNOWLEDGMENTS

We thank Petra Dersch for the CsrB expression plasmid.

## SUPPLEMENTARY MATERIAL

The Supplementary Material for this article can be found online at: <https://www.frontiersin.org/articles/10.3389/fcimb.2018.00323/full#supplementary-material>

## REFERENCES

- Atkinson, S., Goldstone, R. J., Joshua, G. W., Chang, C. Y., Patrick, H. L., Camara, M., et al. (2011). Biofilm development on *Caenorhabditis elegans* by *Yersinia* is facilitated by quorum sensing-dependent repression of type III secretion. *PLoS Pathog.* 7:e1001250. doi: 10.1371/journal.ppat.1001250
- Bobrov, A. G., Kirillina, O., Forman, S., Mack, D., and Perry, R. D. (2008). Insights into *Yersinia pestis* biofilm development: topology and co-interaction of Hms inner membrane proteins involved in exopolysaccharide production. *Environ. Microbiol.* 10, 1419–32. doi: 10.1111/j.1462-2920.2007.01554.x
- Bobrov, A. G., Kirillina, O., Ryjenkov, D. A., Waters, C. M., Price, P. A., Fetherston, J. D., et al. (2011). Systematic analysis of cyclic di-GMP signalling enzymes and their role in biofilm formation and virulence in *Yersinia pestis*. *Mol. Microbiol.* 79, 533–551. doi: 10.1111/j.1365-2958.2010.07470.x
- Bossé, J. T., Sinha, S., Li, M. S., O'Dwyer, C. A., Nash, J. H., Rycroft, A. N., et al. (2010). Regulation of *pga* operon expression and biofilm formation in *Actinobacillus pleuropneumoniae* by sigmaE and H-NS. *J. Bacteriol.* 192, 2414–2423. doi: 10.1128/JB.01513-09
- Bücker, R., Heroven, A. K., Becker, J., Dersch, P., and Wittmann, C. (2014). The pyruvate-tricarboxylic acid cycle node: a focal point of virulence control in the enteric pathogen *Yersinia pseudotuberculosis*. *J. Biol. Chem.* 289, 30114–30132. doi: 10.1074/jbc.M114.581348
- Cerca, N., and Jefferson, K. K. (2008). Effect of growth conditions on poly-N-acetylglucosamine expression and biofilm formation in *Escherichia coli*. *FEMS Microbiol. Lett.* 283, 36–41. doi: 10.1111/j.1574-6968.2008.01142.x
- Chavez, R. G., Alvarez, A. F., Romeo, T., and Georgellis, D. (2010). The physiological stimulus for the BarA sensor kinase. *J. Bacteriol.* 192, 2009–2012. doi: 10.1128/JB.01685-09
- Chen, M. H., Takeda, S., Yamada, H., Ishii, Y., Yamashino, T., and Mizuno, T. (2001). Characterization of the RcsC-→YojN-→RcsB phosphorelay signaling pathway involved in capsular synthesis in *Escherichia coli*. *Biosci. Biotechnol. Biochem.* 65, 2364–2367. doi: 10.1271/bbb.65.2364
- Chen, S., Thompson, K. M., and Francis, M. S. (2016). Environmental regulation of *Yersinia* Pathophysiology. *Front. Cell Infect. Microbiol.* 6:25. doi: 10.3389/fcimb.2016.00025

- Chouikha, I., and Hinnebusch, B. J. (2014). Silencing urease: a key evolutionary step that facilitated the adaptation of *Yersinia pestis* to the flea-borne transmission route. *Proc. Natl. Acad. Sci. U. S. A.* 111, 18709–18714. doi: 10.1073/pnas.1413209111
- Clarke, D. J., Holland, I. B., and Jacq, A. (1997). Point mutations in the transmembrane domain of DjlA, a membrane-linked DnaJ-like protein, abolish its function in promoting colanic acid production via the Rcs signal transduction pathway. *Mol. Microbiol.* 25, 933–944. doi: 10.1111/j.1365-2958.1997.mmi528.x
- Dai, Q., Xu, L., Xiao, L., Zhu, K., Song, Y., Li, C., et al. (2018). RovM and CsrA negatively regulate urease expression in *Yersinia pseudotuberculosis*. *Front. Microbiol.* 9:348. doi: 10.3389/fmicb.2018.00348
- Darby, C., Hsu, J. W., Ghorri, N., and Falkow, S. (2002). *Caenorhabditis elegans*: plague bacteria biofilm blocks food intake. *Nature* 417, 243–244. doi: 10.1038/417243a
- Dillon, S. C., and Dorman, C. J. (2010). Bacterial nucleoid-associated proteins, nucleoid structure and gene expression. *Nat. Rev. Microbiol.* 8, 185–195. doi: 10.1038/nrmicro2261
- Ellison, D. W., and Miller, V. L. (2006). H-NS represses *inv* transcription in *Yersinia enterocolitica* through competition with RovA and interaction with YmoA. *J. Bacteriol.* 188, 5101–5112. doi: 10.1128/JB.00862-05
- Erickson, D. L., Jarrett, C. O., Callison, J. A., Fischer, E. R., and Hinnebusch, B. J. (2008). Loss of a biofilm-inhibiting glycosyl hydrolase during the emergence of *Yersinia pestis*. *J. Bacteriol.* 190, 8163–8170. doi: 10.1128/JB.01181-08
- Erickson, D. L., Jarrett, C. O., Wren, B. W., and Hinnebusch, B. J. (2006). Serotype differences and lack of biofilm formation characterize *Yersinia pseudotuberculosis* infection of the *Xenopsylla cheopis* flea vector of *Yersinia pestis*. *J. Bacteriol.* 188, 1113–1119. doi: 10.1128/JB.188.3.1113-1119.2006
- Erickson, D. L., Lew, C. S., Kartchner, B., Porter, N. T., McDaniel, S. W., Jones, N. M., et al. (2016). Lipopolysaccharide biosynthesis genes of *Yersinia pseudotuberculosis* promote resistance to antimicrobial chemokines. *PLoS ONE* 11:e0157092. doi: 10.1371/journal.pone.0157092
- Erickson, D. L., Waterfield, N. R., Vadyvaloo, V., Long, D., Fischer, E. R., Ffrench-Constant, R., et al. (2007). Acute oral toxicity of *Yersinia pseudotuberculosis* to fleas: implications for the evolution of vector-borne transmission of plague. *Cell Microbiol.* 9, 2658–2666. doi: 10.1111/j.1462-5822.2007.00986.x
- Fang, N., Yang, H., Fang, H., Liu, L., Zhang, Y., Wang, L., et al. (2015). RcsAB is a major repressor of *Yersinia* biofilm development through directly acting on hmsCDE, hmsT, and hmsHFRS. *Sci. Rep.* 5:9566. doi: 10.1038/srep09566
- Fong, J. N., and Yildiz, F. H. (2015). Biofilm matrix proteins. *Microbiol. Spectr.* 3:MB-0004–2014. doi: 10.1128/microbiolspec.MB-0004-2014
- Forman, S., Bobrov, A. G., Kirillina, O., Craig, S. K., Abney, J., Fetherston, J. D., et al. (2006). Identification of critical amino acid residues in the plague biofilm Hms proteins. *Microbiology* 152 (Pt. 11), 3399–3410. doi: 10.1099/mic.0.29224-0
- Goller, C., Wang, X., Itoh, Y., and Romeo, T. (2006). The cation-responsive protein NhaR of *Escherichia coli* activates pgaABCD transcription, required for production of the biofilm adhesin poly-beta-1,6-N-acetyl-D-glucosamine. *J. Bacteriol.* 188, 8022–8032. doi: 10.1128/JB.01106-06
- Guo, X. P., Ren, G. X., Zhu, H., Mao, X. J., and Sun, Y. C. (2015). Differential regulation of the hmsCDE operon in *Yersinia pestis* and *Yersinia pseudotuberculosis* by the Rcs phosphorelay system. *Sci. Rep.* 5:8412. doi: 10.1038/srep08412
- Heroven, A. K., Bohme, K., Rohde, M., and Dersch, P. (2008). A Csr-type regulatory system, including small non-coding RNAs, regulates the global virulence regulator RovA of *Yersinia pseudotuberculosis* through RovM. *Mol. Microbiol.* 68, 1179–1195. doi: 10.1111/j.1365-2958.2008.06218.x
- Heroven, A. K., and Dersch, P. (2006). RovM, a novel LysR-type regulator of the virulence activator gene *rovA*, controls cell invasion, virulence and motility of *Yersinia pseudotuberculosis*. *Mol. Microbiol.* 62, 1469–1483. doi: 10.1111/j.1365-2958.2006.05458.x
- Heroven, A. K., Sest, M., Pisano, F., Scheb-Wetzel, M., Steinmann, R., Bohme, K., et al. (2012). Crp induces switching of the CsrB and CsrC RNAs in *Yersinia pseudotuberculosis* and links nutritional status to virulence. *Front. Cell Infect. Microbiol.* 2:158. doi: 10.3389/fcimb.2012.00158
- Hinnebusch, B. J., and Erickson, D. L. (2008). *Yersinia pestis* biofilm in the flea vector and its role in the transmission of plague. *Curr. Top Microbiol. Immunol.* 322, 229–248. doi: 10.1007/978-3-540-75418-3\_11
- Hinnebusch, B. J., Perry, R. D., and Schwan, T. G. (1996). Role of the *Yersinia pestis* hemin storage (hms) locus in the transmission of plague by fleas. *Science* 273, 367–370.
- Jarrett, C. O., Deak, E., Isherwood, K. E., Oyston, P. C., Fischer, E. R., Whitney, A. R., et al. (2004). Transmission of *Yersinia pestis* from an infectious biofilm in the flea vector. *J. Infect. Dis.* 190, 783–792. doi: 10.1086/422695
- Joshua, G. W., Karlyshev, A. V., Smith, M. P., Isherwood, K. E., Titball, R. W., and Wren, B. W. (2003). A *Caenorhabditis elegans* model of *Yersinia* infection: biofilm formation on a biotic surface. *Microbiology* 149(Pt. 11), 3221–3229. doi: 10.1099/mic.0.26475-0
- Kirillina, O., Fetherston, J. D., Bobrov, A. G., Abney, J., and Perry, R. D. (2004). HmsP, a putative phosphodiesterase, and HmsT, a putative diguanylate cyclase, control Hms-dependent biofilm formation in *Yersinia pestis*. *Mol. Microbiol.* 54, 75–88. doi: 10.1111/j.1365-2958.2004.04253.x
- Lillard, J. W. Jr., Fetherston, J. D., Pedersen, L., Pendrak, M. L., and Perry, R. D. (1997). Sequence and genetic analysis of the hemin storage (hms) system of *Yersinia pestis*. *Gene* 193, 13–21. doi: 10.1016/S0378-1119(97)00071-1
- Liu, L., Fang, H., Yang, H., Zhang, Y., Han, Y., Zhou, D., et al. (2016). CRP is an activator of *Yersinia pestis* biofilm formation that operates via a mechanism involving *gmhA* and *waaAE-coaD*. *Front. Microbiol.* 7:295. doi: 10.3389/fmicb.2016.00295
- Lucchini, S., Rowley, G., Goldberg, M. D., Hurd, D., Harrison, M., and Hinton, J. C. (2006). H-NS mediates the silencing of laterally acquired genes in bacteria. *PLoS Pathog.* 2:e81. doi: 10.1371/journal.ppat.0020081
- Onal Okay, T., and Frigi Rodrigues, D. (2013). High throughput colorimetric assay for rapid urease activity quantification. *J. Microbiol. Methods* 95, 324–326. doi: 10.1016/j.mimet.2013.09.018
- Perry, R. D., Bobrov, A. G., Kirillina, O., Jones, H. A., Pedersen, L., Abney, J., et al. (2004). Temperature regulation of the hemin storage (Hms+) phenotype of *Yersinia pestis* is posttranscriptional. *J. Bacteriol.* 186, 1638–1647. doi: 10.1128/JB.186.6.1638-1647.2004
- Perry, R. D., Pendrak, M. L., and Schuetze, P. (1990). Identification and cloning of a hemin storage locus involved in the pigmentation phenotype of *Yersinia pestis*. *J. Bacteriol.* 172, 5929–5937. doi: 10.1128/jb.172.10.5929-5937.1990
- Potts, A. H., Vakulskas, C. A., Pannuri, A., Yakhnin, H., Babitzke, P., and Romeo, T. (2017). Global role of the bacterial post-transcriptional regulator CsrA revealed by integrated transcriptomics. *Nat. Commun.* 8, 1596. doi: 10.1038/s41467-017-01613-1
- Redelman, C. V., Chakravarty, S., and Anderson, G. G. (2014). Antibiotic treatment of *Pseudomonas aeruginosa* biofilms stimulates expression of the magnesium transporter gene *mgtE*. *Microbiology* 160(Pt. 1), 165–178. doi: 10.1099/mic.0.070144-0
- Romeo, T., and Babitzke, P. (2018). Global regulation by CsrA and its RNA antagonists. *Microbiol. Spectr.* 6:RWR-0009–2017. doi: 10.1128/microbiolspec.RWR-0009-2017
- Sebbane, F., Devalckenaere, A., Foulon, J., Carniel, E., and Simonet, M. (2001). Silencing and reactivation of urease in *Yersinia pestis* is determined by one G residue at a specific position in the ureD gene. *Infect. Immun.* 69, 170–176. doi: 10.1128/IAI.69.1.170-176.2001
- Shiba, Y., Matsumoto, K., and Hara, H. (2006). DjlA negatively regulates the Rcs signal transduction system in *Escherichia coli*. *Genes Genet. Syst.* 81, 51–56. doi: 10.1266/ggs.81.51
- Sun, F., Gao, H., Zhang, Y., Wang, L., Fang, N., Tan, Y., et al. (2012). Fur is a repressor of biofilm formation in *Yersinia pestis*. *PLoS ONE* 7:e52392. doi: 10.1371/journal.pone.0052392
- Sun, Y. C., Guo, X. P., Hinnebusch, B. J., and Darby, C. (2012). The *Yersinia pestis* Rcs phosphorelay inhibits biofilm formation by repressing transcription of the diguanylate cyclase gene *hmsT*. *J. Bacteriol.* 194, 2020–2026. doi: 10.1128/JB.06243-11
- Sun, Y. C., Hinnebusch, B. J., and Darby, C. (2008). Experimental evidence for negative selection in the evolution of a *Yersinia pestis* pseudogene. *Proc. Natl. Acad. Sci. U. S. A.* 105, 8097–8101. doi: 10.1073/pnas.0803525105
- Sun, Y. C., Jarrett, C. O., Bosio, C. F., and Hinnebusch, B. J. (2014). Retracing the evolutionary path that led to flea-borne transmission of *Yersinia pestis*. *Cell Host Microbe* 15, 578–586. doi: 10.1016/j.chom.2014.04.003
- Sun, Y. C., Koumoutsis, A., Jarrett, C., Lawrence, K., Gherardini, F. C., Darby, C., et al. (2011). Differential control of *Yersinia pestis* biofilm formation *in vitro* and

- in the flea vector by two c-di-GMP diguanylate cyclases. *PLoS ONE* 6:e19267. doi: 10.1371/journal.pone.0019267
- Suzuki, K., Wang, X., Weilbacher, T., Pernestig, A. K., Melefors, O., Georgellis, D., et al. (2002). Regulatory circuitry of the CsrA/CsrB and BarA/UvrY systems of *Escherichia coli*. *J. Bacteriol.* 184, 5130–5140. doi: 10.1128/JB.184.18.5130-5140.2002
- Tan, L., and Darby, C. (2004). A movable surface: formation of *Yersinia* sp. biofilms on motile *Caenorhabditis elegans*. *J. Bacteriol.* 186, 5087–5092. doi: 10.1128/JB.186.15.5087-5092.2004
- The UniProt, C. (2017). UniProt: the universal protein knowledgebase. *Nucleic Acids Res.* 45, D158–D169. doi: 10.1093/nar/gkh131
- Timmermans, J., and Van Melder, L. (2010). Post-transcriptional global regulation by CsrA in bacteria. *Cell Mol. Life Sci.* 67, 2897–2908. doi: 10.1007/s00018-010-0381-z
- Wang, X., Dubey, A. K., Suzuki, K., Baker, C. S., Babitzke, P., and Romeo, T. (2005). CsrA post-transcriptionally represses pgaABCD, responsible for synthesis of a biofilm polysaccharide adhesin of *Escherichia coli*. *Mol. Microbiol.* 56, 1648–1663. doi: 10.1111/j.1365-2958.2005.04648.x
- Willias, S. P., Chauhan, S., Lo, C. C., Chain, P. S., and Motin, V. L. (2015). CRP-mediated carbon catabolite regulation of *Yersinia pestis* biofilm formation is enhanced by the carbon storage regulator protein, CsrA. *PLoS ONE* 10:e0135481. doi: 10.1371/journal.pone.0135481
- Wiśniewski, J. R., Zougman, A., Nagaraj, N., and Mann, M. (2009). Universal sample preparation method for proteome analysis. *Nat. Methods* 6, 359–362. doi: 10.1038/nmeth.1322
- Wortham, B. W., Oliveira, M. A., Fetherston, J. D., and Perry, R. D. (2010). Polyamines are required for the expression of key Hms proteins important for *Yersinia pestis* biofilm formation. *Environ. Microbiol.* 12, 2034–2047. doi: 10.1111/j.1462-2920.2010.02219.x
- Zhao, R., Song, Y., Dai, Q., Kang, Y., Pan, J., Zhu, L., et al. (2017). A starvation-induced regulator, RovM, acts as a switch for planktonic/biofilm state transition in *Yersinia pseudotuberculosis*. *Sci. Rep.* 7:639. doi: 10.1038/s41598-017-00534-9
- Zhao, X., Koestler, B. J., Waters, C. M., and Hammer, B. K. (2013). Post-transcriptional activation of a diguanylate cyclase by quorum sensing small RNAs promotes biofilm formation in *Vibrio cholerae*. *Mol. Microbiol.* 89, 989–1002. doi: 10.1111/mmi.12325
- Zhou, D., and Yang, R. (2011). Formation and regulation of *Yersinia* biofilms. *Protein Cell* 2, 173–179. doi: 10.1007/s13238-011-1024-3
- Zhou, W., Russell, C. W., Johnson, K. L., Mortensen, R. D., and Erickson, D. L. (2012). Gene expression analysis of *Xenopsylla cheopis* (Siphonaptera: Pulicidae) suggests a role for reactive oxygen species in response to *Yersinia pestis* infection. *J. Med. Entomol.* 49, 364–370. doi: 10.1603/ME11172

**Conflict of Interest Statement:** The authors declare that the research was conducted in the absence of any commercial or financial relationships that could be construed as a potential conflict of interest.

Copyright © 2018 Schachterle, Stewart, Schachterle, Calder, Kang, Prince and Erickson. This is an open-access article distributed under the terms of the Creative Commons Attribution License (CC BY). The use, distribution or reproduction in other forums is permitted, provided the original author(s) and the copyright owner(s) are credited and that the original publication in this journal is cited, in accordance with accepted academic practice. No use, distribution or reproduction is permitted which does not comply with these terms.





# BfvR, an AraC-Family Regulator, Controls Biofilm Formation and pH6 Antigen Production in Opposite Ways in *Yersinia pestis* Biovar Microtus

Haihong Fang<sup>1,2†</sup>, Lei Liu<sup>3†</sup>, Yiquan Zhang<sup>4</sup>, Huiying Yang<sup>1</sup>, Yanfeng Yan<sup>1</sup>, Xiaojuan Ding<sup>5</sup>, Yanping Han<sup>1</sup>, Dongsheng Zhou<sup>1\*</sup> and Ruifu Yang<sup>1\*</sup>

<sup>1</sup> State Key Laboratory of Pathogen and Biosecurity, Beijing Institute of Microbiology and Epidemiology, Beijing, China, <sup>2</sup> Division of Biology, Beijing Academy, Beijing, China, <sup>3</sup> Department of Blood Transfusion, Wuhan General Hospital of PLA, Wuhan, China, <sup>4</sup> School of Medicine, Jiangsu University, Zhenjiang, China, <sup>5</sup> Department of Microbiology, Anhui Medical University, Hefei, China

## OPEN ACCESS

### Edited by:

Matthew S. Francis,  
Umeå University, Sweden

### Reviewed by:

Vladimir L. Motin,  
The University of Texas Medical  
Branch at Galveston, United States  
Michael Marceau,  
Université Lille Nord de France, France  
David Erickson,  
Brigham Young University,  
United States

### \*Correspondence:

Dongsheng Zhou  
dongshengzhou1977@gmail.com  
Ruifu Yang  
ruifuyang@gmail.com

<sup>†</sup>These authors have contributed  
equally to this work

### Specialty section:

This article was submitted to  
Molecular Bacterial Pathogenesis,  
a section of the journal  
Frontiers in Cellular and Infection  
Microbiology

**Received:** 06 May 2018

**Accepted:** 11 September 2018

**Published:** 02 October 2018

### Citation:

Fang H, Liu L, Zhang Y, Yang H, Yan Y,  
Ding X, Han Y, Zhou D and Yang R  
(2018) BfvR, an AraC-Family  
Regulator, Controls Biofilm Formation  
and pH6 Antigen Production in  
Opposite Ways in *Yersinia pestis*  
Biovar Microtus.  
Front. Cell. Infect. Microbiol. 8:347.  
doi: 10.3389/fcimb.2018.00347

Biofilm formation is critical for blocking flea foregut and hence for transmission of *Y. pestis* by flea biting. In this study, we identified the regulatory role of the AraC-family transcriptional regulator BfvR (YPO1737 in strain CO92) in biofilm formation and virulence of *Yersinia pestis* biovar Microtus. Crystal violet staining, *Caenorhabditis elegans* biofilm assay, colony morphology assay, intracellular c-di-GMP concentration determination, and BALB/c mice challenge were employed to reveal that BfvR enhanced *Y. pestis* biofilm formation while repressed its virulence in mice. Further molecular biological assays demonstrated that BfvR directly stimulated the expression of *hmsHFRS*, *waaAE-coaD*, and *hmsCDE*, which, in turn, affected the production of exopolysaccharide, LPS, and c-di-GMP, respectively. In addition, BfvR directly and indirectly repressed *psaABC* and *psaEF* transcription, respectively. We concluded that the modulation of biofilm- and virulence-related genes by BfvR led to increased biofilm formation and reduced virulence of *Y. pestis* biovar Microtus.

**Keywords:** *Yersinia pestis*, BfvR, biofilm, virulence, transcriptional regulation

## INTRODUCTION

*Yersinia pestis*, which causes severe and even fatal zoonotic diseases, has been responsible for the three plague pandemics throughout human history. *Y. pestis* can form biofilm not only *in vitro*, but also in the infected fleas that leads to a blockage in the proventriculus and enhances the flea-borne transmission (Hinnebusch et al., 1996). Studies on biofilm formation in *Y. pestis* have focused on the synthesis and degradation of: (i) extracellular matrix (Bobrov et al., 2008); (ii) intracellular secondary messengers, such as 3',5'-cyclic diguanylic acid (c-di-GMP) (Kirillina et al., 2004; Bobrov et al., 2011); and (iii) lipopolysaccharide (LPS) (Knirel and Anisimov, 2012). Transcription regulation can also modulate the expression of biofilm-related genes through multiple cellular pathways (Sun et al., 2009; Sun Y. C. et al., 2012; Willias et al., 2014, 2015).

Bacterial exopolysaccharide (EPS) is the primary component of the biofilm extracellular matrix. The *hmsHFRS* operon, located in the 102-kb *pgm* locus, coordinates the synthesis and transport of EPS in *Y. pestis* (Bobrov et al., 2008). The secondary signaling molecule c-di-GMP promotes EPS production in *Y. pestis*. This signaling molecule is catalyzed by diguanylate cyclases (DGC) and

degraded by phosphodiesterase (PDE). In *Y. pestis*, DGC is encoded by two genes, *hmsT* and *hmsD* (derived from the three-gene operon *hmsCDE*); while PDE is encoded by *hmsP* (Kirillina et al., 2004). In general, a high concentration of intracellular c-di-GMP can stimulate biofilm formation and interfere with virulence (Hengge, 2009). DGC and PDE inversely regulate biofilm formation, which is dependent on control of HmsHFRS-based poly- $\beta$ -1, 6-N-acetylglucosamine synthesis in *Y. pestis* (Bobrov et al., 2011).

LPS also plays a vital role in biofilm formation and is synthesized by a three-gene operon *waaAE-coaD*, containing genes *waaA*, *waaE*, and *coaD*, in *Y. pestis*. Deletion of *waaA*, which encodes a 3-deoxy-D-manno-octulosonic acid transferase involved in the synthesis of LPS (Tan and Darby, 2005), results in a biofilm-defective phenotype in *Y. pestis* (Liu et al., 2014).

It was reported that the expression of 214 genes significantly increased in the flea compared with all *in vitro* growth conditions, including *y2570* (YPO1737 in CO92 and *bfvR* in Microtus strain 91001). Whole-genome microarrays in *Y. pestis* KIM6+ showed that *y2570* had significantly higher expression levels in the flea gut but not the rat *bubo* (Vadyvaloo et al., 2010). We predicted and identified that *bfvR*, located between the bases 1,639,340 and 1,639,726 on the genome of Microtus strain 91001, can participate in biofilm formation *in vivo* (Song et al., 2004; Mao et al., 2016). In this research, we also studied the regulation mechanisms on biofilm formation for the mentioned genes by BfVR in *Y. pestis*.

Moreover, we found *bfvR* could inhibit the virulence of BALB/c mice in 91001. The AraC family transcription regulator typically binds to the target DNA and regulates bacterial virulence by sensing small molecule inducers such as urea, bicarbonate, or cellobiose etc. The molecular inducers were abundant at the sites where the bacterial pathogen colonizes and damages its host (Yang et al., 2011).

The protein Psa, known as pH 6 antigen, is one of the surface proteins involved in adhesion to the host cellular surface during initiation of *Y. pestis* pathogenesis. Psa proteins result from the polymerization of single PsaA pilin subunits (Bao et al., 2012), and the assembly of pH 6 antigen is mediated by the secretion of PsaB and PsaC, which constitutes the chaperone/usher machinery on the cell surface (Price et al., 1995). PsaABC is highly expressed following a temperature shift from 26 to 37°C and acidic media, while PsaEF is responsible for the transcriptional activation of *psaABC* (Yang and Isberg, 1997). pH 6 antigen mediates the entry of *Y. pestis* into human pulmonary epithelial cells (Liu et al., 2006; Galvan et al., 2007) and promotes the delivery of Yops (effectors of the plasmid pCD1-encoded type III secretion system) into target host cells via cell-to-cell contact between *Y. pestis* and eukaryotic cells (Felek et al., 2010). pH 6 antigen does not strengthen the attachment to mouse macrophages, however, the resistance to phagocytosis can be developed independent of *Yersinia* outer proteins and capsule antigen in *Y. pestis* KIM5 (Huang and Lindler, 2004). However, loss of Psa has no effect on the virulence of *Y. pestis* strain 231 following subcutaneous challenge of naive and pH 6 antigen-immunized mice (Anisimov et al., 2009). In our opinion, the role of pH 6 antigen in *Y. pestis* virulence appears to be dependent

on the strains tested and the animals challenged. In our study, we showed that by decreasing the transcription of *psaABC* and *psaEF*, BfVR could influence the survival of mice infected with strain 91001.

There are 7–19 AraC- or AraC-like-family transcription regulatory genes deposited in the GenBank database from *Yersinia* genomes. *Y. pestis* biovar Microtus strain 91001, Orientalis strain CO92, and Medievalis strain KIM D27 possess 19, 13, and 14 AraC family transcription regulators, respectively. YbtA, a previously reported AraC family transcription regulator in *Y. pestis*, can promote the transcription of *psn* (receptor for yersiniabactin) and *irp2* (yersiniabactin biosynthesis gene), but inhibit the transcription of *ybtA* itself (Fetherston et al., 1996). MarA can affect bacterial drug sensitivity (Gillette et al., 2000), both MarA47 and MarA48 in the KIM strain of *Y. pestis* can regulate drug sensitivity and virulence (Lister et al., 2010). LcrF, similar to ExcA (an AraC family transcription regulator in *Escherichia coli*), can also regulate the transcription of the Ysc-Yop genes of type III secretion system in *Y. pestis* (King et al., 2013; Li et al., 2014). However, none of the AraC family transcription regulators have been reported to regulate biofilm formation in *Y. pestis*.

In this study, we firstly revealed the regulation of biofilm formation by BfVR in *Y. pestis*. In addition, our findings offer insights into the coordination of virulence and biofilm formation in *Y. pestis*.

## MATERIALS AND METHODS

### Bacterial Strains and Mutant Preparation

The wild-type (WT) *Y. pestis* strain 91001 is avirulent in humans but highly lethal to mice (Zhou et al., 2004). The entire coding region of *bfvR* was replaced with the kanamycin resistance cassette using the one-step inactivation method based on the lambda Red recombination system (Datsenko and Wanner, 2000) and the *Y. pestis* *bfvR* null mutant was designated as  $\Delta bfvR$ . All primers used in this study were listed in Table S1.

A PCR-generated DNA fragment containing the *bfvR* coding region with its 609-bp upstream promoter-proximal region and 267-bp downstream transcriptional terminator region was cloned into the pACYC184 vector (GenBank accession number X06403). The recombinant plasmid was introduced into  $\Delta bfvR$ , yielding the complementary strain *C-bfvR*.

For *psaABC*-related gene regulation experiments, supplemented BHI (sBHI) broth [3.7% Bacto brain heart infusion (BD Biosciences), 0.5% Oxoid yeast extract, 2.5 mM CaCl<sub>2</sub>, 0.2% xylose, pH 6.0] was used for bacterial cultivation (Lindler et al., 1990). An overnight bacterial culture with an optical density (OD<sub>620</sub>) value of about 1.0 was diluted 1:20 into fresh sBHI for further growth at 26°C with 230-rpm shaking. The cell culture with an OD<sub>620</sub> of about 0.6 was transferred to 37°C for a further 3-h culture prior to the harvesting of cells.

For *bfvR* gene regulation and phenotypic experiments, an overnight cell culture in Luria–Bertani (LB) broth with an OD<sub>620</sub> of about 1.5 was immediately diluted 1:20 into fresh LB broth for the second generation cultivation at 26°C to reach an OD<sub>620</sub> of about 1.0 and the culture was stored at 4°C for up to 24 h. The

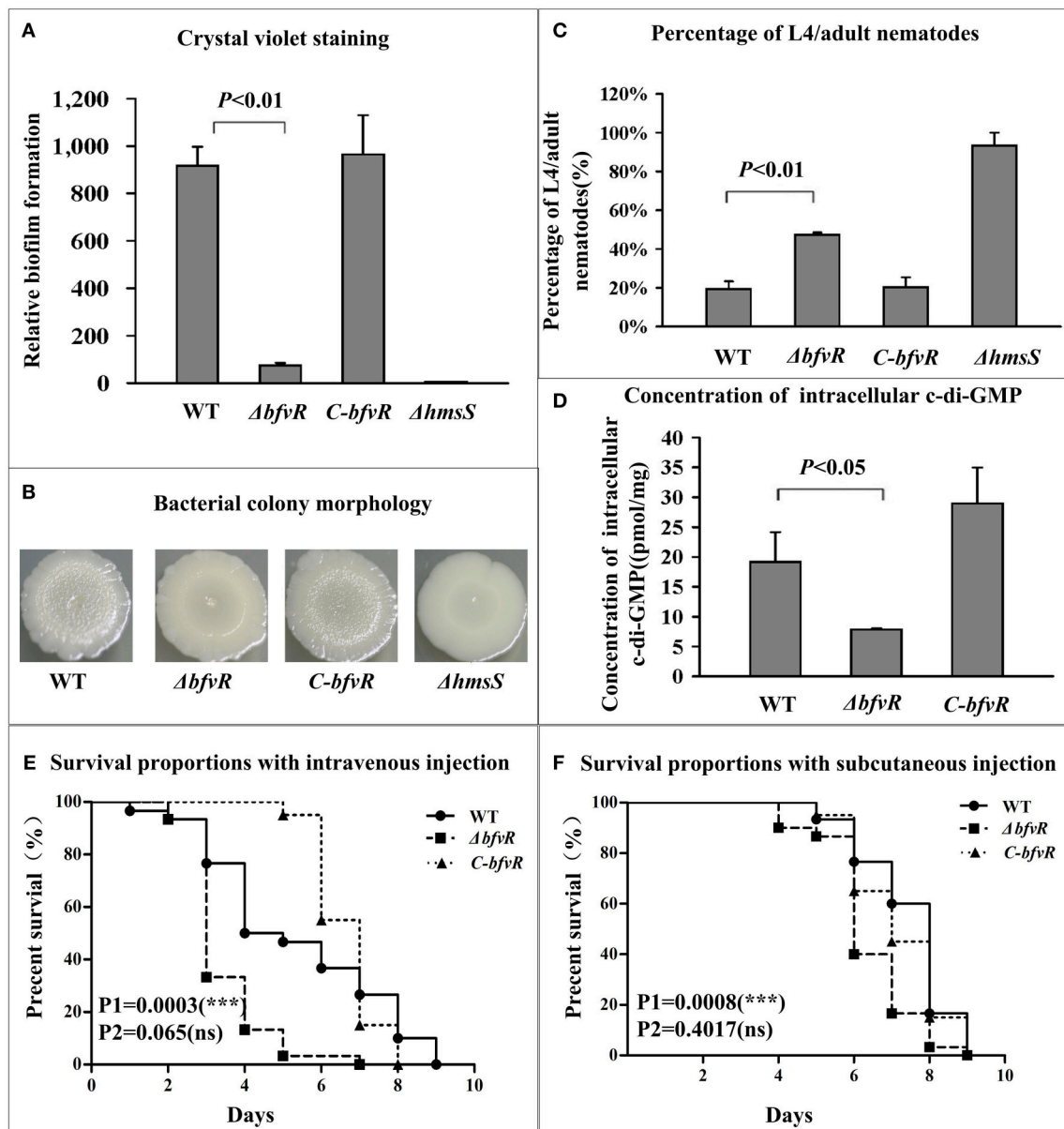


**FIGURE 1 |** BfVR-mediated phenotypes. **(A)** Crystal violet staining of biofilms. Cultured for 48 h in 24-well polystyrene dishes and evaluated by the OD570/OD620 value. **(B)** Bacterial colony morphology. Spotted on the LB agar with the glycerol stocks and cultured for 1 week at 26°C and then analyzed. **(C)** Biofilms on nematodes. Calculated by the percentage of L4/adults after 48-h feeding with different strains. **(D)** Intracellular c-di-GMP concentrations. Isolated c-di-GMP from the logarithmic bacteria and determined the concentrations by UPLC-MS/MS. **(E,F)** Virulence in BALB/c mice. Infected with 50–150 CFU by intravenous injection via the tail vein **(E)** and the subcutaneous injection at the inguinal region **(F)** and evaluated the virulence by the survival curve and P value with the GraphPad Prism 5.0 software. This is a representative experiment. P1 and P2 represented the P values between WT and  $\Delta bfvR$  or  $C-bfvR$ , respectively. \*\*\* Shows significant difference, ns indicates no significant difference.

culture was also diluted 1:20 into fresh LB broth for the third cultivation at 26°C for 6–8 h to reach an OD620 of about 1.0.

## Biofilm-Related Assays

Four different methods (Fang et al., 2013, 2015) of biofilm-related assays were employed: (i) Crystal violet staining of biofilms, the *in vitro* biofilm masses attached to the well walls were stained by crystal violet when bacteria were grown

in polystyrene microtiter plates; (ii) *Caenorhabditis elegans* biofilm assay, the nematode eggs were inoculated onto *Y. pestis* lawns and the percentages of fourth-stage larvae and adults (L4/adult) of *C. elegans* were determined for evaluating the bacterial ability to produce biofilms; (iii) the colony morphology assay, the rugose colony morphology of bacteria grown on LB agar plates was observed at different times for assessing the bacterial ability to synthesize biofilm matrix exopolysaccharide;

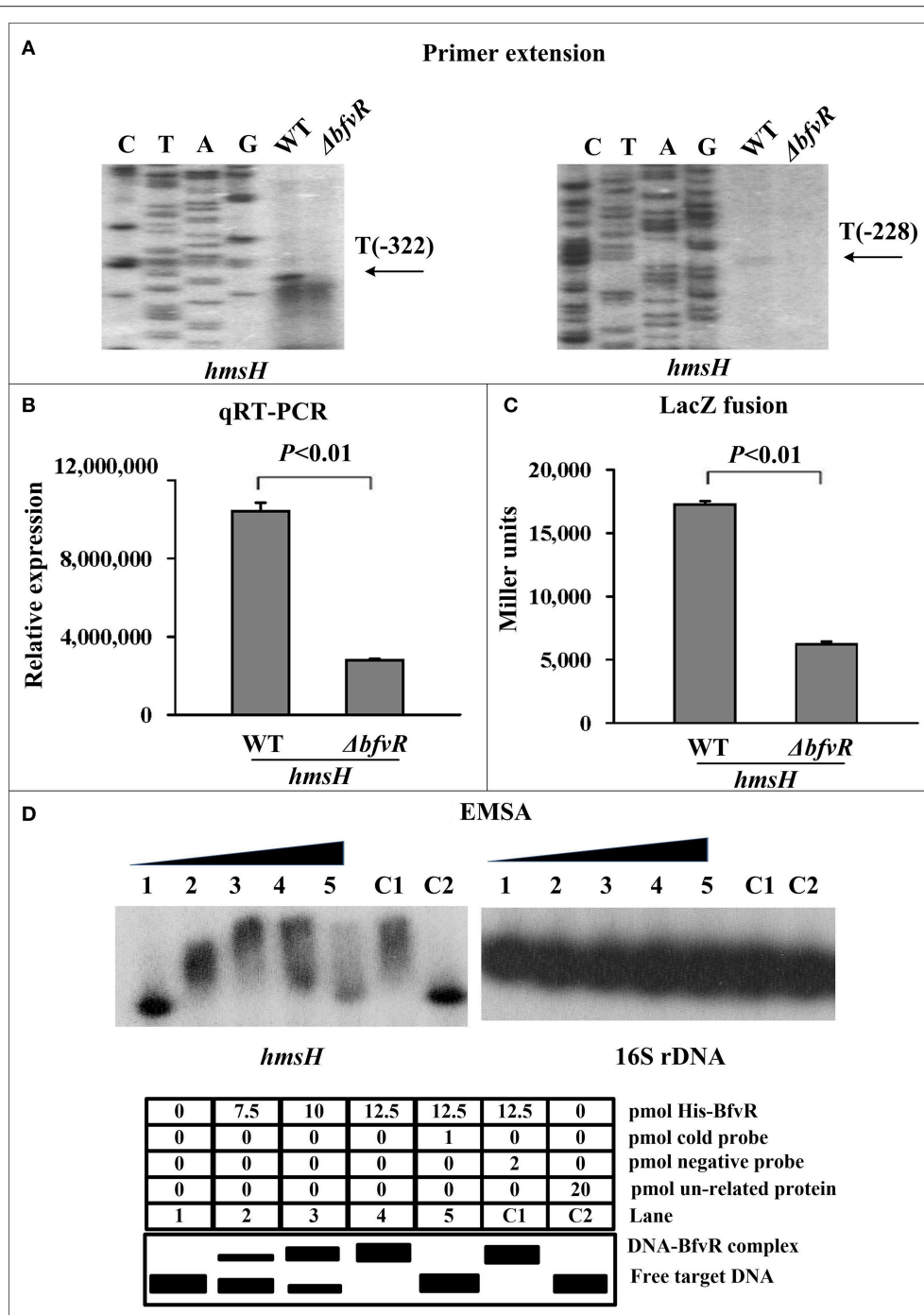


**FIGURE 2 |** Regulation of *hmsH* transcription by BfvR. Lanes G, A, T, and C represented Sanger sequencing reactions. Symbols + and – indicated the nucleotide positions downstream and upstream of the translation start site of target gene, respectively. **(A)** Primer extension. A(–128) represents the transcription start site of *hmsH*. **(B)** Quantitative RT-PCR. The relative mRNA expression was determined by calculating the threshold cycle (Ct) of *hmsH* via the classic  $2^{-\Delta\Delta Ct}$  method through standardized by the 16S rRNA gene. **(C)** LacZ fusion. LacZ reporter fusion with the promoter-proximal region (–451...+103) of *hmsH* and  $\beta$ -galactosidase in cellular extracts were determined. **(D)** EMSA. Purified His-BfvR protein bound to the promoter-proximal fragment of *hmsH* labeled radioactively and the retarded DNA band were shown in the amount-dependent manner.

and (iv) determination of intracellular c-di-GMP levels by a chromatography-coupled tandem mass spectrometry method (Spangler et al., 2010).

## Murine Infection Model

All animal experiments were carried out in accordance with the principles of the Basel Declaration and recommendations of



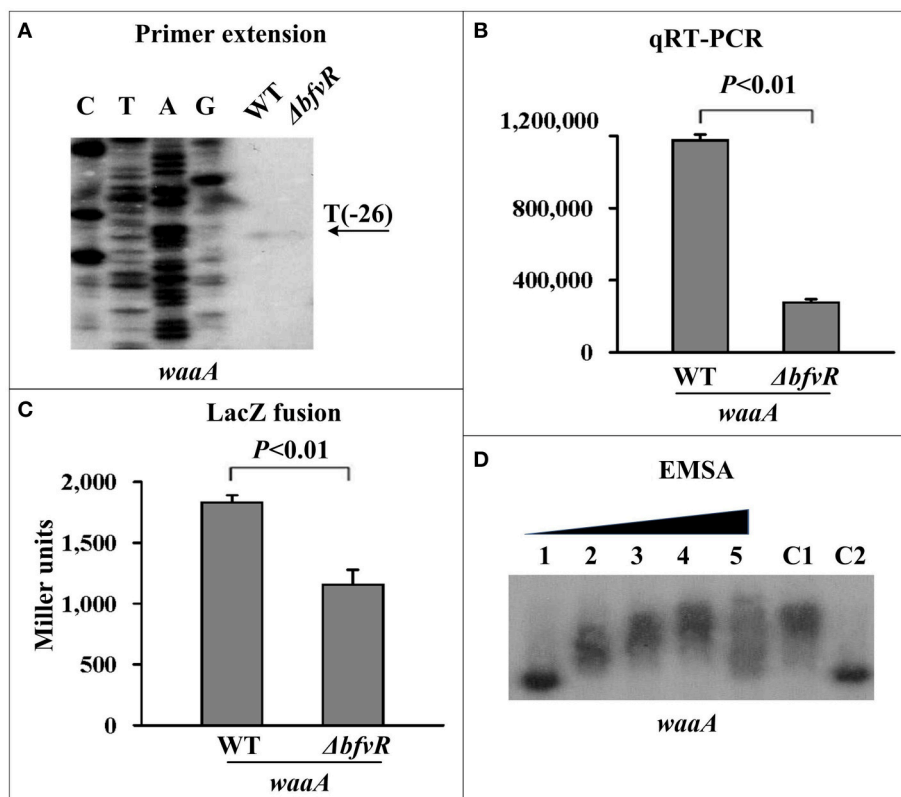


**FIGURE 3 |** Regulation of *waaAE-coaD* by BfVR. Reference to **Figure 2** for the explanation of primer extension **(A)**, quantitative RT-PCR **(B)**, LacZ fusion **(C)**, and EMSA **(D)**. The promoter-proximal region from -574 to +62 was amplified.

the Guidelines for Welfare and Ethics of Laboratory Animals of China, the Committee on Animal Research of the Academy of Military Medical Sciences. The protocol was approved by the Committee on Animal Research of the Academy of Military Medical Sciences. Bacterial cultures were washed twice with PBS (pH 7.2), and then subjected to serial 10-fold dilutions with PBS. Appropriate dilutions were plated onto He's agar plates (1 L powder containing pig blood peptone 12 g,  $K_2HPO_4$  1 g, NaCl 4 g, and agar 13 g, LandBridge, China) to calculate the number of colony-forming units (CFU). For each strain tested, 0.1 ml of the  $10^3$  CFU/ml bacterial suspensions were inoculated by subcutaneous injection at the inguinal region or by intravenous injection via the tail vein into each of 10 female BALB/c mice (aged 6 to 8-week-old). The numbers of mice that died at specified times were recorded and used to create a survival curve with the GraphPad Prism 5.0 software. *P*-values were calculated with the log-rank (Mantel-Cox) test and the Gehan-Breslow-Wilcoxon test affiliated in this software.  $P < 0.01$  was considered to indicate statistical significance.

### Primer Extension (PE) Assay

For the PE assay (Ghosh et al., 1978; Sun F. et al., 2012; Zhang et al., 2013), an oligonucleotide primer complementary to a portion of the RNA transcript of each indicated gene was used to synthesize cDNAs. About 10–30  $\mu$ g of total RNA from each strain

was annealed with 1 pmol of [ $\gamma$ - $^{32}$ P] end-labeled reverse primer using a Primer Extension System (Promega) in accordance with the manufacturer's instructions. The same labeled primer was also used for sequencing with the fmol<sup>®</sup> DNA Cycle Sequencing System (Promega). The PE products and sequencing DNAs were concentrated and analyzed in a 6% polyacrylamide/8 M urea gel. The results were detected by autoradiography (Kodak film) and then analyzed.

### Quantitative RT-PCR

Gene-specific primers were designed to produce amplicons for the target genes. Contaminating DNA in the RNA samples was removed using the Ambion DNA-free<sup>™</sup> Kit (Applied Biosystems). cDNAs were generated using 5  $\mu$ g of RNA and 3  $\mu$ g of random hexamer primers. Real-time PCR was performed using the LightCycler system (Roche) and the SYBR Green master mix (Takara) (Zhan et al., 2008; Sun et al., 2014). Based on the standard curves of 16S rRNA gene expression, the relative mRNA level was determined by calculating the threshold cycle (Ct) of target genes via the classic  $2^{-\Delta\Delta CT}$  method. Negative controls used cDNA generated without reverse transcriptase as templates. Reactions containing primer pairs without template were also included as blank controls. The 16S rRNA gene was used as an internal control for normalization.

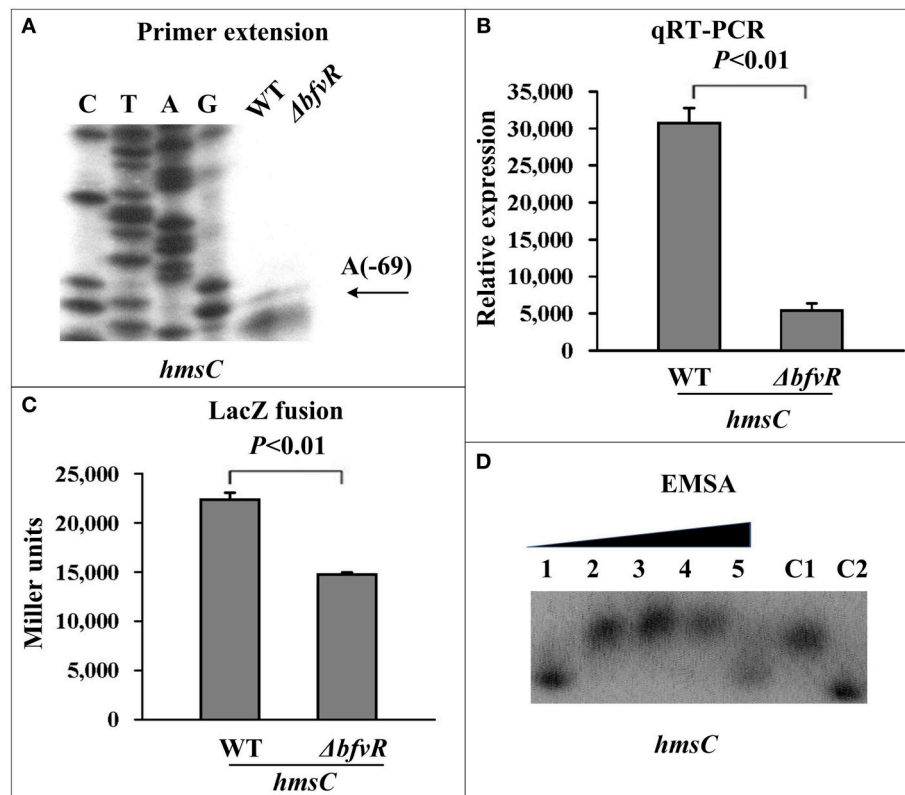


**FIGURE 4 |** Regulation of *hmsC* by BfvR. Reference to **Figure 2** for the annotations of primer extension **(A)**, quantitative RT-PCR **(B)**, LacZ fusion **(C)**, and EMSA **(D)**. The promoter-proximal region from -456 to +55 was amplified.

## LacZ Reporter Fusion and $\beta$ -Galactosidase Assay

The promoter-proximal DNA region of each gene tested was prepared by PCR with Takara ExTaq DNA polymerase using *Y. pestis* strain 91001 genomic DNA as the template. This purified fragment was then cloned directionally into the *HindIII*-*Bam*HI site of the transcriptional fusion vector pRW50 (El-Robh and Busby, 2002) that contained a promoterless *lacZ* reporter gene. The clone was verified by DNA sequencing. Each *Y. pestis* strain tested was transformed with the recombinant plasmid and the empty plasmid pRW50 as a negative control.  $\beta$ -galactosidase activity in extracts was measured from the cells cultivated as described above according to the  $\beta$ -Galactosidase Enzyme Assay System (Promega) (Sun F. et al., 2012; Zhang et al., 2013).

## Preparation of 6xHis-Tagged BfvR Protein

The preparation of purified BfvR protein was performed as previously described (Heroven and Dersch, 2006). The entire coding region of *bfvR* was amplified from *Y. pestis* strain 91001 and cloned directionally into the *Bam*HI and *Hind*III sites of plasmid pColdI (Qing et al., 2004) (Novagen, GenBank accession number AB186388). The recombinant plasmids were transformed into *E. coli* BL21 (DE3) cells (Novagen). Expression of His-BfvR protein was induced by the addition of 1 mM or 2 mM isopropyl-beta-D-thiogalactoside at 16°C

overnight. His-BfvR was purified under native conditions using QIAexpressionist™ Ni-NTA affinity chromatography (Qiagen). The purified eluted protein was concentrated with an Amicon Ultra-15 column (Millipore) to a final concentration of 0.5–0.7 mg/ml in storage buffer containing 10 mM Tris-HCl, 1 mM EDTA, 0.1 mM DTT, and 5 mM  $\beta$ -mercaptoethanol (pH 7.0) plus 20% glycerol. The protein purity was verified by sodium dodecyl sulfate–polyacrylamide gel electrophoresis with Coomassie brilliant blue staining.

## Electrophoretic Mobility Shift Assay (EMSA)

For EMSA, we have made minor modifications according to the Hellman's method (Hellman and Fried, 2007). Promoter-proximal DNA region was prepared by PCR amplification. The 5' end of the DNA was labeled using [ $\gamma$ - $^{32}$ P] ATP and T4 polynucleotide kinase. DNA binding was performed in a 10  $\mu$ l volume containing binding buffer [100  $\mu$ M  $MnCl_2$ , 1 mM  $MgCl_2$ , 0.5 mM DTT, 50 mM KCl, 10 mM Tris-HCl (pH 7.5), 0.05 mg/ml sheared salmon sperm DNA, 0.05 mg/ml BSA, and 4% glycerol], labeled DNA (1,000 to 2,000 c.p.m./ $\mu$ l), and increasing amounts of His-RovA or His-BfvR. Two control reactions were included: one contained the specific DNA competitor (unlabeled promoter DNA regions; cold probe), while the other was the non-specific protein competitor (rabbit anti-F1-protein polyclonal

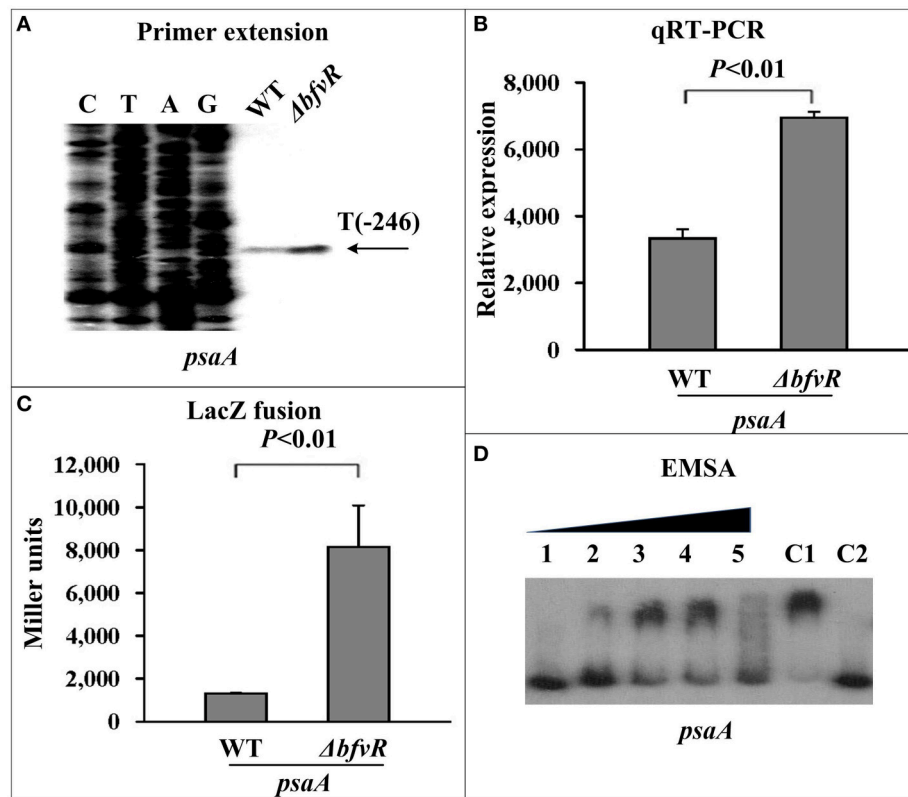


**FIGURE 5 |** Regulation of *psaA* by BfvR. Reference to **Figure 2** for the annotations of primer extension **(A)**, quantitative RT-PCR **(B)**, LacZ fusion **(C)**, and EMSA **(D)**. The promoter-proximal region from -491 to +65 was amplified.

IgG antibody). After incubation at room temperature for 30 min, the products were loaded onto a native 4% (w/v) polyacrylamide gel and electrophoresed in 0.5×Tris-borate buffer containing 100  $\mu$ M MnCl<sub>2</sub> for 30 min with 220 V at 8°C. Radioactive species were detected by autoradiography.

## Experimental Replicates and Statistical Methods

For real-time RT-PCR, the  $\beta$ -galactosidase activity assay, crystal violet staining of biofilms, the determination of L4/adult nematodes, c-di-GMP experiments and murine infection were performed with at least three independent bacterial cultures/lawns, and values were expressed as the mean  $\pm$  standard deviation. The paired Student's *t*-test was performed to determine significant differences;  $P < 0.01$  was considered to indicate statistical significance. For primer extension, EMSA, and colony morphology observations, representative data from at least two independent biological replicates were shown.

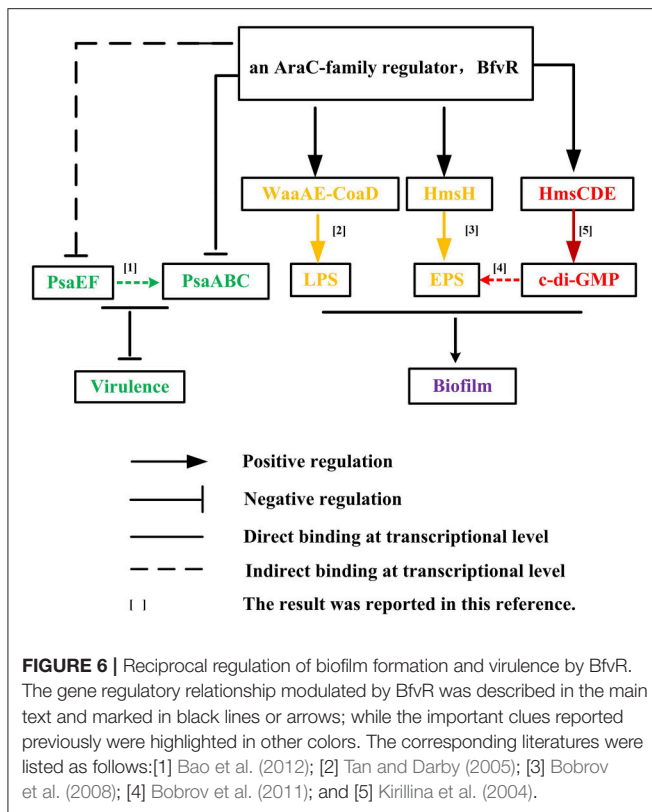
## RESULTS

### Involvement of BfvR in Biofilm Formation and Virulence in Mice

To investigate the potential role of BfvR in biofilm formation, the phenotypes of relevant mutant strains were analyzed. We selected four experimental strains: (i) wild-type (WT); (ii) *bfvR*

mutant strain ( $\Delta bfvR$ ); (iii) pACYC184- $\Delta bfvR$  complementary strain (*C-bfvR*); and (iv) a strain containing a mutation in the biofilm-related gene *hmsS* ( $\Delta hmsS$ ), a typical biofilm negative strain.

Deletion of *bfvR* had no effect on the growth in LB (**Figure S1**) but led to a dramatic reduction in biofilm formation in *Y. pestis* strain 91001. Compared with the WT and *C-bfvR* strains, the  $\Delta bfvR$  mutant strain showed less crystal violet staining (**Figure 1A**), with smoother colony morphology (**Figure 1B**), similar to the  $\Delta hmsS$  mutant. After the nematode eggs were fed with  $\Delta hmsS$  strain, 93% of the eggs developed into L4/adult nematodes, compared with 19.3, 47.3, and 20.3% for the WT,  $\Delta bfvR$ , and *C-bfvR* strains, respectively (**Figure 1C**), indicating *bfvR* might affect *C. elegans* development. In general, when fed with WT strain, about 20% or fewer larvae grew and developed into L4/adult nematodes (Zhou and Yang, 2011; Fang et al., 2013); however, the exact ratio of nematode adults did not directly correlate with the biofilm formation ability of *Y. pestis*. The concentration of intracellular c-di-GMP was quantitatively detected by UPLC-MS/MS analysis (Spangler et al., 2010). Lower production of cellular c-di-GMP was observed in strain  $\Delta bfvR$  (11.45 nmol/ $\mu$ g) compared with the WT (19.68 nmol/ $\mu$ g) and *C-bfvR* (32.70 nmol/ $\mu$ g) strains (**Figure 1D**). These phenotypes suggested that deletion of *bfvR* resulted in an obvious reduction in biofilm/c-di-GMP production.



Wild type bacteria, the BfvR mutant and the complemented strain were used to infect mice through both subcutaneous injection and intravenous injection. This was repeated three times independently for WT and the BfvR mutant, and repeated two times for the complemented strain. Finally, we calculated all the results and drew the survival curves with Graphpad 5.0. Compared with WT,  $\Delta bfvR$  displayed a significant increase in virulence in BALB/c mice after intravenous ( $P = 0.0003$ ) or subcutaneous ( $P = 0.0008$ ) injection. Moreover, compared to WT, the complementary effect of  $C-bfvR$  also showed no significant differences during the intravenous ( $P = 0.065$ ) or subcutaneous ( $P = 0.4017$ ) routes of infection (Figures 1E,F).

Taken together, BfvR could enhance biofilm formation and inhibit the virulence of *Y. pestis* strain 91001 in BALB/c mice.

## BfvR Acts as an Activator of EPS and c-di-GMP

In order to reveal the mechanisms by which BfvR modulated the synthesis of EPS, we analyzed expressions of the related genes including *hmsH* and *waaA*. The genes encoding DGC and PDE, namely *hmsC*, *hmsT*, and *hmsP* in *Y. pestis*, were also evaluated by qRT-PCR, PE,  $\beta$ -galactosidase activity assays and EMSA.

BfvR directly promoted *hmsH* expression. The mRNA levels of *hmsH* in WT and  $\Delta bfvR$  strains were analyzed by primer extension. The levels of mRNA from the two transcriptional start sites (Sun F. et al., 2012) were found to be lower in  $\Delta bfvR$  than in the WT strain (Figure 2A). Quantitative real-time PCR (qRT-PCR) assay indicated a significant reduction in relative mRNA expression in  $\Delta bfvR$  compared with the WT

strain (Figure 2B). A  $\beta$ -galactosidase activity assay also indicated that the promoter activity of *hmsH* (Figure 2C) was attenuated in  $\Delta bfvR$  relative to the WT. EMSA showed that His-BfvR could bind to the promoter-proximal regions of *hmsH* in a dose-dependent manner (Figure 2D). These results indicated that BfvR in *Y. pestis* strain 91001 could promote biofilm formation by directly stimulating *hmsH* expression.

BfvR directly induced *waaAE-coaD* expression. The transcription of *waaA* (Liu et al., 2014), the first gene in the *waaAE-coaD* operon, was investigated in both WT and  $\Delta bfvR$  strains. Both primer extension (Figure 3A) and qRT-PCR assays (Figure 3B) revealed a significant reduction in *waaAE-coaD* expression in  $\Delta bfvR$  compared with the WT strain. The promoter activity of *waaA* (Figure 3C) was attenuated in  $\Delta bfvR$  relative to the WT, as shown by the  $\beta$ -galactosidase activity assay. EMSA revealed that His-BfvR could bind to the upstream regions of *waaA* promoter (Figure 3D) in a dose-dependent manner. These results showed that BfvR in *Y. pestis* could promote biofilm formation by directly stimulating the expression of *waaAE-coaD*.

The c-di-GMP synthesis- and degradation-related genes *hmsT*, *hmsCDE*, and *hmsP* were also regarded as major targets of biofilm formation at the post-transcriptional level in *Y. pestis*. The mRNA levels and binding activities to His-BfvR of these three genes were investigated by PE, qRT-PCR,  $\beta$ -galactosidase activity assay, and EMSA. Compared with WT,  $\Delta bfvR$  only showed a significant decrease in mRNA levels of *hmsCDE* (Figures 4A–C) but not *hmsT* (Figures S2A–C) or *hmsP* (Figures S3A–C). EMSA also showed that only the promoter-proximal regions of *hmsC* (Figure 4D) but not *hmsT* (Figure S2D) or *hmsP* (Figure S3D) could bind His-BfvR *in vitro*. These results indicated that BfvR in *Y. pestis* could promote c-di-GMP synthesis and regulate biofilm formation by directly stimulating the expression of *hmsCDE*.

## Regulation of the *psa* Loci by BfvR

Two loci, *psaABC* and *psaEF* located upstream of *psaA*, responsible for expression of pH 6 antigen (Psa) in *Y. pestis*, were selected as target genes for investigating the regulatory action of BfvR in virulence. PE, qRT-PCR, and  $\beta$ -galactosidase activity assays showed that deletion of *bfvR* led to elevated expression of *psaA* (Figures 5A–C) and *psaE* (Figures S4A–C). EMSA showed that His-BfvR could not bind the promoter-proximal region of *psaE* (Figure S4D) but could bind that of *psaA* (Figure 5D). In our opinion, BfvR might regulate *Y. pestis* virulence through acting on many unknown factors at the same time, but BfvR could at least influence *Y. pestis* virulence by controlling the expression of *psaABC*.

## DISCUSSION

The AraC/XylS family of polypeptides is broadly distributed among Gram negative and positive bacteria (Tobes and Ramos, 2002). Biofilm formation modulation mediated by the AraC-type regulator has been reported for various types of bacteria but, prior to this study, not for *Y. pestis*. In this work, we showed for the first time that BfvR could similarly regulate biofilm formation in *Y. pestis* strain 91001.



Production of extracellular matrix was an important mechanism modulated by the AraC-type transcriptional regulator during biofilm formation. Polysaccharide intercellular adhesin (PIA)/poly-N-acetylglucosamine production was shown to be vital for *Staphylococcus epidermidis* biofilm formation, and this was encoded by the *icaADBC* operon, which in turn was modulated by the AraC-type regulator Rbf (Rowe et al., 2016). In *Enterococcus faecium*, the putative AraC type of regulator EbrB, regulated by *esp* operon expression, was shown to be responsible for the production of the enterococcal surface protein and was implicated in biofilm formation (Top et al., 2013). Another putative AraC-type transcriptional regulator PerA in a clinical isolate of *E. faecalis* strain E99 was detected to be involved in survival within macrophages, pathogenesis in mice, and biofilm formation (Coburn et al., 2008). Similarly, data also showed that BfvR could promote biofilm formation by increasing the synthesis of bacterial EPS and LPS, by directly stimulating the expression of *hmsHFRS* and *waaAE-coaD*, respectively.

WaaA plays an important role in the synthesis of lipid A (Dentovskaya et al., 2011) in *Yersinia*, which is responsible for endotoxin and virulence in mice in *Y. pestis* KIM6+ (Sun et al., 2013). It seems to be contradiction that there could be an ~75% reduction in *waaA* gene expression (Figure 3B) and therefore presumably reduced LPS core oligosaccharide production, yet the virulence of the mutant is still enhanced. In fact, the direct effect of WaaA on mice virulence of *Y. pestis* strain 91001 has not been specifically reported. We found that deletion of PhoP or RcsB dramatically induced the downregulation or upregulation of *waaA*, respectively (Liu et al., 2014). However, loss of PhoP or RcsB had no significant effect on *Y. pestis* strain 91001 virulence tested by us (data not shown). In our opinion, downregulation of *waaA* in the BfvR mutant will not necessarily led to a notable alteration of *Y. pestis* strain 91001 virulence in mice. The mechanisms by which WaaA modulates strain 91001 virulence in mice still needs further investigation.

Within current sequence databases, the AraC/XylS family proteins are the most common positive regulators (Tobes and Ramos, 2002). It has been found that deletion of *bfvR* in *Y. pestis* strain 91001 resulted in a dramatic reduction in biofilm production through biofilm-related phenotypic assays. Until now, there has been no report to indicate that c-di-GMP production is regulated by an AraC-family protein. In this study, we demonstrated that deletion of *bfvR* in *Y. pestis* affected the intracellular c-di-GMP levels shown in the biofilm phenotypic assay. Similar to most AraC/XylS family regulators, BfvR displayed positive regulation during biofilm formation in *Y. pestis*.

The AraC/XylS family of transcription factors have been shown to play an important role in regulating bacterial virulence by modulating the expression of virulence-related genes in *Citrobacter rodentium* (Hart et al., 2008) and *Salmonella enterica* serovar Typhimurium (Bailey et al., 2010). Work reported here also indicated that a similar mechanism existed on virulence modulation by BfvR in *Y. pestis*. BfvR can repress *Y. pestis* virulence in mice by directly and indirectly inhibiting the expression of *psaABC* and *psaEF* at the transcriptional level, respectively. This work further extended our knowledge of

regulation mechanisms under the control of the AraC regulator and their biological relevance *in vitro* (Figure 6).

Based on the results of an NCBI conserved domain assay (<https://www.ncbi.nlm.nih.gov/Structure/cdd/wrpsb.cgi>), the structure of BfvR was found to be homologous to that of SoxS of *Xenorhabdus ishikashii* with 100% coverage and 78% identity aligned by BlastP. SoxS protein was a direct transcriptional activator of the oxidative stress genes of the SoxRS regulon (Li and Demple, 1994), and was widely investigated in strains of family Enterobacteriaceae (Gallegos et al., 1997). SoxS regulated the expression of *ompW* gene, which was involved in osmoregulation as a minor porin, in *Salmonella enterica* serovar Typhimurium (Gil et al., 2009). *ydbK* gene (involved in superoxide resistance) and *ompN* (participating in the minor porins like *ompW*), which were coexpressed in an operon, were indirectly activated by SoxS in a multidrug-resistant *E. coli* strain NorE5 (Fabrega et al., 2012). Redox-cycling drugs rather than superoxide can directly activate the SoxRS response in *E. coli* (Gu and Imlay, 2011). Whether there is a similar SoxRS response shown by BfvR in *Y. pestis* remains to be investigated.

Taken together, our findings suggested that the AraC-family regulator BfvR was firstly found to be involved in the modulation of both biofilm formation and pathogenesis in *Y. pestis* strain 91001. In this study we only focused on biofilm formation and pathogenesis regulated by this regulator, the regulatory role of BfvR in other processes, such as sensing the redox pressure in *Y. pestis*, requires elucidation in future studies.

## AUTHOR CONTRIBUTIONS

DZ and RY conceived the study and designed the experimental procedures. HF, LL, YZ, HY, YY, XD, and YH performed the experiments and carried out data analysis. DZ, HF, LL, YZ, and RY wrote the paper.

## FUNDING

This work was supported by the National Natural Science Foundation of China (31430006), the National Special Project on Research and Development of Key Biosafety Technologies Grant (2016YFC1200100), the China Postdoctoral Science Foundation (2015M572755), the Hubei Province health and family planning scientific research project (WJ2018H0070), and the Natural Science Research Project from Department of Education of Anhui Province (KJ2015A019).

## ACKNOWLEDGMENTS

We thank Kate Fox, DPhil, from Liwen Bianji, Edanz Group China ([www.liwenbianji.cn/ac](http://www.liwenbianji.cn/ac)) for critically reading and language editing the manuscript.

## SUPPLEMENTARY MATERIAL

The Supplementary Material for this article can be found online at: <https://www.frontiersin.org/articles/10.3389/fcimb.2018.00347/full#supplementary-material>

## REFERENCES

- Anisimov, A. P., Bakhteeva, I. V., Panfertsev, E. A., Svetoch, T. E., Kravchenko, T. B., Platonov, M. E., et al. (2009). The subcutaneous inoculation of pH 6 antigen mutants of *Yersinia pestis* does not affect virulence and immune response in mice. *J. Med. Microbiol.* 58, 26–36. doi: 10.1099/jmm.0.005678-0
- Bailey, A. M., Ivens, A., Kingsley, R., Cottell, J. L., Wain, J., and Piddock, L. J. (2010). RamA, a member of the AraC/XylS family, influences both virulence and efflux in *Salmonella enterica* serovar Typhimurium. *J. Bacteriol.* 192, 1607–1616. doi: 10.1128/JB.01517-09
- Bao, R., Esser, L., Sadhukhan, A., Nair, M. K., Schifferli, D. M., and Xia, D. (2012). Crystallization and preliminary X-ray diffraction analysis of PsaA, the adhesive pilin subunit that forms the pH 6 antigen on the surface of *Yersinia pestis*. *Acta Crystallogr. Sect. F Struct. Biol. Cryst. Commun.* 68, 1243–1246. doi: 10.1107/S1744309112033076
- Bobrov, A. G., Kirillina, O., Forman, S., Mack, D., and Perry, R. D. (2008). Insights into *Yersinia pestis* biofilm development: topology and co-interaction of Hms inner membrane proteins involved in exopolysaccharide production. *Environ. Microbiol.* 10, 1419–1432. doi: 10.1111/j.1462-2920.2007.01554.x
- Bobrov, A. G., Kirillina, O., Ryjenkov, D. A., Waters, C. M., Price, P. A., Fetherston, J. D., et al. (2011). Systematic analysis of cyclic di-GMP signalling enzymes and their role in biofilm formation and virulence in *Yersinia pestis*. *Mol. Microbiol.* 79, 533–551. doi: 10.1111/j.1365-2958.2010.07470.x
- Coburn, P. S., Baghdayan, A. S., Dolan, G. T., and Shankar, N. (2008). An AraC-type transcriptional regulator encoded on the *Enterococcus faecalis* pathogenicity island contributes to pathogenesis and intracellular macrophage survival. *Infect. Immun.* 76, 5668–5676. doi: 10.1128/IAI.00930-08
- Datsenko, K. A., and Wanner, B. L. (2000). One-step inactivation of chromosomal genes in *Escherichia coli* K-12 using PCR products. *Proc. Natl. Acad. Sci. U.S.A.* 97, 6640–6645. doi: 10.1073/pnas.120163297
- Dentovskaya, S. V., Anisimov, A. P., Kondakova, A. N., Lindner, B., Bystrova, O. V., Svetoch, T. E., et al. (2011). Functional characterization and biological significance of *Yersinia pestis* lipopolysaccharide biosynthesis genes. *Biochemistry* 76, 808–822. doi: 10.1134/S0006297911070121
- El-Rohb, M. S., and Busby, S. J. (2002). The *Escherichia coli* cAMP receptor protein bound at a single target can activate transcription initiation at divergent promoters: a systematic study that exploits new promoter probe plasmids. *Biochem. J.* 368, 835–843. doi: 10.1042/bj20021003
- Fabrega, A., Rosner, J. L., Martin, R. G., Sole, M., and Vila, J. (2012). SoxS-dependent coregulation of ompN and ydbK in a multidrug-resistant *Escherichia coli* strain. *FEMS Microbiol. Lett.* 332, 61–67. doi: 10.1111/j.1574-6968.2012.02577.x
- Fang, N., Gao, H., Wang, L., Qu, S., Zhang, Y. Q., Yang, R. F., et al. (2013). Optimized methods for biofilm analysis in *Yersinia pestis*. *Biomed. Environ. Sci.* 26, 408–411. doi: 10.3967/0895-3988.2013.05.012
- Fang, N., Yang, H., Fang, H., Liu, L., Zhang, Y., Wang, L., et al. (2015). RcsAB is a major repressor of *Yersinia* biofilm development through directly acting on hmsCDE, hmsT, and hmsHFRS. *Sci. Rep.* 5:9566. doi: 10.1038/srep09566
- Felek, S., Tsang, T. M., and Krukons, E. S. (2010). Three *Yersinia pestis* adhesins facilitate Yop delivery to eukaryotic cells and contribute to plague virulence. *Infect. Immun.* 78, 4134–4150. doi: 10.1128/IAI.00167-10
- Fetherston, J. D., Bearden, S. W., and Perry, R. D. (1996). YbtA, an AraC-type regulator of the *Yersinia pestis* pesticin/yersiniabactin receptor. *Mol. Microbiol.* 22, 315–325. doi: 10.1046/j.1365-2958.1996.00118.x
- Gallegos, M. T., Schleif, R., Bairoch, A., Hofmann, K., and Ramos, J. L. (1997). AraC/XylS family of transcriptional regulators. *Microbiol. Mol. Biol. Rev.* 61, 393–410.
- Galvan, E. M., Chen, H., and Schifferli, D. M. (2007). The Psa fimbriae of *Yersinia pestis* interact with phosphatidylcholine on alveolar epithelial cells and pulmonary surfactant. *Infect. Immun.* 75, 1272–1279. doi: 10.1128/IAI.01153-06
- Ghosh, P. K., Reddy, V. B., Swinscoe, J., Lebowitz, P., and Weissman, S. M. (1978). Heterogeneity and 5'-terminal structures of the late RNAs of simian virus 40. *J. Mol. Biol.* 126, 813–846. doi: 10.1016/0022-2836(78)90022-0
- Gil, F., Hernandez-Lucas, I., Polanco, R., Pacheco, N., Collao, B., Villarreal, J. M., et al. (2009). SoxS regulates the expression of the *Salmonella enterica* serovar Typhimurium ompW gene. *Microbiology* 155, 2490–2497. doi: 10.1099/mic.0.027433-0
- Gillette, W. K., Rhee, S., Rosner, J. L., and Martin, R. G. (2000). Structural homology between MarA of the AraC family of transcriptional activators and the integrase family of site-specific recombinases. *Mol. Microbiol.* 35, 1582–1583. doi: 10.1046/j.1365-2958.2000.01803.x
- Gu, M., and Imlay, J. A. (2011). The SoxRS response of *Escherichia coli* is directly activated by redox-cycling drugs rather than by superoxide. *Mol. Microbiol.* 79, 1136–1150. doi: 10.1111/j.1365-2958.2010.07520.x
- Hart, E., Yang, J., Tauschek, M., Kelly, M., Wakefield, M. J., Frankel, G., et al. (2008). RegA, an AraC-like protein, is a global transcriptional regulator that controls virulence gene expression in *Citrobacter rodentium*. *Infect. Immun.* 76, 5247–5256. doi: 10.1128/IAI.00770-08
- Hellman, L. M., and Fried, M. G. (2007). Electrophoretic mobility shift assay (EMSA) for detecting protein-nucleic acid interactions. *Nat. Protoc.* 2, 1849–1861. doi: 10.1038/nprot.2007.249
- Hengge, R. (2009). Principles of c-di-GMP signalling in bacteria. *Nat. Rev. Microbiol.* 7, 263–273. doi: 10.1038/nrmicro2109
- Heroven, A. K., and Dersch, P. (2006). RovM, a novel LysR-type regulator of the virulence activator gene rovA, controls cell invasion, virulence and motility of *Yersinia pseudotuberculosis*. *Mol. Microbiol.* 62, 1469–1483. doi: 10.1111/j.1365-2958.2006.05458.x
- Hinnebusch, B. J., Perry, R. D., and Schwan, T. G. (1996). Role of the *Yersinia pestis* hemin storage (hms) locus in the transmission of plague by fleas. *Science* 273, 367–370. doi: 10.1126/science.273.5273.367
- Huang, X. Z., and Lindler, L. E. (2004). The pH 6 antigen is an antiphagocytic factor produced by *Yersinia pestis* independent of *Yersinia* outer proteins and capsule antigen. *Infect. Immun.* 72, 7212–7219. doi: 10.1128/IAI.72.12.7212-7219.2004
- King, J. M., Schesser Bartra, S., Plano, G., and Yahr, T. L. (2013). ExsA and LcrF recognize similar consensus binding sites, but differences in their oligomeric state influence interactions with promoter DNA. *J. Bacteriol.* 195, 5639–5650. doi: 10.1128/JB.00990-13
- Kirillina, O., Fetherston, J. D., Bobrov, A. G., Abney, J., and Perry, R. D. (2004). HmsP, a putative phosphodiesterase, and HmsT, a putative diguanylate cyclase, control Hms-dependent biofilm formation in *Yersinia pestis*. *Mol. Microbiol.* 54, 75–88. doi: 10.1111/j.1365-2958.2004.04253.x
- Knirel, Y. A., and Anisimov, A. P. (2012). Lipopolysaccharide of *Yersinia pestis*, the cause of plague: structure, genetics, biological properties. *Acta Nat.* 4, 46–58.
- Li, L., Yan, H., Feng, L., Li, Y., Lu, P., Hu, Y., et al. (2014). LcrQ blocks the role of LcrF in regulating the Ysc-Yop Type III secretion genes in *Yersinia pseudotuberculosis*. *PLoS ONE* 9:e92243. doi: 10.1371/journal.pone.0092243
- Li, Z., and Demple, B. (1994). SoxS, an activator of superoxide stress genes in *Escherichia coli*. Purification and interaction with DNA. *J. Biol. Chem.* 269, 18371–18377.
- Lindler, L. E., Klempner, M. S., and Straley, S. C. (1990). *Yersinia pestis* pH 6 antigen: genetic, biochemical, and virulence characterization of a protein involved in the pathogenesis of bubonic plague. *Infect. Immun.* 58, 2569–2577.
- Lister, I. M., Mecsas, J., and Levy, S. B. (2010). Effect of MarA-like proteins on antibiotic resistance and virulence in *Yersinia pestis*. *Infect. Immun.* 78, 364–371. doi: 10.1128/IAI.00904-09
- Liu, F., Chen, H., Galvan, E. M., Lasaro, M. A., and Schifferli, D. M. (2006). Effects of Psa and F1 on the adhesive and invasive interactions of *Yersinia pestis* with human respiratory tract epithelial cells. *Infect. Immun.* 74, 5636–5644. doi: 10.1128/IAI.00612-06
- Liu, L., Fang, N., Sun, Y., Yang, H., Zhang, Y., Han, Y., et al. (2014). Transcriptional regulation of the waaAE-coaD operon by PhoP and RcsAB in *Yersinia pestis* biovar Microtus. *Protein Cell* 5, 940–944. doi: 10.1007/s13238-014-0110-8
- Mao, Y., Yang, X., Liu, Y., Yan, Y., Du, Z., Han, Y., et al. (2016). Reannotation of *Yersinia pestis* strain 91001 based on omics data. *Am. J. Trop. Med. Hyg.* 95, 562–570. doi: 10.4269/ajtmh.16-0215
- Price, S. B., Freeman, M. D., and Yeh, K. S. (1995). Transcriptional analysis of the *Yersinia pestis* pH 6 antigen gene. *J. Bacteriol.* 177, 5997–6000. doi: 10.1128/jb.177.20.5997-6000.1995
- Qing, G., Ma, L. C., Khorchid, A., Swapna, G. V., Mal, T. K., Takayama, M. M., et al. (2004). Cold-shock induced high-yield protein production in *Escherichia coli*. *Nat. Biotechnol.* 22, 877–882. doi: 10.1038/nbt984
- Rowe, S. E., Campbell, C., Lowry, C., O'donnell, S. T., Olson, M. E., Lindgren, J. K., et al. (2016). AraC-type regulator Rbf controls the *Staphylococcus epidermidis* biofilm phenotype by negatively regulating the icaADBC repressor SarR. *J. Bacteriol.* 198, 2914–2924. doi: 10.1128/JB.00374-16

- Song, Y., Tong, Z., Wang, J., Wang, L., Guo, Z., Han, Y., et al. (2004). Complete genome sequence of *Yersinia pestis* strain 91001, an isolate avirulent to humans. *DNA Res.* 11, 179–197. doi: 10.1093/dnares/11.3.179
- Spangler, C., Bohm, A., Jenal, U., Seifert, R., and Kaever, V. (2010). A liquid chromatography-coupled tandem mass spectrometry method for quantitation of cyclic di-guanosine monophosphate. *J. Microbiol. Methods* 81, 226–231. doi: 10.1016/j.mimet.2010.03.020
- Sun, F., Gao, H., Zhang, Y., Wang, L., Fang, N., Tan, Y., et al. (2012). Fur is a repressor of biofilm formation in *Yersinia pestis*. *PLoS ONE* 7:e52392. doi: 10.1371/journal.pone.0052392
- Sun, F., Zhang, Y., Qiu, Y., Yang, H., Yang, W., Yin, Z., et al. (2014). H-NS is a repressor of major virulence gene loci in *Vibrio parahaemolyticus*. *Front. Microbiol.* 5:675. doi: 10.3389/fmicb.2014.00675
- Sun, W., Six, D. A., Reynolds, C. M., Chung, H. S., Raetz, C. R., and Curtiss, R. III. (2013). Pathogenicity of *Yersinia pestis* synthesis of 1-dephosphorylated lipid A. *Infect. Immun.* 81, 1172–1185. doi: 10.1128/IAI.01403-12
- Sun, Y. C., Guo, X. P., Hinnebusch, B. J., and Darby, C. (2012). The *Yersinia pestis* Rcs phosphorelay inhibits biofilm formation by repressing transcription of the diguanylate cyclase gene hmsT. *J. Bacteriol.* 194, 2020–2026. doi: 10.1128/JB.06243-11
- Sun, Y. C., Koumoutsis, A., and Darby, C. (2009). The response regulator PhoP negatively regulates *Yersinia pseudotuberculosis* and *Yersinia pestis* biofilms. *FEMS Microbiol. Lett.* 290, 85–90. doi: 10.1111/j.1574-6968.2008.01409.x
- Tan, L., and Darby, C. (2005). *Yersinia pestis* is viable with endotoxin composed of only lipid A. *J. Bacteriol.* 187, 6599–6600. doi: 10.1128/JB.187.18.6599-6600.2005
- Tobes, R., and Ramos, J. L. (2002). AraC-XylS database: a family of positive transcriptional regulators in bacteria. *Nucleic Acids Res.* 30, 318–321. doi: 10.1093/nar/30.1.318
- Top, J., Paganelli, F. L., Zhang, X., Van Schaik, W., Leavis, H. L., Van Luit-Asbroek, M., et al. (2013). The *Enterococcus faecium* enterococcal biofilm regulator, EbrB, regulates the esp operon and is implicated in biofilm formation and intestinal colonization. *PLoS ONE* 8:e65224. doi: 10.1371/journal.pone.0065224
- Vadyvaloo, V., Jarrett, C., Sturdevant, D. E., Sebbane, F., and Hinnebusch, B. J. (2010). Transit through the flea vector induces a pretransmission innate immunity resistance phenotype in *Yersinia pestis*. *PLoS Pathog.* 6:e1000783. doi: 10.1371/journal.ppat.1000783
- Willias, S. P., Chauhan, S., Lo, C. C., Chain, P. S., and Motin, V. L. (2015). CRP-mediated carbon catabolite regulation of *Yersinia pestis* biofilm formation is enhanced by the carbon storage regulator protein, CsrA. *PLoS ONE* 10:e0135481. doi: 10.1371/journal.pone.0135481
- Willias, S. P., Chauhan, S., and Motin, V. L. (2014). Functional characterization of *Yersinia pestis* aerobic glycerol metabolism. *Microb. Pathog.* 76, 33–43. doi: 10.1016/j.micpath.2014.08.010
- Yang, J., Tauschek, M., and Robins-Browne, R. M. (2011). Control of bacterial virulence by AraC-like regulators that respond to chemical signals. *Trends Microbiol.* 19, 128–135. doi: 10.1016/j.tim.2010.12.001
- Yang, Y., and Isberg, R. R. (1997). Transcriptional regulation of the *Yersinia pseudotuberculosis* pH6 antigen adhesin by two envelope-associated components. *Mol. Microbiol.* 24, 499–510. doi: 10.1046/j.1365-2958.1997.3511719.x
- Zhan, L., Han, Y., Yang, L., Geng, J., Li, Y., Gao, H., et al. (2008). The cyclic AMP receptor protein, CRP, is required for both virulence and expression of the minimal CRP regulon in *Yersinia pestis* biovar microtus. *Infect. Immun.* 76, 5028–5037. doi: 10.1128/IAI.00370-08
- Zhang, Y., Wang, L., Han, Y., Yan, Y., Tan, Y., Zhou, L., et al. (2013). Autoregulation of PhoP/PhoQ and positive regulation of the cyclic AMP receptor protein-cyclic AMP complex by PhoP in *Yersinia pestis*. *J. Bacteriol.* 195, 1022–1030. doi: 10.1128/JB.01530-12
- Zhou, D., Tong, Z., Song, Y., Han, Y., Pei, D., Pang, X., et al. (2004). Genetics of metabolic variations between *Yersinia pestis* biovars and the proposal of a new biovar, microtus. *J. Bacteriol.* 186, 5147–5152. doi: 10.1128/JB.186.15.5147-5152.2004
- Zhou, D., and Yang, R. (2011). Formation and regulation of *Yersinia* biofilms. *Protein Cell* 2, 173–179. doi: 10.1007/s13238-011-1024-3

**Conflict of Interest Statement:** The authors declare that the research was conducted in the absence of any commercial or financial relationships that could be construed as a potential conflict of interest.

Copyright © 2018 Fang, Liu, Zhang, Yang, Yan, Ding, Han, Zhou and Yang. This is an open-access article distributed under the terms of the Creative Commons Attribution License (CC BY). The use, distribution or reproduction in other forums is permitted, provided the original author(s) and the copyright owner(s) are credited and that the original publication in this journal is cited, in accordance with accepted academic practice. No use, distribution or reproduction is permitted which does not comply with these terms.



# The Infection Process of *Yersinia ruckeri*: Reviewing the Pieces of the Jigsaw Puzzle

José A. Guijarro\*, Ana I. García-Torrico, Desirée Cascales and Jessica Méndez

Área de Microbiología, Departamento de Biología Funcional, Facultad de Medicina, Instituto de Biotecnología de Asturias (IUBA), Universidad de Oviedo, Oviedo, Spain

## OPEN ACCESS

### Edited by:

Victoria Auerbuch,  
University of California, Santa Cruz,  
United States

### Reviewed by:

Petra Dersch,  
Helmholtz-Zentrum für  
Infektionsforschung (HZI), Germany  
Gokhlesh Kumar,  
Veterinärmedizinische Universität  
Wien, Austria

### \*Correspondence:

José A. Guijarro  
jaga@uniovi.es

**Received:** 13 April 2018

**Accepted:** 08 June 2018

**Published:** 26 June 2018

### Citation:

Guijarro JA, García-Torrico AI,  
Cascales D and Méndez J (2018) The  
Infection Process of *Yersinia ruckeri*:  
Reviewing the Pieces of the Jigsaw  
Puzzle.  
Front. Cell. Infect. Microbiol. 8:218.  
doi: 10.3389/fcimb.2018.00218

Finding the keys to understanding the infectious process of *Yersinia ruckeri* was not a priority for many years due to the prompt development of an effective biotype 1 vaccine which was used mainly in Europe and USA. However, the gradual emergence of outbreaks in vaccinated fish, which have been reported since 2003, has awakened interest in the mechanism of virulence in this pathogen. Thus, during the last two decades, a large number of studies have considerably enriched our knowledge of many aspects of the pathogen and its interaction with the host. By means of both conventional and a variety of novel strategies, such as cell GFP tagging, bioluminescence imaging and optical projection tomography, it has been possible to determine three putative *Y. ruckeri* infection routes, the main point of entry for the bacterium being the gill lamellae. Moreover, a wide range of potential virulence factors have been highlighted by specific gene mutagenesis strategies or genome-wide transposon/plasmid insertion-based screening approaches, such as *in vivo* expression technology (IVET) and signature tagged mutagenesis (STM). Finally, recent proteomic and whole genomic analyses have allowed many of the genes and systems that are potentially implicated in the organism's pathogenicity and its adaptation to the host environmental conditions to be elucidated. Altogether, these studies contribute to a better understanding of the infectious process of *Y. ruckeri* in fish, which is crucial for the development of more effective strategies for preventing or treating enteric redmouth disease (ERM).

**Keywords:** *Yersinia ruckeri*, infection route, virulence genes, comparative genome, proteome analysis

## INTRODUCTION

*Yersinia ruckeri* is able to infect different fish species such as carp, catfish, sturgeon, perch and burbot (Tobback et al., 2007; Kumar et al., 2015), although it mainly affects salmonids. Interestingly, *Y. ruckeri* has recently been isolated as an unusual microorganism in a human wound infection (De Keukeleire et al., 2014) as well as in milk, cheese, chicken and minced meat (Özdemir and Arslan, 2015). In salmonids it causes enteric red mouth disease (ERM), which is important owing to the economic losses it causes in the aquaculture industry. ERM is a systemic disease affecting fish in all stages of development, causing a high degree of mortality. The disease occurs acutely in juveniles and has a tendency to become chronic in adult fish (Tobback et al., 2007). Some infected fish are asymptomatic, becoming carriers of the pathogen and acting as reservoirs of the bacterium. It is important to highlight that *Y. ruckeri* is a facultative intracellular bacterium, capable of surviving inside macrophages (Ryckaert et al., 2010).



*Y. ruckeri* strains have been classified into four serotypes (Romalde et al., 1993), the main outbreaks in fish farms being caused by serotype O1 biotype I, although other serotypes, particularly serotype O2, can also be involved (Romalde et al., 2003). Vaccination is the most effective way to control the disease. ERM biotype 1 vaccine, which was the first to be available for fish (Amend et al., 1983), has been used since the early 80s and is very effective in the prevention of the disease. However, during recent years worldwide outbreaks have been produced mainly by novel non-motile and lipase-negative strains, belonging to biotype II (Austin et al., 2003; Fouz et al., 2006; Arias et al., 2007; Calvez et al., 2014). These phenotypes have no appreciable effect on the virulence of the pathogen (Evenhuis et al., 2009; Welch et al., 2011), but the biotype 2 strains are able to elude the protection provided by the vaccine, probably due to the antigenic differences existing in their O-antigen with respect to biotype 1 strains (Tinsley et al., 2011). This has promoted the development and subsequent commercialization of a new vaccine which simultaneously confers protection against the two biotypes (Tinsley et al., 2011).

Owing to the prompt development of the vaccine, the study of the virulence mechanisms of this bacterium has been side-lined for a long time. Nevertheless, during the last few years a considerable number of reports related to the route of *Y. ruckeri* infection or its virulence, as well as several comparative genomic and proteomic analyses have been published. All of this knowledge about the infectious process of this bacterium is condensed and critically reviewed in the present article.

## YERSINIA RUCKERI INFECTION ROUTE

Studies aimed at determining the infection path and invasion mechanism of fish by *Y. ruckeri* have been carried out with different strains, modes of infection and experimental conditions, which sometimes makes it difficult to draw a conclusion. In addition, various tools have been developed and used for elucidating the interaction between *Y. ruckeri* and rainbow trout, its natural host.

Bacterial counting in fish tissues at different times after experimental infection (Tobback et al., 2009, 2010); GFP tagging of *Y. ruckeri* and further visualization by epifluorescence or flow cytometry in tissues (Welch and Wiens, 2005); *in situ* hybridization (Khimmakthong et al., 2013); bioluminescence imaging using strains harboring the *luxCDABE* operon from *Photobacterium luminescens* (Méndez and Guíjarro, 2013) and optical projection tomography (OPT) (Ohtani et al., 2014), a recently developed three-dimensional bioimaging technique combined with immunohistochemical assay (IHC) (Tobback et al., 2009; Ohtani et al., 2014), have all been used. Each of these technologies provides a different approach to determining the route of entry and tissue distribution of *Y. ruckeri*. Although all of them have limitations, if we analyse the results obtained as a whole, it seems that the gills are the portal of entry for the bacterium into the fish. In effect, most studies have established this organ as the first to be infected (Tobback et al., 2009; Khimmakthong et al., 2013; Ohtani et al., 2014, 2015), and more

specifically the pavement cells of the gill lamellae, from which the bacterium would spread to blood (Ohtani et al., 2014). Thus, *Y. ruckeri* was detected only 1 min post infection in the blood, where the number of bacteria increased for 40 min, reaching  $2.3 \times 10^5$  CFU/ml (Ohtani et al., 2014). Although gills seem to be the main point of entry of *Y. ruckeri*, other sites in the fish cannot be excluded. In effect, most studies establish the presence of *Y. ruckeri* in the intestine shortly after infection (Khimmakthong et al., 2013; Ohtani et al., 2014, 2015). It is known that the mucus of the gills is twice as efficient as that of the intestine in enabling the adherence of the bacterium (Tobback et al., 2010). Moreover, after infection, twice as many bacteria were detected in the gills as in the intestine (Tobback et al., 2009; Khimmakthong et al., 2013). However, bacteria have been detected in the intestine from 1 min (Khimmakthong et al., 2013) to 30 min post-infection (Ohtani et al., 2014). Additionally, intestinal dissemination is the main sign of the pathology (Figure 1) (Méndez and Guíjarro, 2013; Ohtani et al., 2014). This, together with the fact that it is unusual for an intestinal pathogen to enter the host by any other route than the oral one means that the digestive tract cannot be excluded as another portal of entry. In addition, Ohtani et al. (2014) used OPT analysis to establish a third route of infection for *Y. ruckeri*, through the skin surface on the lateral line, from which it would penetrate to internal cell layers, a similar result to that found by Khimmakthong et al. (2013). A recent study reported the ability of two isolates of *Y. ruckeri* to invade different types of salmon epithelial cells (Menanteau-Ledouble et al., 2018), the biotype 1 isolate (ATCC 29473) being more infectious than the non-motile biotype 2 strain (A7959-11). The authors suggested that the bacterium could enter host cells by means of several mechanisms that take advantage of cytoskeletal systems. The capacity to invade the epithelium would undoubtedly facilitate entry into the host.

In conclusion, all the results indicate that *Y. ruckeri* can access the interior of rainbow trout by at least three different paths: the gills, lateral line and digestive tract. From these locations bacteria would spread to the blood circulation system to further colonize

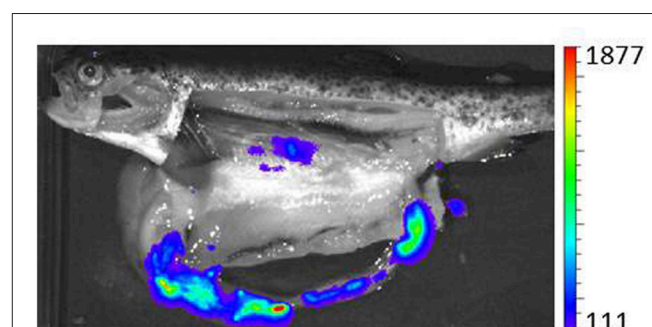


**FIGURE 1** | Bioluminescent tracking of *Y. ruckeri* harboring pGS26-Pac in a fish infected by bath immersion with  $10^7$  cfu ml<sup>-1</sup> for 1 h. Bioluminescence emitted by the bacterium was captured three days postinfection by Ivis-Lumina equipment. Color standards represent “RLU max.” This measure expresses the highest number of counts in a pixel inside the region analyzed (Figure taken from Méndez and Guíjarro, 2013).

and infect other internal organs, causing in many cases the death of the fish.

## DEFINED GENES RELATED TO VIRULENCE

Despite its being a microorganism responsible for a high proportion of losses in continental aquaculture, there are few studies on *Y. ruckeri* virulence factors, perhaps as a consequence of the early development of a vaccine, which made their study unattractive. Many of the virulence factors described so far refer to extracellular factors (ECF) that are common to a wide range of gram-negative pathogenic bacteria, particularly the enterobacteria group (Table 1, Figure 2). Indeed, extracellular proteases, haemolysins and siderophores are among the main extracellular molecules involved in the *Y. ruckeri* infection process.

Yrp1 is a serralyisin family extracellular metalloprotease, widely characterized from an enzymatic point of view (Secades and Guijarro, 1999) and secreted through an ABC transport system (Fernández et al., 2002). It is able to degrade different matrix and muscle proteins such as laminin, fibrinogen, gelatin, actin, and myosin (Fernandez et al., 2003). Although it was shown not to be present in all virulent *Y. ruckeri* strains (Secades and Guijarro, 1999), its presence makes the bacteria more virulent. Transcriptional fusion between the *luxCDABE* operon and the *yrp1* promoter demonstrated that *yrp1* is induced more *in vivo* than *in vitro* (Méndez and Guijarro, 2013). This is consistent with the expression of *yrp1* in fish tissues and the observation that an *yrp1* mutant strain is significantly attenuated in virulence (Fernández et al., 2002). Interestingly, a heat-inactivated Yrp1 toxoid was able to elicit a strong protection against the ERM disease (Fernandez et al., 2003). All of this established a clear and important role for this protease in the pathogenic process.

Additional degrading enzymes were identified in *Y. ruckeri*, such as two putative peptidases belonging to the U32 family which are encoded by the *yrpAB* operon (Navais et al., 2014b). Both genes, *yrpA* and *yrpB*, are present in a similar genetic organization in different pathogens of the enterobacteria group, including human pathogenic *Yersinia* species (Navais et al., 2014b). A synergistic effect occurred in the induction of the *yrpAB* operon under low oxygen conditions when peptones were also present in the culture medium (Navais et al., 2014b). Infection studies with a *yrpA* mutant strain suggest that the YrpA peptidase contributes to virulence in a similar way to the U32 peptidases of *Proteus mirabilis* (Zhao et al., 1999) and *Helicobacter pylori* (Kavermann et al., 2003). A more detailed analysis of the role of these peptidases in the virulence of pathogenic *Yersiniae* could be interesting from a public health point of view.

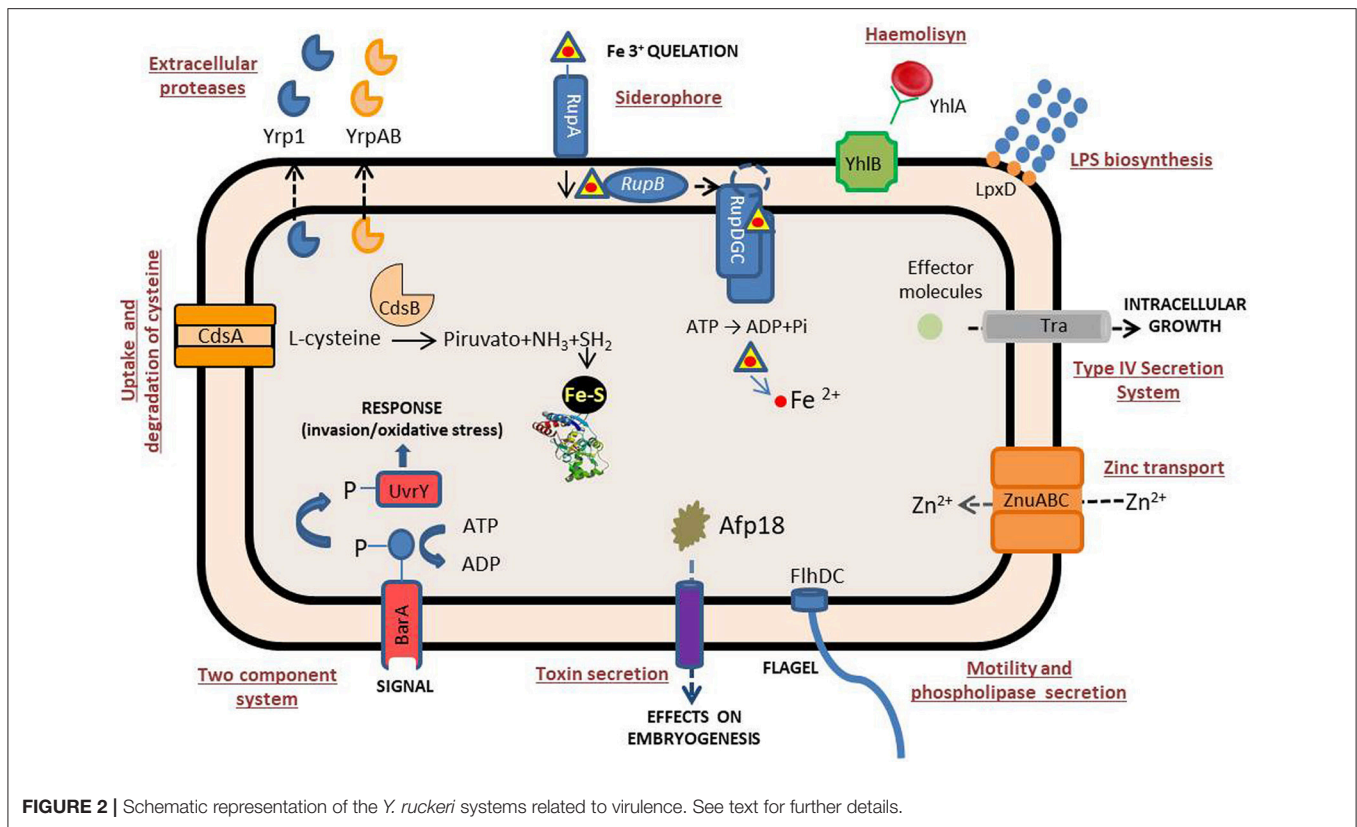
Two different genetic approaches have been applied to allow the selection and further identification of *Y. ruckeri* genes related to the infection process: *in vivo* expression technology (IVET) (Fernandez et al., 2004) and signature-tagged mutagenesis (STM) (Dahiya and Stevenson, 2010a). Each of these has advantages and disadvantages, but undoubtedly, their application has led to the identification of a number of genes related to *Y. ruckeri* pathogenesis.

IVET allowed the identification of up to 14 genes specifically induced *in vivo*, during the infection process of *Y. ruckeri*. Among them, those related to two-component and type IV secretion systems, adherence, haemolytic activity and iron acquisition were further analyzed. It has been found that the genes involved in iron acquisition through the catechol siderophore ruckerbactin have a genetic organization similar to those of the *E. coli* enterobactin gene cluster (Fernandez et al., 2004). Regulation of this cluster depends on iron availability and temperature in such a way that low iron conditions and low temperature (18°C in relation to 28°C) induced its expression (Fernandez et al., 2004). It was shown that production of the siderophore is upregulated during the infection of fish (Fernandez et al., 2004; Fernández et al., 2007a) and it is also involved in virulence since 100-fold attenuation, in relation to the parental strain, was obtained when an isogenic mutant in *rucC*, a gene from the ruckerbactin cluster, was used in LD<sub>50</sub> experiments (Fernandez et al., 2004).

A putative additional system of *Y. ruckeri* for obtaining iron is the *yhlBA* cluster, also identified by IVET. The *yhlA* gene encodes a *Serratia*-type haemolysin, whereas the *yhlB* product is related to the secretion/activation of YhlA (Fernández et al., 2007b) (Figure 2). Analysis of *yhlB::lacZY* transcriptional fusion indicated that higher levels of expression of *yhlB* were obtained under iron-starvation conditions, and also at 18°C than at 28°C (Fernández et al., 2007b). Interestingly, the involvement of the two genes in bacterial virulence is indicated not only by the virulence attenuation obtained when *yhlA* and *yhlB* insertional mutants were used, but also by the cytolytic properties of YhlA against the BF-2 fish cell line (Fernández et al., 2007b). *In vivo* monitoring of *yhlBA* promoter showed that it was highly expressed (Méndez and Guijarro, 2013), as was expected, since the system had been previously isolated as an IVET clone. In

TABLE 1 | Virulence related genes of *Y. ruckeri*.

Gene	Function	References
<i>yrp1</i>	Extracellular protease	Secades and Guijarro, 1999
<i>yrpAB</i>	Peptidases	Navais et al., 2014b
<i>rucC</i>	Iron captation. Ruckerbactin Siderophore synthesis	Fernandez et al., 2004
<i>yhlA</i>	Hemolysine	Fernández et al., 2007b
<i>tral</i>	Type IV secretion system	Méndez et al., 2009
<i>cdsBA</i>	Cysteine transport and degradation	Méndez et al., 2011
<i>znuA</i>	Zinc transport	Dahiya and Stevenson, 2010b
<i>uvrY</i>	Response regulator. Two component system	Dahiya and Stevenson, 2010c
<i>lpxD</i>	Lipid A biosynthesis	Altinok et al., 2016
<i>afp18</i>	Toxin. Glycosyltransferase	Jank et al., 2014
<i>flhD</i>	Motility regulation	Jozwick et al., 2016



contrast to *yrp1*, the *yhlaB* operon is present and the haemolytic activity is detectable in different *Y. ruckeri* strains from different origins and geographical locations. This indicates that this operon is of importance for virulence in this species (Fernández et al., 2007b).

The analysis of a chromosomally located *traHIJKLMN* operon of *Y. ruckeri* that was identified by IVET showed that it was structurally related to the DNA transfer system present in the pADAP virulence-related plasmid of *Serratia entomophila* (Hurst et al., 2003). The cluster was present in different *Y. ruckeri* strains but it was not found in the genomic analysis of human pathogenic *Yersinia* (Méndez et al., 2009). This operon is composed of at least eight genes displaying homology with type IV secretion systems (T4SS). Indeed, *traH*, *traI*, *traJ*, and *traK* genes encoded for proteins similar to those encoded by the *dot/icm* genes of the T4SS of *Legionella pneumophila* (Komano et al., 2000). Thus, it is likely that the gene products of the *tra* operon constitute parts of the T4SS involved in the transfer of virulence factors. In fact, insertional mutagenesis of the *traI* gene resulted in attenuation of the virulence (Méndez et al., 2009). Like other virulence factors, the *tra* operon was more highly expressed at 18°C than at 28°C.

A novel two-gene operon *cdsBA* involved in the transport and further degradation of L-cysteine was also selected by IVET. Attenuation of a *cdsA* mutant supported a role in virulence (Méndez et al., 2011). The *cdsB* gene encoded an L-cysteine desulfidase involved in cysteine degradation, previously

characterized in the archaeal *Methanocaldococcus jannaschii* (Tchong et al., 2005), whereas *cdsA* is a cysteine permease (Méndez et al., 2011). Interestingly, the operon was shown to be present in several anaerobic and facultative bacterial groups, particularly in some species of enterobacteria, including *Y. enterocolitica*, although it was absent in *Y. pseudotuberculosis* and *Y. pestis* (Méndez et al., 2011). This operon was specifically induced by L-cysteine under low oxygen conditions and the uptake of this amino acid was an energy-dependent process (Méndez et al., 2011). Transcriptional fusion of the *cdsBA* promoter with the *luxCDABE* operon showed that the *cdsA* and *cdsB* genes were barely expressed under routine laboratory conditions but were found to have high activity inside the fish. Therefore, virulence attenuation of the *cdsA* mutant underlines the importance of this operon for the bacterium during the infection process. Although the precise role of the CdsAB system remains unknown, it was suggested that it could be involved in the generation of iron-sulfur-centers for Fe-S proteins or in the accumulation of glutathione, an important detoxification and redox buffer molecule in the cell (Méndez et al., 2011).

Interestingly, more of these IVET-selected genes are induced at 18°C, the temperature around which outbreaks of the disease take place, than at 28°C, the optimal temperature for growth of the bacterium (Fernández et al., 2007b; Méndez et al., 2009). This finding points to the existence in *Y. ruckeri* of specific mechanisms (thermo-induced changes of DNA supercoiling, RNA and protein thermometer, etc.) for the temperature



regulation of virulence at temperatures below the optimal for its growth, as seems to occur in a good number of microorganisms that infect ectothermic animals (Guíjarro et al., 2015).

STM was also able to select *Y. ruckeri* mutants that can survive *in vitro* but not in the fish host (Dahiya and Stevenson, 2010a). Further identification of the inactivated genes in these mutants revealed up to 25 different ORFs (Dahiya and Stevenson, 2010a), among which the *znuA* gene, coding a zinc binding protein, and the *uvrY* gene, coding a response regulator, were chosen for deeper study. The *znuA* gene forms part of the *znuABC* operon encoding a high-affinity zinc transporter, which has a genetic organization similar to that found in *E. coli* (Patzer and Hantke, 2000) and *S. Typhimurium* (Campoy et al., 2002). In fact, the introduction of the *Y. ruckeri* *znuABC* locus was able to restore the growth of a *znuABC* mutant of *E. coli* in zinc-deficient media (Dahiya and Stevenson, 2010b). The *znuABC* system is widely distributed in bacteria such as *Brucella abortus* (Kim et al., 2004), *Campylobacter jejuni* (Davis et al., 2009) and *Neisseria gonorrhoeae* (Lim et al., 2008), contributing to their virulence. Interestingly, mutations in the *znuABC* system of *Y. pestis* did not affect virulence (Bobrov et al., 2014, 2017). The reason is that this bacterium has an additional zinc transport system mediated by some components of the yersiniabactin siderophore (Ybt) which is able to sequester zinc in addition to iron (Bobrov et al., 2014, 2017). In mouse models of bubonic and pneumonic plague this system compensates for the loss of *znuABC*. However, the simultaneous absence of both systems leads to a decrease in *Y. pestis* virulence (Bobrov et al., 2014, 2017). However, in *Y. ruckeri* it seems that the *znuABC* system is the main Zn acquisition system, since the *znuA* mutant had nearly 150- to 350-fold lower infection loads in the kidney of rainbow trout than the parental strain, which demonstrates that this Zn transport system has an important role in the infection process (Dahiya and Stevenson, 2010b).

In another mutant selected by STM, the BarA-UvrY two-component system was inactivated. This mutant was recovered from fish in 5- to 15-fold lower numbers compared to the parental strain at the beginning of the infection (Dahiya and Stevenson, 2010c), suggesting that this system is involved in the invasion of gills or gut tissues, as occurred in the *uvrY* mutants of *Y. pseudotuberculosis* (Heroven et al., 2008), *E. coli* (Herren et al., 2006) and *S. Typhimurium* (Johnston et al., 1996). In addition, the *Y. ruckeri* *uvrY* mutant was more sensitive to H<sub>2</sub>O<sub>2</sub>, which suggests an increasing susceptibility to oxidative killing by phagocytic cells. All of this resulted in a lower recovery (10<sup>3</sup>- to 10<sup>5</sup>-fold) of the *uvrY* mutant than the parental strain at the end of co-infection experiments which were carried out by immersion of rainbow trout in water containing both strains (Dahiya and Stevenson, 2010c).

As expected, LPS is important for the pathogenesis of *Y. ruckeri* (Altinok et al., 2016). Specific deletion of the *lpxD* gene, involved in the lipid A biosynthesis, resulted in an LPS-deficient strain. This *lpxD* mutant showed a significant attenuation of virulence (10<sup>3</sup>-fold) in relation to the parental strain when LD<sub>50</sub> determination was carried out by injection (Altinok et al., 2016). It is important to highlight that *lpxD* mutation reduced the overall number of invasive bacteria, which in turn, may influence

the process of invasion and colonization, leading to a decrease in virulence. Special attention must be paid to a virulence factor related to legionaminic acid, a component of the *Y. ruckeri* LPS that will be addressed in the next section.

Another interesting virulence factor that has been described in *Y. ruckeri* is the Afp18 toxin, although it should be noted that its effect has hitherto only been tested in zebrafish embryos (Jank et al., 2014). This is encoded by a gene that is part of the antifeeding prophage gene cluster (*afp*), consisting in a 25 Kb DNA segment involved in the production of a prophage contractile tail. This cluster is similar to the one found in *Serratia entomophila* (Rybakova et al., 2013; Jank et al., 2014), which has common characteristics with the R-pyocins type VI secretion system delivery apparatus of *Pseudomonas aeruginosa* (Heymann et al., 2013). This contractile tail is thought to capture the Afp18 toxin and inject it into the cell cytoplasm of zebrafish blastoderm cells (Jank et al., 2014). The Afp18 protein has a glycosyltransferase domain. Its activity alters the early phase of zebrafish embryogenesis, whereas a non-functional Afp18 lacking the glycosyltransferase domain has no effect on development (Jank et al., 2014). The effect of the Afp18 glycosyltransferase is through a process of specific tyrosine mono-O-GlcNAcylation of RhoA, a regulatory GTPase associated with cytoskeleton development, resulting in actin depolymerization and the abrogation of early zebrafish development (Jank et al., 2014). Interestingly, genome analysis indicates that this antifeeding prophage system is widely distributed among prokaryotes and archaea (Sarris et al., 2014). In *S. entomophila* the Afp18 toxin acts as a virulence factor during the infection of insects (Rybakova et al., 2013), and could also be important as a virulence factor in human pathogenic bacteria. Since all this work was carried out on zebrafish embryos, it could be interesting to study the role of Afp18 on *Y. ruckeri* infection of rainbow trout by generating a mutant strain and following the progression of the disease.

Finally, two elements that should be taken into account are the *flhDC* operon, whose inactivation results in a more virulent strain and the heat sensitive factor (HSF), which has been considered as a virulence factor for a good number of years. The *flhDC* is a flagellar master operon of *Y. ruckeri* involved in the regulation of motility and phospholipase secretion, among other processes (Jozwick et al., 2016). In fact, mutation of the *flhD* gene resulted in significant changes in the bacterial transcriptome (Jozwick et al., 2016). Interestingly, no differences were found between the *flhD* mutant and the wild type strain when a standard experimental challenge model with mortalities as an endpoint was used. However, there was a significant increase in the *flhD* mutant density within the spleen in relation to the wild type strain in competition experiments, a characteristic which was reverted in the complemented strain (Jozwick et al., 2016). The result indicated that mutation of the *flhDC* operon gives a competitive advantage over the parental strain during the infection process. Although it is not known how the mutation in this operon affects bacterial virulence, the result is similar to that found in the *S. Typhimurium* *flhD* mutant in the sense that it was more virulent than the parental strain (Schmitt et al., 2001).



It is also worth mentioning that for many years it was thought HSF was required for virulence in *Y. ruckeri* (Furones et al., 1993). However, this assumption was recently discarded, since HSF was found to be an alkylsulphatase enzyme encoded by the *yraS* gene, whose mutation did not produce any modification in the virulence of the strain in relation to the wild type (Navais et al., 2014a).

## PREDICTED VIRULENCE FACTORS DEDUCED FROM PROTEOMIC AND GENOMIC ANALYSIS

During recent years the development of alternative technologies based on proteomic, transcriptomic and genomic analyses has provided new tools to identify potential virulence factors in bacteria. It is important to consider that this type of analysis is based on comparison and only predicts the potential role of some of the genes or proteins identified as virulence factors. In *Y. ruckeri*, proteomic studies have been carried out under very specific culture conditions. Thus, differentially regulated proteins were identified and quantified in normal and iron-limited media using a label-free, gel-free shotgun proteomic approach (Kumar et al., 2016). Iron is an essential nutrient for bacteria that is difficult to obtain during the infection process, so a limited-iron environment is expected to induce a set of genes, some of which are related to pathogenesis. Under reduced iron availability, the majority of up-regulated proteins in biotype 1 and biotype 2 *Y. ruckeri* strains were related to iron-binding proteins (YfuA, YiuA and YfeA), iron-binding transporters (HemS and Feo), hemin transport (YhlBA) and TonB-dependent iron binding receptor, the latter probably being involved in the transport of ruckerbactin into the periplasm of cells and siderophore biosynthesis proteins. YfeA and YhlBA systems have

previously been described as important virulence factors in *Y. pestis* (Bearden and Perry, 1999) and *Y. ruckeri* (Fernández et al., 2007b), respectively. Another up-regulated protein under iron-limited conditions was a superoxide dismutase, involved in protective mechanisms against oxidative stress, and particularly important in intracellular pathogens such as *Y. ruckeri*. Interestingly, this study revealed no significant differences in protein profile, using liquid chromatography-mass spectrometry analyses, between motile and non-motile *Y. ruckeri* strains, corresponding with biotype 1 and biotype 2, when they were cultured under iron-limited conditions, indicating that iron availability it is not involved in the differential virulence behavior of the two biotypes (Kumar et al., 2016).

A similar study was conducted in order to establish the differential protein profile between virulent and avirulent strains of *Y. ruckeri* grown under standard conditions (Kumar et al., 2017). Interestingly, in virulent strains, a total of 16 proteins were shown to be upregulated, including the haemolysis expression regulator HtrA, DegQ proteases, an anti-sigma regulator factor, different transcriptional regulators belonging to the LuxR, AsnC, and PhoP families, RNA-binding protein Hfq, invasion protein Inv, Cu-Zn superoxide dismutase, among others. All of these have been previously described as virulence-related proteins in different bacterial pathogens, which strongly suggests a role for them in the infection process of *Y. ruckeri*.

Invasins play an essential role in the initial colonization and attachment of *Y. enterocolitica* and *Y. pseudotuberculosis* (Chauhan et al., 2016). In *Y. ruckeri*, invasin (*yrInv*) and invasin-like molecule (*yrllm*) are two putative inverse autotransporter genes that, according to qRT-PCR analysis, were upregulated in a medium that mimics the environmental conditions present in the fish host (Wrobel et al., 2018), so they are likely to be involved in the infection process of *Y. ruckeri* although there are no conclusive data.

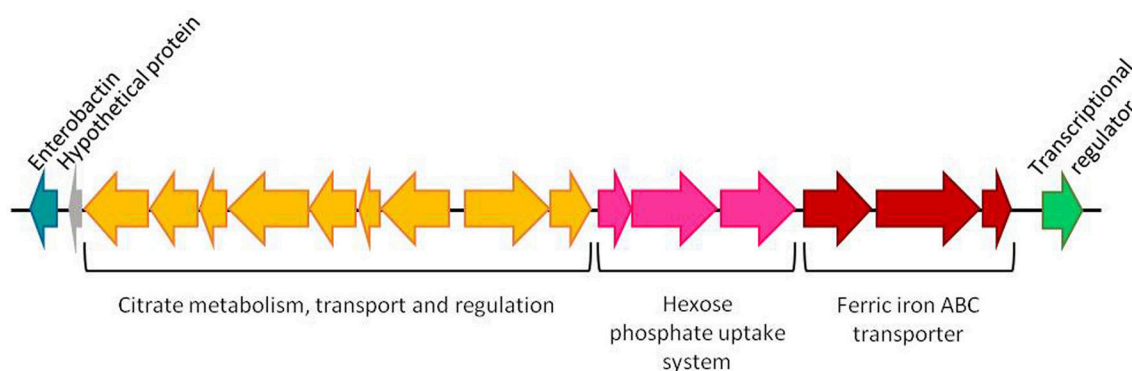


**FIGURE 3 |** Cluster of genes absent from *Y. ruckeri* ATCC29473 type strain and present in the strains *Y. ruckeri* 150, CSF007-82, Big Creek and SC09. The region contains genes encoding for an enterobactin-like siderophore (blue), nine genes involved in the uptake and metabolism of citrate (yellow), a group of three genes related to hexose phosphate uptake (pink), three genes involved in iron transport (red) and a Crp-Fnr family transcriptional regulator (green). (1) Citrate succinate antiporter, (2) 2-(5'-triphosphoribosyl)-3'-dephosphocoenzyme-A synthase, (3) Apo-citrate lyase phosphoribosyldephospho-CoA transferase, (4) Citrate lyase alpha chain, (5) Citrate lyase beta chain, (6) Citrate lyase gamma chain acyl carrier protein, (7) [Citrate[pro-3S]-lyase] ligase, (8) Sensor kinase, (9) Transcriptional regulatory protein, (10) Transcriptional regulatory protein, (11) Sensor histidine protein kinase glucose-6-phosphate specific, (12) Hexose phosphate uptake regulatory protein, (13) Ferric iron ABC transporter iron-binding protein, (14) Ferric iron ABC transporter permease protein, (15) Ferric iron ABC transporter binding subunit (Figure taken from Cascales et al., 2017).

Whole genome analysis of *Y. ruckeri* strains provides a new approach to identifying putative virulence factors. Indeed, genome analysis of the *Y. ruckeri* SC09 strain isolated from catfish (*Ictalurus punctatus*) showed that it harbors a *ysa* locus containing all the genetic components of a type III secretion system (T3SS) quite similar in gene sequence and genetic structure to the *Salmonella enterica* pathogenicity island 1 and chromosomally encoded T3SS of *Y. enterocolitica* 1B (Liu et al., 2016). It should be remembered that T3SS are present only in virulent strains of human pathogenic *Yersinia* (Chen et al., 2010). For this reason, it is possible that the T3SS of *Y. ruckeri* contributes to the survival of the bacterium in fish macrophages and helps in the invasion of gill and gut epithelia. Other putative systems in *Y. ruckeri* SC09 that, according to the genomic analysis carried out by Liu et al. (2016), could be involved in the development of the infection in fish are: a type II secretion system, different two-component signal transduction systems and a phage shock protein system (Psp), which is distributed among enterobacteria and is implicated in the virulence of *Salmonella*, *Shigella* and *Yersinia* species (Huvet et al., 2011). Interestingly, a type IV secretion system described as a putative virulence factor by Liu et al. (2016) is unique to *Y. ruckeri* SC09 strain and it is not present in the other four *Y. ruckeri* strains analyzed by Cascales et al. (2017).

The comparative analysis of the genome sequences of five *Y. ruckeri* strains showed that, although they share approximately 75% of their genes, significant genetic differences were detected depending on the serotype or virulence of these strains (Cascales et al., 2017). Thus, a cluster of 18 genes related to the biosynthesis of legionaminic acid, the major component of the LPS, was exclusively present in serotype O1 strains. This cluster was absent in serotype O2 strains as well as in other *Yersinia* species, but present in different aquatic pathogenic bacteria such as *Vibrio vulnificus*, *Aeromonas salmonicida*, *Vibrio fischeri* (Cascales et al., 2017) and also in *Campylobacter jejuni*, where it is involved in virulence (Zebian et al., 2016). In addition to this cluster, serotype O1 strains share a total of 268 genes, among which are the *invasin* and the type IV secretion system corresponding with the *traHIJKLMN* operon (Méndez et al., 2009).

These genes shared by serotype O1 strains could adapt the bacterium to a particular host, since the three serotype O1 strains analyzed (150, CSF007-82, and ATCC29473) were isolated from rainbow trout. In the same way, a serotype O2 strain (Big Creek 74) together with *Y. ruckeri* SC09, a putative O2 strain, which were isolated from chinook salmon and catfish respectively, share 122 genes which are absent in serotype O1 strains. These include a cluster involved in fimbriae biosynthesis similar to the *Stf* cluster of *S. Typhimurium*, associated with virulence (Emmerth et al., 1999) and an insecticidal toxin complex similar to the one found in *Vibrio parahaemolyticus*, involved in hepatopancreatic necrosis disease in penaeid shrimps (Tang and Lightner, 2014).

In the study of Cascales et al. (2017) it is proposed that the characteristic attenuation in virulence of the ATCC29473 type strain is a consequence of the lack of 21 genes that were present in the other virulent strains. It should be noted that 17 out of these 21 genes are clustered in all four genomes analyzed (Figure 3). This region includes genes encoding a Crp-Fnr family

transcriptional regulator, enzymes related to enterobactin-like siderophore and gene clusters involved in iron transport, hexose phosphate uptake and citrate metabolism. Most of these genes are related to virulence in different bacteria (Gray et al., 2006; Urbany and Neuhaus, 2008; Moisi et al., 2013) so the absence of this region could be responsible for the attenuation of the type strain.

## CONCLUSIONS AND FURTHER STUDIES

The results lead to the conclusion that there exist at least three different routes of infection by *Y. ruckeri*. The most important pathway for the development of ERM has still to be elucidated, but it seems clear that, although the primary bacteremia is generated by the entry of the bacterium into the fish through the gills, the very significant presence of the bacterium in the intestine and also the signs of the disease, strongly suggest that the digestive route must play a relevant role. The virulence of *Y. ruckeri* is multifactorial and it depends not only on the presence of certain genes in each strain but also on certain environmental factors, particularly, temperature. In fact, a temperature below the optimal for bacterial growth and close to the one at which outbreaks occur seems to be important in the expression of some of the genes encoding virulence factors. This appears to be one of the areas for future research, since presently unknown regulation systems could be involved in this temperature-dependent response. Although a lot of genes involved in the pathogenesis of the bacterium have recently been identified, there are still many points that need to be addressed, such as the temporal and spatial expression pattern of each virulence factor and their specific function or the identification of the regulatory mechanisms which modulate the virulence gene expression. The new techniques and methodologies developed in recent years, including CLIQ-BID, a method allowing quantification of damage in eukaryotic cells infected by bacteria (Wallez et al., 2018), the new RNA-seq techniques such as Term-seq (Dar et al., 2016) and Dual RNA-seq (Westermann et al., 2016), useful for the analysis of pathogens under complex environmental conditions and Single Cell RNA-seq (Avraham et al., 2015; Saliba et al., 2017) can help to develop different approaches. Moreover, analysis of the data provided by the genetic and proteomic studies may be a good starting point for elucidating the role of new genes in the infectious process of *Y. ruckeri*. In fact, two specific gene clusters should be considered for their potential role in virulence. This is the case of a cluster involved in legionaminic acid biosynthesis that could be important in the pathogenesis of serotype O1 strains, and the 21 genes absent from the virulence-attenuated *Y. ruckeri* type strain, some of them encoding putative virulence factors.

## AUTHOR CONTRIBUTIONS

JG and JM drafted the first version of the manuscript. DC, JM, AG-T, JG contributed to bibliography analysis and manuscript improvement. All authors have reviewed the final version of the manuscript.

## FUNDING

This research was supported by the AGL2015-66018-R grant from the Ministerio de Economía y Competitividad of Spain.

## REFERENCES

- Altinok, I., Ozturk, R. C., Kahraman, U. C., and Capkin, E. (2016). Protection of rainbow trout against yersiniosis by *lpxD* mutant *Yersinia ruckeri*. *Fish Shellfish Immunol.* 55, 21–27. doi: 10.1016/j.fsi.2016.04.018
- Amend, D. F., Johnson, K. A., Croy, T. R., and McCarthy, D. H. (1983). Some factors affecting the potency of *Yersinia ruckeri* bacterins. *J. Fish Dis.* 6, 337–344.
- Arias, C. R., Olivares-Fuster, O., Hayden, K., Shoemaker, C. A., Grizzle, J. M., and Klesius, P. H. (2007). First report of *Yersinia ruckeri* biotype 2 in the USA. *J. Aquat. Anim. Health* 19, 35–40. doi: 10.1577/H06-011.1
- Austin, D. A., Robertson, P. A., and Austin, B. (2003). Recovery of a new biogroup of *Yersinia ruckeri* from diseases rainbow trout (*Oncorhynchus mykiss*, Walbaum). *Syst. Appl. Microbiol.* 26, 127–131. doi: 10.1078/072320203322337416
- Avraham, R., Haseley, N., Brown, D., Penaranda, C., Jijon, H. B., et al. (2015). Pathogen cell-to-cell variability drives heterogeneity in host immune response. *Cell* 162, 1309–1321. doi: 10.1016/j.cell.2015.08.027
- Bearden, S. W., and Perry, R. D. (1999). The Yfe system of *Yersinia pestis* transports iron and manganese and is required for full virulence of plague. *Mol. Microbiol.* 32, 403–414.
- Bobrov, A. G., Kirillina, O., Feterston, D., Miller, M. C., Burlison, J. A., and Perry, R. D. (2014). The *Yersinia pestis* siderophore, yersiniabactin, and the ZnuABC system both contribute to zinc acquisition and the development of lethal septicaemic plague in mice. *Mol. Microbiol.* 93, 759–775. doi: 10.1111/mmi.12693
- Bobrov, A. G., Kirillina, O., Fosso, M. Y., Fetherston, J. D., Miller, M. C., VanCleave, T. T., et al. (2017). Zinc transporters YbtX and ZnuABC are required for the virulence of *Yersinia pestis* in bubonic and pneumonic plague in mice. *Metallomics* 21, 757–772. doi: 10.1039/c7mt00126f
- Calvez, S., Gantelet, H., Blanc, G., Douet, D. G., and Daniel, P. (2014). *Yersinia ruckeri* biotypes 1 and 2 in France: presence and antibiotic susceptibility. *Dis. Aquat. Organ.* 109, 117–126. doi: 10.3354/dao02725
- Campoy, S., Jara, M., Busquets, N., de Rozas, A. M. P., Badiola, I., and Barbe, J. (2002). Role of the high-affinity zinc uptake *znuACB* system in *Salmonella enterica* serovar *Typhimurium* virulence. *Infect. Immun.* 70, 4721–4725. doi: 10.1128/IAI.70.8.4721-4725.2002
- Cascales, D., Guijarro, J. A., García-Torrico, A. I., and Méndez, J. (2017). Comparative genome analysis reveals important genetic differences among serotype O1 and serotype O2 strains of *Yersinia ruckeri* and provides insights into host adaptation and virulence. *Microbiologyopen* 6. doi: 10.1002/mbo3.460
- Chauhan, N., Wrobel, A., Skurnik, M., and Leo, J. C. (2016). *Yersinia* adhesins: an arsenal for infection. *Proteomics Clin. Appl.* 10, 949–963. doi: 10.1002/prca.201600012
- Chen, P. E., Cook, C., Stewart, A. C., Nagarajan, N., Sommer, D. D., et al. (2010). Genomic characterization of the *Yersinia* genus. *Genome Biol.* 4:11. doi: 10.1186/gb-2010-11-1-r1
- Dahiya, I., and Stevenson, R. M. W. (2010a). *Yersinia ruckeri* genes that attenuate survival in rainbow trout (*Oncorhynchus mykiss*) are identified using signature-tagged mutants. *Vet. Microbiol.* 144, 399–404. doi: 10.1016/j.vetmic.2010.02.003
- Dahiya, I., and Stevenson, R. M. W. (2010b). The *ZnuABC* operon is important for *Yersinia ruckeri* infections of rainbow trout, *Oncorhynchus mykiss* (Walbaum). *J. Fish Dis.* 33, 331–340. doi: 10.1111/j.1365-2761.2009.01125x
- Dahiya, I., and Stevenson, R. M. W. (2010c). The UvrY response regulator of the BarA–UvrY two-component system contributes to *Yersinia ruckeri* infection of rainbow trout (*Oncorhynchus mykiss*). *Arch. Microbiol.* 192, 541–547. doi: 10.1007/s00203-010-0582-8
- Dar, D., Shamir, M., Mellin, J. R., Koutero, M., Stern-Ginossar, N., Cossart, P., et al. (2016). Term-seq reveals abundant ribo-regulation of antibiotics resistance in bacteria. *Science* 352:aad9822. doi: 10.1126/science.aad9822

## ACKNOWLEDGMENTS

DC and AG-T were the recipients of FPU and FPI fellowships, respectively.

- Davis, L. M., Kakuda, T., and DiRita, V. J. (2009). A *Campylobacter jejuni* *znuA* orthologue is essential for growth in low-zinc environments and chick colonization. *J. Bacteriol.* 191, 1631–1640. doi: 10.1128/JB.01394-08
- De Keukeleire, S., De Bel, A., Jansen, Y., Wauters, G., and Pierard, D. (2014). *Yersinia ruckeri*, an unusual microorganism isolated from a human wound infection. *New Microbe. New Infect.* 2, 134–135. doi: 10.1002/nmi2.56
- Emmerth, M., Goebel, W., Miller, S. I., and Hueck, C. J. (1999). Genomic subtraction identifies *Salmonella typhimurium* prophages, F-related plasmid sequences, and a novel fimbrial operon, *stf*, which are absent in *Salmonella typhi*. *J. Bacteriol.* 181, 5652–5661.
- Evenhuis, J. P., La Patra, S. E., Verner-Jeffreys, D. W., Dalgaard, I., and Well, T. J. (2009). Identification of flagellar motility genes in *Yersinia ruckeri* by transposon mutagenesis. *Appl. Environ. Microbiol.* 75, 6630–6633. doi: 10.1128/AEM.01415-09
- Fernandez, L., Lopez, J. R., Secades, P., Menendez, A., Marquez, I., and Guijarro, J. A. (2003). *In vitro* and *in vivo* studies of the Yrp1 protease from *Yersinia ruckeri* and its role in protective immunity against enteric red mouth disease of salmonids. *Appl. Environ. Microbiol.* 69, 7328–7335. doi: 10.1128/AEM.69.12.7328-7335.2003
- Fernandez, L., Marquez, I., and Guijarro, J. A. (2004). Identification of specific *in vivo*-induced (*ivi*) genes in *Yersinia ruckeri* and analysis of ruckerbactin, a catecholate siderophore iron acquisition system. *Appl. Environ. Microbiol.* 70, 5199–5207. doi: 10.1128/AEM.70.9.5199-5207.2004
- Fernández, L., Méndez, J., and Guijarro, J. A. (2007a). Molecular virulence mechanisms of the fish pathogen *Yersinia ruckeri*. *Vet. Microbiol.* 125, 1–10. doi: 10.1016/j.vetmic.2007.06.013
- Fernández, L., Prieto, M., and Guijarro, J. A. (2007b). The iron- and temperature-regulated haemolysin YhlA is a virulence factor of *Yersinia ruckeri*. *Microbiology* 153, 483–489. doi: 10.1099/mic.0.29284-0
- Fernández, L., Secades, P., Lopez, J. R., Márquez, I., and Guijarro, J. A. (2002). Isolation and analysis of a protease gene with an ABC transport system in the fish pathogen *Yersinia ruckeri*: insertional mutagenesis and involvement in virulence. *Microbiology* 148, 2233–2243. doi: 10.1099/00221287-148-7-2233
- Fouz, B., Zarza, C., and Amaro, C. (2006). First description of non-motile *Yersinia ruckeri* serovar I strains causing disease in rainbow trout, *Oncorhynchus mykiss* (Walbaum), cultured in Spain. *J. Fis. Dis.* 29, 339–346. doi: 10.1111/j.1365-2761.2006.00723.x
- Furones, M., Gilpin, M. L., and Munn, C. B. (1993). Culture media for the differentiation of isolated of *Yersinia ruckeri*, based on detection of a virulence factor. *J. Appl. Microbiol.* 74, 360–366.
- Gray, M. J., Freitag, N. E., and Boor, K. J. (2006). How the bacterial pathogen *Listeria monocytogenes* mediates the switch from environmental Dr. Jekyll to pathogenic Mr. Hyde. *Infect. Immun.* 74, 2505–2512. doi: 10.1128/IAI.74.5.2505-2512.2006
- Guijarro, J. A., Cascales, D., García-Torrico, A. I., García-Domínguez, M., and Méndez, J. (2015). Temperature-dependent expression of virulence genes in fish-pathogenic bacteria. *Front. Microbiol.* 6:700. doi: 10.3389/fmicb.2015.00700
- Heroven, K. A., Bohme, K., Rhode, M., and Dersch, P. A. (2008). Csr-type regulatory system, including small non-coding RNAs, regulates the global virulence regulator RovA of *Yersinia pseudotuberculosis* through RovM. *Mol. Microbiol.* 68, 1179–1195. doi: 10.1111/j.1365-2958.2008.06218.x
- Herren, D., Mitra, A., Palaniyandi, S. K., Coleman, A., Elankumaran, S., and Mukhopadhyay, S. (2006). The Bar-UvrY two-component system regulates virulence in avian pathogenic *Escherichia coli* O78:K80:H9. *Infect. Immun.* 74, 4900–4909. doi: 10.1128/IAI.00412-06
- Heymann, J. B., Bartho, J. D., Rybakova, D., Venugopal, H. P., Winkler, D. C., Sen, A., et al. (2013). Three-dimensional structure of the toxin-delivery particle antifeeding prophage of *Serratia entomophila*. *J. Biol. Chem.* 288, 25276–25284. doi: 10.1074/jbc.M113.456145



- Hurst, M. R. H., O'Callaghan, M., and Glare, T. R. (2003). Peripheral sequences of the *Serratia entomophila* pADAP virulence-associated region. *Plasmid* 50, 213–229. doi: 10.1016/S0147-619X(03)00062-3
- Huvet, M., Toni, T., Sheng, X., Thorne, T., Jovanovic, G., Engl, C., et al. (2011). The evolution of the phage shock protein response system: interplay between protein function, genomic organization, and system function. *Mol. Biol. Evol.* 28, 1141–1155. doi: 10.1093/molbev/msq301
- Jank, T., Eckerle, S., Steinemann, M., Trillhaase, C., Schimpl, M., et al. (2014). Tyrosine glycosylation of Rho by *Yersinia* toxin impairs blastomere cell behavior in zebrafish embryos. *Nat. Comm.* 6:7807. doi: 10.1038/ncomms8807
- Johnston, C., Pegues, D. A., Hueck, C. J., Lee, C. A., and Miller, S. I. (1996). Transcriptional activation of *Salmonella typhimurium* genes by a member of the phosphorylated response-regulator superfamily. *Mol. Microbiol.* 22, 715–727.
- Jozwick, A. K., Graf, J., and Welch, T. J. (2016). The flagellar master operon *flhDC* is a pleiotropic regulator involved in motility and virulence of the fish pathogen *Yersinia ruckeri*. *J. Appl. Microbiol.* 122, 578–588. doi: 10.1111/jam.13374
- Kavermann, H., Burns, B. P., Angermüller, K., Odenbreit, S., Fischer, W., Melchers, K., et al. (2003). Identification and characterization of *Helicobacter pylori* genes essential for gastric colonization. *J. Exp. Med.* 197, 813–822. doi: 10.1084/jem.20021531
- Khimmakthong, U., Deshmukh, S., Chettri, J. K., Bojesen, A. M., Kania, P. W., Dalsgaard, I., et al. (2013). Tissue specific uptake of inactivated and live *Yersinia ruckeri* in rainbow trout (*Oncorhynchus mykiss*): visualization by immunohistochemistry and *in situ* hybridization. *Microbial. Pathog.* 59–60, 33–41. doi: 10.1016/j.micpath.2013.03.001
- Kim, S., Watanabe, K., Shirahata, T., and Watarai, M. (2004). Zinc uptake system (*znuA* locus) of *Brucella abortus* is essential for intracellular survival and virulence in mice. *J. Vet. Med. Sci.* 66, 1059–1063. doi: 10.1292/jvms.66.1059
- Komano, T., Yoshida, T., Narahara, K., and Furuya, N. (2000). The transfer region of Inc1 plasmid R64: similarities between R64 *tra* and *Legionella icm/dot* genes. *Mol. Microbiol.* 35, 1348–1359. doi: 10.1046/j.1365-2958.2000.01769.x
- Kumar, G., Hummel, K., Ahrens, M., Menneteau-Ledouble, S., Welch, T. J., Eisenacher, M., et al. (2016). Shotgun proteomic analysis of *Yersinia ruckeri* strains under normal and iron-limited conditions. *Vet. Res.* 47, 100–113. doi: 10.1186/s13567-016-0384-3
- Kumar, G., Hummel, K., Welch, T. J., Razzazi-Fazeli, W., and El-Matbouli, M. (2017). Global proteomic profiling of *Yersinia ruckeri* strains. *Vet. Res.* 48, 55–66. doi: 10.1186/s13567-017-0460-3
- Kumar, G., Menanteau-Ledouble, S., Saleh, M., and El-Matbouli, M. (2015). *Yersinia ruckeri*, the causative agent of enteric redmouth disease in fish. *Vet. Microbiol.* 46:103. doi: 10.1186/s13567-015-0238-4
- Lim, K. H., Jones, C. E., vanden Hoven, R. N., Edwards, J. L., Falsetta, M. L., Apicella, M. A., et al. (2008). Metal binding specificity of the MntABC permease of *Neisseria gonorrhoeae* and its influence on bacterial growth and interaction with cervical epithelial cells. *Infect. Immun.* 76, 3569–3576. doi: 10.1128/IAI.01725-07
- Liu, T., Wang, K.-Y., Wang, J., Chen, D.-F., Huang, X.-L., Ouyang, P., et al. (2016). Genome sequence of the fish pathogen *Yersinia ruckeri* SC09 provides insights into niche adaptation and pathogenic mechanism. *Int. J. Mol. Sci.* 17:557. doi: 10.3390/ijms17040557
- Menanteau-Ledouble, S., Lawrence, M. L., and El-Matbouli, M. (2018). Invasion and replication of *Yersinia ruckeri* in fish cell cultures. *BMC Vet. Res.* 14:81. doi: 10.1186/s12917-018-1408-1
- Méndez, J., Fernandez, L., Menendez, A., Reimundo, P., Perez-Pascual, D., Navais, R., et al. (2009). A chromosomally located *traHIJKL* operon encoding a putative Type IV secretion system is involved in the virulence of *Yersinia ruckeri*. *Appl. Environ. Microbiol.* 75, 937–945. doi: 10.1128/AEM.01377-08
- Méndez, J., and Guijarro, J. A. (2013). *In vivo* monitoring of *Yersinia ruckeri* in fish tissues: progression and virulence gene expression. *Environ. Microbiol. Rep.* 5, 179–185. doi: 10.1111/1758-2229.12030
- Méndez, J., Reimundo, O., Perez-Pascual, D., Navais, R., Gomez, E., and Guijarro, J. A. (2011). A novel *cdsAB* operon is involved in the uptake of L-cysteine and participates in the pathogenesis of *Yersinia ruckeri*. *J. Bacteriol.* 193, 944–951. doi: 10.1128/JB.01058-10
- Moisi, M., Lichtenegger, S., Tutz, S., Seper, A., Schild, S., and Reidl, J. (2013). Characterizing the hexose-6-phosphate transport system of *Vibrio cholerae*, a utilization system for carbon and phosphate sources. *J. Bacteriol.* 195, 1800–1808. doi: 10.1128/JB.01952-12
- Navais, R., Méndez, J., Cascales, D., Reimundo, P., and Guijarro, J. A. (2014a). The heat sensitive factor (HSF) of *Yersinia ruckeri* is produced by an alkyl sulphatase involved in sodium dodecyl sulphate (SDS) degradation but not in virulence. *BMC Microbiol.* 14:221. doi: 10.1186/s12866-014-0221-7
- Navais, R., Mendez, J., Perez-Pascual, D., Cascales, D., and Guijarro, J. A. (2014b). The *yrpAB* operon of *Yersinia ruckeri* encoding two putative U32 peptidases is involved in virulence and induced under microaerobic conditions. *Virulence* 5, 619–624. doi: 10.4161/viru.29363
- Ohtani, M., Villumsen, R., Koppang, E. O., and Raida, M. K. (2015). Global 3D imaging of *Yersinia ruckeri* bacterin uptake in rainbow trout fry. *PLoS ONE* 10:e0117263. doi: 10.1371/journal.pone.0117263
- Ohtani, M., Villumsen, R., Kragelund, H., and Raida, M. K. (2014). 3D visualization of the initial *Yersinia ruckeri* infection route in rainbow trout (*Oncorhynchus mykiss*) by optical projection tomography. *PLoS ONE* 9:e89672. doi: 10.1371/journal.pone.0093845
- Özdemir, F., and Arslan, S. (2015). Genotypic and phenotypic virulence characteristics and antimicrobial resistance of *Yersinia* spp. Isolated from meat and milk products. *J. Food Sci.* 80, 1306–1313. doi: 10.1111/1750-3841.12911
- Patzner, S. I., and Hantke, K. (2000). The zinc-responsive regulator Zur and its control of the *znu* gene cluster encoding the ZnuABC zinc uptake system in *Escherichia coli*. *J. Biol. Chem.* 275, 24321–24332. doi: 10.1074/jbc.M001775200
- Romalde, J. L., Magariños, B., Barja, J. L., and Toranzo, A. E. (1993). Antigenic and molecular characterization of *Yersinia ruckeri* proposal for a new intraspecies classification. *Syst. Appl. Microbiol.* 16, 411–419.
- Romalde, J. L., Planas, E., Sotelo, J. M., and Toranzo, A. E. (2003). First description of *Yersinia ruckeri* serotype O2 in Spain. *Bull. Eur. Ass. Fish Pathol.* 23, 135–138.
- Rybakova, D., Radjainia, M., Turner, A., Sen, A., Mitra, A. K., and Hurst, M. R. (2013). Role of antifeedant prophage (Afp) protein Afp16 in terminating the length of the Afp tailocin and stabilizing its sheath. *Mol. Microbiol.* 89, 702–714. doi: 10.1111/mmi.12305
- Ryckaert, J., Bossier, P., D'Herde, K., Diez-Fraile, A., Sorgeloos, P., Hasebrouck, F., et al. (2010). Persistence of *Yersinia ruckeri* in trout macrophages. *Fish Shellfish Immunol.* 29, 648–655. doi: 10.1016/j.fsi.2010.06.009
- Saliba, A.-E., Santos, S. C., and Vogel, J. (2017). New RNA-seq approaches for the study of bacterial pathogens. *Curr. Opin. Microbiol.* 35, 78–87. doi: 10.1016/j.mib.2017.01.001
- Sarris, P. F., Ladoukakis, E. D., Panopoulos, N. J., and Scoulica, E. V. (2014). A phage tail-delivered element with wide distribution among both prokaryotic domains: a comparative genomic and phylogenetic study. *Genome Biol. Evol.* 6, 1739–1747. doi: 10.1093/gbe/evu136
- Schmitt, C. K., Ikeda, J. S., Darnell, S. C., Watson, P. R., Bispham, J., Wallis, T. S., Weinstein, D. L., Metcalf, E. S., et al. (2001). Absence of all components of the flagellar export and synthesis machinery differentially alters virulence of *Salmonella enterica* serovar Typhimurium in models of typhoid fever, survival in macrophages, tissue culture invasiveness, and calf enterocolitis. *Infect. Immun.* 69, 5619–5625. doi: 10.1128/IAI.69.9.5619-5625.2001
- Secades, P., and Guijarro, J. A. (1999). Purification and characterization of an extracellular protease from the fish pathogen *Yersinia ruckeri* and effect of culture conditions on production. *Appl. Environ. Microbiol.* 65, 3969–3975.
- Tang, K. F., and Lightner, D. V. (2014). Homologues of insecticidal toxin complex genes within a genomic island in the marine bacterium *Vibrio parahaemolyticus*. *FEMS Microbiol. Lett.* 361, 34–42. doi: 10.1111/1574-6968.12609
- Tchong, S.-I., Xu, H., and White, R. H. (2005). L-cysteine desulfidase: and [4Fe-4S] enzyme isolated from *Methanocaldococcus jannaschii* that catalyzes the breakdown of L-cysteine into pyruvate, ammonia, and sulfide. *Biochemistry* 44, 1659–1670. doi: 10.1021/bi0484769
- Tinsley, J. W., Lyndon, A. R., and Austin, B. (2011). Antigenic and cross-protection studies of biotype 1 and biotype 2 isolates of *Yersinia ruckeri* in rainbow trout, *Oncorhynchus mykiss* (Walbaum). *J. Appl. Microbiol.* 111, 8–16. doi: 10.1111/j.1365-2672.2011.05020.x
- Toback, E., Decostere, A., Hermans, K., Haesebrouck, F., and Chiers, K. (2007). *Yersinia ruckeri* infections in salmonid fish. *J. Fish Dis.* 30, 257–268.



- Tobback, E., Decostere, A., Hermans, K., Ryckaert, J., Duchateau, L., Haesebrouck, F., et al. (2009). Route of entry and tissue distribution of *Yersinia ruckeri* in experimentally infected rainbow trout *Oncorhynchus mykiss*. *Dis. Aquat. Org.* 84, 219–228. doi: 10.3354/dao02057
- Tobback, E., Hermans, K., Decostere, A., Broeck Van de, Haesebrouck, F., and Chiers, K. (2010). Interactions of virulent and avirulent *Yersinia ruckeri* strains with isolated gill arches and intestinal explants of rainbow trout *Oncorhynchus mykiss*. *Dis. Aquat. Org.* 90, 175–179. doi: 10.3354/dao02230
- Urbany, C., and Neuhaus, H. E. (2008). Citrate uptake into *Pectobacterium atrosepticum* is critical for bacterial virulence. *Mol. Plant. Microbe. Interact.* 21, 547–554. doi: 10.1094/MPMI-21-5-0547
- Wallez, Y., Bouillot, S., Soleihac, E., Huber, P., Atrée, I., and Faudry, E. (2018). CLIQ-BID: A method to quantify bacteria-induced damage to eukaryotic cells by automated live-imaging of bright nuclei. *Sci. Rep.* 8:5. doi: 10.1038/s41598-017-18501-9
- Welch, T. J., Verner-Jeffreys, D. W., Dalsgaard, I., Wiklund, T., Eenhuis, J. P., Garcia Cabrera, J. A., et al. (2011). Independent emergence of *Yersinia ruckeri* biotype 2 in the United States and Europe. *Appl. Environm. Microbiol.* 77, 3493–3499. doi: 10.1128/AEM.02997-10
- Welch, T. J., and Wiens, G. D. (2005). Construction of a virulent, green fluorescent protein-tagged *Yersinia ruckeri* and detection in trout tissues after intraperitoneal and immersion challenge. *Dis. Aquat. Org.* 67, 267–272. doi: 10.3354/dao067267
- Westermann, A. J., Forster, K. U., Amaman, F., Barquist, L., Chao, Y., et al. (2016). Dual RNA-seq unveils noncoding RNA functions in host-pathogen interactions. *Nature* 529, 496–501. doi: 10.1038/nature16547
- Wrobel, A., Ottoni, C., Leo, J. C., Gulla, S., and Linke, D. (2018). The repeat structure of two paralogous genes, *Yersinia ruckeri* invasin (yrInv) and a “*Y. ruckeri* invasin-like molecule”, (yrIlm) sheds light on the evolution of adhesive capacities of a fish pathogen. *J. Struct. Biol.* 201, 171–183. doi: 10.1016/j.jsb.2017.08.008
- Zebian, N., Merckx-Jacques, A., Pittock, P. P., Houle, S., Dozois, C. M., Lajoie, G. A., et al. (2016). Comprehensive analysis of flagellin glycosylation in *Campylobacter jejuni* NCTC 11168 reveals incorporation of legionaminic acid and its importance for host. *Colonization* 26, 386–397. doi: 10.1093/glycob/cwv104
- Zhao, H., Li, X., Johnson, D. E., and Mobley, H. L. (1999). Identification of protease and *rpoN*-associated genes of urophatogenic *Proteus mirabilis* by negative selection in a mouse model of ascending urinary tract infection. *Microbiology* 145, 185–195. doi: 10.1099/13500872-145-1-185

**Conflict of Interest Statement:** The authors declare that the research was conducted in the absence of any commercial or financial relationships that could be construed as a potential conflict of interest.

Copyright © 2018 Guijarro, García-Torrico, Cascales and Méndez. This is an open-access article distributed under the terms of the Creative Commons Attribution License (CC BY). The use, distribution or reproduction in other forums is permitted, provided the original author(s) and the copyright owner are credited and that the original publication in this journal is cited, in accordance with accepted academic practice. No use, distribution or reproduction is permitted which does not comply with these terms.



# pYR4 From a Norwegian Isolate of *Yersinia ruckeri* Is a Putative Virulence Plasmid Encoding Both a Type IV Pilus and a Type IV Secretion System

Agnieszka Wrobel<sup>1</sup>, Claudio Ottoni<sup>2</sup>, Jack C. Leo<sup>1</sup> and Dirk Linke<sup>1\*</sup>

<sup>1</sup> Department of Biosciences, University of Oslo, Oslo, Norway, <sup>2</sup> Centre for Ecological and Evolutionary Synthesis, University of Oslo, Oslo, Norway

## OPEN ACCESS

### Edited by:

Victoria Auerbuch,  
University of California, Santa Cruz,  
United States

### Reviewed by:

Hanh N. Lam,  
University of California, Santa Cruz,  
United States  
Gokhlesh Kumar,  
Veterinärmedizinische Universität  
Wien, Austria

### \*Correspondence:

Dirk Linke  
dirk.linke@ibv.uio.no

### Specialty section:

This article was submitted to  
Molecular Bacterial Pathogenesis,  
a section of the journal  
Frontiers in Cellular and Infection  
Microbiology

**Received:** 06 July 2018

**Accepted:** 04 October 2018

**Published:** 30 October 2018

### Citation:

Wrobel A, Ottoni C, Leo JC and  
Linke D (2018) pYR4 From a  
Norwegian Isolate of *Yersinia ruckeri* Is  
a Putative Virulence Plasmid Encoding  
Both a Type IV Pilus and a Type IV  
Secretion System.  
Front. Cell. Infect. Microbiol. 8:373.  
doi: 10.3389/fcimb.2018.00373

Enteric redmouth disease caused by the pathogen *Yersinia ruckeri* is a significant problem for fish farming around the world. Despite its importance, only a few virulence factors of *Y. ruckeri* have been identified and studied in detail. Here, we report and analyze the complete DNA sequence of pYR4, a plasmid from a highly pathogenic Norwegian *Y. ruckeri* isolate, sequenced using PacBio SMRT technology. Like the well-known pYV plasmid of human pathogenic *Yersinia*, pYR4 is a member of the IncFII family. Thirty-one percent of the pYR4 sequence is unique compared to other *Y. ruckeri* plasmids. The unique regions contain, among others genes, a large number of mobile genetic elements and two partitioning systems. The G+C content of pYR4 is higher than that of the *Y. ruckeri* NVH\_3758 genome, indicating its relatively recent horizontal acquisition. pYR4, as well as the related plasmid pYR3, comprises operons that encode for type IV pili and for a conjugation system (*tra*). In contrast to other *Yersinia* plasmids, pYR4 cannot be cured at elevated temperatures. Our study highlights the power of PacBio sequencing technology for identifying mis-assembled segments of genomic sequences. Comparative analysis of pYR4 and other *Y. ruckeri* plasmids and genomes, which were sequenced by second and the third generation sequencing technologies, showed errors in second generation sequencing assemblies. Specifically, in the *Y. ruckeri* 150 and *Y. ruckeri* ATCC29473 genome assemblies, we mapped the entire pYR3 plasmid sequence. Placing plasmid sequences on the chromosome can result in erroneous biological conclusions. Thus, PacBio sequencing or similar long-read methods should always be preferred for *de novo* genome sequencing. As the *tra* operons of pYR3, although misplaced on the chromosome during the genome assembly process, were demonstrated to have an effect on virulence, and type IV pili are virulence factors in many bacteria, we suggest that pYR4 directly contributes to *Y. ruckeri* virulence.

**Keywords:** *tra* operon, *pil* operon, conjugative plasmid, *Yersinia ruckeri*, type IV secretion system

## INTRODUCTION

The genus *Yersinia* consists of 17 different species (Reuter et al., 2014; Savin et al., 2014). Although the human pathogens within the genus are closely related to each other, they cause diverse diseases. *Y. pestis*, the causative agent of bubonic and pneumonic plague, is one of the most virulent organisms known (Chauhan et al., 2016). In addition, this genus includes *Y. enterocolitica* and *Y. pseudotuberculosis*, well-known human enteropathogens. *Y. pestis* spreads through fleabites or aerosols, whereas *Y. enterocolitica* and *Y. pseudotuberculosis* are transmitted via ingestion of contaminated food or water (Bottone, 1997; Perry and Fetherston, 1997; Jalava et al., 2006). *Y. enterocolitica* and *Y. pseudotuberculosis* are responsible for a broad range of diseases ranging from mild gastroenteritis to life-threatening septicemia (Bottone, 1997).

*Y. ruckeri* is a fish pathogen causing enteric redmouth disease (ERM), mainly in salmonids (Bullock et al., 1978; Busch, 1978). This bacterium contributes to enormous economic losses in aquaculture throughout the world. *Y. ruckeri* is mostly transmitted through contact with carrier fish (Busch, 1978; Stevenson and Airdrie, 1984). Despite the availability of vaccines, yersiniosis outbreaks still occur in fish farms (Ormsby et al., 2016). The majority of the ERM outbreaks are caused by the highly pathogenic *Y. ruckeri* serotype 1 belonging to biotype 1, characterized as motile with phospholipase activity (Romalde and Toranzo, 1993). For a long time, ERM has played a minor role in Norway, with only a few outbreaks per year (Hjeltnes et al., 2017). The first report of a disease outbreak caused by *Y. ruckeri* among Atlantic salmon was described in Norway in 1985, and this was successfully treated with antibiotics (Sparboe et al., 1986). In recent years, the number of outbreaks in the farmed Atlantic salmon population has substantially increased. The reasons for the most recent outbreaks remain unclear, and *Y. ruckeri* infections are nowadays a major challenge facing the Norwegian aquaculture industry, similar to other countries such as Australia (Barnes et al., 2016), Chile (Avendaño-Herrera et al., 2017), and Scotland (Ormsby et al., 2016).

Each of the human *Yersinia* pathogens harbors chromosomally and plasmid-encoded virulence determinants (Chauhan et al., 2016). *Y. pestis* usually carries two species-specific plasmids, pPCP1 and pMT1, and one highly conserved plasmid shared among the three human pathogenic *Yersiniae*, pYV (also called pCD1) (Ben-Gurion and Shafferman, 1981; Ferber and Brubaker, 1981; Haiko et al., 2009). This large 70-kb plasmid carries a type III secretion system (T3SS), Ysc. T3SS system encodes structural proteins, chaperones as well as effector proteins called Yops (*Yersinia* outer proteins) required for *Yersinia* extracellular survival. The effector proteins and the machinery for their delivery are required for infection and manipulation of host responses to overcome the action of phagocytes (Cornelis et al., 1998). Moreover, the plasmid encodes a major virulence factor, the *Yersinia* adhesin A (YadA) (Mühlenkamp et al., 2015).

Despite the economic importance, the pathogenicity of *Y. ruckeri* has not been studied in detail. Only few virulence factors are known, and to date all of these are encoded on

the chromosome. These include bacterial adhesins important in establishing a successful colonization (Romalde and Toranzo, 1993). In particular, the chromosomally encoded adhesins YrInv and YrIIm might play a role in virulence (Wrobel et al., 2017). They belong to the intimin-invasin family of adhesins, which includes also InvA, the adhesin responsible for the initial bacterial attachment and colonization of host tissues in *Y. enterocolitica* and *Y. pseudotuberculosis* (Isberg and Leong, 1990; Wrobel et al., 2017). Other virulence factors described in *Y. ruckeri* include cytotoxins and haemolysins (Romalde and Toranzo, 1993), the metalloprotease Yrp1 (Secades and Guijarro, 1999), the haemolysin/cytolysin YhlA (Fernández et al., 2007), the iron uptake system ruckerbactin (Fernández et al., 2004), and a chromosomal T3SS (Liu et al., 2016). Recently, a large proteomic study of *Y. ruckeri* strains was performed under standard (Kumar et al., 2017) and iron-limited conditions (Kumar et al., 2016). In total, 1395 proteins were identified in the whole cell lysate of *Y. ruckeri* under standard culture conditions. Among them, several proteins were predicted to be virulence factors, including, among others, HtrA protease, TolB, the lipoprotein NlpD and a LuxR family transcriptional regulator. This global proteomic analysis will help in understanding the biology of the pathogen, as well as in development of new effective treatments against the ERM disease (Kumar et al., 2017).

Plasmid-borne virulence factors have been found in other fish pathogens, including *Vibrio anguillarum* (Crosa, 1980) and *Edwardsiella tarda* (Yu et al., 2012), but not in *Y. ruckeri*. Plasmids in *Y. ruckeri* strains were studied previously due to their possible involvement in virulence in analogy to the human pathogenic *Yersiniae* (De Grandis and Stevenson, 1982). Many authors expected to find the same virulence traits as those described for the human pathogens, such as the plasmid-encoded T3SS. However, none of the plasmid-associated virulence factors of the human-enteropathogenic *Yersiniae* were found in these plasmids. In general, *Y. ruckeri* plasmids have not yet been properly characterized and further research is required to understand their role in bacterial virulence. A study including 183 *Y. ruckeri* strains from different geographical locations reported 8 different plasmid profiles (Garcia et al., 1998). In this study, the most virulent sorbitol-negative *Y. ruckeri* strains of serotype O1 contained a large 75 MDa plasmid (~113 kb), in agreement with earlier studies (Guilvout et al., 1988; Romalde et al., 1993). In addition, smaller plasmids (12.7 MDa; ~19 kb) have been found in most of the strains (Garcia et al., 1998).

More recent studies showed that multidrug resistance plasmids in *Y. ruckeri* strains are a serious aquaculture concern (Toranzo et al., 1983; De Grandis and Stevenson, 1985; Carattoli et al., 2012; Huang et al., 2014). Welch et al. (2007) showed that *Y. ruckeri* strain YR71 carries a multidrug resistance plasmid called pYR1, which has 99% nucleotide identity with the IncA/C (incompatibility A/C) plasmid backbone of the *Y. pestis* isolate IP275, plasmid pIP1202. The IncA/C group comprises a large, low-copy number, multidrug resistance plasmid family within *Enterobacteriaceae* such as *Escherichia coli*, *Salmonella enterica*, *Y. pestis*, and *Klebsiella pneumoniae*, as well as more distantly related species such as *Vibrio cholerae*. Plasmids of this family are unique with regard to their structure and gene content.

They contain putative transfer regions [type IV secretion system (T4SS)], regions involved in integration of mobile genetic elements, as well as regions involved in transcription (Johnson and Lang, 2012). T4SSs are widely distributed in prokaryotes as well as in some archaea. T4SSs are large macromolecular complexes typically composed of a cell-envelope spanning mating channel and an extracellular pilus structure. T4SSs are classified into two major groups type IVA (T4ASSs) and type IVB (T4BSSs). T4ASS resemble the VirB/VirD system of *Agrobacterium tumefaciens* while T4BSSs are related to the conjugation system of IncI plasmids. Typical examples of T4ASSs are found on conjugative plasmids, such as F, RP4 and pKM101, as well as the prototypical VirB system of *A. tumefaciens*. These T4ASSs export nucleoprotein complexes during conjugation. T4BSS is represented by the *Legionella pneumophila* icm/dot system involved in protein translocation into host cells thus allowing the pathogen to replicate intracellularly (Wallden et al., 2010).

In this work, we sequenced a plasmid—which we named pYR4—from the highly pathogenic Norwegian *Y. ruckeri* isolate NVH\_3758 from the 1987 outbreak and performed a comparative bioinformatics analysis of the available *Y. ruckeri* plasmid sequences to evaluate their role in virulence.

## MATERIALS AND METHODS

### Plasmid DNA Sequencing Technology

Genomic DNA as well as plasmid DNA was extracted from a locally important, highly pathogenic Norwegian *Y. ruckeri* isolate NVH\_3758 (biotype 1, serotype 1) recovered from an outbreak of clinical yersiniosis in farmed Atlantic salmon, kindly provided by Prof. Duncan Colquhoun at the Norwegian Veterinary Institute in Oslo, Norway (Gulla et al., 2018). Whole genome sequencing of *Y. ruckeri* NVH\_3758 was performed by the Norwegian Sequencing Centre (Oslo, Norway) using the Single Molecule Real Time (SMRT) sequencing technology of Pacific Biosciences. Sample preparation, reads assembly and consensus polishing were done as previously described (Wrobel et al., 2017). The final assembly yielded two contigs of circularized length of ~3.8 Mb, representing the chromosomal genome (Wrobel et al., 2017), and ~81 kb, corresponding to a new plasmid that we named pYR4. The DNA sequence of pYR4 has been deposited in the National Centre for Biotechnology Information (NCBI) database under the accession number CP032236.

### Plasmid Annotation

The FASTA consensus of pYR4 from *Y. ruckeri* NVH\_3758 was uploaded to RAST (Rapid Annotation using Subsystem Technology) for automatic annotation (Aziz et al., 2008; Seemann, 2014). After initial annotations, all open reading frames (ORFs) with initial annotations were checked using the interactive server HHpred available at the Max Planck Institute for Developmental Biology Toolkit (Söding et al., 2005) against two databases, the PDB and PFAM (Sonnhammer et al., 1998; Sussman et al., 1999). The functional annotations obtained from the HHpred server and RAST were compared and in some cases were corrected manually. Many uncharacterized proteins which

were previously labeled as hypothetical by RAST were annotated based on similarity to characterized proteins. The protein sequences were uploaded into Geneious (Kearse et al., 2012). A circular representation of pYR4 showing the annotated features, the GC content and the GC skew within 50 bp-long genomic regions, was generated with Circos (Krzywinski et al., 2009). The identification of the promoter sequences of the *pil* and *tra* operons was performed with the online server BPROM (Solovyev and Salamov, 2011) as well as bTSSfinder (Shahmuradov et al., 2017) (see **Table 1** and **Supplementary Figure 1**). The mfold Web server was used for RNA secondary structure prediction (Zuker, 2003).

### RepA Phylogeny

The RepA protein sequence of pYR4 was annotated by RAST as “hypothetical.” After the initial annotation, the protein was identified as RepA using HHpred. The protein sequence was then subjected to a search using BLASTP (Altschul et al., 1997). The BLASTP search returned 100 hits, from which the first 29 RepA protein sequences were selected, after excluding sequences of hypothetical proteins and multispecies proteins, and aligned using MUSCLE (Edgar, 2004). In the final alignment, we included RepA protein sequences from pYR1, pYR3, pYR4 in addition to eight RepA protein sequences belonging to the IncA/C plasmid family. The final alignment was then used to construct the phylogenetic tree using MEGA X software by applying the Maximum Likelihood method on the Poisson correction model (Zuckerkanndl and Pauling, 1965; Felsenstein, 1985; Kumar et al., 2018) (see **Supplementary Figure 2**).

### Plasmid Comparative Analysis

We compared the nucleotide sequence of *Y. ruckeri* NVH\_3758 plasmid pYR4 with the nucleotide sequences of the plasmids of *Y. ruckeri* strains YR71 (pYR1), CSF007-82 (pYR2, pYR3) and SC09 (pLT, pWKY) (**Table 2**) deposited in the NCBI database. To keep the same annotation system as for the pYR4 plasmid, the nucleotide sequences of the *Y. ruckeri* plasmids were re-annotated with RAST (see also **Supplementary Figure 3** for pYR4, **Supplementary Figure 4**). Details of the annotation can be found in **Supplementary Tables 1 and 2**.

Plasmid comparisons were also done with sequences of other species containing the *tra* and *pil* operons described in literature, including *Erwinia amylovora* (pEL60, pEA68, pEA72, pEA78), *Serratia entomophila* (pADAP), *Citrobacter freundii* (pCTX-M3), and *Salmonella enterica* subsp. *enterica* serovar Typhimurium (R64) (see **Supplementary Figure 5**). The nucleotide sequence of *Y. ruckeri* NVH\_3758 pYR4 plasmid was also compared to PacBio-sequenced genomic data of *Y. ruckeri* CSF007-82, Big Creek 74, QMA0440, SC09, and Illumina-sequenced genomes of *Y. ruckeri* ATCC29473 and YRB (see **Supplementary Figure 5**). In the comparative survey, we also included the ~57 kb-long scaffold 20 of the *Y. ruckeri* 150 assembly, which contains the *tra* and *pil* operons.

Finally, pYR4 was compared to the Illumina-sequenced genomes of human pathogens *Y. pestis* CO92, *Y. pseudotuberculosis* YPIII, and *Y. enterocolitica* 8081 (see **Supplementary Figure 5**). Pairwise comparisons were



**TABLE 1** | pYR4 promoter predictions by bTSSfinder (Shahmuradov et al., 2017) and BPROM (Solovyev and Salamov, 2011) used in the present study.

Name of operon	Predicted $\sigma$ factor	Sequence of predicted promoter		Location on the pYR4 sequence (nt position)	Score <sup>a</sup>	Software used
		–10	–35			
<i>pil</i> operon	$\sigma^{24}$	TCTGT	TCATT	14,351–14,374	1.77	bTSSfinder
	$\sigma^{38}$	TATTCC	TTTACC	14,339–14,368	1.52	
<i>tra2</i> operon	$\sigma^{24}$	GCGAT	CCACTG	35,014–35,038	0.30	bTSSfinder
	$\sigma^{32}$	CCCCCAGCTG	CTCCAGA	34,989–35,019	1.91	
<i>mob</i> operon	$\sigma^{70}$	TATAAT	TTGATT	60,335–60,306	1.91	bTSSfinder
	$\sigma^{38}$	TATAAT	TTGATT	60,335–60,306	1.80	
	$\sigma^{32}$	TACGCCAGAT	CGATTTT	60,289–60,259	1.86	
<i>stbA</i> operon	$\sigma^{32}$	ATCACTATTA	TGATTGA	72,064–72,035	1.95	bTSSfinder
	$\sigma^{38}$	TACACA	CGTGAG	72,030–72,002	1.94	
	$\sigma^{28}$	TGAGATAA	AAAATCAA	72,011–71,939	1.97	
	$\sigma^{70}$	CAATAT	TTTAAT	71,981–71,961	1.97	
	$\sigma^{24}$	TCAAT	TAATAT	71,992–71,978	1.97	
	$\sigma^{32}$	ATCACTATTA	TGATTGA	72,035–72,064	1.95	
<i>parA</i> operon	$\sigma^{38}$	TACACA	CGTGAG	72,002–72,030	1.94	bTSSfinder
	$\sigma^{28}$	TGAGATAA	AAAATCAA	71,939–72,011	1.97	
	$\sigma^{70}$	CAATAT	TTTAAT	71,963–71,981	1.97	
	$\sigma^{24}$	TCAAT	TAATAT	71,978–71,993	1.97	
<i>pil</i> operon	$\sigma^{70}$	GCGTATTC	TTACCG	14,340–14,367	15; 55	BPROM
<i>tra2</i> operon	$\sigma^{70}$	ATGAAAAAT	TTTAC	34,792–34,817	39; 42	BPROM
<i>tra3</i> operon	$\sigma^{70}$	TCGCAAAAT	TTTCAG	47,970–48,003	30; 47	BPROM
<i>mob</i> operon	$\sigma^{70}$	GGGTATAAT	TTGATT	60,327–60,311	53; 91	BPROM
<i>stbA</i> operon	$\sigma^{70}$	CACTATTAT	TTGACA	72,065–72,038	56; 66	BPROM
<i>parA</i> operon	$\sigma^{70}$	CACTATTAT	TTGACA	72,038–72,065	56; 66	BPROM

<sup>a</sup>A score of 0.81 or higher is considered significant for bTSSfinder, and a score of 0.2 or higher is considered significant for BPROM (Solovyev and Salamov, 2011; Shahmuradov et al., 2017). Two score values provided in the table were predicted for BPROM which correspond to the Pribnow box at the –10 position and at the –35 position, respectively.

**TABLE 2** | *Y. ruckeri* plasmid sequences deposited in GenBank used in the present study.

Plasmid	Strain	Sequencing technology	Size (bp)	G+C content (%)	CDS (predicted by RAST)	GenBank	References
pYR1	YR71	AB 3730xl	158.038	50.9	200	CP000602.1	Welch et al., 2007
pYR2	CSF007-82	PacBio	16.923	41.5	25	LN681229.1	Nelson et al., 2015
pYR3	CSF007-82	PacBio	103.917	48.4	107	LN681230.1	Nelson et al., 2015
pYR4	NVH_3758	PacBio	80.843	49.4	92	PRJNA401093	This study
pLT	SC09	Illumina	57.905	44.3	65	CP025802.1	Liu et al., 2016
pWKY	SC09	Illumina	73.051	40.2	95	CP025801.1	Liu et al., 2016

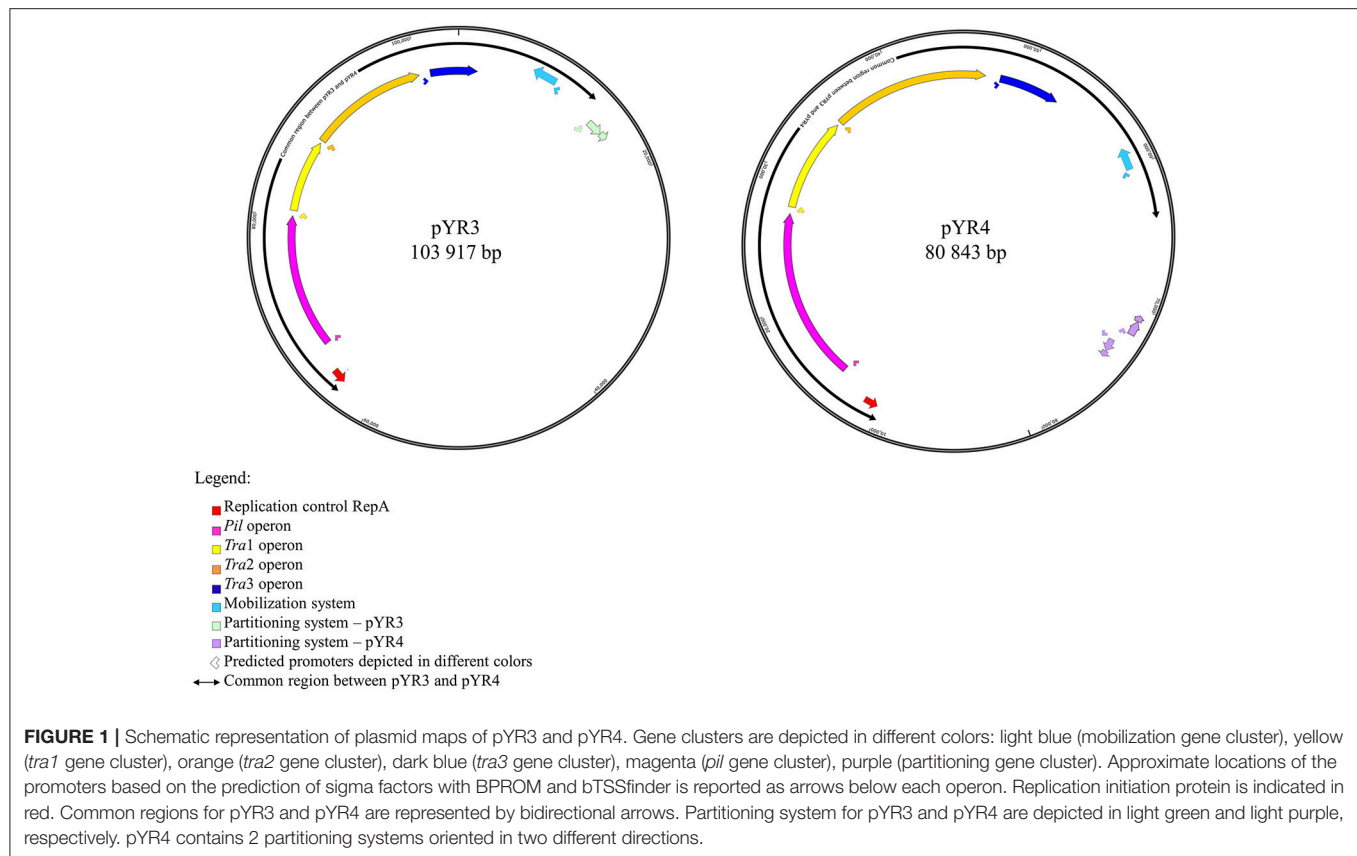
performed with Progressive Mauve (Darling et al., 2010) using default options and the “seed family” option to increase sensitivity. The output backbone file was then used to plot the Locally Collinear Blocks (LCB) in a circular representation with Circos.

## RESULTS

### pYR4 Is a Novel Plasmid Isolated From *Y. ruckeri* NHV3758

In order to define the relationship between the plasmid sequenced in this study and those described in literature,

we performed a comparative analysis of pYR4 with plasmid sequences generated previously by Illumina and PacBio sequencing technologies. The comparative survey with Mauve indicated no obvious similarity between pYR4 and the *Y. ruckeri* plasmids pYR1, pYR2, pLT, and pWKY, as no LCBs (locally collinear blocks) were detected (data not shown). On the other hand, a ~55 kb-long LCB (sequence identity >99%) that included the *pil* and the *tra* operons was present in pYR4 (from nucleotide position 9,100 to 64,005) and in the PacBio-sequenced plasmid pYR3 (Figures 1, 3, Table 2). By re-annotating pYR3 and comparing it with the higher-resolution annotation of



pYR4 obtained through HHPred, we could provide a more in depth characterization of the plasmids under analysis (Nelson et al., 2015) (see Materials and Methods section, **Supplementary Figure 3** for pYR4 and **Supplementary Figure 4** for pYR3).

The remaining portion of the plasmid sequence (>25 kb, 31% of the sequence length) appears to be unique, as no LCB was found in any of the plasmids of *Y. ruckeri* deposited in GenBank so far. This region contains mostly hypothetical proteins ( $n = 10$ ) and mobile genetic elements ( $n = 10$ ). In addition, we found a partial toxin-antitoxin system, a restriction system including both a type I restriction enzyme and a corresponding ArdA-like anti-restriction protein, and a small cluster of genes coding for two alcohol dehydrogenase enzymes and a transcription factor with high similarity to FrmR from *Salmonella*, a formaldehyde-sensitive regulator (**Supplementary Figure 3**). pYR4 contains two potential partitioning systems (ParAG and StbAB) (**Figure 1**). These two partitioning systems are represented by two operons oriented in opposite directions. No obvious sequence similarity with the partitioning system of pYR3 was found. Interestingly, the presence of alternative partitioning systems have already been described before for pYV from *Yersinia* species (Pilla and Tang, 2018). The high abundance of mobile elements may suggest that this plasmid is likely subject to structural rearrangements and that the unique ~25 kb region of pYR4 may be the result of recent horizontal

gene transfer. This is also supported by the difference in G+C content between the ~55 kb region (50.4%) and the remaining portion of the plasmid (47.1%). It is worth noting that in pYR3, this complete region is replaced by a different ~45 kb region (**Figure 1**). These major differences suggest that *Y. ruckeri* NHV3758 contains a plasmid with significant differences to pYR3, which we named pYR4.

## Sequence Analysis of pYR4

The nucleotide sequence of the circular pYR4 plasmid contains 80,842 base pairs (~53 MDa). The G+C content of pYR4 is 49.4%, which is around 2% less than the G+C content of the *Y. ruckeri* NVH\_3758 genome (47.6%), suggesting acquisition by horizontal gene transfer (**Figure 2**) (Nishida, 2012; Hayek, 2013). The annotation of pYR4 with RAST showed 92 putative coding sequences along the entire plasmid sequence. The RAST server could annotate functions for 52 ORFs and we were able to expand this list to 71 ORFs manually, using the HHPred server (Söding et al., 2005) (see **Supplementary Figure 3**), leaving 21 ORFs without putative function. Fifty-five genes are encoded on the positive strand while the remaining 37 are encoded on the negative strand. The entire plasmid sequence can be divided into several gene clusters, including clusters for partitioning (*parA*, *parG*, and *stbAB*), a T4SS (*tra*), and a type IV pilus (TFP) gene cluster (*pil*).

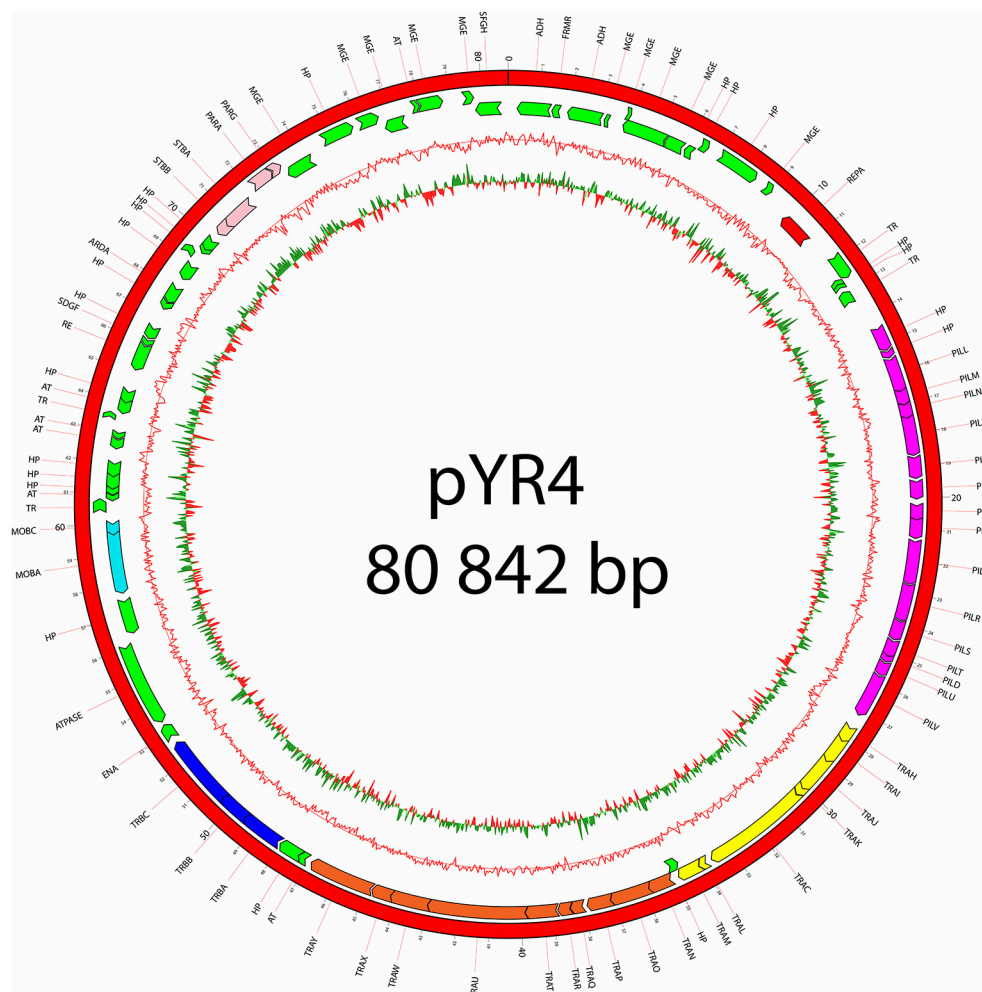


**FIGURE 2 |** Plasmid map of pYR4 isolated from *Y. ruckeri* NVH\_3758. The sequence annotations were generated with RAST (Rapid Annotation using Subsystem Technology) and further analyzed with HHpred. The rings show from inside to outside (1) the GC skew, (2) the G+C content, (3) the position of predicted ORFs in the reverse strand, and (4) the position of ORFs in the forward strand. The gene annotations are positioned in the middle of each gene on the plasmid map. Gene clusters are indicated in different colors: light blue (mobilization gene cluster), yellow (*tra1* gene cluster), orange (*tra2* gene cluster), dark blue (*tra3* gene cluster), magenta (*pil* gene cluster), pink (partitioning gene cluster). Replication initiation protein is indicated in red. Hypothetical proteins (HP) and mobile genetic elements are indicated in green.

In order to understand the pYR4 plasmid physiology as well as to follow its evolution and spread, we classified pYR4 into a plasmid family. A classical method of plasmid classification is based on incompatibility (Inc) groups. In general, plasmids with the same replication system are incompatible while plasmids with different replication system are compatible. In other words, two plasmids of the same Inc group cannot be propagated in the same bacterial cell (Couturier et al., 1988). A set of 30 RepA protein sequences from IncFII plasmid family, together with 9 RepA protein sequences previously characterized as belonging to IncA/C, were aligned in order to classify pYR4. Evaluation of the RepA phylogeny showed that the pYR4 RepA protein is closely related to IncFII plasmids found in other *Yersinia* species (see **Supplementary Figure 2**). A BLASTP search of pYR4 RepA protein returned over 100 hits of homologs

found in different species. The closest RepA homologs were found in Illumina-sequenced genomes of *Y. frederiksenii* and *Y. enterocolitica* with 91 and 90% similarity over the whole protein sequence, respectively. These RepA homologs presumably are part of unnamed plasmids that were incorrectly assigned to chromosomes, since they share only 19% similarity to RepA of the well-described virulence plasmid pYV from *Y. enterocolitica* 8081 (**Table 3**). Thus, pYR4 was classified as a member of the IncFII plasmid family, in contrast to pYR1 which belongs to the IncA/C family and is represented as an outgroup in **Supplementary Figure 2** (Carattoli, 2009). The IncFII plasmid family includes low-copy number plasmids mostly related to virulence, such as pYV, as well as to the dissemination of antimicrobial resistance determinants. Plasmids from this family usually carry the FII replicon alone or in association with

extra replicons such as repFIA and repFIB (Carattoli, 2009; Yang et al., 2015) and are common in *Yersinia* (Villa et al., 2010).

## Comparative Analysis of *Y. ruckeri* Plasmid Sequences Demonstrates Errors in Assemblies of Second Generation Genome Sequencing

Our comparative survey showed that no significant LCBs were found between pYR4 and the chromosomal genomes of *Y. ruckeri* CSF007-82, Big Creek 74, QMA0440, SC09, or YRB (data not shown). However, we found that the ~100 kb-long scaffold 2 of the *Y. ruckeri* ATCC29473 Illumina assembly matched pYR3, except for a mobile element of pYR3 (Figure 3 and Supplementary Figures 4–6). Furthermore, the higher quality of PacBio sequenced plasmids (pYR3 of CSF007-82 and pYR4 of NHV-3758) made it possible in our comparative survey to place scaffolds of previous *Y. ruckeri* assemblies into plasmid locations. In fact, the ~57 kb-long *Y. ruckeri* 150 scaffold 20 that contained the *tra* and the *pil* operons could be mapped entirely to pYR3 (see Supplementary Figure 7). This scaffold included the ~55 kb-long region containing the *pil* and the *tra* operons detected in pYR4 and pYR3. Furthermore, by aligning other unplaced scaffolds of the *Y. ruckeri* 150 assembly, we found that four more scaffolds (23, 31, 32, 34) could be placed within pYR3 (Figure 3 and Supplementary Figures 5, 6). (An unplaced scaffold is a sequence found in an assembly that is not associated with any chromosome). Taken together, the evidence presented here suggests that the *pil* and *tra* operons are localized on plasmids pYR3 and pYR4 and that *Y. ruckeri* 150 and *Y. ruckeri* ATCC29473 contain the plasmid pYR3. In *Y. ruckeri* 150, the presence of plasmid- and chromosomally-borne *tra* clusters has been suggested based on Southern blot hybridization evidence (Méndez et al., 2009). When searching for *tra* genes in the assembly, we could not find copies of *tra* genes other than those matching pYR3 in the scaffold 20 of *Y. ruckeri* 150. Based on our data, chromosomal localization of the *tra* cluster seems very unlikely. However, resequencing or a higher quality assembly of the genome of *Y. ruckeri* 150 could clarify this unambiguously in the future.

Finally, no significant LCBs were found when comparing pYR4 or pYR3 to *Yersinia* human pathogenic species, including the well-studied pYV plasmid from *Y. enterocolitica*. This suggests a very different strategy for host infection in *Y. ruckeri*, as the pYV plasmid is essential for virulence in *Y. enterocolitica*.

## Sequence Analysis of *pil* Operon and Its Potential Involvement in Virulence

Analysis of the pYR4 nucleotide sequence of a putative *pil* operon showed that this region spans a 12.6 kb locus containing 17 ORFs that encode a TFP. TFPs, not to be confused with T4SSs, are surface appendages expressed by many Gram-negative bacterial species. TFPs span both bacterial membranes and they are evolutionary and structurally related to type II secretion systems. TFPs are involved in bacterial adhesion, biofilm formation, horizontal gene transfer, and pathogenesis,

and in addition they mediate cell movement such as gliding motility in *Myxococcus xanthus* and twitching motility in *Pseudomonas* and *Neisseria* species (Shi and Sun, 2002). In the enteropathogenic *Y. pseudotuberculosis*, the TFP gene cluster is composed of 11 open reading frames and contributes to *Y. pseudotuberculosis* pathogenicity (Collyn et al., 2002). The arrangement of the pYR4 *pil* cluster (Figure 2; see also Table 1 and Supplementary Figure 1) resembles the *pil* cluster from the plasmid pADAP, which was described in *S. entomophila* (Hurst et al., 2011), and in plasmid R64 from *S. enterica* serovar Typhimurium (Kim and Komano, 1997). By analogy with the *pil* operon from *S. entomophila*, we adopted the same names for the putative proteins as described there, and designated them as PilLMNNOOPQRSTUDUV [(with the exception of the first two hypothetical proteins, designated as HP (H- for hypothetical and P- for proteins)]. It is worth mentioning that the *pil* operon in *S. enterica* includes only 14 genes (pilIJKLMNOPQRSTUV) in contrast to pYR4 (17 genes). The number of genes for *pil* clusters can vary, as described by Zhang et al. for *S. enterica* serovar Typhi, where the *pil* operon lacks the *pilI*, *pilJ*, and *pilK* genes (Zhang et al., 2000) of *S. entomophila*. The overall G+C content of the *pil* cluster is 51.7%, and thus higher than that of the *Y. ruckeri* NVH\_3758 genome (47.6%) and the average of pYR4 (49.4%). The G+C content of the individual genes in the *pil* locus varies between 55.1% (*pilP*) and 46.8% (*pilN*). The ORFs of the *pil* cluster are encoded on the same strand and the length of the intercistronic region between each ORF ranges from 20 to 205 bp. In the region up to 333 bp upstream of the first hypothetical protein of the *pil* cluster, we could identify binding sites for three sigma factors ( $\sigma 70$ ,  $\sigma 24$ , and  $\sigma 38$ ) using BPROM and bTSSfinder, indicating the presence of putative promoters sequences in that region. In fact, no putative promoter sequence was identified between the *pil* genes suggesting that this region may function as an operon (Figure 2) (see Table 1 and Supplementary Figure 1). Additionally, analysis of the downstream region of *pilV* showed the presence of a palindromic sequence (5'-CTAGACAGAATAGCCTAGTCAATATTATCTATGGCATTAAGATTCTGTCTAG-3') that could serve as a transcription terminator. The analysis of the secondary structure of this region showed a steam-loop like fold with the  $\Delta G = -15$  kcal/mol using the mfold Web server (Zuker, 2003).

The comparison of the protein sequences encoded by the *pil* operon, for example PilO and PilT, of pYR4 with database sequences using BLASTP showed from 64 to 86% identity to PilO and PilT proteins found in the IncI1 plasmid family from *Serratia* species. Accession numbers for the proteins, together with their functions, are given in Table 4.

The biogenesis of TFPs involves a number of proteins. These are all present in the *pil* operon of pYR4, suggesting that the locus is intact and functional. The pYR4 PilS protein encodes a major pilin, which is synthesized as a prePilS. In the prePilS protein sequence we identified a hydrophilic signal peptide comprising 15 residues. A predicted cleavage site lies between the 15th (glycine) and 16th (tryptophan) residues of prePilS, which is recognized by the specific peptidase PilD (Kim and Komano, 1997). The mature PilS contains an N-terminal hydrophobic region (first 23 residues in the mature protein sequence), while



**TABLE 3** | pYR4 RepA homologs detected using BLASTP.

Strain name	Name of the protein	Size (amino acids)	Degree of similarity	Accession number
<i>Y. frederiksenii</i>	Replication protein	316	280/308 (91%)	WP_088130752.1
<i>Y. enterocolitica</i>	Replication protein	316	276/308 (90%)	WP_075339110.1
<i>Y. massiliensis</i>	Replication protein	316	274/308 (89%)	WP_099462805.1
<i>Y. kristensenii</i>	Replication protein	316	270/308 (88%)	WP_087768868.1
<i>Photorhabdus temperata</i> subsp. <i>temperata</i> M1021	Sea7	314	229/308 (74%)	EQB98986.1
<i>S. fonticola</i> AU-P3(3)	Sea7	362	217/308 (70%)	ERK05611.1
<i>S. entomophila</i>	Sea7	362	208/306 (68%)	WP_010895766.1
<i>S. marcescens</i>	Replication protein	312	208/308 (68%)	WP_089197752.1
<i>S. fonticola</i>	Replication protein	312	204/306 (67%)	WP_074032170.1
<i>E. tarda</i>	Replication protein	311	194/303 (64%)	WP_097364799.1

the C-terminal region is rich in cysteine residues, a common feature of TFP pilins (Hurst et al., 2011). Beside the prepilins, we identified two copies of PilO and three copies of PilN, which seems to be a unique feature among plasmids from the same family. PilO and PilN are integral membrane proteins and usually exist only in one copy. An ATPase required for the assembly (PilQ) and an inner membrane protein (PilR) that we identified are also necessary for the assembly of the pili on the bacterial surface.

## Sequence Analysis of the *tra* Regions in pYR4

Annotations of pYR4 by HHpred (Söding et al., 2005) showed the presence of the *tra* region that we presume encodes a T4SS and is involved in conjugation. In fact, the presence of a chromosomally-borne *tra* clusters in *Y. ruckeri* 150 was previously described (Méndez et al., 2009). In our analysis, in addition to the *tra* cluster identified by Méndez et al. (*tra1*) that is probably also plasmid-borne (see above), we could identify another two *tra* clusters, which we named *tra2* and *tra3*. The *tra2* cluster comprises 10 genes with the gene order TraNOPQRTUWXY and an average G+C content of 53.5%, while the *tra3* cluster is composed of 3 genes with a G+C content of 52.6%. These two *tra* clusters are preceded by two putative promoter sequences with one located upstream from the *traN* gene while another one is located upstream from the *trbA* gene. The identification of the putative promoters sequences were based on the prediction of sigma factor binding sites using BPROM and bTSSfinder (see **Table 1** and **Supplementary Figure 1**). The presence of the two identified putative promoter sequences and the small intergenic region between the genes suggests that these genes might function as two operons, in addition to the *tra1* operon (**Figures 1, 2**). The genetic organization of the *tra2* and *tra3* operons resembles the gene order of the *tra* operon found in the pADAP plasmid of *S. entomophila*, the R64 plasmid of *S. enterica* serovar *Typhimurium*, pCTX-M3 of *C. freundii*, pEL60, pEA68, pEA72, and pEA78 of *E. amylovora* (see **Supplementary Figure 5**), as previously suggested for the *tra1* operon (Méndez et al., 2009).

The G+C content of the *tra2* and *tra3* operons (around 53%) differs from the G+C content of the chromosomes of *Y. ruckeri* NVH\_3758 (47.6%), *Y. ruckeri* Big Creek 74 (47.6%), and *Y. ruckeri* CSF007-82 (47.5%). Additionally, the *tra* region was not present in the chromosome of the *Y. ruckeri* strains mentioned above, indicating that the *tra* region may originate from another species. Méndez et al. suggested that *S. entomophila*, the causative agent of amber disease of the New Zealand grass grub, could be the source of the *tra1* region. The G+C content of the *S. entomophila* pADAP *tra* region (*tra1*, *tra2*, *tra3*) is around 52%, which is close to the G+C content of pYR4. In addition, the gene order of that region is very similar. We suggest that the whole *tra* region encompassing *tra1*, *tra2*, and *tra3* could have been acquired from this or a closely related *Serratia* species.

The amino acid sequences of TraH, TraI, TraJ, and TraK showed 29–34% similarity to the *L. pneumophila* T4BSS proteins such as DotD (for “defect in organelle trafficking”), DotC, DotB, and IcmT (for “intracellular multiplication”) (Wallden et al., 2010). The *icm/dot* genes are required for virulence, including intracellular growth and host cell killing (Sadosky et al., 1993; Swanson and Isberg, 1996). The pYR4 Tra proteins and their Tra homologs from *L. pneumophila* are similar in size, ranging from 87 residues (for TraK) to 385 residues (for TraJ). Interestingly, it has been shown before that a *traI* mutant strain of *Y. ruckeri* 150 was attenuated in an *in vivo* assay in rainbow trout and showed difficulty growing inside the fish (Méndez et al., 2009).

## Plasmid Curing Study of pYR4 in *Yersinia ruckeri* NVH\_3758

In order to understand the function of pYR4 and its involvement in pathogenesis, it is desirable to obtain a plasmid-cured strain. There is a wide number of plasmid curing procedures which have been successfully used to remove plasmids in *Yersinia*. They for example include treatments with high temperatures or introduction of an incompatible plasmid (Sheridan et al., 1998; Ni et al., 2008). The genetic stability of the pYR4 plasmid was tested by treating *Y. ruckeri* cells with high temperature. *Y. ruckeri* NVH\_3758 was grown in LB medium for 10 consecutive days at 37°C with dilutions each day (Trevors, 1986). After 10 days, colony PCR was performed on 10 clones using *pil*

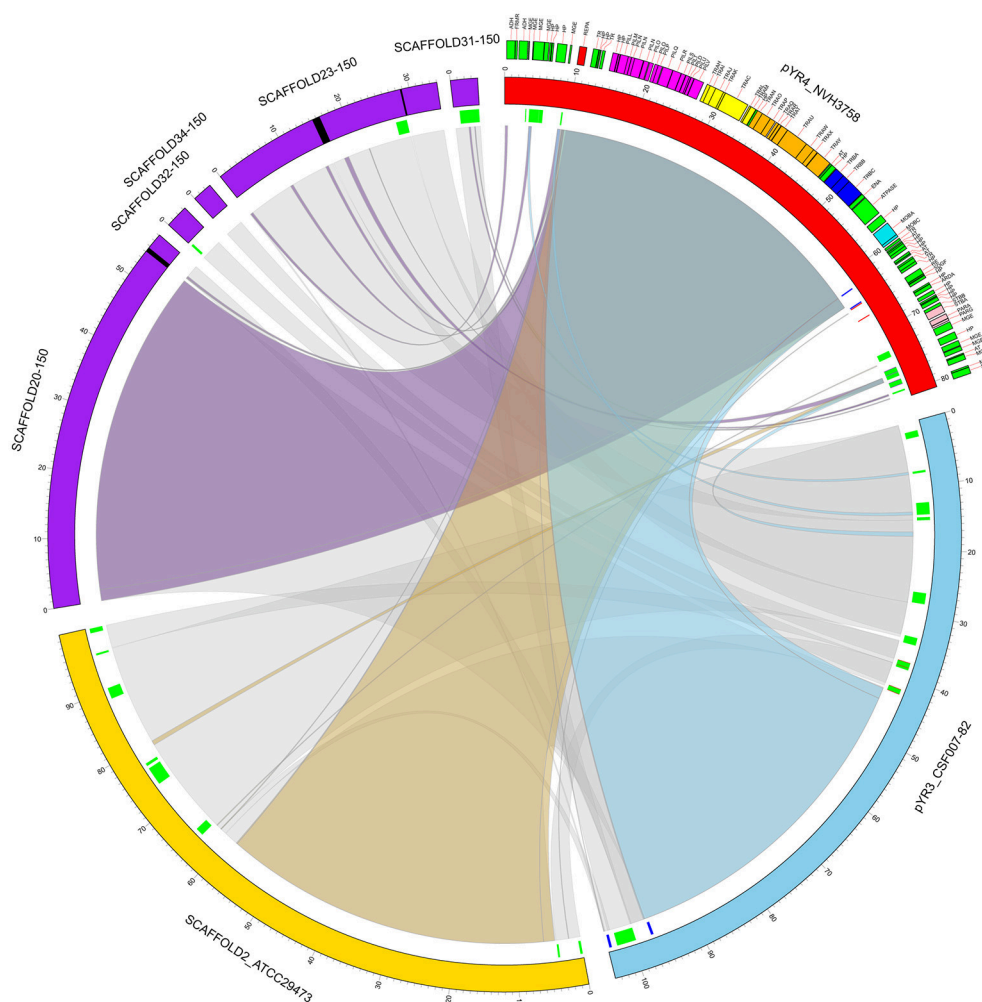


**FIGURE 3 |** Circular representation of a comparative analysis of pYR4 from *Y. ruckeri* NVH\_3758 to pYR3 and scaffolds of genomic assemblies from *Y. ruckeri* ATCC29473 (scaffold 2) and *Y. ruckeri* 150 (scaffolds 20, 23, 31, 32, 34). The pYR4 plasmid is depicted in red, pYR3 in blue, *Y. ruckeri* ATCC29473 scaffold 2 in yellow, and *Y. ruckeri* 150 scaffolds in purple. Sequence gaps (stretches of Ns) within ATCC29473 scaffolds are reported in black. Annotated features in pYR4 are shown and colored as in **Figure 2**. Repetitive DNA regions in pYR3 and pYR4 are colored red and blue, and mobile genetic elements are colored in green (lines in inner ring). Pairwise Locally Collinear Blocks (LCBs) as found in Mauve DNA alignments, are represented as ribbon links colored as follows: pYR4-pYR3 in light blue, pYR4-ATCC29473 in yellow, pYR4-150 in purple, pYR3-ATCC29473, and pYR3-150 in gray. Ribbon links of the ATCC29473 and 150 scaffolds with pYR3 and pYR4 are represented separately in **Supplementary Figures 6, 7**.

primers that could only bind to the plasmid sequence. All tested clones were PCR-positive for the pYR4 plasmid (data not shown). Based on our high quality genomic assembly, the *pil* operon is found only on the pYR4 plasmid and is absent from the chromosome. The results obtained from this analysis indicate that pYR4 is a very stable plasmid. The conjugative ability of the plasmid may maintain it in the population and determine its stability, so that even if individual cells lose it, they get it back from their neighbors. This suggests that the plasmid cannot be cured easily in a short time frame such, as the one that we tested. As we were unable to cure pYR4 within a reasonable amount of time, this precluded performing virulence assays to check the involvement of the plasmid in pathogenesis.

## DISCUSSION

### Higher Quality of pYR4 Assembly and Identification of Unplaced Scaffolds

Comparative analysis of the *pil* region of pYR4 plasmid with other *Y. ruckeri* plasmids revealed that the *pil* region is not a common feature among *Y. ruckeri* strains. Even though we could identify different *pil* regions in some of the *Y. ruckeri* plasmids such as pWKY, we did not detect any significant sequence similarity with the *pil* region described here. Literature suggests that the *pil* operon can be encoded both on plasmids (pADAP of *S. entomophila*) (Hurst et al., 2011) and the chromosome (in *Y. pseudotuberculosis* 32777) (Collins et al., 2002). Our data shows that in *Y. ruckeri* NVH\_3758, the

**TABLE 4 |** The main characteristic features of in *pil* operon identified in the pYR4 plasmid from *Y. ruckeri* NVH\_3758.

CDS	Homolog found by BLASTP	Organism	No. of similar amino acids/total no. of amino acids (similarity %)	Accession number
PilL	Lipoprotein PilL unknown function	<i>Y. pseudotuberculosis</i>	234/356 (66%)	WP_012606417.1
PilM	Lipoprotein PilM unknown function	<i>S. marcescens</i>	109/141 (77%)	CVH07391.1
PilN	TFP formation outer membrane protein, R64 PilN family	<i>S. liquefaciens</i>	106/133 (80%)	OKP16072.1
PilN	PilN family TFP formation outer membrane protein	<i>S. marcescens</i>	338/404 (84%)	WP_089197779.1
PilN	Putative TFP operon lipoprotein	<i>Y. intermedia</i>	151/217 (70%)	CNI92757.1
PilO	Incl1 plasmid pilus assembly protein PilO	<i>S. fonticola</i>	103/160 (64%)	WP_021807907.1
PilO	Incl1 plasmid pilus assembly protein PilO	<i>S. fonticola</i>	126/153 (82%)	WP_021807907.1
PilP	TFP biogenesis protein PilP	<i>Serratia</i> sp. 14-2641	142/195 (73%)	WP_065685464.1
PilQ	Incl1 plasmid conjugative transfer ATPase PilQ	<i>S. fonticola</i>	334/424 (79%)	WP_021807909.1
PilR	General secretion pathway protein GspF	<i>S. marcescens</i>	298/380 (78%)	WP_060442021.1
PilS	Prepilin	<i>Serratia</i> sp. S4	167/197 (85%)	WP_017891024.1
PilT	Lytic transglycosylase	<i>Serratia</i> sp. S4	138/161 (86%)	WP_017891023.1
PilD	Prepilin peptidase	<i>S. marcescens</i>	22/40 (55%)	ASL85991.1
PilV	Shufflon system plasmid conjugative transfer pilus tip adhesin PilV	<i>Y. pekkanenii</i>	297/446 (67%)	CNI31753.1
PilU	Prepilin peptidase	<i>S. fonticola</i> AU-AP2C	101/135 (75%)	ERK05998.1

TFP gene cluster is plasmid-encoded and no other TFP gene cluster was detected on the chromosome. In fact, our genomic comparative survey indicates that previously deposited Illumina-sequenced genomic assemblies containing the *tra* and the *pil* operons—five scaffolds from a *Y. ruckeri* 150 assembly and a scaffold from *Y. ruckeri* ATCC29743—correspond to the plasmid pYR3. In particular for the 150 strain, failure in placing the genomic scaffolds may have occurred due to the presence of repetitive DNA sequences and of mobile elements in the flanking regions, e.g., the repetitive mobile element at positions 37,633–38,328 and 41,885–42,850 of pYR3 (Figure 3). This might also explain the presence of sequence gaps in the scaffolds 20 and 23 of ATCC29743 (Figure 3). These results show the power of the PacBio SMRT technology in producing higher-quality genomic assemblies, thanks to the longer average read lengths available.

Our study highlights the problem related to incorrect assemblies when using second generation sequencing (SGS) technologies. Short-read sequencing is often not enough to properly assemble plasmid sequences. Plasmids often contain many mobile repeat structures whose DNA length exceeds that provided by limitations of SGS technology (ranging 100–600 bp), thus generating unplaced scaffolds and mis-assemblies. The longer average read length provided by the PacBio SMRT sequencing can address some of the limitations of the SGS technologies, making it possible to correctly place genomic scaffolds even when containing repetitive regions and obtain higher quality assemblies. Sequencing the NVH\_3758 genome using the PacBio technology yielded two contigs

representing the chromosomal genome of ~3.8 Mb and the ~81 kb plasmid pYR4. Thanks to the PacBio platform, we could correctly determine the plasmid location of both the *tra* and the *pil* operons. The presence of the *tra* operon on the pYR4 plasmid, not on the chromosome, is reasonable as the *tra* operon encodes genes involved in bacterial conjugation and DNA transfer. We re-emphasize that these two systems, despite having similar names, are very distinct structurally and mechanistically. The T4SS is a secretion system that translocates nucleoprotein complexes or effector proteins into target cells, whereas TFP are contractile appendages mainly mediating adhesion and certain types of motility (Shi and Sun, 2002).

## TFPs in pYR4 And Their Potential Role in Virulence and Conjugation

In the human pathogenic *Yersinia*, pathogenicity is mainly related to the presence of the 70-kb virulence plasmid pYV. This plasmid encodes the Yop proteins and T3SS, which enable the bacteria to survive and multiply in the host tissues (Viboud and Bliska, 2005). Plasmids described so far in *Y. ruckeri* have recently gained more and more attention due to their potential association with virulence, although in-depth knowledge regarding their function is lacking.

Annotations of pYR4 showed 92 open reading frames. We could identify three different functional regions responsible for plasmid partitioning, a T4SS and a TFP. The present study strongly suggests that the pYR4 *pil* cluster belongs to the TFP family. In addition to attachment and motility, TFPs can be

involved in DNA uptake as shown in *N. gonorrhoeae* (Wolfgang et al., 1998). Interestingly, there are examples of TFPs being involved in bacterial conjugation. For example, the PAPI-1 pathogenicity island of *P. aeruginosa* can be transferred to a recipient strain lacking this island. The mobilization of PAPI-1 was dependent on a TFP (Carter et al., 2010). The fact that the *pil* operon clusters together with the *tra* operon suggests that the two are functionally coupled and that the TFPs are involved in conjugative transfer of pYR4. However, it is also possible that the TFP is a virulence factor. We speculate that the *pil* proteins in pYR4, apart from being involved in virulence, can also be responsible for thin pilus formation required for liquid mating (Kim and Komano, 1997). Experiments carried out by Collyn et al. showed that the TFP gene cluster present in *Y. pseudotuberculosis* is not only involved in synthesis of TFPs, but also contributes to its virulence (Collyn et al., 2002). Based on these findings, we speculate that the *pil* operon present in *Y. ruckeri* could play a similarly important role in fish disease.

The difference between the G+C content of the *pil* operon (51.7%) and the average G+C content of the pYR4 plasmid (49.4%) suggests that the *pil* operon could have been acquired relatively recently by horizontal gene transfer. Likewise, the difference in G+C content compared to the *Y. ruckeri* NVH\_3758 chromosome (47.6%) suggests that the plasmid has been acquired from a different species. Previous studies show that for a plasmid to be horizontally transferred, the difference in the G+C composition between the genome and the plasmid should be in the range from 1 to 5% (Hurst et al., 2011). The G+C content of the plasmid pADAP of *S. entomophila* is 53%. Most of the *pil* proteins from pYR4 (PilL, PilN, PilO, PilP, PilQ, PilR, PilS, PilT, PilD) are highly similar to *pil* proteins found in TFPs in *Serratia* species, whereas others (PilL, PilU, PilN) are more similar to those found in other *Yersinia* species. These findings, in addition to the same gene organization of the *pil* cluster, suggest that the TFP locus in pYR4 may have been acquired from *S. entomophila*, which occupies a similar aquatic environment as *Y. ruckeri* (Grimont et al., 1988).

## T4SSs and the *tra* Operon

Analysis of the pYR4 protein encoding sequences allowed us to identify a complete T4SS, which we named *tra*. The corresponding coding region consists of three operons. The genetic organization of the *tra* operons (*tra1*, *tra2*, *tra3*) is very similar to that found in pADAP of *S. entomophila*, pCTX-M3 of *C. freundii* and pEL60, pEA67, pEA72, and pEA78 of *E. amylovora*, as previously described for *tra1* (Méndez et al., 2009). Comparative analysis of the pYR4 *tra* operons to the pYR3 *tra* operons from *Y. ruckeri* CSF007-82 showed 99.9% nucleotide sequence similarity, in contrast to *tra* operons from other *Y. ruckeri* strains, where we did not detect any strong sequence similarity. In 2007, Welch et al. showed the presence of multidrug resistance of the plasmid pYR1 in *Y. ruckeri* YR71. pYR1 also contains a T4SS for conjugative transfer. However, the T4SS of pYR1 does not show high levels of sequence similarity—and no LCB was found in the Mauve

alignment—to the *tra* operons described here (Welch et al., 2007).

Interestingly, similarities between the pYR4 Tra and *L. pneumophila* Icm/Dot proteins implicate a role in *Y. ruckeri* virulence. *L. pneumophila* is the causative agent of Legionnaires' disease. As an intracellular pathogen, *L. pneumophila* is able to grow and multiply within human macrophages, leading to their killing. In *L. pneumophila*, many virulence genes located in *icm* ("for intracellular multiplication") and *dot* ("defect in organelle trafficking") locus have been identified. Some of the Dot/Icm proteins are homologous to the Tra proteins found in plasmid R64 (Komano et al., 2000). pYR4 Tra proteins display amino acid sequence similarity to Icm/Dot proteins ranging from 29 to 34%. They are similar in size and their predicted functions are similar. However, as we could not identify any genes encoding putative effector proteins in pYR4 of NVH\_3758, it is possible that the *tra* locus is purely conjugative. Nevertheless, we cannot conclusively rule out a role for the *tra* locus in virulence. Interestingly, Méndez et al. generated the *traI* mutant strain of *Y. ruckeri* 150 in which the *traI* gene was disrupted. In the *in vivo* competition assays in rainbow trout, the virulence of the *traI* mutant strain was reported to be attenuated when compared to the WT strain, suggesting that TraI is involved in virulence of this bacterium.

## CONCLUSIONS

In conclusion, the results presented here suggest that pYR4 from the 1987 outbreak strain *Y. ruckeri* NVH\_3758 is a conjugative plasmid that encodes a T4SS and a TFP that might contribute to *Y. ruckeri* virulence. The 55 kDa plasmid backbone is identical to that of pYR3 and has presumably been acquired by horizontal gene transfer through conjugation from a *Serratia* species that occupies the same biological niche, as previously suggested (Méndez et al., 2009). In addition, pYR4 contains a previously undescribed ~25 kDa region with a partitioning system completely different from that of pYR3. This region contains a set of mobile elements, several hydrogenase enzymes with a corresponding transcription factor, and additional hypothetical genes that need further investigation.

The plasmid could contribute to the dissemination of *Y. ruckeri* virulence by spreading the TFP-encoding *pil* locus among non-virulent strains. Further experiments are required to elucidate the function of the *pil* and *tra* regions and to clarify their role in virulence. However, we would like to highlight that based on 100% sequence similarity between TraI of pYR4 and TraI of *Y. ruckeri* 150 that we now know is located on pYR3 based on our re-assembly of the *Y. ruckeri* 150 genome, we assume that at least the *tra* region is directly involved in virulence. *traI* deletion in *Y. ruckeri* 150 lead to a significant decrease in virulence (Méndez et al., 2009). Additionally, our study demonstrates the power of PacBio SMRT sequencing technology in producing assemblies of high quality and accuracy, compared to sequencing technologies based on shorter read lengths such as Illumina and 454. The latter methods failed to show the plasmid localization of the *pil* and *tra* regions in multiple cases.



## DATA AVAILABILITY

The sequence of pYR4 described herein has been deposited in GenBank with the accession number CP032236.

## AUTHOR CONTRIBUTIONS

AW and CO conceived, planned, and carried out the experiments. AW, CO, JL, and DL contributed to the discussion and interpretation of the results, and wrote the manuscript. All authors provided critical feedback and contributed to the final shape of the manuscript.

## FUNDING

This work was supported by Departmental funds of the Department of Biosciences, University of Oslo (COMPI), by Research Council of Norway Young Investigator grant 249793

## REFERENCES

- Altschul, S., Madden, T., Schäffer, A., Zhang, J., Zhang, Z., Miller, W., et al. (1997). Gapped BLAST and PSI-BLAST: a new generation of protein database search programs. *Nucleic Acids Res.* 25, 3389–3402. doi: 10.1093/nar/25.17.3389
- Avendaño-Herrera, R., Tapia-Cammas, D., Aedo, A., Saldivia, P., Ortega, C., and Irgang, R. (2017). Disease caused by *Yersinia ruckeri* serotype O2b found in Chilean-farmed coho salmon, *Oncorhynchus kisutch*. *J. Fish Dis.* 40, 279–285. doi: 10.1111/jfd.12502
- Aziz, R., Bartels, D., Best, A., DeJongh, M., Disz, T., Edwards, R., et al. (2008). The RAST server: rapid annotations using subsystems technology. *BMC Genomics* 9:75. doi: 10.1186/1471-2164-9-75
- Barnes, A., Delamare-Deboutteville, J., Gudkovs, N., Brosnahan, C., Morrison, R., and Carson, J. (2016). Whole genome analysis of *Yersinia ruckeri* isolated over 27 years in Australia and New Zealand reveals geographical endemism over multiple lineages and recent evolution under host selection. *Microb. Genomics* 2:e000095. doi: 10.1099/mgen.0.000095
- Ben-Gurion, R., and Shafferman, A. (1981). Essential virulence determinants of different *Yersinia* are carried on a common plasmid. *Plasmid* 5, 183–187. doi: 10.1016/0147-619X(81)90019-6
- Botton, E. (1997). *Yersinia enterocolitica*: the charisma continues. *Clin. Microbiol. Rev.* 10, 257–276.
- Bullock, G., Stuckey, H., and Shotts, J. R. E. (1978). Enteric redmouth bacterium: comparison of isolates from different geographic areas. *J. Fish Dis.* 1, 351–356. doi: 10.1111/j.1365-2761.1978.tb00039.x
- Busch, R. (1978). Enteric redmouth disease. *Mar. Fish. Rev.* 40, 42–51.
- Carattoli, A. (2009). Resistance plasmid families in *Enterobacteriaceae*. *Antimicrob. Agents Chemother.* 53, 2227–2238. doi: 10.1128/AAC.01707-08
- Carattoli, A., Villa, L., Poirol, L., Bonnin, R., and Nordmann, P. (2012). Evolution of IncA /C bla CMY-2 -carrying plasmids by acquisition of the bla NDM-1 carbapenemase gene. *Antimicrob. Agents Chemother.* 56, 783–786. doi: 10.1128/AAC.05116-11
- Carter, M., Chen, J., and Lory, S. (2010). The *Pseudomonas aeruginosa* pathogenicity island PAPI-1 is transferred via a novel type IV pilus. *J. Bacteriol.* 192, 3249–3258. doi: 10.1128/JB.00041-10
- Chauhan, N., Wrobel, A., Skurnik, M., and Leo, J. (2016). *Yersinia* adhesins: an arsenal for infection. *Proteomics-Clin. Appl.* 10, 949–963. doi: 10.1002/prca.201600012
- Collyn, F., Léty, M., Nair, S., Escuyer, V., Younes, A., Simonet, M., et al. (2002). *Yersinia pseudotuberculosis* harbors a type IV pilus gene cluster that contributes to pathogenicity. *Infect. Immun.* 70, 6196–6205. doi: 10.1128/IAI.70.11.6196-6205.2002
- Cornelis, G., Boland, A., Boyd, A., Geuijen, C., Iriarte, M., Neyt, C., et al. (1998). The virulence plasmid of *Yersinia*, an antihost genome. *Microbiol. Mol. Biol. Rev.* 62, 1315–1352.
- Couturier, M., Bex, F., Bergquist, P., and Maas, W. (1988). Identification and classification of bacterial plasmids. *Microbiol. Rev.* 52, 375–395.
- Crosa, J. (1980). A plasmid associated with virulence in the marine fish pathogen *Vibrio anguillarum* specifies an iron sequestering system. *Nature* 284, 566–568. doi: 10.1038/284566a0
- Darling, A., Mau, B., and Perna, N. (2010). Progressive mauve: multiple genome alignment with gene gain, loss and rearrangement. *PLoS ONE* 5:e11147. doi: 10.1371/journal.pone.0011147
- De Grandis, S., and Stevenson, R. (1982). Variations in plasmid profiles and growth characteristics of *Yersinia ruckeri* strains. *FEMS Microbiol. Lett.* 15, 199–202. doi: 10.1111/j.1574-6968.1982.tb00067.x
- De Grandis, S., and Stevenson, R. (1985). Antimicrobial susceptibility patterns and R plasmid-mediated resistance of the fish pathogen *Yersinia ruckeri*. *Antimicrob. Agents Chemother.* 27, 938–942. doi: 10.1128/AAC.27.6.938
- Edgar, R. (2004). MUSCLE: multiple sequence alignment with high accuracy and high throughput. *Nucleic Acids Res.* 32, 1792–1797. doi: 10.1093/nar/gkh340
- Felsenstein, J. (1985). Confidence limits on phylogenies: an approach using the bootstrap. *Evolution* 39, 783–791. doi: 10.1111/j.1558-5646.1985.tb00420.x
- Ferber, D., and Brubaker, R. (1981). Plasmids in *Yersinia pestis*. *Infect. Immun.* 31, 839–841.
- Fernández, L., Marquez, I., and Guijarro, J. (2004). Identification of specific *in vivo*-induced (ivi) genes in *Yersinia ruckeri* and analysis of ruckerbactin, a catecholate siderophore iron acquisition system. *Appl. Environ. Microbiol.* 70, 5199–5207. doi: 10.1128/AEM.70.9.5199-5207.2004
- Fernández, L., Prieto, M., and Guijarro, J. (2007). The iron- and temperature-regulated haemolysin Yhla is a virulence factor of *Yersinia ruckeri*. *Microbiology* 153, 483–489. doi: 10.1099/mic.0.29284-0
- García, J., Dominguez, L., Larsen, J., and Pedersen, K. (1998). Ribotyping and plasmid profiling of *Yersinia ruckeri*. *J. Appl. Microbiol.* 85, 949–955. doi: 10.1111/j.1365-2672.1998.tb05258.x
- Grimont, P., Jackson, T., Ageron, E., and Noonan, M. (1988). *Serratia entomophila* sp. nov. associated with amber disease in the New Zealand grass grub *Costelytra zealandica*. *Int. J. Syst. Bacteriol.* 38, 1–6. doi: 10.1099/00207713-38-1-1
- Guilvout, I., Quilici, M., Rabot, S., Lesel, R., and Mazigh, D. (1988). BamHI restriction endonuclease analysis of *Yersinia ruckeri* plasmids and their relatedness to the genus *Yersinia* 42- to 47-megadalton plasmid. *Appl. Environ. Microbiol.* 54, 2594–2597.

(to JL), and by Research Council of Norway FriMedBio grant 240483 (to DL).

## ACKNOWLEDGMENTS

We would like to thank the sequencing service provided by the Norwegian Sequencing Centre (www.sequencing.uio.no), a national technology platform hosted by the University of Oslo and supported by the Functional Genomics and Infrastructure programs of the Research Council of Norway and the Southeastern Regional Health Authorities. We express gratitude to Prof. Duncan Colquhoun (Norwegian Veterinary Institute) for providing *Y. ruckeri* NVH\_3758.

## SUPPLEMENTARY MATERIAL

The Supplementary Material for this article can be found online at: <https://www.frontiersin.org/articles/10.3389/fcimb.2018.00373/full#supplementary-material>

- Gulla, S., Barnes, A., Welch, T., Romalde, J., Ryder, D., Ormsby, M., et al. (2018). Multi-locus variable number of tandem repeat Analysis (MLVA) of *Yersinia ruckeri* confirms the existence of host-specificity, geographic endemism and anthropogenic dissemination of virulent clones. *Appl. Environ. Microbiol.* 84:e00730–18. doi: 10.1128/AEM.00730-18
- Haiko, J., Suomalainen, M., Ojala, T., Lähdenmäki, K., and Korhonen, T. (2009). Invited review: breaking barriers – attack on innate immune defences by ompT surface proteases of enterobacterial pathogens. *Innate Immun.* 15, 67–80. doi: 10.1177/1753425909102559
- Hayek, N. (2013). Lateral transfer and GC content of bacterial resistance genes. *Front. Microbiol.* 4:41. doi: 10.3389/fmicb.2013.00041
- Hjeltnes, B., Bornø, G., Jansen, M., Haukaas, A., and Walde, C. (2017). *The Health Situation in Norwegian Aquaculture 2016*. Norwegian Veterinary Institute 2017.
- Huang, Y., Michael, G., Becker, R., Kaspar, H., Mankertz, J., Schwarz, S., et al. (2014). Pheno- and genotypic analysis of antimicrobial resistance properties of *Yersinia ruckeri* from fish. *Vet. Microbiol.* 171, 406–412. doi: 10.1016/j.vetmic.2013.10.026
- Hurst, M., Becher, S., and O'Callaghan, M. (2011). Nucleotide sequence of the *Serratia entomophila* plasmid pADAP and the *Serratia proteamaculans* pU143 plasmid virulence associated region. *Plasmid* 65, 32–41. doi: 10.1016/j.plasmid.2010.10.001
- Isberg, R., and Leong, J. (1990). Multiple  $\beta 1$  chain integrins are receptors for invasion, a protein that promotes bacterial penetration into mammalian cells. *Cell* 60, 861–871. doi: 10.1016/0092-8674(90)90099-Z
- Jalava, K., Hakkinen, M., Valkonen, M., Nakari, U., Palo, T., Hallanvuori, S., et al. (2006). An outbreak of gastrointestinal illness and erythema nodosum from grated carrots contaminated with *Yersinia pseudotuberculosis*. *J. Infect. Dis.* 194, 1209–1216. doi: 10.1086/508191
- Johnson, T., and Lang, K. (2012). IncA/C plasmids: an emerging threat to human and animal health? *Mob. Genet. Elements* 2, 55–58. doi: 10.4161/mge.19626
- Kearse, M., Moir, R., Wilson, A., Stones-Havas, S., Cheung, M., Sturrock, S., et al. (2012). Geneious basic: an integrated and extendable desktop software platform for the organization and analysis of sequence data. *Bioinformatics* 28, 1647–1649. doi: 10.1093/bioinformatics/bts199
- Kim, S., and Komano, T. (1997). The plasmid R64 thin pilus identified as a type IV pilus. *J. Bacteriol.* 179, 3594–3603. doi: 10.1128/jb.179.11.3594-3603.1997
- Komano, T., Yoshida, T., Narahara, K., and Furuya, N. (2000). The transfer region of IncI1 plasmid R64: similarities between R64 *tra* and *Legionella icm/dot* genes. *Mol. Microbiol.* 35, 1348–1359. doi: 10.1046/j.1365-2958.2000.01769.x
- Krzywinski, M., Schein, J., Birol, I., Connors, J., Gascoyne, R., Horsman, D., et al. (2009). Circos: an information aesthetic for comparative genomics. *Genome Res.* 18, 1639–1645. doi: 10.1101/gr.092759.109
- Kumar, G., Hummel, K., Ahrens, M., Menanteau-Ledouble, S., Welch, T., Eisenacher, M., et al. (2016). Shotgun proteomic analysis of *Yersinia ruckeri* strains under normal and iron-limited conditions. *Vet. Res.* 47:100. doi: 10.1186/s13567-016-0384-3
- Kumar, G., Hummel, K., Welch, T., Razzazi-Fazeli, E., and El-Matbouli, M. (2017). Global proteomic profiling of *Yersinia ruckeri* strains. *Vet. Res.* 48:55. doi: 10.1186/s13567-017-0460-3
- Kumar, S., Stecher, G., Li, M., Knyaz, C., and Tamura, K. (2018). MEGA X: molecular evolutionary genetics analysis across computing platforms. *Mol. Biol. Evol.* 35, 1547–1549. doi: 10.1093/molbev/msy096
- Liu, T., Wang, K., Wang, J., Chen, D., Huang, X., Ouyang, P., et al. (2016). Genome sequence of the fish pathogen *Yersinia ruckeri* SC09 provides insights into niche adaptation and pathogenic mechanism. *Int. J. Mol. Sci.* 17:557. doi: 10.3390/ijms17040557
- Méndez, J., Fernández, L., Menéndez, A., Reimundo, P., Pérez-Pascual, D., Navais, R., et al. (2009). A chromosomally located traHIJKLMN operon encoding a putative type IV secretion system is involved in the virulence of *Yersinia ruckeri*. *Appl. Environ. Microbiol.* 75, 937–945. doi: 10.1128/AEM.01377-08
- Mühlenkamp, M., Oberhettinger, P., Leo, J., Linke, D., and Schütz, M. (2015). *Yersinia* adhesin A (YadA) – Beauty & beast. *Int. J. Med. Microbiol.* 305, 252–258. doi: 10.1016/j.ijmm.2014.12.008
- Nelson, M., Lapatra, S., Welch, T. (2015). Complete genome sequence of *Yersinia ruckeri* strain CSF007-82, etiologic agent of red mouth disease in salmonid fish. *Genome Announc.* 3:e01491–14. doi: 10.1128/genomeA.01491-14
- Ni, B., Du, Z., Guo, Z., Zhang, Y., and Yang, R. (2008). Curing of four different plasmids in *Yersinia pestis* using plasmid incompatibility. *Lett. Appl. Microbiol.* 47, 235–240. doi: 10.1111/j.1472-765X.2008.02426.x
- Nishida, H. (2012). Comparative analyses of base compositions, DNA sizes, and dinucleotide frequency profiles in archaeal and bacterial chromosomes and plasmids. *Int. J. Evol. Biol.* 2012:342482. doi: 10.1155/2012/342482
- Ormsby, M., Caws, T., Burchmore, R., Wallis, T., Verner-Jeffreys, D., and Davies, R. (2016). *Yersinia ruckeri* isolates recovered from diseased atlantic salmon (*Salmo salar*) in Scotland are more diverse than those from rainbow trout (*Oncorhynchus mykiss*) and represent distinct subpopulations. *Appl. Environ. Microbiol.* 82, 5785–5794. doi: 10.1128/AEM.01173-16
- Perry, R., and Fetherston, J. (1997). *Yersinia pestis* — etiologic agent of plague. *Clin. Microbiol. Rev.* 10, 35–66.
- Pilla, G., and Tang, C. M. (2018). Going around in circles: virulence plasmids in enteric pathogens. *Nat. Rev. Microbiol.* 16, 484–95. doi: 10.1038/s41579-018-0031-2
- Reuter, S., Connor, T., Barquist, L., Walker, D., Feltwell, T., Harris, S., et al. (2014). Parallel independent evolution of pathogenicity within the genus *Yersinia*. *Proc. Natl. Acad. Sci. U.S.A.* 111, 6768–6773. doi: 10.1073/pnas.1317161111
- Romalde, J., Magariños, B., Barja, J., and Toranzo, A. (1993). Antigenic and molecular characterization of *Yersinia ruckeri* proposal for a new intraspecies classification. *Syst. Appl. Microbiol.* 16, 411–419. doi: 10.1016/S0723-2020(11)80274-2
- Romalde, J. L., and Toranzo, A. E. (1993). Pathological activities of *Yersinia ruckeri*, the enteric redmouth (ERM) bacterium. *FEMS Microbiol. Lett.* 112, 291–299. doi: 10.1111/j.1574-6968.1993.tb06465.x
- Sadosky, A. B., Wiater, L. A., and Shuman, H. A. (1993). Identification of *Legionella pneumophila* genes required for growth within and killing of human macrophages. *Infect. Immun.* 61, 5361–5373.
- Savin, C., Martin, L., Bouchier, C., Filali, S., Chenau, J., Zhou, Z., et al. (2014). The *Yersinia pseudotuberculosis* complex: characterization and delineation of a new species, *Yersinia wautersii*. *Int. J. Med. Microbiol.* 304, 452–463. doi: 10.1016/j.ijmm.2014.02.002
- Secades, P., and Guijarro, J. A. (1999). Purification and characterization of an extracellular protease from the fish pathogen *Yersinia ruckeri* and effect of culture condition on production. *Appl. Environ. Microbiol.* 65, 3969–3975.
- Seemann, T. (2014). Prokka: rapid prokaryotic genome annotation. *Bioinformatics* 30, 2068–2069. doi: 10.1093/bioinformatics/btu153
- Shahmuradov, I., Mohamad Razali, R., Bougouffa, S., Radovanovic, A., and Bajic, V. (2017). bTSSfinder: a novel tool for the prediction of promoters in cyanobacteria and *Escherichia coli*. *Bioinformatics* 33, 334–340. doi: 10.1093/bioinformatics/btw629
- Sheridan, J. J., Logue, C. M., McDowell, D. A., Blair, I. S., and Hegarty, T. (1998). A study of the growth kinetics of *Yersinia enterocolitica* serotype O:3 in pure and meat culture systems. *J. Appl. Microbiol.* 85, 293–301. doi: 10.1046/j.1365-2672.1998.00504.x
- Shi, W., and Sun, H. (2002). Type IV pilus-dependent motility and its possible role in bacterial pathogenesis. *Infect. Immun.* 70, 1–4. doi: 10.1128/IAI.70.1.1-4.2002
- Söding, J., Biegert, A., and Lupas, A. N. (2005). The HHpred interactive server for protein homology detection and structure prediction. *Nucleic Acids Res.* 33, 244–248. doi: 10.1093/nar/gki408
- Solov'yev, V., and Salamov, A. (2011). “Automatic annotation of microbial genomes and metagenomic sequences,” in *Metagenomics and its Applications in Agriculture, Biomedicine and Environmental Studies*, ed R. W. Li (New York, NY: Nova Science Publishers), 61–78.
- Sonnhammer, E., Eddy, S., Birney, E., Bateman, A., and Durbin, R. (1998). Pfam: multiple sequence alignments and HMM-profiles of protein domains. *Nucleic Acids Res.* 26, 320–322. doi: 10.1093/nar/26.1.320
- Sparboe, O., Koren, C., Hastein, T., Poppe, T., and Stenwig, H. (1986). The first isolation of *Yersinia ruckeri* from farmed Norwegian salmon. *Bull. Eur. Assoc. Fish Pathol.* 6, 41–42.
- Stevenson, R., and Airdrie, R. (1984). Serological variation among *Yersinia ruckeri* strains. *J. Fish Dis.* 7, 247–254. doi: 10.1111/j.1365-2761.1984.tb00930.x

- Sussman, J. L., Abola, E. E., Lin, D., Jiang, J., Manning, N. O., and Prilusky, J. (1999). The protein data bank. Bridging the gap between the sequence and 3D structure world. *Genetica* 1062, 149–158. doi: 10.1023/A:1003753517358
- Swanson, M. S., and Isberg, R. R. (1996). Identification of *Legionella pneumophila* mutants that have aberrant intracellular fates. *Infect. Immun.* 64, 2585–2594.
- Toranzo, A. E., Barja, J. L., Colwell, R. R., and Hetrick, F. M. (1983). Characterization of plasmids in bacterial fish pathogens. *Infect. Immun.* 39, 184–192.
- Trevors, J. T. (1986). Plasmid curing in bacteria. *FEMS Microbiol. Lett.* 32, 149–157. doi: 10.1111/j.1574-6968.1986.tb01189.x
- Viboud, G. I., and Bliska, J. B. (2005). *Yersinia* outer proteins: role in modulation of host cell signaling responses and pathogenesis. *Annu. Rev. Microbiol.* 59, 69–89. doi: 10.1146/annurev.micro.59.030804.121320
- Villa, L., García-Fernández, A., Fortini, D., and Carattoli, A. (2010). Replicon sequence typing of IncF plasmids carrying virulence and resistance determinants. *J. Antimicrob. Chemother.* 65, 2518–2529. doi: 10.1093/jac/dkq347
- Wallden, K., Rivera-Calzada, A., and Waksman, G. (2010). Type IV secretion systems: versatility and diversity in function. *Cell. Microbiol.* 12, 1203–1212. doi: 10.1111/j.1462-5822.2010.01499.x
- Welch, T. J., Fricke, W. F., Mcdermott, P. F., White, D. G., Rosso, M., Rasko, D. A., et al. (2007). Multiple antimicrobial resistance in plague: an emerging public health risk. *PLoS ONE* 2:e309. doi: 10.1371/journal.pone.000309
- Wolfgang, M., Lauer, P., Park, H., Brossay, L., Hebert, J., and Koomey, M. (1998). PilT mutations lead to simultaneous defects in competence for natural transformation and twitching motility in pilated *Neisseria gonorrhoeae*. *Mol. Microbiol.* 29, 321–330. doi: 10.1046/j.1365-2958.1998.00935.x
- Wrobel, A., Ottoni, C., Leo, J. C., Gulla, S., and Linke, D. (2017). The repeat structure of two paralogous genes, *Yersinia ruckeri* Invasin (yrInv) and a “*Y. ruckeri* Invasin-like molecule”, (yrIlm) sheds light on the evolution of adhesive capacities of a fish pathogen. *J. Struct. Biol.* 201, 171–183. doi: 10.1016/j.jsb.2017.08.008
- Yang, Q., Sun, J., Li, L., Deng, H., Liu, B., Fang, L., et al. (2015). IncF plasmid diversity in multi-drug resistant *Escherichia coli* strains from animals in China. *Front. Microbiol.* 6:964. doi: 10.3389/fmicb.2015.00964
- Yu, J., Cho, M., Kim, J., and Kang, H. (2012). Large antibiotic-resistance plasmid of *Edwardsiella tarda* contributes to virulence in fish. *Microb. Pathog.* 52, 259–266. doi: 10.1016/j.micpath.2012.01.006
- Zhang, X.-L., Tsui, I. S. M., Yip, C. M. C., Fung, A. W. Y., Wong, D. K.-H., Dai, X., et al. (2000). *Salmonella enterica* Serovar typhi uses type IVB Pili to enter human intestinal epithelial cells. *Infect. Immun.* 68, 3067–3073. doi: 10.1128/IAI.68.6.3067-3073.2000
- Zuckerandl, E., and Pauling, L. (1965). “Evolutionary divergence and convergence in proteins,” in *Evolving Genes and Proteins*, eds V. Bryson and H. J. Vogel (New York, NY: Academic Press), 97–166.
- Zuker, M. (2003). Mfold web server for nucleic acid folding and hybridization prediction. *Nucleic Acids Res.* 31, 3406–3415. doi: 10.1093/nar/gkg595

**Conflict of Interest Statement:** The authors declare that the research was conducted in the absence of any commercial or financial relationships that could be construed as a potential conflict of interest.

The reviewer HL and handling Editor declared their shared affiliation.

Copyright © 2018 Wrobel, Ottoni, Leo and Linke. This is an open-access article distributed under the terms of the Creative Commons Attribution License (CC BY). The use, distribution or reproduction in other forums is permitted, provided the original author(s) and the copyright owner(s) are credited and that the original publication in this journal is cited, in accordance with accepted academic practice. No use, distribution or reproduction is permitted which does not comply with these terms.



# Insecticidal Toxicity of *Yersinia frederiksenii* Involves the Novel Enterotoxin YacT

Katharina Springer<sup>1</sup>, Philipp-Albert Sanger<sup>2</sup>, Christian Moritz<sup>1</sup>, Angela Felsl<sup>1</sup>, Thomas Rattei<sup>3</sup> and Thilo M. Fuchs<sup>1,2\*</sup>

<sup>1</sup> Lehrstuhl fur Mikrobielle Okologie, Fakultat fur Grundlagen der Biowissenschaften, Wissenschaftszentrum Weihenstephan, Technische Universitat Munchen, Freising, Germany, <sup>2</sup> Friedrich-Loeffler-Institut, Institut fur Molekulare Pathogenese, Jena, Germany, <sup>3</sup> Department of Computational Systems Biology, University of Vienna, Vienna, Austria

## OPEN ACCESS

### Edited by:

Matthew S. Francis,  
Umea University, Sweden

### Reviewed by:

Mark Robin Holmes Hurst,  
AgResearch, New Zealand  
Louis S. Tisa,  
University of New Hampshire,  
United States

### \*Correspondence:

Thilo M. Fuchs  
thilom.fuchs@fli.de

### Specialty section:

This article was submitted to  
Molecular Bacterial Pathogenesis,  
a section of the journal  
Frontiers in Cellular and Infection  
Microbiology

**Received:** 20 April 2018

**Accepted:** 18 October 2018

**Published:** 14 November 2018

### Citation:

Springer K, Sanger P-A, Moritz C,  
Felsl A, Rattei T and Fuchs TM (2018)  
Insecticidal Toxicity of *Yersinia*  
*frederiksenii* Involves the Novel  
Enterotoxin YacT.  
Front. Cell. Infect. Microbiol. 8:392.  
doi: 10.3389/fcimb.2018.00392

The genus *Yersinia* comprises 19 species of which three are known as human and animal pathogens. Some species display toxicity toward invertebrates using the so-called toxin complex (TC) and/or determinants that are not yet known. Recent studies showed a remarkable variability of insecticidal activities when representatives of different *Yersinia* species (spp.) were subcutaneously injected into the greater wax moth, *Galleria mellonella*. Here, we demonstrate that *Y. intermedia* and *Y. frederiksenii* are highly toxic to this insect. A member of *Y. Enterocolitica* phylogroup 1B killed *G. mellonella* larvae with injection doses of approximately 38 cells only, thus resembling the insecticidal activity of *Photorhabdus luminescens*. The pathogenicity *Yersinia* spp. displays toward the larvae was higher at 15°C than at 30°C and independent of the TC. However, upon subtraction of all genes of the low-pathogenic *Y. enterocolitica* strain W22703 from the genomes of *Y. intermedia* and *Y. frederiksenii*, we identified a set of genes that may be responsible for the toxicity of these two species. Indeed, a mutant of *Y. frederiksenii* lacking *yacT*, a gene that encodes a protein similar to the heat-stable cytotoxic enterotoxin (Ast) of *Aeromonas hydrophila*, exhibited a reduced pathogenicity toward *G. mellonella* larvae and altered the morphology of hemocytes. The data suggests that the repertoire of virulence determinants present in environmental *Yersinia* species remains to be elucidated.

**Keywords:** *Yersinia*, *Galleria mellonella*, insecticidal activity, enterotoxin, YacT

## INTRODUCTION

The genus *Yersinia* so far consists of three human pathogens (*Y. pestis*, *Y. pseudotuberculosis*, and *Y. enterocolitica*), and at least 16 species are considered mostly harmless to humans, namely *Y. aldovae*, *Y. bercovieri*, *Y. frederiksenii*, *Y. intermedia*, *Y. kristensenii*, *Y. mollaretii*, *Y. rohdei*, and the more recently described *Y. ruckeri*, a fish pathogen (Sulakvelidze, 2000), *Y. aleksiciae* (Sprague and Neubauer, 2005), *Y. similis* (Sprague et al., 2008), *Y. massiliensis* (Merhej et al., 2008), *Y. nurmii* (Murros-Kontinen et al., 2010a), *Y. pekkanenii* (Murros-Kontinen et al., 2010b), *Y. wautersii* (Savin et al., 2014), and *Y. entomophaga* (Hurst et al., 2010). These species that are non-pathogenic for humans have been isolated from water, soil, food, domestic and wild animals, and human beings in which they do not cause any clinical infections.

While the virulence properties of the pathogenic species have been characterized during last few decades, much less is known about the determinants that allow *Yersinia* species to survive in the



environment. We have recently demonstrated that the *Y. enterocolitica* strain W22703 (biotype 2, serotype O: 9) is toxic to nematodes and larvae of the tobacco hornworm, *Manduca sexta*, upon oral infection or oral toxin application, and that this insecticidal activity correlates with the presence of the pathogenicity island (TC-PAI<sup>Ye</sup>) (Bresolin et al., 2006; Spanier et al., 2010). This 20-kb fragment is present in the genome of *Y. pestis*, *Y. pseudotuberculosis*, and *Y. enterocolitica* biotype 2–5 strains, but is absent in the genomes of the highly–pathogenic biotype 1B strains, including 8081 and of the most biotype 1A strains, which are considered to be non-pathogenic to humans. The TC-PAI<sup>Ye</sup> carries the toxin complex (TC) genes with high identity to the *tc* genes of entomophagous *Photobacterium luminescens*, and it might be speculated that the TC is required to penetrate the epithelial cell barrier of the insect gut to allow *Y. enterocolitica* cells to enter the hemocoel. In *Y. entomophaga* MH96, an insecticidal pathogenicity island termed PAI<sub>Ye96</sub> was characterized, which is distinct from TC-PAI<sup>Ye</sup> in terms of gene homology and genetic organization (Hurst et al., 2011). A unique feature of this island is that it encodes, besides the type ABC genes, two chitinases that are associated with the mature TC (Busby et al., 2012).

The transcription of the *tc* genes in *Y. enterocolitica* is subject to a strict temperature-dependent regulation as they are completely silenced at 37°C, but strongly upregulated at lower temperatures with a maximal transcription at 10–15°C approximately (Bresolin et al., 2006; Starke et al., 2013; Starke and Fuchs, 2014). Thus, the TC-dependent activity of *Y. enterocolitica* to invertebrates is reciprocally regulated in comparison with that of many *Yersinia* virulence factors directed against humans (Marceau, 2005). Notably, strains lacking the insecticidal genes, including *Y. enterocolitica*, *Y. mollaretii*, *Y. bercovieri*, *Y. ruckeri*, and *Y. aldovae*, are still toxic when subcutaneously injected into *G. mellonella*, indicating the presence of yet unknown insecticidal determinants in these species (Fuchs et al., 2008). More recently, it was demonstrated that *Y. enterocolitica* strains of phylogroup 1 exhibit a strong virulence against *G. mellonella* larvae at temperatures of 25°C and higher upon intrahemocoelic injection, independently of the presence of virulence plasmid pYV (Alenizi et al., 2016). These findings resemble functional redundancy in *P. luminescens* that carries a set of insecticidal factors besides the TC (French-Constant et al., 2007), including the *makes caterpillars floppy* (MCF) toxins (Daborn et al., 2002), the Pir toxins (Waterfield et al., 2005), the protease PrtA (Bishop, 2014), Txp40 (Brown et al., 2006), the XaxAB-like binary toxins (Zhang et al., 2014), and the *Photobacterium* virulence cassettes (Yang et al., 2006). Interestingly, the (partial) loss of some of these insecticidal genes does not result in a lack of toxicity to invertebrates (Wilkinson et al., 2009).

The insecticidal determinants of some *Yersinia* spp. remain to be investigated. Here, we used an established infection assay with *G. mellonella* larvae to monitor the phenotype of the host intrahemocoelically infected with *Y. frederiksenii*, *Y. intermedia*, *P. luminescens*, and *Y. enterocolitica* 8081 and W22703 cells. Dose- and temperature-dependent characteristics of their insecticidal activity were determined, and genome comparison as well as toxin injection were applied to gain further

insights into the entomopathogenic repertoire of environmental *Yersinia* strains.

## RESULTS

Dose-dependent toxicity of *Y. frederiksenii* and *Y. intermedia* to *G. mellonella* larvae. When larvae of the first-instar neonates of *M. sexta* were challenged orally with *Y. frederiksenii* and *Y. intermedia* in preliminary experiments, the toxicity was calculated as 71 and 19%, respectively (Table 1). As both strains used here lack the TC-PAI<sup>Ye</sup>, we switched from this oral infection model to a subcutaneous infection model and injected 5 µl of a 1:100 dilution of *Y. frederiksenii* and *Y. intermedia* overnight culture into *G. mellonella* larvae, and observed a 99–100% lethality after 5 days of incubation at 15°C (Table 1). Thus, the insecticidal activity of *Y. frederiksenii* and *Y. intermedia* is higher than that of all other *Yersinia* strains tested recently in the same infection model, including *Y. enterocolitica* strain W22703 (biotype 2, serotype O:9) (Fuchs et al., 2008). To determine the toxicity of *Y. intermedia* and *Y. frederiksenii* toward *G. mellonella* larvae in more detail, we used defined infection aliquots of approximately 10<sup>3</sup>–10<sup>4</sup> colony forming units (CFU), and monitored the fate of intrahemocoelically infected *G. mellonella* larvae over 5 days at room temperature (20°C) (Figure 1A). The timecourse revealed that all larvae survived for 24 h, but most of them died within the next 2 days. The survival rates of the animals infected with two *Yersinia* species did not significantly ( $p > 0.05$ ) differ under the conditions applied here. In parallel, we homogenized two larvae each day, and monitored the replication of *Y. frederiksenii* within the larvae. The CFU of *Y. frederiksenii* increased from  $1.15 \times 10^3$  to  $3.21 \times 10^3$  (day one) and to  $2.79 \times 10^9$  (day two) directly after the infection, and remained constant for next 3 days ( $1.88$ – $2.62 \times 10^9$ ). This unimpeded bacterial growth resembles the mortality of the larvae that starts only when the *Y. frederiksenii* reaches its stationary phase. This finding suggests that a high cell number of this insect pathogen in the larvae of *Galleria* is a prerequisite for its toxicity and/or that the pathogen has incapacitated the host in the initial phase of intrahemocoelical infection.

We further reduced the infection dose to approximately 100–150 CFU and observed a slightly higher toxicity of *Y. frederiksenii* in comparison with *Y. intermedia*, which, however, started to kill larvae a day earlier (Figure 1B). In contrast, 145 CFU of *Y. enterocolitica* W22703 were not sufficient to kill any larva. Altogether, these data demonstrate a high, dose-dependent toxicity of *Y. frederiksenii* and *Y. intermedia* toward larvae of *G. mellonella*.

## Entomopathogenicity of *Y. enterocolitica* Strain 8081 Resembles That of *P. luminescens*

We compared the injectable insecticidal activity of *P. luminescens*, *Y. frederiksenii*, *Y. intermedia*, and *Y. enterocolitica* strain 8081 (biotype 1B, serotype O:8), which carries a so-called “high-pathogenicity island” encoding the siderophore yersiniabactin (Carniel et al., 1996). In each experiment, the

**TABLE 1** | Oral infection of *M. sexta* and intrahemocoelic infection of *G. mellonella* for 5 days.

Infection model	Strain	tc-PAI <sup>Ye</sup>	Total no.	Dead	Alive	Dead	Alive	Dead	Alive	Dead [%] ± Sd <sup>a</sup>
<i>G. mellonella</i>				1:10		1:100		total		
	<i>Y. intermedia</i>	Absent <sup>b</sup>	52	25	0	27	0	52	0	100 ± 0
	<i>Y. frederiksenii</i>	Plasmid-encoded <i>sep</i> -like genes absent in strain CIP 80.29 <sup>c</sup>	68	28	0	39	1	67	1	99 ± 2
	<b>Controls</b>									
	<i>E. coli</i> DH5α	Absent <sup>b</sup>	63	5	34	2	22	7	56	13 ± 6
<i>M. sexta</i>	LB		64					3	61	5 ± 0
				Undiluted						
	<i>Y. intermedia</i>	Absent <sup>b</sup>	27	5	22					19 ± 14
	<i>Y. frederiksenii</i>	Plasmid-encoded <i>sep</i> -like genes absent in strain CIP 80.29 <sup>c</sup>	21	15	6					71 ± 4
	<b>Control</b>									
	DH5α	Absent <sup>b</sup>	21	1	20					5 ± 7

<sup>a</sup> The average mortality of at least three independently performed experiments with a minimum of six larvae each are shown <sup>b</sup> according to the genome sequence <sup>c</sup> (Fuchs et al., 2008).

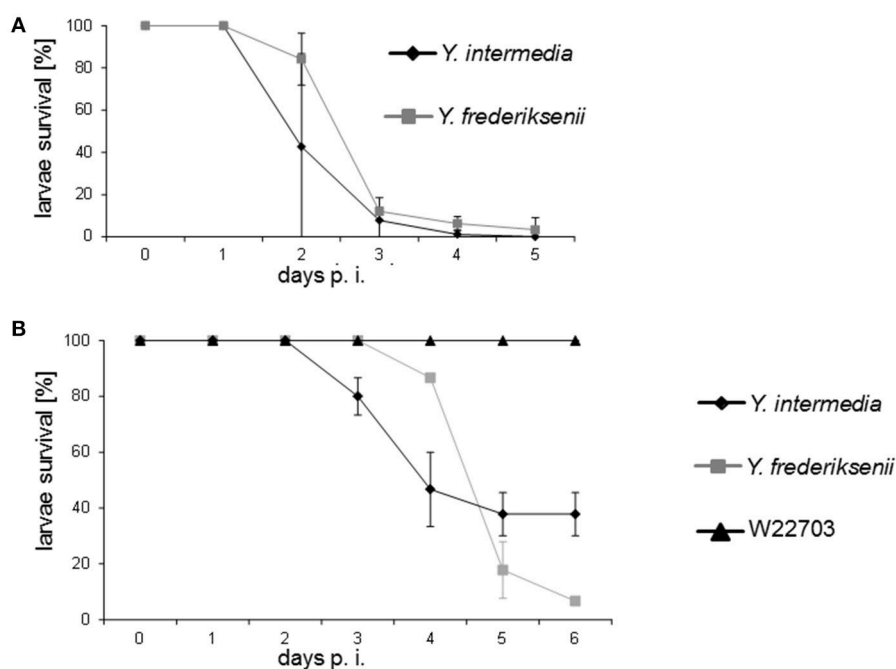


**FIGURE 1** | Time course of *G. mellonella* infection assays with *Y. frederiksenii* and *Y. intermedia*. The strains were pregrown overnight at 30°C, and the cultures were serially diluted. Aliquots of 5–7.5 µl from a 10<sup>4</sup>-fold or a 10<sup>5</sup>-fold dilution were used for infection, corresponding to (A) 1.44–5.50 × 10<sup>3</sup> *Y. intermedia* CFU and 1.43 × 10<sup>3</sup>–10<sup>4</sup> *Y. frederiksenii* CFU, or (B) 120 *Y. intermedia* CFU, 95 *Y. frederiksenii* CFU, and 145 *Y. enterocolitica* W22703 CFU. Three independent experiments per strain were performed, with three groups composed of (A) 25, 29, and 30 larvae (*Y. intermedia*) and 20, 22, and 23 larvae (*Y. frederiksenii*), or (B) 15 larvae each. The larvae were incubated at 20°C and monitored daily. Error bars represent the standard error of the mean of three experiments.

lethality of the larvae decreased with lower numbers of CFU (Figure 2). Interestingly, the survival assays demonstrated that *Y. enterocolitica* 8081 is nearly as toxic as *P. luminescens* toward *G. mellonella* larvae upon intrahemocoelic infection, and is more virulent than *Y. frederiksenii* and *Y. intermedia*. Approximately 38 CFU of *Y. enterocolitica* 8081 were

revealed to be sufficient to kill nearly all larvae, after an infection period of 5 days. For comparison, larvae were intrahemocoelically infected with *Y. enterocolitica* W22703 and DH5α, demonstrating the high insect-pathogenicity of *Y. frederiksenii*, *Y. intermedia*, and *Y. enterocolitica* strain 8081 despite the lack of TC-PAI<sup>Ye</sup>. Altogether, these data

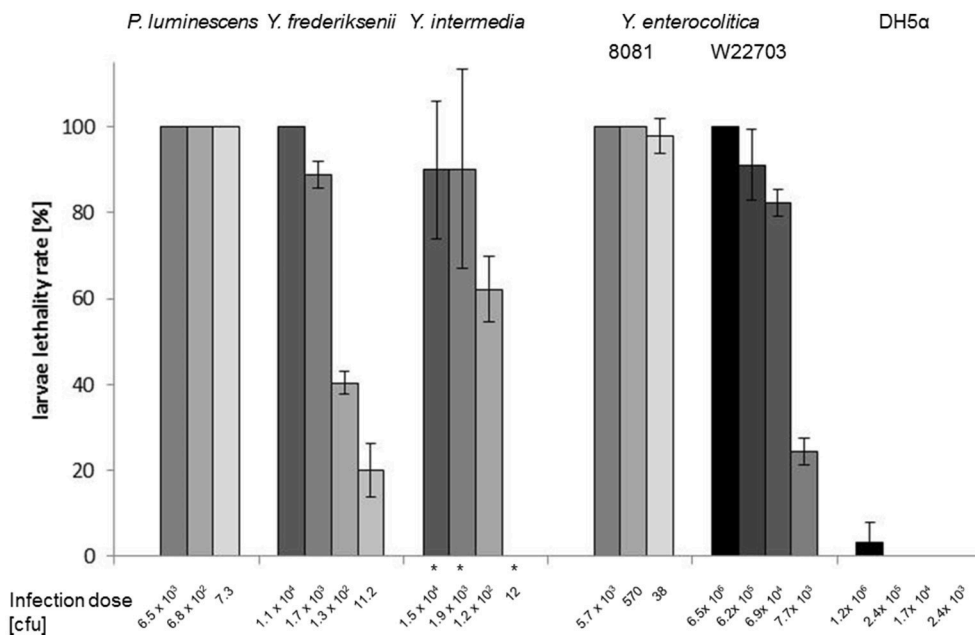


**FIGURE 2 |** Dose-dependent toxicity of *Yersinia* strains. Survival assays were performed by infection of *G. mellonella* larvae with *P. luminescens*, *Y. frederiksenii*, *Y. intermedia*, *Y. enterocolitica* 8081, *Y. enterocolitica* W22703, and *E. coli* DH5α. Infected larvae were incubated at 15°C; few experiments (\*) were performed at 20°C. The CFU used for the injection, the number of larvae, and the error bars (mean of experiments with three groups of larvae) are indicated. Groups of 15 larvae each were independently infected.

show that the lethality toward *G. mellonella* larvae is strictly dose-dependent.

## The Lethality of *Yersinia* Strains Is Temperature-Dependent

Low temperature-dependent toxicity of *Y. enterocolitica* W22703 toward *M. sexta* and *C. elegans*, and of representative strains of *Y. enterocolitica* phylogroups 1–5 against *G. mellonella* has been reported previously (Bresolin et al., 2006; Fuchs et al., 2008; Spanier et al., 2010; Alenizi et al., 2016). Therefore, we tested whether the injectable insecticidal activity described earlier is higher at lower temperature. *G. mellonella* larvae were infected with varying cell numbers of *Y. frederiksenii*, *Y. intermedia*, *Y. enterocolitica* 8081, and *Y. enterocolitica* W22703 and incubated at 15°C and at 30°C. However, upon infection with eight or 95 *Y. frederiksenii* CFU, the larvae showed a higher survival rate at 30°C than at 15°C (Figure 3A). A temperature-dependent pathogenicity toward *G. mellonella* was also observed for *Y. intermedia*. Although this species was found to be slightly low pathogenic at 15°C than *Y. frederiksenii*, we observed that at 30°C, 120 *Y. intermedia* CFU killed more larvae (40% survival rate) in comparison with 95 *Y. frederiksenii* CFU (80% survival rate) (Figure 3B). *Y. enterocolitica* 8081 exhibited a higher toxicity against the larvae at lower temperature as well. Only 57 CFU of this pathogen killed nearly all larvae at 15°C, but 40 CFU killed only 4% at 30°C (Figure 3C). Independent of the infection dose, *Y. enterocolitica* W22703 did not exhibit a significant temperature-dependent toxicity in this model (Figure 3D). A high infection dose of  $9 \times 10^5$  CFU quickly killed all larvae at

15°C and at 30°C, and a low infection dose of 145 CFU killed zero or only 7% of all larvae at these temperatures. Thus, a pronounced dose-dependent insecticidal activity was observed in these experiments with *Y. frederiksenii*, *Y. intermedia*, and both *Y. enterocolitica* strains.

## Phenotypes of Infected Larvae

A healthy *G. mellonella* larva rapidly moves forward and back upon touch, and its exoskeleton is light colored. During the pathogenicity assays described earlier, we observed distinct phenotypes of the larvae at both 15°C and 30°C (Figure 4A). The insects infected with 95 *Y. frederiksenii* CFU were more agile at 30°C, possibly due to the lower toxicity of the pathogen at this temperature. At this temperature, injuries by combats and thus the release of hemolymph is visible from day 3 *post infectionem* (p. i.) due to the high density of insects. From day 4 to 6 p. i., the number of insects in the pupal stage as well as cocoon production increased. At 15°C, all larvae remained undamaged. However, their agility decreased from day 1 p. i. until the larvae moved only their heads or died. They also exhibited a stronger exoskeleton coloring from day 4 p. i. that strengthened until day 6 p. i. Furthermore, while non-infected larvae are sturdy, their body volume decreased upon the loss of liquid as visible in Figure 4B, left, on the larvae's surface.

Another interesting observation was the differential pigmentation of the larvae. Melanization is a defense mechanism of *G. mellonella* larvae to encapsulate pathogens, and the intensity of pigment formation correlates with the number of injected cells (Thomaz et al., 2013). Following infection with *Y.*

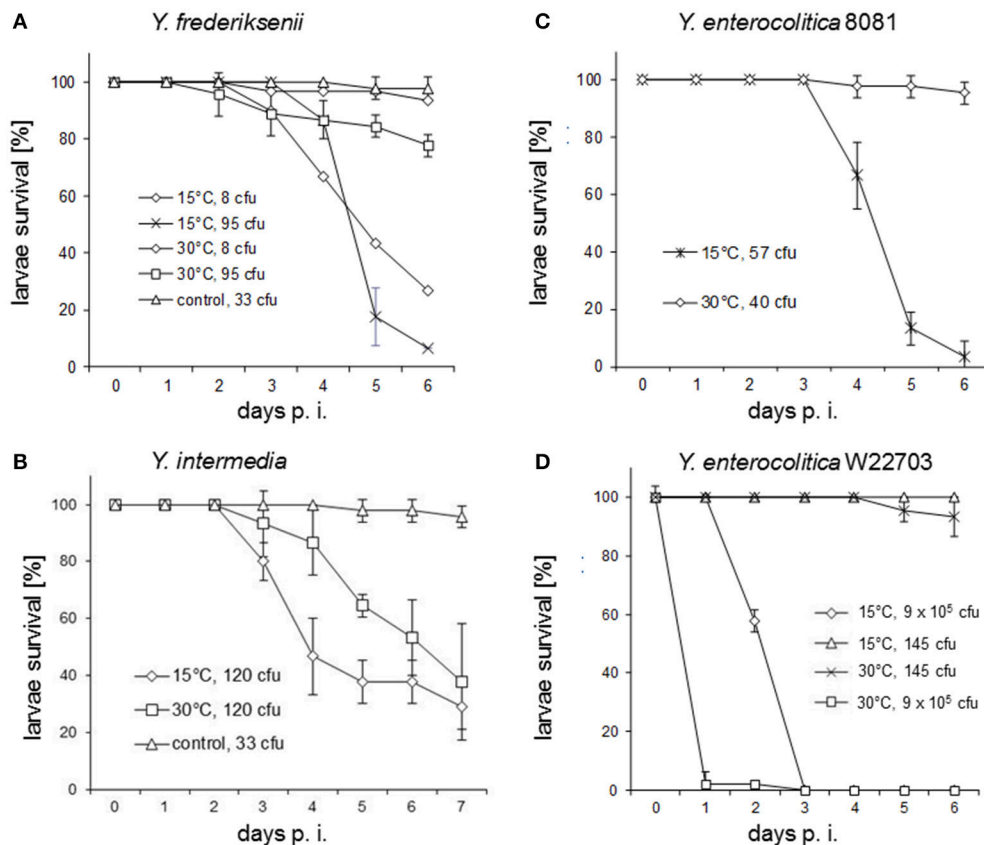


**FIGURE 3 |** Temperature-dependent pathogenicity of *Yersinia* strains against *G. mellonella* larvae. **(A)** Larvae were each infected with eight and 95 *Y. frederiksenii* CFU, respectively, and incubated at 15°C and 30°C; the experiment at 15°C with an infection dose of eight was performed with 30 ungrouped larvae. **(B)** Infection was done with 120 *Y. intermedia* CFU and the larvae incubated at 15°C and 30°C. Infection with *E. coli* DH5α was used here as a control for all experiments. **(C)** 57 *Y. enterocolitica* 8081 CFU were used to infect *G. mellonella* larvae, which were incubated at 15°C; in a further assay, larvae infected with 40 CFU were incubated at 30°C; the experiment with an infection dose of 57 CFU was done with 3 × 10 larvae. **(D)** Infection assays were performed with 9 × 10<sup>5</sup> or with 145 *Y. enterocolitica* W22703 CFU at 15°C and 30°C. In all experiments, three groups of 15 larvae each were independently infected with the exceptions mentioned earlier. Error bars represent the standard deviations. The larvae survival rate was plotted against day's p. i.

*frederiksenii* and *Y. intermedia*, the larvae colored gray-brown to black before they died (Figure 4B); many larvae also exhibited a punctiform pigmentation that resembled that at the injection site. Larvae infected with *P. luminescens*, however, did not show such a pigmentation, but colored red, similar to the effect of red anthraquinones produced by *P. luminescens* following infection (Richardson et al., 1988). These observations point out to different factors that are involved in the injectable insecticidal activity of the three pathogens.

## A Genome Comparison Approach Identifies Potential Virulence Genes Present in Highly and Absent in Weakly Insecticidal Strains

Although their genomes lack the *tc* genes or their homologs, *Y. intermedia* and *Y. frederiksenii* are much more toxic against *G. mellonella* larvae than *Y. enterocolitica* W22703. This finding suggests the presence of yet unknown genetic determinants that contribute to the insecticidal activity of *Yersinia*. Therefore,

we performed a genome comparison that identified 329 genes that are common for *Y. intermedia* strain ATCC 29909 and *Y. frederiksenii* strain ATCC 33641, but absent in *Y. enterocolitica* W22703 (Table S1). This set comprises a large number of genes whose (putative) products belong to categories such as lipoproteins and other membrane proteins (10 + 14), sensing, signaling, and regulation (36), metabolism (28), resistance toward toxic substances (17), transport and secretion (16 + 12), stress response (2), and iron uptake and storage (9). With respect to genetic determinants potentially involved in pathogenicity, the bioinformatics approach identified putative adhesins, toxins, hemolysins, and secretory systems (Table 2). For example, *Y. intermedia* and *Y. frederiksenii* carry a type VI secretion system (T6SS) that, among other functions, contributes to virulence (Filloux, 2013) and is present in all *Yersinia* spp. and in *P. luminescens*, but not in *Y. enterocolitica* W22703. The two species harbor an ATP-binding protein possibly involved in uptake of heme, which is absent in all other species of the *Yersinia* genus, but closely related to a protein in *Klebsiella pneumoniae*.



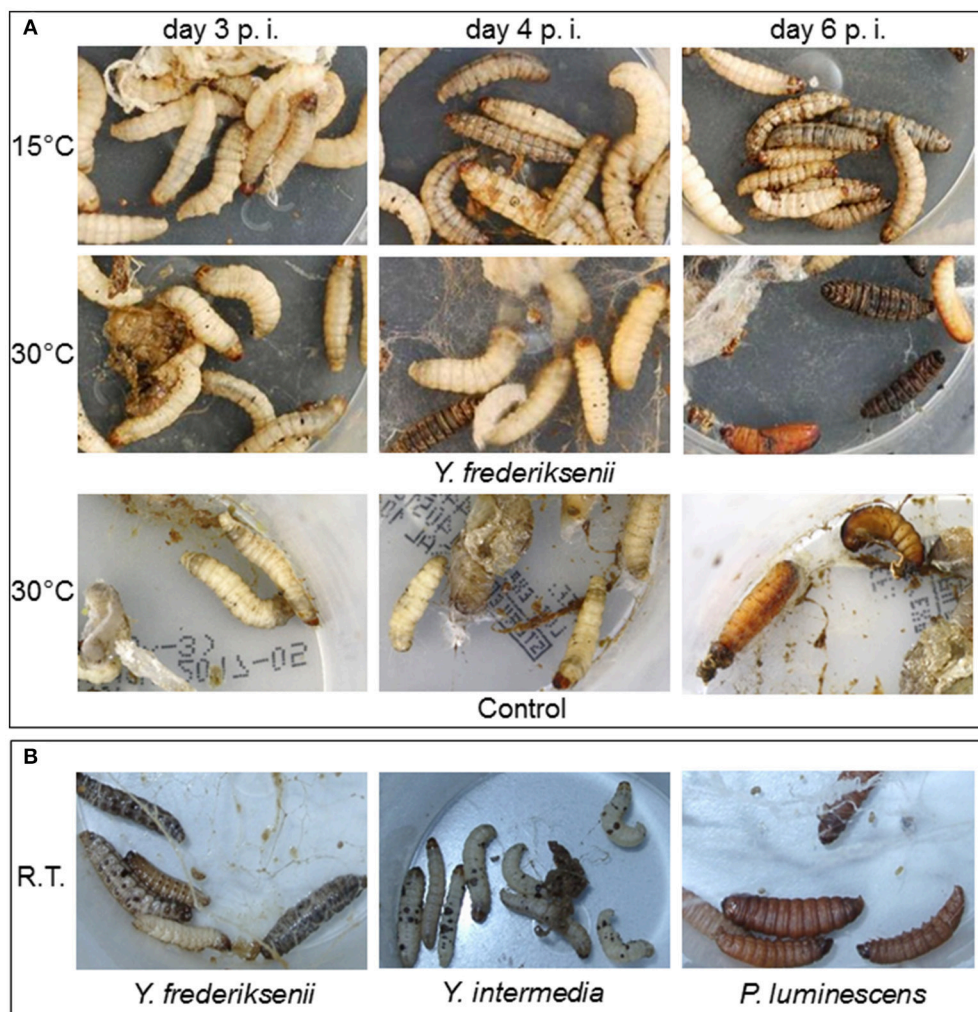


**FIGURE 4 |** Phenotypes of *G. mellonella* larvae after infection. **(A)** Larvae were infected with 95 *Y. frederiksenii* CFU, incubated at 15°C and 30°C, and monitored until day 6 p. i.; larvae injected with 5  $\mu$ l of LB medium served as control. **(B)** Infection was done with *Y. frederiksenii* (5  $\mu$ l of a  $10^3$  dilution of an overnight culture), with *Y. intermedia* (5  $\mu$ l of a  $10^4$  dilution), and with *P. luminescens* (5  $\mu$ l of a  $10^4$  dilution). Photographs were taken 3 days p. i. The larvae were incubated at room temperature (R.T.).

## Attenuated Insecticidal Phenotype of *Y. frederiksenii* $\Delta yacT$

In this genome comparison approach, we identified *yacT* (accession numbers EEQ13070 and WP\_004712324) encoding a protein whose amino acid sequence exhibits a significant homology (*e*-value 0.0, identity 54%; **Supplementary Figure S1**) to the heat-stable cytotoxic enterotoxin (Ast) of *Aeromonas hydrophila*. We termed this protein, with a molecular weight of 71.46 kDa, *Yersinia* Ast-like cytotoxic toxin (YacT), and the corresponding gene *yacT*. Homologs or orthologs of YacT are also encoded by *P. luminescens*, *P. asymbiotica*, and many *Yersinia* spp., but neither by *Y. pestis* or *Y. pseudotuberculosis*, nor by *Y. enterocolitica* strains W22703 and 8081. We generated a deletion mutant of *yacT* termed *Y. frederiksenii*  $\Delta yacT$ , which was also complemented with pACYC-*yacT* carrying the toxin gene. On performing the *G. mellonella* infection assay at 15°C, we

observed a strongly reduced virulence of *Y. frederiksenii*  $\Delta yacT$  (time in days for 50% of the larvae to die,  $TD_{50} = 5.4 \pm 0.22$ ) and of *Y. frederiksenii*  $\Delta yacT$ /pACYC184 ( $TD_{50} = 5.59 \pm 0.01$ ) in comparison to strain *Y. frederiksenii*/pACYC184 ( $TD_{50} = 3.33 \pm 0.18$ ) (**Table 3, Figure 5A**). When the mutant harbored gene *yacT* in trans via plasmid pACYC-*yacT*, its phenotype reverted to that of the parental strain showing a  $TD_{50} = 3.79 \pm 0.46$ . These data clearly demonstrated that *yacT* is required for the high virulence of *Y. frederiksenii* toward the larvae at 15°C.

To understand better the role of the novel toxin during infection, the number of viable *Y. frederiksenii* cells within infected larvae incubated at 15°C was determined daily over a duration of 4 days (**Figure 5B**). We observed a strong growth of *Y. frederiksenii* within 4 days by more than six orders of magnitude. In comparison, a mutant *Y. frederiksenii*  $\Delta yacT$

**TABLE 2 |** Putative virulence factors of *Y. frederiksenii* and *Y. intermedia* absent in *Y. enterocolitica* W22703.

Gene product	<i>Y. frederiksenii</i> <sup>a</sup>	<i>Y. intermedia</i> <sup>a</sup>	Closest homologs/orthologs in	Putative function
ATP-binding protein	yfred0001_42840	yinte0001_30410	<i>Klebsiella pneumoniae</i>	Virulence
Enterotoxin YacT	yfred0001_650	yinte0001_42030	<i>Yersinia</i> spp. excluding <i>Y. pestis</i> , <i>Y. pseudotuberculosis</i> , <i>Enterococcus cloacae</i> , <i>P. luminescens</i>	<i>Yersinia</i> Ast-like cytotoxic toxin
Enterotoxin	yfred0001_3400	yinte0001_16990	<i>Yersinia</i> spp. including <i>Y. pestis</i> , <i>Y. pseudotuberculosis</i>	Ribonuclease E
Hemolysin activator protein large exoprotein	yfred0001_19600 yfred0001_19590	yinte0001_24640 yinte0001_24650	<i>Yersinia</i> spp., <i>P. luminescens</i>	Heme utilization or adhesion
Thermostable hemolysin	yfred0001_34090	yinte0001_3870	<i>Yersinia</i> spp. excluding <i>Y. pestis</i> and <i>Y. pseudotuberculosis</i> , <i>Aeromonas</i> spp.	Cytotoxicity
Autotransporter adhesion	yfred0001_13070	yinte0001_3950	<i>Y. mollaretii</i> , <i>Serratia fonticola</i>	Adhesion
N-acetylglucosamine-binding protein A	yfred0001_36580	yinte0001_6590	<i>Yersinia</i> spp., <i>Aeromonas</i> spp., <i>Erwinia</i> spp., <i>Serratia</i> spp., <i>Pectobacterium</i> spp., <i>E. cloacae</i>	Adhesion
HlyD family	yfred0001_6370	yinte0001_17830	<i>Yersinia</i> spp. excluding <i>Y. pestis</i> and <i>Y. pseudotuberculosis</i> , <i>Serratia</i> spp.	Secretion of RTX toxin
RTX toxin and Ca <sup>2+</sup> -binding protein	yfred0001_38780	yinte0001_10500	<i>Yersinia</i> spp. excluding <i>Y. pestis</i> and <i>Y. pseudotuberculosis</i> , including <i>Y. enterocolitica</i> 8081	Cytotoxicity
Peroxidase-related enzyme	yfred0001_6530	yinte0001_17680	<i>Yersinia</i> spp., <i>Serratia</i> spp.	Defense
T6SS	yfred0001_31470-31660	yinte0001_22540-22350	<i>Yersinia</i> spp., <i>P. luminescens</i> , <i>Pseudomonas</i> spp.	Secretion of effector proteins
Twin-arginine translocation pathway signal	yfred0001_6530	yinte0001_9040	<i>Y. pestis</i> and <i>Y. pseudotuberculosis</i> , <i>Serratia</i> spp.	Virulence (Lavander et al., 2006)

<sup>a</sup>Gene code was taken from the PEDANT 3 database (Walter et al., 2009).

**TABLE 3 |** Infection doses and TD<sub>50</sub> values testing *yacT*.

	CFU/ml inoculum	CFU per 5 µl	TD <sub>50</sub> *(±sd)
<b>15°C</b>			
<i>Y. frederiksenii</i> /pACYC184	2.11 × 10 <sup>6</sup> ± 6.46 × 10 <sup>5</sup>	1.05 × 10 <sup>4</sup>	3.33 ± 0.18
<i>Y. frederiksenii</i> Δ <i>yacT</i>	2.63 × 10 <sup>6</sup> ± 3.05 × 10 <sup>5</sup>	1.31 × 10 <sup>4</sup>	5.4 ± 0.22
<i>Y. frederiksenii</i> Δ <i>yacT</i> /pACYC- <i>yacT</i>	1.94 × 10 <sup>6</sup> ± 3.25 × 10 <sup>5</sup>	9.70 × 10 <sup>3</sup>	3.79 ± 0.46
<i>Y. frederiksenii</i> Δ <i>yacT</i> /pACYC184	2.72 × 10 <sup>6</sup> ± 5.12 × 10 <sup>5</sup>	1.36 × 10 <sup>4</sup>	5.59 ± 0.01
<b>30°C</b>			
<i>Y. frederiksenii</i> /pACYC184	3.35 × 10 <sup>6</sup> ± 2.91 × 10 <sup>5</sup>	1.68 × 10 <sup>4</sup>	—**
<i>Y. frederiksenii</i> Δ <i>yacT</i>	24.11 × 10 <sup>6</sup> ± 7.50 × 10 <sup>5</sup>	2.06 × 10 <sup>4</sup>	—**
<i>Y. frederiksenii</i> Δ <i>yacT</i> /pACYC- <i>yacT</i>	3.90 × 10 <sup>6</sup> ± 3.03 × 10 <sup>5</sup>	1.95 × 10 <sup>4</sup>	—**
<i>Y. frederiksenii</i> Δ <i>yacT</i> /pACYC184	3.15 × 10 <sup>6</sup> ± 1.91 × 10 <sup>5</sup>	1.58 × 10 <sup>4</sup>	—**

Sd, standard deviation; \*, time in days for 50% of the larvae to die; \*\*, more than 50% of the larvae survived.

exhibited a retarded proliferation at day 2 p. i., followed by growth stagnation for 1 day. However, at day 4 p. i., the mutant reached approximately the same cell density as the parental strain. These data confirm that the yersiniae cell numbers increase before the larvae start to die and that YacT contributes to proliferation of *Y. frederiksenii* within the insect host.

## Effect of YacT on Hemocytes

YacT was purified from *E. coli* Bl21 (DE3)/pBAD-HisA(tet)-650. Six microliter of a toxin solution with a concentration of 1.4 µg/µl or of phosphate-buffered saline (PBS) as control were

injected into 20 *G. mellonella* larvae. The larvae of the toxin group showed paralysis of the half rebral abdomen immediately after injection. In addition, some caterpillars of this group displayed a constriction of the head-thorax area and did not react to touching. In comparison, the control group showed none of these symptoms. One day p.i., animals of both groups that were kept at 30°C maintained vigor and formed fine webs. After web removal, 2 or 3 days p. i., the caterpillars of the toxin-treated group showed punctate- to strokelike black discolorations at the dorsal-abdominal areas that we did not observe in the control group (**Supplementary Figure S2**).

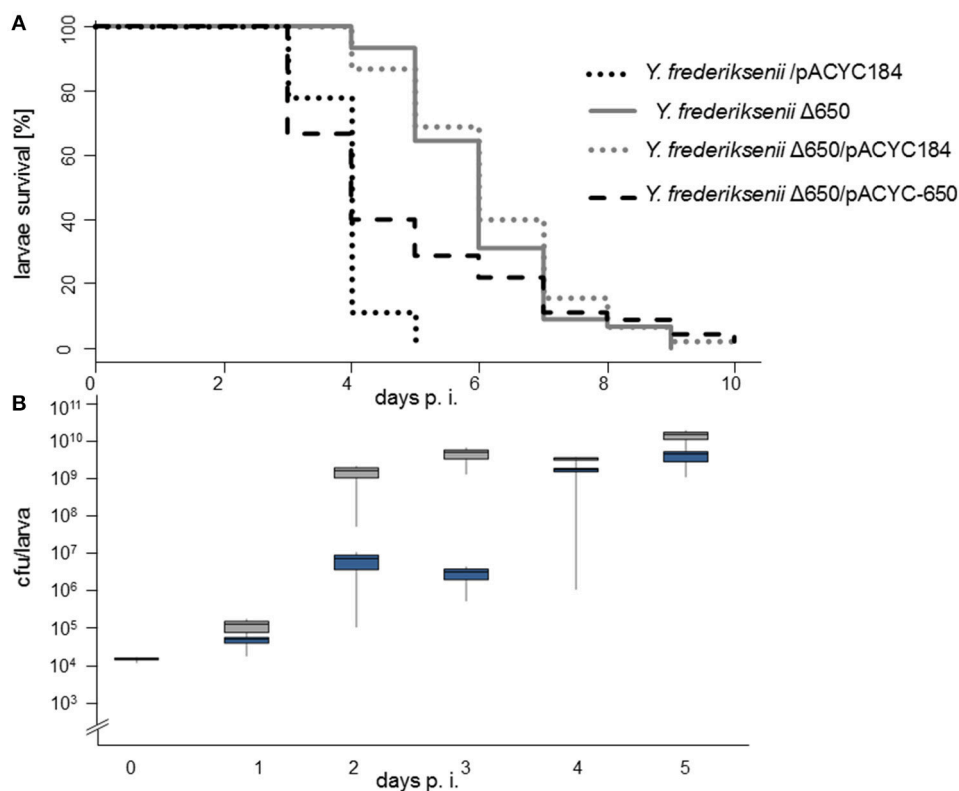


**FIGURE 5 |** *Y. frederiksenii*  $\Delta yacT$  exhibits attenuated virulence. **(A)** *Y. frederiksenii*/pACYC184, *Y. frederiksenii*  $\Delta yacT$ , *Y. frederiksenii*  $\Delta yacT$ /pACYC184, and *Y. frederiksenii*  $\Delta yacT$  /pACYC-yacT were used to infect *G. mellonella* larvae that were incubated for 10 days at 15°C. Infection doses and TD<sub>50</sub> values are indicated in **Table 3**. In all experiments depicted in the Kaplan–Meier plot, three independent infection experiments per strain were monitored, with groups composed of 15 larvae each. **(B)** Additionally, larvae infected in parallel were homogenized at the indicated time points and the number of viable *Y. frederiksenii* cells were enumerated. Gray boxes: *Y. frederiksenii*, black boxes: *Y. frederiksenii*  $\Delta yacT$ . Standard deviations of three replicates are shown.

To study the effect of YacT on hemocytes after 1 day, the hemolymph of larvae was prepared from the aorta and streaked out on microscope slides for staining. Injection of PBS (10 mM phosphate buffer, pH 7.4; 2.7 mM KCl; 137 mM NaCl) served as a control. Upon microscopic analysis, we observed repeatedly several distinct cell phenotypes: hemocytes from animals treated with the toxin showed a round-shaped morphology and they began to form aggregates in comparison to the controls and several cells also enlarged and showed a reduction of chromatin, possibly indicating the beginning of early stages of the cell death (**Figure 6A**).

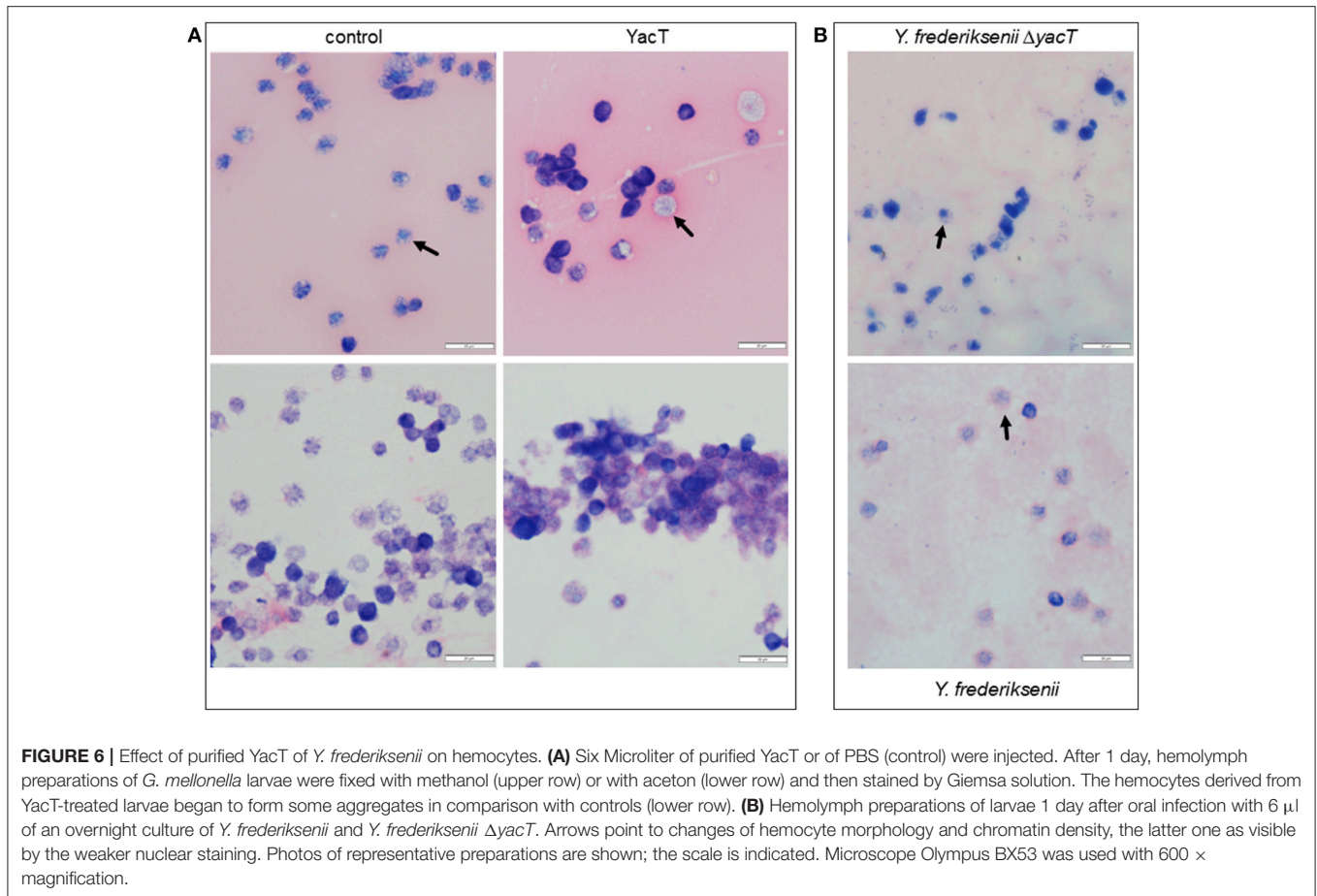
As a complementary experiment, *G. mellonella* larvae were infected orally with *Y. frederiksenii* and its *yacT* deletion mutant. Again, the morphology and chromatin density of hemocytes were modified in the presence of *Y. frederiksenii*, but not of *Y. frederiksenii*  $\Delta yacT$  (**Figure 6B**). In both cases, yersinial cells were visible in the preparations, indicating that penetrating the gut epithelial barrier occurs independent of YacT.

## DISCUSSION

Members of the genus *Yersinia* are fascinating organisms, as they are able to adapt to the environmental life cycle stage as well

as to mammals (Fuchs et al., 2011). During a transition, they encounter a broad spectrum of hostile conditions, and a major clue to overcome these challenges is the temperature-dependent production of host-specific virulence factors. Therefore, the interaction of yersiniae with invertebrates may have been a precursor to human pathogenicity during evolution (Waterfield et al., 2004). In this study, we tested the entomopathogenic potential of a set of *Yersinia* spp. toward larvae of *G. mellonella*. The larvae are considered to be a natural host of yersiniae and other pathogens and, therefore, serve as an indicator of yersinial virulence activities against insects. We identified *Y. enterocolitica* 8081, a representative of the highly pathogenic biovar 1B group, to be the most virulent *Yersinia* strain tested so far against *G. mellonella* larvae, resembling the high insecticidal activity of *P. luminescens*. Data on strain 8081 as the least pathogenic strain among several *Y. enterocolitica* strains tested against *G. Mellonella* are not in contradiction with our findings, because Alenizi et al. performed the infection experiments at 25°C and missed the high toxicity at the environmental temperature of 15°C (Alenizi et al., 2016). *Y. enterocolitica* strain 5303, which belongs to the biovar 1A group and is considered to be apathogenic toward mammals, showed an even higher toxicity toward the *Galleria* larvae, since only ten CFU were sufficient





to kill 50% of the larvae within 5 days (Alenizi et al., 2016). Interestingly, also *Y. intermedia* and *Y. frederiksenii* are more virulent to *Galleria* larvae than other *Yersinia* spp., including *Y. mollaretii*, *Y. bercovieri*, *Y. ruckeri*, *Y. aldovae*, and *Y. kristensenii*, as tested recently (Fuchs et al., 2008). *Y. frederiksenii* and *Y. intermedia* occupy related ecological niches and exhibit very similar phenotypes (Martin et al., 2009). *Y. intermedia*, which is isolated mainly from the environment, animals, food, and (rarely) human beings, received its name due to its genetic and phenotypic properties that are an intermediate between those of *Y. pseudotuberculosis* and *Y. enterocolitica* (Martin et al., 2009). *Y. intermedia* also shares several O antigens with *Y. enterocolitica* (Wauters et al., 1972), of which O:4 and O:17 are probably the prevailing serotypes (Ursing et al., 1980). *Y. frederiksenii* was differentiated from *Y. enterocolitica* in 1980 (Ursing et al., 1980). The high insecticidal potential might point out to yet overlooked natural habitats of these strains.

Temperature is an important signal in the regulation of yersinia virulence factors of that are predominantly produced at 37°C and repressed at temperatures lower than body temperature, or vice versa, as exemplified by the insecticidal *tc* genes in *Y. enterocolitica* W22703. Temperature-dependent mortality of *G. mellonella* upon oral infection, but not

upon intrahemocoelic injection, was observed recently for *Y. entomophaga* (Hurst et al., 2015). Therefore, it is not a surprising outcome of this study that the toxicity of *Y. frederiksenii*, *Y. intermedia*, and *Y. enterocolitica* 8081 increases with lower temperature, thus pointing out to a relevant ecological niche of these strains. Irrespective of the fact that *G. mellonella* has been chosen here as an infection model rather than as a natural host for yersinial infection, the two temperatures applied here correspond to the lifestyle of *G. mellonella* larvae that grow best between 29°C and 35°C, and also develop at 15°C, but not at 10°C or less.

The pronounced contrast between the insecticidal potential of *Y. frederiksenii*, *Y. intermedia*, and *Y. enterocolitica* 8081, on the one hand, and the TC-PAI<sup>Y<sub>e</sub></sup>-harboring *Y. enterocolitica* W22703, on the other hand, at least with respect to the *G. mellonella* model used here, prompted us to perform a genome comparison. This approach aimed to identify the determinants that confer the high insecticidal activity of these strains. **Table 2**, which probably still lacks several factors involved in infection, points out to a broad spectrum of yersinial factors whose role in pathogenicity as well as their host specificity remains to be investigated. One of them is YacT that is highly homologous to the *ast*-encoded heat-stable, cytotoxic enterotoxin of *A. hydrophila* (Chopra et al., 1994) that was associated with gastroenteritis



and non-bloody diarrhea in children and shown to contribute to the fluid secretory response in a murine model (Sha et al., 2002). Cell lysates of *E. coli* cells carrying *ast* elongated Chinese hamster ovary cells, which is a typical response to enterotoxins (Chopra et al., 1994). Besides *Yersinia* strains, YacT orthologs were identified also in *P. luminescens* ssp. *laumondii* ( $e$ -value =  $10^{-177}$ ) and in the human pathogen, *P. asymbiotica* ( $e$ -value =  $10^{-179}$ ), demonstrating that this factor is not unique to *A. hydrophila* as assumed previously (Sha et al., 2002). The prevalence of the Ast and YacT homologs confirms the strong functional relatedness between *Photobacterium* spp. and *Yersinia* spp. with respect to their invertebrate and vertebrate association (Heermann and Fuchs, 2008). It is important to note that YacT is distinct from the heat-stable enterotoxin Yst of yersiniae, for which a homolog is missing in *Y. frederiksenii* ATCC 33641 and *Y. intermedia* (Singh and Virdi, 2004). Our data demonstrate that YacT is required for full pathogenicity toward *G. mellonella*. Moreover, the finding that YacT injection affects the morphology of hemocytes suggests that the immune response of *G. mellonella* controls better the proliferation of *Y. frederiksenii*  $\Delta$ yacT during the first 3 days p. i. as compared with that of *Y. frederiksenii*. The list of determinants in **Table 3** and the variation of *Yersinia* spp. in pathogenesis toward *Galleria* larvae suggest that the yersinial toxicity toward insects upon intrahemocoelic infection is a multifactorial process due to the presence of several cytotoxic determinants. In the light of this assumption, the virulence attenuation upon deletion of *yacT* in *Y. frederiksenii* is remarkably high. Therefore, YacT is a candidate to explain the high toxicity of *Y. frederiksenii* against *G. mellonella*.

## CONCLUSION

A major implication of this study is that the yersinial toxicity toward insects not only depends on the TC, but also on a broader set of insecticidal toxins than known so far. We identified a novel yersinial entomopathogenic factor, whose activity might be associated with the hemocoel rather than with the insect gut as indicated by the distinct oral and intrahemocoelic toxicity of *Y. intermedia* and *Y. frederiksenii*. The findings of this study and other studies suggest that yersiniae strains, regardless of being human pathogens or not, acquire a substantial selection advantage by entering invertebrates. By overcoming infection barriers such as the gut epithelium or the innate immune response of insect larvae or nematodes, they might bioconvert their host, thus getting easy access to energy- and nitrogen-rich nutrients. The resulting proliferation increases the chance of *Yersinia* strains to be transmitted to other hosts including mammals.

## MATERIALS AND METHODS

### Bacterial Strains and Growth Conditions

The strains used in this study were *Y. intermedia* (Collection Institut Pasteur [CIP] 80.28; ATCC 29909), *Y. frederiksenii* (CIP 80.29; ATCC 33641), *Y. enterocolitica* 8081 (Virginia Miller, St. Louis, USA), *Y. enterocolitica* W22703 (Cornelis and Colson,

1975), and *P. luminescens* ssp. *laumondii* strain TT01 BX470251 (Fischer-Le Saux et al., 1999). All cultures were grown in lysogeny broth (LB) (10 g l<sup>-1</sup> tryptone, 5 g l<sup>-1</sup> yeast extract, and 5 g l<sup>-1</sup> NaCl) or on lysogeny broth (LB) agar (LB broth supplemented with 1.5 % w/v agar). *Escherichia coli* were grown at 37°C and *P. luminescens* and *Yersinia* strains at 30°C. If appropriate, the media were supplemented with the following antibiotics: 50 µg ml<sup>-1</sup> streptomycin, 12 µg ml<sup>-1</sup> tetracycline, 50 µg ml<sup>-1</sup> kanamycin, 20 µg ml<sup>-1</sup> chloramphenicol, and 20 µg ml<sup>-1</sup> nalidixic acid.

### General Molecular Techniques

The DNA manipulation was performed according to standard procedures (Sambrook and Russell, 2001). To isolate the chromosomal DNA, 1.5 ml of a bacterial culture was centrifuged, and the sediment was re-suspended in 400 µl of lysis buffer (100 mM Tris pH 8.0, 5 mM EDTA, 200 mM NaCl). After incubation for 15 min on ice, 10 µl of 10% SDS and 5 µl of proteinase K (10 mg/ml) were added, and the sample was incubated overnight at 55°C. The chromosomal DNA was precipitated with 500 µl of isopropanol, washed in ethanol, dried, and dissolved in 500 µl of TE buffer (10 mM Tris-HCl, 1 mM Na<sub>2</sub>EDTA, pH 7.4) containing 1 µl of RNase (10 mg/ml). Polymerase chain reactions (PCR) were carried out with Taq polymerase (Fermentas, Vilnius, and Lithuania) and the following programme: one cycle at 95°C for 2 min; 30 cycles at 95°C for 10 s, at the appropriate annealing temperature for 30 s, at 72°C for 45 s to 180 s depending on the expected fragment length; one cycle at 72°C for 10 min. Four Microliter of chromosomal DNA (100 ng ml<sup>-1</sup>) was used as a template for PCR amplification, and the GeneRuler DNA mix (Fermentas) served as a DNA ladder.

### Genome Comparison

The sequences of genome used for the comparison were that of *Y. enterocolitica* 8081 (accession numbers AM286415 for the chromosome and AM286416 for the plasmid), *Y. intermedia* (genome draft: GCA\_000168035.1), and *Y. frederiksenii* (genome draft: GCA\_000754805.1). Homology searches of predicted proteins were performed by basic local alignment search tool analysis (Altschul et al., 1997). The PEDANT software system [http://pedant.gsf.de; (Walter et al., 2009)] was used for automatic genome sequence analysis and annotation (Frishman et al., 2001). Genomes were recorded and homology searches of predicted proteins were performed by SIMAP (Arnold et al., 2014). The genome comparisons were calculated by using a custom Perl script, which formatted bidirectional-best sequence hits between all predicted proteins ( $E \leq 0.0001$ ).

### Insecticidal Bioassays

*M. sexta* were reared as described (Schachtner et al., 2004). For oral bioassays, bacteria were grown at 15°C (*Yersinia* strains) or 37°C (DH5α) until stationary phase. About 50 µl of a culture was applied to 4 mm<sup>3</sup> disks of an agar-based artificial diet (David and Gardiner, 1965). The liquid was allowed to soak into the agar block, which was dried under a laminar flow. First-instar *M. sexta* neonate larvae were placed on the disk and incubated at 22°C.

The application of bacterial culture aliquots was repeated after 3 days, and the larvae mortality was recorded after 5 days.

Larvae of *G. mellonella* were obtained from the Zoo-Fachmarkt (München, Germany) and stored for less than 1 week at room temperature. Bacterial strains were grown to stationary phase (optical density at 600 nm [OD<sub>600</sub>] ~1–5 × 10<sup>9</sup> cfu/ml) at temperatures between 15°C and 30°C (*Yersinia* spp.), at 30°C (*P. luminescens*), or at 37°C (DH5α), and 10-fold serial diluted. Larvae of 2–3 cm length and of 110–130 mg weight were used. A 5 µl of the bacterial culture or an appropriate dilution thereof were orally applied or injected by a sterilized microsyringe (Hamilton 1702 RN, 25 µl) into the hemocoel through the last left proleg. The aperture reseals after the removal of the syringe, thus preventing the loss of inoculum (Kavanagh and Reeves, 2004).

Infection doses were determined by plating serial dilutions of the cultures used for injection. Control assays had demonstrated that neither the medium nor the wounding by the syringe contributes to the mortality rate of the insects (Fuchs et al., 2008). Infected larvae were incubated for at least 5 days in the dark at the temperature indicated and the number of killed and alive larvae were enumerated each day. Larvae were considered dead if they failed to respond to touch. The TD<sub>50</sub> was calculated using the dose-response curve (drc) package of the R software. To recover bacteria from the larvae, the larvae were surface sterilized with 70% ethanol, washed in H<sub>2</sub>O, and cut into small pieces. The homogenous mass was suspended into 1 ml LB, rigorously shaken for 5 min with a vortex, and centrifuged at 1,000 rpm for 2 min. Serial dilutions were plated on agar plates with LB or with *Yersinia* selective medium (Schiemann CIN medium, Oxoid, Wesel, Germany).

## Deletion Mutants and Complementing Plasmid

In-frame deletion of *yacT* from *Y. frederiksenii* was performed by the one-step method based on the phage λ Red recombinase (Datsenko and Wanner, 2000). In short, PCR products comprising the kanamycin resistance cassette of plasmid pKD4, including the flanking FRT sites, were generated using pairs of 70-nucleotide-long primers that included 20 nucleotides priming sequences for pKD4 as template DNA. Homology extensions of 50 bp overlapped 18 nucleotides of the 5'-end and 36 nucleotides of the 3'-end of the target gene (Link et al., 1997). About 500–1,000 ng of fragment DNA were transferred into *Y. frederiksenii* cells harboring plasmid pKD119. Allelic replacement of the target gene by the kanamycin resistance cassette was controlled by PCR, and nonpolar deletion mutants were obtained via transformation of pCP20. The deletion was confirmed by PCR and sequencing.

Gene *yacT* including 220 bp upstream and 100 bp downstream of the coding sequence was amplified with the oligonucleotides 5'-CGATGAATTCAGTGACCGTCTGTGGGTCTG-3' and 5'-CGGCCATGGGGGGCAGCATCGTGATTTC-3' and ligated into the chloramphenicol resistance cassette of plasmid pACYC184 via *NcoI* und *EcoRI*, resulting in pACYC-*yacT*. The recombinant plasmid was validated by PCR and sequencing.

## Overproduction and Purification of YacT

Gene *yacT* of *Y. frederiksenii* was cloned into plasmid pBAD-HisA(tet) (Starke et al., 2013) via *SacI* and *PstI* using the oligonucleotides 5'-CGATGAGCTCATGCAGAAAATCATACC GAG-3' and 5'-AACTGCAGTTATTGGGTGCTAGCCACAG-3'. An overnight culture of *E. coli* BL21 (DE3)/pBAD-HisA(tet)-650 was diluted 1:100 into 800 ml of LB medium supplemented with 12 µg/ml tetracycline and incubated at 37°C with rotation at 180 rpm. At an OD<sub>600</sub> of 0.6, protein production was induced by adding 0.2% of arabinose. After incubation for an additional 4 h at 37°C and 180 rpm, the cells were harvested by centrifugation at 4°C and 7,500 rpm for 20 min. The pellets were each re-suspended in 5 ml of native lysis buffer (50 mM NaH<sub>2</sub>PO<sub>4</sub>, 300 mM NaCl, and 10 mM imidazole at pH 8.0) in the presence of 1 mM protease inhibitor Pefabloc SC (Sigma-Aldrich, Taufkirchen, Germany) and lysed by 4 passages through a French press (SLM Aminca Instruments, Rochester, NY, USA) at 900 psi; residual cell debris was removed thrice by centrifugation at 4°C and 9,000 rpm for 15 min. Following the filtration, YacT was isolated using the Ni-NTA Fast Start Kit (Qiagen, Hilden, Germany) according to the manufacturer's instructions. For imidazole removal, proteins were dialyzed against 50 mM phosphate buffer plus 0.5 mM MgSO<sub>4</sub>, 0.5 mM ZnSO<sub>4</sub>, and 0.5 mM CaCl<sub>2</sub> and protein extracts were concentrated down to 1 ml with Amicon ultracentrifugal filter units (Millipore). The protein concentration was determined using Roti-Quant solution (Carl, Roth GmbH, Karlsruhe, Germany) according to the Bradford method (Bradford, 1976). The purity of the eluted fractions was analyzed by the separation on a 12.5% sodium dodecyl sulfate (SDS)-PAA gel (Supplementary Figure S3).

## AUTHOR CONTRIBUTIONS

KS, P-AS, and CM performed infection assays and analyzed the results, AF constructed the recombinant strains, TR was responsible for the genome comparison, and TF analyzed the data, conceived the study, and wrote the manuscript. All authors drafted and revised the work and approved of the final version.

## ACKNOWLEDGMENTS

We thank Siegfried Scherer for supporting this study, Luise Ernst for technical assistance, Elisabeth Liebler-Tenorio for support in microscopical analysis, and Henry Derschum, Virginia Miller, Guy Cornelis, and Ralf Heermann for the gift of strains. This study was supported by a grant from the Deutsche Forschungsgemeinschaft (DFG) to TF (FU375/4-2).

## SUPPLEMENTARY MATERIAL

The Supplementary Material for this article can be found online at: <https://www.frontiersin.org/articles/10.3389/fcimb.2018.00392/full#supplementary-material>

## REFERENCES

- Alenizi, D., Ringwood, T., Redhwan, A., Bouraha, B., Wren, B. W., Prentice, M., et al. (2016). All *Yersinia enterocolitica* are pathogenic: virulence of phylogroup 1 Y. *enterocolitica* in a *Galleria mellonella* infection model. *Microbiology* 162, 1379–1387. doi: 10.1099/mic.0.000311
- Altschul, S. F., Madden, T. L., Schaffer, A. A., Zhang, J., Zhang, Z., Miller, W., et al. (1997). Gapped BLAST and PSI-BLAST: a new generation of protein database search programs. *Nucleic Acids Res.* 25, 3389–3402. doi: 10.1093/nar/25.17.3389
- Arnold, R., Goldenberg, F., Mewes, H. W., and Rattei, T. (2014). SIMAP—the database of all-against-all protein sequence similarities and annotations with new interfaces and increased coverage. *Nucleic Acids Res.* 42, 279–284. doi: 10.1093/nar/gkt970
- Bishop, A. H. (2014). Expression of *prtA* from *Photobacterium luminescens* in *Bacillus thuringiensis* enhances mortality in lepidopteran larvae by sub-cutaneous but not oral infection. *J. Invertebr. Pathol.* 121, 85–88. doi: 10.1016/j.jip.2014.07.001
- Bradford, M. M. (1976). A rapid and sensitive method for the quantitation of microgram quantities of protein utilizing the principle of protein-dye binding. *Anal. Biochem.* 72, 248–254. doi: 10.1016/0003-2697(76)90527-3
- Bresolin, G., Morgan, J. A., Ilgen, D., Scherer, S., and Fuchs, T. M. (2006). Low temperature-induced insecticidal activity of *Yersinia enterocolitica*. *Mol. Microbiol.* 59, 503–512. doi: 10.1111/j.1365-2958.2005.04916.x
- Brown, S. E., Cao, A. T., Dobson, P., Hines, E. R., Akhurst, R. J., and East, P. D. (2006). Txp40, a ubiquitous insecticidal toxin protein from *Xenorhabdus* and *Photobacterium* bacteria. *Appl. Environ. Microbiol.* 72, 1653–1662. doi: 10.1128/AEM.72.2.1653-1662.2006
- Busby, J. N., Landsberg, M. J., Simpson, R. M., Jones, S. A., Hankamer, B., Hurst, M. R., et al. (2012). Structural analysis of Ch1 Chitinase from Yen-Tc: the multisubunit insecticidal ABC toxin complex of *Yersinia entomophaga*. *J. Mol. Biol.* 415, 359–371. doi: 10.1016/j.jmb.2011.11.018
- Carniel, E., Guilvout, I., and Prentice, M. (1996). Characterization of a large chromosomal “high-pathogenicity island” in biotype 1B *Yersinia enterocolitica*. *J. Bacteriol.* 178, 6743–6751. doi: 10.1128/jb.178.23.6743-6751.1996
- Chopra, A. K., Pham, R., and Houston, C. W. (1994). Cloning and expression of putative cytotoxic enterotoxin-encoding genes from *Aeromonas hydrophila*. *Gene* 139, 87–91. doi: 10.1016/0378-1119(94)90528-2
- Cornelis, G., and Colson, C. (1975). Restriction of DNA in *Yersinia enterocolitica* detected by recipient ability for a derepressed R factor from *Escherichia coli*. *J. Gen. Microbiol.* 87, 285–291. doi: 10.1099/00221287-87-2-285
- Daborn, P. J., Waterfield, N., Silva, C. P., Au, C. P., Sharma, S., and Ffrench-Constant, R. H. (2002). A single *Photobacterium* gene, makes caterpillars floppy (*mcf*), allows *Escherichia coli* to persist within and kill insects. *Proc. Natl. Acad. Sci. U.S.A.* 99, 10742–10747. doi: 10.1073/pnas.102068099
- Datsenko, K. A., and Wanner, B. L. (2000). One-step inactivation of chromosomal genes in *Escherichia coli* K-12 using PCR products. *Proc Natl Acad Sci USA.* 97, 6640–6645. doi: 10.1073/pnas.120163297
- David, W. A. L., and Gardiner, B. O. C. (1965). Rearing *Pieris brassicae* larvae on a semi-synthetic diet. *Nature* 207, 882–883. doi: 10.1038/207882b0
- ffrench-Constant, R. H., Dowling, A., and Waterfield, N. R. (2007). Insecticidal toxins from *Photobacterium* bacteria and their potential use in agriculture. *Toxicon* 49, 436–451. doi: 10.1016/j.toxicon.2006.11.019
- Filloux, A. (2013). The rise of the Type VI secretion system. *F1000Prime Rep.* 5:52. doi: 10.12703/P5-52
- Fischer-Le Saux, M., Viallard, V., Brunel, B., Normand, P., and Boemare, N. E. (1999). Polyphasic classification of the genus *Photobacterium* and proposal of new taxa: *P. luminescens* subsp. *luminescens* subsp. nov., *P. luminescens* subsp. *akhurstii* subsp. nov., *P. luminescens* subsp. *laumondii* subsp. nov., *P. temperata* sp. nov., *P. temperata* subsp. *temperata* subsp. nov. and *P. asymbiotica* sp. nov. *Int. J. Syst. Bacteriol.* 49, 1645–1656. doi: 10.1099/00207713-49-4-1645
- Frishman, D., Albermann, K., Hani, J., Heumann, K., Metanowski, A., Zollner, A., et al. (2001). Functional and structural genomics using PEDANT. *Bioinformatics* 17, 44–57. doi: 10.1093/bioinformatics/17.1.44
- Fuchs, T. M., Brandt, K., Starke, M., and Rattei, T. (2011). Shotgun sequencing of *Yersinia enterocolitica* strain W22703 (biotype 2, serotype O:9): genomic evidence for oscillation between invertebrates and mammals. *BMC Genomics* 12:168. doi: 10.1186/1471-2164-12-168
- Fuchs, T. M., Bresolin, G., Marcinowski, L., Schachtner, J., and Scherer, S. (2008). Insecticidal genes of *Yersinia* spp.: taxonomical distribution, contribution to toxicity towards *Manduca sexta* and *Galleria mellonella*, and evolution. *BMC Microbiol.* 8:214. doi: 10.1186/1471-2180-8-214
- Heermann, R., and Fuchs, T. M. (2008). Comparative analysis of the *Photobacterium luminescens* and the *Yersinia enterocolitica* genomes: uncovering candidate genes involved in insect pathogenicity. *BMC Genomics* 9:40. doi: 10.1186/1471-2164-9-40
- Hurst, M. R., Beattie, A. K., Jones, S. A., Hsu, P. C., Calder, J., and Van Koten, C. (2015). Temperature-Dependent *Galleria mellonella* mortality as a result of *Yersinia entomophaga* infection. *Appl. Environ. Microbiol.* 81, 6404–6414. doi: 10.1128/AEM.00790-15
- Hurst, M. R., Becher, S. A., Young, S. D., Nelson, T. L., and Glare, T. R. (2010). *Yersinia entomophaga* sp. nov. isolated from the New Zealand grass grub *Costelytra zealandica*. *Int. J. Syst. Evol. Microbiol.* 61, 844–849. doi: 10.1099/ijs.0.024406-0
- Hurst, M. R., Jones, S. A., Binglin, T., Harper, L. A., Jackson, T. A., and Glare, T. R. (2011). The main virulence determinant of *Yersinia entomophaga* MH96 is a broad-host-range toxin complex active against insects. *J. Bacteriol.* 193, 1966–1980. doi: 10.1128/JB.01044-10
- Kavanagh, K., and Reeves, E. P. (2004). Exploiting the potential of insects for *in vivo* pathogenicity testing of microbial pathogens. *FEMS Microbiol. Rev.* 28, 101–112. doi: 10.1016/j.femsre.2003.09.002
- Lavander, M., Ericsson, S. K., Broms, J. E., and Forsberg, A. (2006). The twin arginine translocation system is essential for virulence of *Yersinia pseudotuberculosis*. *Infect. Immun.* 74, 1768–1776. doi: 10.1128/IAI.74.3.1768-1776.2006
- Link, A. J., Phillips, D., and Church, G. M. (1997). Methods for generating precise deletions and insertions in the genome of wild-type *Escherichia coli*: application to open reading frame characterization. *J. Bacteriol.* 179, 6228–6237. doi: 10.1128/jb.179.20.6228-6237.1997
- Marceau, M. (2005). Transcriptional regulation in *Yersinia*: an update. *Curr. Issues Mol. Biol.* 7, 151–177.
- Martin, L., Leclercq, A., Savin, C., and Carniel, E. (2009). Characterization of atypical isolates of *Yersinia intermedia* and definition of two new biotypes. *J. Clin. Microbiol.* 47, 2377–2380. doi: 10.1128/JCM.02512-08
- Merhej, V., Adekambi, T., Pagnier, I., Raoult, D., and Drancourt, M. (2008). *Yersinia massiliensis* sp. nov., isolated from fresh water. *Int. J. Syst. Evol. Microbiol.* 58, 779–784. doi: 10.1099/ijs.0.65219-0
- Murros-Konttinen, A. E., Fredriksson-Ahomaa, M., Korkeala, H., Johansson, P., Rahkila, R., and Björkroth, J. (2010a). *Yersinia nurmii* sp. nov. *Int. J. Syst. Evol. Microbiol.* 61, 2368–2372. doi: 10.1099/ijs.0.024836-0
- Murros-Konttinen, A. E., Johansson, P., Niskanen, T., Fredriksson-Ahomaa, M., Korkeala, H., and Björkroth, J. (2010b). *Yersinia pekkanenii* sp. nov. *Int. J. Syst. Evol. Microbiol.* 61, 2363–2367. doi: 10.1099/ijs.0.019984-0
- Richardson, W. H., Schmidt, T. M., and Neilson, K. H. (1988). Identification of an anthraquinone pigment and a hydroxystilbene antibiotic from *Xenorhabdus luminescens*. *Appl. Environ. Microbiol.* 54, 1602–1605.
- Sambrook, J., and Russell, D. W. (2001). *Molecular Cloning: A Laboratory Manual, 3rd Edn.* Cold Spring Harbor, NY: Cold Spring Harbor Laboratory.
- Savin, C., Martin, L., Bouchier, C., Filali, S., Chenau, J., Zhou, Z., et al. (2014). The *Yersinia pseudotuberculosis* complex: characterization and delineation of a new species, *Yersinia wautersii*. *Int. J. Med. Microbiol.* 304, 452–463. doi: 10.1016/j.ijmm.2014.02.002
- Schachtner, J., Huetteroth, W., Nighorn, A., and Honegger, H. W. (2004). Copper/zinc superoxide dismutase-like immunoreactivity in the metamorphosing brain of the sphinx moth *Manduca sexta*. *J. Comp. Neurol.* 469, 141–152. doi: 10.1002/cne.10992
- Sha, J., Kozlova, E. V., and Chopra, A. K. (2002). Role of various enterotoxins in *Aeromonas hydrophila*-induced gastroenteritis: generation of enterotoxin gene-deficient mutants and evaluation of their enterotoxic activity. *Infect. Immun.* 70, 1924–1935. doi: 10.1128/IAI.70.4.1924-1935.2002
- Singh, I., and Virdi, J. S. (2004). Production of *Yersinia* stable toxin (YST) and distribution of *yst* genes in biotype 1A strains of *Yersinia enterocolitica*. *J. Med. Microbiol.* 53, 1065–1068. doi: 10.1099/jmm.0.45527-0
- Spanier, B., Starke, M., Higel, F., Scherer, S., and Fuchs, T. M. (2010). *Yersinia enterocolitica* infection and *tcaA*-dependent killing of *Caenorhabditis elegans*. *Appl. Environ. Microbiol.* 76, 6277–6285. doi: 10.1128/AEM.01274-10

- Sprague, L. D., and Neubauer, H. (2005). *Yersinia aleksiciae* sp. nov. *Int. J. Syst. Evol. Microbiol.* 55, 831–835. doi: 10.1099/ijs.0.63220-0
- Sprague, L. D., Scholz, H. C., Amann, S., Busse, H. J., and Neubauer, H. (2008). *Yersinia similis* sp. nov. *Int. J. Syst. Evol. Microbiol.* 58, 952–958. doi: 10.1099/ijs.0.65417-0
- Starke, M., and Fuchs, T. M. (2014). YmoA negatively controls the expression of insecticidal genes in *Yersinia enterocolitica*. *Mol. Microbiol.* 92, 287–301. doi: 10.1111/mmi.12554
- Starke, M., Richter, M., and Fuchs, T. M. (2013). The insecticidal toxin genes of *Yersinia enterocolitica* are activated by the thermolabile LTTR-like regulator TcaR2 at low temperatures. *Mol. Microbiol.* 89, 596–611. doi: 10.1111/mmi.12296
- Sulakvelidze, A. (2000). *Yersinia* other than *Y. enterocolitica*, *Y. pseudotuberculosis*, and *Y. pestis*: the ignored species. *Microbes Infect.* 2, 497–513. doi: 10.1016/S1286-4579(00)00311-7
- Thomaz, L., Garcia-Rodas, R., Guimaraes, A. J., Taborda, C. P., Zaragoza, O., and Nosanchuk, J. D. (2013). *Galleria mellonella* as a model host to study *Paracoccidioides lutzii* and *Histoplasma capsulatum*. *Virulence* 4, 139–146. doi: 10.4161/viru.23047
- Ursing, J., Brenner, D. J., Bercovier, H., Fanning, G. R., Steigerwalt, A. G., Brault, J., et al. (1980). *Yersinia frederiksenii*: a new species of Enterobacteriaceae composed of rhamnose-positive strains (formerly called atypical *Yersinia enterocolitica* or *Yersinia enterocolitica*-like. *Curr. Microbiol.* 4, 213–217. doi: 10.1007/BF02605859
- Walter, M. C., Rattei, T., Arnold, R., Guldener, U., Munsterkotter, M., Nenova, K., et al. (2009). PEDANT covers all complete RefSeq genomes. *Nucleic Acids Res.* 37, 408–411. doi: 10.1093/nar/gkn749
- Waterfield, N., Kamita, S. G., Hammock, B. D., and Ffrench-Constant, R. (2005). The *Photobacterium* Pir toxins are similar to a developmentally regulated insect protein but show no juvenile hormone esterase activity. *FEMS Microbiol. Lett.* 245, 47–52. doi: 10.1016/j.femsle.2005.02.018
- Waterfield, N. R., Wren, B. W., and Ffrench-Constant, R. H. (2004). Invertebrates as a source of emerging human pathogens. *Nat. Rev. Microbiol.* 2, 833–841. doi: 10.1038/nrmicro1008
- Wauters, G., Le Minor, L., Chalon, A. M., and Lassen, J. (1972). Supplement to the antigenic schema of *Yersinia enterocolitica*. *Ann. Inst. Pasteur.* 122, 951–956.
- Wilkinson, P., Waterfield, N. R., Crossman, L., Corton, C., Sanchez-Contreras, M., Vlisidou, I., et al. (2009). Comparative genomics of the emerging human pathogen *Photobacterium asymbotica* with the insect pathogen *Photobacterium luminescens*. *BMC Genomics* 10:302. doi: 10.1186/1471-2164-10-302
- Yang, G., Dowling, A. J., Gerike, U., Ffrench-Constant, R. H., and Waterfield, N. R. (2006). *Photobacterium* virulence cassettes confer injectable insecticidal activity against the wax moth. *J. Bacteriol.* 188, 2254–2261. doi: 10.1128/JB.188.6.2254-2261.2006
- Zhang, X., Hu, X., Li, Y., Ding, X., Yang Q., Sun Y., et al. (2014). XaxAB-like binary toxin from *Photobacterium luminescens* exhibits both insecticidal activity and cytotoxicity. *FEMS Microbiol. Lett.* 350, 48–56. doi: 10.1111/1574-6968.12321

**Conflict of Interest Statement:** The authors declare that the research was conducted in the absence of any commercial or financial relationships that could be construed as a potential conflict of interest.

Copyright © 2018 Springer, Sängner, Moritz, Felsl, Rattei and Fuchs. This is an open-access article distributed under the terms of the Creative Commons Attribution License (CC BY). The use, distribution or reproduction in other forums is permitted, provided the original author(s) and the copyright owner(s) are credited and that the original publication in this journal is cited, in accordance with accepted academic practice. No use, distribution or reproduction is permitted which does not comply with these terms.





# An Experimental Pipeline for Initial Characterization of Bacterial Type III Secretion System Inhibitor Mode of Action Using Enteropathogenic *Yersinia*

## OPEN ACCESS

### Edited by:

Matthew C. Wolfgang,  
University of North Carolina at Chapel  
Hill, United States

### Reviewed by:

Deborah Anderson,  
University of Missouri, United States  
Stephanie Rochelle Shames,  
Kansas State University, United States

### \*Correspondence:

Victoria Auerbuch  
vastone@ucsc.edu

### †Present Address:

Sina Mohammadi,  
Merck Exploratory Science Center,  
Cambridge, MA, United States

### Specialty section:

This article was submitted to  
Molecular Bacterial Pathogenesis,  
a section of the journal  
Frontiers in Cellular and Infection  
Microbiology

**Received:** 30 July 2018

**Accepted:** 26 October 2018

**Published:** 22 November 2018

### Citation:

Morgan JM, Lam HN, Delgado J,  
Luu J, Mohammadi S, Isberg RR,  
Wang H and Auerbuch V (2018) An  
Experimental Pipeline for Initial  
Characterization of Bacterial Type III  
Secretion System Inhibitor Mode of  
Action Using Enteropathogenic  
*Yersinia*.  
Front. Cell. Infect. Microbiol. 8:404.  
doi: 10.3389/fcimb.2018.00404

Jessica M. Morgan<sup>1</sup>, Hanh N. Lam<sup>2</sup>, Jocelyn Delgado<sup>2</sup>, Justin Luu<sup>2</sup>, Sina Mohammadi<sup>†</sup>,  
Ralph R. Isberg<sup>3</sup>, Helen Wang<sup>4</sup> and Victoria Auerbuch<sup>2\*</sup>

<sup>1</sup> Department of Chemistry and Biochemistry, University of California, Santa Cruz, Santa Cruz, CA, United States,

<sup>2</sup> Department of Microbiology and Environmental Toxicology, University of California, Santa Cruz, Santa Cruz, CA,

United States, <sup>3</sup> Department of Molecular Biology and Microbiology, Tufts University School of Medicine, Boston, MA,

United States, <sup>4</sup> Department of Medical Biochemistry and Microbiology, Uppsala University, Uppsala, Sweden

Dozens of Gram negative pathogens use one or more type III secretion systems (T3SS) to disarm host defenses or occupy a beneficial niche during infection of a host organism. While the T3SS represents an attractive drug target and dozens of compounds with T3SS inhibitory activity have been identified, few T3SS inhibitors have been validated and mode of action determined. One issue is the lack of standardized orthogonal assays following high throughput screening. Using a training set of commercially available compounds previously shown to possess T3SS inhibitory activity, we demonstrate the utility of an experiment pipeline comprised of six distinct assays to assess the stages of type III secretion impacted: T3SS gene copy number, T3SS gene expression, T3SS basal body and needle assembly, secretion of cargo through the T3SS, and translocation of T3SS effector proteins into host cells. We used enteropathogenic *Yersinia* as the workhorse T3SS-expressing model organisms for this experimental pipeline, as *Yersinia* is sensitive to all T3SS inhibitors we tested, including those active against other T3SS-expressing pathogens. We find that this experimental pipeline is capable of rapidly distinguishing between T3SS inhibitors that interrupt the process of type III secretion at different points in T3SS assembly and function. For example, our data suggests that Compound 3, a malic diamide, blocks either activity of the assembled T3SS or alters the structure of the T3SS in a way that blocks T3SS cargo secretion but not antibody recognition of the T3SS needle. In contrast, our data predicts that Compound 4, a haloid-containing sulfonamidobenzamide, disrupts T3SS needle subunit secretion or assembly. Furthermore, we suggest that misregulation of copy number control of the pYV virulence plasmid, which encodes the *Yersinia* T3SS, should be considered as a possible mode of action for compounds with T3SS inhibitory activity against *Yersinia*.

**Keywords:** type III secretion system, T3SS, T3SS inhibitor, *Yersinia*, pYV

## INTRODUCTION

The type III secretion system (T3SS) is a macromolecular nanosyringe used by dozens of Gram negative pathogens, including *Yersinia*, *Shigella*, *Salmonella*, *Chlamydia*, and *Pseudomonas*, to inject effector proteins into target host cells (Deng et al., 2017). The core structure of the T3SS consists of a basal body that anchors the entire complex in the bacterial membrane and assembles first. The basal body is composed of three proteins, which oligomerize into rings. SctD and SctJ form two rings in the bacterial inner membrane (IM) and SctC, a member of the secretin family of proteins, forms a ring in the bacterial outer membrane (OM) (Bergeron et al., 2013). These three rings are connected in the center by a hollow inner rod and the IM rings are closely associated with the SctN ATPase complex whose integrity is essential to the T3SS (Diepold et al., 2010). In addition to ATP, the proton motive force is also important for T3SS activity (Wilharm et al., 2004), although how the T3SS harnesses the proton motive force remains unclear. Once active, the basal body secretes the SctF needle protein, which polymerizes into a straight, hollow tube protruding into the extracellular space. In *Yersinia* species pathogenic to mammals, the fully assembled Ysc T3SS needle is composed of ~140 SctF subunits, is 65 nm in length, and harbors a tip complex composed of a pentamer of the hydrophilic LcrV translocator protein (Broz et al., 2007). Upon host cell contact, two additional hydrophobic translocator proteins, YopD and YopB, are secreted through the Ysc needle to form a translocon complex that leads to pore formation in the host membrane, facilitating the translocation of effector proteins to the host cytoplasm (Büttner and Bonas, 2002).

The *Yersinia* Ysc T3SS is highly regulated at the transcriptional, translational, and post-translational levels (Francis et al., 2002; Heroven et al., 2012). The transcription factor LcrF directs transcription of genes encoding the T3SS structural, regulatory, and effector proteins, all of which are encoded on the 70 kb pYV virulence plasmid (Schwiesow et al., 2015). Several factors govern regulation of LcrF expression, including temperature and the transcription factor IscR (Schwiesow et al., 2015). Importantly, pYV copy number increases during active type III secretion, and this is important for *Yersinia* virulence (Wang et al., 2016). In addition, the T3SS functions on a positive feedback loop in which active secretion leads to upregulated transcription of T3SS genes (Cornelis et al., 1987; Francis et al., 2002), although the mechanism behind this remains unclear.

A number of pathogens require one or more T3SSs for virulence, as genetic ablation causes attenuation in animal models and clinical isolates harbor plasmids or pathogenicity islands that encode T3SS genes (Coburn et al., 2007). An antibody against the *Pseudomonas aeruginosa* T3SS needle tip protein PcrV is part of a current Phase II clinical trial to treat nosocomial ventilator-associated pneumonia (NCT02696902), indicating that antibodies targeting the T3SS may be used as therapeutics. However, antibodies have low oral bioavailability and must be administered by injection; small molecules with high oral bioavailability are more attractive as therapeutic agents. A number of putative small molecule T3SS inhibitors have been

identified in the past 15 years (Duncan et al., 2012; Marshall and Finlay, 2014; Anantharajah et al., 2017), yet only one class of compounds can be considered validated. Many published T3SS inhibitors have off target effects that may underlie their T3SS disruption. For example, the best studied class of T3SS inhibitors, the salicylidene acylhydrazides, are thought to cause deregulation of T3SS genes through an unknown mechanism, yet the activity of some salicylidene acylhydrazides is dependent on iron chelation (Beckham and Roe, 2014). The phenoxyacetamides represent the only class of compounds that inhibit the T3SS in a physiologically relevant cellular context, protect against a bacterial infection (*P. aeruginosa* abscess formation in mice), and have a validated molecular target, the SctF needle subunit (Bowlin et al., 2014; Berube et al., 2017).

We have developed an experimental pipeline that can be employed to determine initial mode of action for compounds with T3SS inhibitory activity. We chose to use the enteropathogens *Yersinia pseudotuberculosis* and *Yersinia enterocolitica* as the workhorses for this assay pipeline because *Yersinia* is susceptible to the majority of T3SS inhibitors described and because of the wealth of genetic and biochemical tools available. In addition, *Yersinia* are extracellular pathogens that use their T3SS to prevent phagocytosis, negating the need for a T3SS inhibitor to cross the mammalian cell membrane to inhibit the T3SS-host cell interaction. Importantly, the assays selected for the experimental pipeline had to be amenable to miniaturization, as compound availability is often limiting. Since interfering with T3SS gene expression, basal body assembly, needle assembly, and host cell effector protein translocation could all lead to inhibition of T3SS activity, we designed our pipeline to consist of distinct assays that each measure a specific stage of type III secretion. Inhibitors of LcrF and its homolog ExsA from *P. aeruginosa* have been described (Marsden et al., 2015). In addition, it is possible that a small molecule with T3SS inhibitory activity could exert its effect by inhibiting secretion-associated increase of pYV copy number, leading to a decrease in T3SS gene expression. Therefore, two pipeline assays measure pYV copy number and T3SS gene expression. Once T3SS genes are expressed, the T3SS basal body assembles followed by the T3SS needle. Two additional pipeline assays measure SctD (YscD in *Yersinia*) localization to the IM and SctF (YscF) needle assembly. The last two pipeline assays monitor efficiency of T3SS effector protein (Yop) secretion *in vitro* or Yop translocation into target host cells. Each individual assay on its own provides a limited snapshot of a compound's T3SS inhibitory activity. However, when performed as a pipeline of assays, the resulting data can be used to predict the mode of action of a T3SS inhibitor. Furthermore, the training set of T3SS inhibitors we use to validate this pipeline are commercially available, and therefore can serve as controls to compare the activity of other T3SS inhibitors.

## MATERIALS AND METHODS

### Compounds and Antibodies

Compound 3 (CAS# 443329-02-0), compound 4 (CAS# 138323-28-1), and INP0007 (CAS# 300668-15-9) were obtained from Chembridge. INP0010 (CAS# 68639-26-9)

was obtained from ChemDiv. Compound 20 (CAS# 489402-27-9) was obtained from TimTek. The anti-YscF antibody was raised in rabbits against the *Y. pseudotuberculosis* YscF peptide KDKPDNPALLADLQH (Morgan et al., 2017). DMSO concentration did not exceed 0.2%, except where indicated.

## Bacterial Strains and Growth Conditions

Bacterial strains used in this paper are listed in Table 1. *Y. pseudotuberculosis* and *Y. enterocolitica* were grown, unless otherwise specified, in 2xYT (yeast extract-tryptone) at 26°C shaking overnight. In order to induce the T3SS, overnight cultures were diluted into low calcium medium (2xYT plus 20 mM sodium oxalate and 20 mM MgCl<sub>2</sub>) to an optical density (OD<sub>600</sub>) of 0.2 and grown for 1.5 h at 26°C shaking followed by 2–3 h at 37°C to induce Yop synthesis, depending on the assay, as previously described (Auerbuch et al., 2009).

## Construction of YopH Transcriptional Reporter

An expression cassette containing the *yopH* promoter and FLAG (5' terminus)- and *ssrA* (3' terminus)-tagged mCherry was generated using SOEing PCR and cloned into pMMB67EH (Horton et al., 1990; Pettersson et al., 1996; Karzai et al., 2000). The *yopH* promoter was amplified from pHYopT (gift from J. Bliska) using oligonucleotides SMP425 and SMP426 (Table 2). mCherry (gift from R. Tsien) was amplified using oligonucleotides SMP427 and SMP431. FLAG and *ssrA* sequences were incorporated into oligonucleotides SMP426/SMP427 and 431, respectively. Oligonucleotides SMP425 and SMP431 were used to generate the pyopH-FLAG-mCherry-*ssrA* cassette. PCR product was digested with BamHI and EcoRI and cloned into similarly digested pMMB67EH. Site directed mutagenesis using oligonucleotides SMP437 and SMP438 was used to generate the AAV variant of the *ssrA* tag.

## Type III Secretion Assay

Visualization of *Yersinia* T3SS cargo secreted in broth culture by Coomassie staining of SDS-PAGE separated proteins was performed as previously described with some modifications (Auerbuch et al., 2009). After low calcium medium cultures were grown for 1.5 h at 26°C, compounds or DMSO were added and the cultures shifted to 37°C for another 2 h. Post-incubation cultures were spun down at 15,000 × g for 10 min at room temperature. Supernatants were transferred to a new eppendorf tube. Ten percent final trichloroacetic acid (TCA) was added and the mixture was vortexed vigorously. Samples were incubated on ice for 20 min and then spun down at 15,000 × g for 15 min at 4°C. The pellet was resuspended in final sample buffer (FSB) with 20% DTT. Samples were boiled for 15 min prior to running on a 12.5% SDS-PAGE gel. Sample loading was normalized for bacterial culture density (OD<sub>600</sub>) measured prior to centrifugation. Densitometric quantification of the bands was done using Image Lab software (Bio-Rad), setting the relevant DMSO-treated YopE band to 1.00.

The miniaturized secretion assay was done by using *Y. pseudotuberculosis* expressing a YopM-β-lactamase (YopM-Bla) reporter and the chromogenic β-lactamase substrate

nitrocefin to detect secreted YopM-Bla (O'Callaghan et al., 1972; Lee et al., 2007; Green et al., 2016). *Y. pseudotuberculosis* Δyop6 pYopM-Bla and ΔyopN pYopM-Bla (negative control) were grown overnight at 26°C with 250 rpm shaking in 2xYT supplemented with chloramphenicol (25 μg/ml). The bacterial culture was diluted in low calcium media to OD<sub>600</sub> 0.2, incubated at 26°C with 250 rpm shaking for 1.5 h, and 25 μl was distributed into a 384-well plate (Nunc™, Thermo Fisher). Fifty micromolars of compounds or equivalent volume of DMSO was added to each well and the plate incubated at 37°C with 250 rpm shaking for 2 h. The bacterial plate was spun down for 5 min and 10 μl of supernatant transferred to a new plate containing the same volume of nitrocefin (500 μg/ml). Absorbance at 490 nm was measured 30 min after addition of nitrocefin. Three technical replicates for each sample were carried out for each independent experiment.

## Quantitative Real-Time PCR

Indicated concentrations of compounds, or the equivalent volumes of DMSO, were added to 26°C-grown low calcium medium cultures and treated cultures were shifted to 37°C for 3 h. RNA was isolated using an RNeasy Plus Micro Kit (Qiagen) according to the manufacturer's instructions and 2 μg RNA was used to make cDNA, as previously described (Auerbuch et al., 2009; Miller et al., 2014). SYBR Green PCR master mix (Applied Biosystems) was used for qPCR reactions according to the manufacturer's instructions and a 60°C annealing temperature, using the 16s rRNA gene as a reference for each sample. Three technical replicates were averaged for each sample/primer pair per independent experiment. Primers used are listed in Table 3. Results were analyzed using the Bio-Rad CFX software.

## YopH Transcriptional Reporter Assay

Indicated concentrations of compounds, or the equivalent volumes of DMSO, were added to 26°C-grown low calcium medium cultures and treated cultures were shifted to 37°C for 3 h. Two-hundred microliters of cultures were spun down at 3,000 × g for 5 min, resuspended in 200 μl 1X PBS, and mCherry fluorescence and optical density measured in black, clear bottom 96 well plates (Costar®, Corning Inc.) on a Perkin Elmer Victor X3 plate reader. Two technical replicates were averaged for each sample per independent experiment.

## Immunofluorescence Staining of YscF

Quantification of YscF staining on the bacterial surface was carried out as described previously (Morgan et al., 2017). Indicated concentrations of compounds, or the equivalent volumes of DMSO, were added to 26°C-grown low calcium medium cultures and treated cultures were shifted to 37°C for 3 h. Bacteria were fixed by the addition of a mix of 800 μl 4% paraformaldehyde, 1 μl 25% glutaraldehyde, and 40 μl 0.5 M NaPO<sub>4</sub> pH 7.4 to 500 μl of bacterial culture for 15 min at room temperature followed by 30 min or longer on ice. Fixed bacteria were gently sedimented (5,000 × g for 5 min), washed four times with PBS and stored in 250 mM glucose, 10 mM Tris-HCl pH 7.5, and 1 mM EDTA. Eight microliters of the fixed cells were added to coverslips and allowed to set until just dried. Coverslips

**TABLE 1** | Bacterial strains used in this study.

Strain	Description	References
Wild type	<i>Y. pseudotuberculosis</i> IP2666, naturally lacking YopT expression	Bliska et al., 1991
$\Delta yop6$ pYopM-Bl	<i>Y. pseudotuberculosis</i> IP2666 $\Delta yopHEMOJ$ pYopM-Bl	Duncan et al., 2014
$\Delta yop6/\Delta yopB$ pYopM-Bl	<i>Y. pseudotuberculosis</i> IP2666 $\Delta yopHEMOJ/\Delta yopB$ pYopM-Bl	Duncan et al., 2014
pYV40-EGFP-yscD	<i>Y. enterocolitica</i> serotype O9 strain E40	Diepold et al., 2010
Wild type	<i>Y. enterocolitica</i> 8081 serotype O8	Portnoy et al., 1981
YpIII/pIBX	<i>Y. pseudotuberculosis</i> YpIII with Tn5luxCDABE inserted in the Tn1000 resolvase homolog in pCD1 (wild type); Km <sup>r</sup>	Fahlgren et al., 2014
YpIII/(pIBX) <sub>n</sub> = 1	<i>Y. pseudotuberculosis</i> YpIII/pIBX derivative with the pIBX virulence plasmid lacking 3426 bp encoding the IncFII replicon and R6K suicide plasmid, integrated into YPK_3687 in the chromosome; Km <sup>r</sup> , Cm <sup>r</sup>	Wang et al., 2016
pyopH FLAG mCherry	<i>Y. pseudotuberculosis</i> YpIII containing the yopH promoter and YopH with an N-terminal FLAG tag and a C-terminal ssrA-tagged mCherry cloned into pMMB67EH	This study
flhDC <sup>Y.pestis</sup>	<i>Y. pseudotuberculosis</i> $\Delta yopHEMOJ/flhDC^{Y.pestis}$	Auerbuch et al., 2009

**TABLE 2** | Oligonucleotides used to generate pYopH FLAG mCherry.

Number	Sequence	Dir	Function	Enzyme
SMP425	GGAgaatccGCTGCGCGATGTACTGACCCG	>>	pyopH 5'	BamHI
SMP426	CTCCTCGCCCTTGCTCACCATCTTGTCATCGTCGCTCCTTGAATCCAT ATGTCCTCCTTAATTAATACACGCCTATAC	<<	pyopH-FLAG-mCherry/EGFP (for SOE, 3', use with SMP425)	
SMP427	GTATAGCGGTGATTTAATTAAGGAGGGACATatggattacaaggacgacgatgacaag Atggtgagcaaggcgagagag	>>	pyopH-FLAG-mCherry/EGFP (for SOE, 5', use with SMP428)	
SMP428	GAAgaattcTTACTGTACAGCTCGTCCATGCCG	<<	mCherry/EGFP 3'	EcoRI
SMP431	GAAgaattcTTACGCTGCTAACGCGTAATTCATCATTCGCTGC CTTGACAGCTCGTCCATGCCGC	<<	mCherry/EGFP 3' with ssrA (LAA) tag (use with 425,427)	EcoRI
SMP435	CAGCGAATGATGAGAATTACGCGTTAGTAGCGTAAGAATTCTGTTTCCTGTGTG	>>	LAA->LVA mut. for pMMB67EH-PyopH-FLAG-mCherry (top)	
SMP436	CACACAGGAAACAGAATTCCTACGCTACTAACGCGTAATTCATCATTCGCTG	<<	LAA->LVA mut. for pMMB67EH-pyopH-FLAG-mCherry (bottom)	
SMP437	GCAGCGAATGATGAGAATTACGCGCAGCAGTGTAAGAATTCTGTTTCCT GTGTGAAATTG	>>	LAA->AAV mut. for pMMB67EH-pyopH-FLAG-mCherry (top)	
SMP438	CAATTCACACAGGAAACAGAATTCCTACACTGCTGCCGCGTAATTCCT CATCATTCGCTGC	<<	LAA->AAV mut. for pMMB67EH-PyopH-FLAG-mCherry (bottom)	
SMP455	CAAGGCAGCGAATGATGAGAATTACGCGGCATCAGTGTAAGAATTCTGTTT CCTGTGTGAAATTGTTATC	>>	LAA->ASV mut. for pMMB67EH-pyopH-FLAG-mCherry (top)	
SMP456	GATAACAATTCACACAGGAAACAGAATTCCTACACTGATGCCGCGTAATTCCT CATCATTCGCTGCCTTG	<<	LAA->ASV mut. for pMMB67EH-pyopH-FLAG-mCherry (bottom)	

were blocked overnight with PBST with 3% BSA (PBST/BSA) at 4°C. Blocking solution was removed and anti-YscF primary antibody was added at 1:10,000 in PBST/BSA and rocked at 4°C for 4 h. Coverslips were carefully rinsed in ice cold PBST with 0.1% Tween-20 several times and incubated with Alexa fluor 594 or 488 anti-rabbit secondary antibody (Invitrogen) at 1:10,000 in PBST/BSA and rocked at 4°C for 3 h followed by rinsing again in ice cold PBST with 0.1% Tween-20 several times. Coverslips were then stained for nuclear material with Hoechst 33342 (Thermo Scientific) at 1:10,000 in PBST/BSA and left in the dark at room temperature for 30 min. Coverslips were washed in ice cold PBST with 0.1% Tween-20 several times, allowed to dry briefly, mounted onto glass coverslips with Prolong Gold

(Thermo Scientific), and sealed with clear nail polish. Images were taken with the Zeiss Axioimager Z2 widefield microscope under 63X/1.4 oil immersion using Zen software, pseudocolored, and merged in FIJI. YscF puncta were counted using IMARIS software.

## YscD Analysis

*Y. enterocolitica* expressing EGFP-YscD were grown overnight in brain heart infusion (BHI) broth containing nalidixic acid (35 µg/ml) and diaminopimelic acid (80 µg/ml) (Diepold et al., 2010). Overnight cultures were diluted to an OD<sub>600</sub> of 0.2 in M9 minimal medium supplemented with casamino acids. Cultures were grown for 1.5 h at 26°C. Compounds were added



**TABLE 3** | qPCR primers used in this study.

Name	Sequence	References
FqyopE	CCATAAACCGGTGGTGAC	Morgan et al., 2017
RqyopE	CTTGGCATTGAGTGATACTG	Morgan et al., 2017
FqyscN	CTTCGCTTATTCGTAGTGCT	Miller et al., 2014
RqyscN	TCGCCTAAATCAGACTCAAT	Miller et al., 2014
Fq16s	AGCCAGCGGACCACATAAAG	Merriam et al., 1997
Rq16s	AGTTGCAGACTCCAATCCGG	Merriam et al., 1997
FqyscF	TCTCTGGATTACGAAAGGA	Miller et al., 2014
RqyscF	GCTTATCTTTCAATGCTGCT	Miller et al., 2014
FqlcrF	GGAGTGATTTCCGTCAGTA	Miller et al., 2014
RqlcrF	CTCCATAAATTTTGAACC	Miller et al., 2014
FqyscD	TGCCAGAGACGTTACAGGTT	This study
RqyscD	CATCCTGGTTATACTCGCGC	This study
FqErpA	TACCGGTGGTGGATGTAGCGGG	Miller et al., 2014
RqErpA	ATAATCCACGGCACCGCCAC	Miller et al., 2014
FqyopK	ATGTTGCCATTGCTATAAGC	This study
RqyopK	GAGAACGGATGTTTGTCAT	This study
FqyopH	ACACTACAAGACGCCAAAG	This study
RqyopH	GTGAAGGGCTGAATGTGAA	This study
FqlcrV	TGATATCGAATTGCTCAAGA	This study
RqlcrV	CGGCGGTAAAGAGAAAT	This study
FqL9	TGGGTGACCAAGTCAACGTA	This study
RqL9	GTCGCGAGTACCGATAGAGC	This study

at indicated concentrations or the equivalent volumes of DMSO were added and the cultures switched to 37°C for another 3 h. Two microliters of culture were layered on a patch of 1% agarose in water (Skinner et al., 2013) supplemented with 80 µg/ml diaminopimelic acid, 5 mM EDTA, 10 mM MgCl<sub>2</sub>, and either compounds at indicated concentrations or the equivalent volume of DMSO (Diepold et al., 2010). Images were taken with a Zeiss Axioimager Z2 widefield microscope under 63X/1.4 oil immersion using Zen software, pseudocolored, and merged in FIJI. YscD puncta were counted using IMARIS software.

## pYV Copy Number

*Y. pseudotuberculosis* YpIII/pIBX<sub>N=1</sub> and YpIII/pIBX were grown overnight in 2xYT media containing kanamycin (30 µg/ml). Overnight cultures were diluted to an OD<sub>600</sub> of 0.2 in M9 supplemented with casamino acids. Cultures were grown for 1.5 h at 26°C. Compounds were added at indicated concentrations or the equivalent volumes of DMSO were added and the cultures switched to 37°C for another 3 h. Two hundred microliters of each culture was added to clear bottom, white 96 well plates (Costar®, Corning Inc.) and optical density and luminescence were measured using a Perkin Elmer Victor X3 plate reader. Two technical replicates were averaged for each sample per independent experiment.

## YopM Translocation Assay

Measuring translocation of the YopM-β-lactamase (YopM-Bla) reporter effector protein was carried out as previously described (Duncan et al., 2014). A total of 6 × 10<sup>3</sup> CHO-K1

cells were plated in each well of a 384-well plate (Corning™ Falcon™) in 50 µl of F-12K medium plus 10% FBS and 1% glutamine, and incubated overnight. The following day, indicated concentrations of compounds, or the equivalent volumes of DMSO, were added to 26°C-grown low calcium medium cultures of *Y. pseudotuberculosis* expressing YopM-Bla and treated cultures were shifted to 37°C for 3 h. Immediately prior to infection of CHO-K1 cells, the F-12K media was removed and replaced with RPMI plus 10% FBS and compounds or DMSO were added. *Y. pseudotuberculosis* was added to the CHO-K1 plate at an MOI of 7. Five minutes after this transfer, the plate was centrifuged at 290 × g for 5 min to initiate bacterium-host cell contact and incubated for 1 h at 37°C and 5% CO<sub>2</sub>. Thirty minutes prior to the end of the infection, CCF2-AM (Invitrogen) was added to each well, and the plate covered in foil and incubated at room temperature. At the end of the infection, the medium was aspirated and fresh 4% paraformaldehyde added to each well for 20 min to fix the cells. The paraformaldehyde was then aspirated and the DNA dye DRAQ5 (Cell Signaling Technology) in PBS was added to each well. The monolayers were incubated at room temperature for 10 min, washed once with PBS, and visualized using an ImageXpressMICRO automated microscope and MetaXpress analysis software (Molecular Devices). The number of YopM-Bla-positive cells was calculated by dividing the number of blue (CCF2-cleaved) cells by the number of green (total CCF2) cells. Three technical replicates were averaged for each sample per independent experiment.

## Growth Curves

Overnight cultures of *Y. pseudotuberculosis* were diluted to an OD<sub>600</sub> of 0.1 in 2xYT and 200 µl was added to each well of a 96-well plate (Corning™ Falcon™). Compounds were added at 50 µM and kanamycin at 50 µg/ml, plates incubated at 26°C, and the OD<sub>600</sub> of the cultures measured every hour for 13 h using a VersaMax Tunable Microplate Reader (Molecular Devices). The 96-well plates were intermittently shaken throughout the experiment. One technical replicate was used for each sample per independent experiment.

## Motility Assay

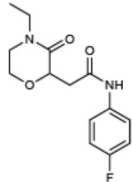
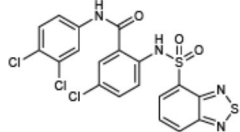
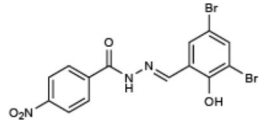
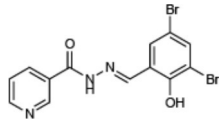
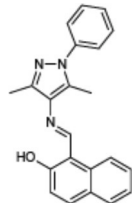
Following overnight growth, 1 µl of *Y. pseudotuberculosis* overnight culture was spotted onto motility medium containing either 1% tryptone/0.25% agar or 1% tryptone/0.25% agar supplemented with 5 mM EGTA and 20 mM MgCl<sub>2</sub> in six-well plates. Each well contained either 0.3% DMSO or 50 µM INP0007 or INP0010. The plates were incubated at 26°C for 24 h before the diameter of swimming motility was measured. One technical replicate was used for each sample per independent experiment.

## RESULTS

### T3SS Inhibitor Training Set for Assay Pipeline

We selected a training set of commercially-available compounds to validate our assay pipeline (Table 4). All compounds selected

**TABLE 4 |** Compounds used in this study and their reported activity.

Compound name	Chemical structure	Shown to inhibit:	References
Compound 3 (CAS: 443329-02-0)		Inhibition of ExoS-Bla and YopE-Bla secretion in <i>Pseudomonas</i> and <i>Yersinia</i> , respectively	Aiello et al., 2010
Compound 4 (CAS: 138323-28-1)		Inhibition of T3SS gene expression and effector secretion in <i>Yersinia</i>	Kauppi et al., 2003
INP0007 (CAS: 300668-15-9)		Inhibition of T3SS gene expression, effector secretion, and motility in <i>Yersinia</i> Inhibition of T3SS (SPI1) gene expression, secretion, and translocation in <i>Salmonella</i>	Kauppi et al., 2003 Nordfelth et al., 2005 Negrea et al., 2007
INP0010 (CAS: 68639-26-9)		Inhibition of T3SS gene expression and effector secretion in <i>Yersinia</i> Inhibition of T3SS gene expression, secretion, and invasion in <i>Salmonella</i> Inhibition of virulence genes, including the T3SS in <i>E. coli</i>	Nordfelth et al., 2005 Negrea et al., 2007 Tree et al., 2009
Compound 20 (CAS: 489402-27-9)		Inhibition of T3SS dependent effector translocation in <i>Yersinia</i>	Harmon et al., 2010

met two strict requirements: demonstrated inhibitory activity on the *Yersinia* T3SS and absence of bactericidal activity within 6 h to accommodate the timeframe of the pipeline assays (Figures 1A–C).

Compound 4 (C4), a haloid-containing sulfonamidobenzamide, was identified through a luciferase-based T3SS gene promoter fusion screen as a potent inhibitor of T3SS gene expression (Kauppi et al., 2003). We chose this compound because it was shown, albeit modestly, to inhibit expression of the LcrF master regulator of the T3SS in *Yersinia* (Kauppi et al., 2003) and we therefore expected that it would have a broad impact on all stages of type III secretion downstream of T3SS expression in our assay pipeline. From the same high throughput screening strategy that identified C4, two members of the salicylidene acylhydrazide class of inhibitors, INP0007 (Kauppi et al., 2003) and INP0010 (Nordfelth et al., 2005), were identified. Despite a large number of studies, the mechanism of action of these compounds remains unclear and there is evidence of off target effects on global virulence gene expression by at least some salicylidene acylhydrazides (Tree et al., 2009). In fact, INP0010 decreased *Yersinia* growth starting 7 h after

initiation of treatment (Figure 1D), consistent with previous reports (Veenendaal et al., 2009). Compound 3 (C3), a malic diamide, was shown to inhibit ExoS secretion in *P. aeruginosa* and YopE secretion in *Yersinia pestis* (Aiello et al., 2010). This compound is structurally related to another class of T3SS inhibitors, the phenoxyacetamides, which were proposed to target the PscF needle subunit in *Pseudomonas* (Bowlin et al., 2014). Based on this structural relatedness, C3 was expected to disrupt T3SS needle assembly without impacting T3SS gene expression. Compound 20 (C20) was identified in a T3SS effector protein- $\beta$ -lactamase reporter translocation screen, but had no significant effect on the ability of the bacteria to secrete T3SS effectors in the absence of host cells, pointing to the possibility that this compound specifically blocks the bacteria–host cell interaction (Harmon et al., 2010). Therefore, C20 was expected to inhibit the translocation of effector proteins into host cells but not impact T3SS gene expression and assembly.

An advantage of using Ysc-expressing *Yersinia* for our assay pipeline is that removing calcium from the culture medium enables T3SS effector proteins to be secreted into the supernatant in the absence host cells (Yother and Goguen, 1985; Perry et al.,

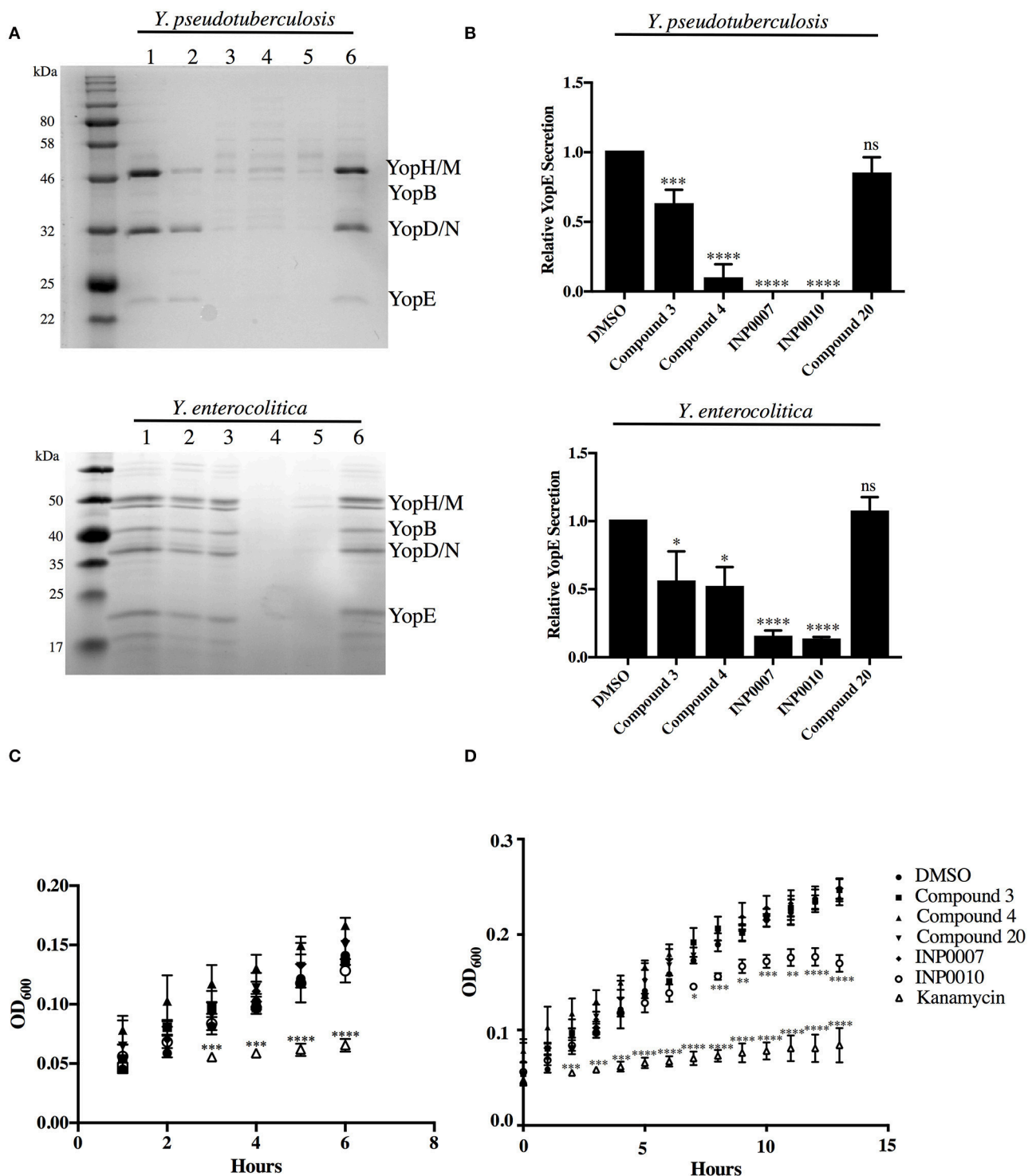


**FIGURE 1 |** Efficiency of T3SS effector protein secretion and bacterial growth in the presence of T3SS inhibitors. **(A,B)** The relative efficiency of effector protein secretion into the culture supernatant was analyzed following bacterial growth for 2 h under T3SS-inducing conditions in the presence of either 50  $\mu$ M compound or equivalent volume of DMSO. **(A)** The secretome of *Y. pseudotuberculosis* IP2666 and *Y. enterocolitica* 8081 was precipitated with trichloroacetic acid, separated by SDS-PAGE, and visualized by staining with Coomassie blue. Samples were normalized to culture optical density. (1) DMSO, (2) Compound 3, (3) Compound 4, (4) INP0007, (5) INP0010, (6) Compound 20. **(B)** Quantification of the YopE protein band by densitometry relative to the DMSO control. The average of 3 (*Y. pseudotuberculosis*) or 4 (*Y. enterocolitica*) biological replicates  $\pm$  standard deviation is shown. **(C,D)** *Y. pseudotuberculosis* IP2666 growth at 26°C in the presence of 50  $\mu$ M compound or DMSO was tracked by measuring optical density. The average of three biological replicates  $\pm$  standard deviation is shown and statistical significance is represented comparing compounds relative to the DMSO control. \* $P < 0.03$ ; \*\* $P < 0.004$ ; \*\*\*\* $P < 0.0001$ ; \*\*\*\*\* $P < 0.0007$  (one way ANOVA with Dunnett's *post-hoc* test).

1986; Straley and Bowmer, 1986; Sample et al., 1987; Forsberg and Wolf-Watz, 1988; Mehig et al., 1989), providing a useful method of monitoring efficiency of T3SS inhibition in order to validate use of a given inhibitor in our assay pipeline. As expected, all test compounds except C20 exhibited significant inhibition of effector Yop secretion (**Figures 1A,B**). Importantly, this secretion assay was used routinely to ensure the efficacy of each batch of compound purchased and after 1 month in storage. Therefore, even when a compound had no effect in a particular assay, we could be confident that it was still active as a T3SS inhibitor.

## Assessment of T3SS Gene Expression

We reasoned that inhibition of the pYV copy number upregulation that occurs during normal induction of type III secretion in *Yersinia* may impact T3SS gene expression, and therefore affect overall T3SS activity. To test this, we employed a *Y. pseudotuberculosis* strain with a luciferase reporter gene cluster integrated onto the pYV virulence plasmid (YpIII/pIBX) (Fahlgren et al., 2014). As a negative control, we used a strain in which a replication deficient copy of the virulence plasmid as well as the luciferase gene cluster was integrated into the chromosome (referred to as YpIII/pIBX<sub>N=1</sub>) (Wang et al., 2016). In this YpIII/pIBX<sub>N=1</sub> strain, the ratio of T3SS and luciferase reporter genes vs. chromosomal genes remains constant even upon induction of type III secretion (Wang et al., 2016). As expected, expression of *lcrF*, the effector protein *yopE*, the integral IM ring protein *ycsD*, and the needle subunit *ycsF* were significantly decreased in the YpIII/pIBX<sub>N=1</sub> strain compared to the YpIII/pIBX strain (**Figure 2A**). While these data demonstrate that inhibition of pYV gene copy number could impact pYV gene expression, four of the five compounds in our training set did not significantly affect virulence plasmid copy number as measured by luciferase activity, while INP0007 significantly increased copy number ( $p = 0.0054$ ; **Figure 2B**) for reasons that are unclear but that may reflect off target effects. In contrast, luciferase expression could be inhibited by blocking general transcription or translation using rifampicin or chloramphenicol (**Figure 2B**). Therefore, while inhibiting pYV copy number in *Yersinia* causes a decrease in T3SS activity, we conclude that none of the compounds in our training set act by inhibiting upregulation of pYV copy number.

In order to determine if the training set compounds negatively impacted T3SS gene expression, we used a *Yersinia* reporter strain containing an unstable YopH-mCherry-AAV transcriptional reporter (Andersen et al., 1998). C4, INP0007, and INP0010 inhibited YopH-mCherry-AAV expression when T3SS activity was induced by incubation in low calcium medium at 37°C (**Figure 3A**). In order to validate and extend these results, we measured transcript levels of T3SS and non-T3SS genes by qPCR. Consistent with the YopH-mCherry-AAV data, C3 and C20 had no significant impact on gene expression (**Figure 4**). However, C4 inhibited expression of all T3SS genes tested, but did not impact expression of two non-T3SS-associated genes: the iron sulfur cluster loading protein *erpA* and the small ribosomal subunit L9. Interestingly, INP0007 and INP0010 significantly inhibited transcript levels of *lcrF*, the needle tip subunit *lcrV*, and effector proteins *yopH*, *yopE*, and *yopK*, but

did not inhibit expression of the ATPase *ycsN*, *ycsF*, and *ycsD* under these conditions (**Figure 4**). To test whether inhibition of secretion via the positive feedback loop indirectly inhibits T3SS gene expression, we measured YopH-mCherry fluorescence and *ycsD* mRNA levels via qPCR during growth at 37°C in high calcium (**Figures 3B,C**). Under these conditions, *Yersinia* can assemble the T3SS (Diepold et al., 2010), but no secretion of Yop effectors occurs (Forsberg and Wolf-Watz, 1988); therefore, the positive feedback loop is not active in high calcium. While overall expression levels of YscD and YopH are lower in high calcium compared to low calcium conditions, C4, INP0007, and INP0010 did not significantly decrease YopH-mCherry-AAV fluorescence in high calcium conditions (**Figure 3B**), suggesting an indirect effect of these compounds on T3SS gene expression through inhibition of secretion in low calcium conditions. Likewise, *ycsD* levels were not decreased by C4 in high calcium (**Figure 3C**). Importantly, *ycsD* expression was significantly lower in the  $\Delta lcrF$  mutant compared to WT under high calcium conditions in the absence of compound. These data indicate that C4 is not likely to target LcrF activity, as *ycsD* is predicted to be under LcrF control (Schwiesow et al., 2015).

## Assessment of T3SS Assembly

In order to monitor T3SS assembly, we used fluorescence microscopy to quantify YscD localization in *Y. enterocolitica* and YscF puncta formation in *Y. pseudotuberculosis* as a proxy for T3SS basal body and T3SS needle assembly, respectively, as previously described (Davis and Mecasas, 2007; Diepold et al., 2010; Morgan et al., 2017). Only INP0007 significantly impacted YscD-EGFP puncta formation (**Figure 5**). Importantly, the level of diffuse fluorescence in INP0007-treated *Yersinia* was greater than that of the non-T3SS-inducing condition (26°C-grown *Yersinia*; **Figure 5A**, inset), indicating that while YscD is expressed at 37°C in the presence of INP0007, it is not assembled into basal bodies in the presence of this compound. In contrast, while C3 and C20 had no significant effect on YscF puncta formation as measured with an anti-YscF antibody, C4, INP0007, and INP0010 significantly inhibited needle assembly (**Figure 6**).

The bacterial flagellar apparatus is composed of a basal body that is structurally related to the injectisome T3SS basal body and mediates secretion of the flagellar hook and filament proteins (Macnab, 2004). Therefore, it is possible that compounds with the ability to inhibit injectisome T3SS basal body assembly may inhibit flagellar assembly and therefore flagellar motility. INP0007 has been shown to inhibit motility in *Yersinia* (Kauppi et al., 2003), but neither INP0007 nor INP0010 inhibited motility in *Salmonella* (Negrea et al., 2007). In our standard *Yersinia* motility agar (Morgan et al., 2017), INP0007 significantly decreased flagellar motility in *Y. pseudotuberculosis*, while INP0010 decreased motility weakly albeit significantly (**Figure 7**). Addition of the chelating agent EGTA in the motility agar, as used in the Kauppi et al study (Kauppi et al., 2003), led to an even greater inhibitory effect on motility by INP0010 (**Figure 7**). The *Y. pseudotuberculosis* *flhDC*<sup>Ypestis</sup> non-motile strain served as the negative control for the motility assay. Taken



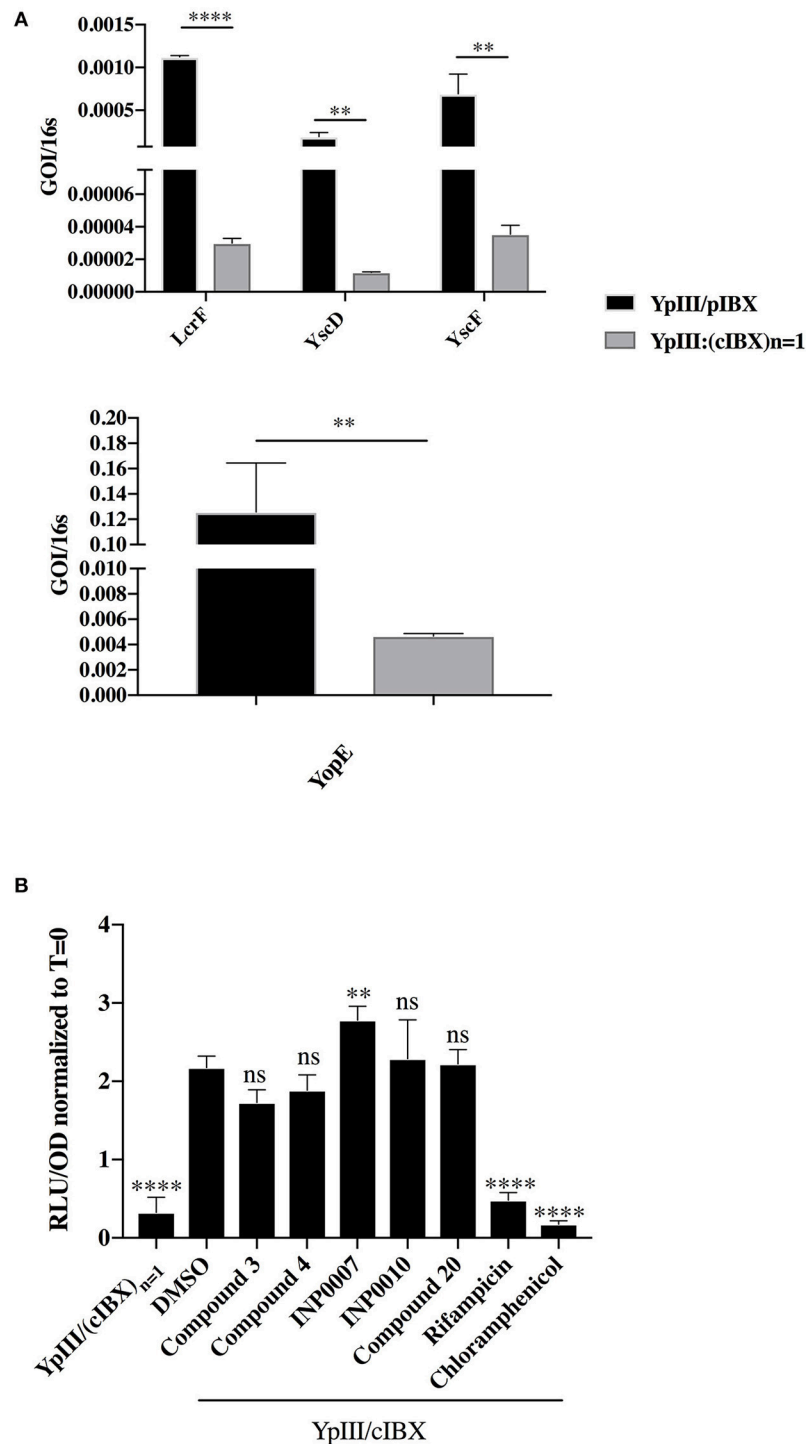


**FIGURE 2 |** Correlation between pYV copy number and T3SS gene expression. **(A)** *Y. pseudotuberculosis* encoding luciferase genes on pYV (YpIII/pIBX) or a strain in which pYV-encoded T3SS and luciferase genes were incorporated into the chromosome in single copy [YpIII/(clBX)<sub>n=1</sub>] were grown for 3 h under T3SS-inducing conditions in 50  $\mu$ M compound or equivalent volume of DMSO and T3SS gene expression evaluated by qPCR. GOI, gene of interest. Expression levels were normalized to 16S rRNA and then the fold change compared to DMSO calculated  $[(GOI)^{compound}/16S^{compound}]/[(GOI)^{DMSO}/16S^{DMSO}]$ . The average of four biological replicates  $\pm$  standard deviation is shown. \*\*\*\* $P < 0.0001$ , \*\* $P < 0.008$  (Student *T*-test). **(B)** *Y. pseudotuberculosis* YpIII/pIBX and YpIII/(clBX)<sub>n=1</sub> were grown under T3SS-inducing conditions for 3 h in 50  $\mu$ M compound or equivalent volume of DMSO and luminescence measured as a readout of pYV gene copy number. The average of four biological replicates  $\pm$  standard deviation is shown and statistical significance is represented comparing compounds relative to the DMSO control. \*\*\*\* $P < 0.0001$ ; \*\* $P = 0.008$  (one way ANOVA with Dunnett's *post-hoc* test).

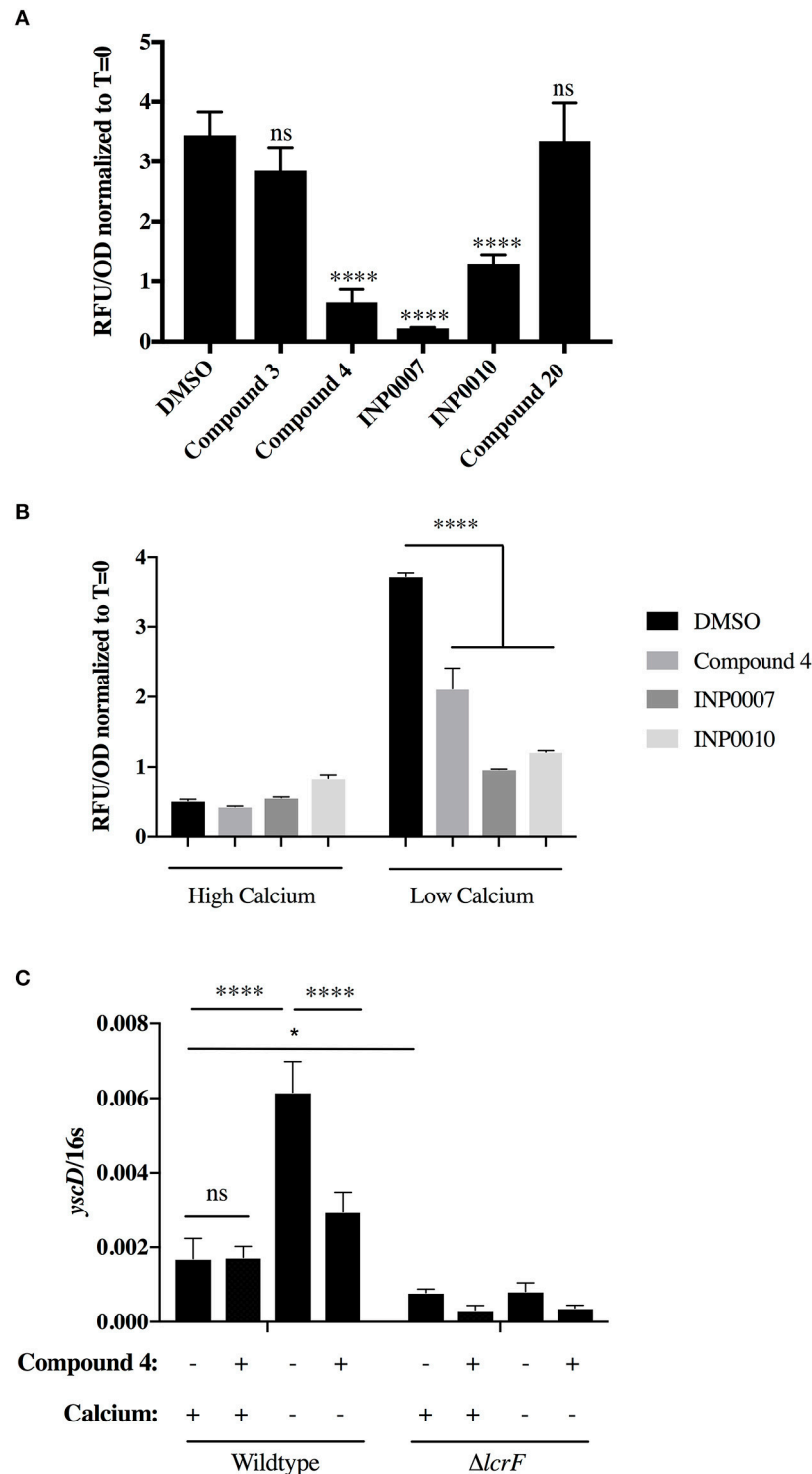


**FIGURE 3 |** Analysis of *yopH*-mCherry fluorescence to assess T3SS gene expression. **(A,B)** *Y. pseudotuberculosis* *pyoH* FLAG mCherry was grown under T3SS-inducing **(A,B)**, low calcium) or non-inducing **(B)**, high calcium) conditions and relative mCherry fluorescence measured at 3 h after addition of 50  $\mu$ M compound or equivalent volume of DMSO. The average of three biological replicates  $\pm$  standard deviation is shown and statistical significance is represented comparing compounds relative to the DMSO control. \*\*\*\* $P < 0.0001$  (one way ANOVA with Dunnett's *post-hoc* test). **(C)** *Y. pseudotuberculosis* wildtype or  $\Delta lcrF$  were grown in low or high calcium media for 3 h in 50  $\mu$ M Compound 4 or equivalent volume of DMSO and *yscD* mRNA levels measured by qPCR. Expression levels were normalized to 16s rRNA. Statistical significance is represented comparing the indicated pairs of conditions. \*\*\*\* $P < 0.0001$ , \* $P < 0.002$  (Student *t*-test).

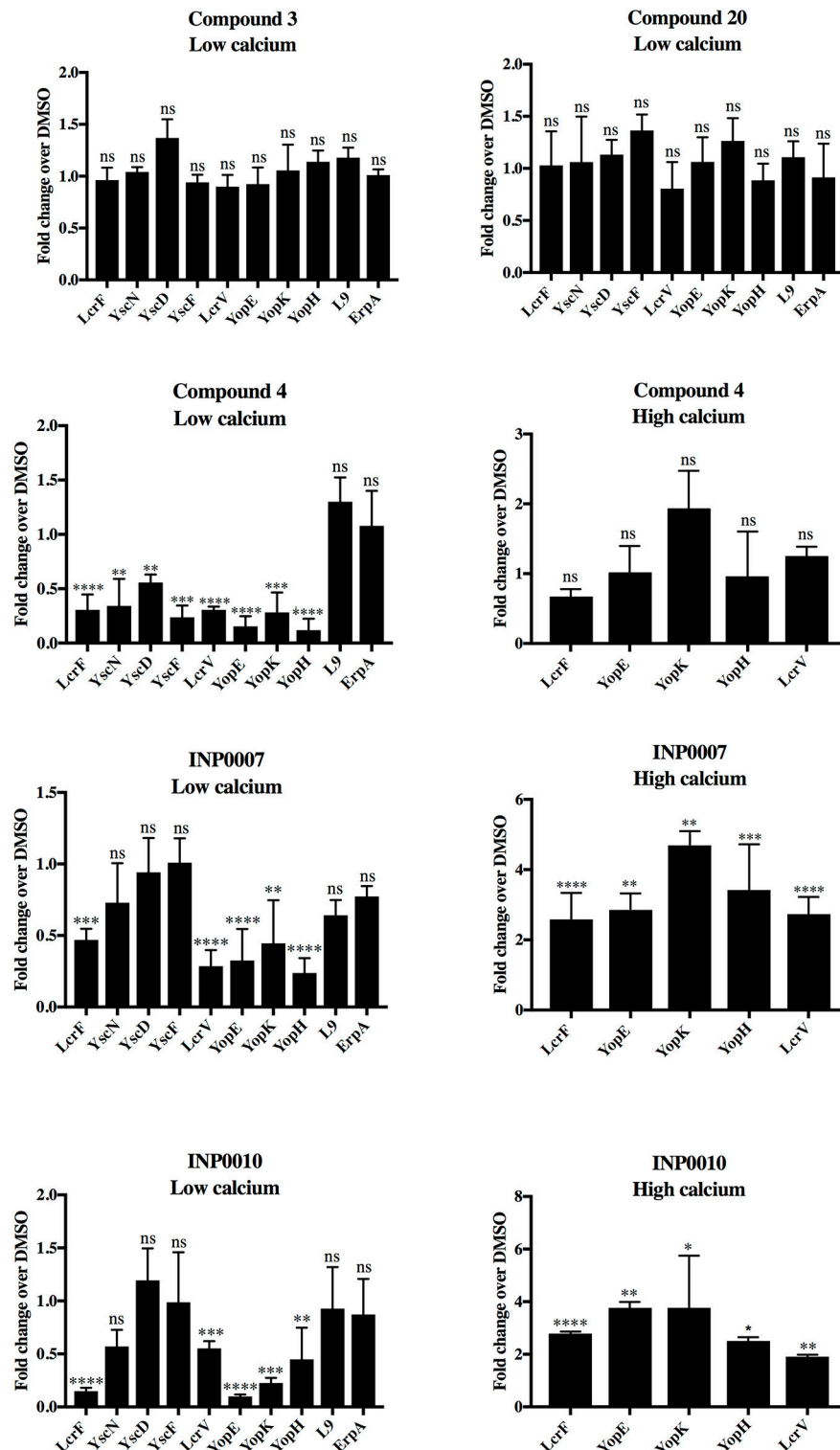
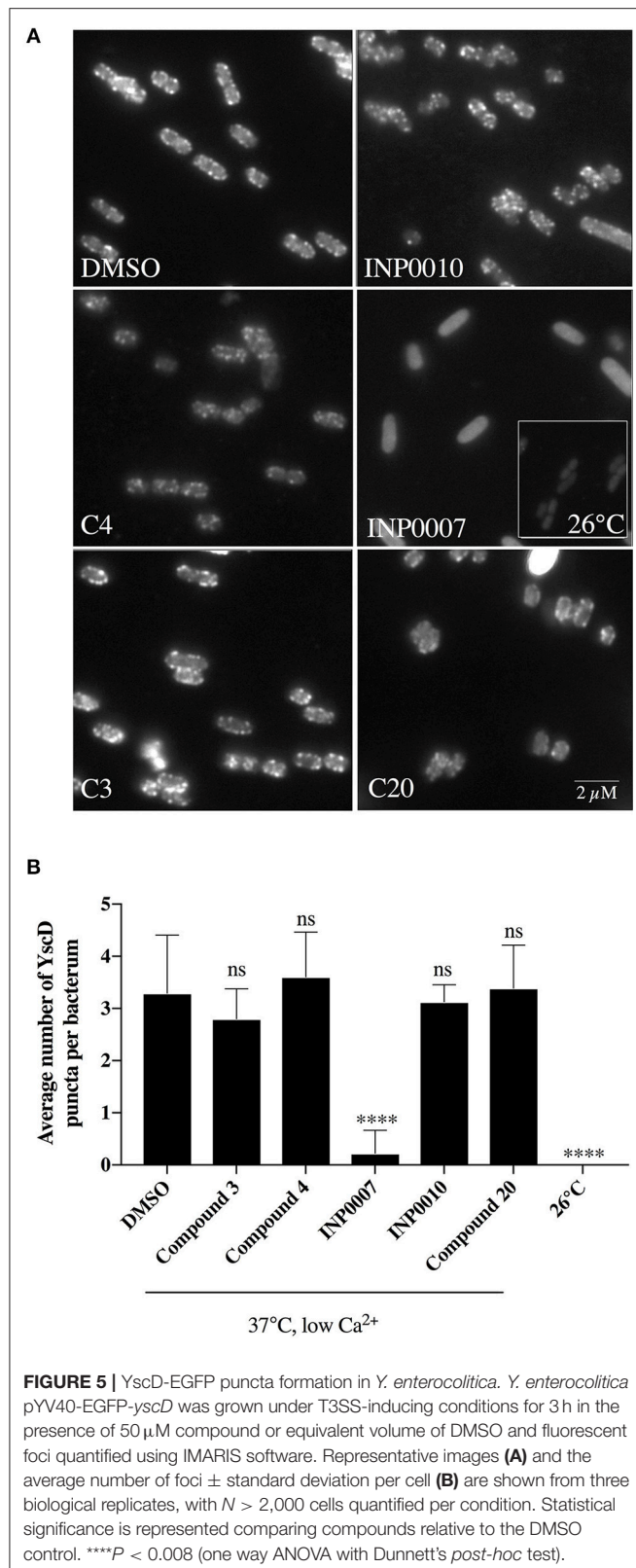
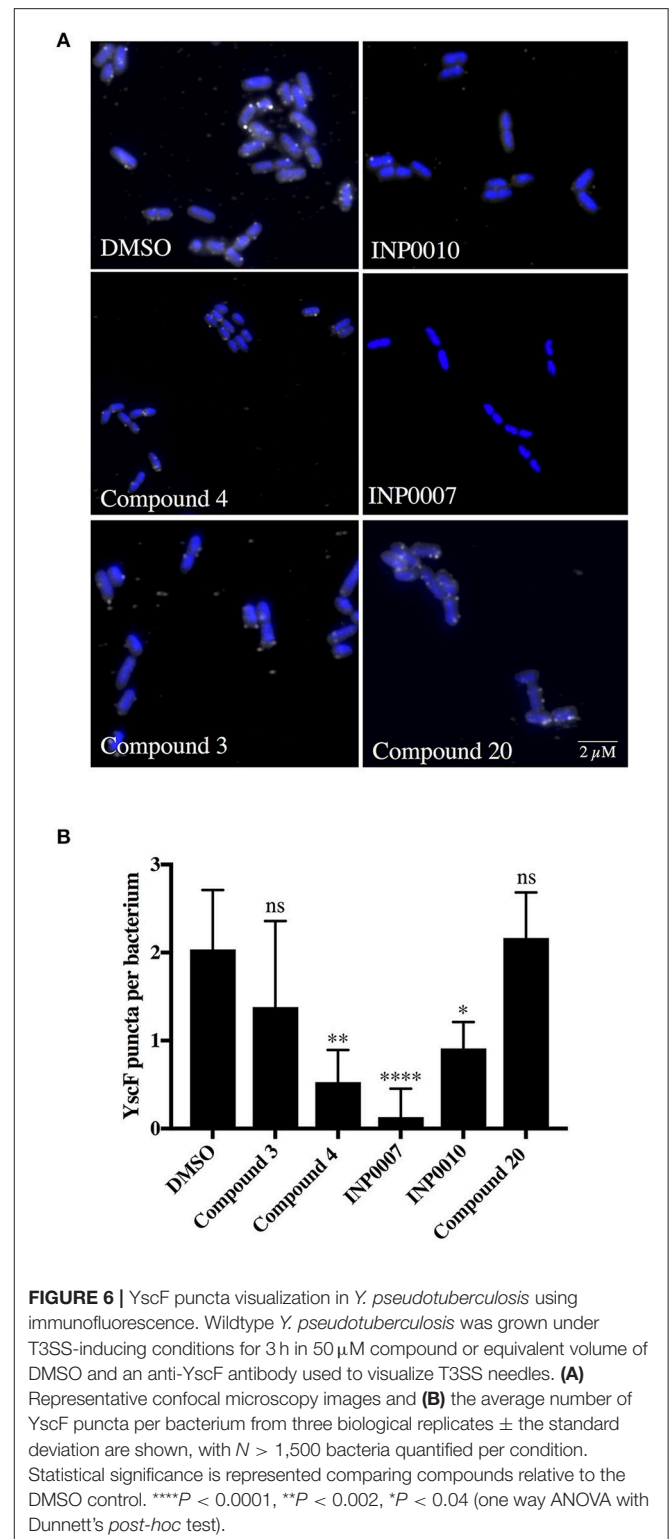


**FIGURE 4 |** T3SS gene mRNA levels under low and high calcium conditions. Wildtype *Y. pseudotuberculosis* was grown under high or low calcium conditions in the presence of 50  $\mu$ M compound or equivalent volume of DMSO and mRNA levels of T3SS (*lcrF*, *yscN*, *yscD*, *yscF*, *lcrV*, *yopE*, *yopK*, *yopH*) and non-T3SS genes (*L9*, *erpA*) assessed by qPCR. The average of four biological replicates  $\pm$  standard deviation is shown and statistical significance is represented comparing compounds relative to the DMSO control for each gene. \*\*\*\* $P < 0.0001$ , \*\*\* $P < 0.0005$ , \*\* $P < 0.003$ ; \* $P < 0.022$  (one way ANOVA with Dunnett's *post-hoc* test). ns, not significant.



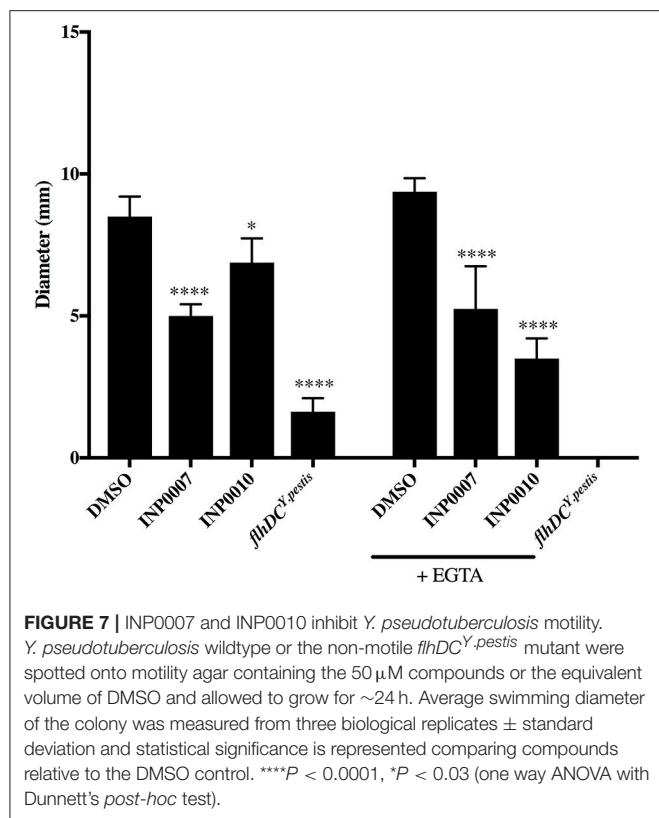
together, these data indicate that INP0007 and INP0010 impact both the flagellar and injectisome T3SS.



## Assessment of Effector Protein Secretion *in vitro*

While the Yop *in vitro* secretion assay shown in Figure 1 is critical for assessing the impact of a compound on overall Yop

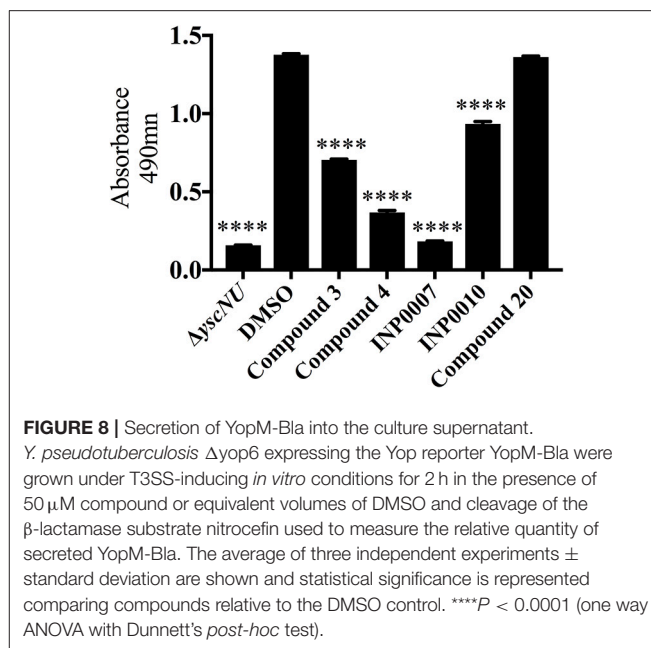




secretion, the method used (Coomassie staining of SDS-PAGE separated proteins precipitated from the culture supernatant) is not amenable to a high throughput format. In order to assess Yop secretion *in vitro* in microtiter plates, *Y. pseudotuberculosis* expressing a YopM- $\beta$ -lactamase (YopM-Bla) reporter was used in conjunction with the chromogenic  $\beta$ -lactamase substrate nitrocefin (O'Callaghan et al., 1972; Lee et al., 2007; Green et al., 2016). Consistent with the block in Yop secretion observed in **Figure 1**, C3, C4, INP0007, and INP0010 significantly blocked YopM-Bla secretion into the culture supernatant while C20 did not (**Figure 8**). Surprisingly, INP0010 blocked YopM-Bla secretion by only 32% as measured using nitrocefin (**Figure 8**), yet appeared to have a much more significant effect on native YopM secretion as measured using Coomassie staining (**Figure 1**). The reason for this discrepancy is unclear; however, we note that INP0010 has cytotoxic effects on bacteria and eukaryotic cells (see below) and is likely to have the greatest off target effects of the compounds in our training set.

## Assessment of Effector Protein Translocation

One of the most important requirements of a T3SS inhibitor is its ability to prevent translocation of effector proteins into target host cells. We employed a different type of YopM-Bla reporter assay to assess translocation of effector proteins into CHO K1 cells loaded with CCF2, a fluorescent  $\beta$ -lactamase substrate that can enter eukaryotic cells (Dewoody et al., 2011). While C3, C4, C20, INP0007, and INP0010 significantly blocked YopM-Bla



translocation at 50  $\mu$ M, INP0010 appeared to be cytotoxic at this concentration (**Figure 9**).

## DISCUSSION

A methodical approach to primary characterization of inhibitors for the T3SS has been lacking in the field. Here, we describe a pipeline of miniaturized assays, using enteropathogenic *Yersinia* as the workhorse organism, that enable rapid, initial characterization of the stage of T3SS expression, assembly, or function targeted by compounds with T3SS inhibitory activity. Furthermore, we used a training set of compounds with previously-identified T3SS inhibitory activity to test the utility of this pipeline (**Table 5**). INP0007 blocked T3SS basal body and needle assembly and therefore inhibited Yop secretion and translocation. C4 and INP0010 did not prevent basal body assembly but blocked needle assembly, secretion, and translocation. However, INP0010 exhibited cytotoxicity, complicating interpretation of some assay results. C3 allowed T3SS assembly but prevented Yop secretion and translocation. Lastly, C20 allowed T3SS assembly and Yop secretion *in vitro*, but blocked translocation of Yops into target host cells. These results demonstrate the ability of our assay pipeline both to validate T3SS inhibitors and provide testable hypotheses on their mode of action.

C3 blocked the ability of the *Yersinia* T3SS to secrete T3SS effector proteins into low calcium culture supernatant and to translocate effector proteins into target host cells. Yet C3 did not block T3SS basal body and needle assembly, as determined by imaging YscD basal body and YscF needle puncta formation. C3 showed a modest inhibition of YopE secretion (28%), but notably inhibited secretion of the translocator protein YopD (**Figure 1A**). These data provide a possible explanation for why C3 strongly inhibited Yop translocation into host cells (40%)

**TABLE 5 |** Summary of experimental pipeline assays using our training set of T3SS inhibitors.

Compound name	pYV copy number <sup>a</sup>	T3SS gene expression (high Ca <sup>2+</sup> ) <sup>b</sup>	T3SS gene expression (low Ca <sup>2+</sup> ) <sup>c</sup>	YscD puncta per bacterium <sup>c</sup>	YscF puncta per bacterium <sup>c</sup>	Secretion (%DMSO) <sup>d</sup>	Translocation <sup>e</sup> (%)
DMSO (control)				~3.3	~2.0	100	~72
C3	No change	No change	No change	~2.8	~1.38	51	~40
C4	No change	No change	All T3SS genes tested	~3.6	~0.5	27	~39
INP0007	Increase	No change	Subset of T3SS genes tested	~0.2	~0.13	13	~27
INP0010	No change	No change	Subset of T3SS genes tested	~3.1	~0.92	68	~55
C20	No change	No change	No change	~3.4	~2.1	99	~44

Dark gray boxes represent statistically significant inhibitory activity at a distinct stage of T3SS deployment. Light gray boxes represent significant inhibitory activity on T3SS gene expression only under low calcium conditions, when the positive feedback loop is active and strong inhibition of secretion leads to a decrease in T3SS gene expression.

<sup>a</sup>Compared to DMSO control, as measured by pYV-encoded luciferase activity.

<sup>b</sup>Compared to DMSO control under high calcium conditions, as measured by qPCR or monitoring YopH-mCherry expression.

<sup>c</sup>Under low calcium conditions.

<sup>d</sup>Compared to DMSO control, as measured by nitrocefin color change resulting from YopM-Bla secreted into the culture supernatant under low calcium conditions.

<sup>e</sup>Percent of cells with  $\beta$ -lactamase substrate CCF2 blue fluorescence in CHO cells.

despite less potent inhibition of YopE secretion, as YopD is required for Yop delivery into host cells (Rosqvist et al., 1994) C3 has structural similarities with the phenoxyacetamides, which target the SctF needle subunit (Aiello et al., 2010; Bowlin et al., 2014). However, our data indicate that C3 blocks a specific activity of the assembled T3SS. Alternatively, the T3SS needle structure may be altered in the presence of C3, still allowing recognition by our anti-YscF antibody but impeding cargo egress.

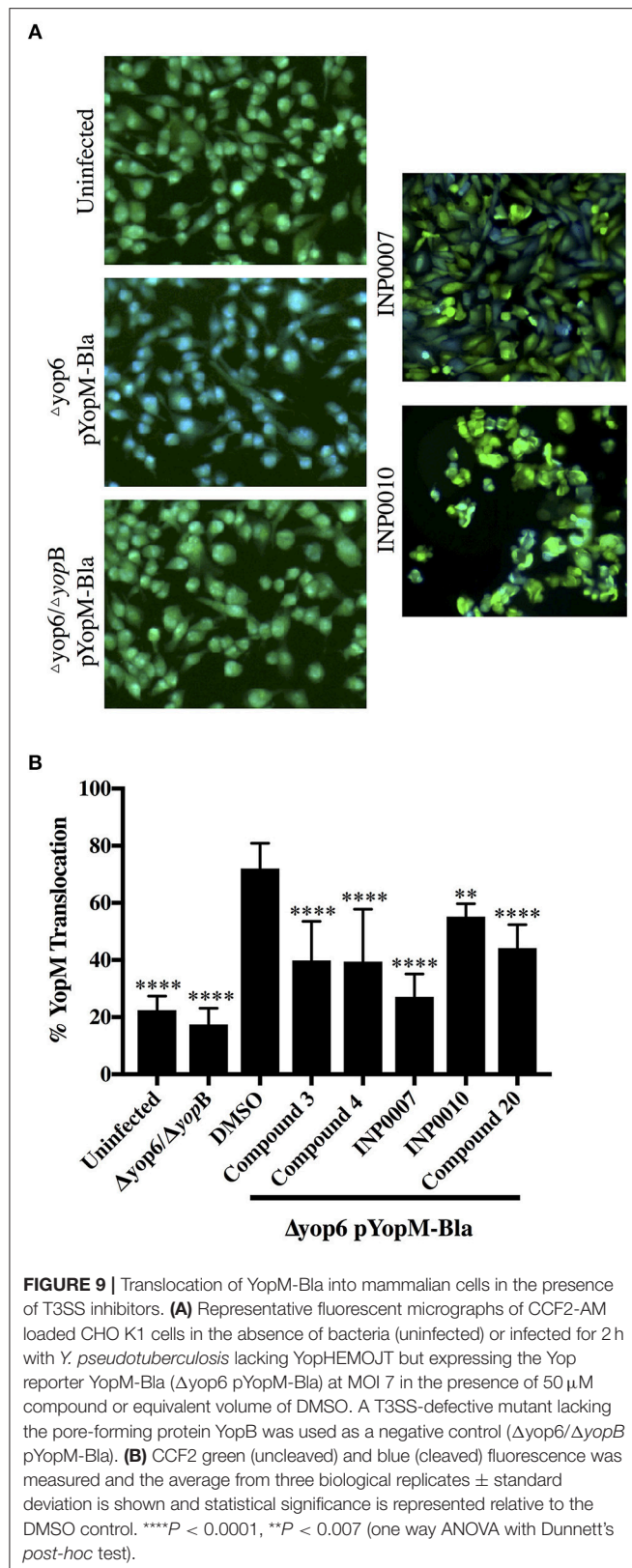
In contrast to C3, C20 specifically blocked translocation of a T3SS effector protein into host cells without blocking any other stage of type III secretion, including T3SS effector protein secretion into low calcium culture. As C20 was previously shown to inhibit only translocation of T3SS effector proteins into target host cells (Harmon et al., 2010), our verification of this finding further demonstrates the robustness of our experimental pipeline. Harmon et al. hypothesized that C20 inhibited the host cell-bacterial interaction, as C20 strongly inhibited adherence of *Y. pseudotuberculosis* to HEp-2 cells. Possible modes of action of compounds that inhibit Yop translocation but not any other stage of type III secretion include interruption of bacterial adhesins, host integrin receptors, or YopBD-mediated pore formation on the host membrane.

C4 was shown to inhibit promoter activity of *lcrF*, the Ysc T3SS master regulator (Kauppi et al., 2003). However, while we observed a C4-dependent decrease in mRNA levels of all T3SS genes tested under low calcium T3SS-inducing conditions, C4 treatment did not impact T3SS gene expression under high calcium conditions when T3SSs are assembled but no Yop secretion occurs. As a  $\Delta lcrF$  mutant had significantly less T3SS gene expression under high calcium conditions compared to wildtype *Yersinia*, this argues against C4 inhibiting LcrF activity. C4 did not alter the number of YscD puncta observed but did decrease the number of YscF puncta per cell by greater than half. These data suggest that C4 does not impact YscD assembly in the plasma membrane but disrupts overall T3SS basal body formation in such a way that needle

formation is compromised or interferes with YscF secretion or assembly.

The salicylidene acylhydrazides INP0007 and INP0010 inhibited expression of *lcrF*, *lcrV*, and *yopKEH*, but did not decrease expression of *yscN*, *yscD*, or *yscF*. While INP0007 and INP0010 are related structurally, INP0010 prevents *Yersinia* growth if the bacteria are exposed longer than 6 h, while INP0007 does not affect bacterial growth even up to 13 h of exposure. Surprisingly, while INP0010 did not inhibit YscD puncta formation, INP0007 caused a 10-fold decrease in YscD puncta. Both compounds significantly inhibited YscF puncta formation, Yop secretion into low calcium culture, and Yop translocation into host cells. However, measuring Yop translocation into host cells in the presence of INP0010 is complicated by the obvious toxic effects of the compound on host cells. Therefore, utilization of the Yop translocation assay of our experimental pipeline is limited to compounds without toxic effects on host cells. However, this also shows the benefit of using microscopy to observe CCF2 green-to-blue fluorescence conversion, as it allows observation of host cell morphology. The salicylidene acylhydrazide class of compounds have been suggested to have a broad impact on expression of horizontally acquired genes (Tree et al., 2009). However, we only observe a defect in T3SS gene expression in low calcium, but not high calcium medium, for INP0007. In addition, we observe a significant defect in flagellar motility by INP0007, suggesting a broader effect of the compound either on the flagellar T3SS, ATP synthesis, or the proton motive force. In total, our results argue that INP0007 inhibits formation of the injectisome T3SS and, either through a similar mechanism or by targeting multiple pathways, also disrupts flagellar T3SS activity. Therefore, we suggest that for T3SS inhibitors that block T3SS basal body assembly, a flagellar motility assay be performed to assess their breadth of action.

Given the previously-demonstrated positive feedback exerted by active type III secretion on T3SS gene transcription (Cornelis et al., 1987), we expected that C3 would inhibit T3SS gene



expression in low calcium medium. C4 and INP0007 inhibited YopE secretion by >70–80% and this correlated with the ability

to affect T3SS gene expression under low calcium conditions. C3 inhibited YopE secretion <50% and this was insufficient to impact the feedback loop on T3SS gene expression. Similarly, the T3SS inhibitor piericidin A1 inhibits YopE secretion by ~40–45% and also does not repress transcription of T3SS genes (Morgan et al., 2017). These data suggest that only compounds that potentially inhibit Yop secretion will affect the T3SS gene expression feedback loop. This indicates that screening strategies based on Yop gene expression as the readout for T3SS inhibition may miss less robust compounds that could be improved by structure-activity relationship analysis.

While none of the inhibitors we tested affected pYV copy number, our data shows that prevention of pYV plasmid copy number upregulation during active type III secretion leads to dramatically reduced T3SS gene mRNA steady-state levels. Therefore, when using *Yersinia* as a model organism for assessing T3SS inhibitor mechanism of action, it is important to consider pYV copy number. Furthermore, as chloramphenicol and rifampicin significantly inhibited luminescence as a readout of pYV copy number, this assay also sheds light on whether a compound affects general transcription or translocation. One caveat is that compounds that act as luminescence quenchers would decrease luminescence in this assay. In this case, analyzing expression of non-T3SS genes, such as the L9 and ErpA genes shown here, via qPCR can serve as a way to test this possibility.

In summary, we propose that the experimental pipeline described here can be used to rapidly bin T3SS inhibitors into categories depending on the stage of type III secretion they inhibit, providing testable hypotheses on mode of action. The commercially available training set shown here can be used to establish these assays in other labs and perhaps enable a more standardized approach to T3SS inhibitor research.

## AUTHOR CONTRIBUTIONS

JM: experimental design, performing experiments, writing paper; HL: experimental design, performing experiments; JD and JL: performing experiments; SM, RI, HW: providing reagents; VA: experimental design, writing paper.

## ACKNOWLEDGMENTS

We thank Benjamin Abrams of the UCSC Life Sciences Microscopy Center and Walter Bray of the UCSC Chemical Screening Center for technical support. We thank Andreas Diepold for providing the fluorescent YscD *Y. enterocolitica* strain. Research reported in this publication was supported by the National Institute of Allergy and Infectious Diseases of the National Institutes of Health under Award Numbers R01AI106930 and R01AI119082. JM was supported by the National Human Genome Research Institute of the National Institutes of Health under Award Number 4R25HG006836-04. RI was supported by NIAID R01AI110684. The content is solely the responsibility of the authors and does not necessarily represent the official views of the National Institutes of Health.



## REFERENCES

- Aiello, D., Williams, J. D., Majgier-Baranowska, H., Patel, I., Peet, N. P., Huang, J., et al. (2010). Discovery and characterization of inhibitors of *Pseudomonas aeruginosa* type III secretion. *Antimicrob. Agents Chemother.* 54, 1988–1999. doi: 10.1128/AAC.01598-09
- Anantharajah, A., Buyck, J. M., Sundin, C., Tulkens, P. M., Mingeot-Leclercq, M. P., and Van Bambeke, F. (2017). Salicylidene acylhydrazides and hydroxyquinolines act as inhibitors of type three secretion systems in *Pseudomonas aeruginosa* by distinct mechanisms. *Antimicrob. Agents Chemother.* 61:e02566-16. doi: 10.1128/AAC.02566-16
- Andersen, J. B., Sternberg, C., Poulsen, L. K., Bjorn, S. P., Givskov, M., and Molin, S. (1998). New unstable variants of green fluorescent protein for studies of transient gene expression in bacteria. *Appl. Environ. Microbiol.* 64, 2240–2246.
- Auerbuch, V., Golenbock, D. T., and Isberg, R. R. (2009). Innate immune recognition of *Yersinia pseudotuberculosis* type III secretion. *PLoS Pathog.* 5:e1000686. doi: 10.1371/journal.ppat.1000686
- Beckham, K. S., and Roe, A. J. (2014). From screen to target: Insights and approaches for the development of anti-virulence compounds. *Front. Cell. Infect. Microbiol.* 4:139. doi: 10.3389/fcimb.2014.00139
- Bergeron, J., Worrall, L., Sgourakis, N., DiMaio, F., Pfuetzner, R., Felise, H., et al. (2013). A refined model of the prototypical *Salmonella* spi-1 t3ss basal body reveals the molecular basis for its assembly. *PLoS Pathog.* 9:e1003307. doi: 10.1371/journal.ppat.1003307
- Berube, B. J., Murphy, K. R., Torhan, M. C., Bowlin, N. O., Williams, J. D., Bowlin, T. L., et al. (2017). Impact of type III secretion effectors and of phenoxycetamide inhibitors of type III secretion on abscess formation in a mouse model of *Pseudomonas aeruginosa* infection. *Antimicrob. Agents Chemother.* 61:e01202-17. doi: 10.1128/AAC.01202-17
- Bliska, J. B., Guan, K. L., Dixon, J. E., and Falkow, S. (1991). Tyrosine phosphate hydrolysis of host proteins by an essential *Yersinia* virulence determinant. *Proc. Natl. Acad. Sci. USA.* 88, 1187–1191.
- Bowlin, N. O., Williams, J. D., Knoten, C. A., Torhan, M. C., Tashjian, T. F., Li, B., et al. (2014). Mutations in the *Pseudomonas aeruginosa* needle protein gene *pscF* confer resistance to phenoxycetamide inhibitors of the type III secretion system. *Antimicrob. Agents Chemother.* 58, 2211–2220. doi: 10.1128/AAC.02795-13
- Broz, P., Müller, C. A., Müller, S. A., Philippsen, A., Sorg, I., Engel, A., et al. (2007). Function and molecular architecture of the *Yersinia* injectisome tip complex. *Mol. Microbiol.* 65, 1311–1320. doi: 10.1111/j.1365-2958.2007.05871.x
- Büttner, D., and Bonas, U. (2002). Port of entry—the type III secretion translocon. *Trends Microbiol.* 10, 186–192. doi: 10.1016/S0966-842X(02)02331-4
- Coburn, B., Sekirov, I., and Finlay, B. (2007). Type III secretion systems and disease. *Clin. Microbiol. Rev.* 20, 535–549. doi: 10.1128/CMR.00013-07
- Cornelis, G., Vanootegeem, J. C., and Sluiter, C. (1987). Transcription of the yop regulon from *Y. enterocolitica* requires trans acting pYV and chromosomal genes. *Microb. Pathog.* 2, 367–379.
- Davis, A., and Mecsas, J. (2007). Mutations in the *Yersinia pseudotuberculosis* type III secretion system needle protein, *yscF*, that specifically abrogate effector translocation into host cells. *J. Bacteriol.* 189, 83–97. doi: 10.1128/JB.01396-06
- Deng, W., Marshall, N. C., Rowland, J. L., McCoy, J. M., Worrall, L. J., Santos, A. S., et al. (2017). Assembly, structure, function and regulation of type III secretion systems. *Nat. Rev. Microbiol.* 15, 323–337. doi: 10.1038/nrmicro.2017.20
- Dewoody, R., Merritt, P. M., Houppert, A. S., and Marketon, M. M. (2011). YopK regulates the *Yersinia pestis* type III secretion system from within host cells. *Mol. Microbiol.* 79, 1445–1461. doi: 10.1111/j.1365-2958.2011.07534.x
- Diepold, A., Amstutz, M., Abel, S., Sorg, I., Jenal, U., and Cornelis, G. R. (2010). Deciphering the assembly of the yersinia type III secretion injectisome. *EMBO J.* 29, 1928–1940. doi: 10.1038/emboj.2010.84
- Duncan, M. C., Linington, R. G., and Auerbuch, V. (2012). Chemical inhibitors of the type three secretion system: disarming bacterial pathogens. *Antimicrob. Agents Chemother.* 56(11):5433–5441. doi: 10.1128/AAC.00975-12
- Duncan, M. C., Wong, W. R., Dupzyk, A. J., Bray, W. M., Linington, R. G., and Auerbuch, V. (2014). An nF-κB-based high-throughput screen identifies piericidins as inhibitors of the *Yersinia pseudotuberculosis* type III secretion system. *Antimicrob. Agents Chemother.* 58, 1118–1126. doi: 10.1128/AAC.02025-13
- Fahlgren, A., Avican, K., Westermark, L., Nordfelth, R., and Fällman, M. (2014). Colonization of cecum is important for development of persistent infection by *Yersinia pseudotuberculosis*. *Infect. Immun.* 82, 3471–3482. doi: 10.1128/IAI.01793-14
- Forsberg, A., and Wolf-Watz, H. (1988). The virulence protein yop5 of *Yersinia pseudotuberculosis* is regulated at transcriptional level by plasmid-plb1 - encoded trans-acting elements controlled by temperature and calcium. *Mol. Microbiol.* 2, 121–133.
- Francis, M. S., Wolf-Watz, H., and Forsberg, A. (2002). Regulation of type III secretion systems. *Curr. Opin. Microbiol.* 5, 166–172. doi: 10.1016/S1369-5274(02)00301-6
- Green, E. R., Clark, S., Crimmins, G. T., Mack, M., Kumamoto, C. A., and Mecsas, J. (2016). Fis is essential for *Yersinia pseudotuberculosis* virulence and protects against reactive oxygen species produced by phagocytic cells during infection. *PLoS Pathog.* 12:e1005898. doi: 10.1371/journal.ppat.1005898
- Harmon, D. E., Davis, A. J., Castillo, C., and Mecsas, J. (2010). Identification and characterization of small-molecule inhibitors of yop translocation in *Yersinia pseudotuberculosis*. *Antimicrob. Agents Chemother.* 54, 3241–3254. doi: 10.1128/AAC.00364-10
- Heroven, A. K., Böhme, K., and Dersch, P. (2012). The Csr/Rsm system of *Yersinia* and related pathogens: a post-transcriptional strategy for managing virulence. *RNA Biol.* 9, 379–391. doi: 10.4161/rna.19333
- Horton, R. M., Cai, Z. L., Ho, S. N., and Pease, L. R. (1990). Gene splicing by overlap extension: tailor-made genes using the polymerase chain reaction. *BioTechniques* 8, 528–535.
- Karzai, A. W., Roche, E. D., and Sauer, R. T. (2000). The *ssrA-smpB* system for protein tagging, directed degradation and ribosome rescue. *Nat. Struct. Biol.* 7, 449–455. doi: 10.1038/75843
- Kauppi, A. M., Nordfelth, R., Uvell, H., Wolf-Watz, H., and Elofsson, M. (2003). Targeting bacterial virulence: inhibitors of type III secretion in *Yersinia*. *Chem. Biol.* 10, 241–249. doi: 10.1016/S1074-5521(03)00046-2
- Lee, V. T., Pukatzki, S., Sato, H., Kikawada, E., Kazimirova, A. A., Huang, J., et al. (2007). Pseudolipase A is a specific inhibitor for phospholipase A2 activity of *Pseudomonas aeruginosa* cytotoxin exoU. *Infect. Immun.* 75, 1089–1098. doi: 10.1128/IAI.01184-06
- Macnab, R. M. (2004). Type III flagellar protein export and flagellar assembly. *Biochim. Biophys. Acta.* 1694, 207–217. doi: 10.1016/j.bbamcr.2004.04.005
- Marsden, A. E., King, J. M., Spies, M. A., Kim, O. K., and Yahr, T. L. (2015). Inhibition of *Pseudomonas aeruginosa* ExsA DNA binding activity by H-hydroxybenzimidazoles. *Antimicrob. Agents Chemother.* 60, 766–776. doi: 10.1128/AAC.02242-15
- Marshall, N. C., and Finlay, B. B. (2014). Targeting the type III secretion system to treat bacterial infections. *Expert Opin. Ther. Targets* 18, 137–152. doi: 10.1517/14728222.2014.855199
- Mehigh, R. J., Sample, A. K., and Brubaker, R. R. (1989). Expression of the low calcium response in *Yersinia pestis*. *Microb. Pathog.* 6, 203–217. doi: 10.1016/0882-4010(89)90070-3
- Merriam, J. J., Mathur, R., Maxfield-Boumil, R., and Isberg, R. R. (1997). Analysis of the *Legionella pneumophila* *fljI* gene: intracellular growth of a defined mutant defective for flagellum biosynthesis. *Infect. Immun.* 65, 2497–2501.
- Miller, H. K., Kwuan, L., Schwiesow, L., Bernick, D. L., Metttert, E., Ramirez, H. A., et al. (2014). IscR is essential for *Yersinia pseudotuberculosis* type III secretion and virulence. *PLoS Pathog.* 10:e1004194. doi: 10.1371/journal.ppat.1004194
- Morgan, J. M., Duncan, M. C., Johnson, K. S., Diepold, A., Lam, H., Dupzyk, A. J., et al. (2017). Piericidin A1 blocks *Yersinia* ysc type III secretion system needle assembly. *mSphere* 2:e00030-17. doi: 10.1128/mSphere.00030-17
- Negrea, A., Bjur, E., Ygberg, S. E., Elofsson, M., Wolf-Watz, H., and Rhen, M. (2007). Salicylidene acylhydrazides that affect type III protein secretion in *Salmonella enterica* serovar typhimurium. *Antimicrob. Agents Chemother.* 51, 2867–2876. doi: 10.1128/AAC.00223-07
- Nordfelth, R., Kauppi, A. M., Norberg, H. A., Wolf-Watz, H., and Elofsson, M. (2005). Small-molecule inhibitors specifically targeting type III secretion. *Infect. Immun.* 73, 3104–3114. doi: 10.1128/IAI.73.5.3104-3114.2005
- O'Callaghan, C. H., Morris, A., Kirby, S. M., and Shingler, A. H. (1972). Novel method for detection of beta-lactamases by using a chromogenic cephalosporin substrate. *Antimicrob. Agents Chemother.* 1, 283–288. doi: 10.1128/AAC.1.4.283



- Perry, R. D., Harmon, P. A., Bowmer, W. S., and Straley, S. C. (1986). A low- $\text{Ca}^{2+}$  response operon encodes the V antigen of *Yersinia pestis*. *Infect. Immun.* 54, 428–434.
- Pettersson, J., Nordfelth, R., Dubinina, E., Bergman, T., Gustafsson, M., Magnusson, K. E., et al. (1996). Modulation of virulence factor expression by pathogen target cell contact. *Science* 273, 1231–1233.
- Portnoy, D. A., Moseley, S. L., and Falkow, S. (1981). Characterization of plasmids and plasmid-associated determinants of *Yersinia enterocolitica* pathogenesis. *Infect. Immun.* 31, 775–782.
- Rosqvist, R., Magnusson, K. E., and Wolf-Watz, H. (1994). Target cell contact triggers expression and polarized transfer of *Yersinia* yopE cytotoxin into mammalian cells. *EMBO J.* 13, 964–972.
- Sample, A. K., Fowler, J. M., and Brubaker, R. R. (1987). Modulation of the low-calcium response in *Yersinia pestis* via plasmid-plasmid interaction. *Microb. Pathog.* 2, 443–453. doi: 10.1016/0882-4010(87)90051-9
- Schwiesow, L., Lam, H., Dersch, P., and Auerbuch, V. (2015). *Yersinia* type III secretion system master regulator LcrF. *J. Bacteriol.* 198, 604–614. doi: 10.1128/JB.00686-15
- Skinner, S. O., Sepúlveda, L. A., Xu, H., and Golding, I. (2013). Measuring mRNA copy number in individual *Escherichia coli* cells using single-molecule fluorescent *in situ* hybridization. *Nat. Protoc.* 8, 1100–1113. doi: 10.1038/nprot.2013.066
- Straley, S. C., and Bowmer, W. S. (1986). Virulence genes regulated at the transcriptional level by  $\text{Ca}^{2+}$  in *Yersinia pestis* include structural genes for outer membrane proteins. *Infect. Immun.* 51, 445–454.
- Tree, J. J., Wang, D., McNally, C., Mahajan, A., Layton, A., Houghton, I., et al. (2009). Characterization of the effects of salicylidene acylhydrazide compounds on type III secretion in *Escherichia coli* o157:H7. *Infect. Immun.* 77, 4209–4220. doi: 10.1128/IAI.00562-09
- Veenendaal, A. K., Sundin, C., and Blocker, A. J. (2009). Small-molecule type III secretion system inhibitors block assembly of the *Shigella* type III secretin. *J. Bacteriol.* 191, 563–570. doi: 10.1128/JB.01004-08
- Wang, H., Avican, K., Fahlgren, A., Erttmann, S. F., Nuss, A. M., Dersch, P., et al. (2016). Increased plasmid copy number is essential for *Yersinia* T3SS function and virulence. *Science* 353, 492–495. doi: 10.1126/science.1235011
- Wilhelm, G., Lehmann, V., Krauss, K., Lehnert, B., Richter, S., Ruckdeschel, K., et al. (2004). *Yersinia enterocolitica* type III secretion depends on the proton motive force but not on the flagellar motor components motA and motB. *Infect. Immun.* 72, 4004–4009. doi: 10.1128/IAI.72.7.4004-4009.2004
- Yother, J., and Goguen, J. D. (1985). Isolation and characterization of  $\text{Ca}^{2+}$ -blind mutants of *Yersinia pestis*. *J. Bacteriol.* 164, 704–711.

**Conflict of Interest Statement:** The authors declare that the research was conducted in the absence of any commercial or financial relationships that could be construed as a potential conflict of interest.

Copyright © 2018 Morgan, Lam, Delgado, Luu, Mohammadi, Isberg, Wang and Auerbuch. This is an open-access article distributed under the terms of the Creative Commons Attribution License (CC BY). The use, distribution or reproduction in other forums is permitted, provided the original author(s) and the copyright owner(s) are credited and that the original publication in this journal is cited, in accordance with accepted academic practice. No use, distribution or reproduction is permitted which does not comply with these terms.



# Discovering RNA-Based Regulatory Systems for *Yersinia* Virulence

Vanessa Knittel<sup>†</sup>, Ines Vollmer<sup>†</sup>, Marcel Volk<sup>†</sup> and Petra Dersch<sup>\*</sup>

Department of Molecular Infection Biology, Helmholtz Centre for Infection Research, Braunschweig, Germany

## OPEN ACCESS

### Edited by:

Matthew S. Francis,  
Umeå University, Sweden

### Reviewed by:

Kai Papenfort,  
Ludwig-Maximilians-Universität  
München, Germany  
Satish Raina,  
Gdansk University of Technology,  
Poland

Erik Holmqvist,  
Uppsala University, Sweden

### \*Correspondence:

Petra Dersch  
petra.dersch@helmholtz-hzi.de

<sup>†</sup>These authors have contributed  
equally to this work

### Specialty section:

This article was submitted to  
Molecular Bacterial Pathogenesis,  
a section of the journal  
Frontiers in Cellular and Infection  
Microbiology

**Received:** 31 July 2018

**Accepted:** 05 October 2018

**Published:** 25 October 2018

### Citation:

Knittel V, Vollmer I, Volk M and  
Dersch P (2018) Discovering  
RNA-Based Regulatory Systems for  
*Yersinia* Virulence.  
Front. Cell. Infect. Microbiol. 8:378.  
doi: 10.3389/fcimb.2018.00378

The genus *Yersinia* includes three human pathogenic species, *Yersinia pestis*, the causative agent of the bubonic and pneumonic plague, and enteric pathogens *Y. enterocolitica* and *Y. pseudotuberculosis* that cause a number of gut-associated diseases. Over the past years a large repertoire of RNA-based regulatory systems has been discovered in these pathogens using different RNA-seq based approaches. Among them are several conserved or species-specific RNA-binding proteins, regulatory and sensory RNAs as well as various RNA-degrading enzymes. Many of them were shown to control the expression of important virulence-relevant factors and have a very strong impact on *Yersinia* virulence. The precise targets, the molecular mechanism and their role for *Yersinia* pathogenicity is only known for a small subset of identified genus- or species-specific RNA-based control elements. However, the ongoing development of new RNA-seq based methods and data analysis methods to investigate the synthesis, composition, translation, decay, and modification of RNAs in the bacterial cell will help us to generate a more comprehensive view of *Yersinia* RNA biology in the near future.

**Keywords:** RNA thermometer, RNA stability, RNA processing, Csr/Rsm system, virulence, gene regulation, small regulatory RNAs

## INTRODUCTION

For a long time it was thought that the RNA make-up and biology of bacteria is rather simple and constitutes mainly of mRNAs, tRNAs, and rRNAs and a few specific RNAs such as the tmRNA/SsrA of the ribosome rescue system. However, over the past 10 years, research on bacterial RNA molecules has proven this to be incorrect, since bacteria possess a huge variety of RNAs. A large repertoire of *cis*- and *trans*-acting non-coding RNAs has been identified and a plethora of different RNA-based regulatory mechanisms and functions has been unveiled mainly in *Enterobacteriaceae*, but lately also in many other prokaryotes. This showed that RNA-based gene expression control is highly complex and global, and almost as diverse and multifarious as transcriptional control. Multiple structured RNA elements have been identified in the 5'-untranslated regions of mRNAs sensing temperatures (RNA thermometers) or metabolites (riboswitches) in order to modulate mRNA translation and/or stability (Kortmann and Narberhaus, 2012; Sherwood and Henkin, 2016; McCown et al., 2017). Moreover, a remarkably large number of small regulatory RNAs (sRNAs) exist in bacteria (i.e., 200–300 in *Enterobacteriaceae*, Barquist and Vogel, 2015; Nuss et al., 2015), which control mRNA expression and decay often in concert with RNA-binding proteins. Among the most prominent RNA-binding proteins are the RNA chaperone Hfq and the carbon storage regulator (Csr) protein CsrA, as well as RNases. Clever variations of different global RNA-sequencing (RNA-seq)-based techniques (Figure 1) used to define the overall RNA-protein interactome and the sRNA-target networks demonstrated that almost 50% of the bacterial mRNAs are subjected to sRNA-mediated regulation (Melamed et al., 2016; Hör and Vogel, 2017; Waters et al., 2017).

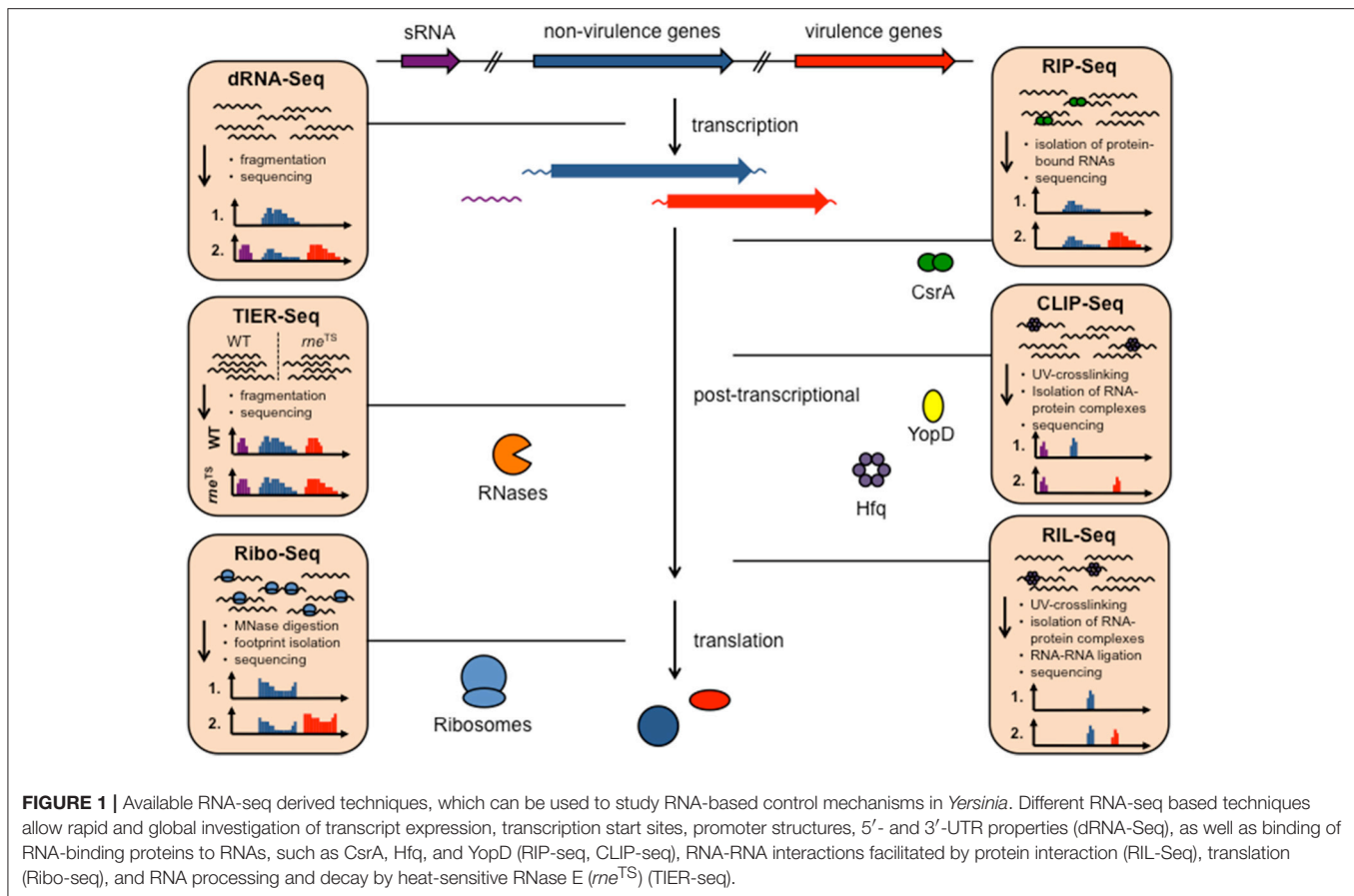
The global analysis of RNA-based control strategies of virulence genes was started with a relatively small number of model bacteria. This included human pathogenic *Yersinia* species, such as *Y. pestis*, the causative agent of bubonic plague and the two enteric pathogens *Y. pseudotuberculosis* and *Y. enterocolitica* causing gut-associated diseases (Yersiniosis), i.e., ranging from enteritis, watery diarrhea, mesenteric lymphadenitis to post-infectious extraintestinal sequelae (Bottone, 1997; Koornhof et al., 1999; Smego et al., 1999; Valentin-Weigand et al., 2014). System level RNA-seq has the advantage that the entire transcriptome of an organism with all included RNA functions can be studied in a cellular and particular environmental (e.g., infection, virulence conditions) context. This allowed a single-nucleotide resolution and a dynamic view of the pathogen's gene expression, which are summarized and discussed in the present review. The establishment of comprehensive RNA maps of *Y. pseudotuberculosis* highlighted not only the breadth and large variety of RNA species, it also revealed new species-specific and conserved principles of RNA-based, post-transcriptional control strategies that contribute to the dynamic, spatial, and fine-tuned control of bacterial pathogenicity.

## GLOBAL TRANSCRIPTIONAL ANALYSIS TO ELUCIDATE FITNESS-RELEVANT TRAITS OF *YERSINIA*

In order to understand how the functional status of *Yersinia* is modulated in response to environmental conditions sensed outside or inside their hosts, detailed knowledge about the bacterial gene expression profile in different surroundings is required. RNA-seq is extremely well-suited for this task due to the high sensibility, high resolution and the possibility for high-throughput analysis of multiple *in vitro* and *in vivo* conditions (Kröger et al., 2013; Nuss et al., 2015, 2017a; Figures 1, 2). In particular transition from exponential to stationary phase and shifts from moderate temperatures to 37°C, mimicking host entry, were found to induce reprogramming of a large set of virulence genes. This includes colonization factors and immune defense mechanisms, encoded on the chromosome and the virulence plasmid, but also many catabolic/energy production genes. For instance, this uncovered the existence of a thermo-regulated “acetate switch,” which seems to prime the bacteria for growth in the digestive tract. This physiological switch occurs when bacteria shift from rapid growth in which they produce acetate from acetogenic carbon sources, e.g., glucose, to a metabolic program of slower growth, which is facilitated by the import and utilization of acetate (Nuss et al., 2015). This is accompanied by a thermo-induced up-regulation of multiple transport and catabolic genes for simple sugars. As the mammalian intestine is rich in short-chain fatty acids, in particular acetate, produced by the intestinal microbiota through consumption of available polysaccharides from diet and host-derived mucus (Cummings and Macfarlane, 1997), flipping the switch may facilitate utilization of these microbiota-derived degradation products.

The RNA-seq approach also allowed us to elucidate the regulatory architecture linking nutritional status to virulence. We identified a massive remodeling of the CRP-controlled network in response to temperature and discovered CRP as a transcriptional master regulator of numerous conserved and newly identified non-coding RNAs which participate in this process (Nuss et al., 2015). This finding highlighted a new level of complexity of the regulatory network in *Yersinia*. The concerted action of several transcriptional regulators and multiple non-coding RNAs controlled by CRP adjusts *Yersinia* fitness and virulence to the requirements of their environmental and virulent life-styles. This discovery showed that CRP is an integral component of a regulatory network that controls life-style switching and highlighted the power of comparative RNA-seq analysis.

Parallel analysis of the transcriptomes of *Y. pseudotuberculosis* during mouse infection (Tissue Dual RNA-seq, Figure 2) has further allowed us to study host-pathogen interaction. It enabled us to correlate gene expression changes of the pathogen with those occurring in the host and revealed genes and regulatory RNAs that are predominantly expressed or repressed during the infection (Avican et al., 2015; Nuss et al., 2015, 2017a). Numerous alterations of host transcripts associated with IL-6-triggered inflammatory and acute phase responses (Mmp8 induction), coagulative activities, metal ion sequestration, tissue repair and damage highlighted that the immune response in the gut-associated lymphoid follicles (Peyer's patches) upon a *Y. pseudotuberculosis* infection is dominated by infiltration of neutrophils and dendritic cells, and elicits a mixed T<sub>H</sub>1/T<sub>H</sub>17 response (Nuss et al., 2017a; Heine et al., 2018). In response, *Yersinia* increases the gene and expression dose of the virulence plasmid-encoded Ysc type III secretion system (T3SS) and the anti-phagocytic Yop effector proteins (Yops) to prevent the phagocytic attack. In addition, the bacteria induce high-affine ion (Fe<sup>2+</sup> and Zn<sup>2+</sup>) sequestration systems, diverse stress response, and nutrient uptake systems to counteract ion deprivation, radical/oxidative stress, anti-microbial peptides, and nutrient restraints (Nuss et al., 2017a). Tissue Dual RNA-seq further showed that the outcome of the observed pathogen-host interactions could vary significantly when expression of certain pathogenicity factors is reduced or abrogated. The cytotoxic necrotizing factor Y (CNF<sub>Y</sub>) expressed by some *Y. pseudotuberculosis* strains, e.g., YPIII and IP2666, is one of these factors. Suppression of CNF<sub>Y</sub> triggers interferon-γ mediated responses fostering non-inflammatory bactericidal activities. Moreover, it promotes Ido1- and Arg1-mediated T<sub>regs</sub> activation and proliferation and other immune suppressing and tolerogenic mechanisms that avoid systemic inflammation, prevent tissue destruction and drive this *Y. pseudotuberculosis* strain into persistency (Heine et al., 2018). This process is accompanied by a preterm reprogramming of the pathogen's transcriptome. Anaerobic and multiple acid and oxidative stress resistance genes (e.g., *arcA*, *fnr*, *frdA*, and *wrbA*) are already induced in the acute phase. It is assumed that this priming gives the bacteria a fitness edge against the host immune defense and facilitates establishment of a persistent microbiota-type life style (Heine et al., 2018). In parallel, the expression profile of many virulence genes changes toward a pattern seen at



moderate temperature under *in vitro* growth conditions. Up-regulation of flagella and adhesion/invasion genes (e.g., *invA*) was observed during the establishment of persistence, whereas genes encoding important components of the T3SS and the Yops were down-regulated. This is accompanied by a change in the expression of the transcription factors of the Crp-CsrA-RovM-RovA regulatory cascade, indicating that these control factors determine the expression switch (Avican et al., 2015; Heine et al., 2018). Our findings suggest a life-style model for *Y. pseudotuberculosis* in which the bacteria change their gene expression profile from a virulent to an adapted phenotype, capable of persisting and spreading by fecal shedding. This further illustrates that the developed Tissue Dual RNA-seq approach is well suited to decipher the complexity of host-pathogen interactions during different stages of the infection. The comparative analysis between different strain isolates or mutants of potential virulence-relevant factors and regulators will help to decipher the complex interplay between of *Y. pseudotuberculosis* and the host response within distinct host niches.

## ANNOTATION AND CHARACTERIZATION OF *YERSINIA* TRANSCRIPTS

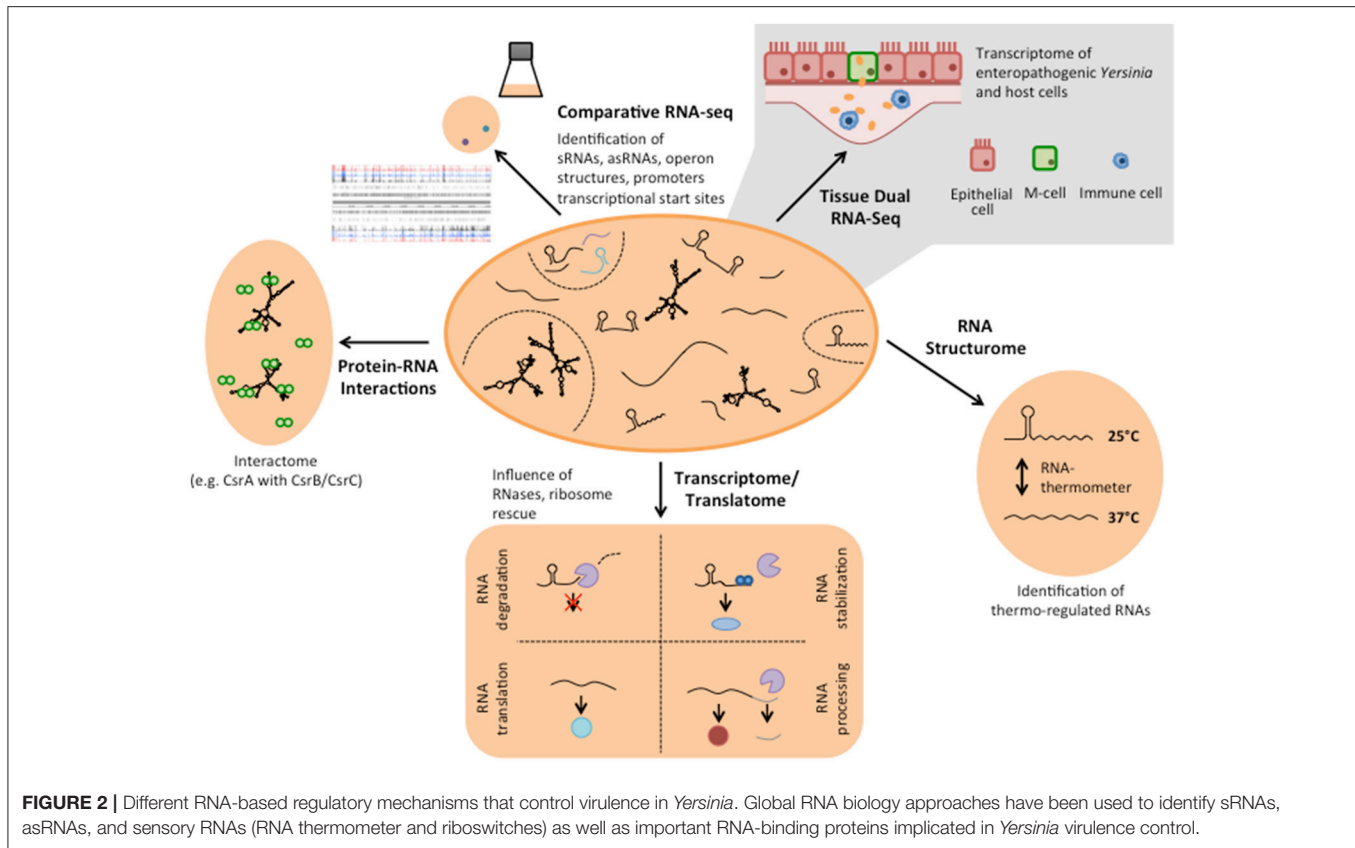
Since RNA-seq provided a single-nucleotide resolution transcriptional landscape of *Y. pseudotuberculosis*, it was

used to map all genes of the chromosome and virulence plasmid (Nuss et al., 2015, 2017a; **Figure 2**). This led to the identification of new, so far not annotated and previously overlooked open reading frames (ORFs) and revealed a large set of antisense RNAs and small *cis*- and *trans*-encoded regulatory RNAs (Koo et al., 2011; Nuss et al., 2015, 2017a). Some of the identified antisense RNAs are long and cover whole genes or multiple genes of the virulence plasmid (Nuss et al., 2015). However, their individual impact on gene expression is still unclear. Moreover, certain variations of the RNA-seq protocols (e.g., treatment of the RNA with the terminator 5'-phosphate-dependent exonuclease short TEX), led to an enrichment of primary transcripts with 5'-triphosphate ends. Comparative analysis between the transcriptomes obtained with or without TEX treatment, called differential RNA-seq (dRNA-seq, Sharma and Vogel, 2014, **Figures 1, 2**), allowed global mapping of the transcription start sites of all transcripts. This led to the identification of promoter elements and the definition of operon structures, and improved the annotation of the *Yersinia* genome and virulence plasmid (Nuss et al., 2015).

## THE *YERSINIA* RNA STRUCTUROME

In contrast to double-stranded DNA, RNA is a single-stranded molecule. However, it can undergo significant intramolecular





base-pairing to take in an individual three-dimensional structure. It is known for quite some time that the intrinsic structure of an RNA impacts many cellular processes, most frequently by modulating its translation and/or decay. Protein synthesis is mainly affected by RNA structures, which influence the accessibility of the ribosome binding site (RBS). Based on the whole-genome transcriptomics study of *Y. pseudotuberculosis* several potential *cis*-regulatory RNA elements have been identified in long 5'-untranslated regions (5'-UTRs; >200 nt) of virulence, stress adaptation and metabolic genes in *Y. pseudotuberculosis* (Nuss et al., 2015). A bioinformatics approach identified 19 riboswitch-like elements (RLEs) among the long 5'-UTRs. Riboswitches are complex RNA structures that undergo structural changes in response to binding of small molecules, typically metabolites or ions, altering the expression of their downstream gene on the transcriptional or post-transcriptional level (Breaker, 2011; Serganov and Nudler, 2013). These features make them ideal to sense small molecule concentrations, e.g., nutrient and ion availability. Five of these RLEs showed features homologous to the threonine operon leader, the Moco (Molybdenum cofactor biosynthesis), FMN and the cobalamin riboswitch of *E. coli* and a cation-responsive riboswitch upstream of an  $Mg^{2+}$  transporter gene (*corA*) similar to *mgtA* of *Salmonella* (Nuss et al., 2015). However, the function of the majority of the riboswitch-like elements remains uncovered.

Structural alteration of a sensory RNA segment can also be triggered by temperature shifts. For instance, a thermo-controlled melting process of a double-stranded region, like a molecular zipper, is used to modulate gene expression of several bacterial heat shock and virulence-relevant genes (Kortmann and Narberhaus, 2012). One of these thermo-sensitive RNA elements (RNA thermometer) was identified upstream of *lcrF* (Table 1), the virulence plasmid-encoding gene for the master regulator of the T3SS/Yop machinery. The *lcrF* RNA thermometer is highly conserved between the human pathogenic *Yersinia* species and consists of a two stem-loop structure of which the second hairpin sequesters and hides the ribosome binding site (RBS) within its stem region at moderate temperatures (20–30°C). Elevated temperatures (37°C) lead to partial unfolding of the stem-loop, which renders the RBS accessible for the small subunit of the ribosome, leading to translation initiation (Hoe and Goguen, 1993; Böhme et al., 2012).

To investigate whether additional RNA thermometers or thermo-sensitive RNA elements are encoded on the *Y. pseudotuberculosis* genome, a structure RNA profile was recently generated of an entire transcriptome (Figure 2). For this purpose total RNA of the bacteria were isolated, incubated at 25, 37, and 42°C, and subsequently treated with single-strand and double-strand specific RNases. RNA-seq analysis of the resulting RNA fragments (PARS: parallel analysis of RNA structures) from 1,750 transcripts identified numerous

temperature-sensitive RNAs (Rhigetti et al., 2016). This revealed that the RNA structurome of this pathogen is highly dynamic and encodes many more RNA thermometers. In total, 16 new RNA thermometers were discovered in 5'-UTRs of metabolic, heat stress, and virulence-relevant genes. Among them are many oxidative stress genes (*sodA*, *sodB*, *sodC*, and *katA*), and two very important virulence genes, encoding the cell adhesion and invasion factor Ail, contributing to host cell colonization and host resistance, and the CNF $\gamma$  toxin, triggering host tissue inflammation and damage (Rhigetti et al., 2016; **Table 1**). Besides the putative RNA thermometer, several small regulatory RNAs and tRNAs were also shown to be thermo-sensitive in this study. It will be interesting to investigate whether they promote and/or participate in the thermo-regulation of their target mRNA(s), and whether they are exploited by the pathogen to modify bacterial metabolism, physiology or pathogenicity upon entering a warm-blooded host, similar to the RNA thermometers.

## CONTROL BY REGULATORY RNAs

Small regulatory RNAs (sRNAs) are central regulators that play an essential role in various physiological and virulence associated processes in bacteria (Papenfort and Vogel, 2010, 2014; Heroven et al., 2017; Quereda and Cossart, 2017; Westermann, 2018). sRNAs are involved in the fine-tuning of these processes, allowing a rapid adaptation of pathogens to new environments. They have unique regulatory characteristics and control target gene expression post-transcriptionally through base-pairing with their transcripts. Such interaction can alter translation initiation or mRNA stability (Fröhlich and Vogel, 2009; Storz et al., 2011; Gorski et al., 2017). Functional analysis of sRNAs in different microorganisms revealed that often several sRNAs are part of the same regulatory cascade and sRNA-target network. This network typically includes multiple feedback loops and mixed regulatory circuits, illustrating the true complexity of RNA-based control system (Nitzan et al., 2017; Hör et al., 2018).

A myriad of sRNAs have been identified in the human pathogenic *Yersinia* species in independent high-throughput RNA-seq studies and are mainly referred to as Ysr (*Yersinia* small RNAs) (Koo et al., 2011; Koo and Lathem, 2012; Qu et al., 2012; Beauregard et al., 2013; Yan et al., 2013; Nuss et al., 2015, 2017a). The Ysrs are presumed *Yersinia*-specific sRNAs that were identified in an sRNA search in *Y. pseudotuberculosis* (Koo et al., 2011). A detailed list and the characteristics of these sRNAs are summarized in two recent reviews (Martínez-Chavarría and Vadyvaloo, 2015; Nuss et al., 2017b) (**Figure 2**, **Table 1**). Two aspects that are particularly striking are that (i) many sRNAs are directly regulated by the cAMP receptor protein (Crp) in response to growth phase and temperature, and that (ii) the majority of sRNAs are specific for *Yersinia*. This indicates that they are important players for the biological fitness and adaptation in their individual environmental and host niches, and reservoirs. A drawback of the latter feature is that most bioinformatic algorithms to identify potential targets of sRNAs rely on comparative genomics, i.e., functional and network analysis depending on sequence conservation between

species (Wright et al., 2013), and are thus not suitable for the analysis of most Ysr sRNAs. Consequently, very little information is available about their molecular function and role for the pathogen. Nonetheless, the RNA chaperone Hfq, which mediates annealing of many sRNAs to their target mRNAs and protects them from ribonuclease cleavage or facilitates sRNA turnover or activity, was found to be required for virulence (**Table 1**). An *hfq* mutant of *Y. pestis* is impaired in its ability to resist phagocytosis and survive within macrophages at the initial stage of infection, and is highly attenuated in mice after subcutaneous or intravenous injection (Geng et al., 2009). Moreover, Hfq was found to regulate biofilm gut blockage that facilitates flea-borne transmission of *Y. pestis* (Rempe et al., 2012). Hfq of *Y. pseudotuberculosis* and *Y. enterocolitica* modulates the expression of multiple virulence-relevant cell surface structures such as adhesins/invasins (e.g., Ail, OmpX, MyfA pili, YadA, InvA) and expression of the T3SS/*yop* genes (Schiano et al., 2010, 2014; Schiano and Lathem, 2012; Kakoschke et al., 2014, 2016). Moreover, several Hfq-dependent alterations in the lipid A structure, motility, and biofilm formation defects, and changes in outer membrane vesicle synthesis were identified, which also impact virulence (Eddy et al., 2014; Leskinen et al., 2017). This strongly indicates that Hfq acts by controlling the expression of virulence-associated genes, probably in conjunction with small non-coding RNAs. However, up to now only very little is known about virulence-associated sRNAs and whether they are Hfq-dependent.

An initial analysis with a few Ysr sRNAs showed that Ysr29, Ysr35, and Ysr141 seem to play a role in pathogenesis (Koo et al., 2011; Schiano et al., 2014; **Table 1**). The specific target of Ysr35 remains unknown, but expression of multiple proteins was found to be affected in an *ysr35* mutant. Among them are several general stress response factors such as the chaperones GroEL and DnaK, the peroxidase AhpC, the translational factors S1 (RpsA) and the ribosome recycling factor Rrf (Koo et al., 2011). The virulence plasmid-encoded sRNA Ysr141 was found to enhance the synthesis of LcrF and many effector proteins (YopJ, YopE, YopK, YpkA), whereby only a direct influence of Ysr141 on YopJ translation was documented (Schiano et al., 2014). Recent work has also identified multiple sRNAs of *Y. pestis*, which are upregulated within macrophages. Among them is Ysr170, which was shown to be important for intracellular replication (Li et al., 2016). Much more is known about conserved sRNAs and their impact on pathogenicity of *Yersinia*. The most prominent influence on pathogenesis has been shown for the global carbon storage regulator system (Csr) (Heroven et al., 2012; Romeo et al., 2013; Vakulskas et al., 2015; Kusmieriek and Dersch, 2017; Nuss et al., 2017b). The Csr system of *Yersinia* consists of the small RNA-binding protein CsrA, which is highly conserved among many bacterial species, and the two non-coding sRNAs CsrB and CsrC. The CsrA protein typically affects the translation and/or stability of target mRNAs by binding to GGA motifs within the mRNA. Activity of CsrA is controlled and antagonized by the sRNAs CsrB and CsrC as these are able to sequester multiple CsrA molecules, which prevents binding of target transcripts (Romeo et al., 1993, 2013; Liu and Romeo, 1997; Liu et al., 1997; Romeo, 1998; Babitzke and Romeo,

**TABLE 1 |** RNA regulators of *Yersinia* important for virulence.

Regulators	Mechanisms/Targets	Virulence-associated processes	Regulation	References
<b>Trans-ENCODED ncRNA</b>				
CsrB/CsrC	Small structured RNAs with multiple GGA sequences that bind and sequester CsrA, Hfq-dependent	Control of RovM, RovA, InvA/PsaA adhesins, T3SS/Yops, host-adapted metabolism, motility, carbon metabolism, stress resistance	Controlled by BarA/UvrY, PhoP/PhoQ, Crp, short chain fatty acids, acidic pH, antimicrobial peptides	(Heroven et al., 2008, 2012; Romeo et al., 2013; Bückner et al., 2014; LeGrand et al., 2015; Kusmierek and Dersch, 2017; Ozturk et al., 2017)
RybB	Hfq-dependent sRNA	Induced in the lung and spleen during infection with <i>Y. pestis</i> biovar microtus	Temperature and growth phase-dependent	(Koo et al., 2011; Yan et al., 2013; Nuss et al., 2015, 2017a)
RyhB1/RyhB2	Homologous Hfq-dependent sRNAs	<i>ryhB1</i> and <i>ryhB2</i> have a small influence on virulence in <i>Y. pestis</i> biovar microtus and <i>Y. pseudotuberculosis</i>	Increased during iron starvation, induced in the lung and spleen during infection with <i>Y. pestis</i> biovar microtus, and induced in Peyer's patches of mice, they depend on growth phase, they are controlled by the regulator Fur, degraded by PNPase	(Deng et al., 2012, 2014; Yan et al., 2013; Nuss et al., 2017a)
GlmZ/GlmY	Homologous sRNAs, GlmZ activates <i>glmS</i> mRNA translation by an anti-antisense mechanism, GlmY acts upstream of GlmZ and positively regulates <i>glmS</i> by antagonizing GlmZ RNA inactivation	Control amino-sugar metabolism, GlmY/GlmZ control <i>glmS</i> , which encodes the enzyme glutamine synthase necessary for the synthesis of <i>N</i> -acetylglucosamine-6-P, which is used for cell wall biosynthesis	Regulated by RNase E and Hfq	(Görke and Vogel, 2008; Urban and Vogel, 2008; Nuss et al., 2017a)
SsrA/tmRNA	A-site of stalled ribosomes, binds together with SmpB to stalled ribosomes by mimicking a tRNA and mRNA, which replaces incomplete/truncated transcripts within stalled ribosomes	Rescues stalled ribosomes, holds the translation machinery in the operation mode	Induced in the lung and spleen during infection with <i>Y. pestis</i> biovar microtus	(Okan et al., 2006, 2010; Yan et al., 2013)
SgrS	SgrS activates synthesis of the phosphatase YigL in a translation-independent fashion the SgrS RNA targets the <i>pldB</i> mRNA and blocks sustained 5'- to 3'-endonucleolytic turnover of the <i>pldB-yigL</i> transcript by RNase E	Phospho sugar stress, SgrS-mediated increase of phosphatase YigL leads to the dephosphorylation of the accumulated sugars and facilitates their export by efflux systems	Glucose-6-P-responsive, accumulation of phospho sugars is toxic and activates SgrS RNA through the SgrR transcription factor	(Vanderpool and Gottesman, 2004; Papenfort et al., 2012, 2013; Bobrovskyy and Vanderpool, 2014, 2016; Nuss et al., 2017a)
Ysr29	–	General stress response (GroEL, DnaK, UreC, S/RpsA, Gst, AhpC, Rrf), required for stress response and full virulence of <i>Y. pseudotuberculosis</i>	Temperature and growth phase-dependent	(Koo et al., 2011)
Ysr35	–	Required for full virulence of <i>Y. pseudotuberculosis</i> and <i>Y. pestis</i> , controls several general stress response factors such as GroEL, DnaK, the peroxidase AhpC and the translation factors RpsA and Rrf	Temperature-induced	(Koo et al., 2011)
Ysr141	–	Influences expression and secretion of T3SS/Yop components and the major regulator LcrF, modulates host immune defense, has direct influence on YopJ translation	–	(Schiano et al., 2014)
Ysr170	–	Important for intracellular replication of <i>Y. pestis</i> in cultured macrophages	–	(Li et al., 2016)
<b>ANTISENSE RNA</b>				
CopA	Complementary to the replicase gene <i>repA</i> of the <i>Yersinia</i> virulence plasmid	Repression of the replication of the virulence plasmid pYV, repression of <i>repA</i> mRNA translation/stability, reduces expression of the T3SS/Yop components	Downregulated during colonization of the Peyer's patches	(Qu et al., 2012; Wang et al., 2016)

(Continued)

TABLE 1 | Continued

Regulators	Mechanisms/Targets	Virulence-associated processes	Regulation	References
<b>RNA THERMOMETER</b>				
<i>Ail</i>	5'-UTR of the adhesin gene <i>ail</i>	Stem-loop structure restricts access of ribosomes to the ribosome binding site at 25°C but not at 37°C, regulation of the expression of the cell attachment and invasion outer membrane protein Ail	Temperature-induced	(Rhigetti et al., 2016)
<i>cnfY</i>	5'-UTR of the toxin gene <i>cnfY</i>	A stem-loop structure restricts access of ribosomes to the ribosome binding site at 25°C but not at 37°C, regulation of the expression of the cytotoxic necrotizing factor CNF <sub>Y</sub>	Temperature-induced, controlled by <i>csrA</i> , <i>crp</i>	(Schweer et al., 2013; Rhigetti et al., 2016)
<i>lcrF</i>	<i>ysw-lcrF</i> intergenic region, FourU RNA thermometer	A two stem-loop structure restricts access of ribosome to the ribosome binding site at 25°C but not at 37°C, proper function required for expression of the T3SS/ <i>yop</i> genes and virulence	Temperature-induced, iron limitation, and oxidative stress, controlled by the transcription factors YmoA, RcsB, IscR	(Hoe and Goguen, 1993; Böhme et al., 2012; Schwiesow et al., 2015; Rhigetti et al., 2016)
<i>kata</i>	5'-UTR of the katalase gene <i>kata</i>	Resistance against oxidative stress	Thermally induced structural changes liberate the ribosomal binding site, induced by oxidative stress	(Rhigetti et al., 2016)
<i>sodA</i>	5'-UTR of the superoxide dismutase gene <i>sodA</i>	Resistance against oxidative stress	Thermally induced structural changes liberate the ribosomal binding site, induced by oxidative stress	(Rhigetti et al., 2016)
<i>sodB</i>	5'-UTR of the superoxide dismutase gene <i>sodB</i>	Resistance against oxidative stress	Thermally induced structural changes liberate the ribosomal binding site, induced by oxidative stress	(Rhigetti et al., 2016)
<i>sodC</i>	5'-UTR of the superoxide dismutase gene <i>sodC</i>	Resistance against oxidative stress	Thermally induced structural changes liberate the ribosomal binding site, induced by oxidative stress	(Rhigetti et al., 2016)
<b>RIBOSWITCH</b>				
<i>mgtA/corA</i>	Mg <sup>2+</sup> binding RNA secondary structure in the 5'-UTR of the Mg <sup>2+</sup> transporter gene <i>mgtA</i> , Mg <sup>2+</sup> binding initiates early Rho-independent termination of <i>mgtA</i> transcription through conformational changes in the RNA	This riboswitch regulates Mg <sup>2+</sup> uptake, essential for survival and replication of macrophages	<i>mgtA</i> expression is induced under high Mg <sup>2+</sup> concentrations	(Korth and Sigel, 2012; Nuss et al., 2015)
<b>RNA-BINDING PROTEINS</b>				
CsrA	CsrA is a global RNA binding protein of the carbon storage regulator system. It interacts with single-stranded GGA motifs within stem-loop structures of mRNAs or the regulatory RNAs CsrB and CsrC, and modulates translation efficiency and stability of mRNAs and regulatory RNAs	CsrA controls multiple virulence- and fitness-relevant traits, e.g., motility, adhesion and invasion factors (YadA, InvA, PsaA), T3SS/Yops, regulatory proteins such as RovM and RovA, various metabolic functions (carbon metabolism), resistance against environmental stresses	CsrA function is controlled by the regulatory RNAs CsrB and CsrC, induced during stationary phase	(Heroven et al., 2008, 2012; Bückner et al., 2014; LeGrand et al., 2015; Williams et al., 2015)
Hfq	Hfq is a global RNA binding protein, preferential binding to AU-rich motifs, interacts with multiple regulatory RNAs and mRNAs, Hfq acts as an RNA chaperone, which enhances and stabilizes interaction of regulatory RNAs with target mRNAs	Loss of the <i>hfq</i> gene affects multiple virulence-related traits, e.g. expression of outer membrane adhesins, biofilm formation and cyclic-di-GMP levels, lipid A structure, outer membrane vesicle synthesis, and motility	Induced during stationary phase, dependent on temperature	(Geng et al., 2009; Schiano et al., 2010; Bellows et al., 2012; Rempe et al., 2012; Schiano and Latham, 2012; Eddy et al., 2014; Kakoschke et al., 2014, 2016; Nuss et al., 2015; Leskinen et al., 2017)
SmpB	SmpB is a specific RNA binding protein that interacts with the A site of ribosomes together with SsrA, SmpB assists SsrA interaction with stalled ribosomes to rescue the translation machinery on mRNAs from truncated transcripts without a stop codon	The SmpB/SsrA system influences <i>ysc/yop</i> expression and type III secretion, affects resistance against environmental stresses experienced within phagocytic cells (e.g., oxidative, nitrosative and acidic stress)	Upregulated during infection with <i>Y. pestis</i> biovar Microtus in the lungs	(Okan et al., 2006, 2010)

(Continued)



TABLE 1 | Continued

Regulators	Mechanisms/Targets	Virulence-associated processes	Regulation	References
YopD	RNA-binding protein, translocator protein, interaction partner of the chaperone LcrH and the protein LcrQ (YscM1 and YscM2 in <i>Y. enterocolitica</i> ), interacts with 5'-UTRs of <i>ysc/yop</i> mRNAs, binds to ribosomes, RNA-binding mechanism and ribosomal interaction partner are unknown	Influences expression of the <i>ysc/yop</i> genes, Ca <sup>2+</sup> -blind/independent expression of the T3SS	LcrF-dependent expression, temperature-regulated, host cell contact-induced	(Williams and Straley, 1998; Anderson et al., 2002; Cambronne and Schneewind, 2002; Chen and Anderson, 2011)
<b>RNases</b>				
RNase E	RNA degradation, endonuclease, cleaves RNA substrates in single-stranded regions followed by a stable stem-loop structure, RNase E is part of the degradosome, a multiprotein complex that includes PNPase	RNase E influences secretion of the T3SS effectors	–	(Yang et al., 2008)
PNPase	RNA degradation, exonuclease, cleaves RNA substrates from the 5'- and 3'-end. PNPase is part of the degradosome, a multiprotein complex, and cooperates with RNase E	PNPase influences secretion of the T3SS effectors, influences resistance against oxidative stress and growth in the cold	–	(Rosenzweig et al., 2005, 2007; Henry et al., 2012; Rosenzweig and Chopra, 2013)
YbeY	RNA decay, processing of 3'-ends of the 16S rRNA, responsible for the late stage 70S ribosome quality control	Pleiotropic, controls many virulence-relevant traits, including acid stress resistance, cell adhesion/invasion properties and T3SS, controls regulatory RNAs CsrB and CsrC	–	(Leskinen et al., 2015)
RNase III	RNA decay, binds and cleaves double-stranded RNA, processing of ribosomal RNA precursors and of some mRNAs	Affects abundance of the RyhB2 transcript	–	(Deng et al., 2014)

2007; Romeo and Babitzke, 2018). In *Yersinia*, similar to other *Enterobacteriaceae*, the Csr system constitutes an important link between metabolic, stress, and virulence gene regulation by sRNAs, and plays a crucial role in virulence (Heroven et al., 2012; Kusmirek and Dersch, 2017; Nuss et al., 2017b). It has been found to control expression of the flagella master regulator FlhDC, the colonization factors InvA and PsaA, and multiple fitness and virulence-relevant cellular processes. These are e.g., motility/chemotaxis, biofilm formation, resistance against various stresses, including antibiotics and oxygen radicals, and adaptation of the central carbon metabolism by regulating the pyruvate-acetyl-CoA-tricarboxylate acid cycle flux (Heroven et al., 2008; Bückner et al., 2014; LeGrand et al., 2015; Willias et al., 2015; Kusmirek and Dersch, 2017). A very recent study of our group further demonstrated that the abundance of both CsrB and CsrC sRNAs in *Y. pseudotuberculosis* is reduced during the colonization of Peyer's patches compared to growth under different *in vitro* conditions (Nuss et al., 2017a). This indicates that more “free” CsrA is required during the infection process. In fact, loss of CsrA was shown to reduce the synthesis and completely abolish the secretion of the Yop effector proteins in *Y. pseudotuberculosis* (Nuss et al., 2017a). Most interestingly,

CsrA also influences Yop secretion in *Y. enterocolitica* (Ozturk et al., 2017), although the overall outcome is quite different. This might be explained by the different growth conditions used for the Yop secretion assay or differences between the species.

Furthermore, RNA-seq approaches used to profile gene expression of *Y. pseudotuberculosis* and *Y. pestis* during host colonization revealed several other conserved sRNAs that are induced during infection. Among these sRNAs are RyhB1 and RyhB2—two sRNAs that are induced during iron starvation experienced in host tissue, SgrS—an sRNA upregulated under glucose-phosphate stress, and GlmY involved in cell wall synthesis (Table 1) (Massé and Gottesman, 2002; Vanderpool and Gottesman, 2004; Reichenbach et al., 2008; Urban and Vogel, 2008; Wadler and Vanderpool, 2009; Deng et al., 2012; Papenfort et al., 2012, 2013; Yan et al., 2013; Bobrovskyy and Vanderpool, 2014, 2016; Nuss et al., 2017a). However, lack of these sRNAs had only a mild effect on host colonization by the pathogens, indicating that they are implicated in the fine-tuning of virulence-relevant fitness processes.

Of the 80 antisense RNAs (asRNAs) that have been discovered to be part of the *Y. pseudotuberculosis* transcriptome, multiple are encoded on the virulence plasmid. Several were complementary

to transcripts of the T3SS/Yop genes, although their influence on the expression of these virulence genes, and the influence on *Yersinia* virulence has not yet been investigated. However, one asRNA, *CopA/incRNA*, has been shown to be extremely important for the virulence process. *CopA* is implicated in the RNA-based control of the copy number of the virulence plasmid. The copy number of the *Yersinia* virulence plasmid, an IncFII plasmid, is controlled by the replicase RepA, which is tightly controlled and negatively regulated at the transcriptional and the post-transcriptional level. Under non-secretion conditions (e.g., in the absence of host cells), synthesis of RepA is repressed by (i) CopB, a transcriptional repressor that interacts with the *repA* promoter, and (ii) the asRNA *CopA*, that binds to the 5' end of the longer of two *repA* transcripts preventing translation of a short leader peptide whose translation is coupled with and required for *repA* translation (Blomberg et al., 1990, 1992; Nordström, 2006; Wang et al., 2016; Pilla and Tang, 2018). Despite other IncFII plasmids, transcription of *copA* and *copB* of the *Yersinia* virulence plasmid are not constitutive. They are temperature-regulated and repressed during infection of the Peyer's patches, leading to a reduction of the ratio of the *CopA* asRNA and the *repA* transcript level, which results in an increase from 1–4 to up to 4–12 plasmid copies per bacterial cell during host tissue colonization (Wang et al., 2016). It could be demonstrated that up-regulation of the virulence plasmid copy number during the infection is crucial for virulence and that one of the secreted T3SS substrates (YopD) is involved. However, the molecular mechanism coupling copy number control to host cell binding still needs to be elucidated.

In summary, the identification of regulatory sRNAs and asRNAs using RNA-seq in the context of an infection process highlights that this approach is a powerful tool for the discovery of new infection-relevant regulatory processes. Application of newly developed RNA-seq technologies such as pulse-chase-expression global target searches (Massé et al., 2005; Papenfort et al., 2006; Westermann et al., 2016), coupling of RNA-seq with ribosome profiling (Guo et al., 2014; Wang et al., 2015), M2-tagged sRNA affinity purification coupled with RNA-seq (Lalaouna et al., 2015; Tomasini et al., 2017), RNA interaction by ligation and sequencing—short RIL-Seq (Melamed et al., 2016), or global small non-coding RNA target identification by ligation and sequencing—short GRIL-Seq (Han et al., 2016) could help to identify direct targets of the regulatory RNAs and their role in *Yersinia* biology.

## TRANSLATIONAL CONTROL

During translation mRNA is decoded for protein synthesis in a multi-step process consisting of initiation, elongation, termination, and recycling (Melnikov et al., 2012). This process is performed by the ribosome and several other translation associated components like tRNAs, initiation factors (IF), elongation factors (EF), and recycling factors (RF and RRF) (Melnikov et al., 2012). In addition to the complex transcriptional control strategies, gene expression of *Yersinia* is extensively regulated on the level of translation. Regulation of translation initiation occurs by changing the accessibility of the RBS for

the small ribosomal subunit (30S, small subunit). As previously described, this can be achieved by masking the RBS with an RNA binding protein such as CsrA (Heroven et al., 2008, 2012) or an RNA thermo-loop (Baba et al., 1991; Böhme et al., 2012).

Other important riboregulators can modulate sRNA-mRNA interaction and influence the function of the translation machinery. For instance, the *trans*-translation control system or ribosome rescue system is composed of a small RNA-binding protein SsrB which transfers the polypeptide chain of ribosomes that are stalled on damaged or incomplete transcripts to the small, stable sRNA SsrA/tmRNA (Okan et al., 2006). The fact that SsrA/tmRNA is strongly upregulated in *Y. pestis* during the colonization of the lung and spleen and an *ssrA* mutant strain is strongly attenuated for virulence in a mouse infection model, strongly indicated that ribosome rescue is crucial for virulence (Okan et al., 2010; Yan et al., 2013). Reduced stress resistance and influence of the expression of the major virulence regulator LcrF in an *ssrA/ssrB* mutant strain could be the reason for this drastic phenotype (Okan et al., 2006, 2010).

One additional and very special translational control pathway of *Yersinia* virulence is mediated by the T3SS protein YopD, which, together with YopB, builds up the translocon pore in the eukaryotic membrane. Under non-secretion conditions, YopD is present in the bacterial cell and interacts with its chaperone LcrH, which prevents its degradation (Francis and Wolf-Watz, 1998; Edgren et al., 2012; Dewoody et al., 2013). Alone or bound to its chaperone LcrH, YopD seems to use sequences within the AU-rich regions in the proximity of the RBS of multiple *yop*-encoding mRNAs. This hinders translation initiation and reduces Yop protein expression (Williams and Straley, 1998; Anderson et al., 2002; Chen and Anderson, 2011). However, other control factors seem to contribute to YopD-mediated translational repression, as the identified 5'-UTR regions are important, but do not seem to be sufficient to promote this process. In fact, the secreted factor LcrQ (LcrM1 and LcrM2 in *Y. enterocolitica*) was found to contribute to post-transcriptional repression by YopD (Cambronne and Schneewind, 2002). Moreover, YopD was found to interact with the small 30S subunits of the ribosome. This indicates the presence of a different population of ribosomes (ribosome heterogeneity, Byrgazov et al., 2013), which negatively influences translation initiation complex formation (Kopaskie et al., 2013). How and to what extent these interactions affect translation of virulence-encoded genes is still unknown. YopD-binding could block the anti-RBS in the 16S rRNA from binding with the RBS. However, this alone would not explain why in particular translation of *yop* mRNAs is abrogated.

## RNA PROCESSING AND DECAY

Fast adaptation to changing surroundings is crucial for bacterial pathogens, such as *Yersinia* cycling between various environmental reservoirs, mammals, and humans in order to efficiently colonize their respective host and thrive in an occupied niche. Essential for this process is a controlled degradation of transcripts, which is mediated by a complex set of ribonucleases (RNases). The amount and type of RNases, their essentiality

and collaboration in RNA metabolism is strongly depending on the investigated pathogen (e.g., *Yersinia pseudotuberculosis* > 15 RNases) (Arraiano et al., 2010; Lawal et al., 2011; Hui et al., 2014). The different RNases vary to a great extent in their mode of action, specificity for certain RNA features, and the nature of their targets in general (Arraiano et al., 2010; Lawal et al., 2011; Hui et al., 2014). Most bacteria, including all human pathogenic *Yersinia* species, contain low-specificity single-stranded endonucleases (e.g., RNase E), double-stranded endonucleases (e.g., RNase III) and 3'-exonucleases (e.g., PNPase) (Mohanty and Kushner, 2016). RNA degradation occurs typically by consecutive endonucleolytic cleavage followed by exonucleolytic degradation from the 3'-end. The 5'-end is generally more stabilized due to the triphosphate end, but also the 3'-end can be rendered more stable toward RNases, e.g., by the presence of hairpin structures, RNA modification/polyadenylation or coverage by translating ribosomes. In addition to maturation and activation of certain transcripts (e.g., rRNA, tRNA), several conserved RNases were found to play a crucial role in global and/or targeted mRNA and sRNA turnover and also virulence in many pathogens (Clements et al., 2002; Ygberg et al., 2006; Lawal et al., 2011; Rosenzweig and Chopra, 2013).

In order to determine global mRNA decay rates, the bacterial culture is generally treated with the RNA polymerase inhibitor rifampicin prior to isolation of total RNA. To identify RNase targets and decay pathways, RNA-seq approaches with a transiently inactivated endoribonuclease followed by RNA-seq—short TIER-seq (Chao et al., 2017, **Figure 1**) or with RNase-deficient mutants were recently used to quantify transcript steady-state levels in Leskinen et al. (2015) and Chen et al. (2016).

In *Yersinia*, especially the RNases PNPase and RNase E were found to occupy well-established roles in the regulation of virulence factors and growth under several infection-relevant conditions (oxidative and cold stress) (Rosenzweig et al., 2007; Yang et al., 2008; Rosenzweig and Chopra, 2013). PNPase forms together with the RNase E, the helicase RhlB and the glycolytic enzyme enolase a multi protein complex, called the degradosome (Rice and Vanderpool, 2011). RNase E represents the scaffolding enzyme for this complex hyperstructure and while some of the affected virulence-relevant properties were associated with an intact buildup of the degradosome, others only require RNase E or PNPase activity and RNA binding ability (Henry et al., 2012; Rosenzweig and Chopra, 2013). A *Yersinia pnp* mutant is significantly less virulent in the mouse compared to the isogenic wild-type strain. It was shown that PNPase is required for optimal functioning of the T3SS. Yet, this did not seem to depend on its ribonuclease activity, but requires its S1 domain. As the *pnp* mutant strain also expressed similar or even enhanced levels of T3SS-encoded transcripts, it is most likely that its virulence attenuation is due to a limiting T3SS activity (Rosenzweig et al., 2005, 2007). Besides the RNases of the degradosome, there is an increasing amount of information that additional RNases contribute to virulence. For instance, the single-strand specific RNase YbeY, which is important for the processing of the 3'-end of the 16S rRNAs, was recently shown to influence the expression of many virulence genes (colonization factors, T3SS,

and the amount of both Csr regulatory RNAs) (Leskinen et al., 2015). How precisely YbeY influences all these processes is still unclear, but the large number of differentially regulated fitness and virulence-relevant genes in the YbeY-deficient mutant correlates with the severe phenotype and illustrates a crucial role in cell homeostasis and virulence. Besides these RNA processing and decay pathways, other RNA degrading enzymes were found to be differentially regulated in response to various virulence-related growth conditions *in vitro* and during infection *in vivo*, indicating that more RNases may play a role in mRNA stability regulation. The exploitation of advanced RNA-seq combined with new target search approaches by coupling a UV crosslinking reaction to covalently link the RNase of interest to its target RNA will elucidate the role of RNases in various cellular processes (Waters et al., 2017). Determination of the cleavage sites and profiling of cleavage products of RNases, as established for other pathogens (Linder et al., 2014; Pobre and Arraiano, 2015; Redko et al., 2016; Chao et al., 2017; Le Rhun et al., 2017), will enable us to obtain genome-wide cleavage maps of different RNases of yersiniae under virulence-relevant conditions and will facilitate unraveling their complex RNA degradation network.

## OUTLOOK: RNA INTERACTOME AND REGULATORY NETWORKS IN *YERSINIA*

The discovery of novel RNA-based regulatory strategies anticipates many exciting new insights into the complex post-transcriptional control network of virulence gene expression. Yet, determining the individual targets and interaction partners (protein and RNA) of the multitude of mRNAs, asRNAs, and sRNAs identified in *Y. pseudotuberculosis* during recent RNA-seq approaches is a time-consuming and very labor-intensive task. However, new approaches have been successfully established to generate a snapshot of the interactome of RNAs that bind to a particular RNA-binding protein, e.g., CsrA, Hfq, or YopD. Such RNA interactomes can be obtained by RNA immunoprecipitation followed by RNA-seq (RIP-seq) (**Figure 2**), by covalently linked protein-RNA interactions followed by RNA-seq (CLIP-seq) (**Figure 2**), RNA interaction by ligation and sequencing (RIL-seq), or cross-linking, ligation and sequencing of hybrids (CLASH) (Bilusic et al., 2014; Holmqvist et al., 2016; Melamed et al., 2016; Waters et al., 2017). These techniques cannot only be used to profile the individual targets and entire binding sites (positions and sequences) of an RNA-binding protein, they will also allow us to improve sRNA target prediction, and facilitate the discovery of new sRNA control circuits and regulatory pathways (Dugar et al., 2016; Heidrich et al., 2017; Michaux et al., 2017). Similarly, RNA-RNA hybrids can be enriched or cross-linked and then sequenced to obtain a genome-wide *Yersinia* RNA-RNA network as done for *E. coli* (Liu et al., 2017).

Other open questions concerning the RNA-based control network of *Yersinia* virulence factors are: How are they conserved or remodeled during evolution between different strains and species, and how do acquired variations change virulence gene

expression and pathogenicity? Numerous species- and strain-specific sensory and regulatory RNAs and many intra-species variations of certain sRNAs have been discovered in human pathogenic *Yersiniae* over the past years. For instance the PhoP regulator, controlling expression of the CsrC sRNA is not expressed in *Y. pseudotuberculosis* strain YPIII, but in IP32953 (Pisano et al., 2014). Moreover, the stability of the CsrC RNAs of strain YPIII and IP32953 differs significantly due to a 20 nt insertion in CsrC of IP32953, which renders the transcript more susceptible to degradation (Nuss et al., 2014). Based on the fact that the Csr system is crucial for T3SS/Yop expression and virulence (Bücker et al., 2014; Nuss et al., 2017a), it seems likely that even small variations (patho-specific alterations) between closely related strains could have a significant influence on the pathogen's potential to readjust and adapt to different hosts, host niches and reservoirs.

Another future task will be to elucidate the precise molecular mechanism how the RNA-binding translocator protein YopD controls translation of *yop* mRNAs. One technique to investigate ribosome-associated regulation, is ribosome profiling (Ribo-seq, **Figure 1**). With this method, all *in vivo* positions of extracted ribosomes on mRNAs (polysomes) can be identified enabling a dynamic view of ribosome movement along all mRNAs of a bacterial cell at a certain growth condition (Li et al., 2012; Ingolia, 2014). The function of ribosome subpopulations, such as those bound by YopD could be investigated by crosslinking of the ribosomes to the mRNA followed by affinity purification of the resulting YopD-ribosomal complex.

Ongoing characterization of the identified RNA-based control mechanisms of *Yersinia* will also have to address how the different riboregulators and RNAs contribute to the colonization of different host niches and whether and how they are implicated in the reprogramming of the pathogen, e.g., *Y. pseudotuberculosis* during the switch from the acute to the persistent infection mode. As regulatory RNAs, such as CsrB and CsrC, are implicated in the control of the regulator RovA, which forms a bistable switch, leading to high- and low-invasive subpopulations (Nuss et al.,

2016), it is important to investigate the impact of riboregulators and non-coding RNAs on the formation of heterogeneous subpopulation with different virulence-relevant features. A major advance for this endeavor would be the development of single-cell RNA-seq approaches, in which the transcriptome of multiple individual bacterial cells could be profiled in different host niches and hosts during the entire course of an infection. So far single-cell RNA-seq has mainly been used for eukaryotic cells, however when applied to single bacteria this approach still suffers from technical limitations, which will have to be overcome in the future. This includes the establishment of more robust analyses and a more effective single-cell lysis and cDNA synthesis (Zhang et al., 2018). The next challenge will then be to analyze and compare the huge amount of generated data in an optimized and standardized integrative manner. This demands the establishment of (i) high quality, and free accessible standardized data-bases and (ii) the development of innovative bioinformatics protocols for data analysis and interpretation that allow integration of different technical and experimental approaches (e.g., different RNA-seq techniques, different OMICs, strains, tissues, and time-points of infection). Once achieved, this will give a comprehensive view on the complex RNA biology of *Yersinia* and will open up a new level of our understanding of virulence control of bacterial pathogens.

## AUTHOR CONTRIBUTIONS

All authors listed have made a substantial, direct and intellectual contribution to the work, and approved it for publication.

## FUNDING

Work on this topic was supported by Deutsche Forschungsgemeinschaft (DE616/6, DE616/7), and the Helmholtz Society. PD is member and supported by the Germany Center for Infection Research (DZIF) under grant number DZIF-TTU 06.801.

## REFERENCES

- Anderson, D. M., Ramamurthi, K. S., Tam, C., and Schneewind, O. (2002). YopD and LcrH regulate expression of *Yersinia enterocolitica* YopQ by a posttranscriptional mechanism and bind to *yopQ* RNA. *J. Bacteriol.* 184, 1287–1295. doi: 10.1128/JB.184.5.1287-1295.2002
- Arraiano, C. M., Andrade, J. M., Domingues, S., Guinote, I. B., Malecki, M., Matos, R. G., et al. (2010). The critical role of RNA processing and degradation in the control of gene expression. *FEMS Microbiol. Rev.* 34, 883–923. doi: 10.1111/j.1574-6976.2010.00242.x
- Avican, K., Fahlgren, A., Huss, M., Heroven, A. K., Beckstette, M., Dersch, P., et al. (2015). Reprogramming of *Yersinia* from virulent to persistent mode revealed by complex *in vivo* RNA-seq analysis. *PLoS Pathog.* 11:e1004600. doi: 10.1371/journal.ppat.1004600
- Baba, K., Takeda, N., and Tanaka, M. (1991). Cases of *Yersinia pseudotuberculosis* infection having diagnostic criteria of Kawasaki disease. *Contrib. Microbiol. Immunol.* 12, 292–296.
- Babitzke, P., and Romeo, T. (2007). CsrB sRNA family: sequestration of RNA-binding regulatory proteins. *Curr. Opin. Microbiol.* 10, 156–163. doi: 10.1016/j.mib.2007.03.007
- Barquist, L., and Vogel, J. (2015). Accelerating discovery and functional analysis of small RNAs with new technologies. *Annu. Rev. Genet.* 49, 367–394. doi: 10.1146/annurev-genet-112414-054804
- Beauregard, A., Smith, E. A., Petrone, B. L., Singh, N., Karch, C., McDonough, K. A., et al. (2013). Identification and characterization of small RNAs in *Yersinia pestis*. *RNA Biol.* 10, 397–405. doi: 10.4161/rna.23590
- Bellows, L. E., Koestler, B. J., Karaba, S. M., Waters, C. M., and Lathem, W. W. (2012). Hfq-dependent, co-ordinate control of cyclic diguanylate synthesis and catabolism in the plague pathogen *Yersinia pestis*. *Mol. Microbiol.* 86, 661–674. doi: 10.1111/mmi.12011
- Bilusic, I., Popitsch, N., Rescheneder, P., Schroeder, R., and Lybecker, M. (2014). Revisiting the coding potential of the *E. coli* genome through Hfq co-immunoprecipitation. *RNA Biol.* 11, 641–654. doi: 10.4161/rna.29299
- Blomberg, P., Nordström, K., and Wagner, E. G. (1992). Replication control of plasmid R1: RepA synthesis is regulated by CopA RNA through inhibition of leader peptide translation. *EMBO J.* 11, 2675–2683. doi: 10.1002/j.1460-2075.1992.tb05333.x



- Blomberg, P., Wagner, E. G., and Nordström, K. (1990). Control of replication of plasmid R1: the duplex between the antisense RNA, CopA, and its target, CopT, is processed specifically *in vivo* and *in vitro* by RNase III. *EMBO J.* 9, 2331–2340. doi: 10.1002/j.1460-2075.1990.tb07405.x
- Bobrovskyy, M., and Vanderpool, C. K. (2014). The small RNA SgrS: roles in metabolism and pathogenesis of enteric bacteria. *Front. Cell. Infect. Microbiol.* 4:61. doi: 10.3389/fcimb.2014.00061
- Bobrovskyy, M., and Vanderpool, C. K. (2016). Diverse mechanisms of post-transcriptional repression by the small RNA regulator of glucose-phosphate stress. *Mol. Microbiol.* 99, 254–273. doi: 10.1111/mmi.13230
- Böhme, K., Steinmann, R., Kortmann, J., Seekircher, S., Heroven, A. K., Berger, E., et al. (2012). Concerted actions of a thermo-labile regulator and a unique intergenic RNA thermosensor control *Yersinia* virulence. *PLoS Pathog.* 8:e1002518. doi: 10.1371/journal.ppat.1002518
- Bottone, E. J. (1997). *Yersinia enterocolitica*: the charisma continues. *Clin. Microbiol. Rev.* 10, 257–276.
- Breaker, R. R. (2011). Prospects for riboswitch discovery and analysis. *Mol. Cell* 43, 867–879. doi: 10.1016/j.molcel.2011.08.024
- Bücker, R., Heroven, A. K., Becker, J., Dersch, P., and Wittmann, C. (2014). The pyruvate-tricarboxylic acid cycle node: a focal point of virulence control in the enteric pathogen *Yersinia pseudotuberculosis*. *J. Biol. Chem.* 289, 30114–30132. doi: 10.1074/jbc.M114.581348
- Byrgazov, K., Vesper, O., and Moll, I. (2013). Ribosome heterogeneity: another level of complexity in bacterial translation regulation. *Curr. Opin. Microbiol.* 16, 133–139. doi: 10.1016/j.mib.2013.01.009
- Cambronne, E. D., and Schneewind, O. (2002). *Yersinia enterocolitica* type III secretion: *yscM1* and *yscM2* regulate *yop* gene expression by a posttranscriptional mechanism that targets the 5' untranslated region of *yop* mRNA. *J. Bacteriol.* 184, 5880–5893. doi: 10.1128/JB.184.21.5880-5893.2002
- Chao, Y., Li, L., Girodat, D., Förstner, K. U., Said, N., Corcoran, C., et al. (2017). *In vivo* cleavage map illuminates the central role of RNase E in coding and non-coding RNA pathways. *Mol. Cell* 65, 39–51. doi: 10.1016/j.molcel.2016.11.002
- Chen, R., Weng, Y., Zhu, F., Jin, Y., Liu, C., Pan, X., et al. (2016). Polynucleotide phosphorylase regulates multiple virulence factors and the stabilities of small RNAs RsmY/Z in *Pseudomonas aeruginosa*. *Front. Microbiol.* 7:247. doi: 10.3389/fmicb.2016.00247
- Chen, Y., and Anderson, D. M. (2011). Expression hierarchy in the *Yersinia* type III secretion system established through YopD recognition of RNA. *Mol. Microbiol.* 80, 966–980. doi: 10.1111/j.1365-2958.2011.07623.x
- Clements, M. O., Eriksson, S., Thompson, A., Lucchini, S., Hinton, J. C., Normark, S., et al. (2002). Polynucleotide phosphorylase is a global regulator of virulence and persistency in *Salmonella enterica*. *Proc. Natl. Acad. Sci. U.S.A.* 99, 8784–8789. doi: 10.1073/pnas.132047099
- Cummings, J. H., and Macfarlane, G. T. (1997). Role of intestinal bacteria in nutrient metabolism. *J. Parenter. Enteral Nutr.* 21, 357–365. doi: 10.1177/0148607197021006357
- Deng, Z., Liu, Z., Bi, Y., Wang, X., Zhou, D., Yang, R., et al. (2014). Rapid degradation of Hfq-free RyhB in *Yersinia pestis* by PNPase independent of putative ribonucleolytic complexes. *Biomed Res. Int.* 2014:798918. doi: 10.1155/2014/798918
- Deng, Z., Meng, X., Su, S., Liu, Z., Ji, X., Zhang, Y., et al. (2012). Two sRNA RyhB homologs from *Yersinia pestis* biovar microtus expressed *in vivo* have differential Hfq-dependent stability. *Res. Microbiol.* 163, 413–418. doi: 10.1016/j.resmic.2012.05.006
- Dewoody, R. S., Merritt, P. M., and Marketon, M. M. (2013). Regulation of the *Yersinia* type III secretion system: traffic control. *Front. Cell. Infect. Microbiol.* 3:4. doi: 10.3389/fcimb.2013.00004
- Dugar, G., Svensson, S. L., Bischler, T., Wäldchen, S., Reinhardt, R., Sauer, M., et al. (2016). The CsrA-FlhW network controls polar localization of the dual-function flagellin mRNA in *Campylobacter jejuni*. *Nat. Commun.* 7:11667. doi: 10.1038/ncomms11667
- Eddy, J. L., Gielda, L. M., Caulfield, A. J., Rangel, S. M., and Lathem, W. W. (2014). Production of outer membrane vesicles by the plague pathogen *Yersinia pestis*. *PLoS ONE* 9:e107002. doi: 10.1371/journal.pone.0107002
- Edgren, T., Forsberg, A., Rosqvist, R., and Wolf-Watz, H. (2012). Type III secretion in *Yersinia*: injectisome or not? *PLoS Pathog.* 8:e1002669. doi: 10.1371/journal.ppat.1002669
- Francis, M. S., and Wolf-Watz, H. (1998). YopD of *Yersinia pseudotuberculosis* is translocated into the cytosol of HeLa epithelial cells: evidence of a structural domain necessary for translocation. *Mol. Microbiol.* 29, 799–813. doi: 10.1046/j.1365-2958.1998.00973.x
- Fröhlich, K. S., and Vogel, J. (2009). Activation of gene expression by small RNA. *Curr. Opin. Microbiol.* 12, 674–682. doi: 10.1016/j.mib.2009.09.009
- Geng, J., Song, Y., Yang, L., Feng, Y., Qiu, Y., Li, G., et al. (2009). Involvement of the post-transcriptional regulator of Hfq in *Yersinia pestis* virulence. *PLoS ONE* 4:e6213. doi: 10.1371/journal.pone.0006213
- Görke, B., and Vogel, J. (2008). Noncoding RNA control of the making and breaking of sugars. *Genes Dev.* 22, 2914–2925. doi: 10.1101/gad.1717808
- Gorski, S. A., Vogel, J., and Doudna, J. A. (2017). RNA-based recognition and targeting: sowing the seeds of specificity. *Nat. Rev. Mol. Cell Biol.* 18, 215–228. doi: 10.1038/nrm.2016.174
- Guo, M. S., Updegrove, T. B., Gogol, E. B., Shabalina, S. A., Gross, C. A., and Storz, G. (2014). MicL, a new sigmaE-dependent sRNA, combats envelope stress by repressing synthesis of Lpp, the major outer membrane lipoprotein. *Genes Dev.* 28, 1620–1634. doi: 10.1101/gad.243485.114
- Han, K., Tjaden, B., and Lory, S. (2016). GRIL-seq provides a method for identifying direct targets of bacterial small regulatory RNA by *in vivo* proximity ligation. *Nat. Microbiol.* 2:16239. doi: 10.1038/nmicrobiol.2016.239
- Heidrich, N., Bauriedl, S., Barquist, L., Li, L., Schoen, C., and Vogel, J. (2017). The primary transcriptome of *Neisseria meningitidis* and its interaction with the RNA chaperone Hfq. *Nucleic Acids Res.* 45, 6147–6167. doi: 10.1093/nar/gkx168
- Heine, W., Beckstette, M., Heroven, A. K., Thiemann, S., Heise, U., Nuss, A. M., et al. (2018). Loss of CNF $\gamma$  toxin-induced inflammation drives *Yersinia pseudotuberculosis* into persistency. *PLoS Pathog.* 14:e1006858. doi: 10.1371/journal.ppat.1006858
- Henry, A., Shanks, J., Van Hoof, A., and Rosenzweig, J. A. (2012). The *Yersinia pseudotuberculosis* degradosome is required for oxidative stress, while its PNPase subunit plays a degradosome-independent role in cold growth. *FEMS Microbiol. Lett.* 336, 139–147. doi: 10.1111/j.1574-6968.12000.x
- Heroven, A., Böhme, K., Rohde, M., and Dersch, P. (2008). A Csr-type regulatory system, including small non-coding RNAs, regulates the global virulence regulator RovA of *Yersinia pseudotuberculosis* through RovM. *Mol. Microbiol.* 68, 1179–1195. doi: 10.1111/j.1365-2958.2008.06218.x
- Heroven, A. K., Böhme, K., and Dersch, P. (2012). The Csr/Rsm system of *Yersinia* and related pathogens: a post-transcriptional strategy for managing virulence. *RNA Biol.* 9, 379–391. doi: 10.4161/rna.19333
- Heroven, A. K., Nuss, A. M., and Dersch, P. (2017). RNA-based mechanisms of virulence control in *Enterobacteriaceae*. *RNA Biol.* 14, 471–487. doi: 10.1080/15476286.2016.1201617
- Hoe, N. P., and Goguen, J. D. (1993). Temperature sensing in *Yersinia pestis*: translation of the LcrF activator protein is thermally regulated. *J. Bacteriol.* 175, 7901–7909. doi: 10.1128/jb.175.24.7901-7909.1993
- Holmqvist, E., Wright, P. R., Li, L., Bischler, T., Barquist, L., Reinhardt, R., et al. (2016). Global RNA recognition patterns of post-transcriptional regulators Hfq and CsrA revealed by UV crosslinking *in vivo*. *EMBO J.* 35, 991–1011. doi: 10.15252/embj.201593360
- Hör, J., Gorski, S. A., and Vogel, J. (2018). Bacterial RNA biology on a genome scale. *Mol. Cell* 70, 785–799. doi: 10.1016/j.molcel.2017.12.023
- Hör, J., and Vogel, J. (2017). Global snapshots of bacterial RNA networks. *EMBO J.* 36, 245–247. doi: 10.15252/embj.201696072
- Hui, M. P., Foley, P. L., and Belasco, J. G. (2014). Messenger RNA degradation in bacterial cells. *Annu. Rev. Genet.* 48, 537–559. doi: 10.1146/annurev-genet-120213-092340
- Ingolia, N. T. (2014). Ribosome profiling: new views of translation, from single codons to genome scale. *Nat. Rev. Genet.* 15, 205–213. doi: 10.1038/nrg3645
- Kakoschke, T., Kakoschke, S., Magistro, G., Schubert, S., Borath, M., Heesemann, J., et al. (2014). The RNA chaperone Hfq impacts growth, metabolism and production of virulence factors in *Yersinia enterocolitica*. *PLoS ONE* 9:e86113. doi: 10.1371/journal.pone.0086113
- Kakoschke, T. K., Kakoschke, S. C., Zeuzem, C., Bouabe, H., Adler, K., Heesemann, J., et al. (2016). The RNA chaperone Hfq is essential for virulence and modulates the expression of four adhesins in *Yersinia enterocolitica*. *Sci. Rep.* 6:29275. doi: 10.1038/srep29275

- Koo, J. T., Alleyne, T. M., Schiano, C. A., Jafari, N., and Lathem, W. W. (2011). Global discovery of small RNAs in *Yersinia pseudotuberculosis* identifies *Yersinia*-specific small, noncoding RNAs required for virulence. *Proc. Natl. Acad. Sci. U.S.A.* 108, E709–E717. doi: 10.1073/pnas.1101655108
- Koo, J. T., and Lathem, W. W. (2012). Global discovery of small noncoding RNAs in pathogenic *Yersinia* species. *Adv. Exp. Med. Biol.* 954, 305–314. doi: 10.1007/978-1-4614-3561-7\_38
- Koornhof, H. J., Smego, R. A. Jr., and Nicol, M. (1999). Yersiniosis. II: The pathogenesis of *Yersinia* infections. *Eur. J. Clin. Microbiol. Infect. Dis.* 18, 87–112. doi: 10.1007/s100960050237
- Kopaskie, K. S., Ligtenberg, K. G., and Schneewind, O. (2013). Translational regulation of *Yersinia enterocolitica* mRNA encoding a type III secretion substrate. *J. Biol. Chem.* 288, 35478–35488. doi: 10.1074/jbc.M113.504811
- Korth, M. M., and Sigel, R. K. (2012). Unusually high-affinity Mg(2+) binding at the AU-rich sequence within the antiterminator hairpin of a Mg(2+) riboswitch. *Chem. Biodivers.* 9, 2035–2049. doi: 10.1002/cbdv.201200031
- Kortmann, J., and Narberhaus, F. (2012). Bacterial RNA thermometers: molecular zippers and switches. *Nat. Rev. Microbiol.* 10, 255–265. doi: 10.1038/nrmicro2730
- Kröger, C., Colgan, A., Srikumar, S., Händler, K., Sivasankaran, S. K., Hammarlof, D. L., et al. (2013). An infection-relevant transcriptomic compendium for *Salmonella enterica* Serovar Typhimurium. *Cell Host Microbe* 14, 683–695. doi: 10.1016/j.chom.2013.11.010
- Kusmirek, M., and Dersch, P. (2017). Regulation of host-pathogen interactions via the post-transcriptional Csr/Rsm system. *Curr. Opin. Microbiol.* 41, 58–67. doi: 10.1016/j.mib.2017.11.022
- Lalaouna, D., Carrier, M. C., Semsey, S., Brouard, J. S., Wang, J., Wade, J. T., et al. (2015). A 3' external transcribed spacer in a tRNA transcript acts as a sponge for small RNAs to prevent transcriptional noise. *Mol. Cell* 58, 393–405. doi: 10.1016/j.molcel.2015.03.013
- Lawal, A., Jejelowo, O., Chopra, A. K., and Rosenzweig, J. A. (2011). Ribonucleases and bacterial virulence. *Microb. Biotechnol.* 4, 558–571. doi: 10.1111/j.1751-7915.2010.00212.x
- Le Rhun, A., Lécrivain, A. L., Reimegard, J., Proux-Wera, E., Broglia, L., Della Beffa, C., et al. (2017). Identification of endoribonuclease specific cleavage positions reveals novel targets of RNase III in *Streptococcus pyogenes*. *Nucleic Acids Res.* 45, 2329–2340. doi: 10.1093/nar/gkw1316
- LeGrand, K., Petersen, S., Zheng, Y., Liu, K. K., Ozturk, G., Chen, J. Y., et al. (2015). CsrA impacts survival of *Yersinia enterocolitica* by affecting a myriad of physiological activities. *BMC Microbiol.* 15:31. doi: 10.1186/s12866-015-0343-6
- Leskinen, K., Pajunen, M. I., Varjosalo, M., Fernández-Carrasco, H., Bengoechea, J. A., and Skurnik, M. (2017). Several Hfq-dependent alterations in physiology of *Yersinia enterocolitica* O:3 are mediated by derepression of the transcriptional regulator RovM. *Mol. Microbiol.* 103, 1065–1091. doi: 10.1111/mmi.13610
- Leskinen, K., Varjosalo, M., and Skurnik, M. (2015). Absence of YbeY RNase compromises the growth and enhances the virulence plasmid gene expression of *Yersinia enterocolitica* O:3. *Microbiology* 161, 285–299. doi: 10.1099/mic.0.083097-0
- Li, G. W., Oh, E., and Weissman, J. S. (2012). The anti-Shine-Dalgarno sequence drives translational pausing and codon choice in bacteria. *Nature* 484, 538–541. doi: 10.1038/nature10965
- Li, N., Hennelly, S. P., Stubben, C. J., Micheva-Viteva, S., Hu, B., Shou, Y., et al. (2016). Functional and structural analysis of a highly-expressed *Yersinia pestis* small RNA following infection of cultured macrophages. *PLoS ONE* 11:e0168915. doi: 10.1371/journal.pone.0168915
- Linder, P., Lemeille, S., and Redder, P. (2014). Transcriptome-wide analyses of 5'-ends in RNase J mutants of a gram-positive pathogen reveal a role in RNA maturation, regulation and degradation. *PLoS Genet.* 10:e1004207. doi: 10.1371/journal.pgen.1004207
- Liu, M. Y., Gui, G., Wei, B., Preston, J. F. III, Oakford, L., Yüksel, U., et al. (1997). The RNA molecule CsrB binds to the global regulatory protein CsrA and antagonizes its activity in *Escherichia coli*. *J. Biol. Chem.* 272, 17502–17510. doi: 10.1074/jbc.272.28.17502
- Liu, M. Y., and Romeo, T. (1997). The global regulator CsrA of *Escherichia coli* is a specific mRNA-binding protein. *J. Bacteriol.* 179, 4639–4642. doi: 10.1128/jb.179.14.4639-4642.1997
- Liu, T., Zhang, K., Xu, S., Wang, Z., Fu, H., Tian, B., et al. (2017). Detecting RNA-RNA interactions in *E. coli* using a modified CLASH method. *BMC Genomics* 18:343. doi: 10.1186/s12864-017-3725-3
- Martínez-Chavarría, L. C., and Vadyvaloo, V. (2015). *Yersinia pestis* and *Yersinia pseudotuberculosis* infection: a regulatory RNA perspective. *Front. Microbiol.* 6:956. doi: 10.3389/fmicb.2015.00956
- Massé, E., and Gottesman, S. (2002). A small RNA regulates the expression of genes involved in iron metabolism in *Escherichia coli*. *Proc. Natl. Acad. Sci. U.S.A.* 99, 4620–4625. doi: 10.1073/pnas.032066599
- Massé, E., Vanderpool, C. K., and Gottesman, S. (2005). Effect of RyhB small RNA on global iron use in *Escherichia coli*. *J. Bacteriol.* 187, 6962–6971. doi: 10.1128/JB.187.20.6962-6971.2005
- McCown, P. J., Corbino, K. A., Stav, S., Sherlock, M. E., and Breaker, R. R. (2017). Riboswitch diversity and distribution. *RNA* 23, 995–1011. doi: 10.1261/rna.061234.117
- Melamed, S., Peer, A., Faigenbaum-Romm, R., Gatt, Y. E., Reiss, N., Bar, A., et al. (2016). Global mapping of small RNA-target interactions in bacteria. *Mol. Cell* 63, 884–897. doi: 10.1016/j.molcel.2016.07.026
- Melnikov, S., Ben-Shem, A., Garreau De Loubresse, N., Jenner, L., Yusupova, G., and Yusupov, M. (2012). One core, two shells: bacterial and eukaryotic ribosomes. *Nat. Struct. Mol. Biol.* 19, 560–567. doi: 10.1038/nsmb.2313
- Michaux, C., Holmqvist, E., Vasicek, E., Sharan, M., Barquist, L., Westermann, A. J., et al. (2017). RNA target profiles direct the discovery of virulence functions for the cold-shock proteins CspC and CspE. *Proc. Natl. Acad. Sci. U.S.A.* 114, 6824–6829. doi: 10.1073/pnas.1620772114
- Mohanty, B. K., and Kushner, S. R. (2016). Regulation of mRNA decay in bacteria. *Annu. Rev. Microbiol.* 70, 25–44. doi: 10.1146/annurev-micro-091014-104515
- Nitzan, M., Rehani, R., and Margalit, H. (2017). Integration of bacterial small RNAs in regulatory networks. *Annu. Rev. Biophys.* 46, 131–148. doi: 10.1146/annurev-biophys-070816-034058
- Nordström, K. (2006). Plasmid R1-replication and its control. *Plasmid* 55, 1–26. doi: 10.1016/j.plasmid.2005.07.002
- Nuss, A. M., Beckstette, M., Pimenova, M., Schmühl, C., Opitz, W., Pisano, F., et al. (2017a). Tissue dual RNA-seq: a fast discovery path for infection-specific functions and riboregulators shaping host-pathogen transcriptomes. *Proc. Natl. Acad. Sci. U.S.A.* 114 E791–E800. doi: 10.1073/pnas.1613405114
- Nuss, A. M., Heroven, A. K., and Dersch, P. (2017b). RNA regulators: formidable modulators of yersinia virulence. *Trends Microbiol.* 25, 19–34. doi: 10.1016/j.tim.2016.08.006
- Nuss, A. M., Heroven, A. K., Waldmann, B., Reinkensmeier, J., Jarek, M., Beckstette, M., et al. (2015). Transcriptomic profiling of *Yersinia pseudotuberculosis* reveals reprogramming of the Crp regulon by temperature and uncovers Crp as a master regulator of small RNAs. *PLoS Genet.* 11:e1005087. doi: 10.1371/journal.pgen.1005087
- Nuss, A. M., Schuster, F., Kathrin Heroven, A., Heine, W., Pisano, F., and Dersch, P. (2014). A direct link between the global regulator PhoP and the Csr regulon in *Y. pseudotuberculosis* through the small regulatory RNA CsrC. *RNA Biol.* 11, 580–593. doi: 10.4161/rna.28676
- Nuss, A. M., Schuster, F., Roselius, L., Klein, J., Bucker, R., Herbst, K., et al. (2016). A precise temperature-responsive bistable switch controlling *Yersinia* virulence. *PLoS Pathog.* 12:e1006091. doi: 10.1371/journal.ppat.1006091
- Okan, N. A., Bliska, J. B., and Karzai, A. W. (2006). A role for the SmpB-SsrA system in *Yersinia pseudotuberculosis* pathogenesis. *PLoS Pathog.* 2:e6. doi: 10.1371/journal.ppat.0020006
- Okan, N. A., Mena, P., Benach, J. L., Bliska, J. B., and Karzai, A. W. (2010). The *smpB-ssrA* mutant of *Yersinia pestis* functions as a live attenuated vaccine to protect mice against pulmonary plague infection. *Infect. Immun.* 78, 1284–1293. doi: 10.1128/IAI.00976-09
- Ozturk, G., Legrand, K., Zheng, Y., and Young, G. M. (2017). *Yersinia enterocolitica* CsrA regulates expression of the Ysa and Ysc type 3 secretion system in unique ways. *FEMS Microbiol. Lett.* 364:fnx204. doi: 10.1093/femsle/fnx204
- Papenfort, K., Pfeiffer, V., Mika, F., Lucchini, S., Hinton, J. C., and Vogel, J. (2006). SigmaE-dependent small RNAs of *Salmonella* respond to membrane stress by accelerating global omp mRNA decay. *Mol. Microbiol.* 62, 1674–1688. doi: 10.1111/j.1365-2958.2006.05524.x
- Papenfort, K., Podkaminski, D., Hinton, J. C., and Vogel, J. (2012). The ancestral SgrS RNA discriminates horizontally acquired *Salmonella* mRNAs through

- a single G-U wobble pair. *Proc. Natl. Acad. Sci. U.S.A.* 109, E757–E764. doi: 10.1073/pnas.1119414109
- Papenfert, K., Sun, Y., Miyakoshi, M., Vanderpool, C. K., and Vogel, J. (2013). Small RNA-mediated activation of sugar phosphatase mRNA regulates glucose homeostasis. *Cell* 153, 426–437. doi: 10.1016/j.cell.2013.03.003
- Papenfert, K., and Vogel, J. (2010). Regulatory RNA in bacterial pathogens. *Cell Host Microbe* 8, 116–127. doi: 10.1016/j.chom.2010.06.008
- Papenfert, K., and Vogel, J. (2014). Small RNA functions in carbon metabolism and virulence of enteric pathogens. *Front. Cell. Infect. Microbiol.* 4:91. doi: 10.3389/fcimb.2014.00091
- Pilla, G., and Tang, C. M. (2018). Going around in circles: virulence plasmids in enteric pathogens. *Nat. Rev. Microbiol.* 16, 484–495. doi: 10.1038/s41579-018-0031-2
- Pisano, F., Heine, W., Rosenheirich, M., Schweer, J., Nuss, A. M., and Dersch, P. (2014). Influence of PhoP and intra-species variations on virulence of *Yersinia pseudotuberculosis* during the natural oral infection route. *PLoS ONE* 9:e103541. doi: 10.1371/journal.pone.0103541
- Pobre, V., and Arraiano, C. M. (2015). Next generation sequencing analysis reveals that the ribonucleases RNase II, RNase R and PNPase affect bacterial motility and biofilm formation in *E. coli*. *BMC Genomics* 16:72. doi: 10.1186/s12864-015-1237-6
- Qu, Y., Bi, L., Ji, X., Deng, Z., Zhang, H., Yan, Y., et al. (2012). Identification by cDNA cloning of abundant sRNAs in a human-avirulent *Yersinia pestis* strain grown under five different growth conditions. *Future Microbiol.* 7, 535–547. doi: 10.2217/fmb.12.13
- Quereda, J. J., and Cossart, P. (2017). Regulating Bacterial Virulence with RNA. *Annu. Rev. Microbiol.* 71, 263–280. doi: 10.1146/annurev-micro-030117-020335
- Redko, Y., Galtier, E., Arnion, H., Darfeuille, F., Sismeiro, O., Coppée, J. Y., et al. (2016). RNase J depletion leads to massive changes in mRNA abundance in *Helicobacter pylori*. *RNA Biol.* 13, 243–253. doi: 10.1080/15476286.2015.1132141
- Reichenbach, B., Maes, A., Kalamorz, F., Hajnsdorf, E., and Gorke, B. (2008). The small RNA GlmY acts upstream of the sRNA GlmZ in the activation of *glmS* expression and is subject to regulation by polyadenylation in *Escherichia coli*. *Nucleic Acids Res.* 36, 2570–2580. doi: 10.1093/nar/gkn091
- Rempe, K. A., Hinz, A. K., and Vadyvaloo, V. (2012). Hfq regulates biofilm gut blockage that facilitates flea-borne transmission of *Yersinia pestis*. *J. Bacteriol.* 194, 2036–2040. doi: 10.1128/JB.06568-11
- Rhigetti, F., Nuss, A. M., Twittenhoff, C., Beele, S., Urban, K., Will, S., et al. (2016). Temperature-responsive *in vitro* RNA structure of *Yersinia pseudotuberculosis*. *Proc. Natl. Acad. Sci. U.S.A.* 113, 7237–7242. doi: 10.1073/pnas.1523004113
- Rice, J. B., and Vanderpool, C. K. (2011). The small RNA SgrS controls sugar-phosphate accumulation by regulating multiple PTS genes. *Nucleic Acids Res.* 39, 3806–3819. doi: 10.1093/nar/gkq1219
- Romeo, T. (1998). Global regulation by the small RNA-binding protein CsrA and the non-coding RNA molecule CsrB. *Mol. Microbiol.* 29, 1321–1330. doi: 10.1046/j.1365-2958.1998.01021.x
- Romeo, T., and Babitzke, P. (2018). Global regulation by CsrA and its RNA antagonists. *Microbiol. Spectr.* 6:RWR-0009-2017. doi: 10.1128/microbiolspec.RWR-0009-2017
- Romeo, T., Gong, M., Liu, M. Y., and Brun-Zinkernagel, A. M. (1993). Identification and molecular characterization of *csrA*, a pleiotropic gene from *Escherichia coli* that affects glycogen biosynthesis, gluconeogenesis, cell size, and surface properties. *J. Bacteriol.* 175, 4744–4755. doi: 10.1128/jb.175.15.4744-4755.1993
- Romeo, T., Vakulskas, C. A., and Babitzke, P. (2013). Post-transcriptional regulation on a global scale: form and function of Csr/Rsm systems. *Environ. Microbiol.* 15, 313–324. doi: 10.1111/j.1462-2920.2012.02794.x
- Rosenzweig, J. A., and Chopra, A. K. (2013). The exoribonuclease polynucleotide phosphorylase influences the virulence and stress responses of *Yersinia* and many other pathogens. *Front. Cell. Infect. Microbiol.* 3:81. doi: 10.3389/fcimb.2013.00081
- Rosenzweig, J. A., Chromy, B., Echeverry, A., Yang, J., Adkins, B., Plano, G. V., et al. (2007). Polynucleotide phosphorylase independently controls virulence factor expression levels and export in *Yersinia* spp. *FEMS Microbiol. Lett.* 270, 255–264. doi: 10.1111/j.1574-6968.2007.00689.x
- Rosenzweig, J. A., Weltman, G., Plano, G. V., and Schesser, K. (2005). Modulation of *Yersinia* type three secretion system by the S1 domain of polynucleotide phosphorylase. *J. Biol. Chem.* 280, 156–163. doi: 10.1074/jbc.M405662200
- Schiano, C. A., Bellows, L. E., and Lathem, W. W. (2010). The small RNA chaperone Hfq is required for the virulence of *Yersinia pseudotuberculosis*. *Infect. Immun.* 78, 2034–2044. doi: 10.1128/IAI.01046-09
- Schiano, C. A., Koo, J. T., Schipma, M. J., Caulfield, A. J., Jafari, N., and Lathem, W. W. (2014). Genome-wide analysis of small RNAs expressed by *Yersinia pestis* identifies a regulator of the Yop-Ysc type III secretion system. *J. Bacteriol.* 196, 1659–1670. doi: 10.1128/JB.01456-13
- Schiano, C. A., and Lathem, W. W. (2012). Post-transcriptional regulation of gene expression in *Yersinia* species. *Front. Cell. Infect. Microbiol.* 2:129. doi: 10.3389/fcimb.2012.00129
- Schweer, J., Kulkarni, D., Kochut, A., Pezoldt, J., Pisano, F., Pils, M. C., et al. (2013). The cytotoxic necrotizing factor of *Yersinia pseudotuberculosis* (CNF<sub>Y</sub>) enhances inflammation and Yop delivery during infection by activation of Rho GTPases. *PLoS Pathog.* 9:e1003746. doi: 10.1371/journal.ppat.1003746
- Schwiesow, L., Lam, H., Dersch, P., and Auerbuch, V. (2015). *Yersinia* type III secretion system master regulator LcrF. *J. Bacteriol.* 198, 604–614. doi: 10.1128/JB.00686-15
- Serganov, A., and Nudler, E. (2013). A decade of riboswitches. *Cell* 152, 17–24. doi: 10.1016/j.cell.2012.12.024
- Sharma, C. M., and Vogel, J. (2014). Differential RNA-seq: the approach behind and the biological insight gained. *Curr. Opin. Microbiol.* 19, 97–105. doi: 10.1016/j.mib.2014.06.010
- Sherwood, A. V., and Henkin, T. M. (2016). Riboswitch-mediated gene regulation: novel RNA architectures dictate gene expression responses. *Annu. Rev. Microbiol.* 70, 361–374. doi: 10.1146/annurev-micro-091014-104306
- Smego, R. A., Frean, J., and Koornhof, and, H. J. (1999). Yersiniosis I: Microbiological and clinicoepidemiological aspects of plague and non-plague *Yersinia* infections. *Eur. J. Clin. Microbiol. Infect. Dis.* 18, 1–15. doi: 10.1007/s100960050219
- Storz, G., Vogel, J., and Wassarman, K. M. (2011). Regulation by small RNAs in bacteria: expanding frontiers. *Mol. Cell* 43, 880–891. doi: 10.1016/j.molcel.2011.08.022
- Tomasini, A., Moreau, K., Chicher, J., Geissmann, T., Vandenesch, F., Romby, P., et al. (2017). The RNA targetome of *Staphylococcus aureus* non-coding RNA RsaA: impact on cell surface properties and defense mechanisms. *Nucleic Acids Res.* 45, 6746–6760. doi: 10.1093/nar/gkx219
- Urban, J. H., and Vogel, J. (2008). Two seemingly homologous noncoding RNAs act hierarchically to activate *glmS* mRNA translation. *PLoS Biol.* 6:e64. doi: 10.1371/journal.pbio.0060064
- Vakulskas, C. A., Potts, A. H., Babitzke, P., Ahmer, B. M., and Romeo, T. (2015). Regulation of bacterial virulence by Csr (Rsm) systems. *Microbiol. Mol. Biol. Rev.* 79, 193–224. doi: 10.1128/MMBR.00052-14
- Valentin-Weigand, P., Heesemann, J., and Dersch, P. (2014). Unique virulence properties of *Yersinia enterocolitica* O:3 - an emerging zoonotic pathogen using pigs as preferred reservoir host. *Int. J. Med. Microbiol.* 304, 824–834. doi: 10.1016/j.ijmm.2014.07.008
- Vanderpool, C. K., and Gottesman, S. (2004). Involvement of a novel transcriptional activator and small RNA in post-transcriptional regulation of the glucose phosphoenolpyruvate phosphotransferase system. *Mol. Microbiol.* 54, 1076–1089. doi: 10.1111/j.1365-2958.2004.04348.x
- Wadler, C. S., and Vanderpool, C. K. (2009). Characterization of homologs of the small RNA SgrS reveals diversity in function. *Nucleic Acids Res.* 37, 5477–5485. doi: 10.1093/nar/gkp591
- Wang, H., Avican, K., Fahlgren, A., Erttmann, S. F., Nuss, A. M., Dersch, P., et al. (2016). Increased plasmid copy number is essential for *Yersinia* T3SS function and virulence. *Science* 353, 492–495. doi: 10.1126/science.aaf7501
- Wang, J., Rennie, W., Liu, C., Carmack, C. S., Prévost, K., Caron, M. P., et al. (2015). Identification of bacterial sRNA regulatory targets using ribosome profiling. *Nucleic Acids Res.* 43, 10308–10320. doi: 10.1093/nar/gkv1158
- Waters, S. A., McAteer, S. P., Kudla, G., Pang, I., Deshpande, N. P., Amos, T. G., et al. (2017). Small RNA interactome of pathogenic *E. coli* revealed through crosslinking of RNase E. *EMBO J.* 36, 374–387. doi: 10.15252/embj.201694639
- Westermann, A. J. (2018). Regulatory RNAs in virulence and host-microbe interactions. *Microbiol. Spectr.* 6:RWR-0002-2017. doi: 10.1128/microbiolspec.RWR-0002-2017

- Westermann, A. J., Förstner, K. U., Amman, F., Barquist, L., Chao, Y., Schulte, L. N., et al. (2016). Dual RNA-seq unveils noncoding RNA functions in host-pathogen interactions. *Nature* 529, 496–501. doi: 10.1038/nature16547
- Williams, A. W., and Straley, S. C. (1998). YopD of *Yersinia pestis* plays a role in negative regulation of the low-calcium response in addition to its role in translocation of Yops. *J. Bacteriol.* 180, 350–358.
- Willias, S. P., Chauhan, S., Lo, C. C., Chain, P. S., and Motin, V. L. (2015). CRP-mediated carbon catabolite regulation of *Yersinia pestis* biofilm formation Is enhanced by the carbon storage regulator protein, CsrA. *PLoS ONE* 10:e0135481. doi: 10.1371/journal.pone.0135481
- Wright, P. R., Richter, A. S., Papenfort, K., Mann, M., Vogel, J., Hess, W. R., et al. (2013). Comparative genomics boosts target prediction for bacterial small RNAs. *Proc. Natl. Acad. Sci. U.S.A.* 110, E3487–E3496. doi: 10.1073/pnas.1303248110
- Yan, Y., Su, S., Meng, X., Ji, X., Qu, Y., Liu, Z., et al. (2013). Determination of sRNA expressions by RNA-seq in *Yersinia pestis* grown *in vitro* and during infection. *PLoS ONE* 8:e74495. doi: 10.1371/journal.pone.0074495
- Yang, J., Jain, C., and Schesser, K. (2008). RNase E regulates the *Yersinia* type 3 secretion system. *J. Bacteriol.* 190, 3774–3778. doi: 10.1128/JB.00147-08
- Ygberg, S. E., Clements, M. O., Rytönen, A., Thompson, A., Holden, D. W., Hinton, J. C., et al. (2006). Polynucleotide phosphorylase negatively controls *spv* virulence gene expression in *Salmonella enterica*. *Infect. Immun.* 74, 1243–1254. doi: 10.1128/IAI.74.2.1243-1254.2006
- Zhang, Y., Gao, J., Huang, Y., and Wang, J. (2018). Recent developments in single-cell RNA-seq of microorganisms. *Biophys. J.* 115, 173–180. doi: 10.1016/j.bpj.2018.06.008

**Conflict of Interest Statement:** The authors declare that the research was conducted in the absence of any commercial or financial relationships that could be construed as a potential conflict of interest.

Copyright © 2018 Knittel, Vollmer, Volk and Dersch. This is an open-access article distributed under the terms of the Creative Commons Attribution License (CC BY). The use, distribution or reproduction in other forums is permitted, provided the original author(s) and the copyright owner(s) are credited and that the original publication in this journal is cited, in accordance with accepted academic practice. No use, distribution or reproduction is permitted which does not comply with these terms.





# All *Yersinia* Are Not Created Equal: Phenotypic Adaptation to Distinct Niches Within Mammalian Tissues

Kimberly M. Davis\*

W. Harry Feinstone Department of Molecular Microbiology and Immunology, Johns Hopkins Bloomberg School of Public Health, Baltimore, MD, United States

## OPEN ACCESS

### Edited by:

Matthew S. Francis,  
Umeå University, Sweden

### Reviewed by:

Igor Brodsky,  
University of Pennsylvania,  
United States  
Petra Dersch,  
Helmholtz Center for Infection  
Research, Germany  
Matthew B. Lawrenz,  
University of Louisville, United States

### \*Correspondence:

Kimberly M. Davis  
kdavi140@jhu.edu

**Received:** 07 May 2018

**Accepted:** 13 July 2018

**Published:** 03 August 2018

### Citation:

Davis KM (2018) All *Yersinia* Are Not  
Created Equal: Phenotypic Adaptation  
to Distinct Niches Within Mammalian  
Tissues.  
*Front. Cell. Infect. Microbiol.* 8:261.  
doi: 10.3389/fcimb.2018.00261

*Yersinia pseudotuberculosis* replicates within mammalian tissues to form clustered bacterial replication centers, called microcolonies. A subset of bacterial cells within microcolonies interact directly with host immune cells, and other subsets of bacteria only interact with other bacteria. This establishes a system where subsets of *Yersinia* have distinct gene expression profiles, which are driven by their unique microenvironments and cellular interactions. When this leads to alterations in virulence gene expression, small subsets of bacteria can play a critical role in supporting the replication of the bacterial population, and can drive the overall disease outcome. Based on the pathology of infections with each of the three *Yersinia* species that are pathogenic to humans, it is likely that this specialization of bacterial subsets occurs during all *Yersinia* infections. This review will describe the pathology that occurs during infection with each of the three human pathogenic *Yersinia*, in terms of the structure of bacterial replication centers and the specific immune cell subsets that bacteria interact with, and will also describe the outcome these interactions have or may have on bacterial gene expression.

**Keywords:** *Yersinia* infections, inflammation, phagocytes, gene expression, heterogeneity

## INTRODUCTION

The genus *Yersinia* contains three species that are pathogenic to humans: *Yersinia pestis*, *Yersinia pseudotuberculosis*, and *Yersinia enterocolitica*. *Y. pseudotuberculosis* and *Y. enterocolitica* are intestinal pathogens that typically cause self-limiting gastroenteritis and mesenteric lymphadenitis (Hubbert et al., 1971; Paff et al., 1976). *Y. pestis* causes bubonic, septicemic, and pneumonic plague, and has acquired a distinct inoculation route over the course of its divergence from an ancestral *Y. pseudotuberculosis*, despite relatively few genetic changes (Achtman et al., 1999). *Y. pestis* is inoculated intradermally into a mammalian host through injection during a flea bite, and *Y. pestis* can also be directly inhaled to cause primary pneumonic plague. Despite distinctions in inoculation route, all three *Yersinia* species have a lymphotropism, meaning they quickly traffic to lymph nodes (LNs) or lymphoid tissues and preferentially colonize these tissues. All *Yersinia* can also spread systemically by accessing the bloodstream and colonizing deep tissue sites, such as the spleen and liver.

Several well-characterized virulence factors play an important role in the disease progression of *Yersinia* and the ability of the bacteria to survive and proliferate within multiple host tissues.

The human pathogenic *Yersinia* all contain a virulence plasmid termed either pCD1 or pYV, which contains genes encoding a central virulence factor for *Yersinia*: the type-III secretion system (T3SS) and its associated effector proteins, Yops (Gemski et al., 1980; Portnoy et al., 1981). The *Yersinia* T3SS is a needle-like structure that injects Yops directly into the host cytosol. Yops collectively function to modulate host signaling pathways to either inhibit or promote inflammation, to inhibit phagocytosis and motility of host cells, and can also inhibit the production and release of antimicrobial substances, such as reactive oxygen species (ROS) (Schesser et al., 1998; Viboud and Bliska, 2005; Songsunthong et al., 2010; Zhang and Bliska, 2010.)

Despite many genetic similarities, there are several well-defined genetic differences between *Yersinia* species. *Y. pestis* has acquired two additional virulence plasmids and 32 additional chromosomal genes since its divergence from *Y. pseudotuberculosis*, but also lost the functionality of as many as 13% of *Y. pseudotuberculosis* gene products (Achtman et al., 1999; Parkhill et al., 2001; Deng et al., 2002; Chain et al., 2004). *Y. pestis* pseudogenes include adhesins, and the lack of these genes may impact the ability of the bacterium to adhere to host cells and inject the T3SS (Simonet et al., 1996; Chain et al., 2004). Multiple adhesins: invasin, Ail, YadA, plasminogen activator protease (Pla, expressed from one of the *Y. pestis*-specific virulence plasmids), and pH 6 antigen, have been shown to play a critical role in adherence to host cells and T3SS injection (Yang and Isberg, 1993; Marra and Isberg, 1997; Felek and Krukoni, 2009; Durand

et al., 2010; Felek et al., 2010; Maldonado-Arocho et al., 2013). *Y. enterocolitica* and *Y. pseudotuberculosis* utilize invasin, Ail and YadA (Yang and Isberg, 1993; Marra and Isberg, 1997; Hudson and Bouton, 2006; Durand et al., 2010; Maldonado-Arocho et al., 2013; Paczosa et al., 2014; Mühlenkamp et al., 2015). *Y. pestis* has acquired inactivating mutations in both *yadA* and invasin, and instead uses Ail, Pla, and pH 6 antigen to promote host cell interactions (Bartra et al., 2008; Felek and Krukoni, 2009; Felek et al., 2010). Ail also plays a major role in promoting serum resistance and preventing complement deposition in all three *Yersinia*, which allows bacteria to survive within the bloodstream and resist neutrophil-mediated killing (Miller and Falkow, 1988; Bliska and Falkow, 1992; Pierson and Falkow, 1993; Kolodziejek et al., 2007; Bartra et al., 2008).

*Yersinia* replicate extracellularly within host tissue sites to form clonal bacterial clusters (Simonet et al., 1990; Logsdon and Mecsas, 2006; Oellerich et al., 2007; Crimmins et al., 2012; Davis et al., 2015). The sites of *Y. pseudotuberculosis* replication have been termed lesions, microcolonies, and recently, pyogranulomas, but each term refers to the same structure, described in **Figure 1** (Davis et al., 2015; Peterson et al., 2017; Zhang et al., 2018). This review will first describe disease progression in mammalian hosts, to introduce the different tissues *Yersinia* replicates within, and then discuss similarities and differences in the inflammatory lesions that form during *Yersinia* infection, with a focus on how interactions with distinct immune cell subsets may alter the gene expression profile of individual *Yersinia* cells within a replicating population.

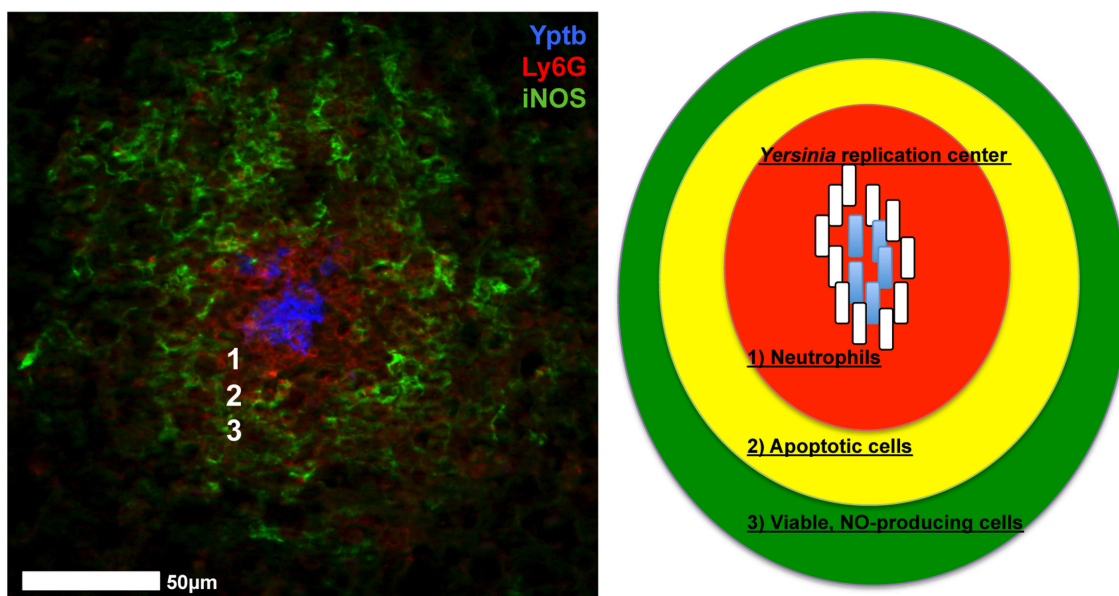


**FIGURE 1 |** *Yersinia* replicate to form inflammatory lesions that contain several different types of immune cells. **Left:** Adapted from Davis et al. (2015). Neutrophils (Ly6G, red) and iNOS<sup>+</sup> cells (iNOS, green) are recruited to replicating centers of *Y. pseudotuberculosis* (Yptb, blue). **Right:** Diagram of inflammatory lesions. (1) Neutrophils (red) form an inner layer surrounded by (2) Apoptotic cells (yellow; monocytes, some neutrophils). (3) Viable, NO producing cells (green; macrophages, dendritic cells, some neutrophils) form an outer layer of phagocytes. Peripheral bacterial cells (white rods) respond to host cell contact and diffusible antimicrobials, and allow interior bacteria (blue rods) to replicate. White numbers in the micrograph correspond with the numbered regions in the diagram.

## YERSINIA HUMAN DISEASE PROGRESSION

### Enteropathogenic *Yersinia* Disease Progression

*Y. pseudotuberculosis* is an enteric pathogen that infects the terminal ileum of the small intestine and also colonizes associated lymphoid tissues, such as Peyer's patches and mesenteric lymph nodes (LNs) (Hubbert et al., 1971; Paff et al., 1976). In healthy individuals, robust neutrophil recruitment is typically sufficient to limit bacterial growth, and can result in clearance. However, in immunocompromised individuals, individuals with hemochromatosis (iron-overload disorder), or in a mouse model of infection, bacteria access the bloodstream and spread to deep tissue sites, such as the spleen and liver (Capron et al., 1981; Abbott et al., 1986; Barnes et al., 2006; Miller et al., 2016). Bacteria replicate within deep tissues to high numbers, which can cause a lethal infection in the mouse model. Replication within intestinal tissues also leads to spread to the cecum, where bacteria associate with cecal lymphoid follicles and can establish a long term, persistent infection in the mouse (Fahlgren et al., 2014; Avican et al., 2015).

Like *Y. pseudotuberculosis*, *Y. enterocolitica* is an intestinal pathogen that initially colonizes the intestinal lumen and associated lymphoid tissues, such as Peyer's patches and mesenteric LNs. *Y. enterocolitica* can also spread to deep tissues following replication at intestinal sites (Heesemann et al., 1993; Viboud and Bliska, 2005; Oellerich et al., 2007). The disease progression for enteric *Yersinia* appears to be very similar, however, *Y. enterocolitica* is a relatively common cause of gastroenteritis, whereas patients rarely present with *Y. pseudotuberculosis* infection. This may be because *Y. enterocolitica* commonly colonizes many different species of livestock and wild game animals, which could lead to increased exposure rates within human populations, or because *Y. enterocolitica* may elicit a heightened inflammatory response resulting in more severe disease (Dube et al., 2001; Chlebicz and Slizewska, 2018; Syczylo et al., 2018).

### *Y. pestis* Disease Progression

*Y. pestis* is inoculated into the dermis of mammalian hosts after replication within the midgut of the flea. Within the flea, bacteria replicate within dense aggregates that partially block the proventricular valve of the flea, thus promoting dissemination into the mammalian host during a flea bloodmeal (Hinnebusch et al., 2017). *Y. pestis* travels from the injection site rapidly into local draining LNs (dLNs), where colonization is established within the mammalian host. In mouse models of infection, bacteria have been shown to traffic to dLNs intracellularly within dendritic cells and monocytes, and also extracellularly within the lymphatic system (Shannon et al., 2013, 2015; St. John et al., 2014; Gonzalez et al., 2015). The exact route depends on the inoculation (intra-dermal or subcutaneous) and also the virulence of the bacterial strain. Following initial trafficking, bacteria appear to occupy an extracellular niche. Bacteria initially replicate within dLNs with limited inflammation, however as bacteria continue to replicate, high levels of inflammatory immune cell recruitment

and tissue damage occurs. This forms the characteristic inflamed LNs, or buboes, that define bubonic plague (Butler, 1994). Tissue damage within LNs promotes bacterial bloodstream access, which initiates septicemic plague, and leads to colonization of deep tissues such as the spleen and liver (Perry and Fetherston, 1997). Septicemic plague can also occur immediately following flea-borne transmission, if the flea bite occurs deep within dermal tissues (Sebbane et al., 2006a). High levels of bacteria within the bloodstream can promote the development of a secondary pneumonic plague. Following bacterial replication in the lung, infected individuals can expel aerosols containing *Y. pestis*, which disseminate and cause primary pneumonic plague in new hosts. Septicemic plague also contributes to dissemination when a flea takes a bloodmeal from an infected host, which then restarts the *Y. pestis* life cycle in the flea vector (Perry and Fetherston, 1997; Hinnebusch et al., 2017).

### Host Response to *Yersinia*, and *Yersinia* Responses to the Host

*Yersinia* encounter many different tissue sites during infection of mammalian hosts, which forces bacteria to adapt to multiple different environments within a single host organism. Recruited inflammatory cells attempt to kill *Yersinia* through phagocytosis or by releasing antimicrobial substances to eliminate extracellular bacteria. *Yersinia*, in turn, can inhibit phagocytosis and detoxify many of these antimicrobials. The genes required to battle the host response have been largely defined by transcriptional data and mutational analyses, that indicate a given gene or pathway contributes to virulence at the population level. Interestingly, distinct subsets of the bacterial population respond differently, depending on their interactions with, and proximity to, different host cell subsets (Marteyn et al., 2010; Burton et al., 2014; Davis et al., 2015). These studies have described host-driven heterogeneity during *Salmonella enterica* serovar Typhimurium and *Shigella flexneri* infections, in addition to *Yersinia*, which may indicate this is a widespread phenomenon within pathogenic bacterial populations. Although much is still unknown concerning *Yersinia* heterogeneity within different tissue sites, we will describe what has been shown thus far, and which pathways may also be utilized in other tissues based on similarities in host cell interactions.

### Lymph Nodes

It has been hypothesized that the ability of *Y. pestis* to disseminate from dermal tissues and replicate within draining lymph nodes (dLNs) is due to the presence of Pla protease, which was acquired on an additional virulence plasmid after *Y. pestis* diverged from *Y. pseudotuberculosis* (Welkos et al., 1997; Lathem et al., 2007). However, *Y. pseudotuberculosis* can also effectively replicate within the dermis and traffic to dLNs following intradermal inoculation (Guinet et al., 2008, 2015). The major pathological difference during infection with the two species was the ability of the immune response to contain bacterial replication. *Y. pseudotuberculosis* elicits robust neutrophil recruitment that surrounds and contains bacteria, whereas *Y. pestis* exists as individual bacteria and reaches heightened bacterial loads (Guinet et al., 2008). *Y. pestis* has



acquired the ability to produce LPS with poor stimulatory activity and also produces an anti-phagocytic capsule, both of which could limit neutrophil interactions (Montminy et al., 2006; Dudte et al., 2017). There were also many examples of *Y. pestis* clustered together within the same infected tissues, but it was unclear if clustering promotes bacterial growth or clearance by the host. In the absence of clustering, *Y. pseudotuberculosis* replication within mesenteric LNs causes a lethal infection in the mouse, suggesting clustering promotes host survival (Peterson et al., 2017). *Y. pseudotuberculosis* was contained by a layer of apoptotic monocytes (**Figure 1**), which may also contain *Y. pseudotuberculosis* within dLNs. These studies suggest that the formation of microcolony, or pyogranuloma, structure contains infection and protects the host, however this structure also allows bacteria to cooperate and promote their own growth (Davis et al., 2015).

*Y. pestis* replication within dLNs is characterized by high bacterial loads and high levels of tissue destruction. Replication of *Y. pestis* within dLNs initially induces very little host cytokine expression, which is actively inhibited by components of the virulence plasmid including the T3SS (Comer et al., 2010). At later timepoints, neutrophils and additional phagocytes are recruited to infected LNs, and IL-17 is produced (Comer et al., 2010). In response, *Y. pestis* increases expression of reactive nitrogen species (RNS) detoxifying genes and iron scavenging genes, indicating *Y. pestis* is being exposed to the antimicrobial diffusible gas, nitric oxide (NO), and has limited access to iron during replication within the dLN (Sebbane et al., 2006b). NO was produced by recruited neutrophils, and likely other phagocytes, within the rat bubo, and the detoxifying gene, *hmp*, played an important role in promoting *Y. pestis* virulence (Sebbane et al., 2006b). It is likely that bacteria in the closest proximity to NO-producing phagocytes may specifically respond to this stress, and detoxify NO to protect other members of the population (Davis et al., 2015), although this hasn't yet been investigated. It will also be interesting to determine if iron limitation is uniformly experienced across LNs, or if this is specific to a subset of cells. Interestingly there was little evidence for a bacterial response to reactive oxygen species (ROS) in dLNs, and only one superoxide dismutase increased in transcript levels. A mutant strain lacking this superoxide dismutase (*sodA*) was fully virulent, which indicates *Y. pestis* effectively inhibits this response within LNs (Sebbane et al., 2006b).

## Deep Tissues

Multiple immune cell types are recruited to deep tissues during infection, and *Yersinia* effectively responds to create a hospitable environment for bacterial replication. Neutrophils directly interact with clustered centers of extracellular *Y. pseudotuberculosis*, and additional phagocytes are maintained at a distance relative to the bacterial centers (**Figure 1**). The layer of NO-producing cells likely contains a mixed population of monocytes, macrophages, and dendritic cells, and is adjacent to an apoptotic cell layer likely composed of monocytes (Davis et al., 2015; Peterson et al., 2017; Zhang et al., 2018). In the spleen, only the bacteria at the periphery of replicating centers respond

to NO, and detoxify NO to prevent further diffusion into the microcolony, thus protecting interior bacteria (Davis et al., 2015). NO was detoxified by Hmp, which was expressed in response to the *Nos2* gene product, inducible nitric oxide synthase, indicating *hmp* expression was a specific response to NO. This example of cooperative behavior likely also exists within mesenteric LNs, based on the recruitment of NO-producing cells, and the similarities in these microcolony or pyogranuloma structures (Zhang et al., 2018). Peripheral *Y. pseudotuberculosis* cells also respond to neutrophil contact in the spleen by expressing heightened levels of the T3SS (Pettersson et al., 1996; Davis et al., 2015). It remains unclear if heightened expression signifies a T3SS translocation event, or if this is due to prolonged host cell contact. Heightened T3SS expression could occur in multiple tissue sites and response to many host cell types, as it is clear that *Yersinia* can inject T3SS effector proteins into many different immune cell types during infection (Durand et al., 2010).

*Y. pestis* and *Y. enterocolitica* actively inhibit immune cell recruitment to the spleen by limiting CCR2 signaling and promoting Gal-1 expression, respectively (Kerschen et al., 2004; Ye et al., 2009, 2011; Davicino et al., 2017). In the liver, inflammatory monocytes and dendritic cells are recruited to sites of *Y. pestis* infection, and YopM promotes cell death of neutrophils and macrophages leading to the formation of an apoptotic layer of host cells around replicating bacterial centers (Ye et al., 2014). This mirrors the layer of apoptotic cells observed within *Y. pseudotuberculosis*-infected mesenteric LNs (**Figure 1**) (Peterson et al., 2017). iNOS<sup>+</sup> cells are also recruited to *Y. pestis* and *Y. enterocolitica* lesions, suggesting that subsets of peripheral cells may also express *hmp* to protect other individuals within the population. This also suggests that there may be quite a few similarities in the host response to *Yersinia* within deep tissues, unlike the pathological distinctions that are observed within infected LNs. This also indicates that all *Yersinia* may respond to similar stresses within deep tissues, and supports the idea that the cooperative behavior described for *Y. pseudotuberculosis* may also occur within other *Yersinia* infections, potentially even by expressing the same stress response pathways in distinct subsets of bacteria.

Neutrophils are a major producer of reactive oxygen species (ROS), but production can be inhibited by the T3SS, so it remains unclear if ROS restricts *Yersinia* growth in tissues. Mutant *Y. enterocolitica* lacking superoxide dismutase (*sodA*) were attenuated within the spleen and liver, but this could be due to sensitivity to endogenous ROS generated during bacterial aerobic respiration, or host-derived ROS (Roggenkamp et al., 1997). Transcriptional responses to ROS have not been observed with *Y. pestis* or *Y. pseudotuberculosis*, and a *Y. pestis* *sodA* mutant was not attenuated for growth in buboes or systemic infection (Sebbane et al., 2006b; Davis et al., 2015). However, a ROS-sensitive *Y. pseudotuberculosis* *dusB-fis* mutant was attenuated in immunocompetent mice, and rescued in the absence of ROS production, suggesting ROS was produced during infection (Green et al., 2016). Fis is a nucleoid-associated protein that likely has pleiotropic effects on the bacterial response to ROS, which may explain why the *dusB-fis* mutant uncovered an impact of ROS on *Y. pseudotuberculosis* growth. WT *Y. pseudotuberculosis*



growth was not impacted by the presence or absence of host-derived ROS, indicating the WT strain can effectively defend itself from ROS without significant transcriptional changes (Davis et al., 2015; Green et al., 2016).

## Intestinal Tissue and Peyer's Patches

Following intestinal colonization, enteropathogenic *Yersinia* traverse M cells to form microcolonies within Peyer's patches, which are specialized lymphoid tissues associated with the intestinal epithelium. The immune response to *Y. pseudotuberculosis* and *Y. enterocolitica* in Peyer's patches is characterized by neutrophil influx and a mixed  $T_H17/T_H1$  response, in contrast to the  $T_H17$ -specific response to *Y. pestis* within dLNs (Comer et al., 2010; Davicino et al., 2017; Nuss et al., 2017). *Y. pseudotuberculosis* responds by expressing genes to prevent phagocytosis and counteract iron deprivation and RNS, similar to *Y. pestis* within dLNs (Sebbane et al., 2006b; Nuss et al., 2017). *Y. enterocolitica* also actively inhibits neutrophil recruitment by a YopH-dependent mechanism that reduces CXCR2 surface expression on neutrophils (Dave et al., 2016). Microcolonies within the lamina propria contain  $CD4^+$  T cells and inflammatory macrophage and/or dendritic cell populations, in addition to  $CD8^+$  T cells. Interaction with  $CD8^+$  tissue-resident memory T cells within the lamina propria can effectively contain *Y. pseudotuberculosis* replication within the terminal ileum (Bergsbaken and Bevan, 2015).

Intestinal infection with sublethal doses of *Y. pseudotuberculosis* can establish a persistent, asymptomatic infection with sustained fecal shedding of bacteria, which may promote dissemination to additional hosts (Fahlgren et al., 2014; Avican et al., 2015). Persistence led to a dramatic shift in bacterial gene expression, which resembled growth at room temperature in bacteriological media, and was characterized by heightened expression of flagella and invasins, and downregulation of the T3SS (Avican et al., 2015; Heine et al., 2018). RovA was involved in these changes, and is known to positively regulate invasins and pH6 antigen expression. RovA expression is bistable in bacteriological media between 30 and 34°C, indicating bacteria utilize a bet-hedging approach to prepare a subset of the population to invade host cells, potentially as bacteria are moving through the host environment and the temperature is increasing (Quade et al., 2012; Nuss et al., 2016). RovA expression was also detected within a subset of the bacterial population replicating within the cecum, suggesting that RovA expression could be another example of cooperative behavior (Nuss et al., 2016).

## Lungs

Very little inflammation is observed early during primary pneumonic *Y. pestis* infection, similar to early timepoints within LNs during bubonic plague (Lathem et al., 2005; Guinet et al., 2008; Comer et al., 2010). However, by 48 h post-infection, inflammatory cells are localized around centers of replicating bacteria and bacteria are responding to the host environment (Lathem et al., 2005). Within the lung, *Y. pestis* upregulates expression of the T3SS, iron acquisition genes, and RNS detoxifying genes, including *hmp* (Lathem et al., 2005). In contrast, expression of pH 6 antigen, Pla, and ROS

detoxifying genes were downregulated, indicating bacteria were not responding to ROS, and these adhesins were not required to replicate within the lungs (Lathem et al., 2005). Similar results were seen in a *Y. pseudotuberculosis* lung infection model, where Ail and YadA contribute to replication and dissemination to deep tissues, but pH 6 antigen was dispensable (Paczosa et al., 2014). It will be interesting to determine if heightened gene expression occurs within all the individual *Yersinia* cells replicating within the lung, or if distinct subsets of cells respond in different ways. Based on experiments with *Y. pseudotuberculosis*, individual *Y. pestis* cells may be expressing heightened levels of the T3SS or heightened levels of *hmp* depending on their spatial location relative to immune cell subsets.

## Concluding Remarks

As *Yersinia* replicate within tissues, they form microcolonies where some individual cells interact directly with host immune cells, and other cells only interact with other bacteria. *Yersinia* species elicit similar inflammatory responses, characterized by recruitment of neutrophils, monocytes, macrophages, and dendritic cells, and all *Yersinia* appear to react similarly by upregulating expression of anti-phagocytic factors, RNS detoxifying genes, and iron scavenging genes. Several key questions remain: Are microcolonies protective for the host, or do they promote bacterial replication? Can we alter the host response to better contain bacterial growth? Limiting the host response impacts the containment of *Yersinia* within microcolonies and increases virulence, suggesting microcolonies protect the host (Peterson et al., 2017). However, disruption of microcolonies by attenuating *Yersinia* can promote clearance of bacteria, suggesting there is also a protective effect for bacteria (Davis et al., 2015). More future studies will be needed to determine if the host immune response can be manipulated to better contain and clear infection.

We are only beginning to understand how host cell interactions are driving differences in bacterial gene expression, and how small subsets of the bacterial population may be producing virulence genes that are critical for promoting disease. Better understanding and characterization of the heterogeneity in gene expression across bacterial populations, specifically in virulence gene expression, will have important implications for identifying potential drug targets for novel therapeutics. We believe the heterogeneity within *Yersinia* populations is likely also present within populations of other bacterial pathogens, and may be a widespread phenomenon that needs to be taken into account when designing antimicrobial therapeutics.

## AUTHOR CONTRIBUTIONS

The author confirms being the sole contributor of this work and approved it for publication.

## ACKNOWLEDGMENTS

The author of this manuscript declares no conflict of interest. This work was supported by the NIAID Career Transition award, 1K22AI123465-01.

## REFERENCES

- Abbott, M., Galloway, A., and Cunningham, J. (1986). Haemochromatosis presenting with a double *Yersinia* infection. *J. Infect.* 13, 143–145. doi: 10.1016/S0163-4453(86)92869-0
- Achtman, M., Zurth, K., Morelli, G., Torrea, G., Guiry, A., and Carniel, E. (1999). *Yersinia pestis*, the cause of plague, is a recently emerged clone of *Yersinia pseudotuberculosis*. *Proc. Natl. Acad. Sci. U.S.A.* 96, 14043–14048. doi: 10.1073/pnas.96.24.14043
- Avican, K., Fahlgren, A., Huss, M., Heroven, A., Beckstette, M., Dersch, P., et al. (2015). Reprogramming of *Yersinia* from virulent to persistent mode revealed by complex *in vivo* RNA-seq analysis. *PLoS Pathog.* 11:e1004600. doi: 10.1371/journal.ppat.1004600
- Barnes, P. D., Bergman, M. A., Mecsas, J., and Isberg, R. R. (2006). *Yersinia pseudotuberculosis* disseminates directly from a replicating bacterial pool in the intestine. *J. Exp. Med.* 203, 1591–1601. doi: 10.1084/jem.20060905
- Bartra, S. S., Styer, K. L., O'Bryant, D. M., Nilles, M. L., Hinnebusch, B. J., Aballey, A., et al. (2008). Resistance of *Yersinia pestis* to complement-dependent killing is mediated by the ail outer membrane protein. *Infect. Immun.* 76, 612–622. doi: 10.1128/IAI.01125-07
- Bergsbaken, T., and Bevan, M. (2015). Proinflammatory microenvironments within the intestine regulate the differentiation of tissue-resident CD8+ T cells responding to infection. *Nat. Immunol.* 16, 406–414. doi: 10.1038/ni.3108
- Bliska, J. B., and Falkow, S. (1992). Bacterial resistance to complement killing mediated by the ail protein of *Yersinia enterocolitica*. *Proc. Natl. Acad. Sci. U.S.A.* 89, 3561–3565. doi: 10.1073/pnas.89.8.3561
- Burton, N., Schürmann, N., Casse, O., Steeb, A. K., Claudy, B., Zankl, J., et al. (2014). Disparate impact of oxidative host defenses determines the fate of salmonella during systemic infection of mice. *Cell Host Microbe* 15, 72–83. doi: 10.1016/j.chom.2013.12.006
- Butler, T. (1994). *Yersinia* infections: centennial of the discovery of the plague bacillus. *Clin. Infect. Dis.* 19, 655–661. doi: 10.1093/clinids/19.4.655
- Capron, J., Delamarre, J., Delcenserie, R., Ginston, J., Dupas, J., and Lorriaux, A. (1981). Liver abscess complicating *Yersinia pseudotuberculosis* ileitis. *Gastroenterology* 81, 150–152.
- Chain, P. S., Carniel, E., Larimer, F. W., Lamerdin, J., Stoutland, P. O., Regala, W. M., et al. (2004). Insights into the evolution of *Yersinia pestis* through whole-genome comparison with *Yersinia pseudotuberculosis*. *Proc. Natl. Acad. Sci. U.S.A.* 101, 13826–13831. doi: 10.1073/pnas.0404012101
- Chlebicz, A., and Slizewska, K. (2018). Campylobacteriosis, salmonellosis, yersiniosis, and listeriosis as zoonotic foodborne diseases: a review. *Int. J. Environ. Res. Public Health* 15:E863. doi: 10.3390/ijerph15050863
- Comer, J. E., Sturdevant, D. E., Carmody, A. B., Virtaneva, K., Gardner, D., Long, D., et al. (2010). Transcriptomic and innate immune responses to *Yersinia pestis* in the lymph node during bubonic plague. *Infect. Immun.* 78, 5086–5098. doi: 10.1128/IAI.00256-10
- Crimmins, G. T., Mohammadi, S., Green, E. R., Bergman, M. A., Isberg, R. R., and Mecsas, J. (2012). Identification of MrtAB, an ABC transporter specifically required for *Yersinia pseudotuberculosis* to colonize the mesenteric lymph nodes. *PLoS Pathog.* 8:e1002828. doi: 10.1371/journal.ppat.1002828
- Dave, M. N., Silva, J. E., Elicabe, R. J., Jeréz, M. B., Filippa, V. P., Gorlino, C. V., et al. (2016). *Yersinia enterocolitica* YopH-deficient strain activates neutrophil recruitment to Peyer's patches and promotes clearance of the virulent strain. *Infect. Immun.* 84, 3172–3181. doi: 10.1128/IAI.00568-16
- Davicino, R. C., Méndez-Huergo, S. P., Elicabe, R. J., Stupirski, J. C., Autenrieth, I., De Genaro, M. S., et al. (2017). Galectin-1-driven tolerogenic programs aggravate *Yersinia enterocolitica* infection by repressing antibacterial immunity. *J. Immunol.* 199, 1382–1392. doi: 10.4049/jimmunol.1700579
- Davis, K. M., Mohammadi, S., and Isberg, R. R. (2015). Community behavior and spatial regulation within a bacterial microcolony in deep tissue sites serves to protect against host attack. *Cell Host Microbe* 17, 21–31. doi: 10.1016/j.chom.2014.11.008
- Deng, W., Burland, V., Plunkett, G., Boutin, A., Mayhew, G. F., Liss, P., et al. (2002). Genome sequence of *Yersinia pestis* KIM. *J. Bacteriol.* 184, 4601–4611. doi: 10.1128/JB.184.16.4601-4611.2002
- Dube, P. H., Revell, P. A., Chaplin, D. D., Lorenz, R. G., and Miller, V. L. (2001). A role for IL-1 alpha in inducing pathologic inflammation during bacterial infection. *Proc. Natl. Acad. Sci. U.S.A.* 98, 10880–10885. doi: 10.1073/pnas.191214498
- Dudte, S. C., Hinnebusch, B. J., and Shannon, J. G. (2017). Characterization of *Yersinia pestis* interactions with human neutrophils *in vitro*. *Front. Cell. Infect. Microbiol.* 7:358. doi: 10.3389/fcimb.2017.00358
- Durand, E. A., Maldonado-Arocho, F. J., Castillo, C., Walsh, R. L., and Mecsas, J. (2010). The presence of professional phagocytes dictates the number of host cells targeted for Yop translocation during infection. *Cell. Microbiol.* 12, 1064–1082. doi: 10.1111/j.1462-5822.2010.01451.x
- Fahlgren, A., Avican, K., Westermark, L., Nordfeith, R., and Fällman, M. (2014). Colonization of cecum is important for development of persistent infection by *Yersinia pseudotuberculosis*. *Infect. Immun.* 82, 3471–3482. doi: 10.1128/IAI.01793-14
- Felek, S., and Krukonis, E. (2009). The *Yersinia pestis* ail protein mediates binding and Yop delivery to host cells required for plague virulence. *Infect. Immun.* 77, 825–836. doi: 10.1128/IAI.00913-08
- Felek, S., Tsang, T. M., and Krukonis, E. S. (2010). Three *Yersinia pestis* adhesins facilitate Yop delivery to eukaryotic cells and contribute to plague virulence. *Infect. Immun.* 78, 4134–4150. doi: 10.1128/IAI.00167-10
- Gemski, P., Lazere, J. R., and Casey, T. (1980). Plasmid associated with pathogenicity and calcium dependency of *Yersinia enterocolitica*. *Infect. Immun.* 27, 682–685.
- Gonzalez, R. J., Lane, M. C., Wagner, N. J., Weening, E. H., and Miller, V. L. (2015). Dissemination of a highly virulent pathogen: tracking the early events that define infection. *PLoS Pathog.* 11:e1004587. doi: 10.1371/journal.ppat.1004587
- Green, E. R., Clark, S., Crimmins, G. T., Mack, M., Kumamoto, C. A., and Mecsas, J. (2016). Fis is essential for *Yersinia pseudotuberculosis* virulence and protects against reactive oxygen species produced by phagocytic cells during infection. *PLoS Pathog.* 12:e1005898. doi: 10.1371/journal.ppat.1005898
- Guinet, F., Avé, P., Filali, S., Huon, C., Savin, C., Huerre, M., et al. (2015). Dissociation of tissue destruction and bacterial expansion during bubonic plague. *PLoS Pathog.* 11:e1005222. doi: 10.1371/journal.ppat.1005222
- Guinet, F., Avé, P., Jones, L., Huerre, M., and Carniel, E. (2008). Defective innate cell response and lymph node infiltration specify *Yersinia pestis* infection. *PLoS ONE* 3:e1688. doi: 10.1371/journal.pone.0001688
- Heesemann, J., Gaede, K., and Autenrieth, I. (1993). Experimental *Yersinia enterocolitica* infection in rodents: a model for human yersiniosis. *APMIS* 101, 417–429. doi: 10.1111/j.1699-0463.1993.tb00130.x
- Heine, W., Beckstette, M., Heroven, A. K., Thiemann, S., Heise, U., Nuss, A. M., et al. (2018). Loss of CNFY toxin-induced inflammation drives *Yersinia pseudotuberculosis* into persistency. *PLoS Pathog.* 14:e1006858. doi: 10.1371/journal.ppat.1006858
- Hinnebusch, B. J., Jarrett, C. O., and Bland, D. M. (2017). “Fleaing” the plague: adaptations of *Yersinia pestis* to its insect vector that lead to transmission. *Annu. Rev. Microbiol.* 71, 215–232. doi: 10.1146/annurev-micro-090816-093521
- Hubbert, W., Petenyi, C., Glasgow, L., Uyeda, C., and Creighton, S. (1971). *Yersinia pseudotuberculosis* infection in the United States. Septicemia, appendicitis, and mesenteric lymphadenitis. *Am. J. Trop. Med. Hyg.* 20, 679–684. doi: 10.4269/ajtmh.1971.20.679
- Hudson, K. J., and Bouton, A. H. (2006). *Yersinia pseudotuberculosis* adhesins regulate tissue-specific colonization and immune cell localization in a mouse model of systemic infection. *Infect. Immun.* 74, 6487–6490. doi: 10.1128/IAI.00718-06
- Kerschen, E. J., Cohen, D. A., Kaplan, A. M., and Straley, S. C. (2004). The plague virulence protein YopM targets the innate immune response by causing a global depletion of NK cells. *Infect. Immun.* 72, 4589–4602. doi: 10.1128/IAI.72.8.4589-4602.2004
- Kolodziejek, A. M., Sinclair, D. J., Seo, K. S., Schnider, D. R., Deobald, C. F., Rohde, H. N., et al. (2007). Phenotypic characterization of OmpX, an ail homologue of *Yersinia pestis* KIM. *Microbiology* 153, 2941–2951. doi: 10.1099/mic.0.2006/005694-0
- Latham, W. W., Crosby, S. D., Miller, V. L., and Goldman, W. E. (2005). Progression of primary pneumonic plague: a mouse model of infection,

- pathology, and bacterial transcriptional activity. *Proc. Natl. Acad. Sci. U.S.A.* 102, 17786–17791. doi: 10.1073/pnas.0506840102
- Latham, W. W., Price, P. A., Miller, V. L., and Goldman, W. E. (2007). A plasminogen-activating protease specifically controls the development of primary pneumonic plague. *Science* 315, 509–513. doi: 10.1126/science.1137195
- Logsdon, L. K., and Mecsas, J. (2006). The proinflammatory response induced by wild-type *Yersinia pseudotuberculosis* infection inhibits survival of yop mutants in the gastrointestinal tract and Peyer's patches. *Infect. Immun.* 74, 1516–1527. doi: 10.1128/IAI.74.3.1516-1527.2006
- Maldonado-Arocho, F. J., Green, C., Fisher, M. L., Paczosa, M. K., and Mecsas, J. (2013). Adhesins and host serum factors drive Yop translocation by *Yersinia* into professional phagocytes during animal infection. *PLoS Pathog.* 9:e1003415. doi: 10.1371/journal.ppat.1003415
- Marra, A., and Isberg, R. (1997). Invasin-dependent and invasin-independent pathways for translocation of *Yersinia pseudotuberculosis* across the Peyer's patch intestinal epithelium. *Infect. Immun.* 65, 3412–3421.
- Marteyn, B., West, N. P., Browning, D. F., Cole, J. A., Shaw, J. G., Palm, F., et al. (2010). Modulation of *Shigella* virulence in response to available oxygen *in vivo*. *Nature* 465, 355–358. doi: 10.1038/nature08970
- Miller, H. K., Schwiesow, L., Au-Yeung, W., and Auerbuch, V. (2016). Hereditary hemochromatosis predisposes mice to *Yersinia pseudotuberculosis* infection even in the absence of the type III secretion system. *Front. Cell. Infect. Microbiol.* 6:69. doi: 10.3389/fcimb.2016.00069
- Miller, V. L., and Falkow, S. (1988). Evidence for two genetic loci in *Yersinia enterocolitica* that can promote invasion of epithelial cells. *Infect. Immun.* 56, 1242–1248.
- Montminy, S. W., Khan, N., McGrath, S., Walkowicz, M. J., Sharp, F., Conlon, J. E., et al. (2006). Virulence factors of *Yersinia pestis* are overcome by a strong lipopolysaccharide response. *Nat. Immunol.* 7, 1066–1073. doi: 10.1038/ni1386
- Mühlenkamp, M., Oberhettinger, P., Leo, J. C., Linke, D., and Schütz, M. S. (2015). *Yersinia* adhesin A (YadA)—beauty & beast. *Int. J. Med. Microbiol.* 305, 252–258. doi: 10.1016/j.ijmm.2014.12.008
- Nuss, A. M., Beckstette, M., Pimenova, M., Schmühl, C., Opitz, W., Pisano, F., et al. (2017). Tissue dual RNA-seq allows fast discovery of infection-specific functions and riboregulators shaping host-pathogen transcriptomes. *Proc. Natl. Acad. Sci. U.S.A.* 114, E791–E800. doi: 10.1073/pnas.1613405114
- Nuss, A. M., Schuster, F., Roselius, L., Klein, J., Bucker, R., Herbst, K., et al. (2016). A precise temperature-responsive bistable switch controlling *Yersinia* virulence. *PLoS Pathog.* 12:e1006091. doi: 10.1371/journal.ppat.1006091
- Oellerich, M. F., Jacobi, C. A., Freund, S., Niedung, K., Bach, A., Heesemann, J., et al. (2007). *Yersinia enterocolitica* infection of mice reveals clonal invasion and abscess formation. *Infect. Immun.* 75, 3802–3811. doi: 10.1128/IAI.00419-07
- Paczosa, M. K., Fisher, M. L., Maldonado-Arocho, F. J., and Mecsas, J. (2014). *Yersinia pseudotuberculosis* uses Ail and YadA to circumvent neutrophils by directing Yop translocation during lung infection. *Cell Microbiol.* 16, 247–268. doi: 10.1111/cmi.12219
- Paff, J. R., Triplett, D. A., and Saari, T. N. (1976). Clinical and laboratory aspects of *Yersinia pseudotuberculosis* infections, with a report of two cases. *Am. J. Clin. Pathol.* 66, 101–110. doi: 10.1093/ajcp/66.1.101
- Parkhill, J., Wren, B. W., Thomson, N. R., Titball, R. W., Holden, M. T., Prentice, M. B., et al. (2001). Genome sequence of *Yersinia pestis*, the causative agent of plague. *Nature* 413, 523–527. doi: 10.1038/35097083
- Perry, R. D., and Fetherston, J. D. (1997). *Yersinia pestis*—etiologic agent of plague. *Clin. Microbiol. Rev.* 10, 35–66.
- Peterson, L., Philip, N., DeLaney, A., Wynosky-Dolfi, M., Asklof, K., Gray, F., et al. (2017). RIPK1-dependent apoptosis bypasses pathogen blockage of innate signaling to promote immune defense. *J. Exp. Med.* 214, 3171–3182. doi: 10.1084/jem.20170347
- Pettersson, J., Nordfeith, R., Dubinina, E., Bergman, T., Gustafsson, M., Magnusson, K. E., et al. (1996). Modulation of virulence factor expression by pathogen target cell contact. *Science* 273, 1231–1233. doi: 10.1126/science.273.5279.1231
- Pierson, D. E., and Falkow, S. (1993). The ail gene of *Yersinia enterocolitica* has a role in the ability of the organism to survive serum killing. *Infect. Immun.* 61, 1846–1852.
- Portnoy, D. A., Moseley, S. L., and Falkow, S. (1981). Characterization of plasmids and plasmid-associated determinants of *Yersinia enterocolitica* pathogenesis. *Infect. Immun.* 31, 775–782.
- Quade, N., Mendonca, C., Herbst, K., Heroven, A. K., Ritter, C., Heinz, D. W., et al. (2012). Structural basis for intrinsic thermosensing by the master virulence regulator RovA of *Yersinia*. *J. Biol. Chem.* 287, 35796–35803. doi: 10.1074/jbc.M112.379156
- Roggkamp, A., Bittner, T., Leitritz, L., Sing, A., and Heesemann, J. (1997). Contribution of the Mn-cofactored superoxide dismutase (SodA) to the virulence of *Yersinia enterocolitica* serotype O8. *Infect. Immun.* 65, 4705–4710.
- Schesser, K., Splik, A. K., Dukuzumuremyi, J. M., Neurath, M. F., Pettersson, S., and Wolf-Watz, H. (1998). The yopJ locus is required for *Yersinia*-mediated inhibition of NF-kappaB activation and cytokine expression: YopJ contains a eukaryotic SH2-like domain that is essential for its repressive activity. *Mol. Microbiol.* 28, 1067–1079. doi: 10.1046/j.1365-2958.1998.00851.x
- Sebbane, F., Jarrett, C. O., Gardner, D., Long, D., and Hinnebusch, B. J. (2006a). Role of the *Yersinia pestis* plasminogen activator in the incidence of distinct septicemic and bubonic forms of flea-borne plague. *Proc. Natl. Acad. Sci. U.S.A.* 103, 5526–5530. doi: 10.1073/pnas.0509544103
- Sebbane, F., Lemaître, N., Sturdevant, D. E., Rebeil, R., Virtaneva, K., Porcella, S. F., et al. (2006b). Adaptive response of *Yersinia pestis* to extracellular effectors of innate immunity during bubonic plague. *Proc. Natl. Acad. Sci. U.S.A.* 103, 11766–11771. doi: 10.1073/pnas.0601182103
- Shannon, J. G., Bosio, C. F., and Hinnebusch, B. J. (2015). Dermal neutrophil, macrophage and dendritic cell responses to *Yersinia pestis* transmitted by fleas. *PLoS Pathog.* 11:e1004734. doi: 10.1371/journal.ppat.1004734
- Shannon, J. G., Hasenkrug, A. M., Dorward, D. W., Nair, V., Carmody, A. B., and Hinnebusch, B. J. (2013). *Yersinia pestis* subverts the dermal neutrophil response in a mouse model of bubonic plague. *MBio* 4, e00170–e00113. doi: 10.1128/mBio.00170-13
- Simonet, M., Richard, S., and Berche, P. (1990). Electron microscopic evidence for *in vivo* extracellular localization of *Yersinia pseudotuberculosis* harboring the pYV plasmid. *Infect. Immun.* 58, 841–845.
- Simonet, M., Riot, B., Fortineau, N., and Berche, P. (1996). Invasin production by *Yersinia pestis* is abolished by insertion of an IS200-like element within the inv gene. *Infect. Immun.* 64, 375–379.
- Songsunthong, W., Higgins, M. C., Rolán, H. G., Murphy, J. L., and Mecsas, J. (2010). ROS-inhibitory activity of YopE is required for full virulence of *Yersinia* in mice. *Cell. Microbiol.* 12, 988–1001. doi: 10.1111/j.1462-5822.2010.01448.x
- St. John, A. L., Ang, W. X. G., Huang, M. N., Kunder, C. A., Chan, E. W., Gunn, M. D., et al. (2014). S1P-dependent trafficking of intracellular *Yersinia pestis* through lymph nodes establishes bubos and systemic infection. *Immunity* 41, 440–450. doi: 10.1016/j.immuni.2014.07.013
- Szczyło, K., Platt-Samoraj, A., Banczerz-Kisiel, A., Szczerba-Turek, A., Pajdak-Czaus, J., Łabuć, S., et al. (2018). The prevalence of *Yersinia enterocolitica* in game animals in Poland. *PLoS ONE* 13:e0195136. doi: 10.1371/journal.pone.0195136
- Viboud, C. I., and Bliska, J. B. (2005). *Yersinia* outer proteins: role in modulation of host cell signaling responses and pathogenesis. *Annu. Rev. Microbiol.* 59, 69–89. doi: 10.1146/annurev.micro.59.030804.121320
- Welkos, S., Friedlander, A., and Davis, K. (1997). Studies on the role of plasminogen activator in systemic infection by virulent *Yersinia pestis* strain CO92. *Microb. Pathog.* 23, 211–223. doi: 10.1006/mpat.1997.0154
- Yang, Y., and Isberg, R. (1993). Cellular internalization in the absence of invasin expression is promoted by the *Yersinia pseudotuberculosis* yadA product. *Infect. Immun.* 61, 3907–3913.
- Ye, Z., Gorman, A. A., Uittenbogaard, A. M., Myers-Morales, T., Kaplan, A. M., Cohen, D. A., et al. (2014). Caspase-3 mediates the pathogenic effect of *Yersinia pestis* YopM in liver of C57BL/6 mice and contributes to YopM's function in spleen. *PLoS ONE* 9:e110956. doi: 10.1371/journal.pone.0110956

- Ye, Z., Kerschen, E. J., Cohen, D. A., Kaplan, A. M., van Rooijen, N., and Straley, S. C. (2009). Gr1+ cells control growth of YopM-negative *Yersinia pestis* during systemic plague. *Infect. Immun.* 77, 3791–3806. doi: 10.1128/IAI.00284-09
- Ye, Z., Uittenbogaard, A. M., Cohen, D. A., Kaplan, A. M., Ambati, J., and Straley, S. C. (2011). Distinct CCR2(+) Gr1(+) cells control growth of the *Yersinia pestis*  $\Delta$ yopM mutant in liver and spleen during systemic plague. *Infect. Immun.* 79, 674–687. doi: 10.1128/IAI.00808-10
- Zhang, Y., and Bliska, J. (2010). YopJ-promoted cytotoxicity and systemic colonization are associated with high levels of murine interleukin-18, gamma interferon, and neutrophils in a live vaccine model of *Yersinia pseudotuberculosis* infection. *Infect. Immun.* 78, 2329–2341. doi: 10.1128/IAI.00094-10
- Zhang, Y., Khairallah, C., Sheridan, B. S., van der Velden, A. W. M., and Bliska, J. B. (2018). CCR2+ inflammatory monocytes are recruited to *Yersinia*

*pseudotuberculosis* pyogranulomas and dictate adaptive responses at the expense of innate immunity during oral infection. *Infect. Immun.* 86, e00782–e00717. doi: 10.1128/IAI.00782-17

**Conflict of Interest Statement:** The author declares that the research was conducted in the absence of any commercial or financial relationships that could be construed as a potential conflict of interest.

Copyright © 2018 Davis. This is an open-access article distributed under the terms of the Creative Commons Attribution License (CC BY). The use, distribution or reproduction in other forums is permitted, provided the original author(s) and the copyright owner(s) are credited and that the original publication in this journal is cited, in accordance with accepted academic practice. No use, distribution or reproduction is permitted which does not comply with these terms.



# Advantages of publishing in Frontiers



## OPEN ACCESS

Articles are free to read  
for greatest visibility  
and readership



## FAST PUBLICATION

Around 90 days  
from submission  
to decision



## HIGH QUALITY PEER-REVIEW

Rigorous, collaborative,  
and constructive  
peer-review



## TRANSPARENT PEER-REVIEW

Editors and reviewers  
acknowledged by name  
on published articles

## Frontiers

Avenue du Tribunal-Fédéral 34  
1005 Lausanne | Switzerland

Visit us: [www.frontiersin.org](http://www.frontiersin.org)

Contact us: [info@frontiersin.org](mailto:info@frontiersin.org) | +41 21 510 17 00



## REPRODUCIBILITY OF RESEARCH

Support open data  
and methods to enhance  
research reproducibility



## DIGITAL PUBLISHING

Articles designed  
for optimal readership  
across devices



## FOLLOW US

@frontiersin



## IMPACT METRICS

Advanced article metrics  
track visibility across  
digital media



## EXTENSIVE PROMOTION

Marketing  
and promotion  
of impactful research



## LOOP RESEARCH NETWORK

Our network  
increases your  
article's readership